Charlotte Boccara

Spatial Coding in the Hippocampal Region

Thesis for the degree of Philosophiae Doctor

Trondheim, March 2014

Norwegian University of Science and Technology
Faculty of Medicine
The Kavli Institute for Systems Neuroscience
Centre for the Biology of Memory/
Centre for Neural Computation

NTNU – Trondheim
Norwegian University of
Science and Technology

NTNU
Norwegian University of Science and Technology

Thesis for the degree of Philosophiae Doctor

Faculty of Medicine
The Kavli Institute for Systems Neuroscience
Centre for the Biology of Memory/
Centre for Neural Computation

ISBN 978-82-326-0122-6 (printed ver.)
ISBN 978-82-326-0123-3 (electronic ver.)
ISSN 1503-8181

Doctoral theses at NTNU, 2014:99

Printed by NTNU-trykk

ENGLISH SUMMARY

The human brain is an extremely complex machine that contains billions upon billions of neurons. These neurons are organized in several overlapping networks distributed across the nervous system, which specialize in specific cognitive functions. Functional specialization occurs also at the neuronal level as precise features can specifically activate the firing of individual neurons. One of the most widely studied neuronal specializations is that of the neurons of the hippocampal region. This region of the medial temporal lobe is involved in cognitive functions such as learning, memory and spatial cognition. Investigations first conducted in rats and later repeated in humans established that the hippocampal network consists of many interconnected areas grouped in two main subregions: the hippocampal formation and the parahippocampal region, each coding for different elements essential for accurate navigation. The exponential precision in techniques observed over the last few decades has revealed a complex network with many uncertainties regarding the nature, origin, and distribution of the spatial code throughout the hippocampal region. This thesis aims to shed light on this subject by adopting two approaches. The first one is to perform *in vivo* unit recording in freely behaving rats for several areas of the parahippocampal region. The second is to focus on the anatomical identification of the hippocampal subareas through the establishment of cyto- and chemo-architectonic markers.

The first approach led to the discovery of a new type of spatial parahippocampal neuron code for the boundaries of a given environment. These so-called border cells completed the hippocampal neural spatial network that includes place cells, head direction cells, and grid cells, which together convey positional, directional, metrics and velocity signal. Using the same approach, the second paper of this thesis revealed the widespread distribution of grid, head direction, and border cells over several interconnected parahippocampal regions (i.e. the presubiculum, the parasubiculum and the medial entorhinal cortex). It confirmed at a larger scale the specialization of some subareas and layers for specific modalities (e.g. layer II of the medial entorhinal cortex and grid cells) and the conjunction of several codes at the single neuron level (e.g. grid by head direction cells). It also delved into the existence of a network code superimposed on the neural code through the summation of unit activity to constitute cell assemblies and the emergence of network oscillations responsible, in turn, for unit

modulation. The discovery of grid cells outside the medial entorhinal cortex constrains the number of mechanisms so far proposed to explain such specific pattern of activity. The work presented here offers some perspectives on the relative contribution of cellular and network properties to the integration of multiple signals that contributes to the generation and the stabilization of the grid, spatial, and border signals.

The second approach provides a much-needed tool for experimentalists in the form of a three-dimensional atlas of the hippocampal region that focuses on anatomical border description and is integrated in a web-based virtual microscope application. The significant advantage of this atlas compared with previous accounts is that the boundaries and markers we describe have been verified in all three major sectional planes (i.e. coronal, sagittal and horizontal). By mapping single plane delineations onto a standard three-dimensional Waxholm rat brain, incoherencies between these dimensions were detected and borders readjusted accordingly. Additionally, this atlas is does not only offer cytoarchitectonic markers of the anatomical borders of the hippocampal region subareas. Given the lack of clear differences in neuronal staining, it also establishes an additional set of chemoarchitectonic criteria made apparent with immuno-staining against two calcium-binding proteins; calbindin and parvalbumin.

The results of this thesis may be read at three different levels. First, they influence the original concept of the cognitive map (O'Keefe and Nadel 1978) and build on the idea of a universal metric map (Moser et al. 2008; Moser and Moser 2008) to show that spatial cognition is supported by dynamic, interdependent, and collaborative widespread systems. Second, the understanding of the spatial neural code offers some insights into general information coding, computation, and the dynamic interaction between mental representation and behavioural outcomes. Learning and memory processes are at the core of spatial cognition, and the hippocampal region is crucial for such functions. Therefore, similar neural mechanisms may be supporting both spatial cognition and memory. Finally, these observations come from the analysis of rat neural activity, yet as the hippocampal region is a highly phylogenetically conserved brain area, many of them may be translated to humans and aid in the understanding and control of neurological pathologies such as epilepsy and Alzheimer’s disease.

NORSK SAMMENDRAG

Menneskehjernen er en ekstremt komplisert innretning som består av milliarder på milliarder med nerveceller. Disse nevronene er organisert i flere overlappende nettverk distribuert utover nervesystemet hvor de spesialiserer seg i spesifikke kognitive funksjoner. Det finnes også en funksjonell spesialisering på enkeltcellenivå hvor eneklte nevroner eller funksjonelle typer aktiveres på sin spesifikke måte. En av de best studerte nervecellespesialiserigene i hjernen er nevronene i den hippocampale region, lokalisert i den mediale delen av tinningslappen. Denne regionen er involvert i kognitive funksjoner som læring, hukommelse og spatial kognisjon.

Studier først gjort i rotter, og senere i mennesker har vist at det hippocampale nervenettverket består av mange sammenkoblete områder gruppert i to underregioner: den hippocampale formasjon og den parahippocampale region. Begge regionene har blitt påvist å kode for ulike elementer som er nødvendige for presis navigasjon. De siste tiårene har vi sett en enorm forbedring i presisjonen til ulike forskningsteknikker, og dette har åpenbart et komplekst nettverk hvor det fortsatt er mye usikkerhet vedrørende funksjon, opphav og distribusjon av den spatiale koden i den hippocampale region. Denne avhandlingen ønsker å belyse disse problemstillingene ved å benytte to ulike tilnærminger. Den første er å gjennomføre in vivo opptak i flere områder av den parahippocampale regionen hos frittløpende rotter. Den andre er å fokusere på anatomisk identifikasjon av hippocampale underområder ved å etablere metoder for cellulær- og kjemoarkitektonisk merking.

Den første tilnærmingen førte til oppdagelsen av en ny type spatial parahippocampal nevral kode for grensene i et gitt miljø. Disse såkalte grensecellene komplementerte det hippocampale nevrospatiale nettverket som innkluderer plassceller, hoderetningsceller og gitterceller. Tilsammen formidler disse cellene de nevrale signalen for posisjon, retning, metrikk og hastighet. Ved å benytte den samme metoden viser den andre artikkelen i denne avhandlingen den utstrakte distribusjonen av gitter-, hoderetnings- og grenseceller i flere underområder av de tett sammenkoblede parahippocampale regionene (presubiculum, parasubiculum og det mediale entorhinal cortex). I store trekk bekreftet disse funnene spesialiseringen i enkelte underområder og lag for spesifikke modaliteter (for eksempel lag II av det mediale entorhinal cortex og gitterceller) og sammenfallet av flere typer koder på enkeltcellenivå (for eksempel

gitteregenskaper på hoderetningsceller). Artikkelen undersøkte også eksistensen av en nettverkskode liggende over enhetsnervecellekoden gjenom summasjon av enhetsaktiviteten som kollektivt danner celleaggregater og nettverksossilasjoner og som igjen er ansvarlige for modulasjon av enhetene. Funnet av gitterceller utenfor det mediale entorhinal cortex begrenser antallet mekanismer som så langt har blitt foreslått til å forklare et slikt spesifikk mønster av aktivitet. Dette avhandlingsarbeidet gir perspektiver på det relative bidraget til cellulære egenskaper og nettverksegenskaper i integrasjonen av multiple signaler som bidrar i generering og stabilisering av gittersignaler, spatiale signaler og grensesignaler.

Den andre tilnærmingen tilbyr eksperimentatorer et nødvendig verktøy i form av et tre-dimensjonalt atlas over den hippocampale region som fokuserer på beskrivelsen av anatomisk grenser. Atlaset er i tillegg integrert i en nettbasert virtuelt mikroskop-applikasjon. Den signifikante fordelen med dette atlaset sammenlignet med tidligere atlas er at grensene og landemerkene som beskrives har blitt verifisert i tre anatomiske plan (koronalt, sagitalt og horisontalt). Ved å legge snitt fra de tre anatomiske plan inn i en standard tredimensjonal Waxholm rottehjerne, ble uoverenstemmelser mellom de tre dimensjonene oppdaget og grensene følgelig justert. Videre tilbyr ikke dette atlaset bare cytoarkitektoniske markører for anatomiske grenser mellom underområder i den hippocampale regionen. Grunnet mangelen på distinkte forskjeller ved farging av nevrale preparater etablerer det også et tillegssett av kjemoarkitektoniske kriterier ved immunofarging mot to kalsiumbindende proteiner; calbindin og parvalbumin.

Resultatene fra denne avhandlingen kan leses på tre ulike nivåer. For det første påvirker den vårt opprinnelige konsept om kognitive kart (O'Keefe and Nadel 1978) og bygger isteden på ideen om et universelt metrisk kart (Moser et al. 2008; Moser and Moser 2008) for å vise at spatial kognisjon støttes av et sett av dynamiske, gjensidig avhengig og samarbeidende systemer. For det andre så kan forståelsen av den spatiale nevrale kode gi bedre innsikt i generell informasjonskoding, beregninger og dynamiske interaksjoner mellom mentale representasjoner og atferd. Lærings- og minneprosesser representerer selve kjernen i spatial kognisjon og de hippocampale regionene er nødvendig for slike funksjoner. Derfor kan de samme nevrale mekanismene støtte både spatial kognisjon og minnedannelser. For det tredje: disse observasjonene kommer fra analyser av nevral aktivitet i rotter, men siden den hippocampale regionen er et

phylogenetisk konservert hjerneområde kan det tenkes at mange av observasjonene kan overføres til mennesker, og dermed bidra til økt forståelse av og kontroll med nevrologiske sykdommer som epilepsi og Alzheimer.

LIST OF PAPERS

Paper #1: **Representation of geometric borders in the entorhinal cortex**
Solstad T, Boccara CN, Kropff E, Moser M-B & Moser EI (2008).
Science, 322, 1865-1868.

Paper #2: **Grid cells in pre- and parasubiculum**
Boccara CN, Sargolini F, Hult V, Solstad T, Witter MP, Moser EI and Moser M-B (2010).
Nature Neurosci., 13, 987-994.

Paper #3: **A three-plane architectonic atlas of the rat hippocampal region**
Boccara CN, Kjønigsen LJ, Hammer I, Bjålie J, Leergaard TB, Witter MP
Manuscript

ACKNOWLEDGEMENTS

This work was conducted at the Kavli Institute for Systems Neuroscience and the Centre for the Biology of Memory at the Norwegian University of Science and Technology in Trondheim. The projects were funded by the Kavli Institute, the Norwegian Research Council, and the European Commission.

I would like to start by saying that I feel privileged to have had the opportunity to conduct my doctoral work in the Moser lab and in the Kavli Institute. I will always be grateful to May-Britt and Edvard Moser for being my supervisors. I have learnt so much by their side. They offered me the best training in *in vivo* recording techniques one could ask for, outstanding theoretical and technical supervision, and built a unique work place sparkling with boundless skills, knowledge, and also friendship. Thank you May-Britt and Edvard for making it possible for me to publish as I did and for giving me the opportunity to continue on this arduous path that is research. Watching you working was extremely impressive and made me want to follow as much as I could in your footsteps. I also wanted to thank you for being there when things were not as smooth as one could wish, and for always being patient and understanding.

I would like to continue by thanking Menno Witter who opened the door of a whole new field for me. One could not wish for a more knowledgeable anatomist. Thank you Menno for teaching me things that will be extremely valuable for the rest of my career. Thank you for your patience in helping the non-neuroanatomist that I am to complete the redaction of a pure anatomy paper.

Now comes the time to thank all my collaborators and colleagues in Trondheim, including a fantastic technical team and visiting professors. There are so many people that I am not able to write the name of everybody, yet I wanted to mention a few.

First of all I wanted to thank Francesca Sargolini who mentored me when I arrived at the CBM and who was at the instigation of paper #2. She taught me so much and is truly a fantastic person. I am sure she will be extremely successful (as she has already started to prove) in Marseille.

I would like next to thank my main collaborators: Trygve Solstad, Emilio Kropff, Veslemøy Hult and Lisa Kjøningsen. I learned a lot from all of them and they made it possible to produce a work that I am proud to have participated in. One can see by the level of publication of this lab that the people who compose it are truly

extraordinary. I was privileged for several years to work alongside some of the most brilliant minds in neuroscience. I tried to learn as much as I could from my colleagues and the visiting professors of the Kavli Institute, and will always be grateful for that opportunity.

That work would not have been possible without the incredible technical team of the Kavli Institute that is the envy of every lab in the world. Thank you Raymond Skjerpeng, Klaus Jenssen, Kyrre Haugen, Ann Mari Amundsgård, Haagen Waade, Ingvild Hammer, Espen Sjulstad, Endre Kråkvik, and Paulo Girao. Thank you to the administrative team who were ever willing to delve into so many papers and administrative issues on my behalf: Ingunn Bakken, Iuliana Hussein, Linda Veres, Elisabeth Ofstad, Anne Vaernes, and Sigrid Wold. Thank you, I know that I was not the easiest to deal with.

Thank you to the NTNU and the Faculty of Medicine for providing such an excellent neurosciences doctoral programme.

I also want to spare a few words for the people who guided me through my Master's degree and with whom I continued to enjoy contact and support during this PhD. Thank you Richard Miles, Georges Chapouthier, Patrice Venault, Lucia Witner, Vincent Navarro, and Desdemona Fricker.

The CBM was also where I met many of my dearest friends: Dori, Ros, Cathrin, Tiffany, Alex, Yadi, Paulo, Jaime, Hill-Aina, Nathalie, Adam, Karoline. I am very lucky to have had you along the road…

I would also like to take the opportunity here to thank Jozsef Csicsvari and my new colleagues at IST. There were all so very supportive and understanding in the difficult period that is starting something new when something else is not completely done yet. I am looking forward to the years I will spend in Vienna with them. A special thanks go to Alice, Desiree and Mike.

I also wanted to open a small parenthesis here to acknowledge how much our work is indebted to laboratory rats. They have walked kilometres and kilometres of various mazes, often motivated by thirst or hunger, sometimes incapacitated in various ways and connected to some kind of recording devices. Their sacrifice made it possible for us to get closer to understanding the brain and it should not be forgotten.

The final thanks go to my family: my father who gave me the taste for research and introduced me for the first time to neurosciences through the work of Laborit. My mother, who always encouraged me and is one of the reasons I went to Norway to reclaim my origins. My brother, who was always supportive and who tried to introduce me to people that could help me on the way. Merci beaucoup! Finally there is Ola. I cannot begin to describe how much he was at the heart of this work. He helped me in so many ways. He is the most wonderful thing that ever happened to me and gave me our Nicolas. Thank you, Ola and Nicolas, for your patience and your sacrifices that permitted me to finish this thesis.

Tusen takk!

Charlotte Boccara
Klosterneuburg, June 2013.

Banksy

FOREWORD AND MANUSCRIPT OVERVIEW

Nowadays, modern science is addressing very specific questions and often we scientists tend to forget the context in which our findings are written and published, and thus we fail to convey their importance for a general audience. To avoid such a shortcoming here, I wanted to start this thesis manuscript with a **very general introduction** (1) that covers the general **context** of my studies by presenting the **fundamental questions** they address that humankind has asked itself for generations and therefore to inscribe the research in a **historical perspective**. This general introduction will be divided into three sections. The first section (1.1) introduces the main topic of this thesis: the **neural localization of cognitive function**. The second section (1.2) presents the specific function investigated here: **spatial cognition** and the third section (1.3) the specific **brain area**: the **hippocampal region**.

The **second part** of the introduction (2) will be more specific to my topic: **single neuron specialization in the hippocampal region**. In my research, I have taken advantage of the improvement of brain recording techniques to correlate with great accuracy the activity of single neurons (i.e. single unit) with the ongoing behaviour of the studied subject (in this thesis, rats). This second part will give an overview of spatial and directional coding at the neuronal level in the hippocampal region. I will specifically discuss the **distribution**, **properties** and **modulation** of place, head direction and grid cells according to the environmental features and interactions within a more **global network**.

Following the introduction, I will present a **synopsis of the results** supporting this thesis work. They consist of three scientific articles. The first one reports the discovery of neurons in the rat whose activities respond specifically to **geometric borders** in the environment (paper #1). The second details the existence of spatially modulated neurons (the so-called **grid cells**) in interconnected areas of the hippocampal region (paper #2). Together with the introduction, this work establishes how a hippocampal neuronal network supports spatial representation. The third article describes the **histology of the hippocampal region** with an emphasis on how to recognize the different anatomical borders between its numerous subareas (paper #3).

In the final part of this manuscript, the **discussion** will elaborate on the results of these three articles and their implications in the light of the work presented in the introduction as well as some very recent findings.

CONTENTS

ENGLISH SUMMARY ..... **iii**

NORSK SAMMENDRAG ..... **v**

LIST OF PAPERS ..... **viii**

ACKNOWLEDGEMENTS ..... **ix**

FOREWORD AND MANUSCRIPT OVERVIEW ..... **xii**

CONTENTS ..... **xiv**

1. GENERAL INTRODUCTION **1**

1.1 LOCALIZATION OF COGNITIVE FUNCTIONS **1**

1.1.1 From the ancient Egyptians to Cartesian dualism: the brain as the seat of the mind 1

1.1.2 Towards the cartography of the brain: from the phrenologists to the neuropsychologists and the Brodmann areas 4

1.1.3 The twentieth century and the advent of imaging techniques: distributed systems of brain functions 7

1.1.4. Neuronal specialization 9

1.2 SPATIAL COGNITION **10**

1.2.1. Space perception and nature of spatial information 11

1.2.2. Navigation processes 12

1.2.3. The cognitive map 14

1.2.4. Neural substrate of spatial memory 15

1.3 HIPPOCAMPAL REGION **17**

1.3.1 Anatomy of the hippocampus 19

1.3.2 Connectivity of the hippocampus 23

1.3.3. Basic physiology of the hippocampus 27

1.3.4 Functions of the hippocampus 38

TRANSITION **46**

2. SINGLE NEURON SPATIAL CODE IN THE HIPPOCAMPAL REGION **47**

2.1 SPATIAL AND DIRECTIONAL MODULATION IN THE HIPPOCAMPAL REGION **49**

2.1.1 Place cell definition and distribution 49

2.1.2 Head direction cell definition and distribution 52

2.1.3 Grid cell definition and distribution 55

2.1.4 Overview of spatial and directional modulation in the hippocampal region 59

2.2 STATIC PROPERTIES **62**

2.2.1 Foreword on cell population studied 63

2.2.2 Spatial and directional properties 64

2.2.3 Discharge properties 75

2.3 DISCHARGE CORRELATES **83**

2.3.1 Prerequisites and concepts 83

2.3.2 Allothetic information 85
2.3.3 Idiothetic information 91
2.3.4 Environment spatial features 95
2.3.5 Non-spatial features 99
2.4 DYNAMIC PROPERTIES 105
2.4.1 Remapping (unit level) 105
2.4.2 Development of firing patterns in a novel environment 111
2.5 NETWORK PROPERTIES 113
2.5.1 Reference frame and multiple active maps 114
2.5.2 Ensemble remapping: Global vs. partial remapping and network coherence 116
2.5.3 Attractor network and pattern completion/separation 117
2.5.4 Global functional network: interaction and coordination between areas 122

OBJECTIVES 126
Objective 1. Neural code for the boundaries of the environment 126
Objective 2. Distribution of the spatial code over the parahippocampal network 127
Objective 3. Origin of the spatial code 127
Objective 4. Anatomical identification of the subareas of the hippocampal region 127

SYNOPSIS OF RESULTS (REVIEW OF THE PAPERS) 129
Paper 1: Representation of geometric borders in the entorhinal cortex 129
Paper 2: Grid cells in the pre- and parasubiculum 134
Paper 3: A three-plane architectonic atlas of the rat hippocampal region. 140

DISCUSSION 147
I. Impact on definitions 148
I.I Refinement of anatomical borders and their architectonic markers (Paper #3) 148
I.II Shift in definition of head direction cell (Paper #2) 149
I.III Shift in grid cell definition (paper #2 and #1) 151
I.IV Establishment of border cell definition (paper #1 and #2) 155
I.V Brief perspective on shift in place cell definition and relation with grid cells 157
II. Modalities of information coding and its distribution over a global coordinated network 158
II.I Spatial information coding at the neural level (paper #2, #1 and #3) 159
II.II Global functional network: coordination and interaction between areas (paper #1 and #2) 161
II.III Contribution of the network to the signal at the single cell level 164
III. On the origin of the spatial signal 165
III.I Mechanisms at the origin of head direction cells (paper #2) 165
III.II Mechanisms at the origin of grid cells (paper #2) 169
III.III Role of directional, grid and border inputs to place cells (paper #1 and #2) 177
III.IV On how to use the anatomy to follow up the spatial signal (paper #3) 182
IV. Perspectives on the behavioural function of the spatial code 183
IV. I Role in navigation 183
IV.II Extrapolation to role in memory and learning 184

CONCLUSION **185**

LEGAL AND ETHICAL ASPECTS **188**

ANNEXES **189**

Annex 1: Basic physiology **189**

Annex 2: Characterization (methodological considerations) **192**

REFERENCES **198**

INDIVIDUAL PAPERS **234**

1. GENERAL INTRODUCTION

1.1 LOCALIZATION OF COGNITIVE FUNCTIONS

1.1.1 From the ancient Egyptians to Cartesian dualism: the brain as the seat of the mind

The human quest to understand its own nature often translates into a quest to understand the concepts of mind, soul and intelligence and their biological substrate, asking the fundamental question: "Are mind and body linked?" (Santoro et al. 2009).

Fig. 1 Hieroglyphic for the word "brain" (The Edwin Smith Surgical Papyrus, c.1700 BC)

The heart and the mind were synonymous in ancient Egyptian. The brain, on the other hand, was considered a minor organ. However, in the fifteenth century BC, the Egyptian physician Imhotep wrote the first known description of the brain and its possible functions by relating 48 cases of brain injury, in what is now known as the Edwin Smith Surgical Papyrus (Mohamed 2008) (Fig. 1). From the sixth century BC to the second century AD, Greek philosophers and physicians speculated about the source of human thought, emotion, perception and voluntary movement (Crivellato and Ribatti 2007). Two main theories were at odds with each other: the **encephalocentric** (i.e. brain centred) and the **cardiocentric** (heart centred). First of the encephalocentric, Alcmaeon of Croton stated, in the early fifth century BC, that the brain was the seat of sensation and understanding, however he placed this in the watery ventricles of the brain. Following on that theory, Hippocrates of Cos (c. 400 BC), articulated that human and animal brains were similar, with the difference that the human brain contained the human mind, placed there like a "holy statue" (Garofalo 1997). In his work known in Latin as *De morbo sacro*, Hippocrates pointed to the brain as the seat of judgment, emotions and aesthetic activity: "our pleasures, joys, laughter and jests arise from no other source than the brain; and so do our pains, grief, anxieties and tears. Through it ... we also discern ugly and beautiful, bad and

good, pleasant and unpleasant" (Crivellato and Ribatti 2007). Plato (427–347 BC) supported the same idea, he viewed the human soul as composed of three parts, one of them: the rational soul is placed in "the head, which is the most divine part and dominates over the rest [of the body] in us. And the gods gave to this part also the whole body as servant." (Crivellato and Ribatti 2007). On the other hand, Aristotle (384–322 BC) advocated the cardiocentric theory and considered the brain to be only a cooling system for the blood. He was followed by Diocles of Carystus (fourth century BC), who initially stated that the heart was the centre for hearing and understanding. Yet Diocles later shifted towards the encephalocentric theory and suggested that the right half of the brain provided sensation and the left intelligence (Crivellato and Ribatti 2007). Galen of Pergamon (AD 129 to c. 216) was a Roman physician in a gladiator school. He opposed the cardiocentric theories supported by the Stoics. He based his views on the work of Greek anatomists from the Alexandrian medical school, like Herophilius and Erastritus, and on his own animal vivisections as well as his treatment of the gladiators' traumas and wounds (Acar et al. 2005). Herophilus of Chalcedon (335–280 BC) accurately described the anatomy of cranial and spinal nerves and identified that there were two kinds of nerves, the sensory (*aisthetika neura*) and the motor nerves (*kinetika neura*), whose origin he placed in the cerebrum and the spinal marrow. He henceforth supposed that the fourth ventricle and possibly the overlying cerebellum was the control centre of human movement (Acar et al. 2005). From the same school, Erasistratus of Ceos (310–250 BC) after initially supposing the dura (i.e. the thick membrane enveloping the brain) to be the command seat of sensitive, motor and cognitive functions, recognized in his old age that the nerves originated from the substance of the brain and proposed that human intelligence correlates with number of brain circumvolutions (Crivellato and Ribatti 2007). Galen postulated that the nerves were tubes transporting the mind-controlling fluid known as pneuma (i.e. animal spirit) from its reservoir, and thus control centre, the ventricle system. This view was later followed by St Augustine of Hippo (AD 400) in his cell doctrine whereby each cell (i.e. ventricles) contained different bodily fluids or humors: blood (lust), mucus (slow response), yellow bile (anger) and black bile (depression) the balance of which dictated the physical functioning (Clarke and Dewhurst 1996). These theories were dominant in the western world until the sixteenth century and work of the anatomist Vesalius (1514–1564) and the

philosopher René Descartes (1596–1650). Vesalius, by studying the corpses of executed criminals, realized that bumps (gyri) and grooves (sulci and fissures) on the brain surface are similar between individuals (Fig. 2). With the same method, he identified that brain tissue is divided into grey and white matter and that the latter is continuous with the nerves. This led him to postulate that the white matter carries information to and from the grey matter (Clarke and Dewhurst 1996).

Fig. 2 Illustration from Andreas Vesalius, *De humani corporis fabrica libri septem* (1543), Plate 606.

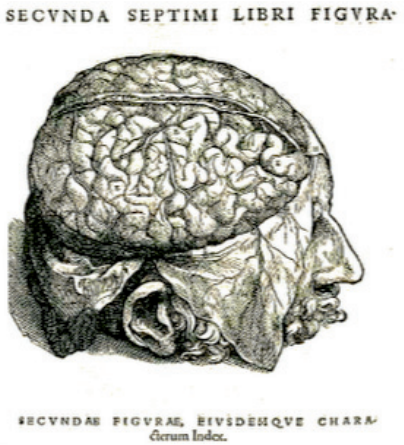

In parallel, Descartes developed his concept of mind-body dualism. However he placed all mental function in the pineal gland, a small brain structure which is now thought to have a role in the regulation of sleep/wake cycles (Lokhorst and Kaitaro 2001) (Fig. 3).

Fig. 3 Illustration from Rene Descartes, The Pineal Gland (1644)

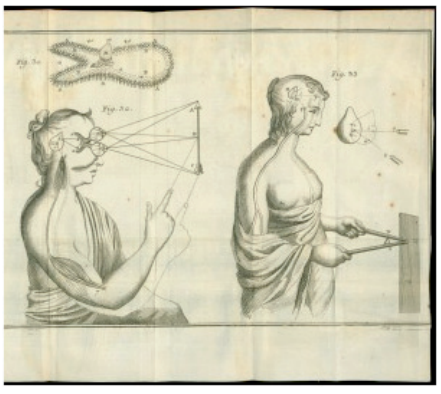

1.1.2 Towards the cartography of the brain: from the phrenologists to the neuropsychologists and the Brodmann areas

The central role of the brain in cognitive functions was commonly accepted in the scientific community of the eighteenth and nineteenth centuries. Furthermore, the work of Luigi **Galvani** and Emile **du Bois-Reymond** (1800), Charles **Bell** and Francois **Magendie** (1810) and Benjamin **Franklin** (1871) established the nerves as the wires communicating the brain information through the body by **electrical impulses** (Piccolino 1998). However, this period was the seat of a new debate between "localizationists" in favour of a theory of brain area specialization in specific functions, and "globalists" opposing that theory.

In the **localizationist** ranks, Franz Joseph **Gall** (1758–1828) developed a method called cranioscopy, which postulated that an individual's personality could be determined by the variation of the bumps on their skull (Fig. 4). Renamed **phrenology** by his follower Johann Spurzheim, that theory popularized the idea that different brain regions were devoted to specific functions (Fodor 1983). However, it was based on cranial shape and proved out to be completely wrong with the result that subsequent brain localization work was abandoned for a while.

Fig. 4 A list of phrenological organs (from Samuel R. Wells, after O.S. Fowler)

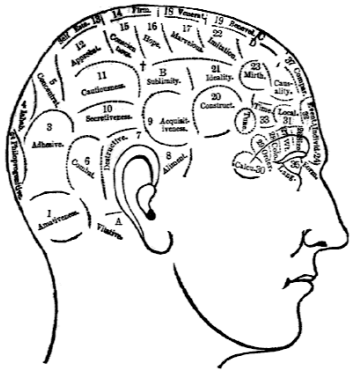

In the **globalist** ranks, the studies of Jean-Pierre **Flourens** of partial brain lesions in hens and pigeons concluded that function loss is dependent on the extent of the lesion rather than on its location and that while sensory inputs were localized, more complex processes such as perception were dependent on the integrity of the entire brain (Flourens 1824). Additionally, he developed the idea of pluripotence of the brain

tissue by arguing that if a lesion is not too severe, remaining healthy tissue will take over the function supported by damaged one.

In the middle of the nineteenth century, the concept of localized brain functions was reintroduced by successive **neuropsychological reports** of patients with accidental partial brain lesions. John **Harlow** initiated this series with his famous 1848 report on Phineas Gage (Harlow 1848). Gage was working as a foreman on a railway when an explosion drove an iron rod through his head, damaging on its way a big portion of his frontal lobes (Damasio et al. 1994) (Fig. 5). After a "stormy recovery", he did not present much physical sequels, yet his behaviour and personality changed so much that he never worked as a foreman again: **Gage was "no longer Gage"** (Macmillan 2000).

Fig. 5 Three-dimensional views of the iron bar in Gage's frontal lobe (Damasio et al. 1994)

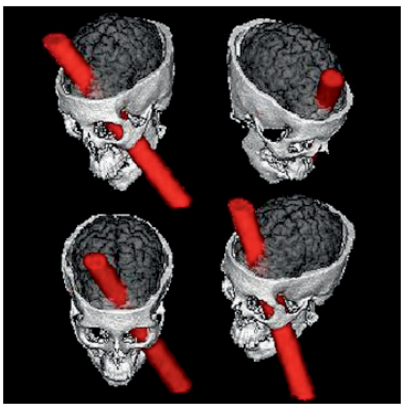

Paul **Broca** really launched the use of "human lesion method" to establish and understand the function of the different brain area. In 1861, he reported the case of a patient who had been able to produce only one syllable, "tan", in the form of stereotyped recurrent utterances: "tan-tan-tan" (Broca 1861). After the death of his patient, a careful examination of his brain revealed a focalized lesion in the left third convolution of the inferior frontal gyrus. Therefore Broca claimed that this area was involved with speech production.

During the century from 1850 to 1950 the rise of neuropsychology led to controversial discussions between scientists arguing for a holistic interpretation of the cortex and those supporting the localization paradigm. The localizationist hypothesis gained more and more support from neuropsychological reports correlating

behavioural disorder and location of brain injury (e.g. (Harlow 1848; Broca 1861; Bernhard 1872; Wernicke 1874; Charcot 1878; Head and Holmes 1911; Scoville and Milner 1957) but also from other methods. In *On the Origin of Species* (Darwin 1859), Charles **Darwin** established that some brain areas were conserved between species, advancing therefore phylogenic arguments in favour of localization. Others, like Langley and **Sherrington**, examined focalized animal brain lesions to understand better the precise role of each area (Langley and Sherrington 1884). In 1870, **Fritsch and Hitzig** discovered the motor cortex through the observation that electrical stimulation of different areas of a dog's brain led to involuntary muscular contractions of specific parts of the body (Fritsch and Hitzig 1870). Further, John **Hughlings Jackson** inferred the organization of the human motor cortex by observing the progression of epileptic seizures through the body of his patients (Hughlings-Jackson 1884). Wilder **Penfield** used a similar stimulating method with a surgical probe on epileptic patients before resection of a focus epilepticus. This led him to map the sensory and motor cortex (Penfield and Erickson 1941) and to link the temporal lobe with memory (Penfield 1952). This accumulation of evidence was however moderated by the work of scientists such as Karl **Lashley,** who studied the performance of rodents with variable sized brain lesions in mazes (Lashley 1950). He claimed, echoing Flourens, that impairments in performance were explained by the amount of the lesion rather than its location.

In spite of this, the localization paradigm became more and more popular: most neurologists saw the brain as a puzzle where each of our abilities fitted neatly into a specific area and this started the work of brain cartography. The desired map was the 1909 **cytoarchitectonic map** of 43 human brain areas published by Korbinian **Brodmann** (Brodmann 1909; Zilles and Amunts 2010) (Fig. 6).

Fig. 6 Brodmann areas lateral and medial side views of the human brain (Brodmann 1909)**.**

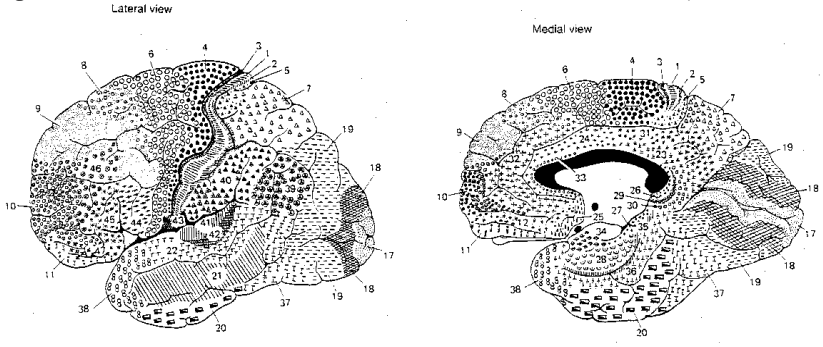

1.1.3 The twentieth century and the advent of imaging techniques: distributed systems of brain functions

Fig. 7 Multimodal brain Imaging

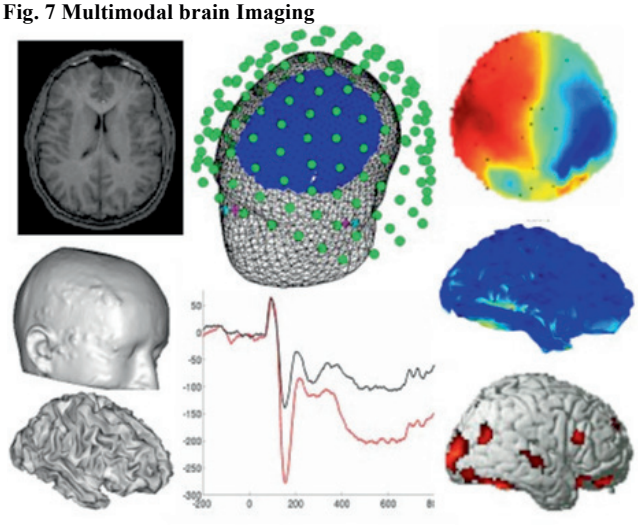

MRI, MEG, EEG, fMRI from Dr Richard Henson profile page (http://www.neuroscience.cam.ac.uk/directory/profile.php?RikHenson)

The twentieth century saw the emergence of increasingly sophisticated **non-invasive *in vivo* brain imaging techniques** that can mainly be divided in two groups: on the one hand, static "brain pictures" and on the other hand, dynamic "brain activity recordings" (Fig. 7). The latter started to be developed at the turn of the century and consisted initially of the recording of surface brain electrical activity (Caton 1875; Beck 1890; Pravdich-Neminsky 1913). These so called electroencephalograms or **EEGs** presented great **time accuracy**, yet they lacked **spatial resolution**, especially when it came to localizing deep structures. On the other end of the spectrum, contemporary methods to take "brain pictures" made it possible to visualize deep structures but did not access any dynamic time component. In the early 1900s, the first "pictures" were obtained by using **X-ray imaging** combined initially with pneumoencephalography (Dandy 1919) but this technique was rapidly abandoned as being too dangerous for the patient. Later on, in the 1970s, neurologists rekindled X-ray techniques especially to assess head trauma with the development of the computed tomography (**CT**) **scan** (Oldendorf 1961; Cormack 1973). In parallel, other techniques emerged using magnetic fields such as magnetic resonance imaging (**MRI**)

(Carr 1952) or magneto-encephalography (**MEG**) (Cohen 1968). MEG was revolutionary because it was taking a "film" of the brain activity and thus allowed researchers to access images of the functioning brain of patients performing tasks in a scanner. MEG temporal resolution is very good but its spatial resolution is still quite poor. Functional imaging techniques continued to be developed with **PET** (positron emission tomography) scans (Phelps et al. 1975) and **fMRI** (functional MRI) (Ogawa et al. 1990). Though their spatial resolution was better than MEG, their temporal resolution was poorer. The advent of functional imaging techniques (Walsh and Cowey 2000; Bjaalie 2002; Brett et al. 2002) allowed **elaboration on the localization paradigm**. It notably made possible the finding that the processing of information, interpretation and elaboration of adapted behavioural response, are computed across **plastic brain networks distributed over interconnected and communicating areas** (Rorden and Karnath 2004; Toga et al. 2006).

The concept of **system of interconnected areas** comes from the fact that, even for the simplest task, functional images showed the activation of several brain areas albeit subtracting the baseline activity (Kosik 2003). Thus it is considerably more complex than a one-to-one mapping of function onto anatomy. Brain areas are highly interconnected and information is processed in a distributed manner (McIntosh 1999; Passingham et al. 2002). However, much of the signal processing is still unclear: in particular whether it is serial or parallel, and to what extent functions are bound together. Partial answers came from recent studies showing that areas that belong to a common interconnected network may **communicate** through global oscillations (Colgin et al. 2009; Siegel et al. 2012). I will develop that point further in 2.5 and the Discussion chapter. Furthermore, not only is one function distributed over several areas but also a given area can be activated by different tasks. Most areas are either **plurimodal** or they discriminate and compute information independently of the modality. The easiest function to map is the perception of primary sensory stimuli. However, even these so-called primary sensory cortices do not have their delineations set in stone. Groundbreaking work was conducted on **brain plasticity** on congenitally blind or deaf people (Cohen et al. 1997; Finney et al. 2001). It revealed that the tactile experience of reading Braille could activate the visual cortex, and reciprocally the visual experience of interpreting sign language could activate the auditory cortex (Merabet and Pascual-Leone 2010). There are however some limits to these

adaptation processes in terms of critical period (Hensch 2005) and amount of adaptation (Kosik 2003). Further plasticity mechanisms are shown when repeating an activity or action: it can lead to an optimization of the brain resources by modifying the volume of the targeted area, its activation threshold and its wiring (intracortical connections). At the scale of the life experience, Woollett and Maguire showed an increase of the size of the **hippocampus for taxi drivers** (Woollett and Maguire 2011). The hippocampus and the surrounding parahippocampus are involved in spatial cognition. This specific function is the subject of this thesis and will be discussed further in greater detail. Adaptation can also be seen in a phylogenic fashion. Indeed, when looking at the distribution of the body representation on the motor cortex, one can see an **over-representation of the hand in the homunculus** (Fig. 8).

Fig. 8 Representation of the cortical homunculus
From http://en.wikipedia.org/wiki/File:Sensory_Homunculus.png (original upload 19/06/2006)

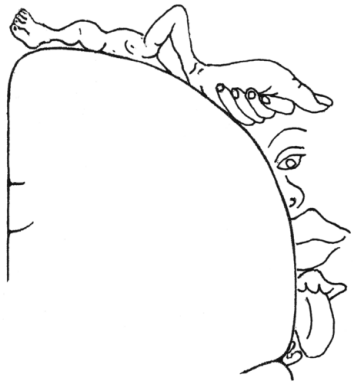

1.1.4. Neuronal specialization

So far I have discussed the distribution of brain functions over areas, systems and networks. However, specialization can take place at a finer resolution. The **basic functional unit** of the brain is the neural cell or neuron. Neurons were defined at the end of the nineteenth century based on the seminal histological work of Camillo **Golgi** and Ramon y **Cajal** giving birth to the **neural doctrine**(Golgi 1886; Ramón y Cajal 1909). As stated while discussing EEG recordings, brain activity, and a fortiori neuron activity, is electrical. For a brief explanation of the basis of this electrical signal, see neuron physiology (insert 1). Since the 1930s, **methods** for **recording** individual neurons have constantly improved in order to record in more and more

integrated systems (from *in vitro* to *in vivo* freely behaving) for longer periods of time and from several neurons at the same time (from larger and larger cell assemblies in one area or distributed over several areas). In 1928, Edgar **Adrian** recorded, for the first time, the electrical discharge from single nerve fibres for which he received the Nobel Prize. About 10 years later, **Renshaw, Forbes and Morrison** developed a method to record from individual pyramidal cells in the hippocampus using glass microelectrodes in cats (Renshaw et al. 1940). At the end of the 1950s, **Hubel and Wiesel** finally characterized brain function at the level of the single neurons with their mapping of the visual cortex (Hubel and Wiesel 1959). This was followed in 1971 with the work of **O'Keefe and Dostrovsky,** seminal for this thesis, who, by recording the activity of hippocampal cells *in vivo* from freely behaving rats, succeeded in correlating their activity with a cognitive function (spatial memory) (O'Keefe and Dostrovsky 1971).

Recording techniques are constantly improving and it is possible nowadays to correlate with great accuracy the activity of single neurons (i.e. single unit) with the on-going behaviour of the subject. In addition, the miniaturization and increased precision of recording devices allows us to analyse in parallel the signal in provenance of many neurons (i.e. multi unit recording). I have taken advantage of these techniques during my **PhD work** and I will present here its results and give examples of **specialization at the neuronal level**. In particular, I will discuss the modalities of that specialization, in terms of its precision, its multimodality, its distribution, its plasticity, its interaction within a network and with the brain states. The function I studied was **spatial cognition** and the area, the **hippocampal region**. Before presenting these results I need to define both spatial cognition (1.2) and the hippocampal region (1.3).

1.2 SPATIAL COGNITION

Spatial cognition is a vital ability. It results from a succession of functional adaptations to **problems of survival** such as search and retrieval of vital locations to ensure reproduction and conservation of the species such as feeding area, nest and herd and the recognition of dangerous areas.

Spatial cognition processes result in constructing a **representation** of the **external space** and **self-position** in that space in order to navigate accurately. Such processes encompass **perception** and **learning** (and memory) of the space and of

accurate **navigation strategies**. In this thesis, I will focus on how spatial representations are coded at the single neuron level.

1.2.1. Space perception and nature of spatial information

The **epistemology** of space perception can be traced back to the Greek philosophers. On the one hand is the **empiricist** conception, which originated with **Aristotle**'s tabula rasa and reached its zenith with the seventeenth- and eighteenth-century British empiricists like **Bacon, Locke** and **Hume**. Empiricism asserts that knowledge comes only and primarily from sensory experiences. Empiricism is often contrasted with **rationalism** such as **Descartes**, **Leibniz** and **Spinoza**. Rationalism claims that reason alone determines knowledge, independently of the senses (Markie 2012). **Kant**, in his critique of pure reason (Kant 1781), argued against both rationalists and empiricists. He assessed that, while it is correct that experience is fundamentally necessary for human knowledge, reason is necessary for processing that experience into coherent thought. Kant's and the **idealists'** vision of space perception thus has its roots in **Platonism**. It can be summarized by saying that individuals have notions of space, pre-existing any experiences and that these conceptual principles and processes **pre-structure the experience** of the world. The data presented in this thesis shed new light on these concepts (see Discussion).

Spatial information can be divided into allothetic and idiothetic information. Allothetic comes from the Greek ἀλλος allos (another) and idiothetic from the Greek ἴδιος idios (self). **Allothetic** information is all information coming from the exterior environment (i.e. from external sensory cues) in opposition to **idiothetic** information, which derives from "internal" perception (i.e. of one's own location and own movement). The **neural substrate** of space perception consists of all the areas processing sensory information, including sensory cortices and thalamus. Allothetic information is based on environmental sensory cues, so its neural substrate is mainly distributed over the visual, olfactory, auditory and tactile **sensory systems.** On the other hand, idiothetic information is derived from the animal's own movements so it includes information provided by the **vestibular, proprioceptive and somatosensory systems** (e.g. efference copies of motor commands, external motion-related information such as optic flow).

1.2.2. Navigation processes

With the birth of experimental psychology and neurosciences at the beginning of the twentieth century, scientists and psychologists tried to understand and conceptualize navigation. One can **define navigation** as the capacity to **plan** and **execute a goal-directed path** (Gallistel 1990). It is **based on space perception** and **self-perception** in that space by the integration of allothetic and idiothetic information.

Both animal and human studies show that accurate navigation can be reached by different strategies. Among these **different navigation strategies**, one can distinguish **landmark navigation** based on allothetic information from **path integration** navigation based on idiothetic information (Kesner and Olton 1990; Redish 1999; McNaughton et al. 2006).

Path integration derived from dead reckoning navigational strategies. The term **dead reckoning** dates from the seventeenth century, probably from the adjective dead in the sense of "absolute" or "exact" (*Encarta World English Dictionary*). It is the process of estimating the position of a ship based solely on speed and direction of travel and time elapsed since the last known position in **contrast to pilotage** (navigation by visible landmarks) and celestial navigation (by reference to the stars or other heavenly bodies). **Historically**, dead reckoning as a cognitive process can be traced back to **Darwin,** who postulated the existence of such a navigation mechanisms for animals and humans was "effected chiefly, no doubt, by eyesight, but partly, perhaps, by the sense of muscular movement, in the same manner as a man with his eyes blinded can proceed" (Darwin 1873). The study of **desert ants and honey bee homing strategies** (Frisch and Lindauer 1954; Dyer and Gould 1981; Wehner and Srinivasan 1981) led to the definition of **path integration** as an important navigation strategy in the animal kingdom, which allows animals to keep track of the straight-line distance and direction of travel, so that an agent can compute the vector home at any point during the journey (Etienne 1980; Mittelstaedt and Mittelstaedt 1980). Path integration can be defined as a **self-contained navigation system** (or internal navigation system, (O'Keefe and Nadel 1978)), for which the **position**, **orientation**, and **velocity** (direction and speed of movement) are **continuously calculated via dead reckoning** without the need for external references.

Landmark navigation includes among others cue navigation strategy and guidance strategy, which are part of the taxon system (O'Keefe and Nadel 1978). In

the **cue navigation strategy**, the subject associates one single sensory cue to its journey's goal. The subject can then navigate by computing its distance from the goal as a function of the perceived cue intensity. The **guidance strategy** is used if the goal cannot be directly associated with one cue, so that the subject can learn the position of several landmarks in respect to his own location when he is at this goal. This could be seen as taking a snapshot of the scene (eidetic image). The strategy then consists in retrieving this specific configuration of landmarks. Another possibility, in the absence of a goal directly associated cue, is the **route learning strategy**. It consists of setting intermediate goals associated to salient cues and then associating motor responses to these intermediate "goals" (like turn to the right). This last strategy is somehow reminiscent of the stimulus-response theory rejected by Tolman, according to which spatial learning consists of chaining together a number of motor responses that link relevant external stimuli (Tolman 1948).

Finally, a very effective strategy to navigate is to use a **map** of the environment. As shown in (1.2.3), much evidence argues for the existence of such a map in the rodent hippocampus (Fig. 9).

Fig. 9 Navigation and representation of space: path integration vs. map-based navigation

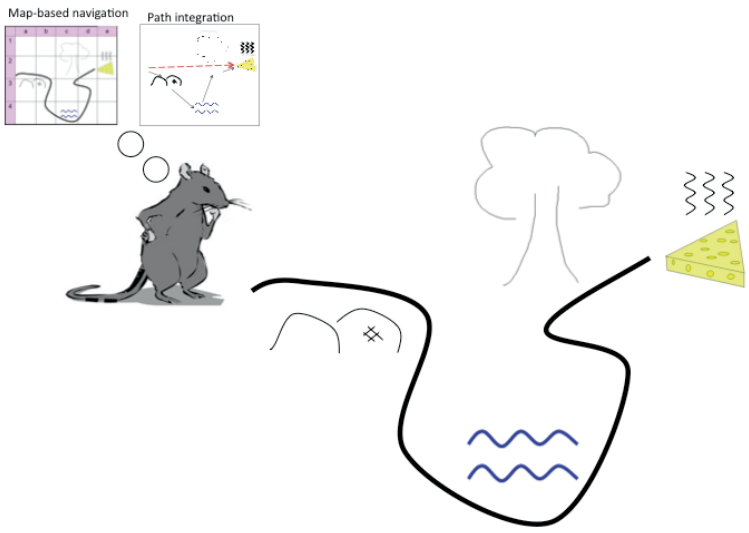

These different navigational strategies can be revealed in mazes such as the **Morris water maze** (Morris et al. 1982) (Fig. 22). This consists of a circular pool filed with opaque water. Though rats are good swimmers, they will attempt to find ground under

their paws. The Morris water maze is designed so that such ground is available for them in the form of a submerged platform. In some cases, the platform is visible, in other cases it is hidden and the rats must learn to find it with the available information. This information can be allothetic based (e.g. a salient visual cue indicating the placement of the hidden platform) or idiothetic based (e.g. a learned trajectory).

Animals use different strategies in function of the type of information available. The neural system described in this thesis supports mostly map-based and path integration strategies.

1.2.3. The cognitive map

O'Keefe and Nadel hypothesized that the four mentioned navigation strategies (i.e. internal navigation, cue navigation, guidance and route learning) form the so-called **taxon system** based on routine and procedures. They opposed this taxon system to a flexible system called the **local system** based on a **cognitive map**. However, they proposed that these different navigational systems are not mutually exclusive (O'Keefe and Nadel 1978; Gallistel 1990; McNaughton et al. 1991).

In rupture with the empiricist view, the idea of a cognitive map was already introduced in **Kant**'s theory of the existence of a pre-structure brain organization preceding all experiences of the world. **Tolman** (Tolman 1948) further supported this intuition based on the results of his experiments conducted on rats (Fig. 10). He argued that: "in the course of learning something like a field map of the environment gets established in the rat's brain" (Tolman 1948). The cognitive map theory was strongly established after the groundbreaking discovery of **place cells**: neurons, in the rat's hippocampus, coding specifically for the location of the animal in an environment, independently of its ongoing behaviour (O'Keefe and Dostrovsky 1971). I will describe the properties of place cells extensively in the second part of this introduction (2).

Fig. 10 Tolman and the intuition of a cognitive map

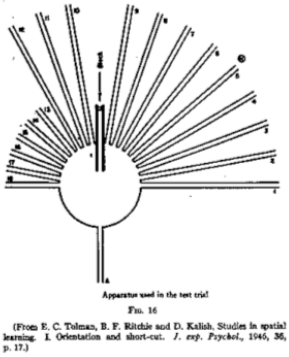

Apparatus used in the test trial

FIG. 16

(From E. C. Tolman, B. F. Ritchie and D. Kalish, Studies in spatial learning. I. Orientation and short-cut. *J. exp. Psychol.*, 1946, 36, p. 17.)

(Left) Edward C.Tolman (Right) One of the maze envisioned by Tolman (from "Cognitive maps in rats and men", 1948)

The key characteristic of the **map-based locale system** is that places are located in a framework of **metric properties** and relations, linked to other places and stimuli (e.g., landmarks) in a map-like fashion. Thus the cognitive map encodes the element of a task and the **spatial relationships** between these elements, which allow the rats to learn relevant location, independently of the specific movements necessary to reach it. Rats can then, for example, find an invisible fixed platform in the Morris water maze, while starting from varying locations in the pool (Morris 1981; Morris et al. 1982).

1.2.4. Neural substrate of spatial memory

Place cells are stable in one environment: every time the animal enters the environment, a given place cell will reproducibly code for a given location (Muller et al. 1987; Thompson and Best 1990). This finding argues for a role of place cells (and hippocampus) in spatial memory. I will briefly discuss here what **spatial memory** is.

The intuition of the existence of **multiple memory system** can be traced back more than a century to psychologists and philosophers such as **Maine de Biran** (Maine de Biran 1804) or **Bergson** (Bergson 1910). Over the years, a wide variety of experiments helped to verify and make precise this original insight.

Nowadays, the classical **taxonomy of memory** is based on work from **Tulving** and **Squire** among others (see (Squire 2004) for review). It distinguishes between declarative (or explicit) and non-declarative (implicit) memory (Fig. 11). Of course, to talk about declarative memory for an animal is only a figure of speech.

Non-declarative memory regroups different memory types like **procedural** memory that we evoked previously (as a part of the taxon system) or simple classical **conditioning**, which are very like **reflexes**. The common determinate to all non-declarative memory, in a human definition, is that it does not require any consciousness of the experience contrary to declarative memory which can be consciously recalled. **Declarative memory** is often divided into **semantic** memory (knowledge, facts about the world) and **episodic** memory (recollection of personal experience of an event). A classic example to illustrate these different types of memory is to consider someone **playing the piano**. To learn and remember how to play the piano requires non-declarative memory (procedural). To remember the fact that you know how to play the piano is semantic memory. To remember that you played the piano at your mother's birthday two years ago is episodic memory (see Figure 11). An **episode** can be considered to have three components: **WHAT** (playing the piano) happens and **WHEN** (two years ago) and **WHERE** (at your mother's place) did it happen. The WHERE component is part of the **spatial memory** and, as stated previously, place cells are thought to be its neural substrate. Some (Eichenbaum et al. 1999) have argued that place cells are in fact "**episodic memory cells**" and that they have been classified as place cells because the "WHERE component" is the most accessible for quantification. I tend to agree with this position and will argue this point further in the course of the discussion.

Fig. 11 Taxonomy of memory classification (adapted from (Tulving 1985; Squire 2004)

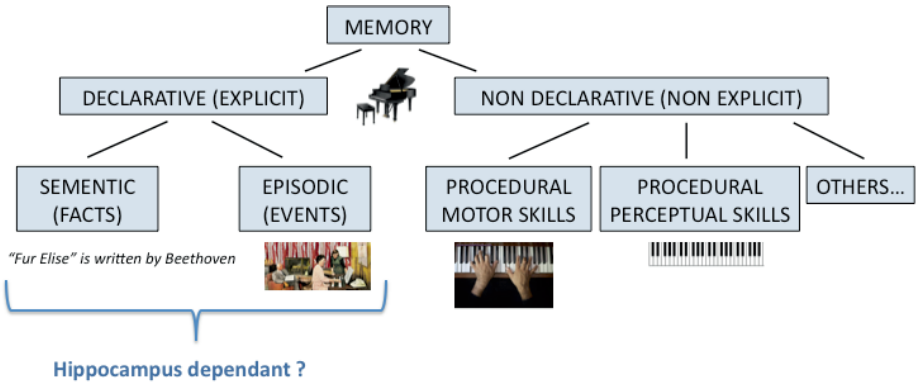

Based on extensive lesion and imaging studies, the taxonomy of the memory system proposes that each memory type is supported by a different **brain area**. In that sense,

the **taxon system**, which is supposed to derive from procedural memory, is mostly supported by the **striatum** (see review: White and McDonald 2002). On the other hand, the **hippocampal region** is the repository of **declarative memory**, and a fortiori of episodic memory (Squire 1986; Squire 2004). The existence of place cells designs the **hippocampal formation** as the substrate of the **cognitive map**. However, other types of spatial and directional modulation have been observed in the **parahippocampal region**. Among them are; **head direction cells**, which are active when the animal has its head in a given direction (Ranck 1984; Taube et al. 1990; Taube et al. 1990); **grid cells**, which resemble place cells but have multiple firing fields that tessellate the whole environment (Fyhn et al. 2004; Hafting et al. 2005; Boccara et al. 2010); paper #2) and **border cells**, which code for the border of the environment ((Solstad et al. 2008); paper #1). I will present in detail these cells in the second part of this introduction (2) and in the synopsis of results.

1.3 HIPPOCAMPAL REGION

Before getting to the core of this thesis, which is the neuron specialization in spatial cognition, I will present the areas they are recorded from. The hippocampal region is part of the **limbic system** in the **medial temporal lobe** (MTL) of the human brain and in the medio-caudal part of the rat brain. Based on cytoarchitectonic criteria, it is divided into two main structures: the **hippocampal formation** (HF) and the **parahippocampal region** (PHR). The term "hippocampus" is derived from the Greek ἵππος, *híppos* (horse) and κάμπος, *kámpos* (sea monster). In 1587, the Italian anatomist Arantius used this term for the first time to describe a structure in the temporal horn of the lateral ventricles that resembles a sea horse, or "hippocampus" in Latin (Lewis 1923; Walther 2002).

Fig. 12 Drawing of the neural circuitry of the rodent hippocampus (Ramón y Cajal 1909)**.**

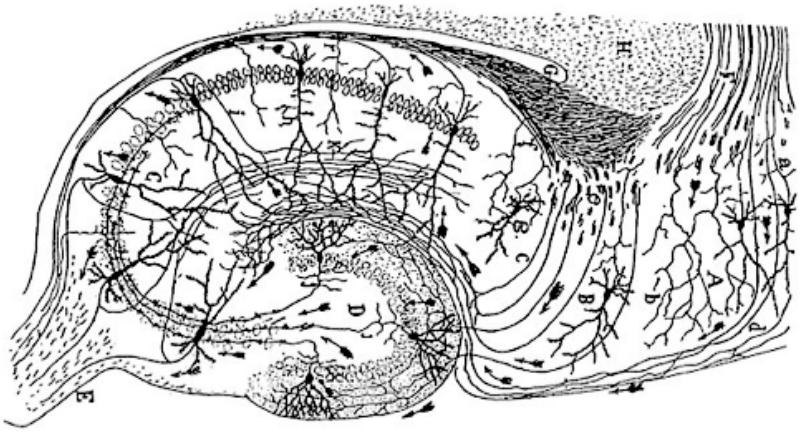

Santiago Ramón y Cajal. *Histologie du Système Nerveux de l'Homme et des Vertebrés*, Vols. 1 and 2. A. Maloine. Paris. 1909.

In the history of neuroscience, few structures have been as intensely studied as the hippocampus. Since Ramon y Cajal (Fig. 12), neuroscientists have taken advantage of its **numerous unique features** to establish both general and region-specific neural and system principles. Why is the hippocampal region so remarkable? First and foremost, as a living tissue, it is quite accessible to isolate and study at different integration levels. Individual neurons can be successfully grown in **ectopic cultures**, which allow the precise examination of their cellular properties. At the circuit level, one can cut a **hippocampal slice** and test it for a **prolonged period in vitro**. This technique was fundamental in the characterization of the propagation of signals from one neuron to the other and was further facilitated by the relative simplicity of the predominantly **unidirectional hippocampal circuit**. Such slice preparations generated the discovery of a major neural mechanism: the **long-term potentiation** (LTP) (Bliss and Lømo 1973). LTP, which is due to the unique **plastic properties** of hippocampal synapses, further positioned the hippocampus as a preferentially studied structure. Finally, the already mentioned discovery of **spatial and directional modulated cells**, the subject of this thesis, opened a whole new world in terms of cognitive/behaviour localization at the scale of the neuron.

The hippocampal region has been intensively studied also because of its involvement in several neurology and psychiatric diseases such as **epilepsy** and **Alzheimer**. Indeed, the specific physiological properties of the hippocampal region

make it one of the most excitable regions of the brain and therefore a frequent point of focus in epilepsy (Wiebe 2000). On the other hand, the initial development of Alzheimer's disease can be observed by the accumulation of amyloid plaques in the entorhinal cortex and the dentate gyrus (Gallagher and Koh 2011).

In this section, I will first present the hippocampal **anatomy**, second its **connectivity**, third its **physiology** and fourth some of its allocated **functions**.

1.3.1 Anatomy of the hippocampus

As is illustrated in Fig. 13, the hippocampal region is a **complex three-dimensional curved** structure with intricate sub-structures. The precise recognition of the borders of these different structures is primordial to the interpretation of many studies. One of the objectives of this thesis is to present the reader with cytoarchitectonic and chemoarchitectonic tools to facilitate this identification. I refer the reader to **paper #3** for an in-depth description of the **anatomy and the cytoarchitecture of each subfield** with the depiction of the borders of the subfields linked to an interactive histological database. In addition, the reader will find there a presentation of the **different axes** (e.g. dorsoventral, septotemporal, mediolateral, raustrocaudal, transversal) used to describe the respective positions of elements in these structures. I will therefore limit myself to presenting in this section the basic nomenclature and some historical facts concerning the description of the hippocampal region.

Fig 13 Three-dimensional views of the hippocampal region (A) Medial side view of one hemisphere. (B) Caudal view. (C) Lateral side view. Colour code as presented in the lower panel

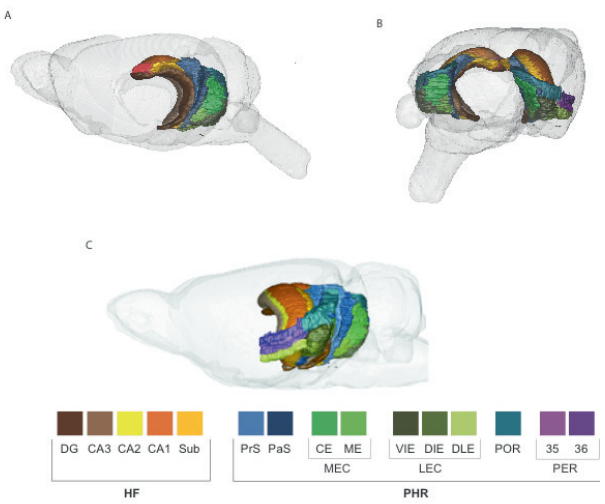

HF: hippocampus formation; PHR: parahippocampal region; DG: dentate gyrus; CA1-3: cornu Ammonis 1-3, Sub: subiculum; PrS: presubiculum; PaS: parasubiculum; EC: entorhinal cortex; PER: perirhinal; POR: postrhinal; MEC: medial entorhinal cortex; LEC; lateral entorhinal cortex; 35: perirhinal area 35; 36: perirhinal area 36; CE: caudal entorhinal area; ME: medial entorhinal area; VIE; ventral intermediate entorhinal area; DIE: dorsal intermediate entorhinal area; DLE: dorsal

1.3.1.1 Nomenclature and historical perspective on the anatomy

In 1923, **Lewis** published a historical and etymological work on the anatomy of the **hippocampus** in which he attributed to **Arantius** (1587) the fatherhood of the appellation and to **Duvernoy** the first illustration of its structure (1729). He further reported that **Winsløw** introduced for the first time the idea of a horn, by comparing the curvature of the structure to that of a ram's horn and that **Garengeot** (1742) proposed the Latin term **cornu Ammonis** (acronym CA), Ammon's horn, in reference to the Egyptian god often depicted as having the head of a ram (Lewis 1923).

As mentioned previously, the hippocampal region is located in the medial temporal lobe (MTL) of the brain and is considered to be part of the **limbic system**. The limbus, from the latin *limbus* (edge) was first evoked by **Willis** (Willis 1664) to refer to the brain area that surrounds the brain stem. About 200 years later, **Broca** (Broca 1861) coined the term with his description of "*grand lobe limbique"*.

The initial histological work of **Golgi** (Golgi 1886), **Sala** (Sala 1891), **Schaffer** (Schaffer 1892) and **Ramón y Cajal** (Ramón y Cajal 1893) helped to establish some of the different subfields of the hippocampal region. The main distinction in the hippocampal region is between the hippocampal formation (HF) and the parahippocampal region (PHR) and is based on the number of layers each area contains. The **HF is a three-layer cortex**, also called the archaeocortex, from the Greek ἀρχαῖος, *arkhaîos* (ancient), while the **PHR is a six-layer cortex** or neocortex, from the Greek νεος, *neos* (new). Both the HF and the PHR are further divided into several **sub-structures**. The original nomenclature is mostly derived from the analysis of Golgi-stained material by **Ramón y Cajal** and his student, **Lorenté de Nó**. This initial work was later revised based on new techniques allowing the observation of the connectivity of these areas (with retrograde and anterograde transporters) and chemical markers (e.g. markers of some specific interneuron types). One of the objectives of this thesis is to describe some of these cyto- and chemoarchitectonic features to help to delineate the borders between the different subareas. I refer the reader for that purpose to paper #3.

1.3.1.2 The hippocampal formation (HF)

The HF is divided into the **dentate gyrus** (DG), the **hippocampus proper** (containing the CA fields) and the **subiculum**. Ramón y Cajal (Ramón y Cajal 1893) highlighted the **trilaminal organization of the** HF and famously in 1911 drew its **functional circuit diagram** (Ramón y Cajal 1909), which still holds for the most part

nowadays. The **first layer** consists of a mixture of afferent and efferent fibres and interneurons. The **second layer** is the single principal cell layer. These cells are called granular cells in the DG and pyramidal cells (or pyramids) in the CA fields and in the subiculum. The **third layer** is a molecular acellular layer, which contains the apical dendrites of the pyramids and the granular cells.

The first description of the **DG** was actually in the description of the hippocampus by Arantius. About 200 years later, Tarin (Tarin 1750) described that structure anew and called it the fascia dentate, derived from the Latin *dentatus* (tooth-like), in reference to its shape. The denomination "dentate gyrus" dates from 1861 (Huxley 1861), yet Cajal used the term "fascia dentata".

Lorenté de Nó (Lorente de Nó 1921; Lorente de Nó 1934) divided the **hippocampus proper** into four subfields and he named them **CA1**, **CA2**, **CA3** and **CA4**, following Garengeot's *cornu Ammonis*. This division is still valid to some extent today. However, the CA4 field defined by Lorente de Nó is now considered to be part of the dentate gyrus (Blackstad 1956; Amaral 1978).

Subiculum is Latin for "support". Ramon y Cajal used that term to describe a supporting area of the hippocampus. However the area designated was in fact part of the PHR. Lorenté de Nó (Lorente de Nó 1934) later corrected this confusion and limited the subiculum to the three-layer cortex adjacent to CA1 where the thin-packed cell layer typical of the DG and the CA fields becomes much wider and less organized.

1.3.1.3 The parahippocampal region (PHR)

The term "parahippocampal region" (PHR) comes from the Greek παρά *para* (next to), designating the area next to the hippocampus. It was first described as the subiculum (Ramón y Cajal 1901) and the appellation PHR was introduced in the 1920s (Smith 1919). The PHR surrounds the thalamus and extends from the septal region dorsally to the amygdaloid complex ventrally. In the rat it lays anterior to the subiculum (Sub). The PHR includes the presubiculum (**PrS**), the parasubiculum (**PaS**), the entorhinal cortex (**EC**), the perirhinal cortex (**PER**) and the postrhinal cortex (**POR**). Some authors include other areas, however, based on connectivity criteria we have not included them (see discussion of paper #3 and Discussion chapter). The PHR is a **six-layer cortex**. Layer I is the molecular layer and mostly acellular. Layers II and III are called the superficial layers. Layer IV, when apparent,

is called the lamina dissecans (Rose 1927) and is mostly acellular. Layers V and VI are called the deep layers. The organization of the different layers in each subfield is portrayed further in paper #3.

The **PrS** and **PaS** are located next to the subiculum and they are named according to their position with the prefixes Latin *prae* (before) and Greek παρά *para* (next to). PrS and PaS have sometimes been regrouped as the subicular complex. However, the differences in the number of layers of these structures give little grounds for this grouping. The PrS and the PaS were clearly established by Blackstad in 1956. The PrS covers part of **Brodmann's areas 27** and **48**. Note that some authors distinguish the dorsal part of the PrS and name it postsubiculum, from Latin *post* (behind). The PaS covers part of **Brodmann's area 29**e and **49**a and b. PrS and PaS are the region that I have investigated extensively in paper #2.

EC, **PER** and **POR** are named after their position relative to the rhinal sulcus with the Greek prefixes ἐντός ento- (within) and περί, *peri* (around) and the Latin *post* (behind). The rhinal sulcus is a constant feature of the mammalian brain where the HF meets the neocortex (Insausti 1993). Historically, **Brodmann** (Brodmann 1909) illustrated three distinct cytoarchitectonic regions near the rhinal sulcus in primates: **area 28** or area entorhinalis, area **35** or area perirhinalis and area **36** or area ectorhinalis. The EC is a central part in the hippocampal region. It has sometimes been considered as part of the hippocampal formation, yet its very clear six layers place it in the PHR. The EC is quite a large area, which regroups several substructures that present cyto- and chemoarchitectonic as well as functional differences. Cajal referred to Hammarberg (Hammarberg 1895) concerning the EC. A first major division is between its medial and lateral parts: the medial entorhinal cortex (**MEC**) and lateral entorhinal cortex (**LEC**). Some authors (Witter et al. 1989) divide the MEC further into a medial entorhinal area (**ME**) and caudal entorhinal area (**CE**), and the LEC into the dorso-lateral area (**DLE**), dorso-intermediate area (**DIE**) and ventro-intermediate area (**VIE**). The MEC is the original repository of the **grid cells**. One of the aims of this thesis is to present a clearer comprehension of the function of its different neurons (see papers #1 and #2). A long lineage of work (Rose 1929); (Krieg 1946; Krieg 1946; von Bonin and Bailey 1947; Deacon et al. 1983; Murray and Mishkin 1986; Amaral et al. 1987; Witter et al. 1989; Mumby and Pinel 1994; Burwell et al. 1995) helped to establish the definitions of PER and POR and that PER

is further divided in **Brodmann areas 35** and **36** (A35 and A36). I will address some of this work in relation to our own observations in paper #3.

1.3.2 Connectivity of the hippocampus

Since the seminal work of Ramon y Cajal, Lorenté de Nó and Rose (see above), many authors have contributed to build up the knowledge of this intricately connected network with more and more precise histological, tracing, electrophysiological and microscopy methods: among them **Blackstad** in the 1950s, **Andersen**, **Powell**, **Cowan**, **Raisman and Hamlyn** in the 1960s and more recently **Amaral**, **Lavanex**, **Witter** and **Burwell,** to cite some of the main authors.

As stated previously, the hippocampal formation (**HF**) circuit is unique and that is one of the reasons for the interest of that structure. It is mainly described as a **tri-synaptic circuit, predominantly unidirectiona**l, with a single cell layer and strictly laminated inputs. The parahippocampal region (**PHR**) receives information from the whole brain, especially from the **sensory and associative structures,** and transmits it to the **HF,** which by a reciprocal connection sends information back, thus forming a **loop.** The intra- and interconnections of the hippocampal region are numerous and of various densities and nature (inihibitory/excitatory), creating a complex circuit and leading some authors to overlook or even leave out some of these connections.

I will attempt here to present first the **standard view** of that network and, second, a more complex view, yet one that is still incomplete. I refer the reader to the following website: http://www.temporal-lobe.com, for detailed and updated information on the rat HR connectivity (based on (van Strien et al. 2009)).

1.3.2. 1 Standard view

The hippocampal region is portrayed as consisting of a unidirectional loop: **PHR-to-DG-to-CA3-to-CA1-to-Sub-to-PHR** which includes a unidirectional tri-synaptic pathway, EC-to-DG-to-CA3-to-CA1 (Andersen et al. 1966) (Fig. 14).

Fig. 14 Standard view of the hippocampal circuit as presented in van Strien et al. (2009).

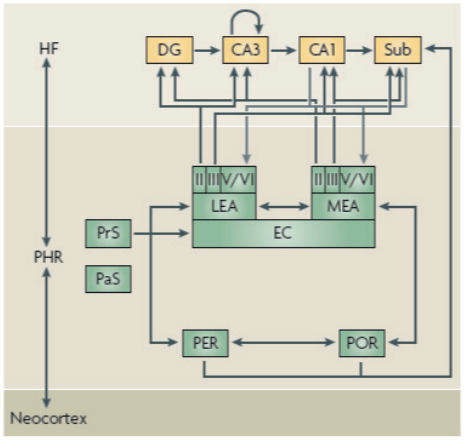

HF: hippocampus formation; PHR: parahippocampal region; DG: dentate gyrus; CA1-3: cornu Ammonis 1-3, Sub: subiculum; PrS: presubiculum; PaS: parasubiculum; EC: entorhinal cortex; PER: perirhinal; POR: postrhinal; MEA: medial entorhinal cortex; LEA; lateral entorhinal cortex; EC: entorhinal cortex

The different substructures of the **PHR** (i.e. PrS, PaS, PER, POR and EC) receive "**unimodal and multimodal information**" (i.e sensory, associative and cognitive information) from many **cortica**l (e.g. prefrontal cortex, associative cortex, sensory cortex, mamillar bodies) and **subcortical** (e.g. amygdala, septum, thalamus, hypothalamus, septum, brainstem) structures. The **EC** has a **central interface position** in that complex: inputs converge on it from a variety of sensory and multimodal association areas (including all the other PHR structures and parietal, temporal and prefrontal cortices). The standard view emphasizes especially the projections from PER and POR and claims that they are organized in two parallel reciprocal pathways: **PER-to-LEC** (lateral EC) and **POR-to-MEC (**medial EC) ((Burwell and Amaral 1998), but see 1.3.2.2). The EC functions as a hub channelling all "external information" to the HF via fibres that merge in the angular bundle and perforate the subiculum, hence their name: the **perforant path** (Ramón y Cajal 1893). The projection from the EC to the HF is highly organized; **EC layer II-to-DG and -to-CA3**, whereas **EC layer III-to-CA1 and -to-Sub** (Kohler 1986; Swanson and Kohler 1986). In addition, this projection is **topological** so that dorsal EC contacts dorsal HF and ventral EC contacts ventral HF (Steward 1976).

The **HF** is the seat of a mostly unidirectional tri-synaptic pathway DG-to-CA3-to-CA1-to-Sub. The DG projects to the CA3 via **mossy fibres** (Ramón y Cajal 1909) and the CA3 pyramids project to CA1 via the **Schaffer collateral** (Schaffer

1892) and the CA1 projects to the subiculum. In addition CA3 is the repository of high recurrent collateral (Amaral and Witter 1989). To close the loop, output from the **HF projects back to the PHR** (Swanson 1977), especially to the EC deep layers.

1.3.2.2 A more complex view

Though the standard view can be used as a reference frame, one should be aware that it includes many **approximations** that can, in some cases, be the source of important **misinterpretations**. I will not detail here all the extrinsic connections of the HR. I refer the reader to the book chapter by Amaral and Witter (Paxinos 2004) and to the review by Van Strien and Witter (van Strien et al. 2009). An **example** of the complexity of these extrinsic connections is given in Fig. 15 and 16 where I present the connections to **PrS** and **PaS**. One of the common misconceptions is about the parallel reciprocal pathway from **PER to LEC and POR to MEC**. PER (A36) and MEC are also reciprocally connected and so are POR and LEC (van Strien et al. 2009). To continue with intrinsic PHR connections, **PrS and PaS** are often portrayed as sending unidirectional information to the **EC**. However, that information is reciprocated to quite some extent (see Fig. 15 and 16 for references). In addition, it is often left unmentioned that **PER/POR and PrS/PaS** are reciprocally connected (Deacon et al. 1983; Furtak et al. 2007). Moreover, **EC** is the seat of quite rich intrinsic long-range connections between subfields (e.g. between MEC and LEC) but also, locally, between layers (Kohler 1986; Kohler 1988; Dolorfo and Amaral 1998).

Fig. 15 Connections of the presubiculum

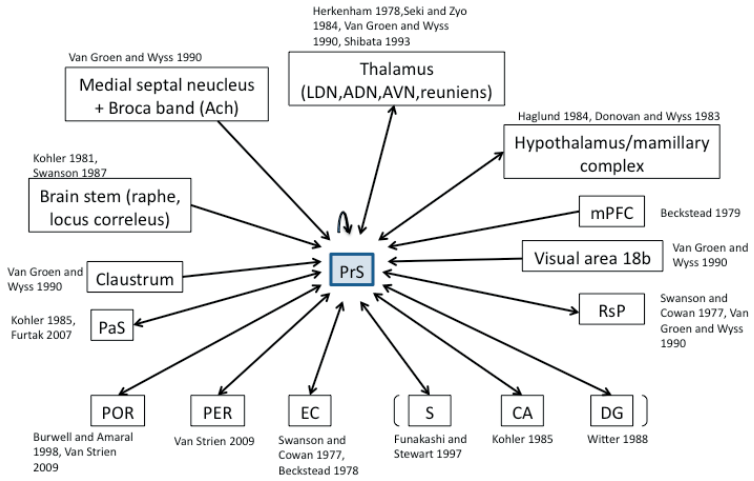

The EC is often described as the gateway of the HF, however this is an oversimplification**: PrS and PaS** do also project to all the subfields of the **HF**, though to a lesser extent. Back projections come mostly from Sub (yet some come from CA1) (see Fig 15 and 16 for references). The PrS-to-DG and PaS-to-DG projections are especially of interest as they occur radially and not transversally, as seen in the case of EC (Fig. 15 and 16).

Fig. 16 Connections of the parasubiculum

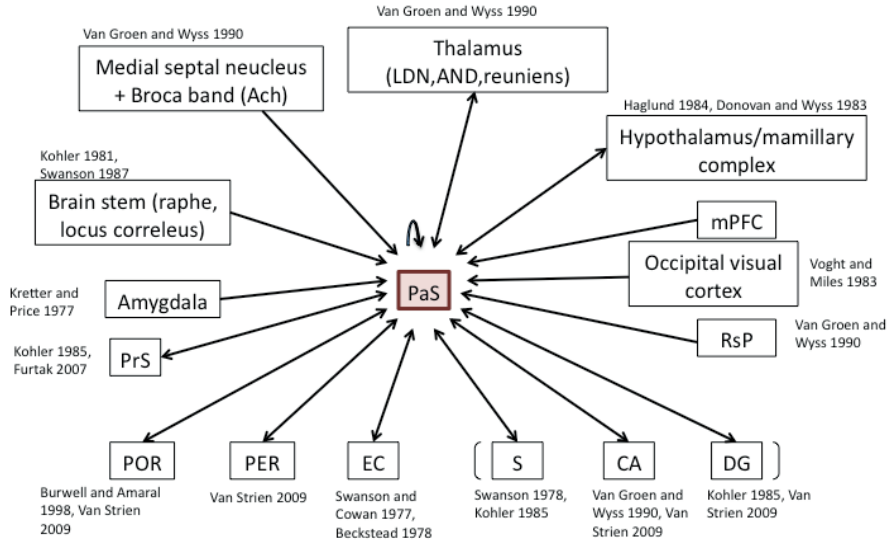

PER and POR also project directly to **CA1 and Sub** (Kosel et al. 1983; Furtak et al. 2007). In addition, EC connectivity is not uniform among its subdivisions (i.e. ME, CE, DIE, VIE and DLE), and different cortical and subcortical areas contact different **subdivisions of the EC** (van Strien et al. 2009). The projection from **EC to the HF** is not as simple as is sometimes described. On the one hand, the connection between **EC** and **CA1/Sub** follows the segregation MEC/LEC, initiated with the PER/POR parallel pathway, with the LEC projecting to the distal CA1 and the proximal Sub and MEC to the proximal CA1 and to the distal Sub (Tamamaki and Nojyo 1995). But on the other hand, there is convergence of inputs from **LEC and MEC** to similar subfields. Regarding the **DG**, the LEC projects to the outer third of the DG molecular layer while the MEC projects to the middle third of that layer (Swanson and Kohler 1986; van Strien et al. 2009). Similar convergence is observed in **CA3** (Sporns and Tononi

2007). The simple schema where EC layer II projects to DG, CA3 and EC layer III to CA1/Sub is also not definite. Indeed, the DG is also contacted by EC layers III, V and VI, and CA1 is also contacted by EC layers II, V and VI (van Strien et al. 2009). In addition, a recent transgenic mice study is now reporting that **CA2** is the main recipient in the HF of the MEC afferences (Rowland et al. 2011), though this projection might not be reciprocated (Cui et al. 2012).

Similarly, **connectivity within the HF** is more complex than the classic unidirectional DG-to-CA3-to-CA1-to-Sub. For once, it is organized so that the segregation between **two parallel pathways** is kept, with the first pathway being "distal CA3"-to-"proximal CA1"-to-"distal Sub" and the other one being "proximal CA3"-to-"distal CA1"-to-"proximal Sub" (Witter et al. 1989; Amaral et al. 1991; Naber et al. 2001); (van Strien et al. 2009). Another modification from the classical view is that the tri-synaptic pathway is not as unidirectional as was formerly envisaged: there are probably **inhibitory feedbacks** from CA3 to DG and from CA1 to CA3 (Laurberg 1979; Li et al. 1994; van Strien et al. 2009). Moreover, CA3 is not the only subfield that receives **recurrent collaterals**. It seems likely that all subfields of the HF do so as well, but to a lesser extent (Segal and Landis 1974; Kohler 1985; Amaral et al. 1991; van Strien et al. 2009). To close the loop, the **back projections from the HF to the PHR** are not only directed to the EC but also to all the other subfields (i.e. **PrS, PaS, PER, POR**) (Fig. 15 and 16) (Burwell and Amaral 1998). The connection from HF to EC follows the same topographical organization on the dorso-ventral axis as the EC-to-HF one, but it is less sharply defined. It mostly projects to the **deep layers of the EC**, yet some **superficial layers** are also contacted (Swanson 1977; Kohler 1985). Finally, one should not forget that both left and right hippocampal regions communicate via **commissural connections** (Ramón y Cajal 1909; Lorente de Nó 1934; Blackstad 1956)).

1.3.3. Basic physiology of the hippocampus

For the non-neuroscientist reader, I give a short overview of the basic principles of neuron physiology in annex 1. The present section is based on several chapters of *The Hippocampus Book* (Andersen 2007), I refer the reader to that book for more detailed information. I will present here three aspects of the physiology of the neurons of the hippocampal region. In the first part, I will describe some of the **neurons' morphological and physiological properties**. The comprehension of these properties

is essential to understanding the mechanisms responsible for the discharge of spatial and directional neurons. In the second part, I will very briefly address the **structural and synaptic plasticity characteristics** of these areas. Finally, I will give some accounts of the **rhythms** observed in the local field potential (LFP) of the hippocampal region, notably the theta rhythms.

1.3.3.1 Morphological and physiological properties of principal neurons

(see also *The Hippocampus Book*, chapter 5 (Spruston and McBain 2007))

As presented in annex1, neurons are classified according to their location and their afferences and efferences. However, they are also classified based on their physiological and morphological properties, which reflect how they process information. These properties include **morphology** (number and organization of the dendrites, shape of their soma, length and branching of their axons), **membrane properties** (resting membrane potential, threshold for action potential), **discharge properties** (AP rate, refractory periods, AP wave-form), **channel and receptor distributions**, **synapse types** and **neurotransmitter type**s (in particular, whether they are excitatory or inhibitory). I will present here some very basic morphological and physiological properties of neurons from the hippocampal region.

In the articles that are the base of this thesis, we did not analyse data from (putative) interneurons, therefore I will not discuss here the **different subtypes of interneurons** of the hippocampal region except to say that they exist in **great variety** (e.g. GABA, CCK, VIP, SP, CRF, Somatostatin, NPY, enkephalin, dynorphin, acetylcholine). I would like to stress that although interneurons are not considered here it does not mean they have a lesser role in cognitive function.

Since Ramon y Cajal and Lorenté de Nó's studies and drawings, the depiction of the neuronal population in the hippocampal region has gained in precision over the years. Most of the **principal excitatory neurons** have been named based on their **morphology** (shape of their cellular body and orientation and branching of their axons and dendrites). In the **HF**, one can distinguish between the **pyramidal neurons** in the CA fields and in the Sub, on one hand, and the **granule** and **mossy neurons** in the DG on the other. The **PHR** has been less intensively studied than the HF. Based on morphological criteria, one can distinguish between **pyramids** and **non-pyramids** (among which are: stellate, horizontal, polymorphic and multipolar cells) (Fig. 17).

Fig. 17 Morphology of a pyramidal neuron

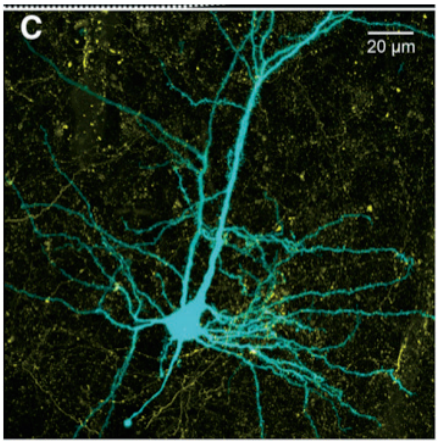

High-magnification confocal image of intracellularly filled LII parasubiculum pyramidal neuron (from Canto and Witter 2012)

1.3.3.1.1 HF principal neurons

The **pyramids** are named for their pyramid-shaped soma from which emerge two elaborated branching dendritic trees, one apical and one basal. Pyramids are very well organized in the **CA fields** in rows that allow a **precise lamination** of excitatory, inhibitory and neuromodulatory inputs. The alignment is **not as neat** in the **Sub**. A single axon emanates from the pyramidal soma and branches extensively, especially in CA3, forming **collaterals** with several targets, both within and beyond the hippocampus. Pyramids can **spike discretely** (at a rate from 1 to 10 Hz *in vitro*) (Henze and Buzsaki 2001). However, **bursts** of activity have been observed *in vivo* with rates exceeding 100 Hz (Frank et al. 2001). This bursting activity is very typical of pyramidal cells and aids in their characterization in vivo as **complex spike cells** (Kandel and Spencer 1961; Ranck 1973). Prolonged activation of pyramid cells *in vitro* results in a diminution of their maximum firing rate (i.e. **spike-frequency accommodation**) (Madison and Nicoll 1984). Membrane properties, ion channels and pumps are not uniformly distributed. Subicular pyramids share many morphological and physiological properties with CA pyramids. They can be divided into bursting and regular spiking pyramids, where the bursting ones have a higher rate than CA pyramids (Mason 1993). Interestingly, bursting cells have been proposed to target the PrS and PaS specifically, while regular spiking ones would specifically target the EC (Stewart 1997; Funahashi et al. 1999). The study of pyramid membrane properties

shows that they exhibit intrinsic resonance properties (Llinas 1988; Hausser et al. 2000) and that they express voltage dependent oscillation (Leung and Yim 1991).

Dentate **granular cells** have a small ovoid cell body with a single, approximately conical dendritic tree and an axon that forms numerous collaterals before projecting to the CA3 (mossy fibres). Their firing is much more sparse than what is observed with pyramidal cells, however they can also burst (Fricke and Prince 1984). Prolonged stimulation leads to spike accommodation similar to what is observed with pyramids (Staley et al. 1992). **Mossy cells** are present in the polymorphic layer of the DG (hilus). They consist of ovoid cell bodies that give rise to several primary dendrites and a single axon that targets the DG molecular layer in an excitatory manner, and often forms collaterals in this region (Scharfman 1995).

1.3.3.1.2 Principal neurons of the PHR

The PHR includes several types of principal neurons, divided into pyramidal and non-pyramidal cells. They are not homogeneously distributed among the subdivisions and layers of the PHR. The **pyramidal cells** can be divided further according to the orientation(s) of their dendrites and axons. The most studied **non-pyramidal cell** type is the **stellate cell**; other types include horizontal, polymorphic and multipolar cells.

The **entorhinal cortex** (EC) shows a great variety of neuron morphologies and physiologies. It seems there is no **correlation between morphology and physiology** in MEC and LEC, with MEC layer II forming an exception (Canto and Witter 2012; Canto and Witter 2012). Many groups have attempted to characterize the physiological properties of the EC neurons. In particular, the work of Alonso and colleagues (e.g. (Alonso and Llinas 1989; Klink and Alonso 1993; Klink and Alonso 1997; Egorov et al. 2002; Tahvildari et al. 2007) and Hasselmo and colleagues (e.g. (Fransen et al. 2006; Giocomo et al. 2007; Koene and Hasselmo 2007; Yoshida et al. 2008) helped to highlight two intriguing phenomena: persistent firing and sub-threshold oscillations. **Persistent firing** translates the ability of EC neurons to maintain firing after an **initial brief stimulation**. The persistent firing pattern varies according to neurons and layers. It can be regular or occurring in bursts, it can be graded and have ON/OFF patterns. **Subthreshold oscillations** in the EC are typical of the stellate cells. **Stellate cells** can be found throughout the whole EC but they are the most abundant cell type in layer II, especially in its medial part. Alonso and Llinas demonstrated that injecting a subthreshold depolarizing current in these cells induces

membrane **oscillations at theta frequency** (Alonso and Llinas 1989). The frequency of oscillation depends on the location of the neuron along the dorso-ventral axis of MEC layer II (Giocomo et al. 2007). These different physiological properties will be discussed in more detail as possible explanatory mechanisms underlying the spatial and directional specificity of MEC neurons (see Discussion chapter, below).

The **PrS** and **PaS** neurons do show somehow similar properties to those of the EC. **Stellate and pyramid cells** are preferentially distributed in **different layers** (stellates: layers II and V, especially in PrS layer II) (Funahashi and Stewart 1997). PrS neurons are, however, more densely packed and have smaller somas compared with the PaS and EC. PrS and PaS neurons usually exhibit **repetitive single spiking** and the deep layer cells have been shown to **burst** in response to the stimulation of the Sub or EC (Funahashi and Stewart 1997). Like in the EC, **persistent firing** (Fricker et al. 2009; Yoshida and Hasselmo 2009) and **subthreshold oscillations** (Glasgow and Chapman 2007; Glasgow and Chapman 2008; Glasgow et al. 2012) are observed in the PrS and PaS. Recently, several clusters of cell population were characterized in the PrS (Simonnet et al. 2012).

Likewise the **PER** and **POR** contain both **pyramids and stellates** (Furtak et al. 2007). Although the pyramids are the most common type of neuron in PER, their number is comparatively lower in PER than in other neocortical areas. Different discharge patterns can be observed in these cells, from **regular spiking** to **fast spiking**, **burst spiking** and **late spiking**. These different patterns are not uniformly distributed among layers (Kealy and Commins 2011). A similar situation is observed in the POR (Sills et al. 2012).

1.3.3.2 Plasticity in the hippocampal region

(see also *The Hippocampus Book*, chapters 9 and 10 (Bliss et al. 2007; Gould 2007))

One of the most striking properties of the hippocampal region, and a reason why it is so intensively studied, is that it is highly plastic. **Neural plasticity** is the ability of the brain to adopt physiological modifications in **response to changes** in the environment, in behaviour or in neural processes. This plasticity is expressed, in the hippocampal region, at both the **structural and the synaptic level**.

The hippocampal region is a relatively **late-developing region** so that it undergoes many **structural rearrangements** after birth (e.g. **axons** and **dendritic trees** sprouting or trimming, apparition and disappearance of **synapses**) (Fricke and

Cowan 1977; Fricke and Cowan 1978; Bayer 1980; Bayer 1980; Pokorny and Yamamoto 1981; Super and Soriano 1994; Jones et al. 2003; Danglot et al. 2006). However, substantial reorganization still occurs in **adulthood** when the hippocampal region is **damaged** but also in response to normal **changes in the environment** and what the subject **experiences**. The most striking expression of this structural plasticity is the **neurogenesis** that occurs in the **DG**. Indeed, thousands of new neurons are born every day throughout adulthood in rats (Kaplan and Hinds 1977; Gage et al. 1998; Cameron and McKay 2001). Neurogenesis, cell death, dynamic rearrangement of synapses and dendritic arborizations have been linked to different behavioural and cognitive states such as **learning and environment complexity** (Rosenzweig et al. 1962), **stress** (Watanabe et al. 1992; Gould and Tanapat 1999), **physical activity** (Barnea and Nottebohm 1994) and **depression** (Santarelli and Saxe 2003).

The other type of plasticity observed in the hippocampal region is **synaptic plasticity**. The synapses are the elements that connect two neurons. Their strength (or efficacy) will determine how well these neurons are connected and how much the activity of one will influence the activity of the other. First postulated by Cajal, this phenomenon resonates with **Hebbs's** famous postulate according to which: "The persistence or repetition of a reverberatory activity (or "trace") tends to induce lasting cellular changes that add to its stability (…) When an axon of cell A is near enough to excite a cell B and repeatedly or persistently takes part in firing it, some growth process or metabolic change takes place in one or both cells such that A's efficiency, as one of the cells firing B, is increased"(Hebb 1949), p62).

Plastic synapses have the ability to **increase or decrease their efficacy** in function of their use or disuse or in response to a **specific pattern of activation**. This change in efficacy can result, for instance, from the alteration of the number and the type of receptors and channels or of the quantity of neurotransmitter released, or the shape and "contact surface" of the synapse. In 1973, **Bliss and Lømo** (in the laboratory of Per Andersen) were the first to characterize such plasticity at the synapses that form the perforant path on the granular cells. They observed a long lasting increase in synaptic strength after a **brief tetanic stimulation** (100 Hz for some seconds) that mimics the intensive use of the synapse by the system. This phenomenon has come to be known as long-term potentiation or **LTP** (Fig. 18). It is now known to involve, among others, **calcium** and **NMDA receptors**. It has been

subsequently observed at many different synapses through the hippocampal region. Some authors even suggested that it might be observed at all excitatory glutamate synapses (Malenka and Bear 2004). LTP has been naturally linked to mechanisms of **learning and memory** (Bliss and Collingridge 1993; Moser and Moser 2000; Whitlock et al. 2006). Mechanisms of depotentiation of the synapse (Lynch et al. 1977) provided the first indication that the synapse could support **reduction of synaptic strength**, necessary to **avoid saturation**.

Fig. 18 Discovery of LTP (long term potentiation)

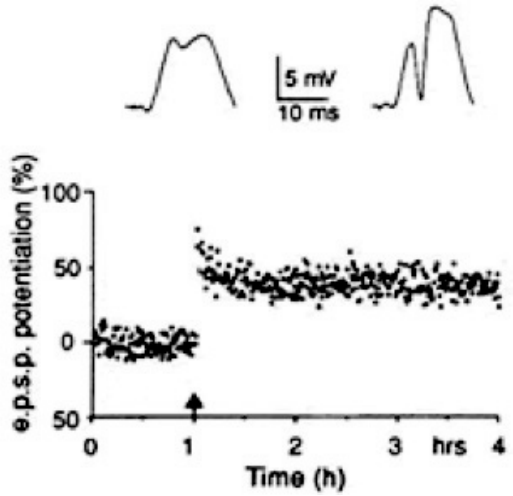

Long-term potentiation was first reported in the perforant path (entorhinal cortex-dentate gyrus in the hippocampal formation) (Bliss and Lømo 1973).

The counterpart of the LTP is the **LTD** or long-term depression. The LTD results from the stimulation of the synapses at a low frequency, over an extended period (1 Hz, 10 to 15 minutes), which mimics an under-use of that synapse by the system (Dudek and Bear 1992).

The understanding of HR structural and synaptic **plasticity** may shed light on the mechanisms behind this at the neural level of **spatially modulated cells**, which is one of their **defining properties** (see 2.1).

1.3.3.3 Rhythms of the hippocampal region

Brain functioning can be studied at different resolutions: neuron activity can be investigated at the single cell level but also as part of the **summation of the collective activity** of all neurons (i.e. principal cells and interneurons) in a given area. This global electric activity when recorded locally in a given brain volume by extracellular

electrode is referred to as **local field potential** (LFP). While observing the LFP of some areas, one can see the emergence of "**brain oscillations**" and other global electrical events which result from the **dynamic coordination of neural activity** across distributed groups of neurons.

The hippocampal neurons frequently show a synchronization of their activity. Three major patterns have been characterized in the hippocampal region: **theta oscillations** (4–12 Hz), **sharp waves and associated ripples** (140–200 Hz), and **gamma oscillations** (25–140 Hz) (Fig. 19). Interestingly, these global rhythms may influence in return the firing of individual neurons whose activity may then be "theta modulated" or "gamma modulated" (see 1.3.3.3.4). For complementary information on hippocampal region rhythms, I refer the reader to a number of reviews (Buzsaki 2002; Buzsaki 2004; Buzsaki 2010; Colgin and Moser 2010; Buzsaki 2011).

Fig. 19 Hippocampal field oscillations in the rat (Bragin et al. 1995; Buzsaki 2002)

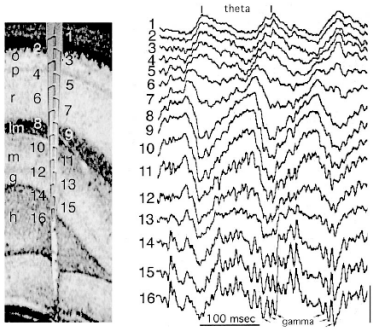

(Left) A 16-site silicon probe in the CA1-dentate gyrus axis. Numbers indicate recording sites (100 m spacing). o, str. oriens; p, pyramidal layer; r, str. radiatum; lm, str. Lacunosum-moleculare; g, granule cell layer; h, hilus.

(Right) Voltage-versus-depth profile: theta waves recorded during exploration. Gamma waves superimposed on theta oscillation are marked by arrows. Vertical bar: 1mV.

1.3.3.3.1 Theta oscillations

In 1938, Jung and Kornmüller (Jung and Kornmüller 1938) published for the first time their observation of regular slow oscillatory activity in the hippocampal field potential. This hippocampal slow oscillation pattern was later characterized at a frequency between 4 and 7 Hz and named the **hippocampal theta rhythm** in analogy with the EEG human rhythm appellation at the same frequency (Green and Arduini 1954). Subsequent studies on rats extended the frequency window to **4 to 12 Hz** and demonstrated that the theta rhythm was appearing when the animal was engaged in some specific behaviours that made it interact with the environment, such as **exploratory behaviour** (e.g. walking, running, sniffing), or when it was **asleep**, during the so-called rapid eye movement (**REM**) sleep phase (Grastyan et al. 1959;

Jouvet 1969; Vanderwolf 1969). It was later shown that theta activity is associated with the **intention to move** rather than with feedback produced by movement (Whishaw and Vanderwolf 1973; Sinnamon 2005). In addition, the theta power has been found to co-vary with **performance in tasks**, involving learning and memory or spatial cognition (Wyble et al. 2004; Sinnamon 2005; Montgomery et al. 2009). These observations, combined with other studies, led scientists to postulate that the theta has a **role in learning/memory** and in **spatial cognition** (Miller 1989; Lisman and Idiart 1995; Buzsaki 2005; Vertes 2005). Some authors suggested that theta rhythms reflect the **"on-line" state** of the hippocampus when the animal is **ready to process incoming signal** (Buzsaki 2002).

Theta is not confined to the HF. It can be observed in other parts of the brain, including the **PHR** and nearly **all areas that interact strongly with the HF** (e.g. septum, amygdala, striatum, prefrontal cortex, retrosplenial cortex, olfactory bulbs). Similarly to what is observed with increase of local theta power in correlation with specific spatial or memory cognitive tasks, **theta coherence between brain regions** does co-vary with **performance** (Montgomery et al. 2009). This argues for a role of theta oscillation as a **coordinator of multiple systems** supported by different brain areas.

The **origin** of the hippocampal theta is not yet completely elucidated and is probably plural. Authors have often distinguished between **two types of theta**. The **first** one is **linked to movement** (running, grooming, swimming), and thus dubbed "translational theta", it is dependent on the activity of the septum and the MEC superficial layers and has the role of pacemaker. The **second** one is **linked to highly aroused states** such as fear, and is thus dubbed "attentional theta". It is dependent on the cholinergic activity of the septum and has more a role of modulation. Yet each of these thetas may result from multiple origins. I refer the reader to reviews on the subject which argue that there are several types of theta whose oscillatory pattern can be imposed by both **external inputs** and by **autonomous internal oscillators** (Buzsaki 2002; Buzsaki and Draguhn 2004; Buzsaki et al. 2012).

These **external inputs** were first thought to come from the **medial septal area** and the diagonal band of Broca (Petsche and Stumpf 1962; Winson 1978) involving its **long-range GABAergic neurons** (Freund and Buzsaki 1996; Klausberger and Somogyi 2008). The septum does indeed project to many of the areas that present

theta oscillations (Witter and Amaral 2004). Others have involved the **supramammillary nucleus** of the hypothalamus in theta generation (Kirk 1998).

The **autonomous internal oscillators** can be based on **autorhythmic neurons** acting either as true oscillators (as pacemakers) or as resonators (responding preferentially to certain firing frequencies). Such **intrinsic oscillatory properties** have been observed in both the HF (Bland 1986); (Mitchell and Ranck 1980); (Leung and Yim 1986) and the PHR (Alonso and Llinas 1989); (Glasgow and Chapman 2007) where cells have the ability to generate **theta-frequency membrane potential oscillations** when stimulated under their depolarization threshold (Nunez et al. 1987; Alonso and Llinas 1989; Ylinen et al. 1995; Kamondi et al. 1998; Glasgow and Chapman 2007).

The autonomous internal oscillations could also emerge as a **network property**, often involving mutual **synaptic inhibition** and **oscillatory coupling** between principal cells and interneurons (Alonso and Garcia-Austt 1987; Csicsvari et al. 1999; Klausberger et al. 2003), and arises from a dynamic interplay between synaptic interactions and the intrinsic electrical properties of the neurons.

Recent studies have proved the existence of **multiple independent oscillators** in the CA field, self-generators of theta (Goutagny et al. 2009). Therefore, it seems that there are several theta oscillators throughout the hippocampal region and that the **septum coordinates** them so that theta oscillations are coherent through the region. It has been observed that theta oscillations recorded at **different positions** can have **different phases** at a given moment (Brankack et al. 1993). This does not indicate an incoherence between areas but more a dynamic view where theta oscillations behave like **travelling waves** carrying the information from one end to the other (Lubenov and Siapas 2009).

1.3.3.3.2 Gamma oscillations

The hippocampal region LFP also exhibits oscillations at a higher frequency including the gamma oscillations (Stumpf 1965). The spectrum of frequency of these oscillations is pretty wide and goes from **25 to 140 Hz** (Leung et al. 1982; Buzsaki et al. 1983; Bragin et al. 1995)). Gamma and theta rhythms are not exclusive. On the contrary, **theta waves shape the gamma bursts** nesting inside the wide theta periods of 100–200 ms (Bragin et al. 1995; Colgin and Moser 2010). They are also linked to the sharp-waves ripple activity (see 1.3.3.3.3; Sullivan, Csicsvari et al. 2011). Gamma

oscillations are present in all structures where **interneurons target the soma** so to provide **fast inhibition** (Whittington et al. 1995; Jonas and Buzsaki 2007). That way, they are maintained by the **interactions between the interneurons and the principal cells**. Neurons that discharge within the time period of a gamma cycle (10–30 msec) define a cell assembly (Harris et al. 2003). There seem to be **two independent generators** of gamma oscillation, one in the **EC** and the other in **CA3,** leading respectively to **fast** and **slow** gamma (Csicsvari et al. 2003). This fast and slow gamma seems to have a role in the **routing and the grouping of information** across different brain areas, as well as in the encoding and the retrieval of this information so that areas will tune to one or another frequency depending on the region they are communicating with (Colgin et al. 2009) and may influence differently separate groups of hippocampal cells (Huxter et al. 2008).

1.3.3.3.3 Sharp waves ripples

When theta oscillations disappear in periods of waking behavioural quiescence or during non-REM (NREM) sleep, they are replaced by **large irregular activity** (LIA) (Vanderwolf 1969) in the waking period and **slow wave oscillation** (delta) during some sleep periods (**SWS**). During these non-theta states, large-amplitude field potentials, or **sharp waves** (SPWs) occur intermittently. These events lead to the synchronous discharge of many neurons distributed over the extent of the hippocampal region. SPWs are initiated by the **self-organized population bursts of the CA3 pyramidal cells** (Buzsaki et al. 1983). SPW are associated with **fast-field oscillations** (**140–200 Hz**), or **ripples**, confined to the **CA1** pyramidal cell layer (O'Keefe and Nadel 1978; Buzsaki et al. 1992). **Though SPW are characteristic of SWS, they can also occur during periods of immobility while awake** (Buzsaki et al. 1983). Recent studies have demonstrated a direct link between suppression of SPW and memory performance (Girardeau et al. 2009; Dupret et al. 2010; Ego-Stengel and Wilson 2010; Jadhav et al. 2012).

1.3.3.3.4 Influence on unit firing

These different rhythms seem to be responsible of the **orchestration of the brain** (Chrobak and Buzsaki 1998). A key issue is then to understand the relationship between single unit activity and the global field activity. In the hippocampal region, the activity of many neurons indeed seems to be **modulated by theta and gamma** rhythms, at least to some degree, and different neuronal populations are preferentially

active at **different phases** during a theta cycle (Alonso and Garcia-Austt 1987; Csicsvari et al. 1999);(Skaggs et al. 1996; Frank et al. 2001; Klausberger et al. 2003). In addition, unit activity seems to be "**reactivated**" during **sharp waves/ripples** (Pavlides and Winson 1989; Wilson and McNaughton 1993).

The specificity of theta (and gamma) modulation of principal neurons of the hippocampal region will be presented in more detail while discussing the properties of the neurons in the second part of this thesis (2.2.3.3) and while presenting the results from papers #1 and #2.

1.3.4 Functions of the hippocampus

1.3.4.1 A multifunctional structure

Since its discovery, the hippocampal region has been postulated to have **several functions** (e.g. olfactory, emotional, attention, memory, spatial cognition). I will present here some of its main functions. The reader should keep in mind that the hippocampal region regroups several **sub-structures** all of which have different specializations for these diverse functions.

Originally the hippocampus was thought to be involved in **olfaction** (Brodal 1947). This theory was later supported by the revelation of numerous **projections** between the hippocampal region and the olfactory bulbs (Scalia and Winans 1975). Though nowadays other functions have taken over the spotlight, the implication of the hippocampus in solving **olfactory memory tasks** or its **neuron olfactory code** do argue for some role in olfaction even if it does not seem to be its primary function (Eichenbaum et al. 1987; Eichenbaum et al. 1988; Eichenbaum et al. 1989; Otto et al. 1991; Wood et al. 1999; Alvarez et al. 2001; Eichenbaum and Robitsek 2009; Diekelmann et al. 2011).

In 1937 Papez placed the hippocampal region at the heart of the "**Papez circuit system for emotional expression**" (Fig. 20). He proposed that the hippocampus was responsible for the perception of emotionally salient situations, their collection and their channelling towards the hypothalamus where the appropriate emotional response was then generated. This link is still relevant today. The hippocampal region is now considered to interact with the **amygdala** in emotional situations (Phelps 2004; Richardson et al. 2004). Moreover, stress and depression have an impact on the morphological and physiological properties of hippocampal region neurons so that they are the target of some **anti-depressors** and **anti-**

anxiolytics (Sheline et al. 1996); (Lee et al. 2002; Dranovsky and Hen 2006). Animal lesion studies show that the **ventral hippocampus** is specifically involved in **the** expression of **fear** (Kjelstrup et al. 2002).

Fig. 20 Papez circuit (Bloom et al. 2006)**.**

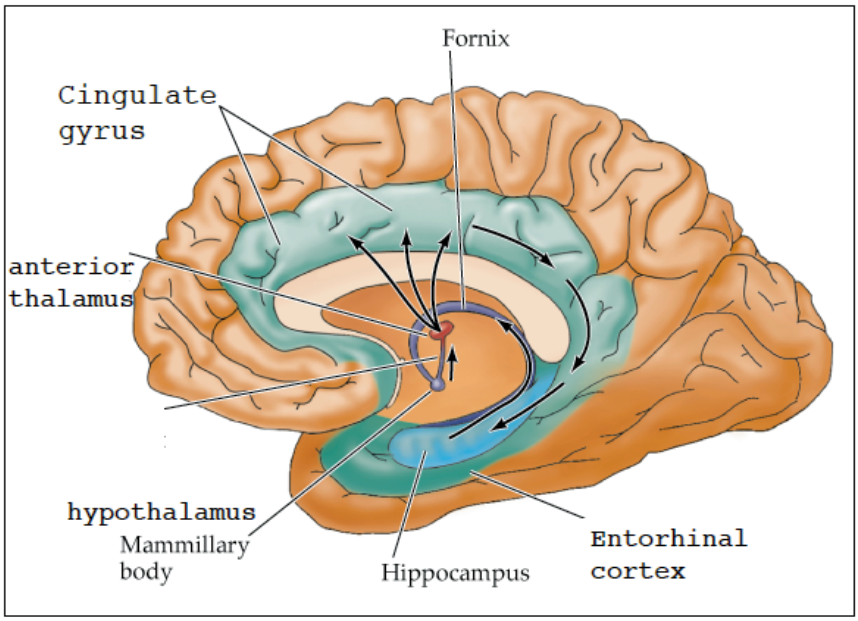

Historically, the third function suggested for the hippocampal region is the **control of attention**. This was notably based on the discovery of the hippocampal **theta rhythm** characteristic of the engagement of the animal in voluntary movement (Jung and Kornmüller 1938). Recent studies argue for the activity of the hippocampal cells as being influenced by and reflecting attention processes (Vinogradova 2001; Fenton et al. 2010).

Probably the main functions now associated with the hippocampus are **memory and learning**. In fact, some of the involvement of the hippocampal region in olfaction and emotion can be seen as **olfactive memory** and **emotional memory**. Since the famous case reported by Scoville and Milner (Scoville and Milner 1957), many studies and theories have placed the hippocampal region at the heart of **episodic memory,** as previously discussed (1.2.4). As a young man, Henry Molaison (HM) suffered from severe epilepsy, which led William Scoville to surgically remove the

epileptic focus (Fig. 21). This left HM with a **bilateral hippocampal lesion** covering the whole HF and a large portion of the PHR as well as the amygdala.

Fig. 21 The case of Henry Molaison (HM)

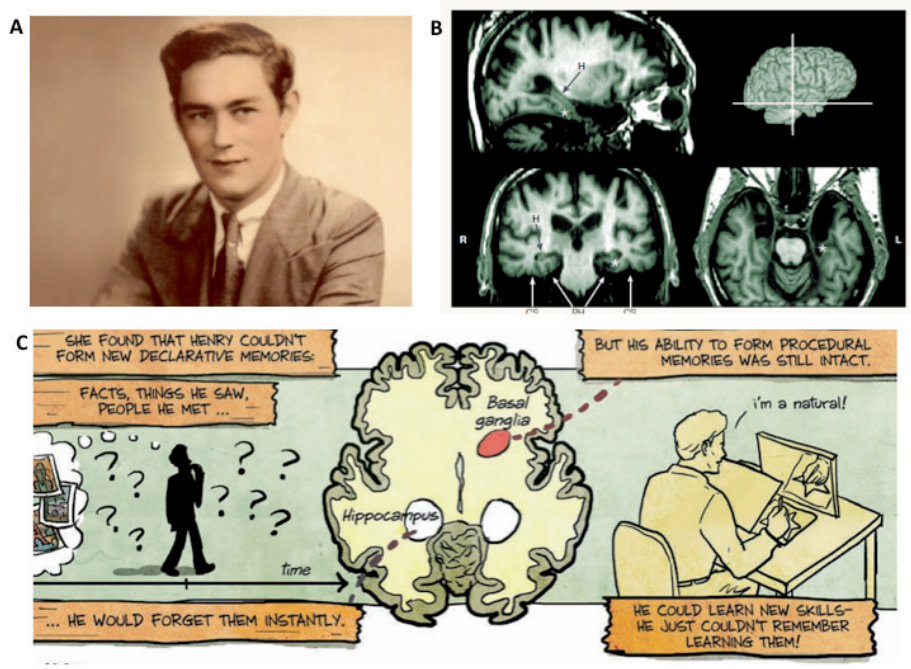

(A) Photograph of Henry Malaison (HM) before the intervention **(B)** Multiplanar views of MRI volumes showing preserved structures in HM's MTL. The asterisk marks the intersection of the three viewing planes, just caudal to the left medial temporal lobe (MTL) resection, seen best in the transaxial view. Top left, sagittal view; bottom left, coronal view; bottom right, transaxial view; top right, surface rendering showing locations of transaxial and coronal planes. Abbreviations: CS, collateral sulcus; EC, entorhinal cortex; H, hippocampus; L, left; PH, parahippocampal gyrus; R, right. Corkin 2002 **(C)** Excerpt of a comic in *Scientific American* relating the condition of HM, by Dwayne Godwin and Jorge Cham http://www.scientificamerican.com/article.cfm?id=memories-of-henry .

The first report from **Scoville and Milner**, followed by hundreds of neuropsychological investigations throughout HM's life, reported that the main sequels of the lesion were a deficit in the ability to form new episodic memories, regardless of type of memory test, stimulus material, sensory modality (**global anterograde amnesia**) and a **moderate graded retrograde amnesia** (loss of memory of events prior to the surgery, especially in the two years preceding the ablation). In spite of this quite severe amnesia, HM's working and procedural memory (abilities to learn mechanical tasks such as drawing with the help of a mirror), as well as his language abilities were mostly preserved and he was of relatively normal

intelligence (Scoville and Milner 1957; Milner 1958; Corkin 2002; Smith and Kosslyn 2007).

HM's case was the first of its kind and therefore one of the central pieces at the base of the **multiple memory system** and the role of the hippocampal region in the episodic memory (Squire 1992; Eichenbaum and Cohen 2001). This role has since been further confirmed by many investigations, notably of patients affected by the terrible affliction of **Alzheimer's** disease. Alzheimer's is a neurodegenerative disorder that leads to memory loss and ultimately to dementia. The neurodegeneration consists of loss of neurons and synapses in the cerebral cortex and certain subcortical regions, especially in the region of the hippocampal region (Braak and Braak 1991). There accumulate both **amyloid plaques** (insoluble deposits of amyloid-beta peptide and cellular material outside and around neurons) and **neurofibrillary tangles** (aggregates of the microtubule-associated protein tau which has become hyperphosphorylated and accumulate inside the cells themselves). The **EC** and the **DG** are among the first regions to present an accumulation of amydoloid plaques (Chen et al. 2000; Thal et al. 2000; Teipel et al. 2006; Gallagher and Koh 2011)).

Other hippocampal functions that can be seen as a variant of the memory function are its role in **novelty detection** (Nyberg 2005), in **pattern completion** and **pattern separation** (or discrimination) (Rudy and Sutherland 1989; Rolls 2007) and in **sequences** of events and **prospective coding** (Lisman and Redish 2009).

1.3.4.2 Focus on spatial cognition

1.3.4.2.1 Animal studies

The study of spatial cognition is at the heart of this thesis. This function was originally hinted at by a series of studies in which **rats** and other mammals with **hippocampal lesions** performed poorly in tasks demanding some sort of spatial cognition. These tasks involved discrimination and **learning of mazes** or some sort of orientation toward a stimulus (e.g. (Kimble 1963; Kveim et al. 1964; Lash 1964); (Rogozea and Ungher 1968; Hendrickson et al. 1969; Jackson and Strong 1969). In 1971, **O'Keefe and Dostrevsky** changed everything with their discovery of **place-modulated cells** in the CA fields (O'Keefe and Dostrovsky 1971). O'Keefe and Nadel (O'Keefe and Nadel 1978) later formulated that the hippocampus was the recipient of the **cognitive map** envisioned by **Tolman** in 1948. In this seminal book, they demonstrate their theory based on the account of the mentioned lesions studies

alongside more recent ones (Kimble and Kimble 1970; Ungher et al. 1971; Harley 1972; Olton 1972); (Riches 1972; Plunkett et al. 1973; Winocur and Breckenridge 1973; de Castro 1974; Myhrer 1975; O'Keefe et al. 1975; Olton 1977). Consecutively, mazes were specifically designed to address different components of spatial cognition and to evaluate the impairment caused by hippocampal lesions in such conditions (e.g. (Barnes 1979; Olton 1979; Morris et al. 1982), see example of the Morris water maze in Fig. 22).

Fig. 22 Watermaze and hippocampal lesions.

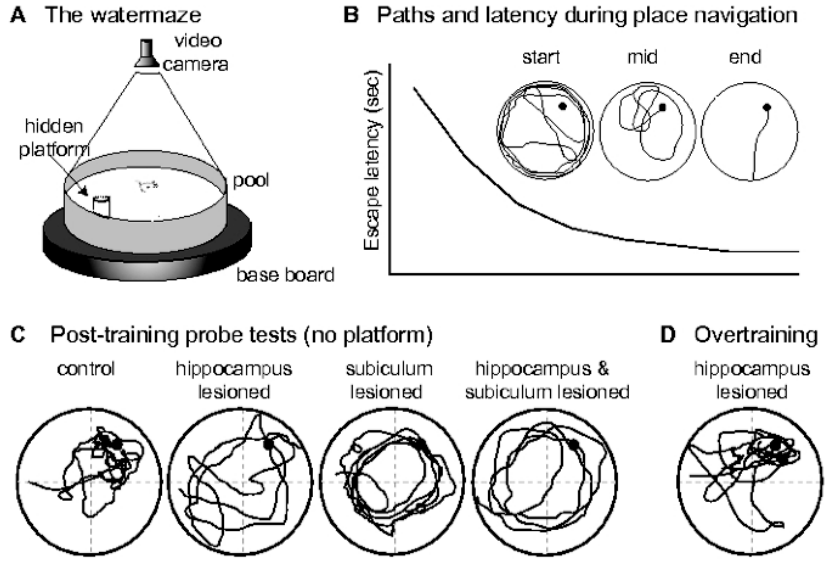

(A) Drawing of a typical watermaze set-up with overhead videocamera and rat swimming to find the hidden platform. **(B)** Representative escape latency graph and swim paths from successive stages of training – initial swimming at the side-walls, then circuitous paths across the area of the pool, and finally directed path-navigation. **(C)** The hidden platform is removed for post-training probe tests. Whereas normal or sham-lesion controls swim to the target quadrant (NE, within dotted grey lines), rats with hippocampus, subiculum or combined lesions do not. **(D)** Overtraining of hippocampus lesioned rats can result in quite focused search patterns in a probe test. After Morris et al. (1990) scholarpedia http://www.scholarpedia.org/article/Morris_water_maze

At that point in time, the number of studies on the hippocampal regions went exponential. Work conducted on **monkeys** extended the implication of the hippocampal region in spatial cognition to species than other rodents (e.g. (Mishkin 1978; Zola-Morgan and Squire 1984; Zola-Morgan et al. 1986; Zola-Morgan et al. 1989; Gaffan and Parker 1996; Buckley and Gaffan 1997; Malkova and Mishkin 2003; Lavenex et al. 2006; Lavenex and Lavenex 2009).

By the late 1970s and the beginning of the 1980s, the next concern was to address the specific roles of the diverse **substructures** presenting some spatial modulation. This mapping was mostly done through the evaluation of spatial performances of rats with **lesions** increasing in precision. The breadth of the literature on that subject is very important. I mention here a few of these studies for illustrative purposes. Some concentrated on the **HF subfields** (CA1-Sub: (Jarrard 1978); CA3-Sub: (Jarrard 1983); CA3-CA4-DG: (Sutherland et al. 1983); CA3-DG: (Whishaw 1987); Sub: (Morris et al. 1990); all subfields: (Good and Honey 1997; Galani et al. 1998)). Others attempted to assess the role of the **PHR** and its subregions (e.g. PHR: (Schenk and Morris 1985); EC: (Olton et al. 1982; Glasier et al. 1995; Nagahara et al. 1995; Galani et al. 1997; Good and Honey 1997; Hardman et al. 1997; Kirkby and Higgins 1998; Eijkenboom et al. 2000; Oswald and Good 2000; Parron and Save 2004); PrS-PaS: (Taube et al. 1992; Good and Honey 1997; Kesner and Giles 1998; Liu et al. 2001); PER-POR: (Wiig and Bilkey 1994; Nagahara et al. 1995; Ennaceur et al. 1996; Liu and Bilkey 1998; Wiig and Burwell 1998; Aggleton and Brown 1999; Bussey et al. 1999; Bussey et al. 2000; Liu and Bilkey 2002)). Interestingly, some lesion studies attempted to determine whether specific parts within each substructure were specifically important for spatial cognition. That way the **dorsal part of the hippocampus** was revealed as more important for spatial cognition (Moser et al. 1993; Moser et al. 1995) and so were the **medial** (Kesner and Giles 1998) and **dorsal** (Steffenach et al. 2005) parts of the **EC**. Spatial cognition regroups different functions, therefore some studies focused on specific components of spatial cognition such as the sense of direction (e.g. (Pearce et al. 1998; Whishaw and Maaswinkel 1998; Oswald and Good 2000; Eacott and Norman 2004; Tse et al. 2007)). In addition to classic lesion studies, **disconnection studies** are a powerful paradigm to understand the relative roles of the different part of the hippocampal region (e.g. (Cassel et al. 1998; Warburton et al. 2001; Galani et al. 2002; Steffenach et al. 2002; Parron et al. 2006)). With time not only the anatomical precision of the lesion increased but also its modalities. Indeed research on the hippocampal region in the last two or three decades has seen the emergence of new tools such as **transient pharmacological inactivation** (e.g. (Moser et al. 1998)), genetic tools allowing researchers to specifically modulate the activity of a region, a cellular type or a protein **via transgenic mice** (e.g. (Wirak et al. 1991; Silva et al. 1992) or **virus induced transgenic expression** (Geller and Freese 1990), and, very recently,

optogenetic tools can activate or inactivate a target with the temporal resolution of a laser light (Deisseroth et al. 2006; Fenno et al. 2011).

The reader should note that, in parallel to lesion and inactivation studies, many ***in vivo* recording** studies in freely behaving rats, adapted and modernized after those of O'Keefe and Dostrovsky, were conducted to further characterize the hippocampal region unit neural activity. I will describe some of the main results from these studies in the second part of this introduction (2). Some of these *in vivo* studies were **combined with inactivation/lesion** of hippocampal substructures. I will describe and analyse some of the results of these manipulations on the firing patterns of the spatially and directionally modulated neurons in the Discussion chapter of this thesis.

1.3.4.2.2 Human studies

The hippocampal region's role in spatial cognition was further affirmed and extended by several human studies. The volume of literature on that subject is quite overwhelming, so I will only cite two famous studies and refer the reader to numerous reviews on the subject (Moscovitch et al. 2006; Carr et al. 2010).

Fig. 23 London taxi drivers

Upper panel: Activation in the right hippocampus during the recall of routes around London by 11 taxi drivers compared with recall of a famous landmark (from Maguire 1997). Lower panel: Virtual navigation and map of London (from Maguire et al. 2006)

One of the most famous studies is the work initiated by **Maguire** and colleagues measuring the hippocampal region characteristics of **London taxi drivers** (Fig. 23). Their original discovery was an increase in the activation of the taxi drivers' right HF (Maguire et al. 1997). Another famous strain of studies originated with the characterization of the so-called **parahippocampal place area** (PPA) by **Kanwisher**

and Epstein (Epstein and Kanwisher 1998), specifically activated while subjects were visualizing scenes.

What about patients with **hippocampal lesions,** such as the famous HM? His limitations in spatial cognition were quite moderate and in no way as extended as one could expect (Corkin 2002). In general, **navigation skills** in patients with hippocampal region lesions are **sometimes preserved** (Teng and Squire 1999; Rosenbaum et al. 2000; Stefanacci et al. 2000; Rosenbaum et al. 2005) and **sometimes impaired** (Maguire et al. 1996; Kessels et al. 2001; Spiers et al. 2001; Hassabis et al. 2007). For review see (Squire 2004; Moscovitch et al. 2006). These variations can be comprehended at different levels. First, hippocampal lesions rarely cover the **whole extent of the hippocampal region**. In the case of HM, for instance, PER and POR were preserved. Second, regions neighbouring and highly connected to the hippocampal region (e.g. parietal cortex, retrosplenial cortex) are thought to be involved in spatial cognition and could thus support it in specific conditions (Aguirre and D'Esposito 1999). Third, as mentioned before, accurate navigation can be achieved by **different strategies** involving completely different structures, such as the striatum or the caudate nucleus (White and McDonald 2002). This switch in strategy has been observed in patients with hippocampal lesions or in imaging studies (Hartley et al. 2003; Iaria et al. 2003; Maguire et al. 2006; Moscovitch et al. 2006). Finally, even in rats spatial memory is preserved after hippocampal lesion if there has been an extensive training in that environment prior to the lesion (Winocur et al. 2005).

TRANSITION

In the first part of this introduction (1), I presented evidence supporting the **localization of different functions** in different areas. As stated in 1.1.4, this specialization can even take place at a very fine resolution such as the basic functional unit of the brain that is the **neuron**. In the second section (1.2), I presented the brain function focus of this thesis: the **spatial cognition**. As argued in the third section (1.3), many lesion and imaging studies prove that this function is partly supported by both main divisions of the **hippocampal region**: the hippocampal formation (**HF**) and the parahippocampal region (**PHR**). In the second part of this introduction (2), I will now address the main focus of this thesis and discuss the **neuron spatial specialization in HF and PHR**.

2. SINGLE NEURON SPATIAL CODE IN THE HIPPOCAMPAL REGION

In the 1940s, **Renshaw** and colleagues recorded, for the first time, ***in vivo*** **unitary discharge** of **hippocampal neurons** (pyramidal cells) (Renshaw et al. 1940). Time saw the improvement of unit recording methods, which evolved from **single wire** to more sophisticated recording techniques such as **tetrode** recordings. The latter technique is used in the studies supporting this thesis (cf. methods sections in paper #1 and #2). These technical advances have made it possible to **increase the number of units** (neurons) one could record from a behaving animal and allowed a **better isolation** of single unit activity. Recordings from single neurons in **HF** and **PHR** highlight a unique feature of these areas: most of the principal neurons there have their activity modulated by **spatial features**. The three main (most studied) spatially modulated cells are the **place cells**, the **head direction** (HD) **cells** and the **grid cells**. Note that a new type of spatially modulated cells, the **border cells**, is the focus of paper #2 and will therefore be discussed in the synopsis of results. I will focus here on results obtained from **rats**. One could argue that the HF and PHR area are **highly phylogenetically conserved** among mammals so that it is reasonable to conceive that some of these results can be extended to other species (including human).

The goal of this thesis is to give a **comprehensive overview of place, HD, grid and border cells** and to discuss how the results of papers #1, #2 and #3 can integrate in this view.

In the first section (2.1), I will consider the **distribution** of **spatial and directional modulation** among the different hippocampal and parahippocampal structures. I will start by describing **initial reports** of place, HD and grid cells and their **definitions** based on their antonymic fundamental qualities: **stability** and **plasticity**. Border cells will be defined below in the Synopsis of results and Discussion chapters. I will then give an **overview** of how space and direction are represented in the different structures of the **hippocampal region**. Paper #2 contains additional information on the distribution of HD and grid cells while paper #3 offers a clearer definition of the anatomical borders of these areas (see Synopsis of results and Discussion).

In the second section (2.2), I will define more thoroughly place, HD and grid cells by presenting their "**static properties**", which characterize the cell activity in conditions of **environmental stability**. I will specify for each cell type, considered in

a stable familiar environment, their **directional and spatial properties**, including specific **field and grid properties** and their **discharge properties**, including modulation by global oscillatory rhythms (theta and gamma). I will attempt to highlight here differences between similar cell subtypes recorded in **different subfields**. I refer the reader to annex 2 for more **detailed methodological** considerations on how to measure these different properties.

In the third section (2.3), I will discuss the influence of place, HD and grid cell activity. The primary **discharge correlates** of these cells are by definition supposed to be spatial and directional. Yet this coding is the result of what the rat experiences and processes. The rat experiences the world through **allothetic** and **idiothetic information** that allow it to assess the **environment spatial features** (**geometry**, **borders**, **object**) and changes in these features. **Non-spatial information** such as **experience** or **behavioural relevance** completes this representation. In this section, I will discuss the type of control (generation, modulation, stabilization, anchoring) allothetic and idiothetic information, environment spatial and non-spatial features exercise upon place, HD and grid cell activity.

In the fourth section (2.4), I will present the **dynamic properties** of place, HD and grid cells. By "dynamic properties", I mean here all response of the cell activity to a **change in the environment**. This section is in two parts, the first one dealing with changes between **familiar environments** and consequent **remapping** of place, HD and grid cells, and the second on the development of their firing patterns in a **new environment**.

The last section (2.5) of this introduction will address the **network properties** of place, HD and grid cells. Here I will stop considering the units in their individuality but rather as **ensembles of cells**, belonging to one or several types and possibly distributed over several subareas. This will allow me to discuss how those ensembles are attached to a r**eference frame** and how they homogenously (or not) remap. I will also introduce the notion of **pattern completion/separation**. Finally, I will show how the **interaction and coordination between areas** (and ensembles) supports a **global spatial network**.

This overview of place, HD and grid cells properties will allow me to introduce how the work of paper #1, #2 and #3 is fundamental in refining the understanding of the spatial network distributed code over the hippocampal region.

The pre-requisite to study field properties is to define how to **delineate** such a field. When comparing studies, one should be aware of possible variation in this **definition**. A firing field is often estimated as a **contiguous region of at least X cm^2** where the firing rate is above Y% of the peak rate (X and Y depending on studies, see annex 2). Place fields can be described according to several parameters: their **numbers**, their **shape**, their **size** (or scale), their **spatial distribution** (in the environment), their "**intensity**" (as measured by maximum firing rate) and their **sharpness** (or specificity, relation between in- and extra-field firing rates). I will discuss these different parameters in the following paragraphs.

2.1 SPATIAL AND DIRECTIONAL MODULATION IN THE HIPPOCAMPAL REGION

Since 1960, several classes of spatially or directionally modulated neurons have been defined in the hippocampal region (HR). I will here present the three classes that are the most studied: **place cells** (2.1.1), head direction (HD) cells (2.1.2) and **grid cells** (2.1.3). For each of them, I will give an account of how they were **initially reported**. I will then define them based on their antonymic fundamental properties of **stability** and **plasticity**, while their other properties and discharge correlates will be discussed in detail below. Thirdly, I will address their **distribution** in the HR.

Place, HD and grid cells are essential to the spatial network, yet many other HR neurons are spatially and directionally modulated without qualifying for place, HD or grid definition, and paper #2 was instrumental in characterizing one of these cell types corresponding to the border of the environment (see Synopsis of results and Discussion chapters). In the last part of this section (2.1.4), I will give an **overview of the distribution of spatial and directional modulation throughout the HR**.

2.1.1 Place cell definition and distribution

2.1.1.1 First characterization

Place cells are cells that seem to **code for an animal's location**. These cells are generally silent when the animal is exploring an environment except when it enters a specific portion of this environment referred to as the **place field** of this cell (Fig. 24). **O'Keefe and Dostrovsky** first characterized them about four decades ago in the **rat** hippocampus (O'Keefe and Dostrovsky 1971).

Fig. 24 Representative example of a place cell

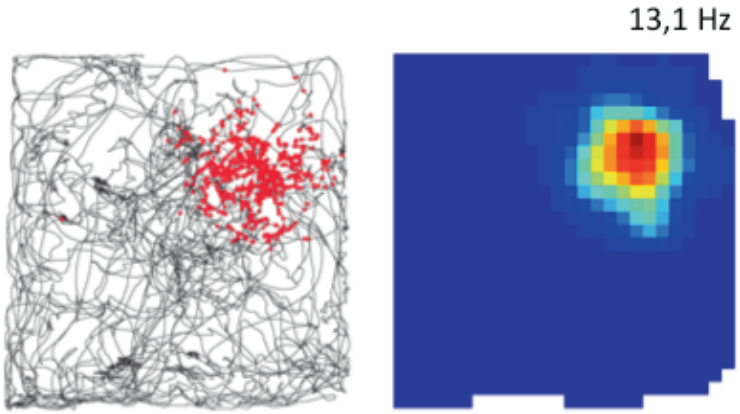

Path trajectory with spike positions (in red); colour-coded rate map (maximum firing in dark red, minimum in dark blue). Peak firing rate indicated in the upper right corner. (Tora Bonnevie data)

Based on this groundbreaking finding, **O'Keefe and Nadel** proposed that the hippocampus was the neural substrate of the **internal cognitive map** envisioned some decades earlier by **Tolman** (Tolman 1948; O'Keefe and Nadel 1978). Indeed, an ensemble of place cells can span a whole environment so that the rat's position could be tracked constantly by the activity of these neurons. **Wilson and McNaughton** confirmed this hypothesis by r**econstructing** accurately the animal movement through their environment based on **ensemble activity** (Wilson and McNaughton 1993). Place-responsive neurons have been described in species other than rodents (e.g. **monkeys**: (Ono et al. 1991); **humans**: (Ekstrom et al. 2003); **bats** (Ulanovsky and Moss 2007)).

One should note that originally place cell activity was observed in **complex spike cells** (CS) (i.e. **principal cells** or putative excitatory cells) and not theta cells (i.e. putative interneurons). Moderate spatial modulation was later described in putative interneurons (McNaughton et al. 1983).

2.1.1.2 Stability

An intrinsic property of place cells is that they are **stable** over very long periods of time (Muller et al. 1987) (Fig. 25). This means that given a hippocampal neuron in a given rat with a specific place field in a given environment, each time the rat will be in that environment, that neuron will always have the **same place field**. The only time limitation seems to be due to the technical difficulties of recording **over weeks and**

weeks from the same neuron (153 days in (Thompson and Best 1990)). This argues for place cells as being a neural substrate for **spatial memory**.

Fig. 25 Place cell stability (Muller et al. 1987)

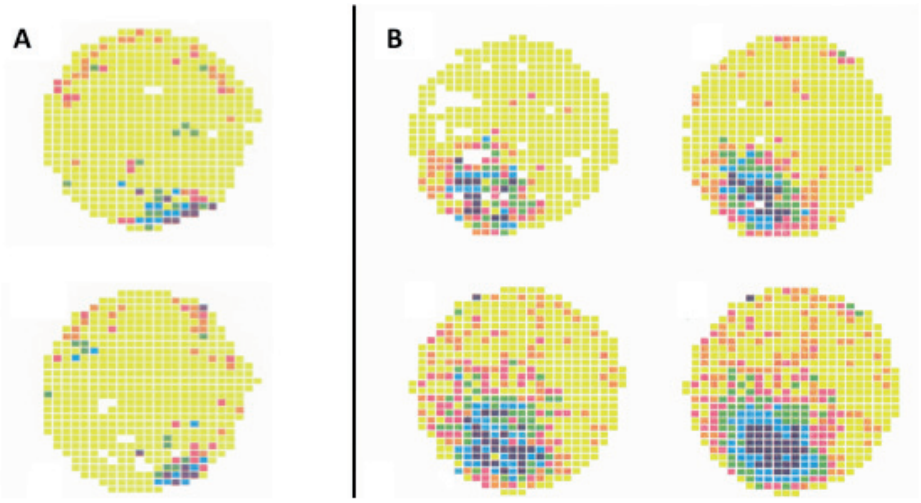

(A) Rate maps of the same place cell with six-day intervals between both session. Note similarity between the maps. Maximum firing in dark blue, minimum in yellow.
(B) Rate maps of a single place cell for total recording times of 4, 8, 16, and 32 min (from upper left to lower right). Note similarity between the maps and emergence of the place field. Maximum firing in dark blue, minimum in yellow.

2.1.1.3 Plasticity

The second fundamental property of place cells is that they are **not specific to one environment**. When comparing the behavioural correlates of one set of place cells in two environments, some neurons might be active in only one environment and silent in the other, while others might be active in both (O'Keefe and Conway 1978).

The percentages of active place cells can be quantified. Indeed, all principal hippocampal neurons can be identified during slow-wave sleep or light anaesthesia. Depending on the studies, 30 to 80% of them are considered **active** in a given environment (Thompson and Best 1989; Wilson and McNaughton 1993; Lee et al. 2004; Henriksen et al. 2010). This means that 20 to 70% have such low spontaneous activity that they are considered **silent** in that environment. Some cells seem to be silent in all environments.

The phenomenon of loading different representations/maps for each environment is called **remapping** (Muller et al. 1987; Quirk et al. 1990) (Fig. 26). The dynamic of remapping will be discussed later in more detail (2.4). Plasticity and

stability are antonymic: the activity of place cells results from a balance between these two fundamental properties.

Fig. 26 Place cell plasticity

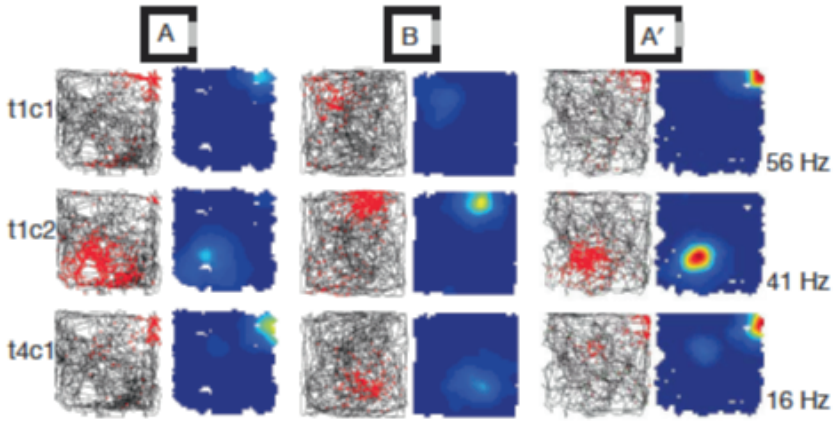

Maps of three simultaneously recorded place cells recorded in two different environments (A and B). Trajectory with spike positions; colour-coded rate map (from Fyhn et al. 2007) Peak firing rate indicated in the bottom right corner. Note the dissimilarity of firing patterns between the environments.

2.1.1.4 Distribution in the hippocampal region

Place cells were originally discovered in **CA1** (O'Keefe and Dostrovsky 1971). Shortly after, Ranck described two types of neurons in the hippocampal formation: the complex spike (CS) cells and the theta cells (Ranck 1973). The CS cells were shown to present some spatial modulation notably linked to reward and were classified in two categories: approach-consummate and approach-consummate mismatch. These cells were recorded from both CA1 and **CA2/CA3**. Later, it was suggested that the CS are principal cells and the theta cells are interneurons (Fox and Ranck 1975). Finally, in 1978, place modulation was clearly reported in the **DG** (Olton et al. 1978).

2.1.2 Head direction cell definition and distribution

2.1.2.1 First characterization

Approximately a decade after the discovery of place cells, James **Ranck**, while investigating the **rat** parahippocampal region, described neural correlates of directional signals: the head direction (HD) cells (Ranck 1984) and later, a then post-doctoral fellow of his laboratory, Jeffrey **Taube,** published a complete account of HD cells properties (Ranck 1984; Taube et al. 1990). A given HD cell is active whenever

the animal faces a particular direction in the environment, irrespective of where it is or what it is doing (Fig. 27). They were first observed in the rat **dorsal presubiculum** (also known as postsubiculum), a region that gives strong indirect inputs to the hippocampus.

Fig. 27 Representative example of a head direction cell

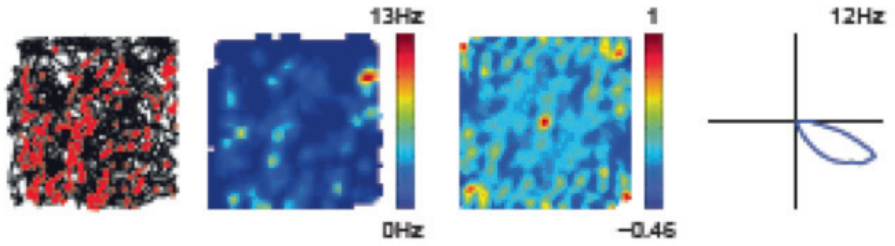

Trajectory with spike positions; colour-coded rate map and autocorrelation map; directional plot. Peak firing rate indicated in the upper right corner (from Boccara et al. 2010).

This completed the requirement for accurate navigation. Indeed, the sense of location provided by place cells is not sufficient to find one's way, a **sense of direction** is crucial to know in which direction to go. Similarly to what has been done with place cells, one can **reconstruct** the direction faced by the rat by computing the activity from an **ensemble of HD cells** (Johnson et al. 2005).

HD cells, or cells similar to them, were also recorded in **mice** (Khabbaz et al. 2000), and **monkey** presubiculum (Robertson et al. 1999), independently of eye movements or gaze direction. Others (Doeller et al. 2010; Jacobs et al. 2010) report cells coding for sense of direction in **humans**.

2.1.2.2 Stability

Like place cells, HD cells are **stable in a given environment**: they code preferentially for the same orientation for as long as the rat stays in the environment and, moreover, each time the animal re-enters that environment, the HD cells will keep the **same preferred firing direction** indicating some sort of **spatial memory** (Taube et al. 1990) (Fig. 28).

Fig. 28 Head direction cell stability

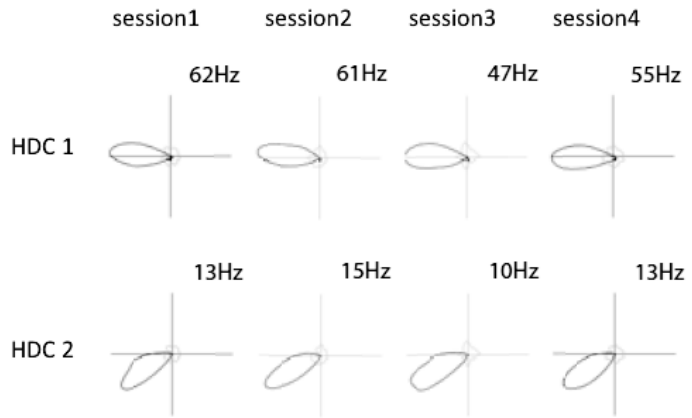

Polar plots of two head direction cells over four consecutive sessions in the same environment. Peak firing rate indicated in the upper right corner of each polar plot (from Solstad et al. 2008).

2.1.2.3 Plasticity

HD cells **do not behave like a magnetic compass**. Their **preferred direction is not absolute but relative** to the environment the rat is exploring (Taube et al. 1990). This means that the same neuron might be active when the rat is looking towards the north in an environment A, towards the east in environment B and towards the south in environment C.

Fig. 29 Head direction cell plasticity

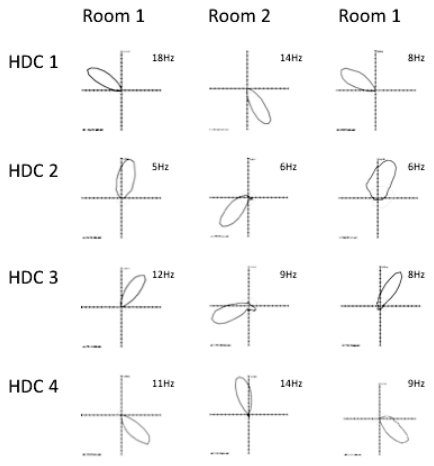

Polar plot of four simultaneously recorded head direction cells recorded in two different rooms. Peak firing rate indicated in the upper right corner of each polar plot. (unpublished data)

Unlike place cells, there are **no "silent" HD cells**: all the HD cells within a network are used for encoding directional headings at all times (Fig. 29). One could argue that this is due to the fact that a rat will have the opportunity to face all possible directions, even in a very small environment. One could also possibly argue that HD cells are **purely directional** while place cells have some non-spatial correlates (see 2.2).

2.1.2.4 Distribution in the hippocampal region

As stated above, **HD cells** were **first recorded** and characterized in the **dorsal PrS** (also referred to as the postsubiculum). Consequently, HD cells have been reported in several other areas of the brain. In the PR, they can also be found in the **MEC**, more specifically in **layer III, V and VI**, but not layer II (Sargolini et al. 2006; Boccara et al. 2010). **Additionally, paper #2** ((Boccara et al. 2010) see synopsis of results) presents HD cells in the dPaS.

2.1.3 Grid cell definition and distribution

2.1.3.1 First characterization

Fig. 30 Representative example of a grid cell

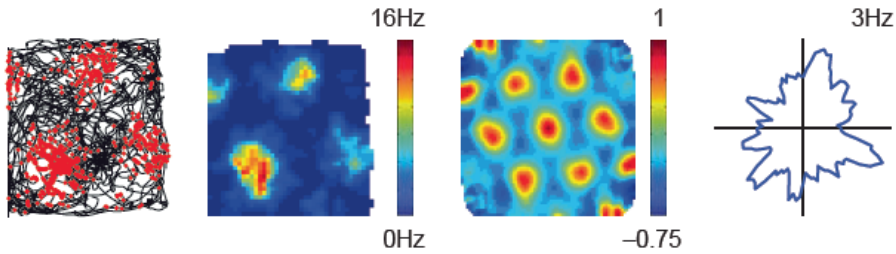

Trajectory with spike positions; colour-coded rate map and autocorrelation map; directional plot. Peak firing rate indicated in the upper right corner (from Boccara et al. 2010)

The **entorhinal cortex** (EC) is the hub of the hippocampal region. This quite large parahippocampic area connects sensory, association and directional inputs with the hippocampus proper (Witter et al. 1989; Burwell 2000; Lavenex and Amaral 2000; van Strien et al. 2009). Original recordings of activity in the EC showed variable spatial modulation (Barnes et al. 1990; Quirk et al. 1992; Frank et al. 2000). Insights from **neuroanatomical work** suggested that this heterogeneity could be due to the existence of a gradient of specialization. Indeed the dorsal part of the hippocampus shows the clearest spatial selectivity (Jung et al. 1994) and receives projections

specifically from the dorsolateral band of the medial EC (MEC) (Witter et al. 1989; Dolorfo and Amaral 1998). Therefore, specific recordings targeted at the **dorsal MEC** show a high amount of **spatial modulation** (Quirk et al. 1992; Fyhn et al. 2004; Hargreaves et al. 2005). These spatially modulated neurons are **different from place cells**. They present **multiple firing fields** organized in a very **regular grid pattern** so that they tessellate the whole environment: hence their name: **grid cells** (Hafting et al. 2005). The pattern has been described in an open field environment as a repetition of **isosceles triangular** or hexagonal array (with a 60-degree rotational symmetry) (Fig. 30). In addition, the collective activity of a small number of simultaneously recorded grid cells is sufficient to **reconstruct** accurately the **trajectory** of a rat (Fyhn et al. 2004). A large portion of the grid cells code for head direction in addition to their spatial modulation (Sargolini et al. 2006). Such cells were dubbed conjunctive cells and will be discussed in 2.2.3.3.3 (Fig. 31).

Fig. 31 Representative example of a conjunctive grid by head direction cell

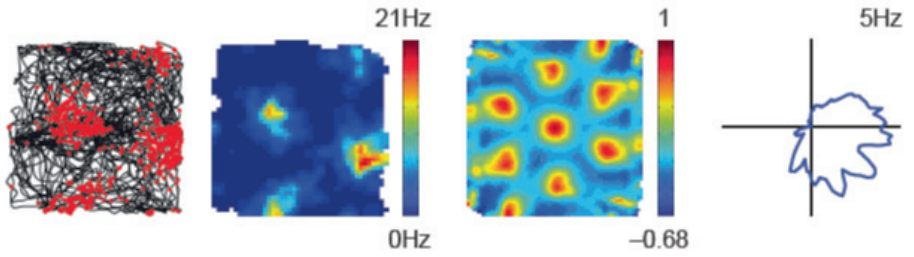

Trajectory with spike positions; colour-coded rate map and autocorrelation map; directional plot. Peak firing rate indicated in the upper right corner (from Boccara et al. 2010).

Grid cells have been observed in other species, such as **mice** (Fyhn et al. 2008) and **bats** (Yartsev et al. 2011), and indirectly in **humans** (Doeller et al. 2010). The definition of grid cells is increasingly challenged through a series of recent studies, including those presented here (see Discussion chapter for references). I will present the basis for this shift in the Discussion chapter, below.

2.1.3.2 Stability

As is observed for place and HD cells, grid cells are **stable over a period of weeks**. This means that the same neuron will present the same grid pattern repeatedly in a given environment ((Fyhn et al. 2004; Hafting et al. 2005); personal data) (Fig. 32). This suggests that **mnesic processes** might be involved in the retrieval of the same grid pattern over and over.

Fig. 32 Grid cell stability

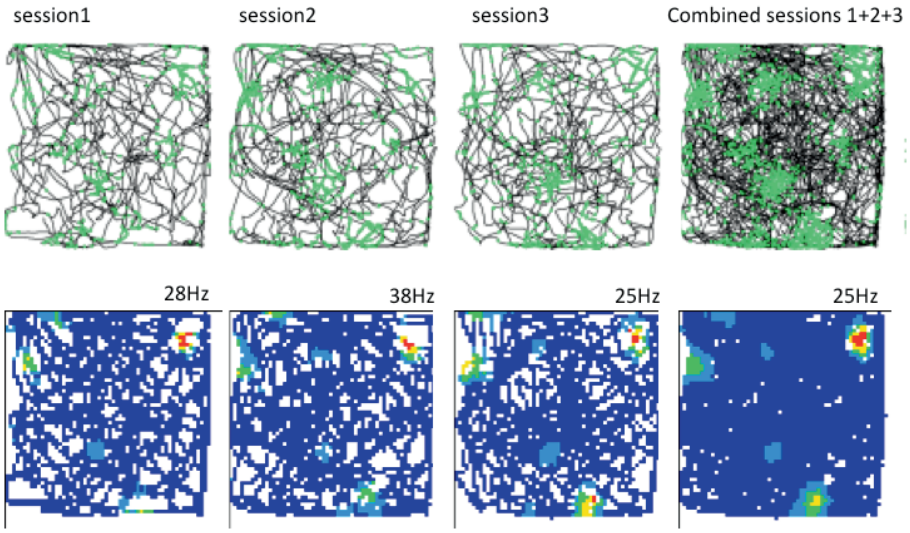

Trajectory with spike positions and colour-coded rate map of a representative grid cell recorded over three consecutive individual sessions and when combined in a single session. 2.2 X 2.2 m environment Peak firing rate indicated in the upper right corner. (unpublished data)

2.1.3.4 Plasticity

Fig. 33 Grid cell Plasticity

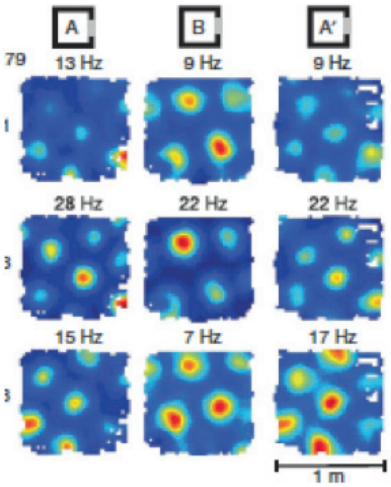

Rate maps for representative simultaneously recorded MEC cells in two different environments (A and B). Note the dissimilarity of firing patterns between environments (from Fyhn et al. 2007).

Like place and HD cells, grid cells **remap** between different environments (Fyhn et al. 2007) (Fig. 33). However, like HD cells and unlike place cells, they are active in

all environments (i.e. there are **no silent grid cells**) and they **preserve their internal spatial firing relationships** when the animal moves from one environment to another. This suggests that these cells, unlike the place cells of the hippocampus, are part of a **path integration-dependent metric** applied universally across environments (see 2.5.2).

2.1.3.4 Distribution in the hippocampal region

Before the publication of paper #2, grid cells had only been reported in **MEC** principal cell layers (II, III, V and VI). That paper shows an abundance of grid cells in dorsal **PrS** and **PaS** (see Synposis of results and Discussion). In addition this paper gives a **quantitative analysis** of the proportions of grid cells in the different layers of the MEC, PrS and PaS.

2.1.4 Overview of spatial and directional modulation in the hippocampal region

Spatial and directional modulation has been observed in almost all areas of the HR. Yet, as proposed above, the distribution of cells following the definition of place, HD and grid cells is more specific. CA and DG are the main neural repository of place cells. When considering the HR, HD cells were mostly characterized in the PrS and the MEC and grid cells were unique to the MEC. Paper #2 reports the existence of HD cells in the PaS and grid cells in both the PaS and PrS.

To give a reader a complete overview of the state of the art of the HR neuron, I am reporting here the spatial and directional modulation observed in the **different sub-structures** of **HF** (DG, CA, Sub) and **PHR** (EC, PrS, PaS, PER, POR). I will present the specific spatial and directional properties of place, HD and grid cells in (2.2).

2.1.4.1 Cornu Ammonis (CA) fields and the dentate gyrus (DG)

CA and DG neurons are highly **spatially modulated,** as they are the deposit of **place cells** (see 2.1.1.4). The spatial and **directional properties** of place cells will be discussed in (2.2.1). **Direction modulation of putative interneurons** has been reported in CA fields (Leutgeb et al. 2000).

2.1.4.2 Subiculum (Sub)

Spatial modulation has been reported in the subiculum, yet whether the subiculum does contain **place cells** is still a **subject of debate**. **Barnes** and colleagues reported that subiculum units did not exhibit the highly localized patterns of spatial firing observed in the CA fields and that they only found evidence for **spatially consistent**

but dispersed firing in some cells (Barnes et al. 1990). Other studies from **Sharp** and colleagues do report **place cells** in the subiculum (Sharp and Green 1994; Sharp 1997). Recent recordings performed in the **Moser** lab show only **very weak spatial modulation** in the subiculum (personal communication from E. Henriksen). Four explanations could reconcile these apparently contradictory results. A re-analysis of the waveforms of the "place cells" (at the time recorded with stereotrodes) could show that the signal was in fact a **grid signal picked up from bypassing fibres** from the perforant path in a similar fashion to what is shown in (Leutgeb et al. 2007). A second possibility is that these recordings were not from the subiculum, but rather from the **fasciola**, which could be described as a "mini-hippocampus" curved on top of the subiculum, and therefore containing the DG, CA fields and the subiculum (see paper #3). Alternatively they could come from different positions along the **proximo-distal axis** of the subiculum and, as recently demonstrated, proximal cells are more spatially selective than distal ones (Kim et al. 2012). Finally, these cells could code for spatial features without qualifying for the definition of place cells. Indeed, a recent report has presented a new type of spatial response in subicular neurons. The activity of these cells depends solely on the rat's location relative to environmental boundaries (Lever et al. 2009). They were therefore named **boundary vector cells** (BVC). These BVC share some properties with the **border cells** recorded in the MEC, PaS and PrS (see paper #1) (Solstad et al. 2008). See the chapters below: Synopsis of results and Discussion.

2.1.4.3 Entorhinal cortex (EC)

Prior to the discovery of **grid cells** in the MEC (2.1.3), several studies reported **weak to strong spatial modulation** in EC neurons (Mitchell and Ranck 1977; Barnes et al. 1990; Mizumori et al. 1992; Quirk et al. 1992; Frank et al. 2000; Fyhn et al. 2004; Hargreaves et al. 2005). Comparison between lateral and medial EC shows that **LEC** units are only **very weakly spatially modulated** (Fyhn et al. 2004; Hargreaves et al. 2005) and mostly respond to objects (Zhu et al. 1995; Young et al. 1997; Wan et al. 1999; Deshmukh and Knierim 2011). The MEC also contains another type of spatially modulated cells: the **border cells** (see synopsis of results: papers #1 and #2). It is currently admitted that the entorhinal cortex (both MEC and LEC) **does not contain place cells**.

Many **MEC** neurons are **very much directionally modulated**. As stated previously (2.1.2.4), MEC **layers III, V and VI** contain an abundance of HD cells (Sargolini et al. 2006; Boccara et al. 2010). These HD cells **intermingle with grid cells,** establishing a representation of space and direction in the same local network. Moreover, many neurons are **conjunctively modulated by grid and by head direction** (i.e. conjunctive cells). This means that for a neuron to be active the rat must be in one of the grid nodes and have its head in the preferred firing direction (Sargolini et al. 2006) (see 2.2.3). This direction modulation is not dependent on the rat behaviour or constrained by the environment. More detailed **quantification** of directional modulation between MEC layers is presented in **Paper #2** (Boccara et al. 2010). On the other hand, the **LEC** does **not** present absolute **direction modulation**, but only direction related to the position of objects (Deshmukh and Knierim 2011).

2.1.4.4 Presubiculum (PrS) and Parasubiculum (PaS)

Spatial modulation (often linked to head direction modulation) has been reported in PrS and PaS (Taube 1995; Sharp et al. 1996; Cacucci et al. 2004; Hargreaves et al. 2005; Hargreaves et al. 2007). However the study presented in **paper #2** ((Boccara et al. 2010) (see synopsis of results) suggests that most of this modulation was the activity of **grid** and **border cells**. In the same study I present a **quantitative analysis** of these different cell types among the different subareas.

As stated above, **HD cells** were **first recorded** and characterized in the **dorsal PrS** (also referred to as the postsubiculum). In addition, some **conjunctive place-by-direction** modulation has been reported in **both the PaS and PrS** (Taube 1995; Cacucci et al. 2004). I will present in **Paper #2** (Boccara et al. 2010), see synopsis of results) robust **"pure" direction modulation** of many neurons in the PaS, in addition to PrS. Furthermore, I will show that **both areas** contain **conjunctive grid by head direction** cells and I will quantify these different cell types among the different subareas.

2.1.4.5 Perirhinal (PER) and postrhinal (POR)

There is **no** report of **spatial modulation in PER** neurons (Burwell et al. 1998; Hargreaves et al. 2005), but only object recognition modulation (Kealy and Commins 2011). S**ome** spatial modulation has been observed in **POR** neurons. However, this spatial modulation is very different from that of place cells and more reflective of the **changes in visual stimuli** (Burwell and Hafeman 2003). In their 2004 study where

they discovered grid cells, Fyhn and colleagues recorded the portion of the POR just dorsal to the MEC. They found that there was **no clear spatial modulation** in that area, with cells presenting very low information rates and average stability of the spatial firing across trials (Fyhn et al. 2004).

I did not find any report of **directional modulation** in the PER or POR.

2.2 STATIC PROPERTIES

As stated previously, I have defined "static properties" as characterizing cell activity in conditions of **environmental stability** and in opposition to "dynamic properties", characterizing changes in cell activity in response to environmental changes. This distinction is reminiscent of that in (2.1) between stability and plasticity: the two fundamental properties of place, grid and HDC. I will discuss "dynamic properties" extending to plasticity in (2.4).

Static properties can mainly be divided into two categories. The first one concerns the specialization of the cell in coding for space or direction (2.2.1). These **spatial and directional properties** range from the quantification of general spatial/directional modulation to specific properties linked to each cell type, such as field or grid properties. The second category concerns the **discharge properties** (2.2.2) that qualify the cell's firing pattern independently of its specialization. This encompasses the **proportion** of cells active in one environment, their **discharge pattern,** including their mean firing rate and waveform, and finally whether their firing is modulated by the rhythms recorded in the local field potential (**LFP**) such as theta and gamma rhythms.

To extend the description of spatial and directional signal **distribution** initiated in (2.1), a key point of the discussion generated by the findings of papers #1, #2 and #3 (see Discussion chapter), I will attempt to highlight differences between similar cell subtypes (i.e. place, HD and grid cells) recorded in **different subfields** and therefore supporting different neuronal properties and connectivity patterns. When appropriate, I will also stress the differences of activity along a given subfield giving an **anatomical gradient**.

I refer the reader to annex 2 for more **detailed methodological** considerations on how to measure these different properties. Many of the parameters presented here are also used in describing cells in the MEC, PrS and PaS in paper #1 and #2.

2.2.1 Foreword on cell population studied

While describing the properties of place cells, I will consider here only the **HF place cells**. I will not present spatially modulated cells from the PHR, either because they do not fit the definition of place cells, or alternatively because they were recently identified as grid cells.

When I defined HD cells in section 2.1.2, I mainly considered **dPrS** and **MEC** HD cells, however the **HD cell system** is **distributed** over several interconnected areas. They have been recorded in many brain areas outside the hippocampal region, including the dorsal sector of the **retrosplenial** cortex (Chen et al. 1994), the caudal lateral dorsal thalamic nucleus (**LDN**) (Mizumori and Williams 1993), the anterior dorsal thalamic nucleus (**ADN**) (Taube 1995), the dorsal tegmental nuclei of Gudden (**DTN)** (Bassett and Taube 2001), portions of extra-striate cortex (**Oc2M** and **Oc2L**), the lateral mammillary nuclei (**LMN**) (Stackman and Taube 1998), the dorsal **striatum** (Wiener 1993), and the **parietal cortex** (McNaughton et al. 1994) (yet in the parietal cortex, the observed direction modulation was mostly movement related). This thesis is about the hippocampal region. Therefore I will not present the properties of HD cells found outside this region (for a review of HD cells outside the hippocampal region, see (Muller et al. 1996; Sharp et al. 1996; Taube 1998; Taube and Bassett 2003; Taube 2007). The reader should however keep in mind that some of these areas, like the ADN, present a very high proportion of HDC cells (55%) (Taube 1995) with properties different from what is observed in the parahippocampal areas. Therefore HD cells observed in the parahippocampal areas may well be inherited from HD cells in other areas. Lesion studies support this hypothesis (Goodridge and Taube 1997; Blair et al. 1999) (see Discussion chapter).

The third preliminary remark to this section is that there is **no clear definition** that allows distinction **between HD and directionally modulated cells**. It is commonly assumed that HD cells have a very specific preferred firing direction, with negligible firing outside of that direction. I will discuss this point in the following section (2.2.2) and the Discussion chapter.

Grid cell properties presented here are mostly from the **MEC**. Some recordings that claimed to be in the MEC were in fact, after re-examination of the histology, probably in **the PaS** (see paper #3). Paper #2 presents an account of PaS and **PrS** grid cells and highlights differences and similarities between the MEC, PrS

and PaS that I will discuss further in the Synopsis of results and the Discussion chapters.

2.2.2 Spatial and directional properties

2.2.2.1 Place cells

2.2.2.1.1 General spatial properties

Spatial modulation is mainly measured by three parameters (see annex 2). The first one, often called **spatial information**, is a measure of how informative about the animal's whereabouts is the cell activity. A limitation to that measure is that it is intrinsically linked to the size of the place field relative to the size of the environment: the larger the ratio of field/environment, the less informative it will be. The second parameter can be designated as spatial **coherence**. It measures how spatially distributed the cell activity is by comparing the average firing rate in contiguous bins. A limitation of that measure is that an overall active or overall inactive cell will have a high spatial coherence. The third parameter measures how stable and reliable the spatial specificity is and consists of intra- or inter-trial **spatial correlations**.

Original studies showed a **non-uniform distribution** of spatial modulation between DG, CA3 and CA1. CA3 cells were classified as conveying more spatial information while CA1 cells were more reliable (Barnes et al. 1990; Markus et al. 1995). Yet studies conducted in **several environments** argue that spatial information is not systematically higher in either CA3 or CA1 (Leutgeb et al. 2004). DG cells exhibit clear spatially selective discharge similar to that of CA3 pyramidal cells recorded under the same conditions (Jung and McNaughton 1993); (Leutgeb et al. 2007), though the number of active cells is much sparser (see 2.2.3). Recent studies showed that spatial modulation is not uniform within the CA1 subfield and that spatial information, spatial coherence and spatial correlation are gradually distributed along the **longitudinal axis CA1** with proximal CA1 place cells more spatially tuned than distal ones, respecting in that the distribution of inputs of medial vs. lateral EC (Henriksen et al. 2010). No consensus has been reached yet regarding the **subiculum**. According to some studies, subicular cells have almost no spatial specificity (Barnes et al. 1990); E. Henriksen personal communication), while others claim that they are spatially modulated, though they might not be qualified as place cells (Sharp 1997; Lever et al. 2009). These differences argue for a varied role in spatial cognition between the different HF subfields (see 2.5.3 and Discussion chapter).

2.2.2.1.2 Field properties

Field stability

As stated previously, **CA1 and CA3** firing fields are mostly **stable** in constant environments **within and between recording sessions** lasting for minutes or even hours and separated by long time intervals (up to several months) (Best and Thompson 1984; Muller et al. 1987; Thompson and Best 1990). Under similar conditions of environmental constancy, **granule cell place fields** are stable too (Jung and McNaughton 1993).

Place cells are stable regardless of whether the rat spends all its time between sessions in its home cage or some of its time in a different recording apparatus. This **resistance to interferences** might be dependent on other variables such as the age of the rat (Shen et al. 1997). If sessions are run in two or more apparatuses over extended times, specific fields are stable in each different environment (Muller and Kubie 1987; Thompson and Best 1989). The long-term stability of firing fields implies that the representation is **recalled** and not created *de novo* each time the rat enters a familiar environment. The stability of different patterns specific to each familiar environment implies that many representations can be stored without interference (Muller et al. 1996). I will discuss this point further in 2.4.5.2.

Number of fields

A single CA1 place cell may present **more than one field** in a given apparatus (Muller et al. 1987). The number of fields seen **depends on the size** of the environment. It appears that, if the recording environment is big enough, all place cells will present multiple **irregularly spaced** place fields (Park et al. 2011). In same dimension environments, **granular place cells** present **more fields** than CA place cells (Jung and McNaughton 1993; Leutgeb et al. 2007).

A recent study challenges the homogenous distribution of field number within hippocampal substructures. Indeed, an **increasing gradient** of field number per place cells was observed from **proximal to distal** CA1 (Henriksen et al. 2010).

Field shape

Field shapes are **not uniform** between place cells and they seem to **depend on the environment's own shape** (Muller et al. 1987; O'Keefe and Burgess 1996). This environmental influence will be studied in more detail in 2.4.4.1. Variations in field shape are of special interest, since they suggest that **boundaries** are recognized and

treated in special ways. This point will be examined in the Discussion chapter based on observation from **paper #1** (Solstad et al. 2008).

Field size (scale)

While original studies show similar size properties between CA3 and CA1 place cells (Muller et al. 1987), more recent ones present **smaller field size for CA3** (Barnes et al. 1990; Markus et al. 1995; Leutgeb et al. 2004; Park et al. 2011). **Granular cells** seem to have **smaller** place fields than pyramidal cells (Jung and McNaughton 1993). In case of place cells with multiple fields, it is the bigger field that is considered (CA1>CA3 = DG; Park 2011). The proportion of active pixels in an environment gives a similar measure (CA1>CA3 = DG; Park 2011). The majority of place cells analyses are based on recordings in the most dorsal part of the hippocampus. **Ventral hippocampal cells** were first thought to code for non-spatial features (Jung et al. 1994; Wood et al. 1999). This might be true. But the lack of observation of spatial modulation in these early studies might also have been due to the size of the apparatus used. Indeed, recent studies using much larger environments have shown that the ventral hippocampus does contain place cells. However, these place cell fields are much bigger than their dorsal counterparts. By studying systematically the size of place fields along the dorso-ventral axis (i.e. septo-temporal axis), several authors have highlighted a **dorso-ventral scale gradient** along which place field size increases almost linearly from 1 m in the most dorsal part to 10 m in the most ventral tip (Kjelstrup et al. 2008) (Fig. 34). Therefore, when comparing the scale of place cells recorded in different subfields, one should be careful to match them according to their dorso-ventral position. Whether this septo-temporal scale gradient is the **by-product** of another feature gradient is not yet clear (velocity gain: (Maurer et al. 2005) see 2.4.3.1, grid scale: (Brun et al. 2008), channel distribution: (Giocomo et al. 2011; Hussaini et al. 2011)). It is possible that this gradient reflects the distribution of conjunctive coding (2.3.5 and Discussion chapter).

Fig. 34 Place cell properties

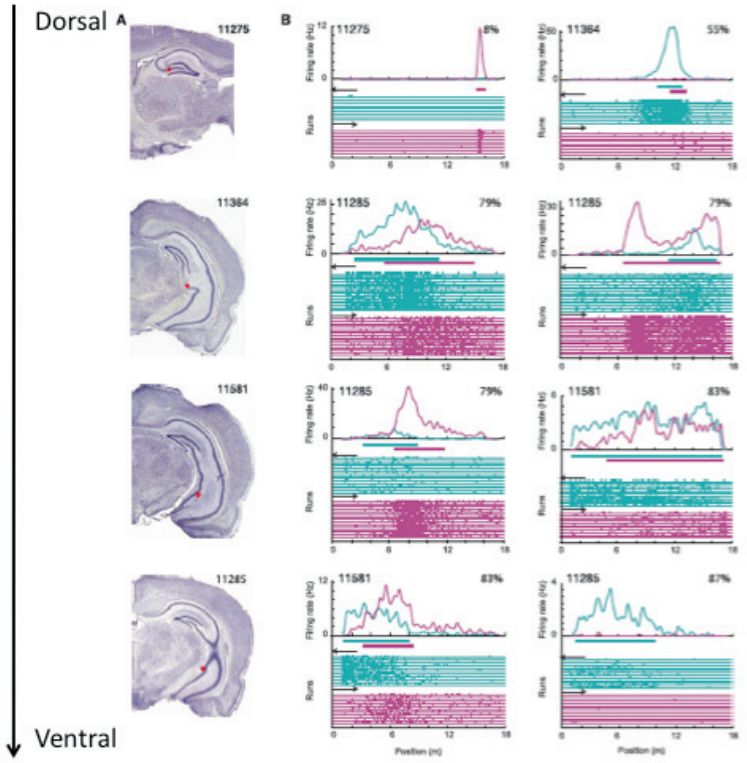

Distribution of place cell scale along a dorso-ventral gradient (from Kjelstrup et al. 2008). **(A)** Nissl-stained sections showing recording locations in four animals (red dots). **(B)** Place fields of eight pyramidal cells recorded at different longitudinal levels of CA3 during animals running on a linear 18-m track. Percentages indicate location along the dorso-ventral axis. Smoothed spike density function indicates firing rate as a function of position. Horizontal bar indicates estimated place field. Left runs, pink; right runs, green. (Bottom of each panel) Raster plot showing density of spikes on individual laps. Each vertical tic indicates one spike and each horizontal line shows one lap.

It should be pointed out that the place field size might also be influenced by **the size of the environment** itself. This environmental influence will be studied in more detail in 2.4.4.

Field spatial distribution (in the environment)

Contrary to what is seen in other cortices (e.g. receptive fields in visual and somatosensory cortices) there is **no topographical organization** of the place cells in the hippocampus. Anatomically contiguous (i.e. collocated) place cells do not tend to represent neighbouring places (O'Keefe and Conway 1978; Jung and McNaughton 1993; Redish et al. 2001). Some studies will even argue the contrary (Dombeck et al. 2010) as if there were a mechanism of lateral inhibition. The **environment**, the

context and the **behaviour** might influence the field spatial distribution. These features will be studied in more detail in 2.4.4 and 2.4.5.

Field intensity and coherence

Place fields are defined based on their spatial coherence (i.e. how coherent is the activity of neighbouring pixels, see annex 2). Well sampled fields generally have a **single maximum** rather than two or more local maxima (Muller et al. 1987). Rate surfaces resemble mountains rather than plateaus and contours become smoother as recording time increases (Muller et al. 1996). There is no significant difference between subfields for **maximum firing rate** (Leutgeb et al. 2004; Leutgeb et al. 2007). Variations in field intensity might be just Gaussian noise around population means, but also might reflect a hierarchy of place cells with similar or overlapping firing fields (Muller et al. 1996). **Sparsity** is a measure of how **spatially compacted** (or **sharp**) a place field is (see annex 2). The sparsity is consistently **higher in CA1** compare to CA3. This means that CA3 place fields are sharper than CA1 (Leutgeb et al. 2004).

2.2.2.1.3 Directional properties

In an **open field**, the activity of a **place cell** is usually **independent of the orientation** with which the rat enters the place field (O'Keefe and Conway 1978). However, **place fields can be directional** when the **behaviour is restricted** to a route due to constraints of the environment (e.g. on a **linear track**) (McNaughton et al. 1983) or of the experimental conditions (e.g. stereotypic behaviour between **static rewards**) (Markus et al. 1995). These directional properties of place cells **can be acquired**: place cells with no directional preference in unrestricted open-field environments become directional over time when the rat behaviour is restricted to routes (Muller et al. 1994; Markus et al. 1995; Navratilova et al. 2012) (see 2.4). Furthermore, the running direction seems to influence the place cell **temporal code** (Huxter et al. 2008) (see 2.2.3).

Several studies show some **discrepancy** in how direction is preferentially represented in the **different subfields**, yet they are not in concordance with each other (McNaughton et al. 1983; Barnes et al. 1990; Jung and McNaughton 1993; Leutgeb et al. 2004).

2.2.2.2 Head direction cells

Head direction (HD) cells are classified as "head direction cells" because they discharge as a function of the animal's head direction in the horizontal plane, **independent** of the animal's **behaviour**, **location**, or **trunk position**.

2.2.2.2.1 Directional properties

Directional tuning curve

The directional tuning curve correlates the neuron's firing rate versus the rat's head direction. Irrespective of whether it is plotted on a **linear graph** or on a **polar plot**, it characterizes a HD cell quite precisely. These tuning curves present generally **triangular** or **Gaussian** shapes (Taube et al. 1990; Blair and Sharp 1995; Taube 1995). This means that, contrary to place cells that often present several place fields in one environment, most HD cells exhibit generally **only one preferred direction**. These curves are relatively **symmetric** in the dPrS (Taube et al. 1990). The amount of symmetry has not been systematically studied in the MEC. Most of the directional parameters I will examine in the following paragraphs can be extrapolated from the directional tuning curve (Fig. 35).

Fig. 35 Head direction cell properties

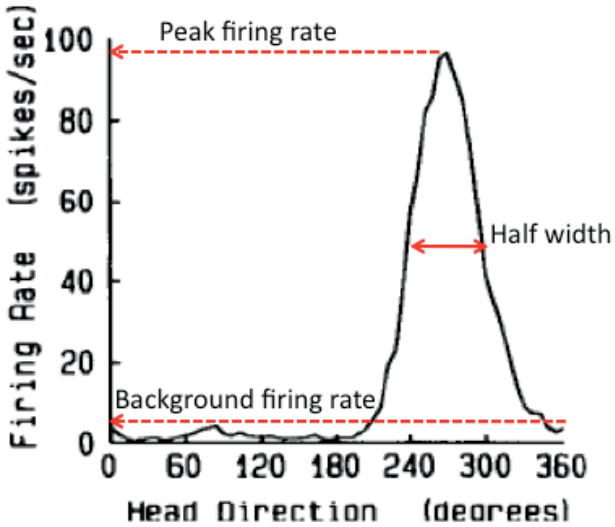

Directional tuning curve of a representative head direction cell, figuring peak firing rate (intensity), half width (tuning range) and background firing rate (specificity), adapted from Taube (1990).

Directional intensity (peak firing rate) and rate curve

Peak firing rates vary across different HD cells and range from about **5 Hz to 100 Hz**

with the mean peak around **35 Hz** in **dPrS** (Taube and Muller 1998). **MEC** HD cell peak firing rates vary less and range from **5 Hz to 40 Hz** (Sargolini et al. 2006). However, the very high firing cells recorded in the PrS may be **interneurons** (excluded from Sargolini's study). Firing rate decreases from maximum as the rat moves its head to either side of an HD cell's preferred direction, until it reaches a baseline firing rate on average 45° away from the preferred direction (see also directional tuning below, and (Muir and Taube 2002)).

Directional specificity (ratio with background firing rate)

The **background-firing rate** (outside the preferred firing direction) of HD cells both in dPrS and MEC is **usually quite low**, less than 1 Hz and less than 0.5 Hz respectively. This means that most HD cells are usually **quite specific**. However this should be put into perspective with the **definition criteria of HD cells**. Indeed paper #2 shows a much higher background firing for some directionally modulated cells. This point will be taken up in the Discussion chapter.

Directional tuning range – Sharpness

The **range of directional headings** over which activity is elevated **above baseline** levels is referred to as the directional firing range. It may vary quite a lot in the **dPrS**, from **60° up to 150°**, with a mean of **90°** (Taube et al. 1990; Taube and Bassett 2003). The breadth of directional tuning is defined differently in Sargolini's MEC study (Sargolini et al. 2006), where it is expressed by the **angular standard deviation of the mean vector,** which for **MEC** HD cells varies from about **5° to 90°**. Breadth of tuning is not significantly different between MEC layers II, V and VI. I will address later, in the light of the results from paper #2, how these differences in tuning range affect the definition of HD cells (see Discussion chapter).

Very recent results might suggest that there is a gradient of directional tuning range along the dorso-ventral axis in layer III of the MEC (Giocomo et al. 2012).

Directional stability

For each head-direction cell, the **preferred direction**, **peak firing rate**, and **directional firing range** has been observed to remain quite **stable for days** in both dPrS (Taube et al. 1990) and MEC (Sargolini et al. 2006). There can sometimes be, after a long period, some small variation in the peak firing rate and preferred firing direction.

Polar distribution

Similarly to the **absence of topographical organization** of place cells in the hippocampus, there is an apparent uniform distribution of the preferred firing direction of the HDC over a 360° range. This is true for both the dPrs (Taube et al. 1990) and the MEC (Sargolini et al. 2006).

Directional information

The **directional information content** (IC) measure takes into consideration many of the previously mentioned parameters in order to give a general sense of how directionally modulated a cell is. The mean directional IC for HDC in dPrS is at 1.3 (Taube and Muller 1998), yet see paper #2. In MEC it varies from 2 to 8 (Sargolini et al. 2006). See annex 1 for details of the calculations.

2.2.2.2.2 Spatial modulation

Quantitative analysis has shown that the location of the animal has **minimal effect** on directional cell firing in the **dPrS** (Taube et al. 1990). In the **MEC**, a large portion of the neuron population presents **conjunctive properties of grid and HD cells**. These so-called conjunctive cells will be presented in 2.2.2.3. **Paper #2** also presents such **conjunctive cells** in the **PrS** and **PaS**.

2.2.2.3 Grid cells

Grid cells are characterized by three main properties: their spatial phase, their orientation and their spacing (Fig. 36). I will present here these specific properties along with the more general field and spatial properties applying to grid cells.

2.2.2.3.1 Grid properties

Fig. 36 Grid cell properties

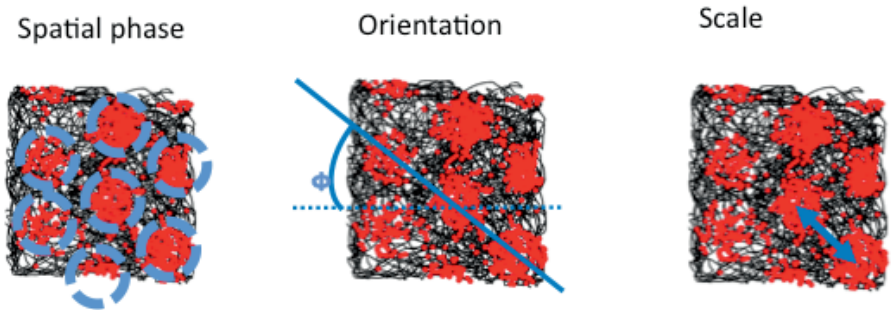

Trajectory with spike positions of a representative grid cell figuring the three main grid cell properties: spatial phase, orientation and scale.

Grid spatial phase

The spatial phase of a grid is given by **the crossing of its vertices in the plane**. The grid phase seems to be **randomly distributed** in all layers of the MEC without following any topography (Fyhn et al. 2004; Hafting et al. 2005). The vertices of most nearby grid cells seem to be offset relative to each other (Sargolini et al. 2006). **No topographical organization** of the grid spatial phase seems to exist in the MEC.

Grid orientation

The orientation of a grid is given by **tracing lines between its different nodes**. In a perfect grid, all these lines will present three different orientations separated by **60°** angles. The orientation of a grid is defined differently according to studies. In Hafting (2005), it is expressed in the spatial autocorrelogram as the angle f between a camera-defined reference line (0 degrees) and a vector to the nearest vertex of the inner hexagon in the counterclockwise direction.

In this pioneering study, the entire range of orientations was represented in the population as a whole (from 1° to 59°), but among cells recorded **in the same rat**, **orientation varied minimally** and even less in neighbouring neurons (Hafting et al. 2005). There seems to be no systematic change from dorsal to ventral in the dMEC (Hafting et al. 2005) or between layers (Sargolini et al. 2006). **Recent studies**, including those presented in this thesis, have pondered on these results on grid orientation, and thus influenced the **grid cell definition** (Doeller et al. 2010), (Krupic et al. 2012; Stensola et al. 2012). I will present and examine these results in the Discussion chapter.

Grid scale (field size) and spacing

Grid spacing is the **distance from one node to another**. In a perfect grid this distance should be **constant**. The grid spacing often (but not always) **correlates** with the scale of the fields. The **grid scale** is the **size of each grid field** (i.e. grid node). In a perfect grid this grid field size should be **invariant**. In Hafting (2005) and Sargolini (2006), spacing was expressed for each grid as the distance from the central peak to the vertices of the inner hexagon in the spatial **autocorrelogram** (the median of the six distances).

The spacing seems to be linked to the location of the grid cells in the brain. According to Hafting (2005) and Sargolini (2006), collocated grid cells (i.e. cells

recorded in the same area) do have similar orientation and similar spacing. Moreover, by comparing grid spacing and grid scale along the **dorso-ventral** (or septo-temporal) axis, one can see a **scale gradient similar** to what is seen for **hippocampal place cells**. Indeed, **spacing and field size increased with distance from the postrhinal border** with smaller and tighter fields in the dorsal portion of all layers of the MEC and bigger and more dispersed ones in more ventral portions ((Hafting et al. 2005; Sargolini et al. 2006; Brun et al. 2008). This pattern is observed both within and between animals.

According to **Brun (2008)**, the spatial scale of the grid pattern **increases gradually** along the dorsoventral axis, beginning with firing fields **0.3–0.5 m** in width, and a spacing of 0.5–1.5 m in the dorsal region, and reaching a width of 1.5–3 m and a spacing of **2.5–5 m** at the ventral end of the map. However, others (Barry et al. 2007) reported a more **stepped size variation** with more tightly clustered rather than evenly distributed grid spacing. They also report a constant ratio of grid sizes across rats, such that the grids in each rat varied in size by a fixed non-integer ratio. This step variation of grid size is consistent with recent reports of an **organization of grid cells** in **patches** (Burgalossi et al. 2011) and large-scale recording studies in multiple dorso-ventral and medio-lateral planes (Stensola et al. 2012). I will discuss these results in more detail below.

Grid score (grid cell classification)

The proportions of grid cells and grid properties are dependent on the definition and classification of grid cells. This unfolds in two ways: the first is **how to calculate** the grid scores and the second is where and how to set an acceptance **threshold** for such a score. Most grid scores are based on the **60-degree rotational symmetry** between each node. I will weigh the pros and cons of this score in the Discussion chapter, especially in the light of recent new findings mentioned previously ((Barry et al. 2007; Lever et al. 2009; Doeller et al. 2010; Krupic et al. 2012); (Stensola et al. 2012) and the studies presented here. Until 2010, thresholds were set in a empirical yet subjective way. From that time, the Moser and O'Keefe labs agreed on how to determine the **threshold** in a more subjective and **statistical way**. For more details, see annex 2 and Discussion below.

2.2.2.3.2 Spatial properties

Spatial information

In order to characterize the grid cell activity precisely, Fyhn and colleagues compared the spatial firing parameter of a group of MEC grid cells with those of CA1 place cells demonstrated to receive direct projection from the MEC area where the grid cells were recorded. I will refer to these place cells as "**target place cells**".

A comparison of grid fields of dorso-lateral MEC and place fields of the target CA1 shows that the **average information rate** in bits/s was not different: spatial information rate of **0.91 for dorsolateral MEC** and **0.95 for target CA1** (Fyhn et al. 2004). For methodology, see annex 2.

The measure of spatial information **varies from one study to another**. Some authors, like (Sargolini et al. 2006), found quite high spatial information centred around 1.2, while others, like (Hargreaves et al. 2005) showed much lower spatial information in the MEC compared with the CA1. These differences can be explained by the **heterogeneity** of the properties of grid and place cells **along the dorso-ventral axis** and between the different MEC **layers**.

Field properties

Grid fields can additionally be characterized, like place fields, in terms of their **stability**, their **shape**, their **intensity** and their **sharpness**. Some of these parameters have been studied in the first studies on grid cells. Nevertheless, there is still lot to uncover. I refer the reader to annex 2 for a detailed definition of these parameters.

While the **stability** of grid field seems similar to that of target CA1 place field, **sparsity** is higher in MEC compared with target CA1 (Fyhn et al. 2004). However, one should take into consideration that this measure includes, for the MEC, all putative excitatory cells, and that grid cells represent only a fraction of them.

The average distribution of grid **peak rate** moves slightly toward higher values compared with target CA1 place cells (Fyhn et al. 2004), and peak rate can reach 40 Hz (Sargolini et al. 2006). All nodes of activity are often sharply delineated from the background, yet the individual peak firing rates varied one from another (Hafting et al. 2005). This **individual field rate variation** is consistent from one session to another and several nodes can have such a low firing rate that they will reproducibly not appear on the map (unpublished observations).

2.2.3.3.3 Directional properties

Direction modulation (conjunctive properties)

Many grid cells present conjunctive properties of grid and head direction cells (hence they are also referred to as conjunctive cells). For such cells to be **active**, the rat needs to be in one of the **grid nodes** and have its head in the **preferred firing direction**. The **proportion** of grid cells with conjunctive properties is **layer-dependent**. According to (Sargolini et al. 2006), the largest proportion is encountered in layers **III** and **V**, where 66% and 90% of the grid cells have dual response properties, respectively. In layer **VI**, the proportion is 28%. Layer **II** is virtually **devoid** of conjunctive cells. **Paper #2** (Boccara et al. 2010) presented in this thesis will examine these proportions in further detail, by using new classification criteria (see Synopsis of results and Discussion chapters).

Direction tuning curve

According to (Sargolini et al. 2006), the degree of directional tuning in cells that met selection criteria for both gridness and directionality is **not significantly different**. Some authors have argued that the mean firing directions of directional grid cells are aligned with the grid (Doeller et al. 2010). Yet, finer analyses of a larger sample have proven that it seems not to be the case (unpublished data, see Discussion chapter).

Differences in preferred **firing direction peak** and **tuning width** of conjunctive cells had not been investigated until the research published in **paper #2**. This study presents results not only from the MEC but also from the PrS and PaS. For more details see Synopsis of results and Discussion chapters below.

2.2.3 Discharge properties

2.2.3.1 Proportions

2.2.3.1.1 Place cells

Nearly all CA1 putative principal cells active in an environment satisfy the criteria for **place cells** (Henriksen et al. 2010). However, only **30 to 80% are active** in one environment, the rest being silent (percentages differ from one study to another); see 2.1.1.3 (O'Keefe and Conway 1978; Thompson and Best 1989; Wilson and McNaughton 1993); (Lee et al. 2004; Henriksen et al. 2010). Similar findings can be applied to the other CA fields. Recent *in vivo* intra- or juxtacellular studies have suggested that putative silent/active cells seem to be **predetermined** prior to the entrance of the animal into the environment due to some specific **cellular**

mechanisms (Epsztein et al. 2011; Lee et al. 2012).

The vast majority of **DG** place cells are **silent** during sleep, resting or explorative behaviours (Jung and McNaughton 1993; Leutgeb et al. 2007). The proportion of active granule cells, as estimated from studies of immediate early gene activation, varies from **2 to 5%** of the cell population (Chawla et al. 2005; Ramirez-Amaya et al. 2006; Tashiro et al. 2007). However, most of the cells active in a given environment remain active in a second environment (Jung and McNaughton 1993; Leutgeb et al. 2007). The DG is quite unique in the brain in the sense that it is one of the few structures where there is neurogenesis in the mature brain (Altman and Das 1965); (Kaplan and Hinds 1977; Kuhn et al. 1996). These **newborn neurons** exhibit a period of **enhanced excitability** (higher proportion active) and **plasticity** (prone to more differences between environments). This period, depending on experimental paradigm, lasts from **two weeks to five months** (Wang et al. 2000; Snyder et al. 2001; van Praag et al. 2002; Ambrogini et al. 2004; Schmidt-Hieber et al. 2004; Esposito et al. 2005; Ramirez-Amaya et al. 2005; Song et al. 2005; Ge et al. 2006; Overstreet-Wadiche et al. 2006; Overstreet-Wadiche et al. 2006); see (Alme et al. 2010) for more references).

Subicular cells seem to be active in all environments, however it is difficult to cluster them and to isolate them as place cells (E. Henriksen, personal communication). Very few data exist for the moment.

2.2.3.1.2 Head direction cells

Contrary to what is observed in the hippocampus where all principal cells are thought to be place cells, HD cells represent only a **small fraction** of the total number of recorded **principal cells**. A large portion of these **anatomically contiguous** non-HD neurons has been identified as **grid cells** in the MEC (Sargolini et al. 2006), in dPrs and in dPaS (see paper #2). However, many of these putative principal cells have **no identified firing correlates**.

The reader should keep in mind that to be able to compare proportions of HD cells in different areas, one needs a robust definition of what is a head direction based on objective criteria. So far that **definition** is quite blurry and the difference between HD and directionally modulated cells is not clear. In **paper #2**, we propose **objective criteria** to determine whether a neuron is **HD modulated**. However the threshold for being identified as a HD cell has not yet been established.

With these limitations in mind, the **proportion** of HD cells in **dPrS** varies according the studies from about **25% to about 35%** (Taube et al. 1990; Sharp et al. 1996; Taube 1998). In the **MEC**, HD cells (or HD modulated cells) represent **about 50%** of the putative principal cells (Sargolini et al. 2006). There are some differences between individual layers of the MEC. The most superficial cell layer, layer II, does not contain any while deeper layers present an abundance of HD cells (LIII: 46%, LV: 76%, LVI: 62%) (Sargolini et al. 2006). I will discuss these numbers further and apply new criteria in **paper #2** and in the Discussion chapter.

In contrast with pyramidal place cells that are silent in some environments, HD cells are **active in all environments**. This fundamental difference will be discussed more at length later (see Discussion).

2.2.3.1.3 Grid cells

Grid cells had only been characterized in the **MEC** (Fyhn et al. 2004; Hafting et al. 2005) before the publication of the work presented in this thesis, which shows that they also exist in **PrS** and **PaS**. See synopsis of results: **Paper #2**. **All MEC principal cell** layers do contain grid cells but grid prevalence and grid properties can vary from one layer to another (Sargolini et al. 2006). As is observed with HD cells, grid cells represent only a **fraction** of the total number of recorded principal cells. The most superficial layer (layer II) is the richest in grid cells: about **60% of layer II** principal cells are grid cells. **Layer III** is close to **35%**. This value drops to about **15%** and **20%** respectively for the deep **layers V** and **VI**. In contrast with pyramidal place cells that are silent in some environments, grid cells, like HD cells, are **active in all environments**. This is a fundamental property of grid cells and will be investigated more in detail in 2.4.1.1 and in the Discussion chapter.

2.2.3.2 Discharge pattern

2.2.3.2.1 Place cells

I have already addressed some of the basic physiological properties of the hippocampal neurons in 1.3.3.1. The following paragraph will give some complementary information on the *in vivo* discharge. I also refer the reader to annex 2 for more details on the parameters used to characterize the discharge.

The **mean overall firing rate** of **CA1** place cells oscillates around **1Hz** (Markus et al. 1995; Muller et al. 1996; Gothard et al. 2001). Both **CA3** and **DG** place cells have the same or a lower mean firing rate (between **0.4 to 1 Hz** on average for

CA3: (Barnes et al. 1990; Markus et al. 1995; Leutgeb et al. 2004; Leutgeb et al. 2007); between **0.5 Hz and 1 Hz** for DG (granular cells): (Jung and McNaughton 1993), 0.7 Hz (Gothard et al. 2001), 1 Hz (Leutgeb et al. 2007). **Subicular cells** have a much **higher firing rate** ((Barnes et al. 1990); E. Henriksen personal communication).

A characteristic of hippocampal pyramidal cells is their tendency to fire **complex spike bursts** when the animal is sitting quietly (Ranck 1973). Granule cells also exhibited burst discharges reminiscent of complex spikes from pyramidal cells while the animals sat quietly; however, the **spike duration** of **granule cells** was significantly **shorter** than for CA pyramidal cells (Jung and McNaughton 1993). Recent developments in *in vivo* recording techniques now make it possible to study the discharge properties at the cellular level in the behaving animal (Lee et al. 2006); (Lee et al. 2009); (Dombeck et al. 2010); (Epsztein et al. 2010); (Epsztein et al. 2011); (Lee et al. 2012) and notably characterized the sub-threshold potential variation and correlate them with the rat behaviour.

2.2.3.2.2 Head direction cells

HD cell **firing persists** if the rat's head remains in the preferred firing direction of the cell (Taube and Muller 1998) and there is **no indication that adaptation of firing** rate occurs if the animal continues to face a preferred direction (Taube and Bassett 2003). This persistent firing is **also observed *in vitro*** in dPrS and EC cells (Yoshida and Hasselmo 2009), see 1.3.3). Most cells have a constant regular firing pattern while the rat has its head in the preferred direction. A few directional cells were observed to discharge a burst of spikes as the head passed through the preferred direction, while on other occasions they discharged only one or two spikes (Taube et al. 1990). I will discuss this point in more detail in the Discussion chapter.

As already discussed in 2.2.2, the HD cell **background-firing rate** (outside the preferred firing direction) both in the dPrS and MEC is **usually quite low** (below 1 Hz) and peak firing rates vary from **5 Hz to more than 100 Hz** (Taube et al. 1990; Taube and Muller 1998; Sargolini et al. 2006), yet there is a high probability that cells with such a high firing rate are interneurons.

2.2.3.2.3 Grid cells

The **average mean firing rate** of the putative excitatory cells in the superficial layers of the MEC is in the same range as what is observed in CA1 place cells around 1 Hz

(Fyhn et al. 2004) or **a few Hz** (Sargolini et al. 2006). It is **higher in the** grid cells in the **deeper layers** and rises to 10 Hz in layer VI grid cells, which record the highest mean firing rates (Sargolini et al. 2006). Similarly to place cells, grid cells are characterized by the occasional occurrence of **bursts** (Fyhn et al. 2004). In the data set of Fyhn (2004), the proportion (including many non-grid cells) of bursts (**ISI**s < 10 ms) was **0.13** ± 0.01 Hz. (ISI = interval interspike, see annex 2). The development of recent *in vivo* juxtacellular recording tools will make it possible to identify precisely the discharge properties of grid cells (Burgalossi et al. 2011).

2.2.3.3 Modulation by global oscillatory rhythms

I established in 1.3.3.3 that the HR neurons frequently show a **dynamic coordination of** their activity that results in the emergence of global electrical events. Three major oscillatory patterns have been characterized in the hippocampal region: **theta oscillations** (4–12 Hz), **sharp waves and associated ripples** (140–200 Hz), and **gamma oscillations** (25–140 Hz) (see 1.3.3.3). These rhythms can be observed *in vivo* by using local field potential (LFP) recordings, which are obtained with extracellular electrodes.

2.2.3.3.1 Theta modulation

When the animal moves through a place or grid field, **place cells** (Vanderwolf 1969; O'Keefe and Nadel 1978); (Buzsaki et al. 1983) and **grid cells** (Hafting et al. 2008) often fire in a bursting pattern with an interburst frequency in the same range as the concurrent LFP theta: these cells are thus **theta-modulated** (Fig. 37–39). As far as I know, Paper #2 is the first publication to show that a portion of **HD cells** are theta modulated (see Synopsis of results and Discussion chapters).

Fig. 37 Theta modulation and phase precession in place cells (from Buzsaki and Moser 2013).

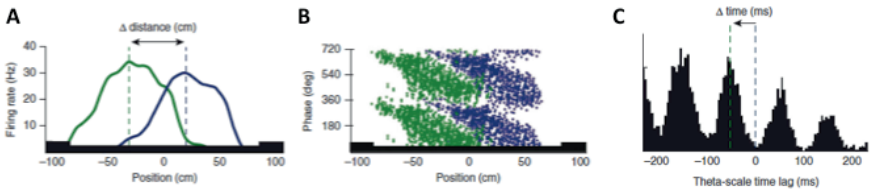

(A) Overlapping place fields of two hippocampal neurons (green and blue) on a track. **(B)** Theta phase of each spike as a function of position in the place fields of the two neurons. Note precession of spikes from late to early phases as the rat crosses the place fields (i.e. phase precession). Two theta cycles are shown for clarity. **(C)** Cross-correlation between the reference (blue) and overlapping (green) place cells. Δ time is the time lag between the spikes of two neurons within the theta cycle ('theta time')

Link between theta rhythm and running speed

As stated in 1.3.3.3.1, many studies show that one type of theta oscillation frequency is determined by the animal's travelling velocity (Buzsaki 2002). Since most place and grid cells, and many HD cells, are both theta and speed modulated, one can consider that they behave as **speed-dependent oscillators** (see 2.3.3) (Geisler et al. 2007); http://www.scholarpedia.org/article/Hippocampus). Actually, when comparing slow and fast speeds, speed affects the intrinsic oscillation frequency (and power) of place cells more than LFP (Geisler et al. 2007). It is interesting to observe that both place and grid cells in **bats** are modulated by running speed in the **absence of theta** modulation in these animals (Ulanovsky and Moss 2007; Yartsev et al. 2011). A possible explanation is that for bats the functions covered by theta in the rat are supported by a **different frequency** (probably lower). The consequences of this **hypothesis** are very important for grid cell generation and spatial coding (see Discussion chapter).

Theta phase precession, phase locking and temporal code

Temporally precise recordings of place cells activity show that they **burst** at a slightly **higher frequency** than the LFP theta (O'Keefe and Recce 1993). Consequently, as the animal traverses a place field, the **spikes** of its corresponding place cells are not locked to a particular phase of the theta cycle, but rather **shift progressively forward** on each **theta cycle**. This phenomenon is called **theta phase precession** (O'Keefe and Recce 1993). The phase at which the cell is firing is more correlated with the rat's **spatial location** than with temporal aspects of his behaviour, such as the time after entry to the place field or the animal's running speed. When considering an **ensemble population**, most place cells show **maximal activity** at the **same phase** of the theta cycle (Skaggs et al. 1996). The phase at which the **first spikes** occur when a rat enters a place field comes 90–120^{o} after that. The **phase shift** never exceeds **360^{o}** and the phase advance is typically an **accelerating**, rather than linear, **function of position** within the place field. This gives a stereotypical banana shape to the temporal distribution of the spikes. The **precession rate** is tightly coupled with the **place field size**, suggesting that a single cycle of theta phase precession could be used to define unitary place field boundaries: the larger the place field, the slower the slope of the theta phase distribution function (Maurer et al. 2006). If the rat is trained to follow a **stereotypical linear path**, place cell sequences are organized both spatially and

temporally. In such situations, the place fields of sequentially active place cells can overlap and their temporal relationships are governed by a **compression** rule: within the theta cycle, the spike timing sequence of neurons predicts the upcoming sequence of locations in the path of the rat, with larger time lags representing larger distances (Skaggs et al. 1996; Dragoi and Buzsaki 2006); http://www.scholarpedia.org/article/Hippocampus) (Fig. 37). Thus place cells code for location through both a rate and a **temporal code** that are highly correlated. The temporal encoding of place sequences is plastic and depends on **experience** (Mehta et al. 1997; Mehta et al. 2000; Mehta et al. 2002). At **faster running speeds** place cells are active for fewer theta cycles but oscillate at a higher frequency and emit more spikes per cycle and the **number** of the place cells compressed in one theta cycle sequence **increase** (Geisler et al. 2007; Maurer et al. 2012). These results confirmed two hypotheses: one was that **speed-correlated acceleration** of place cell assembly oscillation is one of the mechanisms responsible for the correlation between the distance in the field and the phase at which the place cells spike (Geisler et al. 2007). The second is that hippocampal networks generate short time-scale **predictions of future** events to optimize behaviour (Maurer et al. 2012). Recent studies have demonstrated that temporal coding was **not restricted to stereotypic linear behaviour** and could also be observed in running wheel (Harris et al. 2002) and open field (Huxter et al. 2008) behaviour. Theta modulation may support several functions of **information encoding, retrieval and prediction** (Manns et al. 2007); Huxter et al. 2008(Gupta et al. 2012).

Fig. 38 Theta modulation and phase precession in a MEC LII grid cell (Hafting et al. 2008)

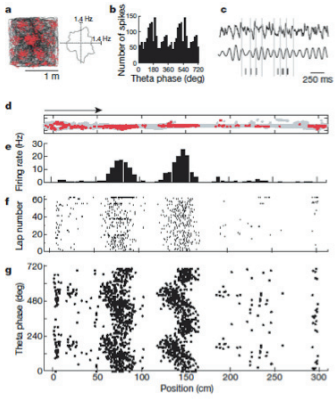

a, Firing field (left) and directional tuning (right) of a layer II grid cell in the open field. **b**, Phase distribution for the cell in a. **c**, Entorhinal EEG with spike times for the same layer II cell during 2.3 s of track running. **d–g**, Trajectory with spike positions **d–g**, (**d**), linearized rate maps (**e**), raster plot for successive laps (**f**), and theta phase as a function of position (**g**). Note the gradual advance of firing phase as the rat passes through each field.

Phase precession and temporal code has mostly been studied in hippocampal place

cells, especially in CA1. Yet, both phenomena have been observed in **all place cells** independently of their anatomical location. As stated previously, most **MEC grid** cells are theta modulated. However, only a portion of them present **phase precession** mechanisms (mostly in **layer II**, Fig. 38), while the others have their activity "**phase-locked**" to a specific phase of the theta cycle (mostly in **layer III**, Fig. 39) (Hafting et al. 2008). One should note that this distribution follows the **distribution of directionality** between layers and that most phase-locked grid cells are in truth conjunctive grid and HD cells. I will discuss that point in more detail during the discussion. Preliminary results showed that grid cells do also present phase precession in a 2D environment (Climer et al. 2012; Jeewajee et al. 2012; Reifenstein et al. 2012).

Fig. 39 Theta modulation and phase locking in a MEC LIII grid cell (Hafting et al. 2008)

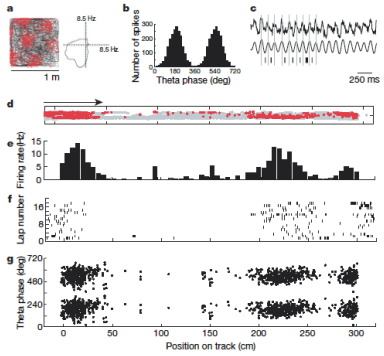

a, Firing field (left) and directional tuning (right) of a layer III grid cell in the open field. **b**, Phase distribution for the cell in a. **c**, Entorhinal EEG with spike times for the same layer III cell during 2.3 s of track running. **d–g**, Trajectory with spike positions (**d**), linearized rate maps (**e**), raster plot for successive laps (**f**), and theta phase as a function of position (**g**). Note phase locking to the trough of the theta cycle.

2.2.3.3.2 Gamma modulation

The other main oscillations observed in the HR are regrouped in the gamma band. They have been associated with decision-making, increased attention, and improved reaction times (Ahmed and Mehta 2012). As stated in 1.3.3.3.2, it seems that there are **two independent generators** of gamma oscillation, one in the **EC** and the other in **CA3,** leading respectively to **fast** and **slow** gamma oscillations (Csicsvari et al. 2003). One of the main influences of gamma modulation has been observed in CA1 place cells whose population can alternate fast and slow gamma modulation (Colgin et al. 2009). It has been postulated that this dual modulation has a role in the **routing and the grouping of the information** across different brain areas, as well as in the encoding and the retrieval of this information so that areas will tune to one or another

frequency depending on the region they are communicating with (Colgin et al. 2009; Colgin and Moser 2010; Colgin 2011).

It has recently been demonstrated that **running speed** alters the frequency of hippocampal gamma oscillations, supporting an increased synchrony between anatomically distant CA1 regions (Ahmed and Mehta 2012). Possible gamma modulation of grid and HD cells remains to be more precisely investigated.

2.3 DISCHARGE CORRELATES

In this section, I will specify the influences upon place, HD and grid cell activity. I will start by defining some **prerequisites and concepts** (2.4.1), notably what type of control (generation, modulation, stabilization, anchoring) a determinant can exercise upon place, HD and grid cells. The primary discharge correlates of these cells are by definition supposed to be **spatial and directional** (see 2.2.2). Yet this coding is the result of what the rat experiences and processes. The rat experiences the world through allothetic and idiothetic information that allows it to assess the spatial features of the environment (geometry, borders, object) and changes in these features. I will review how **allothetic** (2.4.2) and **idiothetic** (2.4.3) **information** influences the firing of these cells. I will then present the influence of the **spatial features** of the environment (2.4.4) and its topology on cell activity, notably its shape (i.e. geometry) and size. Since the original studies, **non-spatial information** has been thought to modulate place cells' activity while HD cells and grid cells were more part of a universal navigation system. I will discuss how non-spatial features exercise influence upon place, HD and grid cell activity, and distinguish the relative influence of context, behaviour and behavioural relevance (e.g. reward).

2.3.1 Prerequisites and concepts

Spatial and directional coding in place, HD and grid cells are the result of what the rat experiences and processes. Consequently, what influences the **rat's perception**, **processing** and **behaviour** may influence these cells' activity. Thus one should be aware that the **brain distorts the "reality"** of the physical world: it weights its informational content, ponders the salience of the available cues and transforms, more or less accurately, its physical properties into **physiological codes**. Like any representation, the cognitive representation of space is thus not an exact replica of the "reality".

Various behavioural tasks, apparatuses and types of sensory stimulation have helped to reveal the determinants of spatial and directional cell firing. It is important to keep in mind that there are different ways to influence the cells' activity: which may be classified as **generating**, **controlling**, **stabilizing** and **anchoring**. I will attempt in the next sections to specify as much as possible which **type of control** is exercised by each of the different factors presented.

In order to investigate what is controlling the discharge, experiments are designed in such a way that the **putative determinant factor**, or the neuronal **system/mechanism supporting** it, is permanently or transiently **disrupted** (i.e. removed or modified). This leads to two major types of experiment. Thos in the first set focus on **modifying the environment** in order to **isolate the considered factor**. For instance, in order to test the influence of visual cues one can turn off the light, remove the cues, move them or, using several cues, introduce conflicts between them and see which ones the neuronal discharge follows. In such experiments, if the modifications are consequent, it may lead the rat to consider that it is exploring a whole new environment. That configuration can lead to the loading of new "cognitive maps". This phenomenon is known as remapping. Alternatively, the **disruption** can be more **invasive** and concern the **physiology** of the animal itself. To follow on the example of the visual cues effect, the animal can be transiently or permanently blinded, the visual cortex activity may be disrupted by a lesion centred on the cortex or by cutting projection fibres. Some proteins involved in the studied system can be transiently or permanently, pharmacologically or genetically modified or disrupted (e.g. transgenic mice, KO mice, local transgenic expression via virus, iRNA, drugs).
I will hereafter discuss the influence of **diverse types of cues** on cell firing. One should note that cues have **different valiances** and we can infer **different concepts**. For instance, a cue can be an object or a distal landmark, but it can also be a border of the environment. A cue can be more or less salient so that the animal pays more or less attention to it. This is even more accentuated for cues with a behavioural relevance such as a goal or a reward location. In addition the stability of the cue modulates how influential it is. I will develop these notions in more detail in this sub-section (2.4.5).

As indicated by their names, the **primary correlates** of place, HD and grid cells are thought to be **spatial and directional**. In the example of place cells, it was described in 1976 that they "do not seem to be tuned to specific sensory stimuli,

tolerate radical changing in lighting, (are) omnidirectional and uninfluenced by reward (Andersen 2007), p. 491). However a growing body of work proves that different types of information can potentially **influence the activity** of spatial and directional neurons. As presented in (1.2), numerous authors differentiate between two navigational strategies in spatial cognition. One is based on **allothetic information** extracted from external sensory information or sensory cues. It is sometimes called the cue landmark navigation system. The second is based on **idiothetic information** extracted from internal perception and calculation of movement and position in space (e.g. vestibular information, proprioception, optic flow, speed). This second strategy is equivalent to a dead reckoning system and is named path integration. Behavioural experiments have established that animals use both strategies to navigate.

2.3.2 Allothetic information

As stated previously, allothetic information is extracted from **external sensory** information or sensory cues. The major sensory inputs are **visual**, **olfactory**, **auditory** **somatosensory** (touch and wiskering) and **taste** (Whishaw and Kolb 2005). I will here review the **influence** of sensory inputs on **place, HD and grid cell** activity.

2.3.2.1 Place cells

When place cells were discovered, the "**sensory hypothesis**" was proposed, that place cells fire in only one place because of a specific combination of sensory stimuli that occurs in this location. Quite soon afterwards, this theory was proved **inaccurate**: sensory inputs influence the firing of place cells, but it seems that they are not necessary for the generation or the maintenance of their activity. Their role is more to **control**, **stabilize** and **anchor** the preferred firing location, as I will discuss hereafter. I will predominantly support my argumentation with the results of experiments testing the role of visual cues, vision being the most studied of the senses in navigation. Many of these findings may be transferable to other senses.

2.3.2.1.1 Disruption of the sensory input

The most straightforward experiment to test the influence of visual cues is to turn off the light. O'Keefe (1976) conducted the first **dark experiment** (see also (Quirk et al. 1990; Markus et al. 1994). The abolition of all visual inputs had three consequences for place cell activity. The first was a **transient decrease of firing rate** during the first exposures to darkness until it increased again after a period of **habituation**. The

second was more permanent and consisted of a **loss of stability** in the position of the firing field(s) compared with the light conditions. The third was a **permanent change in the preferred firing location** in dark conditions as if the animal considered the dark environment to be a new environment and the place cells consequently **remapped**. To measure the influence of visual inputs, Save and colleagues studied place cell activity in **rats blinded before eye opening** and found that these rats had **place cells very similar** to those recorded from **sighted rats** (Save et al. 1998). These results confirmed that **visual cues**, or even ability to see, are **not essential** for the firing of place cells. However, the transient block of visual inputs will confuse the rat at first until it resets its perception of the environment after a little while, though not optimally. Thus visual cues seem to have a **role of stabilization/anchoring** of place cells, notably in recognizing the environment in which the animal is located (and which map to load, see 2.4.6). When analysing such experiments, one should also take into consideration the amount of stress the animal experiences in such conditions.

2.3.2.1.2 Manipulation of the sensory cues

To test further the control of visual cues upon place cells, one can place a rat in an environment with no recognizable landmark (for example, a black circular box surrounded by black curtains) with the exception of a **single prominent visual cue** (for instance, a large white cue card on the inside of the apparatus). Then the experimenter can rotate this cue and observe if the firing follows it. In 1987, Muller and Kubie published the results of similar **rotation experiments** (Muller and Kubie 1987). They observed that most of the time the rotation of the cue card produced an **equal rotation of the fields** of single pyramidal cells. Similar results were obtained in the dentate gyrus (Jung and McNaughton 1993). These types of experiments consist of "**tricking**" the rat into thinking that its environment rotated while it was actually only the walls. After multiple repetitions, the rat often becomes less naïve and rotation of the field is less clear as the rat is more in a situation of cue conflict. In the same configuration as described previously (i.e. circular environment with one salient visual cue), the **removal of the cue card** altogether left the size, the shape and the radial position of the firing field unaffected but caused the fields to be **less stable** and **drift to unpredictable angular positions** (Muller and Kubie 1987). It seems also that their **firing rate** is affected depending on how close the cue card is (Hetherington and Shapiro 1997). Taken together, these results confirm that visual cues anchor and

stabilize place field cells' activity.

Some studies have investigated the effect of a **partial removal of visual cues** and found that **some fields** are affected preferentially by **one specific visual cue** while **other**s respond in more complex ways ((O'Keefe and Conway 1978; Shapiro et al. 1997) to **several cues**. The results of such experiments show that some cues exercise more control than others, based on **difference in saliency** but mostly on how **relevant** the cue is. Some authors showed that **stability** of the cue has great impact on its control upon place cell firing. Furthermore, depending on the experiments, **cue control hierarchy** may vary from one animal to another or even from one session to another (see 2.5 for references). These considerations introduce the notion of reference frame that I will address later, notably while analysing the situation of cue conflicts and taking into consideration not only place cell ensembles but also HD and grid cells (2.5.1).

Some authors (Sharp et al. 1990) tested the influence of the **introduction of a second symmetrical cue card** in a cylinder. In such a configuration most cells are unaffected while a few cells present the transient apparition of a second symmetrical field that disappears rapidly after some experience. Other authors introduced the second cue card in an **asymmetric** way (Fenton et al. 2000). In some cases, a modification of the angle between the two cue cards could induce a displacement of the firing fields so that the global representation by an ensemble of place cells was **distorted**. Additionally the modification of a visual cue might have some effect on the firing field position. For instance, **changing the width** of the cue card in a circular maze can sometimes induce the fields to **rotate to a modest extent** (Muller and Kubie 1987). Thus, place cell activity is not strictly dependent on visual cues but the **rat's perception** of the environment is **influenced by visual inputs** and **controls the position of the firing field**. In many experiences, it has been shown that – when available – visual cues tend to influence place cell activity more than other types of sensory cues. However, one should be aware that it is difficult to match equally the saliency of different type of cues. I will discuss more cue rotation experiments in (2.4. and 2.5) while addressing how place cells' properties are linked to a reference frame. There, I will present results from conflicting cue experiments, notably when opposing distal and proximal cues.

Looking at non-visual sensory inputs, initial reports suggested that **olfactory**, **tactile and auditory** cues exert some **influence** upon place fields, though in most

studies it was **minimal** (O'Keefe 1976; O'Keefe and Conway 1978; O'Keefe and Speakman 1987); (Thompson and Best 1989; Save et al. 2000). Yet, it was demonstrated that a fraction of **hippocampal cells** do **respond to specific odours** (Eichenbaum et al. 1987; Wood et al. 1999) or to **taste** (Ho et al. 2011).

2.3.2.2 Head direction cells

HD cells have been recorded in **many different brain areas**. They form a **heterogeneous population** with variable properties, especially concerning the factors that control/influence their activity. In this thesis I will present the properties of HD cells recorded in the **parahippocampal area** (PrS: (Ranck 1984), MEC: (Sargolini et al. 2006)). Papers #1 and #2 present further results concerning the PrS and MEC. I will compare them with PaS HD cells in the synopsis of results and discussion. To list and compare the different properties between regions is beyond the scope of this work. I refer the reader to the numerous reviews addressing these issues (e.g. (Taube 2007). As in the discussion of place cells above, I will mainly focus on vision.

2.3.2.2.1 Disruption of the sensory input

Dark experiments (turning off the light or blindfolding the rats) do not result in the suppression of the direction-specific firing of dPrS HD cells. Yet this preferred direction is **less stable** than in normal condition and **drifts** along the session ((Goodridge et al. 1998); unpublished results mentioned in (Taube 1998). Thus, visual inputs seem **unnecessary for the generation and maintenance** of HD cell activity but do have a **role of stabilization/anchoring** as they do for place cells (Taube 1998). As I will discuss later, **place and HD** cells could be part of the **same system** and thus be influenced in similar manners.

2.3.2.2.2 Manipulation of the sensory cues

It seems that specific visual cues have the **role of anchor** and can exert control over HD cells' preferred firing direction. This control has been confirmed in **rotation experiments** similar to what I described previously for place cells (Muller et al. 1987). In such experiments, the rotation of a cue card produced near-equal rotation in the preferred firing direction of HD cells with **minimal changes** in **peak firing** or **directional firing range** (Taube et al. 1990; Kudrimoti et al. 1996; Sargolini et al. 2006). In the same line of thoughts, the **removal of salient visual cues** does **not affect** peak **firing rate** or directional range but can provoke a shift of the preferred direction that may be reminiscent of a **remapping** (Taube et al. 1990). The animal's

perception of cue stability seems essential for reliable HD cell responses (Knierim et al. 1995). Indeed, a novel visual cue should be available for a minimum amount of time (between 3 and 8 min) to systematically gain control over the preferred direction of HD cells (Goodridge et al. 1998). Thus, the extent to which a known cue is perceived as stable **defines the amount of contro**l it will exert over the directional firing of a HD cell (Muir and Taube 2002). However once a cue is familiar, it can re-anchor HD cells extremely rapidly, as attested by experiments where rats, in a cue orientated familiar environment, were subjected after turning the **light off** to very **slow rotation** (Zugaro et al. 2003). The rotation was not detected by the rat and the preferred directions of its HD cells followed the rotation, yet as soon as the light was turn on, the directions **very rapidly re-orientated** themselves following the visual cues (latency: 80 msec).

Similar **rotation experiment**s were conducted with auditory and olfactory cues. The **auditory cue** was a click sound and did not lead to a corresponding shift (Muir and Taube 2002). The **absence of rotation** could be explained either by the **lack of control** of auditory cues over HD cell firing or by the fact that an auditory click, as a cue, was **not salient enough** compared with uncontrolled environmental cues. The rotation of salient **olfactory cues** was **followed by 50% of HD cells** from the dPrS (Muir and Taube 2002). The type of olfactory cues used in that experiment were thus not as salient as the visual cue of white card. I will discuss more cue rotation experiments in (2.4.6) while addressing how the properties of HD cells are linked to a reference frame. There, I will present results from conflicting cues experiments, notably when opposing distal and proximal cues.

2.3.2.3 Grid cells

Here I present results for the MEC grid cells. I will compare them with the PrS and PaS grid cells in the synopsis of results of paper #2 and the discussion.

2.3.2.3.1 Disruption of sensory input

Grid cells maintain their grid like activity during **dark experiments** (light off). Darkness had **no significant effect** on the **spacing** of the grid and there was no change in **average firing rate** or **spatial information per spike**. Yet, in the majority of the cells the onset of total darkness caused a **weak dispersal or displacement of the vertices**, expressed as a moderate decrease in the spatial correlation of the rate maps (Hafting et al. 2005). These results are similar to those obtained with place and

HD cells where a drift in preferred firing place or direction occurs after disruption of visual cues. Of the three main grid parameters, it is the spatial phase that drifts. Thus, visual inputs seem **unnecessary for the generation and maintenance** of grid pattern and activity, but do have a **role of stabilization/anchoring** of its vertices to an external reference frame, the same as for place and HD cells (Fig. 40). I will discuss later (2.5) whether place, HD and grid cells are tight together to unique frame of reference at a time.

Fig. 40 Example of control of visual cues over grid cell activity

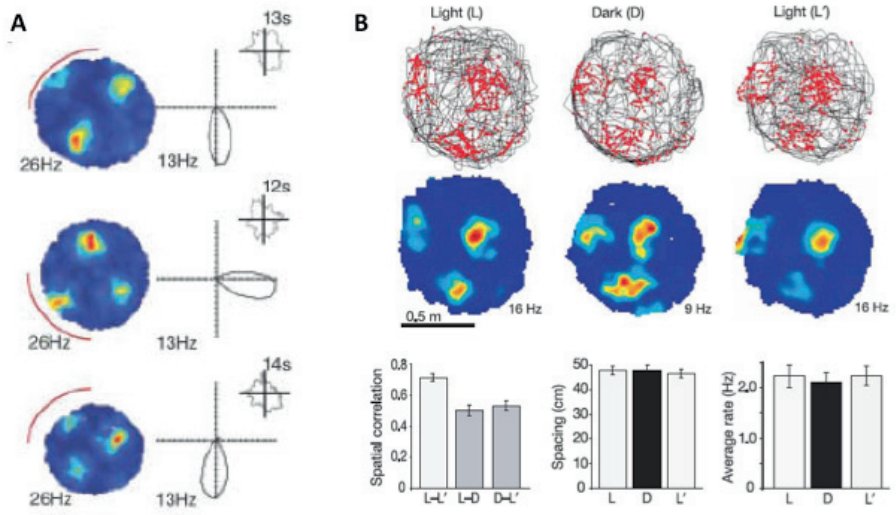

(A) Rotation experiment (Sargolini et al. 2006): rate maps and polar plot of a conjunctive (head direction and grid) cell following the rotation of a white cue card (figured by a red curved line in the figure). **(B)** Dark experiment (Hafting et al. 2005). Upper panel: representative behaviour of a grid cell during the deprivation of light in the environment, trajectory with spike position and rate map. Lower panel: Differences in spatial correlation, spacing and average rate of a grid cell set during the same experiment. Note the absence of strong differences between light and dark conditions.

2.3.2.3.2 Manipulation of the sensory cues

Rotation experiments further test how salient visual cues anchor grid cell vertices. The original study (Hafting et al. 2005) consisted of a 90° rotation of a white cue card on the wall of a circular box while curtains masked distal cues. **Grid** cells' vertices systematically **followed** the rotation. The same result was observed in later studies (Sargolini et al. 2006; Boccara et al. 2010), though it seems that the fidelity of the rotation depends on how well non-rotating cues are masked. **Removal** or **distortion** of two cue cards in a similar fashion to what had been done in the past while testing

the response of CA place cells (Fenton et al. 2000) led to a similar response (see above) from MEC grid cells (Song et al. 2012).

2.3.3 Idiothetic information

As stated previously, idiothetic cues are extracted from **internal perception and calculation** of one's own **movement** and **position** in space (e.g. vestibular information, proprioception, motor efferent copy, optic flow, speed). The navigation strategy they support is equivalent to a **dead reckoning system** and is named **path integration**. Rats are able to navigate in the absence of any external sensory cues and using only path integration (O'Keefe and Speakman 1987).

2.3.3.1 Place cells

In specific experimental conditions, place cell firing rates may be related to variables other than spatial location such as the **speed**, **direction**, and **turning angle** of the rat as it moves through the place field and performs task-relevant **approach movements** (Wiener et al. 1989).

The first basis for the influence of idiothetic cues on place cells is that place fields remain relatively **stable during dark** experiments or other cue deprivation experiments (2.3.2.1). Additionally, **place field** locations are often **maintained** when the recording box is **transformed smoothly** into another familiar box (Leutgeb et al. 2005). These various results suggest that an internal representation is preserved independently of allothetic cues and probably based on idiothetic information.

This claim was further supported by the fact that place cells present different patterns of activity in **two visually identical boxes connected by a corridor** (Skaggs and McNaughton 1998). Furthermore, inverting which box the rat starts in results in a transient inversion of the maps attached to each environment for the length of time the rat is "tricked". Alternatively, physical interchange of the two boxes does not induce the field to move along with the box. Finally, rotating the proximal environment leads the fields to follow the rotation (Tanila 1999). These joint results revealed the **influence of the perceived orientation and animal's own movement** on the field cell firing and that it is not based on a lack of salience of the proximal cues.

Another classic study consisted of recording hippocampal place cells while the rat was running on a **linear track** from a **fixed reward** site to another, **movable reward** site mounted on a **sliding box** (Gothard et al. 1996) (Fig. 41). While the rat ran toward the fixed site, the box was moved before the rat returned to the box's new

position. The place field locations on the return run are modified by this action: on the initial part of all journeys, cells fire at fixed distances from the origin, whereas on the final part, they shift to fire at fixed distances from the destination. It was calculated that the time elapsed since leaving the box in fact provided a better predictor of the shift position than the distance (Redish et al. 2000). Thus, on outward journeys from the box, with the box behind the rat, the position representation must have been updated by **path integration**, and idiothetic and allothetic cues conjointly influence the firing field positions.

Fig. 41 Linear path integration updates the positional firing of hippocampal pyramidal cells

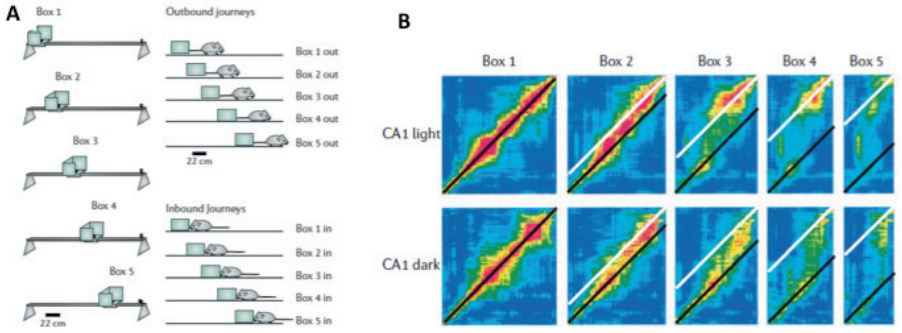

(McNaughton et al. 2006)
(A) Presentation of the task in which a rat runs on a linear rail from a moveable box to a fixed goal at the end of the track. The figure illustrates the configurations of the start box on the track and the journey types, which were presented in random order.
(B) Pyramidal cells in area CA1 fire in relation to distance from the box as the animal leaves it (over distances of more than several body lengths), before shifting reference frames to fire in relation to visual cues (CA1 light) or, in darkness, the end of the track (CA1 dark). Here are shown the correlation matrices of the CA1 neuronal ensemble population vectors for each location on the full track versus every location on the full track (Box 1), and for each location on the shortened tracks, in which the box was shifted closer to the fixed goal site (Box 2–Box 5), versus every location on the full track. The black lines represent the reference frame of the box; white lines represent the laboratory/track reference frame. Note the shift from one reference to another.

Disorientating a rat's internal **sense of direction** prior to exploration induces **instability** in place cells (Knierim et al. 1995). Moreover it influences the **anchoring effect** of idiothetic information by rendering it unreliable. I will discuss this experiment at greater length in 2.3.5.1, as it is strongly linked to experience. The actual **inactivation of the vestibular system** results in the **disruption of the location-specific firing** of hippocampal place cells (Stackman et al. 2002). Whether this is a direct consequence or due to the disruption of the HD system remains to be proven.

The influence of the animal's own movement on place cell activity was further

established by the discovery that most place cell **activity ceases** if the animal is **restrained** (Foster et al. 1989). Furthermore, their firing is a function of the running speed of the rat but tends to asymptote well before half-max speed (McNaughton et al. 1983; Geisler et al. 2007). On the other hand, running speed also correlates, in the rat, with the global **theta rhythm** observed in the local field potential. Thus, place cells are **speed-dependent oscillators** (Geisler et al. 2007) http://www.scholarpedia.org/article/Hippocampus. The running speed gain is not uniform across all place cells and increases along a **dorso-ventral gradient** (Maurer et al. 2005), similarly to field scale (see 2.2.2.1).

To understand better how place cell activity is influenced by motion signal, experiments were developed in which rats either **actively drove a car** between locations on a circular track or experienced **pseudomotion** by being stationary while the environment was rotated. These two situations were compared with a control in which the animal walked between the two locations (Terrazas et al. 2005). Decoupling movement in space from ambulation disrupts the location specificity of most hippocampal cells to a large extent. The few that still qualified as place cells in this condition exhibited substantially **larger place fields,** as if the track circumference was reduced and the animal moved around it at a correspondingly slower speed. This confirmed that **spatial scale and speed could be linked.** The emergence of virtual reality tools (Hafting et al. 2008; Harvey et al. 2009; Dombeck et al. 2010) allows these questions to be addressed in more detail.

A recent study showed that the **cerebellum** is probably involved in **processing self-motion signals** essential to the shaping of hippocampal spatial representation. Indeed, the perturbation of its plasticity results in the disruption of spatial specificity of place cells, concomitant with impaired navigation capabilities selectively during a **path integration task** (Rochefort et al. 2011).

2.3.3.2 Head direction cells

Most studies on the influence of idiothetic information on HD cell activity were conducted on the anterior dorsal nucleus (**ADN**). I will therefore report here some of these results as comparative material with parahippocampal HD cells.

I established previously (2.4.2.2.1) that HD cells mostly maintain their firing **directional specificity** in the **absence of salient sensory cues** or when a rat travels from a familiar environment to a novel one, deprived of cues (Taube and Burton

1995). This suggests that, without familiar landmarks, the preferred firing direction can be maintained by a process called **directional path integration** using idiothetic cues such as vestibular information, proprioception, motor efference copy, optic flow and speed. One may distinguish between what is necessary to generate and maintain the directional signal and what modulates it.

The **maintenance** of the directional signal is **not dependent on optic flow, speed inputs** or even **self-motion information** as HD cells preserved their firing in the absence of visual information (2.4.2.2.1), when the rat is motionless (Taube and Bassett 2003) or during passive movement (Shinder and Taube 2011); but see (Taube et al. 1990); (Golob et al. 1998). On the other hand, the directional signal is **dependent on the integrity of the vestibular system** (Stackman and Taube 1997; Stackman et al. 2000; Muir et al. 2009; Yoder and Taube 2009).

The **anchoring roles** of visual, motor, and proprioceptive inputs on the HD signal were further investigated by manipulating the idiothetic cues available to a rat as it moved from a familiar to a novel environment (Stackman et al. 2003). Disrupting **optic flow cues** (by darkening the room) or **self-motion information** (by passive transport) led to a **shift** in the preferred firing directions of HD cells. However, one should consider that the rat might experience these abrupt transitions as complete changes in reference frame and that the observed shift in this situation could be the expression of remapping.

The **disorientation** of a rat (by slow rotation) leads to HD cell **instability** (Knierim et al. 1995; Dudchenko et al. 1997) probably rendering unreliable the anchoring effect of **idiothetic information**. I will discuss this experiment at greater length in 2.3.5.1, as it is strongly linked to experience.

HD cell activity may be modulated by **angular head velocity** and **running speed**. This influence varies from one area to another. **Angular head velocity** influence seems to be maximal in the **ADN** where the cell directional firing preference shifts towards the direction in the head is rotating, as if anticipating the future head direction (Sharp et al. 1995). Furthermore, the firing rate of HD cells is often positively modulated by angular head velocity, even in the absence of active locomotion (Zugaro et al. 2000). **PrS** HD cell activity may also be modulated by angular head velocity (Sharp et al. 1996). However, there is no shift in their directional firing preference in response to head movement. **Running speed** has been shown to positively modulate a portion of HD cell activity in both the **MEC**

(Sargolini et al. 2006) and **dPrS** (Sharp et al. 1996). However, it is not clear whether this correlation is a **by-product** of the influence of theta modulation (see synopsis of results in paper #2 and discussion).

The influence of idiothetic information on the generation, maintenance and stability of the directional signal will be further discussed in the light of the experimental work of this thesis (see discussion).

2.3.3.3 Grid cells

As an animal walks in an environment, the **periodicity** and **scale** of the grid cells remain **constant** in spite of constant changes in the animal's **speed** and **heading**. This is also true in situations where salient landmarks are removed or in the **dark** (2.4.2.3.1). Thus, the constant **updating** of the **spatial representation** needed to keep the grid periodicity is not dependent on external visual information and must be linked to some **internal processing** based on idiothetic information. It has been proposed that the grid cells are a **key** element of the **path integration** system (Moser and Moser 2008), notably because animals with lesion to the MEC cannot perform homing behaviour based only on self-motion information (Parron and Save 2004).

Like place cells, the firing rates of most grid cell are positively **modulated by running speed** in the rat (Sargolini et al. 2006). As running speed also correlates, in the rat, with the global **theta rhythm** frequency observed in the local field potential (LFP), grid cells may be considered as **speed-dependent oscillators** (Geisler et al. 2007); http://www.scholarpedia.org/article/Hippocampus). The link between running speed and LFP theta modulation was discussed at greater length above, in 2.2.3.3.1.

Future work is needed to assess precisely the modalities of the influence of idiothetic information on grid cell activity. It will be especially interesting to observe the effects of the modification/disruption of vestibular and self-motion information, as has been done for HD and place cells (see discussion on the origin of grid cells). The advent of **virtual reality tools** for electrophysiological recordings will help in this task to complete already existing data on how grid cells behave when the rat is stationary or when it is constrained.

2.3.4 Environment spatial features

In the previous sections, I considered how the activity of place, HD and grid cells is linked to the **animal's perception** of its **environment** and its **position** using allothetic and idiothetic information. I have not yet discussed how the environmental

features, and changes in these features, affect the firing of these cells, besides the anchoring effect of salient visual white cue cards. In this section, I will reflect on the **influence** of the spatial features of the environment: its **geometry** (**shape**, **borders**, **size, dimensions**) and whether it contains **objects** or **barriers**.

The reader should note that **laboratory** environments are often **very simple** in order for experimentalists to be able to control their different elements. They are very seldom representative of **natural environments** and it seems that increasing the complexity of the environment leads to **more complex** spatial patterns of **place cell** firing (Battaglia et al. 2004; Fenton et al. 2008).

2.3.4.1 Geometry

The **shape** of the recording box has been tested for its effect on the activity of place, HD and grid cells (Muller and Kubie 1987; Taube et al. 1990; Fyhn et al. 2007). In these studies, the rats were exposed to two familiar environments: one **circular** and one **square**. Between the two shapes, all three cell types **remapped**. **Place cells** either **changed** their preferred firing **location** in an **unpredictable** manner or became **silent**. For **HD cells, the** firing directions **shifted,** and enthorinal **grid** fields **realigned**. The offset was similar in all simultaneously recorded HD and grid cells. The direction of the offset was uniformly distributed between experiments. HD cell tuning width and grid spacing and orientation were not much affected by the shape change. To limit the number of variables between the two situations, other studies looked at the influence of shape when the **circular** and the **square** boxes were positioned at exactly the **same location** in the room (Lever et al. 2002; Fyhn et al. 2007). If the rat is **familiar with only one** of the shapes, its place cells will have **similar firing locations** in both environments at first. With more and more exposure, the novel shape will see the **gradual emergence of new firing** patterns (change in location or even silencing) to the point of a configuration of remapping similar to what is described above. Further experiments attempted to address the **transition point** between these two representations by slowly **morphing** one environment into another using intermediate boxes of octagonal shape between a circle and a square (Lever et al. 2002; Leutgeb et al. 2005; Colgin et al. 2010). Both **abrupt** and **smooth** transitions were found. The results were influenced by the **rat's experience**, **training procedures** and the **subfield** (CA3 vs CA1). I will discuss these in more detail in 2.3.5.1.

To establish further how the geometry of the environment controls HD cell

firing, some studies used **asymmetrically** shaped boxes (Knight et al. 2011; Clark et al. 2012). They assessed the influence of the geometry of the box by **rotating** it and observing if the fields rotated accordingly. They found that in **some conditions** (disorientation, little allothetic information), the preferred **direction followed** the rotation of the box. I will consider these experiments further when discussing reference frame (2.3.5.1).

Another classic way to address the role of geometrical boundaries is by **expanding the environment** (Fig. 42). This manipulation either leads to **parametric expansion** of **place field** or has **no effect** (Muller and Kubie 1987). **Stretching** the box in **one dimension** induced the **expansion** of the place **field** in that direction, according to some authors who link this result to a **mathematical model** based on the distance from the wall (O'Keefe and Burgess 1996). In similar conditions, **grid cells** present comparable **expansion** patterns (Barry et al. 2007). I will discuss these experiments and model bases further in results from paper #2 (Solstad et al. 2008) in the discussion, where I will link the distortion of the field to the **experience** of the rat and the **salience** of the cue. Additionally, preliminary results suggest that the shift or rotation of the boundaries of the environment may affect the grid cell firing pattern (Savelli and Knierim 2012).

Fig. 42 Grid and place field distortion following geometrical changes of the recording environment (O'Keefe and Burgess 1996; Barry et al. 2007)

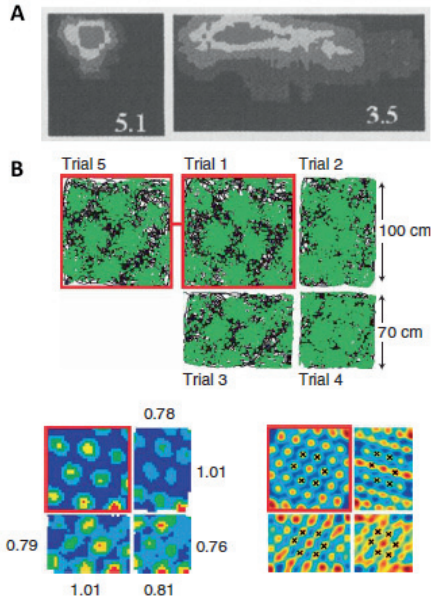

(A) Elongation of a place field following the extension in one dimension of the recording environment from squared to rectangular.

(B) Compression of grid fields following the successive compression of a squared environment. Upper: Trajectory with spike positions. Lower left: rate maps. Lower right: autocorrelograms.

Constraining the path of the animal – either by placing it in a one-dimensional environment (**1D**) such as a linear or a circular track or by training it to follow a **stereotypic path** (by going directly to a goal, for example) – influences the cell properties. Place cells become orientated: they fire preferentially in one **direction** (Markus et al. 1995; Battaglia et al. 2004). This could be interpreted as the animal considering both orientations on the path as two different environments or at least as two different journeys. The development of this preferred firing direction is a **plastic** phenomenon linked to **experience** (Navratilova et al. 2012). Other authors have attempted to reduce a two-dimensional (2D) environment to 1D in a **hairpin maze**. They observed the repetition of the same two patterns of expression, specific to either the inbound arms or the outbound arms, while the head direction signal remained stable (Derdikman et al. 2009; Whitlock and Derdikman 2012).

Most studies characterize place, HD and grid cells in 1D or 2D environments. Several authors have attempted to address their characteristics in a three-dimensional (**3D**) environment; by building 3D structures (Stackman et al. 2000; Knierim and McNaughton 2001; Calton and Taube 2005; Hayman et al. 2011; Taube 2011), by Placing the animals in a no-gravity environment (Knierim et al. 2000) or by studying species that navigate in 3D environment such as bats (Ulanovski, personal communication). This is a very important and exciting path of experimentation but I will not discuss it further here for length consideration.

2.3.4.2 Walls, barriers and objects

An environment is limited by its borders. In a laboratory, most of the time these borders are walls. Walls seem to **anchor** the place fields in the current map. **Removing these walls** leads to a **loss of stability** of place cells or even their **remapping** as if the rat considered the environment as being new (Barry et al. 2006). As far as I know, the influence on grid and HD cells of complete removal of the wall has not been explored prior to the research conducted for paper #2. There we found similar results as with place cells. I will discuss these data further in the synopsis of results and the discussion.

Not only are walls perceived by the animal and influential on cell firing but **place cells** also tend to be in higher numbers **close** to **borders**, **cues** and **objects** (Hetherington and Shapiro 1997).

In **specific conditions** where distal cues are minimized and rendered

irrelevant, such as a non-spatial radial maze task, place cell activity can be dependent on the proximity of visual-tactile cues. In some extreme cases, some hippocampal cells code only for the cue, independently of the rat's location, and thus they can be named **cue cells** (Young et al. 1994). Hippocampal cells can be modulated by or develop conjunctive coding for place and object (Fyhn et al. 2002; Komorowski et al. 2009; Manns and Eichenbaum 2009) (see 2.3.5.2 on the modality of this development). Similarly, in different conditions, hippocampal cells' firing fields can follow specifically barriers placed in an environment when they are rotated, translated or even put in a new environment and thus they can be named **barrier cells** (Muller et al. 1987; Rivard et al. 2004). Three-dimensional objects do influence **place cell** activity, especially those receiving direct inputs from the **LEC** and **PER**, parahippocampal areas whose cells' activity is related to **objects** (Aggleton and Brown 1999; Murray et al. 2007; Burke et al. 2011; Burke et al. 2012; Deshmukh et al. 2012). One can suppose that the influence of walls, barriers, cues and objects on spatially modulated cells is linked to their use as **spatial landmarks** for navigation (especially in the absence of other reliable and salient landmarks) and thus is linked to their **behavioural relevance**. I will discuss this point in (2.3.5.2) and in the discussion.

Recent studies (Savelli et al. 2008; Solstad et al. 2008; Lever et al. 2009) reported cells in the subiculum and the PHR whose activity is closely linked to the border of the environment. I will present and discuss these results in the synopsis of results and in the discussion.

2.3.5 Non-spatial features

Place cell activity is not determined only by the position of the rat. Indeed, almost all place cells present what is called "**extra field firing**", some more than others. This is also referred to as **overdispersion** (Wikenheiser and Redish 2011). Overdispersion also qualifies as **"field firing variation":** even with a very robust place field, a place cell might be absolutely silent on a pass through the field. Vice versa, the firing rate at the place field sometimes greatly exceeds what can be determined by the time-averaged positional firing rate distribution (Fenton et al. 1998). This overdispersion could result from the existence of a **temporal code** lying on top of the spatial code ((Muller et al. 1996) (see 2.2.3.3) or from the influence of **non-spatial features**. In fact, non-spatial features such as **context, attention, on-going behaviour,**

behavioural relevance, goal/reward, current state of the animal, experience and **novelty** were found to influence greatly the activity of **place cells** and maybe to a lesser extent that of **HD** and **grid cells**. The latter are thought to be part of a **universal navigation system** ((Moser and Moser 2008), see discussion). I will here briefly present some of the data supporting these claims. As the reader can see, the list of non-spatial features encompasses overlapping notions.

2.3.5.1 Experience

I presented in 2.3.4 how manipulations of the environment's spatial features induce changes in place, HD and grid cell firing. Yet often the emergence of a **different pattern** of activity requires **repeated exposures** to the new configuration and is thus linked to experience, as observed for **geometrical changes** (O'Keefe and Burgess 1996; Mehta et al. 1997; Mehta et al. 2000). Such results seem to be linked to plasticity properties (Ekstrom et al. 2001). Similar backward shifts were observed with the preferred firing direction of HD cells (Yu et al. 2006).

To this point, I have focused on how the cell activity was changed by these manipulations. One could consider, alternatively, how their firing specificity is preserved in some conditions. For example, rotation experiments show that allothetic visual information (cue card) is important to **anchor** the firing spatial specificity (see 2.3.2), yet this spatial specificity remains more or less stable after removal of the cue. Thus the activity of the cell is influenced by the rat's **experience** and memory of the card (O'Keefe and Speakman 1987). Such **reverberatory activity** or **mnemonic trace** also exists in HD and grid cells (2.4.2). One study (Sharp et al. 1990) showed very convincingly the existence of reverberatory activity in place cells by recording their activity in a simple circular box with one cue card. The manipulation consisted of introducing a **second cue card** and then removing it. In some place cells, the presence of a new card led to the development of a **new place field**, which r**emained after the removal** of the card.

The effect of a **cue control** upon the cell firing specificity depends on how salient the cue is, but also on how stable it is. The **stability** of a cue is linked to the **animal's experience**, which thus could not only influence the activity of a cell but also the degree to which a cue controls the spatial and directional firing specificity. To test this hypothesis, rats were trained to navigate in a circular environment with a single salient cue card. They were divided into two groups: half of the rats were

disoriented before being placed in the cylinder, in order to disrupt their internal sense of direction, while the other half were not. Subsequent testing of the cue card control upon the firing specificity of place and HD cells showed that it was much weaker for the rats that had been disorientated during training (Knierim et al. 1995). Several other studies confirmed that the strength of cue control over place cells and HD cells depends on the **rat's learned perception of the stability** of the cues (Dudchenko et al. 1997; Jeffery 1998; Jeffery and O'Keefe 1999; Chakraborty et al. 2004).

Few studies discuss the influence of experience on **grid cell** firing pattern. In the discussion I will address some results, such as those obtained in the expansion boxes (Barry et al. 2007), in the light of the data presented in paper #2 (Solstad et al. 2008).

Experience and **novelty** are related. I will discuss how novelty affects the firing of place, HD and grid cells in 2.4 when discussing how these patterns emerge in novel environments.

2.3.5.2 Behaviour and behavioural relevance

In this paragraph, I will briefly present how on-going behaviour, behavioural relevance, goal/reward, attention and context influence HR principal cells.

Reward and task performance

Fig. 43 Influence of non-spatial features upon place cell activity (Dupret et al. 2010)

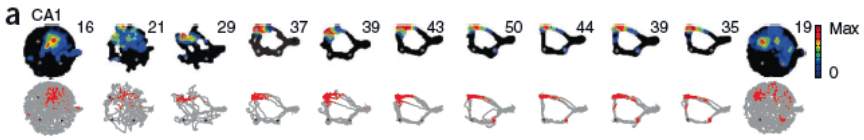

Progressive association of the CA1 place field to the goal location concomitant with the learning of a spatial task on the cheeseboard maze. Rate maps and trajectory with spikes.

One of the strongest associations seen is between **reward** location and place cell activity, whose place fields can follow the shift of a reward location (Breese et al. 1989; Kobayashi et al. 1997; Kobayashi et al. 2003; Ho et al. 2008; Dupret et al. 2010) (Fig. 43). Moreover, the progressive association between **reward object** and location (2.3.4.2) correlates with task **learning** and is thus dependent on the animal's behaviour (Komorowski et al. 2009; Dupret et al. 2010) and place cells seem to code for values of experienced events (Lee et al. 2012). Additionally, **changes in task demands** affect the firing statistics of place cells. For example, reducing the **number**

of reward points leads to less variability within a session (Wikenheiser and Redish 2011) or choosing a **behavioural strategy** in an object-place association task changes the prospective firing correlates (Lee and Kim 2010). It was recently shown that place cells can encode several task-related cognitive aspects via rate remapping (Allen et al. 2012). Contrary to place field location, the preferred firing direction of HD cells does **not seem influenced** by **reward** position and does not correlate with **behavioural choices** (Dudchenko and Taube 1997; Golob et al. 2001; Muir and Taube 2004) in spite of early reports stating a correlation with behaviour in LDN HD cells (Mizumori and Williams 1993), for disambiguation see (Muir and Taube 2002). The influence of **reward** or association with **performance** in spatial tasks for **grid cells** remains to be explored.

Ongoing behaviour and attention

The animal's **ongoing behaviour** can also influence place, grid and HD cell activity. I showed in 2.2.3.3 how the cells' firing rate is modulated by **movement** (i.e. heading and angular speed). The relation between firing rate and speed is intrinsically linked to theta rhythm modulation (but see (Ulanovsky and Moss 2007; Yartsev et al. 2011). Besides movement, **cognitive processing**, **attention** and **sleep** also influence both LFP and unit activity (Whishaw 1972; Eichenbaum and Lipton 2008; Ahmed and Mehta 2009; Diekelmann and Born 2010).

Attention-like modulation of **place cell** discharge has been shown by decoding global, attention-like states from ensemble discharge. Both the discharge rates and the spatial firing patterns of individual cells are distinct between "**attentive states**" and "**non-attentive states**" such that during the latter there is an excess of noise (Fenton and Muller 1998; Olypher et al. 2002; Fenton et al. 2010). Furthermore, identifying **attention-like states** improves reconstructions of the rat's path from ensemble discharge. These dynamic attention-like processes modulate discharge on an approximately **one-second time scale**. Attention processes **stabilize** place cell firing locations (Kentros et al. 2004).

One should be aware that such attention processes are linked to novelty/experience and involve **acetylcholine modulation** (Hasselmo and McGaughy 2004). **The firing properties** of hippocampal and EC principal cells (putative place and grid cells) are modulated ***in vitro*** by the application of a cholinergic agonist/antagonist. Furthermore, ***in vivo*** modulation of the cholinergic pharmacology

influences **place cells'** spatial **specificity** (Brazhnik et al. 2003; Hasselmo and Giocomo 2006; Heys et al. 2012). Attention-like modulation of HD and grid cells remains to be properly investigated.

Context

The definition of "context" is not clear and is linked to the features considered. Some have defined "context" in terms of **background cues** but it can also be considered in terms of **behavioural demands**, **temporal sequence of actions** or even **emotion**. Therefore examining the influence of context upon place, HD and grid cell firings overlaps with the reward, task and ongoing behavioural modulation mentioned above.

The literature on **place cell** activity **modulation** by spatial and behavioural context is wide (Nadel et al. 1985; Markus et al. 1995; Skaggs and McNaughton 1998; Mizumori et al. 1999; Wood et al. 2000; Song et al. 2005; Griffin et al. 2007). To illustrate this statement, I can cite a few experiments. For example, **different colour of the wall or a change of odour** can induce changes in the firing rate of place cells (Anderson and Jeffery 2003). Likewise, changes in task demands, such as retrieving a food **reward from two different locations** in an unchanging environment, lead to the development of highly context-specific place-cell firing patterns (Smith and Mizumori 2006). **Temporal context** for odour-sampling events is supported by a gradual change in the pattern of hippocampal activity (Manns et al. 2007; Ginther et al. 2011). One can also observe, as animals learn different meanings for items in distinct behavioural contexts (reward or no reward), the development of robust **conjunctive item-place coding** by hippocampal neurons that parallels the learning curve (Komorowski et al. 2009). Place cells respond differently according to the **task** the animal is performing (i.e. continuous spatial alternation, delayed spatial alternation or tactile-visual conditional discrimination) (Hallock and Griffin 2012). **Finally, emotional context,** such as fear, may lead to changes in preferred firing location (Moita et al. 2004).

Grid cell activity seems also to be modulated by spatial and behavioural context. Similarly to place cells, **different colour of the wall or different odour** can induce changes in the firing rate of grid cells (Alenda et al. 2010; Marozzi et al. 2012). Moreover, recordings of spatially modulated MEC cells (putative grid cells) show that their firing is dependent on **behavioural context** depending on where the animal had come from or where it was going (Frank et al. 2000). Simultaneous

recordings in the MEC and CA1 in animals continuously alternating left-turn and right-turn routes through a T-maze show that putative grid cells in the MEC more strongly distinguished left-turn from right-turn trials compared with CA1 place cells (Lipton et al. 2007). **HD cell** recordings have not yet shown any evidence of influence of context on their activity (Wiener et al. 2002).

Non-spatial coding

Until now I have mainly drawn a picture where all dorsal **hippocampal principal cells** were either **spatially modulated** or silent. This picture seems to be very **simplistic**, however, and only valid for very simple environments with no behavioural demands. In more complex environments, the activity of hippocampal cells is **not only modulated** by non-spatial features but also some cells seem to **code for behaviour variables** either **combined with or independently of location**. I started to present in 2.3.4.2 how hippocampal cells could code for cue or barrier independently of location. This association might depend on the behavioural relevance of the cue to performing a required task. There are many other examples of non-spatial coding in the hippocampus: units responding to **sniffing behaviour** (O'Keefe 1976), to **cue sampling** (Eichenbaum et al. 1987; Wiener et al. 1989), to **goal (or goal approach)** (Eichenbaum et al. 1987; O'Keefe and Speakman 1987; Wiener et al. 1989; Wood et al. 1999), to **events** (such as a jump) (Lenck-Santini et al. 2008), cells whose firing discriminates between **trial types** in a non-matching-to-sample task (Otto and Eichenbaum 1992; Wood et al. 1999), in an alternation T-maze task (Wood et al. 2000) or in a delayed-non-match-to-place task (Griffin et al. 2007). Recently, "**time cells**" were identified, coding for time delay independently of location (MacDonald et al. 2011). Therefore, as hinted in 1.3.4, to call hippocampus cells place cells might be a restrictive definition and one could rather use the term **"memory cells"** (Eichenbaum et al. 1999). The situation in the **PHR** is different: the cell population is more **heterogeneous** than in the HF such that HD and grid cells are intermingled with cells which do not code for space and direction. Among them some PHR cells were identified as coding for non-spatial features (Vann and Albasser 2011), yet no HD or grid cells were shown to switch their response from directional/spatial to non-spatial only, as has been shown in the hippocampus.

2.4 DYNAMIC PROPERTIES

I will present here the dynamic properties of place, HD and grid cells. As stated above, "dynamic properties" here are the **changes in** cell **activity** in response to **changes in the environment**. I have already presented (section 2.3) experiments using environmental changes in order to determine the cell discharge correlates: to what type of information the cell type responds preferentially, especially in a situation of conflict between different cues. In this section I will focus on cells' dynamic response to environmental changes and thus explore their **plastic properties**. I will continue to describe dynamic properties in the next section (2.5) where I will consider the response of ensemble cells as opposed to **single cells** that are the subject of the current section. This section is divided in two parts. The **first** part presents how the firing patterns of place, HD and grid cells change between two familiar environments – the situation often known as **remapping** (2.4.1). In the **second** part, I will discuss how such firing patterns develop in a **novel environment** (2.4.2).

2.4.1 Remapping (unit level)

It is considered that place cells and, by extension, HD and grid cells, by their spatial and directional specific firing, together map the environment. A change in their preferred firing location or direction is thus called **remapping**. Historically remapping was first introduced and quantified in place cells by recording their activity when exposed to small changes in simple environments (Muller et al. 1987) or by radically changing the environment (Thompson and Best 1989). Related effects were consequently observed for **HD cells** (Taube et al. 1990), **grid cells** (Fyhn et al. 2007) and border cells ((Solstad et al. 2008), see discussion) shortly after their respective discovery. Though all the mentioned cell types remap, their firing patterns adapt in different ways when exposed to multiple environments. I will attempt here to describe their **respective remapping properties**. Such properties can be considered at the unit or the network level. As mentioned previously, in this section I will discuss remapping at the **unit level** before moving on to the network level in the next section (2.5). This distinction is of course artificial, as a cell should always be considered as part of a network. However, this will help me to introduce the relevant concepts and mechanisms progressively.

I will start here by describing the different **degrees of intensity of remapping** (2.4.1.1): the different (or orthogonalized) representations of each environment and how much overlap subsists, both for **spatial/directional** and **discharge** properties

(see 2.2 for definitions of such properties). Secondly, I will take into consideration the many **factors modulating** the "degree" of remapping and how their influence can differ between cell types or areas (2.4.1.2). Finally, I will examine remapping **kinetics** (2.4.1.3).

2.4.1.1 Degrees of remapping

Firing patterns can be modified principally in three different manners. **The first** is a change in the cell's **preferred firing direction/location** compared with a common reference frame. **The second** is a change in the **firing rate**. Its most extreme situation would be complete silence of the cell in one of the environments. **The third** is a change in **spatial/directional specificity** that would translate to an increase or decrease of spatial/directional information or grid score. Its most extreme situation would be a cell firing independently of direction/location in one of the environments. These three types of modification of firing pattern can be observed independently or conjointly (Fig. 44 and 45).

Change in preferred firing direction/location: global remapping

When first described, remapping was referred to as a **change in preferred firing direction/location** compared with a common reference frame. This situation was later termed **global remapping**. All the mentioned cell types perform "global remapping" when confronted with a substantially different environment. It is not clear in situations of global remapping whether the **field characteristics** of **place cells** in one environment **predict** those of the other environment, in terms of field shape, firing rate, spatial information or number. Yet some studies have found some correlation of field size between environments (McHugh et al. 2007).

Fig. 44 Place cell global and rate remapping (Fyhn et al. 2007)

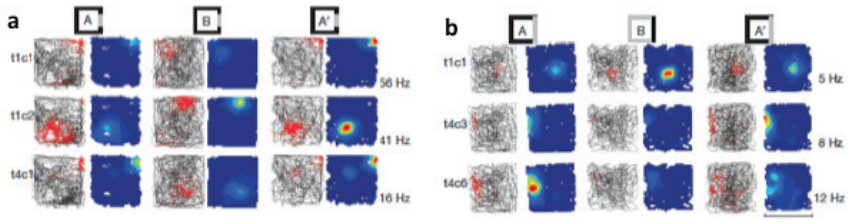

(a) Maps of three simultaneously recorded place cells in two different rooms (A and B) showing global remapping. **(b)** Maps of three simultaneously recorded place cells in two slightly different environments (A and B) showing rate remapping. Environment B is identical to A with the exception of A having three black walls and one white, and B three white walls and one black.Trajectory with spike positions; colour-coded rate map. Peak firing rate indicated in the bottom right corner.

The preferred firing direction of **HD cells** seems uncorrelated in two substantially different environments and neither is the **spatial phase** of **grid cell** nodes (Taube et al. 1990; Fyhn et al. 2007). Both HD cells and grid cells do conserve some properties from one environment to another, however. For HD cells, the **tuning curve half widths** remain stable (Taube et al. 1990) and also (to some extent) **grid scale** (Fyhn et al. 2007). **Grid orientations** do change in some conditions but not when both recording environments are located in the same room with the same distal cues available, introducing the notion of **two categories of global grid cell remapping**: one encompassing only a translation of the grid field phase, the other supporting both translation and rotation of the field, completely changing the reference frame. I will discuss the experiment supporting this conclusion in more detail while addressing network properties (2.5.4).

Fig. 45 Grid cell remapping (Fyhn et al. 2007)

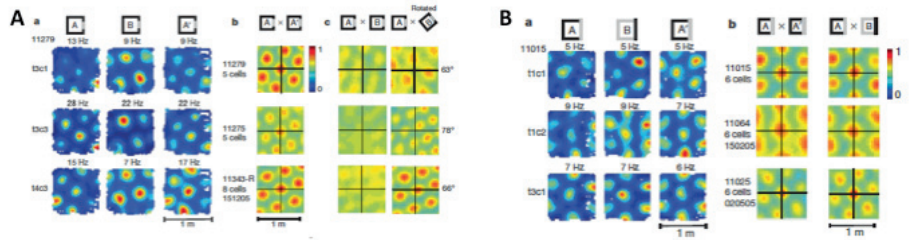

(A) Behaviour of simultaneously recorded grid cells in a situation inducing a global remapping of place cells. Note both a translation and a rotation of the fields. **(B)** Behaviour of simultaneously recorded grid cells in a situation inducing a rate remapping of place cells. Note the sole translation of the fields (and the lack of rotation).
For both (A) and (B): **(a)** shows representative examples of the rate maps of a three-cells ensemble. **(b)** shows the stacked autocorrelograms of three different grid cell ensembles.

Change in firing rate: from rate remapping to complete silence

As stated previously (2.1), place cells are fundamentally different from HD and grid cells regarding their **plastic properties**. Indeed, the latter two are active in all environments while **place cells** are often **silent** in a given environment. It is considered that **HD and grid cells** together form a **universal directional and metric system,** where universal means that it is applicable to all environments (Moser et al. 2008). The remapping expression of place cells is not uniform across **subfields** as one can see differences between **CA1** vs. **CA3** vs. **DG,** as will be discussed below (Leutgeb et al. 2004; Leutgeb et al. 2005; Leutgeb et al. 2007). In particular, though

DG principal cells are seldom active in a given environment, those that are **active** are active in almost **all environments** (Leutgeb et al. 2007; Alme et al. 2010).

Complete silencing of **place cell** activity in a given environment is often considered to be **global remapping**. However, in some situations when two environments present minor differences, place cells retain the same firing field location in both environments but present different field firing rates. Such a situation is called **rate remapping** (Leutgeb et al. 2005; Fyhn et al. 2007; Colgin et al. 2008). Rate remapping has been postulated as a way for the place cell to convey changes in non-spatial features (see 2.3.5). Experimentally, rate remapping has not yet been characterized in grid or HD cells. I will discuss further what factors influence whether place cells experience global or rate remapping in the next paragraph (2.4.1.2).

Decrease of spatial/directional specificity

When comparing firing patterns of a given cell between two environments, a crucial element to establish is whether the cell investigated is still spatially/directionally modulated with measures such as **spatial/directional information and coherence**. It is not clear whether a reduction of spatial/directional specificity can be qualified as remapping: it does not entail the emergence of a second map, but rather the disintegration of the first one. **Experimentally**, a reduction in spatial/directional specificity often emerges after withdrawal of allothetic or idiothetic information (see 2.3), when introducing conflicts between the cues (see below) or when the animal is placed in a completely novel environment (see 2.4.3). In theory such a situation can emerge from several scenarios: (1) the animal's **confusion** about its whereabouts which leads the representation to flicker between **multiple representations**, (2) the **weak anchoring** of the animal's representation in a stable **reference frame** which leads the representation to keep **drifting**, (3) the **slow kinetics** for a new representation to become established in a **new environment**, (4) unexplained **disparities** of spatial/directional **modulation** between environments due to external factors.

Finally, in a situation of cue conflicts, one can see the emergence of a new code superimposed on the former one (Knierim and Hamilton 2011) or its deformation concomitant with the change in the environment (O'Keefe and Burgess 1996; Barry et al. 2007). This mixed code is somehow reminiscent of what happens

with **partial remapping**, however, partial remapping is applied to an ensemble of cells and will thus be discussed in 2.4.2.

2.4.1.2 Factors influencing remapping expression

I have already presented in section 2.3 several remapping experiments while considering which features were controlling place cell activity. There I have shown that a remapping can be induced by changes in both spatial and non-spatial features inferred from allothetic or idiothetic information.

As remapping is induced by a change in **environmental features**, it is logical that the **saliency** of these features and the **intensity of the change** are highly influential in remapping expression (see 2.3 for examples) (Leutgeb et al. 2005; Wills et al. 2005). It is often admitted that minor changes in environmental features will induce rate remapping in place cells while more drastic changes will induce global remapping (Leutgeb et al. 2005; Fyhn et al. 2007).

Prior experience of the two different environments is also an essential factor, as can be the **number of exposures** to the remapping situation (Quirk et al. 1990; Bostock et al. 1991; Lever et al. 2002). The mode of **learning** of the environment is also very important, notably in which context it was first presented and differentiated from others (Colgin et al. 2010).

As demonstrated previously (2.4.1.1), **coherence** in the change of environmental features or introduction of **cue conflicts** is also an important factor.

Finally, strong differences exist in remapping expression not only between cell types (see 2.4.1.1) but also across **subfields**, as has been demonstrated for place cells recorded in **CA1** vs. **CA3** vs. **DG** (Leutgeb et al. 2004; Leutgeb et al. 2005; Leutgeb et al. 2007) affirming different roles for different hippocampal subfields. These differences between subfields are not yet clearly asserted. I will discuss them in more detail when presenting network remapping in 2.5.3. It seems that the integrity of external inputs to these different regions can influence remapping expression (Lu et al. 2012; Von heimendahl and Brecht 2012).

2.4.1.3 Kinetics

To complete the analysis of remapping expression of each cell type, it is crucial to consider its **kinetics** or **time course**. It is only quite recently that kinetic has started to be studied by the development of better performing analytic tools and behavioural installation. The study of remapping kinetic requires almost **instantaneous**

transformation of the environment, which can be achieved by switching the light off (Quirk et al. 1990; Fyhn et al. 2007) or other more sophisticated behavioural switching protocols (Jezek et al. 2011), or by rapid manipulations of the environment that take place while the rat is not aware of it (Knierim et al. 1998; Redish et al. 2000). This type of experiment allows access to two fundamental parameters: whether the new representation is established **progressively or at once** (i.e. fast remapping), and whether once established the second map is **stable or flickers** between representations.

Time-dependent processes govern **realignment** from one representation to another (Redish et al. 2000). In a situation of abrupt cue conflict generated by visual cue rotation while the light is switched off, both place cells and HD cells realigned quite fast with the new visual cues. However, when the rotation angle is very important, **place cells** stabilize their firing pattern faster according to visual cues than **HD cells**, which need a delay of over one minute before re-orienting (Knierim et al. 1998). However, this might only translate as differences in the nature of the control exerted by visual cues and not dynamic mechanisms. Other studies have shown that HD cells realigned as rapidly as 80 msec (Zugaro et al. 2003). Grid cells have also been shown to realign at least as fast as place cells (Fyhn et al. 2007, sup fig 11). It was demonstrated very recently that the transformation of the spatial context does not change the hippocampal representation all at once but is followed by temporary bistability in the discharge activity of **CA3** ensembles. Rather than sliding through a continuum of intermediate activity states, the CA3 network undergoes a short period of fast **theta-paced flickering between representations** of the past and present environment before settling on the latter (Jezek et al. 2011). One should be aware that the remapping dynamic is linked to the level of familiarity of the different environments. This will be discussed in 2.4.3.

2.4.2 Development of firing patterns in a novel environment

Fig. 46 Effect of novelty and experience on place and grid cells

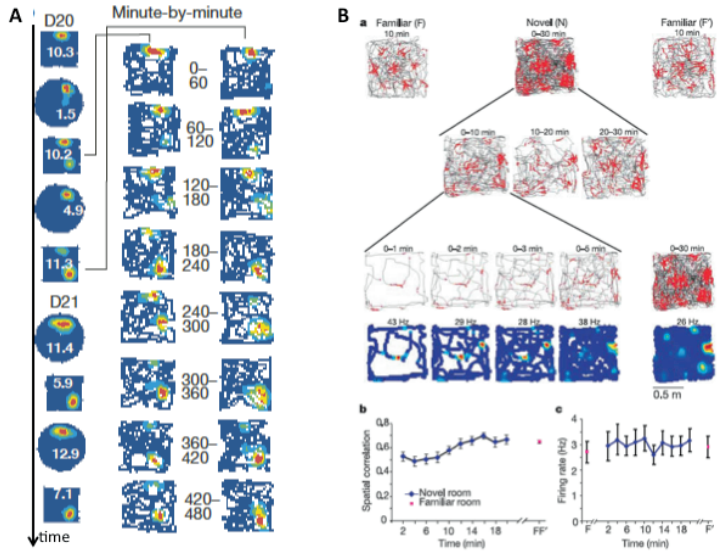

(A) Progressive dissociation with experience of a place field developed in a familiar (circle) and a novel (square) environment (from Lever 2002). Note the initial similarity between the field location and the progressive emergence of a new pattern in the square box**. (B)** Quasi-instantaneous development of a new firing pattern in a similar novel environment (from Hafting et al. 2005). Note that the grid pattern is not developed clearly at once when the novel environment is much bigger than the familiar one.

When considering environmental changes, a crucial distinction to establish is whether both environments are familiar or one is new. I will here address the latter situation and discuss how specific spatial and directional firings emerge in **novel environments** (Fig. 46). Before going further on that subject, I would like to open a parenthesis on the **definition of novelty**. Experience and novelty are tied to each other and it is difficult to assess how unfamiliar new environmental features are compared with what the animal has previously experienced. Thus, one should keep in mind that some "new environments" might be more familiar than others.

Place, HD and grid patterns do have **different dynamics** of emergence in a novel environment. It seems that HD cells establish faster than place and grid cells (see below). Originally, grid cell patterns were reported to become stable more quickly than place cells (Hafting et al. 2005), yet several recent studies report findings that do not support this (Barry et al. 2012).

Place cells form stable representations in a new environment after some minutes (Muller et al. 1987; Leutgeb et al. 2005). At first, their spatial **specificity** is

less robust (Wilson and McNaughton 1993), their average **firing rate** is higher (Nitz and McNaughton 2004) and other **firing and network properties** are transiently modified (Jeewajee et al. 2008; Lever et al. 2010), but these values reset rapidly on average to their baseline as the animal explores the new environment. The **kinetic** of the new field formation seems linked to how **unfamiliar** the new environment is. Indeed, if it presents only minor changes, the orthogonalization of firing patterns may happen gradually (Lever et al. 2002) while in other conditions previously silent neurons developed a place field over the course of a single passage through the environment (Frank et al. 2004). It has also been shown that orthogonalizing processes observed in CA3 are stronger in a novel environment. In general, **experience** influences place field parameters in predictive ways, possibly linked to plastic changes in synaptic weight (i.e. **backward shift**) (Mehta et al. 1997) or according to mechanisms assumed to be linked to **attention** (Olypher et al. 2002) and the **cholinergic system** (Ikonen et al. 2002). Interestingly, it seems that place fields require the rat to have **direct experience** of the environment to become established (Rowland et al. 2011). Remapping kinetic is also faster in CA3 than in CA1, supporting the hypothesis that CA3 plays a key role in the rapid formation of representations (Lee et al. 2004).

HD cells develop specific directional firing almost **instantaneously** (Mizumori and Williams 1993; Taube and Burton 1995; Stackman et al. 2003; Dudchenko and Zinyuk 2005). So far there are no reports of significant changes in rate and other firing properties of HD cells in a novel environment. Yet **experience** does influence HD cells' firing direction (Dudchenko and Zinyuk 2005) and plastic phenomena similar to place cells' **backward shift** have been described in ADN HDC (Yu et al. 2006).

Early studies of **grid cells** showed that firing location in a novel environment was mostly stable from the first time the rat passed through the area, both in light and in total darkness (Hafting et al. 2005). Though the grid pattern was present almost at once, the **firing rate** of the cells was initially lower and the specific spatial **stabilization** required some minimal exposure. It was reported that the grid pattern in a new environment is very similar to the familiar one in terms of scale but that direction and spatial phase will shift unpredictably. Yet detailed analyses showed that during the first exposure to a novel environment, grid **fields** are generally **bigger** (Fyhn et al. 2007), often **more elliptical** (meaning that they are skewed respective to

their 60^{o} symmetry), with a **lower gridness score** and changed **firing properties** (e.g. theta modulation) (Barry et al. 2012). These results are more similar to what is known about place cells than HD cells: they are not accountable for changes in running speed and, like place cells, these values progressively reset to their baseline with **experience** (Barry et al. 2012). **Acetylcholine** might be involved in many of these phenomena (Barry et al. 2012). Moreover, it seems that grid cells' responses to a novel environment are **not homogeneous**: some being almost unaffected while others have their pattern completely disrupted (Barry et al. 2012; VanCauter et al. 2012). I will discuss this point in more detail in the discussion alongside the experience-modulation of border cell patterns. Interestingly, contrary to place and HD cells, no backward shift is observed in the MEC (Frank 2002; (Hafting et al. 2008). Field symmetry can be observed, however it is independent of experience (Hafting et al. 2008).

2.5 NETWORK PROPERTIES

Until now I have mostly treated cells as individual units, yet, as mentioned above, this distinction does not reflect the reality. Units are indissociable from the network they belong to and only a consequent number of neurons make possible the **decoding** of the rat's trajectory/position/head direction by use of **vectors** instead of single points of activity. Moreover, it is essential to record from a large assembly of cells in order to **distinguish rules, as opposed to trends from isolated examples**. Finally, as established above (2.2.3), unit discharge is modulated by **network global rhythmic activity** (theta, gamma).

The constant improvement of recording techniques allows recording from larger and larger cell assemblies and from multiple areas. This plays a very important role in better understanding the **dynamic properties** of place, HD and grid cells, especially while creating **cue conflict situations** and observing what **reference frame** is followed by co-recorded cells (2.5.1). Such experiments make it possible to highlight whether there is only one perception and representation of space at a given time or if there is a dissociation and incoherence between units belonging to a local (or multiple) network. **Global and partial remapping** situations are fundamental to point out **network (in)coherences** (2.5.2). Some influential theories portray place, HD and grid cell networks as **continuous or discrete attractor networks**. I will explore this notion while discussing **pattern completion/separation** theories and

experiments (2.5.3). Finally, I will present some examples on how the activity of **multiple cell types and areas** can be influenced/coordinated in a more **global functional network** (2.3.4).

2.5.1 Reference frame and multiple active maps

Cue conflict situations have been essential to determine some **hierarchy** between **cues** and to define which cue(s) are followed by some or all concomitantly recorded units, thus setting a reference frame. It is especially useful to highlight whether there are **multiple representations of space** at a given time by showing incoherent responses of units belonging to the same network (Fig. 47).

Place cells have been recorded in environments presenting a mixture of both local and distal cues of different modalities (visual, olfactory, sensory) and sporting **double or triple rotations** that induce cue conflicts (Shapiro et al. 1997; Tanila et al. 1997). Such experiments have promoted the idea that there are **no strict rules** on what types of cue place cells follow even though they tend to be more influenced by **visual distal cues**. Moreover, co-recorded place cells do not necessarily see their place fields rotate together: place cell networks are sometimes **non-uniform** (see notion of partial remapping below). One should note that some conflict configurations disrupt completely the firing patterns and result in global or partial remapping (see 2.5.2). Furthermore, a close examination of place cells, even in a **stable multi-cued environment**, shows for many of them clear **"extra-field" activity** supporting the "**multi-map**" theory (Fenton and Muller 1998; Olypher et al. 2002). This **"overdispersion"** seems linked to **fluctuation of spatial attention** that alternates between distal cues and local/self-motion cues (Kentros et al. 2004; Fenton et al. 2010) and is accentuated by reward-related events (Jackson and Redish 2007). Recently, **theta-paced fast alternation** between maps in a single environment has been demonstrated in specific fast remapping situations (Jezek et al. 2011), see 2.4.1.3.

Fig. 47 Heterogeneity of place cell responses to a conflict reference frame situation (Knierim 2002)

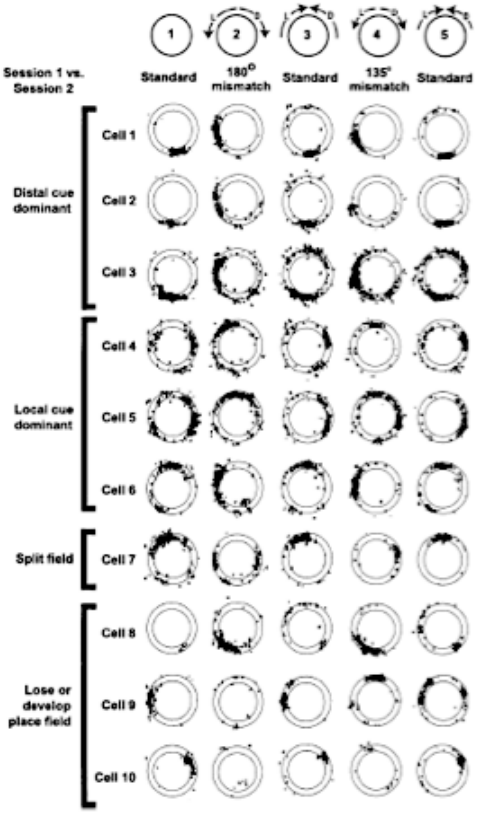

Mismatch between distal and local cues. Activity of 10 simultaneously recorded cells. Note the existence of four types of responses. The *black dots indicate* the location of the rat when each spike was fired.

Contrary to what is observed for place cells, the **properties of HD cell ensembles are rigid**: relationships between cells are retained from one environment to another (Taube et al. 1990; Taube 1998; Hargreaves et al. 2007). Furthermore, studies inducing **conflicts between cues** show that the preferred directions of co-recorded HD cells shift (remap) by **similar amounts** in a coherent manner, yet not necessarily following a specific cue (Knierim et al. 1995; Kudrimoti et al. 1996; Muller et al. 1996; Zugaro et al. 2000; Zugaro et al. 2004; Yoganarasimha et al. 2006; Knight et al. 2011; Clark et al. 2012). In spite of these differences, one should note that in situations where place fields rotate following a cue, **strong coupling** exists between rotation of preferred firing location/direction in **place cells** and HD cells (Knierim et al. 1995; Knierim et al. 1998).

Simple rotation experiments with concomitantly recorded **grid** and **HD** cells show that they are tightly **coupled** and rotate by similar amounts (Sargolini et al. 2006). Multisite recordings of place, HD and grid cells show that the cell population is usually coherent; yet rather more discrepancies can be observed with place cells (Knierim et al. 1998; Hargreaves et al. 2007). More results on the subject of the effect on cue rotation on all cell types can be found in (Knierim and Hamilton 2011). I refer the reader to the discussion for the description of the behaviour of border cells and PrS/PaS grid cells in such experiments.

2.5.2 Ensemble remapping: Global vs. partial remapping and network coherence

When **theorizing** on the remapping of an **ensemble of cells**, **three configurations** are possible. **First**, all cells could remap in a **uniform manner**, respecting the **topological constraints** between each other's representations. This situation would be, in an extreme case, equivalent to a combined **translation and rotation of a rigid map** and in a more flexible case in a high percentage of overlap between concomitant firing cells in both environments. **Second**, **all cells** could remap in a **non-predictive way** such that the new preferred firing location and directions would emerge randomly, independently of the previous configuration. **Third**, a subset of cells within the population could present a global remapping, others a rate remapping and a different subset could appear unaffected by the environmental changes. Such a **non-uniform** situation is referred to as **partial remapping** (Quirk et al. 1990).

Experimentally, similarly to what is observed at the single cell level (2.4.1), network dynamic remapping expression depends on the intensity of the change in the environment, the cell type considered and its anatomical location.

HD cell (Taube and Burton 1995; Kudrimoti et al. 1996; Zhang 1996; Zugaro et al. 2003; Johnson et al. 2005; Yoganarasimha and Knierim 2005; Sargolini et al. 2006; Yoganarasimha et al. 2006) and **grid cell** ensembles (Fyhn et al. 2007; Colgin et al. 2008; Jeffery 2011; Marozzi et al. 2012) are both active in all environments and exhibit **coherent remapping** as described in the first theoretical configuration outlined above of a **rigid universal map**. While remapping, they maintain their relative firing direction/spatial phase relationship between **co-localized cells**. However, it is not clear yet whether these rigid relationships extend to all the HD and grid cells of the animal, forming a **continuous map**, or whether cells from different areas (or subareas) cluster into independent modules supporting **multiple maps** (Fyhn

et al. 2007). Recent findings on the influence of **compression of the environment** on grid cells support the latter (Stensola et al. 2012).

Place cells exhibit different remapping dynamics. As mentioned above, these dynamics strongly depend on the intensity of the change in the environment and the anatomical location of the cell type. When presented with an **intense change**, all place cells display **global remapping**. Only a fraction of cells are active in both environments while the others are silent either in one or both. Cells co-active in one environment are not necessarily co-active in another. The **absence of coherence** is also seen at the spatial phase level: two cells with neighbouring field in one environment do not necessarily have neighbouring field in the second environment (Kubie and Muller 1991). **Partial remapping** is observed in situations of cue conflicts leading to the existence of multiple references of frame (Fig. 47). Such configurations emerge from multiple rotations of different cues (see 2.5.1) (Knierim et al. 1998) or when the two environments are quite similar (Skaggs and McNaughton 1998; Anderson and Jeffery 2003). Recording of place cell location influences partial remapping dynamics: in a multiple rotation situation leading to partial remapping, the **population coherence** is **stronger in CA3** than in CA1 (Lee et al. 2004).

Multi-site recordings have determined that some **remapping coherence** exists between multiple cell types and areas (Knierim et al. 1995; Yoganarasimha and Knierim 2005); Hargreaves, 2007; (Sargolini et al. 2006; Fyhn et al. 2007; Hargreaves et al. 2007), yet not in a systematic rigid manner. Strong links have however been highlighted between the dynamic behaviours of the cell types: for example, whether the **grid cell** population is **remapping or not** in response to an environmental change, dictates the type of remapping (respectively **global or rate remapping**) expressed by CA **place cells** (Fyhn et al. 2007).

2.5.3 Attractor network and pattern completion/separation

Remapping encompasses the notion of **pattern separation**, which is an **orthogonalization process** maximizing differences between correlated input patterns in order to reduce interferences between stored information, as opposed to **pattern completion**, which is a process that reconstructs a complete memory (e.g. map) from a fragment of it (Leutgeb et al. 2004) (Fig. 48 and 49).

Fig. 48 Cell assemblies with attractor dynamics (from Leutgeb et al. 2005)

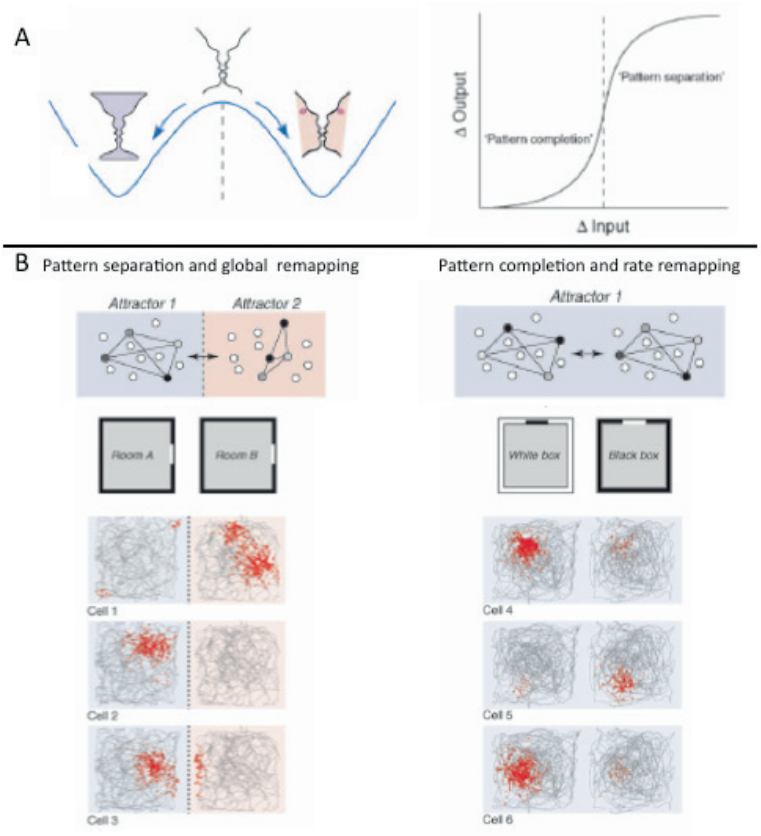

(A) Patterns that are ambiguous converge to a matching familiar pattern (pattern completion) and, at the same time, diverge from similar interfering patterns (pattern separation). The perceived image fluctuates between two familiar images (blue or pink) instead of stabilizing in the middle (white). Attractor networks are thought to induce sharp transitions between network states during progressive changes in the input pattern. **(B)** Spikes (red dots) were recorded from pyramidal cells in CA3 of a rat that was running in a square box. Grey lines indicate the path of the rat. (left) Place fields were tested after the recording room was changed but not the local cues, (right) or after the local cues were changed but not the recording room. Three cells are shown for each condition. When the room changed (left), the distributions of firing rate and firing position were completely orthogonalized, suggesting that the population vector spanned statistically independent vector subspaces and switched between attractors 1 and 2 (pattern separation). When only the cue configuration was changed (right), there was a substantial change in firing rates but no change in firing location, suggesting that the population vector spanned the same subspace as different states of the same attractor (pattern completion).

Because of its **collateral recurrent** network, it has been proposed that **CA3** has the role of an **auto-associative network** leading to **pattern completion**. The fact that the CA3 population remains more coherent in a slightly altered environment situation pleads for that case (Lee et al. 2004; Vazdarjanova and Guzowski 2004) as do other studies demonstrating the crucial role for CA3 in memory acquisition (Nakazawa et

al. 2003). However the propensity of CA3 units toward pattern orthogonalizsation in response to environment modification versus CA1 units is **not yet clearly established**. Some studies have shown that when exposed to minor or major modification of the environment, respectively, CA3 units are more prone to rate or global remap while CA1 unit patterns remain unchanged (Leutgeb et al. 2004; Leutgeb et al. 2005), this effect being even stronger in novel environments (see 2.4.1.1). Yet other studies have shown that CA1 were more prone to global remapping in response to different behavioural manipulations (Lee et al. 2004; Dupret et al. 2010). It is clear that CA1 and CA3 have different ratios of remapping-strength vs. environmental-alterations-intensity, as suggested by co-activation studies (Vazdarjanova and Guzowski 2004).

On the other hand, it has been hypothesized that the **DG** is a source of pattern separation based on the **sparse** level of firing of the granular cells (Jung and McNaughton 1993; Chawla et al. 2005) and the sparse connection from DG to CA3 (Amaral et al. 1990). Recent studies support this theory by showing that, compared with CA3, granular cells firing pattern are even more **sensitive to small environmental changes** (Leutgeb et al. 2007). Furthermore, when exposed to gradual modification of the environment (i.e. **morphing** of the shape of the recording box from a square to a circle), CA3 place cells show gradual changes in rate, mirroring environmental changes (rate remapping), while granular cells **remap** in a **non-coherent** way (more on morph experiments below) (Leutgeb et al. 2007). Very recently, it was shown that young dentate granule cells mediate pattern separation, whereas old granule cells facilitate pattern completion (Nakashiba et al. 2012).

A large theoretical body of work proposes that the generation of spatial and directional signal is based on a self-organizing and self-sustaining system, as originally proposed in Hebb's cell assembly theory (Hebb 1949). Such systems have been described as **attractor networks** (Hopfield 1982; McNaughton et al. 1996; Samsonovich and McNaughton 1997; McNaughton et al. 2006) where representations oscillate between stable attractor nodes of lowest energy. To picture that concept, one can imagine a **landscape of energy** made of hills and valleys. If a marble is dropped in that landscape, it will roll until it finds the lowest point of a valley. In that metaphor, the valleys represent the stable attractor nodes and the marble is the spatial/directional representation. An attractor network can be continuous or discrete.

In a **continuous attractor network**, each possible node has equal energy and thus they all are equal stable attractor **points** as if the energy landscape were flat. A **discrete network contains** only a **few stable nodes** and, when enough energy is applied, the representation will "**jump**" from one to another, abruptly, without passing by intermediate representations.

Fig. 49 Pattern completion/separation processes in the grid-place cell system (Leutgeb et al. 2007)

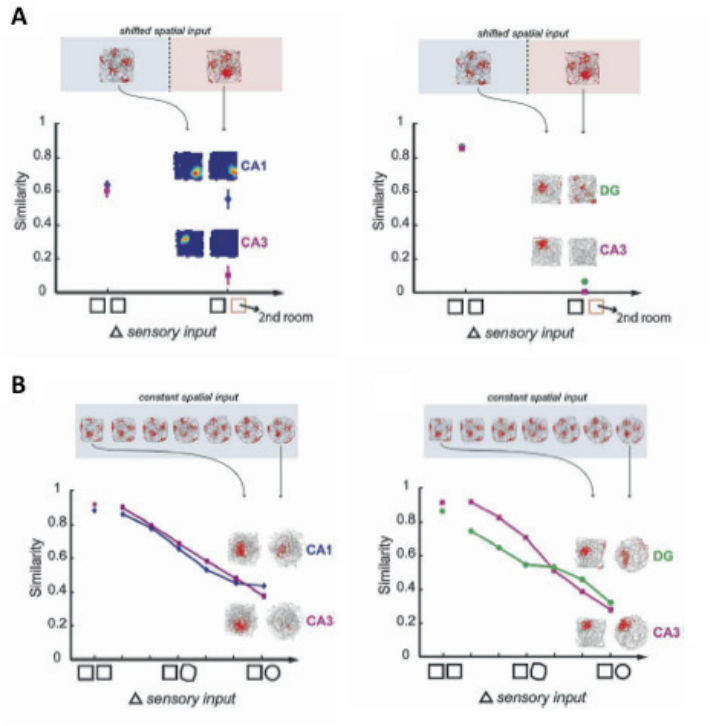

(A) Comparison between the different fields of the hippocampal formation (CA1, CA3 and DG) of place cells recorded in similar squared environment located in the same or in different room. Note an orthogonalization of the patterns in DG and CA3 that contrast with conservation of the patterns in CA1. Note the situation in two different rooms leads to an orthogonalization of the grid patterns in the MEC (represented by the annotation shifted spatial inputs above the graph). **(B)** Comparison between the different fields of the hippocampal formation (CA1, CA3 and DG) of place cells recorded in a "morphing" environment that morphs from a square to a circle. DG, CA3, and CA1 cells showed robust rate remapping while their firing locations remained unchanged. Note the morphing situation leads to constant grid patterns in the MEC (represented by the annotation constant spatial inputs above the graph).

Direction representation has been hypothesized to be supported by a continuous attractor network (McNaughton et al. 1991; Zhang 1996; Goodridge and Touretzky 2000; Sharp et al. 2001; Xie et al. 2002; McNaughton et al. 2006). In those models, **HD cells** are connectively organized in a circle according to their preferred firing direction: when the animal rotates, successive HD cells are activated. The transfer of

energy could then be supported by the presence of conjunctive HD and angular velocity cells. Extensions of these models were subsequently proposed to explain mechanisms for the generation and path integration of **place cells** and **grid cells** (Skaggs et al. 1995; Sharp et al. 1996; Touretzky and Redish 1996; McNaughton et al. 2006). I will discuss some of these models in the light of the results of this thesis in the discussion.

To resolve whether continuous or discrete attractors represent space in **place cells**, "**morph experiments**" were designed, in which rats were taught to distinguish two environments (i.e. square vs. circle). Once two different stable representations were established, the animals were exposed to intermediate environments between the two configurations. If the space is a **continuous attractor**, one should see a **progressive smooth transformation** from one representation into another with intermediate representations mirroring intermediate environments. On the other hand, if the space is a **discrete attractor**, one should see a **brusque jump** in representations. Experimentally, both abrupt and gradual transitions between representations can be observed, depending on the amount of **prior exposure** to the original environments and whether they were initially presented during the **learning period**, as a continuous compartmented environment or two different ones (Leutgeb et al. 2005; Wills et al. 2005; Leutgeb et al. 2007; Colgin et al. 2010). In practice, it translated to the fact that when the animal initially learned the mazes in two different locations the transition between representations was abrupt, but if the mazes they learned to discriminate were initially presented to them in the same location, the transition was smooth.

As stated previously, different **cell types**, or similar cell types recorded from different **subfields,** express **different dynamics** when exposed to such "morph experiments". More specifically, it was shown that in some specific experimental conditions leading to coherent rate remapping in **CA3**, **DG** place cells show erratic remapping between their different place fields and **grid cells** seem unaffected (Leutgeb et al. 2007).

The existence of **partial remapping** in situations of cue conflict cast doubt on attractor network theories (Knierim 2002; Jeffery 2011). These difficulties could be circumvented by supposing that, in some situations, attractors fragment in **sub-maps**. Another explanation reconciling attractor network theory with partial remapping is that, in a situation of cue conflict, the confused rat's representation of space could

oscillate between several maps. Finally, place cells could indeed be parts of a hippocampal attractor network, that may be weak relative to the inputs from external sources, such as representations of the sensory environment and representations of heading direction, in a familiar, well explored environment. I will discuss further below how network theory and results of remapping experiments, in the light of the results presented in this thesis, integrate in the latest grid/place/HD cell formation theory (see discussion).

2.5.4 Global functional network: interaction and coordination between areas

Throughout this introduction I have attempted to present where and how spatial cognition is processed in the brain. An important conclusion point here is that it is computed in an interactive and coordinated manner over several brain areas. In this subsection I will present evidence in support of that statement based on studies of connectivity, lesion/inactivation, postnatal development and coordination of ensemble activity. Moreover, for as much as spatial and directional signal is distributed over a widespread circuit of interconnected areas within the **HR network**, this network **interacts and communicates with areas external to the HR,** such as the thalamus, the vestibular system, the cerebellum, the lateral mammillar nuclei, the septum, the retrosplenial cortex and several others. The functional ramifications of that complex network is further strongly supported by a large literature based on lesion or inactivation of specific HR subareas or of connected areas that lead (or not) to the impairment of navigation skill or of the spatial/directional code in intact areas. I will give further consideration to that subject in the discussion.

2.5.4.1 Lesion and inactivation studies

In 1.3.4 above, I mentioned some studies giving insights in the mapping of different subareas role in spatial cognition by correlating rat's spatial performances with the location and the spread of eventual brain lesion/inactivation. This question was further addressed by assessing how place, HD and grid cell static, dynamic and network properties as well as discharge correlates are affected by specific lesion/inactivation of subarea that they received projections from.

The literature is quite abundant on whether there is loss of stability or of anchoring ability in **place cells** in response to the lesion/inactivation/disconnection of other HR areas such as the EC (Miller and Best 1980; Brun et al. 2008; Van Cauter et al. 2008), subfields of the HF (McNaughton et al. 1989; Mizumori et al. 1989; Brun et

al. 2002; Nakashiba et al. 2008), the PrS or PaS (Calton et al. 2003); (Liu et al. 2004), the POR and PER (Muir and Bilkey 2001; Muir and Bilkey 2003; Nerad et al. 2009); or non-HR areas like the septum (Mizumori et al. 1989; Leutgeb and Mizumori 1999; Ikonen et al. 2002; Koenig et al. 2011; Brandon et al. 2012), the lateral dorsal thalamic nucleus (LDN)(Mizumori et al. 1994), the locus correleus (LC) (Berridge et al. 1993), the vestibular system (Stackman et al. 2002), the prefrontal cortex (PFC) (Kyd and Bilkey 2003; Kyd and Bilkey 2005), the retrosplenial cortex (Cooper and Mizumori 2001), the cerebellum (Rochefort et al. 2011), and the ventral tegmental area (VTA) (Martig and Mizumori 2011).

Similar studies have tested **HD cell** stability by lesioning/inactivating the HF (Golob and Taube 1999; Hafting et al. 2008; Bonnevie et al. 2012), the thalamic nuclei (N): antero-dorsal (ADN) (Goodridge and Taube 1997) and latero-dorsal (LDN) (Golob and Taube 1999), dorso-tegmental nuclei of Gudden (DTN) (Bassett et al. 2007), the latero-mamillar nuclei (LMN) (Blair et al. 1999) (Bassett et al. 2007; Sharp and Koester 2008), the vestibular system (Stackman and Taube 1997; Stackman et al. 2002; Muir et al. 2009), the septum (Brandon et al. 2011; Koenig et al. 2011).

Finally some studies have tested changes in **grid cell** properties in response to a lesion/inactivation of the HF (Hafting et al. 2008; Bonnevie et al. 2012), the LMN (Sharp and Koester 2008) or the septum (Mizumori et al. 1992; Brandon et al. 2011; Koenig et al. 2011). The results of these studies are essential to understand the **origin of the spatial signal**. I will discuss this in more detail in the discussion.

2.5.4.2 Cell ensemble spatial coordination

The vast literature on lesion/inactivation partially presented above clearly establishes that spatial and directional signals are dependent on the integrity of several specific areas belonging to a **global network**. However, it is not completely defined how these areas i**nteract** and **coordinate** their respective activities. To address this issue, one can analyse the behaviour of cell ensembles during **remapping** and simple or conflictual **cue rotation**/modification. There are several **levels of cell ensembles**: (**1**) ensemble of the same type of cells all belonging to the same area (e.g. CA1 place cells), (**2**) ensemble of different types of cells (e.g. CA1 and DG place cells), (**3**) different types of cells all belonging to the same area (e.g. MEC HD and grid cells), (**4**) different types of cells from different types of areas (e.g. PrS HD and CA1 place cells). I have already presented in 2.5 how place and HD cells behave in situation (1)

and (2) and grid cells in situation (1). Situations (3) and (4) were assessed by further studies (Knierim et al. 1995; Taube and Burton 1995; Fyhn et al. 2007) (Knierim et al. 1998; Sargolini et al. 2006); (Hargreaves et al. 2007). I will address in the discussion how paper #1 and #2 complete this picture by showing how border cells seem to behave in situation (1) and grid cells in situation (2).

The main conclusion of this review is that **HD and grid cells** seem to behave as a **quite rigid ensemble,** while **place cells** show much **less coherence,** especially when **divided by subareas**. I will nuance this conclusion further in the discussion in the light of papers #1 and #2 as well as other recent studies.

2.5.4.3 Temporal coordination

The results reviewed above settled that spatial and directional signals are distributed across a relatively **coherent network**. They do not address, however, how cells belonging to different areas **coordinate and communicate** together. The investigation of these cells' firing properties makes it possible to answer such questions. Temporal coordination of activity can be seen by the **coherence between synchronous neural activities** detected in the LFP of connected areas. These **synchronous oscillations** cover different frequencies (e.g. **theta**, **gamma**) and their occurrence often reflects a **specific brain state** (see 2.2.3.3). They are thought to regulate communication between areas by **facilitating inputs** on the targeted area at a certain brain state or by **tuning to the same frequency** areas, whose dialogue is privileged at a given point against potentially interfering information from different sources (Colgin et al. 2009; Buschman and Miller 2010; Colgin 2011; Peyrache et al. 2011; Kim et al. 2012). Some hypothesize the existence of **synchrony generators**, such as the septum for the theta, that allow tuning in the brain to a certain frequency while being engaged in a specific behaviour. Such activity might be influenced by **neuromodulation** (Newman et al. 2012).

Coherence has also been shown at the **single neuron level**: between single unit activities or between unit sequences belonging to at least two areas. This phenomenon has been observed during specific brain states, such as sleep, where multi-cells firing-sequences evoked by awake-experience were replayed. Recently, it was shown that specific network electrical events such as **sharp wave ripples**, occurring both during sleep and wakefulness, were temporally coordinating the **unit reactivation** over different areas to reflect the same experience (Ji and Wilson 2007),

and that they could be **orchestrated by gamma synchrony** (Carr et al. 2012) and **silence neocortical inputs** to avoid any interferences (Logothetis et al. 2012). Temporal coordination has also been observed in situations of learning and novelty (Cheng and Frank 2008).

OBJECTIVES

At the core of this thesis are the modalities of **distribution and coding of spatial information** in the **hippocampal region** (HR). In itself, this subject resonates with the more general question of the **localization of cognitive processes**.

As stated previously, **cognition** is a generic term that encompasses many different notions. One can think of it as a course of action that covers several stages: **(1) perception** of the information, **(2) encoding**/acquisition of knowledge (learning), **(3)** the actual **processing** whose output in the case of spatial cognition is a representation of the external space and of one's self-location, and **(4) "recall"** of the information to use it in a given behaviour, which is **navigation** in the case of spatial cognition.

In this thesis I focus on the **processing of information**, which, for **spatial cognition**, takes place to a great extent in the HR. As discussed earlier, processing is a generic term that includes several mechanisms such as integration, transformation/translocation, consolidation/stabilization, enhancement/silencing, and comparison of the signal. These definitions of cognition and information processing are partly inspired by the memory stages theory (Atkinson and Shiffrin 1968). The study of the properties and distribution of spatially modulated cells gives insights into spatial information coding which can be extrapolated to general information coding.

Objective 1. Neural code for the boundaries of the environment

A first question here was the **nature of the information coded at the neural level**. As demonstrated in the introduction, three cell types had been characterized in the HR as coding for spatial variables: the place cells, the head direction (HD) cells and the grid cells. Together, these cells encode the **information needed to navigate accurately**: information on position, direction, metrics, and velocity. Yet, the **code for the border of the environment**, though an essential component of spatial cognition, had until then only been expressed as a factor influencing the firing of place and grid cells. The main objective of paper #1 was to supply this surprising lack and to demonstrate the existence of HR neurons specifically coding for the geometrical borders of an environment.

Objective 2. Distribution of the spatial code over the parahippocampal network

The second question concerned **distribution of the spatial information over the hippocampal network**. In the introduction I showed that place cells have been characterized in several subareas of the hippocampal formation, that the HD cells had been observed in two subareas of the parahippocampal region (PHR): the presubiculum (PrS) and the medial entorhinal cortex (MEC), and that the grid cells had only been seen in one of these subareas: the MEC. The main objective of paper #2 was to test whether **grid cells are found outside of the MEC** by recording in two PHR subareas that gives afferences to the MEC (i.e. the pre and parasubiculum: PrS and PaS). The second objective of that paper was to observe how the **properties** of the three main PHR subtypes (i.e. HD, grid and border cells) **are distributed over three PHR subareas** (i.e. MEC, PrS and PaS). This resonates with the question of modalities of information processing: serial or parallel. To achieve the second objective, a parallel objective was uncovered: the development of **new quantitative methods** for the characterization of HD, grid and border cells.

Objective 3. Origin of the spatial code

Together, paper #1 and #2 gave rise to the third question enunciated in this thesis: the **origin of the signal**. Indeed, the analysis and comparison of the HD grid and border cell properties over a distributed network led to the understanding of how different brain areas may be involved in the **generation and stabilization** of the signal. Some of the main mechanisms addressed here were the role of the **network oscillations** such as theta oscillations and the relative **need for directional and boundary information** to obtain a spatial signal. Finally the distribution of several properties over different subareas makes it possible to test whether some **cellular properties** typical of only some specific areas are necessary to generate a given signal.

Objective 4. Anatomical identification of the subareas of the hippocampal region

The fourth question here was the **anatomical discrimination** between the different subareas of the HR by the establishment of **clear architectonic markers**. As shown in the introduction and highlighted by the objectives of papers #1 and #2, the hippocampal region is constituted of several functional systems distributed over very precise subareas. The increase in accuracy of recording and manipulation techniques has led to a more and more **sophisticated and detailed positioning of neural properties and functions**. However, the scientific community was confronted with

the problem of a lack of clear markers of the HR anatomical borders valid in all major plans of sectioning and easily recognizable, even by the non-specialist. Paper #3 attempts to solve that problem by proposing a fine-grained anatomical description of the parahippocampal-hippocampal region, its subdivisions and their anatomical borders, integrated in a web-based application, providing an **interactive three-dimensional atlas**. This interactive and flexible framework offers a **didactic tool for experimentalists** to help them to find their way in the often complex anatomy of the hippocampal region.

SYNOPSIS OF RESULTS (REVIEW OF THE PAPERS)

Paper 1: Representation of geometric borders in the entorhinal cortex

As reviewed in the introduction, the **navigational system** of the hippocampal region (HR) is supported by a set of specialized neurons coding for location (place cells), direction (head direction cells) and metrics (grid cells). However, a large portion of the HR cells seem to be spatially modulated and their specific correlates have not yet been identified. Paper #1 reports the **discovery of a new type of cell** in the parahippocampal region: the **border cells**.

Fig. 50 Border cell

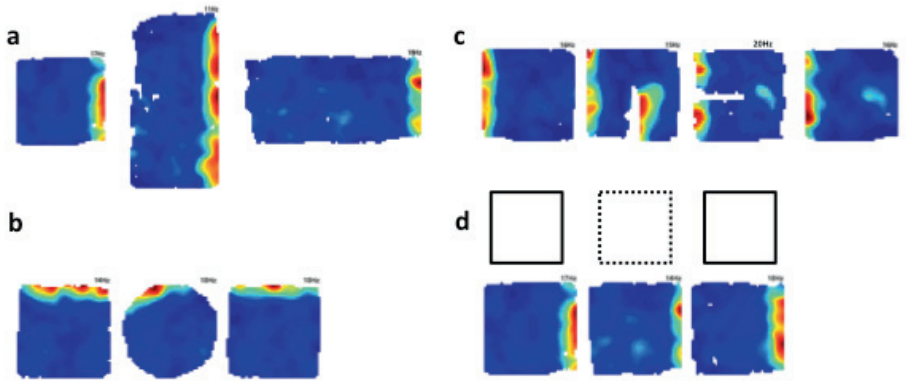

Colour-coded rate maps of a representative border cell in different environments **(a)** Original squared environment stretched in a rectangle in either the longitudinal or the latitudinal dimensions. **(b)** Environments of different shapes. **(c)** Introduction of a discrete wall (visible as a line of white pixels). Note the reminiscence of a field after removal of the wall in the far right map. **(d)** Removal of the walls surrounding the environment. Maximum firing rate in red, minimum in dark blue, pixels not covered are white. Peak firing rate is indicated above each panel.

Border cells are **defined** by the fact that they **fire specifically** when the animal is close to the **borders of the environment**. Their specificity of activity is **stable** within and between sessions even when separated by several days. The orientation-specific, edge-apposing activity of these cells is maintained when the environment is **stretched** and during testing in enclosures of **different shape** in a **different room** (Fig. 50a and b). Their **plasticity** properties are thus reminiscent of those of the MEC grid cells **active in all environments**.

The specificity of coding for the border of the environment was verified by inserting a **discrete wall** in the enclosure, which led to the emergence of an **additional field** following the initial field but with the same orientation (Fig. 50c). To

test if these cells were responsive only to physical walls or to the more general concept of environment boundaries, the **walls were removed** to leave the rat on an elevated platform so high that it could not jump from it. In such conditions, the specificity of **firing remained attached to the border** of the environment (Fig. 50d).

To identify cells quantitatively as border cells, their "**border score**" was computed by the difference between the maximal length of a wall touching a single firing field and the average distance of the fields from the nearest wall, divided by the sum of those values. However, paper #2 showed later that this score is not optimal (see discussion).

Analysis of the distribution of border cells shows that these cells are relatively **sparse**, making up less than 10% of the local cell population, but they are present in the **MEC**, **PaS** and **PrS**, often intermingled with HD cells and grid cells. Paper #2 gives a more precise account of the distribution of border cells, notably between layers.

The study of the **static properties** of border cells shows that their spatial modulation may vary from one cell to another. Differences concern the **number of walls** their firing is attached to: it seems that all possibilities may exist (i.e. in a square environment, it can be one, two, three or four walls, see Fig. 51), the "**wideness**" of the firing field (i.e. distance from the wall during which the field is continuous), or their "**sharpness**" (i.e. ratio intra vs. extra field firing). Moreover, a consequent proportion of border cells **code conjunctively for head direction** in addition to their spatial code and independently of the constraints of the rat's position in the firing field (see paper #2 for quantitative analysis). The main difference in **discharge properties between** border cells and grid cells is that only a portion of them (i.e. **about half**) see their activity modulated by the **theta oscillations** recorded in the local field potential (see paper #2).

Fig. 51 Number of walls

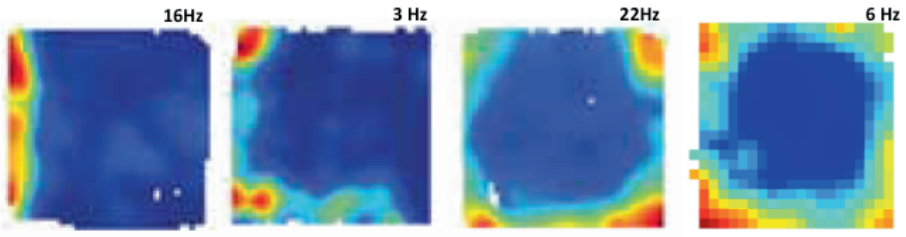

Colour-coded rate map of representative border cells with their firing attached to (from left to right one, two, three or four walls). Maximum firing rate in red, minimum in dark blue, pixels not covered are white. Peak firing rate is indicated above each panel.

Rotation experiments show that their **discharge correlates** with **allothetic** visual cues. The control from idiothetic information was not tested. **Spatial features** such as barriers did influence their firing pattern. Activity seemed independent of the context. However, the great variation in **sharpness** from one border cell to another (and their sometimes consequent extra field firing) may be explained by the influence of **unidentified secondary correlates** and **experience** (see discussion).

The study of the **dynamic properties** of border cells revealed some fundamental differences from place cells, as they are active in all environments, in a similar manner to grid and HD cells. Their **remapping** properties should be studied in greater detail, however. In addition, the development of their firing pattern in a **novel environment** remains to be explored (see discussion).

The study of the **network properties** of border cells showed that, in situations of remapping or cue rotation, all border cells concomitantly recorded do remap or rotate in a coordinated manner between themselves and with the grid and HD systems.

Border cells may thus be instrumental in **planning trajectories** and **anchoring grid fields and place fields** to a geometric reference frame in a similar way to the theoretical model of **boundary vector cells** (BVC) (see discussion).

Recent studies (Savelli et al. 2008; Solstad et al. 2008; Lever et al. 2009) reported cells in the subiculum and PHR whose activity is tightly linked to the border of the environment. I will present and discuss these results in the discussion.

In addition to the description of border cells, paper #1 tests further the **influence of boundaries and the geometry of the environment on grid and HD cell** activity. The spatial and directional specificity of these cells was maintained in situations of **complete removal of the wall**, yet one could observe in some cases a

loss of stability or even remapping as if the rat considered the environment as new. The directional specificity of these cells was also mostly maintained in situations of **distortion** (expansion in one dimension) of the environment. Its effect on the spatial specificity of grid cells led to non-homogeneous response. In some instances, grid fields were distorted following the distortion of the environment (Fig. 52A) as shown previously (Barry et al. 2012). However, in other cases the firing fields remained unchanged and the extension of the environment led to a change in the number of the fields (Fig. 52B). In both cases, all cells recorded simultaneously responded in a similar fashion. This leads to the conclusion that this response is governed by the rat's perception of its environment. I will elaborate further on these results in the discussion, where I will link the distortion of the field to the **experience** of the rat and the **salience** of the cue.

Fig. 52 Grid cells in "distorted environments"

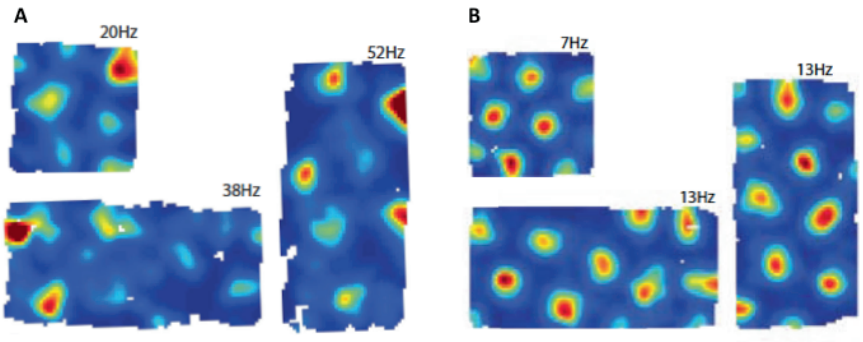

(A) Concomitant distortion of the fields with **(B)** Multiplication of the fields. Colour-coded rate 1aps, maximum firing rate in red, minimum in dark blue, pixels not covered are white. Peak firing rate is indicated above each panel.

Finally, one should note that we observed a small number of **"unclassified cells"** whose activity was dependent on the border of the environment, yet not attached to it (Fig. 53). Some of these cells showed a central firing (i.e. "anti-border cells"), others had their firing remote from the borders, in a fashion similar to that which was hypothesized previously (Barry et al. 2006).

Fig. 53 Other code for border

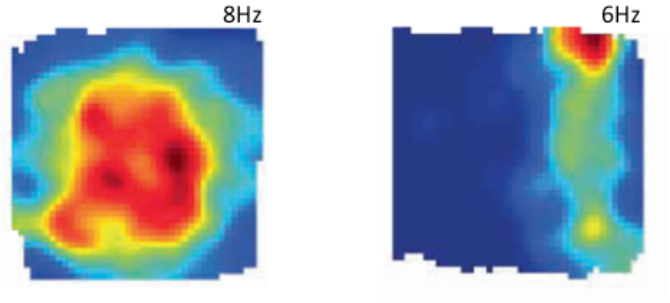

Colour-coded rate map of two representative “unclassified cells” whose activity was dependent on the border of the environment. Maximum firing rate in red, minimum in dark blue, pixels not covered are white. Peak firing rate is indicated above each panel.

Paper 2: Grid cells in the pre- and parasubiculum

Fig. 54 Localization in three-dimensional side view (A) and caudal view (B) of the hippocampal formation (HF). (C) Simplified schematization of the local spatial functional circuit

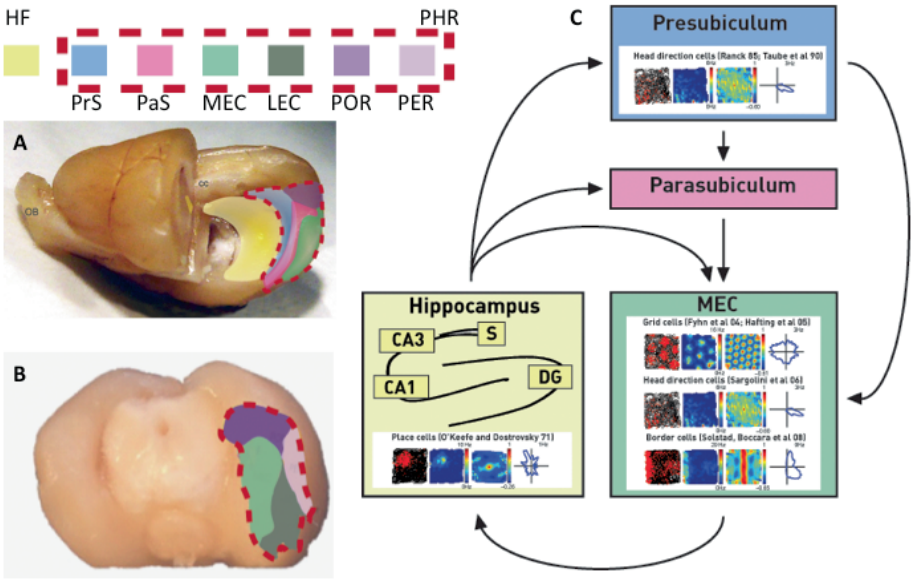

(A-B) In light yellow and the diverse subareas belonging to the parahippocampal region (PHR) circle with red dashes: the presubiculum (PrS, light blue), the parasubiculum (PaS, light pink), the medial entorhinal cortex (MEC, light green), the lateral entorhinal cortex (LEC, dark green), the postrhinal cortex (POR, dark purple) and the perirhinal cortex (PER, light purple).
(C) Simplified schematization of the local spatial functional circuit involving the hippocampal formation (hippocampus), the pre- and parasubiculum, and the MEC. Figured inside the rectangle corresponding to each areas the principal cell type that had been characterized in the literature previous to the study: place cells in the HF, head direction cells in the PrS and grid, head direction and border cells in the MEC (from left to right: path of the animal with spikes in red, rate map, spatial autocorrelation map and polar plot).

As reviewed in the introduction, the **grid cell system** has recently been discovered in the **MEC** and is thought to be part of a **universal path integration system** together with the HD cells instrumental in navigation. One of the main objectives of paper #2 was to determine whether grid cells were specific to the MEC or could be found in other brain regions. The areas of investigation were the **dorsal portion of the pre- and parasubiculum** (Fig. 54). These targets were chosen based on several premises. They are both l**ocated "upstream" of the MEC** and share with this structure **similar cytoarchitecture and connectivity** (van Strien et al. 2009) (see paper #3). Notably, those three structures are at the interface between hippocampal, associative and sensory inputs. I will describe and comment at length on the traits shared between the

MEC, PaS and PrS in the discussion. Paper #2 establishes that **grid cells indeed exist both** in the **PrS** (Fig. 55) and **PaS** (Fig. 56).

Fig. 55 Spatially modulated cells in the presubiculum (PrS)

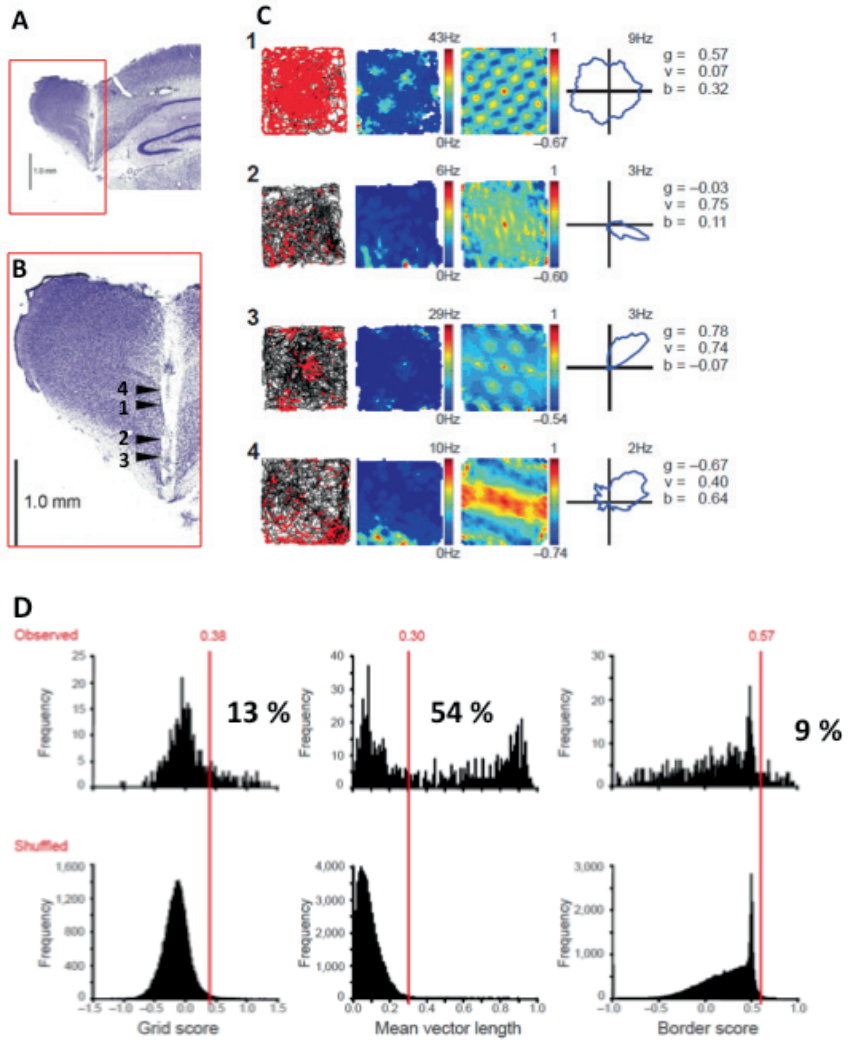

(A) Sagittal Nissl-stained section showing a track left by recording tetrodes in the PrS. **(B)** Magnification of the track presented in A showing the recorded position of the cells presented in C. **(C)** Representative examples recorded in the PrS of a grid cell (1), head direction cell (2), conjunctive head by direction cell (3) and border cell (4); For each cell from left to right: path of the animal with spikes in red, rate map, spatial autocorrelation map, polar plot and grid score (g) mean vector length score (v) and border score (b). **(D)** Distribution for the entire sample of presubiculum cells of grid scores, mean vector length and border scores (top, observed, number of cells = 654), as well as randomly shuffled rate maps from the same sample of presubiculum cells (bottom, shuffled; 65,400 permutations). Red line and number indicate 99th percentile for the shuffled data. Black percentages indicate portion of the presubiculum sample that reached the 99th percentile threshold.

Fig. 56 Spatially modulated cells in the parasubiculum (PaS)

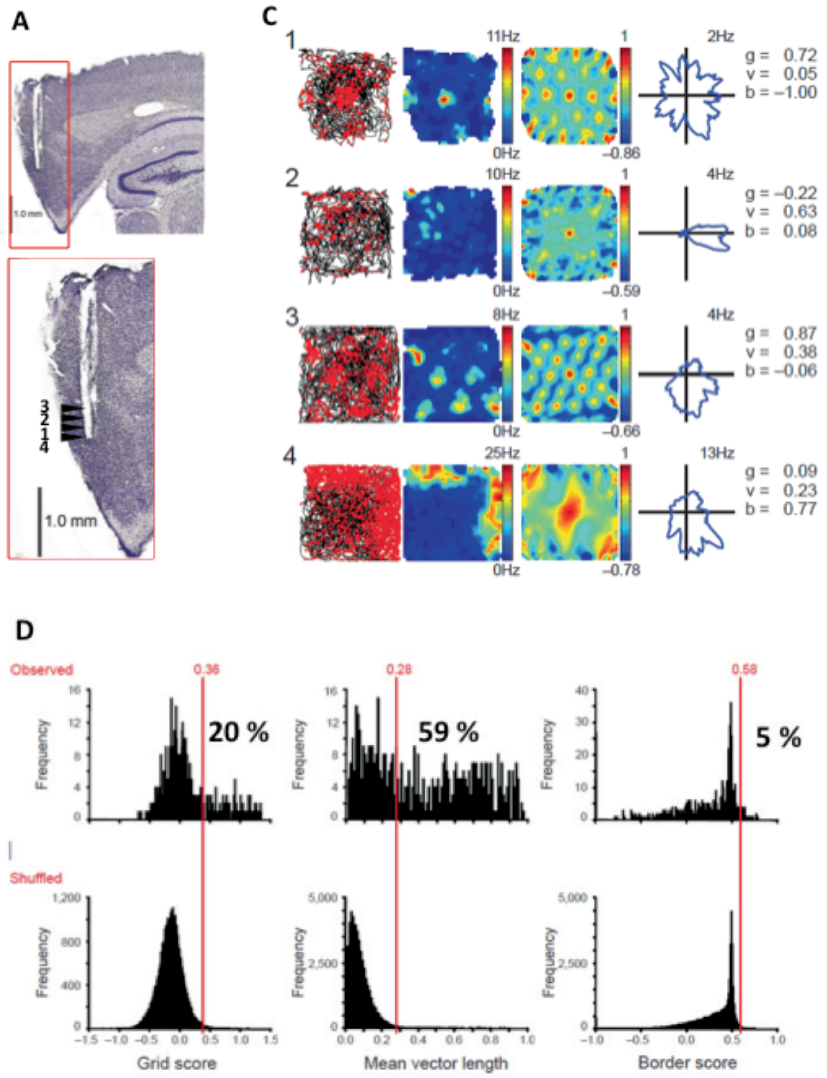

(A) Sagittal Nissl-stained section showing a track left by recording tetrodes in the PaS. **(B)** Magnification of the track presented in A showing the recorded position of the cells presented in C. **(C)** Representative examples recorded in the PaS of a grid cell (1), head direction cell (2), conjunctive head by direction cell (3) and border cell (4); For each cell from left to right: path of the animal with spikes in red, rate map, spatial autocorrelation map, polar plot and grid score (g) mean vector length score (v) and border score (b). **(D)** Distribution for the entire sample of parasubiculum cells of grid scores, mean vector length and border scores (top, observed, number of cells = 528), as well as randomly shuffled rate maps from the same sample of parasubiculum cells (bottom, shuffled; 65,400 permutations). Red line and number indicate 99th percentile for the shuffled data. Black percentages indicate portion of the parasubiculum sample that reached the 99th percentile threshold.

The second objective of paper #2 was to **analyse spatial and directional modulation of principal neurons** in the **MEC, PrS and PaS** (i.e. mainly grid, HD and border cells) **quantitatively** and to compare the distribution of their properties between areas and layers. To achieve that goal, paper #2 was instrumental in **defining statistical tools** to measure the modulation of grid, HD and border cells quantitatively (see annex 2) and thus to **address a subjectivity bias at the core of previous studies**. The rather large sample of spatially and directionally modulated cells distributed over several areas helped to test and verify the properties of grid, HD and border cells, and to investigate **how homogeneous those properties are between different areas and layers** with a dataset of 650 MEC cells, 654 PrS cells and 528 PaS cells.

Fig. 57 Distribution of the entire sample of MEC cells

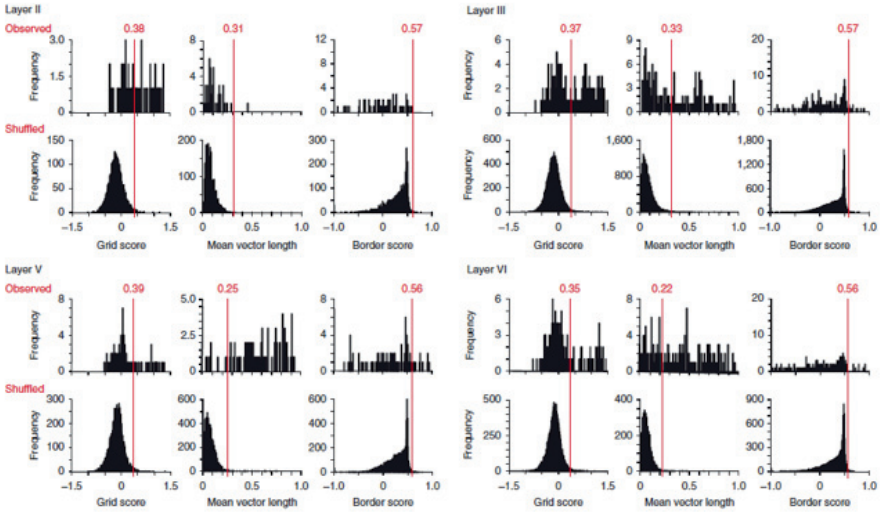

Distribution of the entire sample of MEC cells of grid scores, mean vector length and border scores, sorted by layers. In each panel, the top row shows the distributions of values in the recorded data, whereas the bottom row shows the corresponding distributions for randomly shuffled rate maps from all cells in the respective layers. The red lines indicate the 99th percentile values. (Percentages over 99th percentile threshold: grid modulated cells (LII 50%, LIII 47%, LV 21%, LVI 25%), head direction modulated cells (LII 2%, LIII 46%, LV 89%, LVI 69%) and border modulated cells (LII 2%, LIII 6%, LV 12%, LVI 6%)

The main finding is that grid, HD and border cells can be recorded in those three PHR areas (Fig. 55–57). The properties, discharge correlates and distribution of each cell type are **quite homogeneous between areas, with the exception of the MEC superficial layers** which show a much **higher proportion of grid cells** (i.e. about half of the principal cells) both in layer III (LIII) and II (LII). In addition, **LII is singled out by its absence of direction and border modulation**. Additionally, the

average grid scores (based on the 60° symmetry of the grid pattern) are higher in superficial layers of the MEC. These local differences in grid properties argue for **different pools of grid cells** and initiate the **reappraisal of the definition of grid cells** (see discussion).

Fig. 58 Theta modulation of functional cell types in presubiculum, parasubiculum and MEC

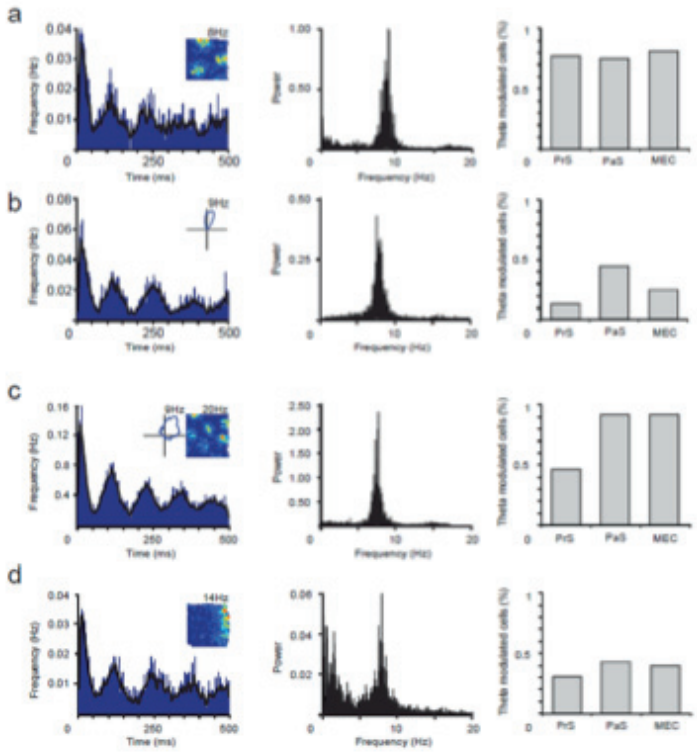

(a–d) Four theta-modulated cells are shown (**a**, grid cell; b**,** head-direction cell; **c**, conjuctive (head direction X grid cell); **d**, border cell). Left to right, panels show spike-time autocorrelation diagrams (inserts, spatial or directional rate maps), EEG power spectra and percentages of theta-modulated cells in each parahippocampal region.

Theta modulation of cell activity was assessed for all cell types in all areas (Fig. 58). Results show that the **majority of grid cells**, independently of their recording location, have their activity theta-modulated. However, some do not show strong theta modulation, in spite of high theta power in the local field potential. On the other hand, less than half of the HD and border cells have their activity modulated by theta. In addition, paper #2 establishes an interesting correlation between proportion of grid cells and proportion of cells whose activity is theta-modulated in the same area (Fig. 59). The significance of these results will be further analysed in the discussion.

Fig. 59 Distribution of grid, head direction and theta modulation

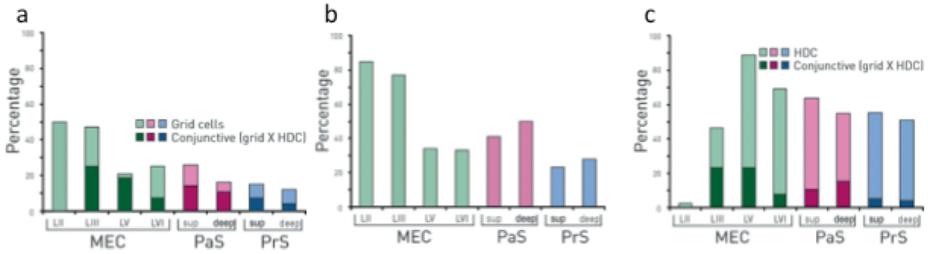

Distribution of grid cells **(a)**, theta-modulated cells **(b)** and head direction-modulated cells **(c)** in the parahippocampal cortex. The distributions of each cell type across layers of MEC, presubiculum and parasubiculum are shown. Green bars MEC, Pink bars PaS, Blue bars PrS. The subset of cells with conjunctive grid X head direction properties are indicated in dark grey in a and c. Note the parallel decrease in numbers of grid cells and theta-modulated cells from the superficial (sup) layers of MEC to the deep MEC layers.

It is interesting to note that **direction modulation** can be observed both as the only observable correlate (i.e. "pure" HD cells) and in conjunction with grid properties (i.e. conjunctive cells) in all three areas. Robust "pure" direction modulation had not been characterized in the PaS prior to this study. Moreover, quite a **large variety of tuning range** was expressed from one cell to another both in conjunctive and non-conjunctive cells. The rationale behind this heterogeneity will be discussed in the discussion and will initiate the debate on the definition of HD cells.

Preliminary results from the same data set show that dynamic and network properties seem similar to what has been observed in recording limited to the MEC (Fig. 60).

The demonstration of a **common pool of space-responsive cells in architecturally diverse subdivisions** became essential for testing the predicates of mechanistic theories of grid cells (see discussion). Furthermore, it highlighted the existence of a circuit of functionally specialized neurons distributed across several connected hippocampal areas.

Fig. 60 Ensemble remapping

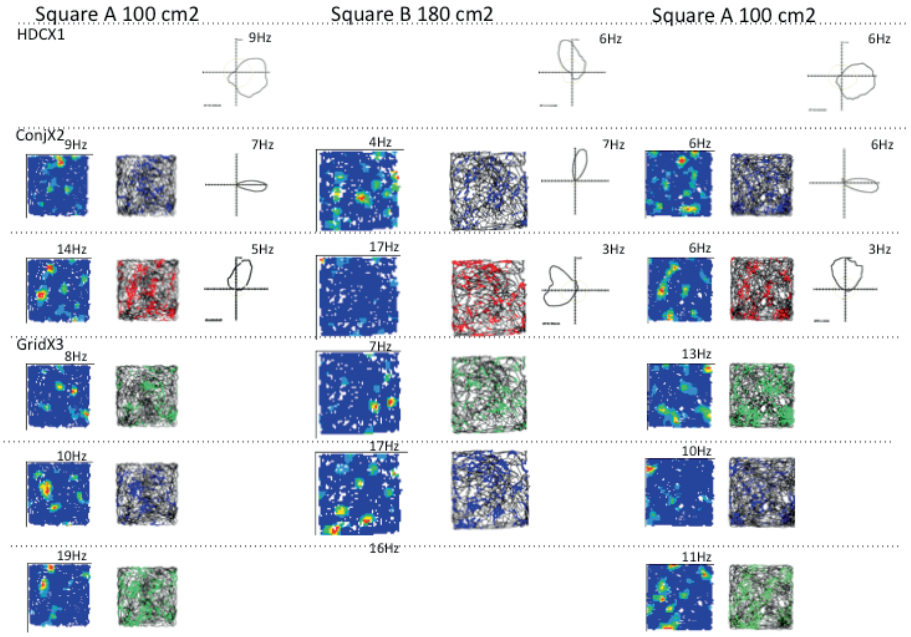

Rate map, path with spikes and polar plot of six simultaneously recorded cells (1 HD, 2 conjunctive HD by grid and 3 "pure" grid cells) in two different rooms. Peak firing rate indicated in the upper right corner of each rate plot. (Unpublished data from observations of parasubiculum cells)

Paper 3: A three-plane architectonic atlas of the rat hippocampal region.

Paper #3 establishes a set of precise criteria that allows the **identification of anatomical borders between the subareas of the rat hippocampal region**. The resultant **atlas** is based on a series of adjacent sections stained for neurons and for a number of chemical marker substances.

Here we described the hippocampal region as consisting of **two main structures**: the **hippocampal formation** (HF) and the **parahippocampal region** (PHR). The HF, also sometimes referred to as the hippocampus, includes the **dentate gyrus** (DG), the **cornu Ammonis** (CA) regions 1, 2, and 3, or the hippocampus proper, and the **subiculum** (Sub). We additionally differentiate a separate, yet poorly understood, part referred to as the **gyrus fasciolaris**, or fasciola cinereum (Stephan 1975). The PHR comprises the **presubiculum** (PrS), the **parasubiculum** (PaS), the **entorhinal cortex** (EC), the **perirhinal cortex** (PER) and the **postrhinal cortex** (POR). The distinction between the HF and PHR is a difference in their layering: the HF is a three-layer cortex, while the PHR is considered to have six different layers. Some of the PHR areas may be subdivided further. Here we detailed the subdivision

of the PER into PER 35 and 36 and that of the EC into a lateral entorhinal cortex (LEC) and a medial entorhinal cortex (MEC). Following the previous descriptions (Insausti et al. 1997), we further subdivided the MEC into caudal entorhinal (CE) and medial entorhinal (ME) areas and the LEC into dorsal lateral entorhinal (DLE), dorsal intermediate entorhinal (DIE) and ventral intermediate entorhinal (VIE) areas (Fig. 61).

Fig. 61 Three-dimensional views of the hippocampal region

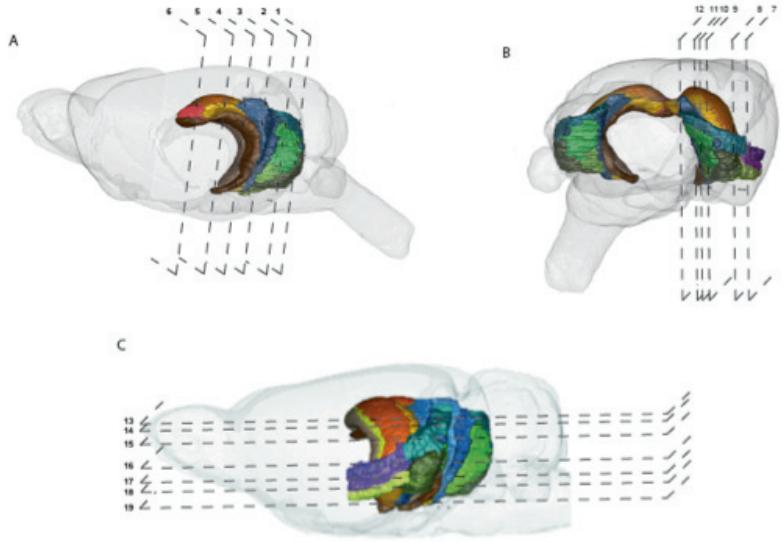

(A) Medial side view of one hemisphere. **(B)** Caudal view. **(C)** Lateral side view. Colour code as presented in Fig. 62. Dashed lines: numbers corresponding to sections presented in S15, S16 and S17.
HF: hippocampus formation; PHR: parahippocampal region; DG: dentate gyrus; CA1-3: cornu Ammonis 1-3, Sub: subiculum; PrS: presubiculum; PaS: parasubiculum; EC: entorhinal cortex; PER: perirhinal; POR: postrhinal; MEC: medial entorhinal cortex; LEC; lateral entorhinal cortex; 35: perirhinal area 35; 36: perirhinal area 36; CE: caudal entorhinal area; ME: medial entorhinal area; VIE; ventral intermediate entorhinal area; DIE: dorsal intermediate entorhinal area; DLE: dorsal lateral entorhinal area

In recent decades, many studies have highlighted **functional and connectional heterogeneity of neighbouring hippocampal subareas**. A resumé of connectional heterogeneity can be found in a fairly recent review (van Strien et al. 2009). Heterogeneity of spatial correlates has been presented throughout this whole thesis. However, other types of coding have been observed in the hippocampal region. Notably, cells coding for objects were recorded in the lateral entorhinal (Zhu et al. 1995; Young et al. 1997; Wan et al. 1999; Deshmukh and Knierim 2011). Similar neural correlates of object recognition memory or novelty were observed in the

perirhinal cortex (Zhu et al. 1995; Burke et al. 2012), but also in the postrhinal cortex (Burwell and Hafeman 2003) and the subiculum (Chang and Huerta 2012).

The **absence of clear standard markers** has caused **imprecision in the anatomical identification of experimental observations and manipulations** (Hafting et al. 2005; Barry et al. 2007; Burgalossi et al. 2011). Such interpretation errors may multiply as the **accuracy of current experimental tools is increasing very fast** (Lee et al. 2006; Dombeck et al. 2010; Gradinaru et al. 2010; Burgalossi et al. 2011; Domnisoru et al. 2012; Gu et al. 2012; Raimondo et al. 2012; Zhang et al. 2013).

Previously published anatomical descriptions are lacking in precision or reliability, for either considering criteria only valid for one sectioning plane or by not focusing on the whole hippocampal region (see discussion). They generally described the architectonical features of the hippocampus subareas but failed to highlight the markers of the borders between those areas.

The atlas presented here focuses on these markers and defines a set of **cytoarchitectonic criteria apparent in simple neuronal staining** that makes it possible to distinguish between neighbouring hippocampal areas. In the absence of clear differences in neuronal staining, the present work establishes an **additional set of chemoarchitectonic criteria made apparent with immuno-staining against either the calbindin or the parvalbumin protein**. Contrary to previous accounts, the architectonical markers described here are verified to be **visible in all three major sectional planes** (i.e. coronal, sagittal and horizontal, Fig. 62–64).

Monoplanar border delineations thus obtained were integrated in a three-dimensional atlas and readjusted until **all dimensions were coherent with each other**. The majority of the anatomical borders of the resultant atlas are similar to what had been presented in previous accounts. However **some borders were reappraised** (see discussion). For example, one can note that a portion of parasubiculum has often been confused with the medial-dorsal tip of the entorhinal cortex. The use of differential staining and notably calbindin highlights that misconception and establishes the curvature of the parasubiculum around the entorhinal cortex.

Fig. 62 Selected coronal sections

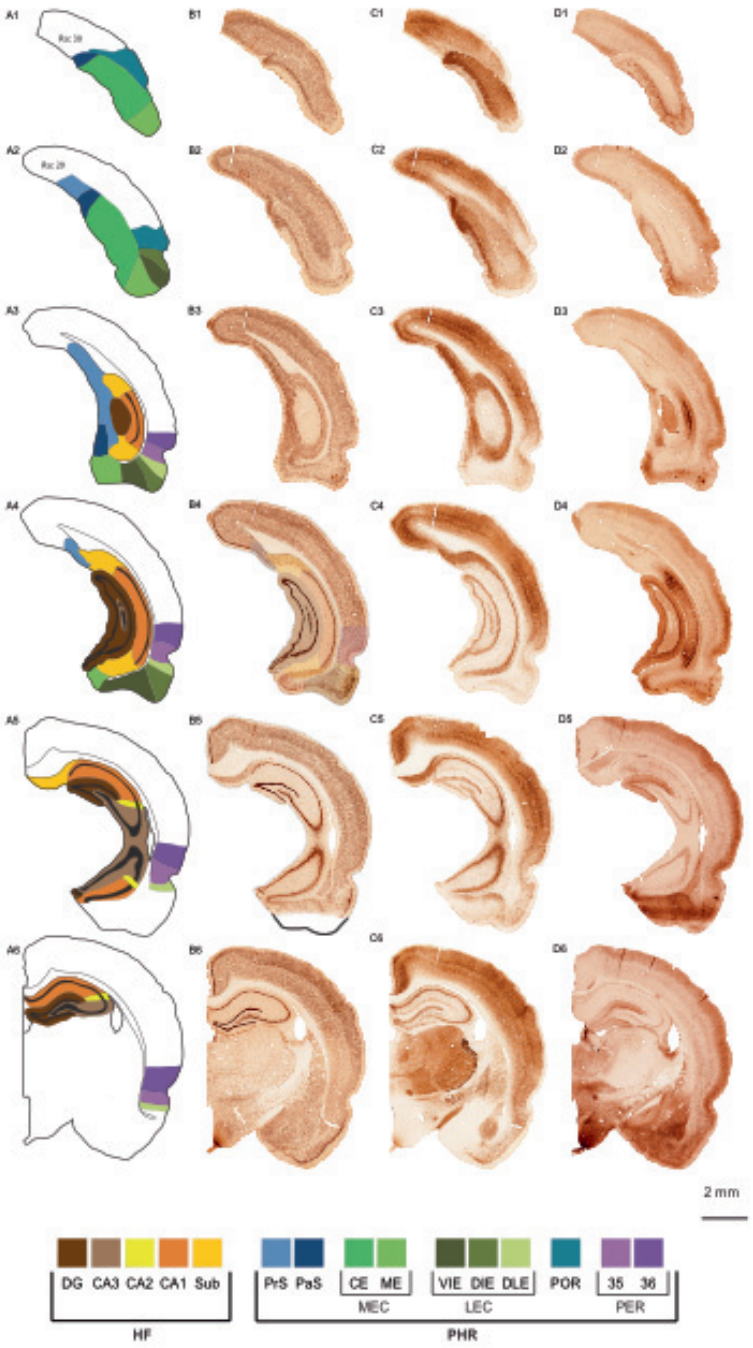

(A) Delimitation of the subareas of the hippocampal region. Colour code as presented in the lower panel. **(B)** Nissl sections. **(C)** Parvalbumin sections. **(D)** Calbindin sections. Numbers correspond to levels presented in Fig. 61. Rsc: retrosplenial cortex; see Fig. 61 for other acronyms.

Fig. 63 Selected sagittal sections

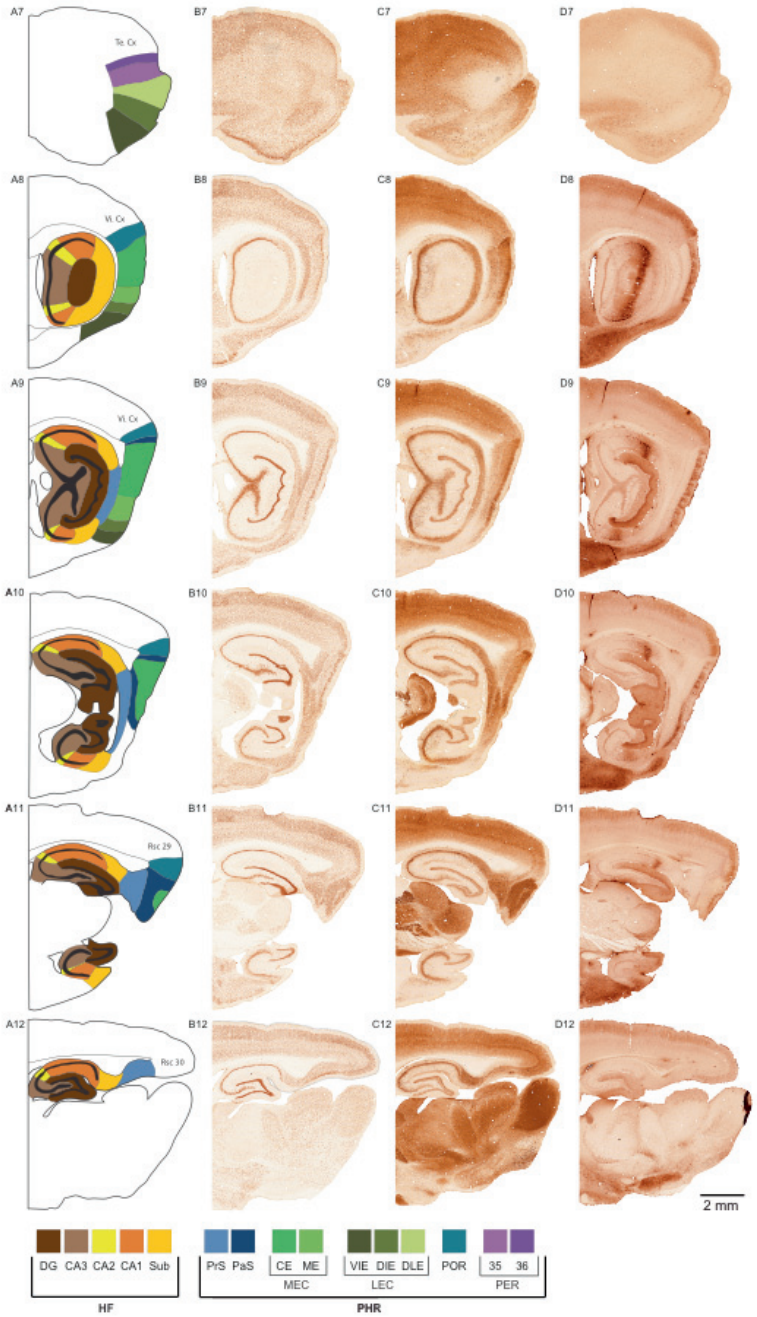

(A) Delimitation of the hippocampal region subareas. Colour code as presented in the lower panel. **(B)** Nissl sections. **(C)** Parvalbumin sections. **(D)** Calbindin sections. Numbers correspond to levels presented in Fig. 61. Te.Cx: temporal cortex; Vi.Cx: visual cortex; Rsc: retrosplenial cortex; see Fig. 61 for other acronyms.

Fig. 64 Selected horizontal sections

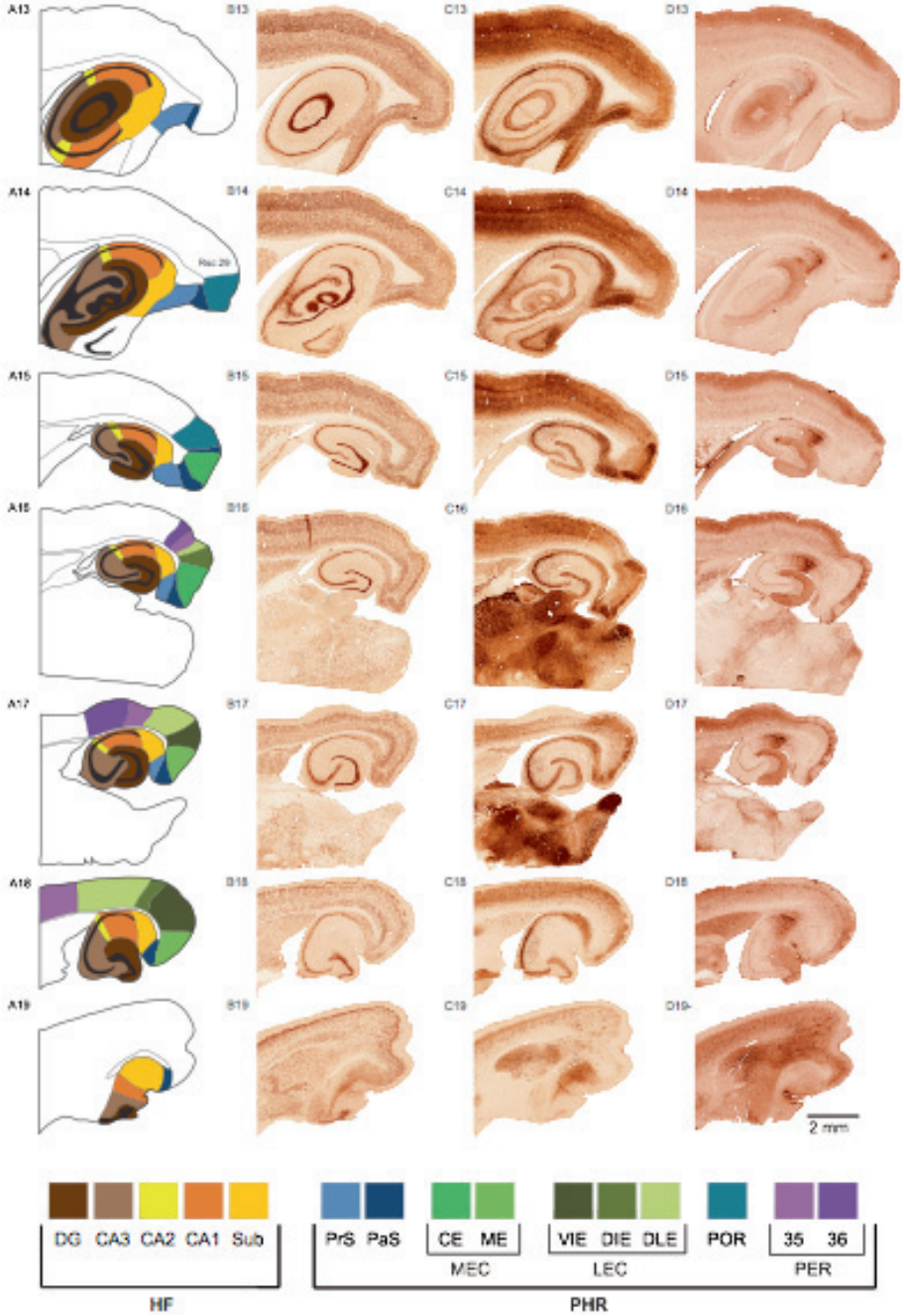

(A) Delimitation of the subareas of the hippocampal region. Colour code as presented in the lower panel. **(B)** Nissl sections. **(C)** Parvalbumin sections. **(D)** Calbindin sections. Numbers correspond to levels presented in Fig. 61. Rsc: retrosplenial cortex; see Fig. 61 for other acronyms

The current database is integrated with an **on-line application** (http://www.rbwb.org), which currently consists of the updated architectonic description of each of the subareas and an interactive coronal atlas mounted in a **virtual microscope** that allows one to zoom in on each section stained for all three markers (Kjonigsen et al. 2011). Soon, the remaining sectioning planes (i.e. sagittal and horizontal) will be implemented in this application, which will also allow the generation of **three-dimensional renditions** of the hippocampal region structures in the rat brain.

With its **focus on border recognition and didactic approach**, this atlas is intended to become a **standard tool for experimentalists** both in the planning and in the interpretation phase of their work. It will give them the opportunity to carefully decide beforehand the best plan of sectioning and whether multiple stains are needed in order to determine a given anatomical border.

DISCUSSION

The question central to my thesis is that of a **neural substrate for cognition** (see 1.1 for historical perspective on localization of cognitive function). I addressed it by focusing on a specific function: **spatial cognition** (see 1.2), in a specific brain region: the **hippocampal region** (HR) (see 1.3), at a specific level of investigation: the basic functional brain unit, i.e. the **neuron**. One can see spatial cognition as a generic term that encompasses all conscious and unconscious **mental processes** that allow the subject to **perceive**, acquire **knowledge** and construct a **dynamic mental representation** of its **environment** (and self-location in that environment) in order to **navigate** accurately. In this discussion I will attempt to initiate a global reflection on **how and where spatial information is coded, and to what end**. This thesis presents the hippocampal region (HR) as a complex and heterogeneous system involved to a great extent in spatial coding. The HR is anatomically divided in two principal components: the **hippocampal formation** (HF) and the **parahippocampal region** (PHR), each of them further subdivided as detailed in paper #3.

While the first part of the introduction (1) establishes the sub mentioned premises, the second part (2) provides a large cohort of data predominantly from **HR unit recording** obtained in **freely behaving rats** in order to show that individual HR neurons **code** for **positional**, **directional**, **self-motion**, **metric** and other **environmental information**. It focuses on reviewing three cell types: place cells, head direction cells and grid cells (see definitions in 2.1). The electrophysiological work presented in the scientific articles supporting this thesis focuses on the parahippocampal region (PHR) and completes this dataset in two ways. Paper #1 shows the existence of PHR neurons that **code for the boundaries** of the environment: the **border cells**. Paper #2 demonstrates the **distribution** of positional, directional, metric and boundaries **coding over interconnected PHR areas** (i.e. grid HD and border cells in the MEC, the presubiculum and the parasubiculum).

Four main points of discussion arise from the three articles supporting this thesis:

I- A reappraisal and establishment of several definitions (i.e. of grid, HD and border cells as well as of anatomical boundaries and architectonic markers)

II- A reflection on the modalities of information coding and its distribution over a global coordinated network

III- A reflection on the origin of the spatial signal

IV- Some brief perspectives on the behavioural function of the neural code

One should note that the study of spatial cognition and coding goes beyond space. First, it is intimately linked to **learning and memory**. Knowledge acquisition is central to spatial cognition and a large number of studies point to the HR as crucial for both spatial cognition and declarative memory. Second, spatial cognition is representative of the **dynamic interaction** between mental **representation** and **behavioural** outcome. Finally, understanding the spatial neural coding modalities allows insights in **information coding and computation** in a general context.

I. Impact on definitions

I.I Refinement of anatomical borders and their architectonic markers (Paper #3)

Paper #3 describes clear markers of the anatomical borders of subareas of the HR. It is **innovative** both in the resultant **reappraisal of some of the HR subareas borders** and in the **methods** used to reach its conclusions.

One of the methodological strengths of this study is to combine information from both cyto- and chemo-architectonic markers. C**yto-architectonic features** are revealed by neural staining, a method widely used for histological *post hoc* analyses. It illustrates how the neurons are organized in a considered section in terms of size, shape and density. This technical procedure is relatively **simple** and **fast, and** its popularity ensures the existence of a **large database** that facilitates comparison between studies. However, as it is demonstrated in paper #3, cyto-architectonic features are not informative enough to distinguish between some areas/subareas. The use of **chemo-architectonic** features is useful in these situations. We (re-) established some of these features for paper #2 in the anatomical distinction between MEC, PrS, PaS, Sub and POR. Paper #3 is the extension of that procedure to the whole HR. This work led us to observe that even today, several studies are wrongly reporting the anatomical location of their recordings. This is especially problematic as often a large part of the **interpretation of electrophysiological/lesion/inactivation studies** is based on the **correct identification** of the anatomical region manipulated or recorded from. For example, one can note that a portion of parasubiculum has often been confused for the medial-dorsal tip of the entorhinal cortex. The use of differential staining and notably calbindin highlights that misconception and establishes the curvature of the parasubiculum around the entorhinal cortex.

Another methodological advancement in this study is to consider the brain in its three dimensions. All boundaries defined in any of the three major planes is systematically verified in the other two, to assure that they are consistent throughout. Inconsistencies are easily detected and borders readjusted by mapping the single plane delineations onto a **standard three-dimensional rat brain** (Kjonigsen et al., in prep). This work is based on a standardized representation of the rat brain, the so-called Waxholm rat brain (Johnson et al. 2010). The current database is integrated with an on-line application (http://www.rbwb.org), which currently consists of the updated architectonic description of each subarea and an interactive coronal atlas made available through a virtual microscope (Kjonigsen et al. 2011). The sagittal and horizontal sections will be entered into this application in the near future.

I.II Shift in definition of head direction cell (Paper #2)

HD cells have been defined as cells coding for the head direction of the animal in a stable manner (2.1.2). They are active in all environments and thus quite different from place cells. Based on their static (2.2), dynamic (2.4) or network (2.5) properties, it has been proposed that they are part of a **universal, path integration-based map** (see IV). Supporting this theory, the study of their discharge correlates (2.3) show that non-spatial features have very little influence on their activity. Principal component analysis establishes that many are **speed/velocity modulated**. HD cells were originally defined based on non-quantifiable criteria. Paper #2 clearly demonstrates the **need for objective and quantifiable criteria** to distinguish HD cells from **directional modulation**. This paper provides quantifiable criteria to define directional modulation, yet it does not dive immediately into the issue of HD cell definition.

How to define a head direction cell

There are **three main parameters** one needs to address when measuring direction modulation. The first is **the sharpness of** the preferred firing direction: this is represented by the width of its tuning range. The second is **the specificity** of the firing modulation: in other words the ratio between the firing rate in the bins allocated to the preferred range and the background-firing rate. The last one is a measure of **stability** of the preferred firing direction, which is given by a directional coherence parameter. One can see at once that binning, smoothing and defining the firing range are essential to these measures (see annex 1).

There are three main aspects to the problem of **defining HD cells**. The first one is **which score** to use that translates the three mentioned parameters best, the second is **how to define thresholds** for that score, and the third is whether HD cell may **code for other parameters** such as location or velocity.

HD score

The strength of directional tuning (i.e. **HD score**) has been estimated by different methods: (1) computing the **length of the mean vector** for the circular distribution of firing rate. (2) Calculating a **directional information rate** (or content) in a similar way to the spatial information rate (or spatial information content). (3) Using a non-parametric **Watson's U2 test** to obtain a score of circular distribution of the firing (for more details, see annex 1). For paper #2, we decided to use the first method (mean vector length), as it was the method that seemed to reflect best the sharpness and specificity of directional tuning.

HD score threshold: directional modulation

Before the joint effort of (Langston et al. 2010; Wills et al. 2010) and the authors of paper #2, HD score thresholds were decided empirically. These three papers developed a method for **score thresholds** (i.e. cut-off between directionally and non-directionally modulated cells) to be calculated by the use of a **statistical criterion** that computed for each area studied the degree of directional tuning that would be expected by chance. The chance level was estimated based on **"shuffled" polar maps** artificially generated on a cell-by-cell basis, by time-shifting the entire sequence of spikes fired by the cell along the animal's path by a random time interval and this procedure 100 times for each cell, yielding, for example, a total of 10,000 permutations for 100 cells (for more details, see annex 1). However, this method only provides a statistical threshold for direction modulation, yet not for HD cells.

Conjunctive properties

The last aspect for HD cell definition is that many directionally modulated cells **conjunctively code** for spatial information (e.g. place, grid or border cells). Additionally, experience and constraints in the environment can influence the directionality of some place cells. A hypothesis to explain the heterogeneity in the HD score is that cells with low scores code for other modalities beside HD, yet this is not verified for all examples of conjunctive HD and grid cells. Nevertheless, I would guess that HD cells should be defined as cells that code only for head direction

information with a high specificity (with the possible exception of acceptance of conjunctive coding for speed/velocity information). However, I have no answer on how strict the specificity should be. A statistical analysis of HD cell-rich areas could perhaps give an idea of the distribution (and concordance with other criteria such as directional coherence) and be the basis for new criteria. I can imagine that not all non-directional coding is spatial and is therefore more difficult to isolate. A possible solution could be to define HD cells by their **accuracy in predicting the HD of the animal**. I will discuss below whether HD cells with conjunctive properties are homogenously distributed over the PHR (II), their implication in the directional signal generation (III) and their role in a global functional system (IV).

As a final note on the properties of HD cells, I wanted to mention that more in-depth analysis of the results of paper #1 could help to give more detail on the dynamic properties of HD cells and the influence of geometry (square/circle) and walls on their firing to complete some recent studies (Clark et al. 2012).

I.III Shift in grid cell definition (paper #2 and #1)

As mentioned above, grid cells – by their regular firing fields tessellating the whole environment – code for distance, self-motion and metric information (see extended definitions in 2.1). They have been proposed to be part of a **universal, path integration-based map** together with the HD cells. A pillar of this theory is that they express similar firing patterns in all environments.

This thesis experimental work, especially paper #2, contributes greatly to the redefinition of the properties of grid cells, together with sub mentioned studies (see 2.2, 2.3, 2.4, 2.5). I will discuss here how these **new data have challenged the original rigid definition** of the **grid cell** (see 2.1.3) and whether one should see a **concomitant evolution of the gridness score**, which is still based, for the most part, on that definition. To do so I will review data on grid cell discharge correlates (2.3) as well as static (2.2), dynamic (2.4) and network properties (2.5).

Static properties

A widening of the definition of grid cells occurred very shortly after they were originally reported, through a fundamental complementary study showing that many grid cells, in addition to their spatial code, support a directional code (Sargolini et al. 2006). A precise distribution between subareas of such **conjunctive grid-by-head direction cells** was further established (see II).

At the heart of the grid definition is its **60° rotational symmetry.** However, the analyse of a larger cohort of grid cells in paper #2 demonstrates that many of them do not inscribe a perfect circle, but are rather elliptical. Very recent work from the Moser lab (Stensola et al. 2012) addresses that specific point and whether one can see a distribution of different **ellipse/circles** between subregions (see II). It may be interesting to investigate whether ellipticity of grid cells is higher among those that present conjunctive properties.

The divergence from the "perfect grid" is further exposed when considering the **differences of firing rate between nodes** (i.e. single grid fields). According to preliminary observations of the data collected for papers #1 and #2, these rate differences seem to be conserved in a given environment, from one session to another. Based on this observation, grid cells may well **code for more than pure metric information** and the rate modulation could be due to mechanisms similar to the **context gating information** theory hypothesized to explain place cell activity (Hayman and Jeffery 2008). It would be very informative to see if there is a distribution of heterogeneity of grid field rate between grid cells recorded in different subareas (see II). Further influence of the "context" on grid cell activity has been observed when some cells remap in response to changes in the colour or the scent of the environment (Alenda et al. 2010; Marozzi et al. 2012).

Discharge correlates

One of the first studies to do so reported the **influence of geometry** on grid cell discharge (Barry et al. 2007). It showed that, in a similar fashion to what is observed with place cells (O'Keefe and Burgess 1996), the deformation of the environment (expansion of a square recording box in one dimension) led to a proportional deformation of the grid fields (see 2.3.4 for more details). We use the same experimental paradigm of expansion of the environment to qualify border cells in paper #1. Our results on grid cell behaviour in such a situation are not as homogeneous as those reported in (Barry et al. 2007). Indeed, in some sessions, grid fields were distorted and in others they remained stable. Our explanation for these discrepancies is that, in such a behavioural paradigm, the grid cell deformation is linked to an anchoring of the firing field to the wall of the environment. Yet, changes in **cue control and experience** would affect the perception of the animal of the wall as a reliable and stable cue. We believed that, on the occasions when the fields remain

unchanged in spite of the deformation of the environment, the animal either had extensive experience of the environment or had access to more external cues (curtain open). Nevertheless, this experiment was instrumental in showing how external environmental features can influence grid cell firing structure. This also influenced the view on grid cell signal generation (see III). The influence of task demands has recently been pointed out as contributing to the fragmentation of grid patterns in some circumstances (Gupta et al. 2013).

I would like to open a parenthesis here on the fact that the data collected in paper #1 contains many experiments testing the influence of the environmental geometry, borders, walls and barrier on border cells. Yet many grid cells were concomitantly recorded. It would be interesting to analyse further the behaviour of the grid cells in situations of wall/no wall, square/circle and barrier introduction, in order to complete the view on discharge correlates of grid cells. Furthermore, I could observe that, in a square or circular environment, grid fields close to the wall are on average more "deformed" than those in the centre of the apparatus. This "**border effect"** is reminiscent of what was observed in some early grid cell models (see III.II).

Network properties

As stated in 2.2.2.3, grid cells are principally characterized according to three static properties: their spatial phase, their grid orientation and their grid scale, which includes both field size and grid spacing. Strict **network rules** were at first assumed or reported for these properties: constant proportion between grid field size and grid spacing, constant scale among collocated grid cells (at a given depth), constant orientation in a given rat in a given environment. However, recent reports (including paper #2) are moderating these views.

Though a general proportional trend can be observed between **grid field size and grid spacing**, the proportional relation is not strict. It would be interesting to study this relation in more detail, whether other factors can influence it, such as context, anatomical location or conjunction. However, to do so, one should start by discussing the method used to define the boundaries of a grid field.

The other rule considering grid scale of **one scale per depth** has also been increasingly challenged. As paper #2 points out, anatomically collocated grid cells may present different grid scale (for the distribution of grid scale see II).

Similarly, paper #2 challenged the rule of **one grid orientation per rat** in a given environment. Consecutive studies (Stensola et al. 2012) confirmed that result by showing that (1) some grid cells are ellipsoid (see above) and (2) ellipses of different orientations co-exist in anatomically co-located grid cells. Recent studies reported that the preferred firing directions of conjunctive grid and HD cells aligned with their grid orientation (Doeller et al. 2010). Finer analyses of a bigger sample go against this finding, however (unpublished data, analyses of both data sets by both the Moser and O'Keefe labs). Further analyses are needed to explain the rationale behind the effect observed by (Doeller et al. 2010).

Two recent studies are challenging another fundamental dynamic property of grid cells: the fact that as part of a predetermined rigid structure (see Kant), grid cells have their specific **firing pattern expressed at once in a novel environment** (see 2.4.2). One study showed that grid scale transiently increases in a novel environment before going back to its original scale with experience (Barry et al. 2012), while the other showed that some grid cells have their characteristic pattern completely disrupted (VanCauter et al. 2012). It seems that there are different categories of grid cells responding differently to novelty (see II). These results also have implications for the grid signal generation (see III).

Firing properties

Paper #2 also introduced some discrepancies between grid cells regarding their firing properties (see 2.2.3.2.3). It shows that **theta modulation** is not uniform among grid cells, independently of the theta power recorded in the LFP. It is possible that this result reflects the existence of different categories of grid cells (see II). These results also have implications for the grid signal generation (see III).

Beyond grid cells

A recent study (Krupic et al. 2012) has further challenged the definition of grid cells by reporting that the majority of PaS and MEC cells have spatially periodic firing patterns composed of plane waves (or bands) drawn from a discrete set of orientations and wavelengths. They claimed that this new class of cell, identified by **Fourier-like analyses**, includes grid cells as an important subset that corresponds to three bands at 60° orientations and has the most stable firing pattern. This result could explain the variation in extra-field firing observed in grid cells.

Gridness score

The shift in grid cell properties calls for a re-evaluation of the method of calculation of the gridness score. Most methods currently available are based on the **60° rotational symmetry** (see annex 1). This score is **limited** in two ways: first, as stated above, recent results are questioning the strictness of this rotational symmetry, second, it does not take into consideration the grid field **periodicity**. By this, I mean that the autocorrelation map of a perfect grid is not the triple alternation of an active sextant with an inactive sextant (see figure 64) but the multiplication of this representation by one showing the alternation of concentric circle of activity.

Fig. 64 Maps for cells with perfect 60° rotational symmetry (a) or perfect periodicity score (b)

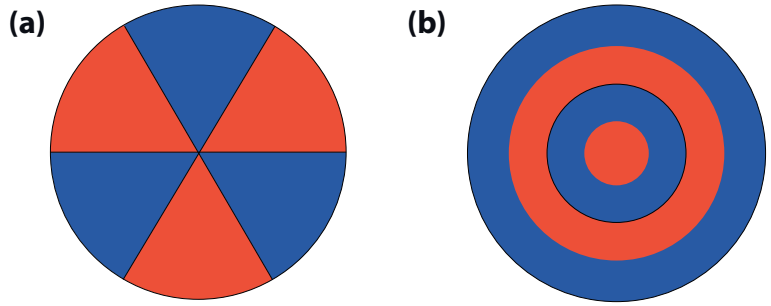

In addition, paper #2 was instrumental in defining a **gridness score threshold** by similar statistical methods as explained in (I.II), see annex 1 for more information.

I.IV Establishment of border cell definition (paper #1 and #2)

Paper #1 identifies a **new class of PHR cell** coding for spatial information: the border cells. Border cells are defined as cells stably coding for the environment border. Similar activity was also reported in (Savelli et al. 2008; Lever et al. 2009).

Border cell properties

Border cells can be **distinguished from place cells** based on three main properties: (1) their firing field expends together with the environment, independently of the animal's experience or control of external cues; (2) they are never silent in a given environment (though further sleep analysis is required to establish clearly the distinction with DG cells); and (3) they are recorded in the PHR.

Border cells **code for the environmental border**, independently of whether this is a physical wall, though border cells respond to the introduction of movable

barriers in the environment. **Several categories** of border cell have been reported coding for one, two, three or four walls.

The dynamic properties of border cells are **active in all environments** similarly to grid and HD cells. However, they seem to be more labile than the latter two. Indeed they exhibit much higher **disparities in scores** of the same cell recorded in two different environments (personal observation, not quantified). Furthermore, as presented in the synopsis of results, the placement of an extra barrier in the middle of an environment may lead to the apparition of a new field. After the removal of that barrier, one can observe a **residual field**.

In paper #2 in-depth analyses of square/circle data could give more insight into the influence of geometry on border cell firing (e.g. whether they cover the same proportion of the environment wall, the shape of the field). That dataset should also contain information on the establishment of border cell firing in a new environment, but it remains to be further analysed.

Comparison with boundary vector cells (BVC)

One of the main points of discussion emerging from paper #1 is how border cells relate to the theoretical boundary vector cells (BVC) (Barry et al. 2006), which are neurons that encode the perpendicular distance from walls. Only a few examples were originally reported, leading to the discussion in paper #1 on whether these cells were actually principal cells of the **subiculum** or signals from PHR border cells. A larger proportion of cells corresponding to this definition were subsequently reported in the subiculum, however, with a waveform characteristic of principal cells (Derdikman 2009; Lever et al. 2009). One of the main differences between BVC and border cells lies in what these **cells code** for: the **environment** (border cells) or the **position/relation of the animal within that environment** (BVC). It translates experimentally in the fact that, by definition, all border cells have their **firing attached to the wall** of the environment while BVCs can be remote (so-called long-range BVCs). One should note that such cells were additionally reported in paper #1 alongside other spatially modulated cells whose firing patterns follow the deformation of the environment (central cell/anti border cell). Lever and colleagues discussed how some of the border cells reported in paper #1 do behave like short range BVCs, however, the fact that most border cells **remap in a no-wall experiment** led them to conclude that those do not follow BVC properties. In addition, they mention that

"**four-walls border cells**" are not accounted for by their theory. A possible explanation would be that there are **several categories** of cells whose firing is border/boundary-related distributed over diverse subregions (see II).

Borderness score

Border cells may be characterized by three parameters: (1) the **extent of the wall** they are coding for (and in non-circular environments: how many walls), (2) the **thickness** of the firing field, (3) their **stability** in a given environment or in different environments. The score developed in paper #1 attempted to address these diverse criteria, yet the distribution of the borderness score data in paper #2 shows that a peak appears very close to the statistically determined threshold. This informed us that the borderness score developed in paper #1 is unsatisfactory. Furthermore, it does not account for circular environments. Recent studies (Giocomo et al. 2011; Bjerknes et al. 2012) attempted to address these limitations by defining border cells based on their response to the **introduction to a new wall** in the environment.

I.V Brief perspective on shift in place cell definition and relation with grid cells

Neither paper #1 nor #2 reports direct recordings from place cells. However, it is interesting to compare how the definition of place cells has shifted in recent years by analogy to the grid and HD cells. Furthermore, the studies presented here give insights into how spatial modulation in the PHR (MEC, PrS and PaS) was probably mistaken for place cell activity when they were in fact grid or border cells. Finally, it gives insight into how the HR spatial circuit is organized and the origin of the place cell signal (see II and III)

Place cells were originally defined as hippocampus cells coding for an animal's location in a stable manner (see 2.1.1). A cell is identified as a place cell mainly on the basis of two parameters: **spatial information** and **spatial coherence**. A third **anatomical** criterion (i.e. being a hippocampal cell) is often tacitly implied. As far as I know, there is still no strict definition today of **place cell versus place-modulated cells** (which in the broad sense of the term includes grid and border cells). This might be due to the fact that the hippocampal place cell population is quite **heterogeneous** regarding its static (2.2), dynamic (2.4) or network (2.5) properties. Some of these discrepancies are very apparent, such as a much higher field number in DG as well as a tendency for a cell to be either silent or active in all environments.

In addition, the determination of place cell correlates showed that hippocampal cells **code for non-spatial features**, either independently or conjunctively with spatial features (2.3), especially when the animal is confronted with more complex tasks/environments. This non-spatial coding operates in a very plastic way, being strongly **linked to experience and behavioural needs**. These observations have led some to expand the definition of place cells towards that of **memory cells** (see IV).

One can actually discriminate between **different categories of place cells** distributed over **diverse subregions** (see II). This population heterogeneity may support **functional differences** between subfields (see IV), as well as differences in **signal generation** (see III).

II. Modalities of information coding and its distribution over a global coordinated network

The study of the **properties and distribution** of **place, HD, grid and border cells** gives insights into spatial information coding which can be extrapolated to general information coding. Papers #1 and #2 were instrumental in clarifying how the spatial/directional signal is **distributed over a large network** that includes several subsystems (HD, grid, place and border systems). The final output (representation) of these systems seems to be the most accessible in the HR yet other brain areas are involved in the generation and stabilization of the signal. Paper #3 presents a method to establish the precise anatomical position of the components of this network by identifying the general area, the specific layer and even the dorso-medial position of a given cellular type. The purpose here is to discuss, in the light of papers #1, #2 and #3, how the spatial signal is distributed in a heterogeneous yet coordinated network.

In **II.I** I will present how the spatial information is **coded at the neural level**. I will especially consider how the **signal** is **distributed**: Is a given cell type population homogeneous in its properties? What is the finest level of distribution of cell types/properties: subareas, layers, linear or discrete gradient, neurons? Is there some clustering of properties?

In **II.II** I will examine how spatial information is **coded at the network level**. I will first focus on the coherency of the spatial network. I will then explore the notion of temporal coordination of the units within that network to see the emergence of a global code.

In **II.III**, I will discuss in greater detail the contribution of the network to the neural code and the degree to which parts of these networks may be interdependent.

II.I Spatial information coding at the neural level (paper #2, #1 and #3)

Spatial coding at the single cell level

Many cells withhold both a **rate and a temporal code**. The rate code translates the fact that a cell's firing rate is modulated by location/direction. The temporal code is especially apparent for place and grid cells and consists, for these cells, of the precise phase of the theta cycle at which they fire. The spatial accuracy of this temporal code may be higher than the rate code and, in the case of the Sub, subsist even in the absence of a clear spatial rate code (Kim et al. 2012).

One single neuron may code for **conjunctive features** (both spatial and non-spatial, see 2.3). Such cells have been clearly defined in (Sargolini et al. 2006) and paper #2, under the form of conjunctive grid-by-HD cells. The idea of a conjunctive code leads to the discussion of code vs. modulation: does the fact that a given feature modulates a cell activity necessarily mean that this cell codes for this feature?

Finally, the code observed at the single cell level does not necessarily apply to the current representation of location/direction but may be predictive of the future location/direction or retrospective, mirroring past location/direction. The concomitant existence in the network of **retrospective, current and prospective coding** may be instrumental in learning processes and could well extend to general signal processing mechanisms (Ferbinteanu and Shapiro 2003; Shapiro and Ferbinteanu 2006; Ferbinteanu et al. 2011; Mankin et al. 2012).

Head direction cell distribution of properties

HD cells are distributed over a **large network** including many regions **outside the HR**. Very thorough reviews address the comparison between PrS and extra-HR HD cells (Taube and Muller 1998; Muir and Taube 2002; Taube 2007). Paper #2 compiles most of the static and proportional differences one can see in directional modulation between the **PrS**, **PaS** and **MEC**: Regarding proportion distribution, the most striking feature is that **LII MEC** contains virtually no HD or directionally modulated cells. Other than that, proportions are relatively uniform between all layers of the PrS, PaS and MEC except for LIII MEC, which presents substantially less direction modulation. HD cell static properties are not strongly predictive of where the cell is located; however, one can see a tendency for **PrS** directional cells to be **sharper** than

PaS and MECs. This could be due to the fact that PrS contains a higher proportion of cells uniquely coding for direction ("true HD cells") while **PaS** and **MEC** have more cells presenting a **conjunctive code** such as that seen with grid-by-HD cells and border-by-HD cells, yet it is possible that more type of conjunctive HD-by-X cells remain to be discovered. Furthermore recent studies found a **continuous dorso-ventral increasing tuning gradient** of HD cells (i.e. sharpness**)** in **MEC LIII** but not in LV (Giocomo et al. 2012). I will be interesting to see if this gradient reflects a gradient in the conjunctive properties (e.g. grid or velocity modulation) of these cells. Finally, when originally describing the HD cells in the dPrS, Taube and colleagues observed that a few directional cells discharged a burst of spikes as the head of the animal passed through the preferred direction, while on other occasions they discharged only one or two spikes (Taube et al. 1990). An attractive explanation could be that these cells may be conjunctive cells. It would be interesting to check how firing rate is different from one ensemble to another.

Grid cell distribution of properties

As shown in paper #2, grid cell proportions are distributed in almost a reverse fashion compared with the HD cells: they are **over represented in the superficial layers of the MEC** (around 50%) and represented in decreasing proportions in **deep layers of the MEC, PaS and PrS**. Similarly to HD cells, the static properties of grid cells are not strongly predictive of where the cell is located. Yet, a similar tendency followed that of the proportion distribution with an average **higher gridness score among MEC LII grids**. The existence of an over-representation of grid-by-X conjunctive coding in the other areas might account for this observation. Average cell **theta modulation** roughly respects this distribution. It will be interesting to **quantify which parameters** explain best the inhomogeneous distribution of gridness score: outside of field firing, ellipticity, heterogeneity of rate between nodes. Moreover, it will be very meaningful to test whether **dynamic properties** would follow such a distribution (especially in novelty conditions). This would allow a distinction between at least **two different pools of grid cells** with appealing mechanistic and theoretical application (see III). Besides, a **dorso-ventral grid scale gradient** has been observed in MEC mirroring that of the hippocampal place cells (Hafting et al. 2005; Brun et al. 2008). It has been shown recently that this gradient is not continuous, but rather reflects the

discrete distribution of properties over small areas (Stensola et al. 2012), which could correspond to recently discovered entorhinal cell patches (Burgalossi et al. 2011).

Border cell distribution of properties

Very little is known at present on the properties of border cells and their distribution besides the distinction established between **subiculum** BVCs and PHR border cells (see I.III). Paper #2 shows that besides the virtual absence of border cells in MEC layer II, there are no other significant differences between **MEC**, **PrS** and **PaS**.

Cluster of properties

Preliminary observations of the paper #2 dataset led me to hypothesize that cell type and properties tend to cluster (e.g. the conditional probability to record a second grid is higher than for the first one). The existence of **connective patches** was recently confirmed (Burgalossi et al. 2011) and so was the **discrete distribution** of some grid properties (Stensola et al. 2012). Further analyses are however required to establish the fine microstructure of spatial and directional modulation in the HR.

Another level of investigation is whether **specific cell types** (e.g. stellates, pyramids) support preferentially certain types of modulation. It was demonstrated, for instance, that **place cells are pyramidal cells** (Henze and Buzsaki 2001; Lee et al. 2006; Lee et al. 2009; Epsztein et al. 2010). Yet more data is needed to conclude about granular and mossy cells. The PHR contains many different cell types. Based on **LII MEC stellate** proportions, it has been hypothesized t**hat grid cells** are stellate cells (Giocomo et al. 2007). Other work confirmed the observation of grid signal in stellate cells, however, it did not exclude the existence of this signal in pyramidal or multipolar cells (Burgalossi et al. 2011; Domnisoru et al. 2012; Schmidt-Hieber and Hausser 2012; Zhang et al. 2013). Future work will continue to focus on that cellular aspect of the spatial/directional signal in terms of morphology but also in terms of proteonomic and cellular mechanisms. This will make it possible to resolve some of the questions on the origin of the signal (see III).

II.II Global functional network: coordination and interaction between areas (paper #1 and #2)

The spatial/directional code may be read at the network level through both the **collective activity of individual neurons** (i.e. neural assemblies) and the **synchronized oscillation of a neuronal population**.

Cell ensembles spatial (in)-coherence

As stated in 2.5.4.2, there are several **levels of cell ensembles**: (**1**) ensemble of cells coding for the same feature and belonging to the same area (e.g. CA1 place cells), (**2**) ensemble of cells coding for the same feature but not necessarily belonging to the same area (e.g. CA1 and DG place cells), (**3**) cells belonging to the same area but not necessarily coding for the same feature (e.g. MEC HD and grid cells), (**4**) cells belonging to the same network but not necessarily coding for the same feature or belonging to the same area (e.g. PrS HD and CA1 place cells).

Paper #1 data shows that border cells from a given area (situation 1) when confronted with a change in the environment behave as a coherent ensemble and either all or none remap. This behaviour is similar to what is observed with HD and grid cells and contrary to place cells. The relationships between their respective firing fields are conserved in a situation of cue rotation, yet they are not conserved from one environment to another, again in a similar fashion as what is observed with HD and grid cells. In addition, a small, unpublished remapping dataset collected for paper #2 show the same tendency for grid cells in situation (2). The addition of these results to the studies presented in 2.5.4.2 suggest a system where **HD, grid, border cells** seem to belong to a **coherent (yet not rigid) network** that behaves as one **tight ensemble,** while **place cell** ensembles, though often showing **strong coupling** with each other and with HD, grid and border cells, are **less rigid and less coherent** in all situations of comparison, especially when the rat is **disorientated.**

Paper #2 shows a decrease in border specificity in the no-wall configuration. An attractive explanation for this result may be that it is due to the novelty of the no-wall configuration. According to that hypothesis, border cells would follow the same behaviour as some grid cells and have their specific firing pattern disrupted in a **novel environment**, in a non-coherent way between concomitantly recorded cells.

Representation of the spatial signal at the network level: neural assemblies

As discussed above, neural assemblies are mostly coherent and their collective activity permits to compute with great accuracy the position of the rat in the environment. This neural network is the substrate for the **cognitive map** (O'Keefe and Nadel 1978), now extended to the whole HR and including place, HD, grid and border cells. A divergence from the original concept is that the PHR seem to support a **universal path integration based navigation system** (see 2.3.5), while the HF supports a representation less rigid and more influenced by non-spatial information.

In addition to their activity *in situ*, place cells assemblies may be defined by their activity outside of the preferred firing field either in the behaving animal or during sleep. It was shown that **place cell sequences** represent **retrospective or prospective location** (Wilson and McNaughton 1994; Foster and Wilson 2006; O'Neill et al. 2006; Johnson and Redish 2007; Karlsson and Frank 2009; Dragoi and Tonegawa 2011). Such phenomena are involved in the **consolidation** of spatial representation and correlate with **performances in navigation tasks** (Dupret et al. 2010; Jadhav et al. 2012). At present, HD, grid and border cell assemblies have not be shown to present such prospective or retrospective activity (Brandon et al. 2012).

Representation of the spatial signal at the network level: local field oscillations

The neural code is not only apparent by the firing patterns of individual cells but also by the variation of potential observed in the local field. The **synchronized activity** of a majority of neurons in an area results in the **oscillation** of the global network activity. The frequency of oscillation may be imposed by an **external generator** or **locally generated**. I will discuss this point at greater length in (III). The global oscillations may in return modulate the discharge of individual neurons. Similarly to what has been observed for HF place cells and MEC grid cells (see 2.2.3), papers #1 and #2 show that an important portion of the cells in the PrS, PaS and MEC see their activity modulated according to a global theta rhythm. In 2.5.4.2, I presented the principles of temporal coordination in the HR. A **two-dimensional phase precession analysis** of the database in paper #1 and #2 could provide precious data on the activity of border cells and grid cells in several areas of the PHR.

Local field oscillations may be mirroring a particular **brain state** or **ongoing behaviour**. In addition, the observation of the synchronisation of these oscillations between connected areas led to the hypothesis that they facilitate the coordination of the network and that they support **communication inside** and **outside** that network. The existence of temporal coordination between interconnected areas addresses a fundamental question of cognition localization, which is that of **serial or parallel processing**. It provides evidence for a parallel processing. However, several studies, mostly based on lesions/inactivation/knock out studies have hypothesized that the spatial/signal is inherited from one area to another, thus leaning towards serial processing (see III). The two theories are not mutually exclusive.

II.III Contribution of the network to the signal at the single cell level

This point will be discussed in more details in the chapter on the origin of the spatial signal (see III). Yet I wanted to mention here a few pointers.

The vast literature on lesion/inactivation (see 2.5.4.1) establishes that spatial and directional signals are dependent on the integrity of several specific areas belonging to a **global network**. The spatial/directional signal is distributed over several areas in the HR forming a spatial network.

I will discuss in (III) evidences suggesting that the spatial/directional code emerges from the **transformation of the signal** inherited from one area to another, through the **integration** of complementary inputs coming from all over the brain, and that both **serial and parallel processing** can be observed, as is demonstrated by the results from lesion/inactivation and developmental studies. The **gradual transformation** of the signal can even be observed within a structure like in CA1 and Sub, which show proximo-distal gradients of spatial selectivity (Henriksen et al. 2010; Kim et al. 2012). A question raised by this discussion is that of the existence of **organization centres** (e.g. directional signal distributed by dorsal PaS patch, theta signal imposed through septum innervations).

Furthermore, the existence of cells coding for several features gives insights into the integration/transformation of the signal. One can see, notably with the example of HD cells, that units with conjunctive properties have been hypothesized as both upstream and downstream of the signal processing chain (e.g. AHV-by-HD cells give inputs to "pure" HD cells which give inputs to HD-by-grid cells, see III). Thus a single feature code may both result from the integration of conjunctive codes and participate in the generation of a **conjunctive code**.

The signal is further **stabilized and anchored** in a spatial/temporal reference frame by the **summation** of complementary inputs, the **enhancement** of the determinant inputs and the **silencing** of the noise and interfering inputs through the action of mechanisms such as inhibitory and excitatory network, reverberant activity and strengthening/weakening of the synapses by plastic processes. One can consider the spatial/directional network as composed of several sub-systems that stabilize each other through the action of constant feed forward and feedback between them in a functional "loop" circuit. The existence of a network also allows the **comparison** between **prospective, current and retrospective coding** to support **learning**, or

between the current experience and previous similar experiences to maximize similarity or differences in order to induce **pattern completion or separation**.

Finally, many of these mechanisms are facilitated by the **synchronization of the oscillatory activity** (see II.II). The **coherence** of neural activity privileges **communication** and **interaction** between parts of the network.

III. On the origin of the spatial signal

Central to this thesis is the question of the directional/spatial signal origin. The signal can be treated either as a global signal or by focusing on individual cell types. When delving in this matter, one should be careful to distinguish between **signal origin and signal stabilization** (see 2.3.1). To answer these questions, the most important sources of information come from the **lesion/inactivation and KO studies** evoked in the introduction (2.5.4.1), from in-depth studies of the **cellular mechanisms** of each cell type and from **developmental data**. I will discuss further these results below while assessing the **cellular and network mechanism**s at the origin of HD, grid and place cells.

III.I Mechanisms at the origin of head direction cells (paper #2)

I will focus here on the mechanisms accounting for the directional signal observed in the **HR** and will neglect data not linked to it. I refer the reader to four excellent reviews for complementary information on the **HD cell system** (Taube 1998; Taube and Bassett 2003; Taube 2007; Clark and Taube 2012).

Network mechanisms at the origin of head direction cells

Paper #2 was instrumental in showing how HD cells are distributed over a large network of PHR regions (**dPrS**, **dPaS**, **MEC**). Yet the HD cell network also includes **many regions outside the HR**: the retrosplenial cortex, several thalamus nuclei (latero-dorsal: LDN, antero-dorsal: ADN), the dorso-tegmental nuclei (DTN), the lateral mammillary nuclei (LMN), portions of extra-striate cortex, the dorsal striatum and the parietal cortex (see 2.2.1 and (Muller et al. 1996; Sharp et al. 1996; Taube 1998; Muir and Taube 2002; Taube and Bassett 2003; Taube 2007). HD cell **proportions vary** from one area to another. They are very high in the PHR and the ADN (over 50%, (Taube 1995), paper #2).

Several studies point to the **origin** of the directional signal as **located outside the HR**. Some of the primary supports for this hypothesis come from **lesion studies**. The first step was to establish the relative role of **dPrS** and **ADN** in their respective

directional signal (Goodridge and Taube 1997). ADN complete lesions result in the total loss of direction in dPrS, while dPrS lesions lead to changes in HD cell properties. PrS lesions result in less sharp, more predictive and less anchored HD cells (i.e. the ability of visual landmark cues to control HD cell tuning is most significantly disrupted) (Yoder et al. 2011). Thus, the directional signal does not originate in dPrS, yet it is the seat of some information integration stabilizing that signal. Lesions focused on another thalamic nucleus, the **LDN,** do not have any significant effects on dPrS HD cells (Golob et al. 1998). **Retrosplenial** cortex complete lesions seem to destabilize considerably the HD signal in the ADN, by impairing landmark control over the cell firing (Clark et al. 2010). That area might have an important role in conveying visual information to the HD cell circuitry (Taube 2007). Both **DTN** and **LMN** individual lesions disrupt the directional signal in the ADN, dPrs, PaS, MEC (Blair et al. 1999; Bassett et al. 2007; Sharp and Koester 2008). Both these regions have in common the task of conveying the signal in provenance from the vestibular system, thus it is not surprising to see that the lesion/inactivation of the **vestibular system** leads to the total disruption of the directional signal both in the ADN and the dPrS (Stackman and Taube 1997; Stackman et al. 2002), as does the occlusion of its semi-circular canals (Muir et al. 2009) or the genetic ablation of otolith organs (Yoder and Taube 2009). It was recently shown that the **supragenual nuclei** act as a relay of the vestibular information and that its lesion disrupts the directional signal in the ADN (Clark et al. 2012). Beside vestibular information, the DTN is also the recipient of motor information via projections from the interpeduncular nucleus (IPN). Lesions of the **IPN** disrupt the directional signal in ADN in a very similar fashion to dPrS lesions (Clark et al. 2009). Interestingly, the inactivation of the vestibular system, in spite of disrupting the directional signal, does not inhibit the firing of ADN putative HD cells, which present, in these conditions, intermittent firing bursts of activity that could result from IPN inputs (Stackman and Taube 1997).

If instead of disrupting "upstream" of the dPrs, one observed the effect of "downstream" lesions, one can see that a transient inactivation of the **HF** does not have a significant effect on the firing properties of MEC and dPaS HD cells, and might even make them have a slightly higher HD score (Bonnevie et al. 2012). This result contradicts former studies showing that HF lesion leads to a loss of stability of dPrS HD cells, in spite of a conserved ability to follow a cue (Golob and Taube 1999). However, in that study, lesions were not restricted to the HF but included large

portions of **overlying neocortex** such as the occipital cortex, thus it is difficult to draw a conclusion without more specific experimental results. Moreover, ADN HD cells were almost unaffected by **MEC** lesion, except for an increased tendency for prospective firing (Clark and Taube 2011). A recent **septum** inactivation study (Brandon et al. 2011) showed that MEC HD cells seem unaffected by the loss of septum activity.

These lesion studies were completed by **systematic comparisons** in intact rats of the **properties of HD cells in each region** in order to understand the directional signal code transformation in the HD cell network (Taube 1998). As dPrS HD cells are dependent on ADN and LMN integrity, it is interesting to compare them to see whether one can observe a progression in "directional code integration". Several differences exist between the HD cells of the **PrS** and **ADN** and **LNM**. ADN and LMN HD cells are less sharp that in the dPrS. This larger range of direction can be explained by two linked observations: first, most ADN and LMN HD cells are on average more strongly modulated by angular head velocity (AHV) (Blair and Sharp 1995; Taube 1995; Taube 1998); second, time shift analysis shows, on average, stronger anticipatory firing in ADN and LNM, while dPrS cells tend to code for the current HD (Blair and Sharp 1995; Blair et al. 1997; Taube 1998; Taube and Muller 1998). These observations were used to build the theory according to which direction representation is supported by a **continuous attractor network** (see 2.5.3) (McNaughton et al. 1991; Zhang 1996; Goodridge and Touretzky 2000; Sharp et al. 2001; Xie et al. 2002; McNaughton et al. 2006; Clark and Taube 2012). In those models, HD cells are connectively organized in a schematic circle according to their preferred firing direction: when the animal rotates, successive HD cells are activated. The transfer of energy could then be supported by the presence of **conjunctive head-by-angular velocity cells** (HD X AHV**)**. Such cells as well as "pure" AHV cells have been recorded in many areas including ADN and LMN.

Beside the models, it is clear that the source of HD cells is in the vestibular system that sends its information to the ADN via the **DTN** and the **LMN**, which contains **AHV** cells. The HD cells in those areas respond preferentially to **motor and motion inputs**. The ADN then project to the **dPrS** (among others with the retrosplenial cortex, for example), where the "motion" directional signal may be stabilized by its anchoring to a reference frame based on sensory information. The directional signal there is the "purest", coding strictly for the **current HD** and nothing

else (those could be the "real" HD cells, while other areas present more directional cells, see HD cell shift in definition in I.II). The **dPrS back projection** to the ADN and the LMN has a **stabilizing effect** on the directional signal. Interestingly, these projections arise from different cell populations within the dPrS (Yoder and Taube 2011). "Downstream" of the dPrS, the directional signal is combined with spatial and maybe contextual information to allow more integrated processes (see section on the origin of grid cells).

Cellular mechanisms at the origin of head direction cells in the HR

I refer the reader to section 1.3.3.1.2 where I briefly listed the morphological and physiological properties of PrS, PaS and MEC principal cells and distinguish several clusters of cell populations within each area. Also discussed in the introduction are the discharge properties of HD cells (see 2.2.3.2.2). One of the main *in vivo* firing characteristics of HD cells is that they keep firing when the rat is maintained in one direction, independently of motion, on-going behaviour, visual or auditory stimulation, motor signals, or vestibular modulation, and present very little adaptation in their firing rate (Taube and Bassett 2003). This **lack of adaptation** has been reproduced in *in vitro* whole cell patch recordings where it was shown that a short-triggering stimulus (as few as five induced spikes) could initiate **persistent firing** in MEC cells (Egorov et al. 2002) and in dPrS cells (Fricker et al. 2009; Yoshida and Hasselmo 2009). These results suggest that persistent firing of HD cells of the HR could be supported by an intrinsic mechanism. Recent work conducted *in vitro* on the ADN showing persistent firing of single cells supports that hypothesis (Kulkarni et al. 2011). Pharmacological results indicated that a **calcium-sensitive nonselective cation current** drives this persistent firing in presubicular cells (Yoshida and Hasselmo 2009) that could be modulated by the **cholinergic system** (Zilli and Hasselmo, cited in (Taube 2010)). Other authors found that a component of the specific **sodium current of** presubicular cells was **insensitive to tetrodotoxin** and hypothesized that such a (TTX-I) current may be responsible for the reduced adaptation observed in many PrS cells (Fricker et al. 2009). Furthermore, cells with persistent firing were distributed in both superficial and deep layers of the PrS, as shown in paper #2 for HD cell distribution (Yoshida and Hasselmo 2009). Yet, recent *in vitro* data shows small differences in electrophysiological and dendritic properties between deep and

superficial layers (Simonnet et al. 2012). In depth investigation of paper #2 data could give insights into whether these *in vitro* differences translate *in vivo*.

Recent *in vivo* **interspike interval** (ISI) analyses of HD cells of the ADN, LMN and dPrS showed that **HD cell firing was irregular**, even when the animal's HD was maintained within ± 6° of the cell's preferred firing direction (Taube 2010). The degree of variability in cell spiking was a characteristic property for each cell. There was little correlation between ISIs and angular head velocity or translational speed. In contrast to the high variability observed for the ISI, firing rate within the cell's preferred direction over longer time intervals was more consistent (regular) and predictable. This supports the idea that HD cell activity is based on a **rate code** rather than a temporal one. Most evidence points to external synaptic inputs as the most likely source of the high variability in ISIs (see discussion in (Taube 2010)).

Based on the septum lesion data (Brandon et al. 2011), and the fact that many HD cells are **not theta modulated** (see paper #2), theta does not seem to be involved in the generation of the HD signal. However, it is possible that different populations of HD cells with different locations within the network may react differently regarding septal lesions.

Finally, the advent of new ***in vivo*** recording techniques makes it possible to measure the **properties** of HD cell **membranes** in behaving rats, especially in the PaS (Burgalossi et al. 2011).

III.II Mechanisms at the origin of grid cells (paper #2)

The discovery of grid cells is quite recent and paper #2 is the first to show their existence outside the MEC. Because of their unique and fascinating **hexagonal firing pattern**, grid cells have arouse great interest among the scientific community, especially regarding their origin. Many have attempted to **model** how the cellular network could translate idothetic and allothetic information into a neuronal grid pattern. I will here focus on what is experimentally known about the **mechanisms** supporting grid cell generation, delving in both **signal origin** and **signal stabilization**. I will attempt briefly to link these observations to the current dominant models outlined below.

Grid cell models

As reviewed in (Moser et al. 2008; Giocomo et al. 2011; Zilli 2012), most models of grid cell generation are linked to **path integration** and implement **velocity-related**

inputs. Those can mainly be divided into two classes: the **oscillatory interference (OIF) models** and the **continuous attractor network (CAN) models**. Besides the variations or combinations of OIF and CAN models, one should mention one model based on the idea that a grid arrangement is the most efficient way to tile a plane with circles, and hypotheses that the grid pattern emerges from **Hebbian self-organization** in the network of competitive spatial inputs (Kropff and Treves 2008).

The oscillatory interference (OIF) models derived from **phase precession** models. In these models, the grid cell pattern emerges from the **interference between independent oscillators** with **different phase** or **frequencies** applied on different **sub-cellular compartments** (Burgess et al. 2007; Hasselmo et al. 2007; Blair et al. 2008; Burgess 2008; Hasselmo 2008). These interfering oscillations are often controlled by velocity and may be **locally or externally generated.** Generation of local oscillations have been observed trough the activity of the cells themselves (e.g. membrane subthreshold potential oscillation (MSPO), cell firing) or through the **oscillatory network** of units. The septum is often considered as an external generator of oscillations. Those models were mainly criticized for their **susceptibility to noise**. Later models were stabilized by the addition of either a constant update of the fields through **external sensory inputs** (Hasselmo 2008), or by coupling the neural oscillators via **excitatory or inhibitory connectivity** (Zilli and Hasselmo 2010). Other models emancipated themselves from velocity modulation (Welday et al. 2011).

The basic principles of the **continuous attractor network (CAN) model** have already been explained in 2.5.3. This model is based on the existence of a **strong recurrent connectivity** (McNaughton et al. 1996; Samsonovich and McNaughton 1997; Fuhs and Touretzky 2006; McNaughton et al. 2006; Burak and Fiete 2009; Si et al. 2012) and often postulate the existence of a **separate layer of cells** coding for **conjunctive velocity by position** or **head direction** by position cells. **Edge effects** were observed in the first CAN models resulting in an overall firing at the edge of the environment. That can be corrected by organizing the neural network in such a way that neurons at the edge of the network connect with neurons at the opposite edge, like, for instance, in a **torus** (McNaughton et al. 1996; McNaughton et al. 2006). Those models were criticized for not addressing the dynamic properties of grid cells such as **phase precession**, yet later versions corrected that (Navratilova et al. 2012).

Recently, **second generation models** have been developed, using elements from both OIF and CAN models and taking into consideration new experimental data,

notably about the shift in the grid cell definition (see I.III). As pointed out in (Zilli 2012), grid models are made of different components such that a division between OIF and CAN may seem artificial. The question of grid cell origin is very current and work in this area is fast moving. All models have been criticized for not being biologically realistic in one way or another (Remme et al. 2010; Taube 2010).

Recent data from the Trondheim Kavli Institute led to the formulation of a promising new model from the Roudi lab (Dunn et al. 2012) where **HF is an external excitatory drive** necessary for the formation of the grid pattern, which arises by **velocity-dependent translation** across an **inhibitory recurrent network**.

Signal inherited or locally generated?

As related in I.III, several recent studies (including paper #2) demonstrated that grid cell properties are not homogenous and that one could distinguish between **different grid categories** that for some properties follow an **anatomical distribution** (see II.II), though their **dynamic properties** are quite **tightly linked** (see II.III). Yet the discovery that **grid cells exist outside the MEC** (see paper #2) led to a fundamental question about the origin of the grid pattern: can it be inherited? Or in other words: can the signal coming from a grid cell generate another grid cell? Interestingly a recent study (Koenig et al. 2011) identified a **subpopulation** of grid cells different from the other grid cells, seemingly **not directly participating in the generation of the grid pattern**. Once the grid pattern of those cells was disrupted, they did not regain their spatial regularity, even after the elimination of the cause of disruption. Yet, one should note that in some of these cases the injection led to brain lesions. Many of the models mentioned above suppose transmission of the grid pattern from one cell to another. If not inherited from one area to another, then grid cells are **locally generated** in **anatomically and physiologically different areas**. In such a configuration, the conditions needed to generate the grid signal must be common to these areas. I will hereafter present some of the **common properties between PrS, PaS and MEC**, and discussed how they may participate in the grid signal generation.

Need for directional inputs

The **PrS**, **PaS** and **MEC** have in common that they **receive directional inputs**. As a matter of fact, in all areas except MEC LII, **grid cells intermingle with HD cells** and a large proportion of them present conjunctive HD-by-grid properties.

The study of the **postnatal development** of spatial and directional firing patterns established that when rat pups aged two and a half weeks explore an open environment outside the nest for the first time, their PrS and PaS **HD cells have adult-like properties from the beginning**. Place and grid cells are also present but evolve more gradually. **Grid cells show the slowest development.** The presence of adult-like directional signals at the onset of navigation raises the possibility that such signals are instrumental in setting up networks for place and grid representation (Langston et al. 2010; Wills et al. 2010).

Recent preliminary **lesion data** further supported that idea by showing the **disruption of the grid cell patterns** in the MEC and PaS in response to lesion of the HD cell system (i.e. **ADN lesions**) (Clark et al. 2011). Other data confirmed that grid cells receive HD signal as "pure" **grid cells do transform in HD cells** after the **inactivation of the HF** (see also below, (Bonnevie et al. 2012)). Thus the HD cell system would be instrumental not only in setting up but also in maintaining the grid system when the animal is moving. This notion is well integrated in most grid cell models, which require directional inputs. It was recently shown that both **PaS** and **PrS** are sending **projections** to **all layers of MEC** (Canto et al. 2012) and *in vivo* studies showed that at least one particular **PaS dorsal patch** seem to behave as an **organizational centre** sending **directional information** to all **MEC LII "grid patches"** (Burgalossi et al. 2011).

Need for anchoring inputs

As demonstrated in 2.3.2.3, though **visual inputs** are not necessary for the generation and maintenance of grid pattern and activity, they have a role of **stabilization/anchoring** of its vertices to an **external reference frame**. Furthermore, the **environment spatial features** seem to influence the grid pattern (see 2.3.4 and I.III) and my personal observations are that, in a regular square or circular environment, grid fields close to the wall are on average more "deformed" than those in the centre of the apparatus which is evocative of the **edge effect** seen in the first CAN models. To explain these effects, it has been postulated that grid cells were anchored to the environment border through projections from the border cells or the subicular **BVC** (Barry et al. 2006; Lever et al. 2009; Burgess and O'Keefe 2011). Experimentally, border responsive cells were found in the MEC, PrS, PaS and Sub and those areas **project to the grid cell system** (paper #1, paper #2) (Savelli et al.

2008; Lever et al. 2009). **Developmental data** shows that border cell maturation precedes that of the grid cells (Bjerknes et al. 2012).

Moreover, recent data shows that some **grid cell properties** are **unstable in a new environment** (see 2.4.2), especially in big environments. These observations establish that the grid signal stability, in some if not all grid cells, is dependent on **cue experience** and **perception**.

Hippocampal inputs

PrS, **PaS** and **MEC** all receive **inputs from the HF** (though CA1 inputs to the MEC are more important than the PrS and PaS). Some unpublished data from the Moser lab (Bonnevie et al. 2012) demonstrated that the **grid pattern is disrupted** in response to a transient **inactivation of the HF**. The authors show that the pattern disruption is gradual and selective and that the affected cells become tuned to the animal's head direction. Short-window and spike-triggered analysis led them to conclude that the pattern disruption was **not reflecting a pattern drift** due to a lack of anchoring and that the hippocampal inputs were needed per se to generate the grid signal. Finer analyses show that the disrupted cells still express **weak non-periodic spatial firing** fields and directional modulation, thus revealing the influence of other inputs on the grid cells and confirming the existence of a directional component. They interpret these by hypothesizing that the **HF is an external excitatory drive** necessary for the formation of the grid pattern, which arises by velocity-dependent translation across an inhibitory recurrent network (Dunn et al. 2012).

Specific organization of the local network

Many grid cell models are based on the specific organization of the local network. Most **CAN models** hypothesized that the grid pattern arises from an **excitatory recurrent network** based on connectivity strength with local excitation and surround inhibition.

Some experimental data have supported the local network involvement in grid cell theory, while other data refutes it. **Developmental** studies showed that the gradual maturation of the grid pattern in pups mirrors an **increase in network synchrony among entorhinal stellate cells** (Langston et al. 2010). The highest proportion of grid cells is found in **MEC LII**, however, where **excitatory recurrent connections are sparse** or non-existent (Dhillon and Jones 2000). However, recent unpublished data from the Witter lab shows that MEC LII stellate cells are

interconnected only through a **local recurrent inhibitory network of constant magnitude** (Couey et al. 2012). These results support the same model as in the Bonnevie data (see above) (Dunn et al. 2012), inspired by (Burak and Fiete 2009). The existence of an inhibitory recurrent network is further supported by recent data obtained by **photostimulation of the MEC PAV interneurons** showing a strong **inhibition of grid cell activity** (Buetfering et al. 2012).

As suggested by compelling new results, these networks could be organized locally at the scale of **MEC anatomical patches** (Burgalossi et al. 2011; Stensola et al. 2012).

Theta modulation

Many **OIF models** are based on the **theta modulation** of **grid cells** and are developed after **phase precession** models (see 2.2.3.3). Paper #2, besides confirming that most grid cells are theta modulated, shows an **association between the proportion of theta-modulated cells and the proportion of grid cells** in given subareas. Putative grid cells (i.e. MEC LII stellate cells) show subthreshold membrane potential oscillation (**SMPO**) at a theta frequency (Alonso and Llinas 1989). This argues for a **local generation of theta** signal by **cellular intrinsic ionic mechanisms**. These observations were shown to be true for other grid-cell rich areas such as the PaS (Glasgow and Chapman 2007; Glasgow and Chapman 2008). Furthermore, SMPO properties are organized following a similar **dorso-ventral gradient** as seen for grid scale, Specifically, the inverse of the frequency of SMPO in entorhinal neurons increased according to that gradient establishing another link between SMPO and grid cells (Giocomo et al. 2007). This effect seems **modulated by cholinergic inputs** (Heys et al. 2010; Glasgow et al. 2012; Tsuno et al. 2012) and to involve the time constant of an **Ih current** (i.e. an hyperpolarization-activated cation current I(h) observed in patch-clamp) (Giocomo and Hasselmo 2008). This action was hypothesized to be mediated through a hyperpolarization-activated cyclic nucleotide-gated (HCN) subform (i.e. HCN1) (Giocomo and Hasselmo 2009). Yet, in *in vivo* **KO HCN1** mice the grid cell pattern is intact and so is their dorso-ventral scale gradient although there is a probably a **loss of subthreshold theta** (Giocomo et al. 2011) at odds with many IOF models (Mehta 2011). However, these HCN1 KO mice show a concomitant **increase of grid scale** and **theta modulation period**, arguing for a role

of Ih in the **gain of the transformation from movement signals to spatial firing** fields (Giocomo et al. 2011).

The other main source known of theta modulation in the MEC is coming from the **septum**. It was recently shown that an **inactivation** of the septum (Mizumori et al. 1992) leads to the **disruption of the grid patterns** (Brandon et al. 2011; Koenig et al. 2011), while **CA1 place cells** are only **mildly affected** by similar manipulation (Mizumori et al. 1989; Koenig et al. 2011). However, it is not clear yet what are the mechanisms responsible for the disappearance of the grid signal. Besides the obvious, it could also occur through **indirect mechanisms** affecting the coding of the **velocity signal** or disrupt the **synchrony of the network** or the **balance** between activation and inhibition. One should note that **CA3 place cells** are deeply affected by septum inactivation (Mizumori et al. 1989). Whether this is linked to grid cell disruption and, if yes, whether this is a cause or a consequence, remains to be shown.

As previously stated, a **subpopulation of the grid cells,** whose pattern was disrupted by the septum inactivation, did not regain their spatial regularity, at odds with the other grid cells (Koenig et al. 2011). This result argues for the existence of several categories of grid cells (II), including some **that may inherit the signal** from others. This extends the finding that several grid cells in the rat do **not present strong theta modulation**, in spite of strong theta power in the local field potential (paper #2). It will be interesting to know whether the "Koening grid cell sub-population" (1) were strongly theta modulated to start with; (2) were recorded in specific anatomical location (outside LII); (3) showed conjunctive properties (with HD, with velocity).

Controversially, a recent study argues against the role of theta in grid cell generation by showing that **grid cells in bats** exist in the **absence of continuous theta oscillations**, and with almost no theta modulation of grid-cell spiking (Yartsev et al. 2011). Several authors object that these grids were recorded in very unnatural conditions (crawling vs. flying) and at low speed (Colgin 2011; Barry et al. 2012; Zilli 2012). However, preliminary results suggest that there are no changes in the theta of flying bats (Ulanovsky, personal communication). Thus how should we reconcile the bat and the septum inactivation studies? A good explanation would be that what is observed in the septum inactivation is a **by-product of the inactivation of the transformation of the speed** (Colgin 2011). Indeed, it has been shown that rat running speed modulates septum theta activity (King et al. 1998). Furthermore, **bat grid cells** are indeed **speed modulated** (Ulanovsky, personal communication). It

would be interesting to see whether frequencies other than theta correlate with speed in the bat. Such a hypothesis was recently confirmed by the finding of **SMPO in bat** hippocampus slices, which oscillated at a **lower frequency** (2–3 Hz) than in rats (Heys et al. 2012).

Speed modulation

Almost all grid cell models are based on the integration of the velocity signal and many suppose the interaction of **velocity control oscillators** (VCOs) (Jeewajee et al. 2008). It has been shown that the **firing rate** of most **grid cells** is **positively modulated by running speed** in the rat (Sargolini et al. 2006). As stated above "the **bat/septum**" controversy experimentally suggest that velocity modulation has a role in the generation and maintenance of grid cell pattern.

Supporting that hypothesis, it has been shown that rat **running speed modulates septum theta activity** (King et al. 1998), place cell activity (Rivas et al. 1996; Geisler et al. 2007) and grid cell activity (Sargolini et al. 2006; Jeewajee et al. 2008). A recent study recording in the septum, the ADN and the HF showed that **theta cell** burst frequencies varied as the cosine of the rat's direction of movement in these areas (Welday et al. 2011). Based on these results, the authors build up a model where neurons receiving inputs from such theta cells could, when the inputs were synchronized, compute a location as it is observed in place, grid, or border cells.

As stated above, some have hypothesized a role for **Ih** in the transformation from movement signals to spatial firing fields (Giocomo et al. 2011). It is likely that some of the mechanisms described for theta modulation can apply to velocity modulation. The advent of **virtual reality** studies should help to investigate these questions in more details.

Specific cellular properties

Though grid cells have been recorded across several areas they are the most abundant in their "non conjunctive form" in **MEC LII** where they represent approximately 50% of the principal cell population. In an attempt to understand which cellular properties are at the origin of the grid pattern, several studies have focused on MEC LII cells. Recent ***in vivo*** **studies** confirmed that MEC LII grid cells were in the vast majority **stellate cells**, yet some **pyramids** in MEC LII have also been shown to express a grid pattern (Burgalossi et al. 2011); (Domnisoru et al. 2012); Schmidt-Hieber, 2012).

An extensive and still growing body of work has made it possible to establish many of putative cellular properties of grid cells (see 1.3.3.1, and see (Canto and Witter 2012) for a comprehensive overview of all layers of the MEC). Studies focusing on MEC LII stellates led to the hypothesis of a role for **SMPO mechanisms mediated by HCN1** channel (see above). In addition, other cellular mechanisms have been postulated to participate to the grid pattern generation, notably **spike frequency adaptation** (Yoshida et al. 2012) or **persistent firing** (Hasselmo 2008) (see (Giocomo et al. 2011; Pastoll et al. 2012; Zilli 2012) for a discussion on how some of these cellular properties are included in grid cell models). The recent development of ***in vivo* studies** of the cellular properties of individual cells in behaving rats allowed the observation of the **potential variation** of **membrane subthreshold** in function of the rat's behaviour and the further investigation of grid cellular mechanisms of generation and maintenance (Burgalossi et al. 2011); (Domnisoru et al. 2012; Schmidt-Hieber and Hausser 2012).

III.III Role of directional, grid and border inputs to place cells (paper #1 and #2)

Place cells are much **less rigid** than HD and grid cells. They are not active in all environments and show rate/global remapping in a non-coherent way or even partial remapping. Moreover, they have different spatial and non-spatial features. The spatial code observed is dual: **rate and temporal code**. This code may encompass more than just spatial features. This heterogeneity and complexity of place cell activity may be explained by the **abundance of inputs** they receive and process. Therefore, their origin and stabilization may result from complex interactions between several mechanisms. .

Discussing the origin of place cells is not a simple matter as they present **different properties** depending on their **anatomical location** (II.II). Thus the **origin of place cells may be plural**, yet many models focus on **CA1** place cells as being the "final product" of converging inputs principally from **DG, CA3 and MEC**.

A large body of work including **lesion/inactivation** (II.III) and **connectivity** (1.3.2) studies has helped us to understand that place cell generation or stability requires the **integrity of the circuits** within the **HF** and the **PHR** but also **external** to the HR. The advent of new tracing and inactivating tools allow these studies to be more and more precise in discriminating inputs, even at the functional scale. Central

to the subject of this thesis, it was recently shown that **CA1 place cells receive monosynaptic projection from MEC grid, border and HD cells** (Ye et al. 2012).

I will here mainly observed the relations between place cells and HD, grid and border cell activity. I will discuss how this activity is linked to path integration, navigation and memory in the last section of the discussion

Local network

As discussed in 2.5.3, some of the properties of place cells seem linked to the **specific wiring of the local network**: in particular, the role of the CA3 recurrent excitatory network in pattern completion or the role of the DG inputs sparsity in pattern separation. Each hippocampal subfield may have a different role in the processing of the spatial signal (see IV) and as demonstrated by partial remapping data, the place cell network does not behave coherently (2.5.2). Focused lesion/deafference of specific HF subfields (McNaughton et al. 1989; Mizumori et al. 1989; Brun et al. 2002; Nakashiba et al. 2008) show that place cells may be generated in the absence of inputs of other HF subfields. However, their activity suffer from it, especially in terms of stability. This led to the conclusion that: (1) place cells are **independently generated in each subfield from external inputs**, (2) place cells are **stabilized by their interaction within a HF network**. I will not discuss here the involvement of local hippocampal properties in the generation and stabilization of place cells but the reader should be aware that a large body of work shows a strong contribution from specific excitatory and inhibitory hippocampal networks, as well as from specific cellular properties and ionic currents of hippocampal cells ((McHugh et al. 1996; Csicsvari et al. 1999; Nakazawa et al. 2004; Nolan et al. 2004; Epsztein et al. 2010; Epsztein et al. 2011; Lee et al. 2012; Resnik et al. 2012; Royer et al. 2012)).

Directional input

Several **models** have supposed that the **HD system contributes to establish and maintain place fields activity** (McNaughton et al. 1996; Touretzky and Redish 1996). This hypothesis is supported by the fact that in certain circumstances (e.g. behavioural constraints and experience), place cells may be directional (2.2.2.1.3). Furthermore, development studies have established that the directional signal precedes the place signal and that grid cells show the slowest development (Langston et al. 2010; Wills et al. 2010). As explained in III.I, the root of the directional signal is in the **vestibular system**. Its inactivation results in the disruption of the location-

specific firing of hippocampal place cells (Stackman et al. 2002). The **lesion or inactivation** of other areas supporting the HD cell system does not necessarily impair place cells, however. LMN lesions have little effect (Sharp and Koester 2008), retrosplenial cortex inactivation leads to remapping (Cooper and Mizumori 2001), LDN inactivation diminishes the spatial selectivity of half of the place cells while increasing that of the other half (Mizumori et al. 1994). It is not clear, however, whether this effect is due to impairment of the HD system, as PrS HD cells are not affected by similar lesions (Golob et al. 1998). Some authors have shown that PrS and ADN lesions affect the stability of place cells (Calton et al. 2003), while others have shown that PrS/PaS lesion impaired their spatial specificity (Liu et al. 2004). This **heterogeneity in results** may be explained by the variety of areas withholding HD cells. However both LMN and ADN lesions lead to the disruption of the directional signal in downstream structures (see III.I), therefore the results observed may be explained by the disruption of other cellular types such as grid cells. That **place cells receive HD cells inputs** is clear (Ye et al. 2012), yet what exactly is the contribution(s) of these inputs remains to be further investigated.

Grid inputs

Since the discovery of grid cells, several theoretical **model**s have been based on grid inputs either for place cell generation or place cell stabilization (O'Keefe and Burgess 2005; Fuhs and Touretzky 2006; McNaughton et al. 2006; Solstad et al. 2006; Blair et al. 2008; de Almeida et al. 2009; Cheng and Frank 2011); (Jeffery 2011; de Almeida et al. 2012). Here I discuss the experimental data on that subject.

Place cells received inputs from the grid cells (Ye et al. 2012). The silencing or activation of stellate MEC LII cells (i.e. putative grid cells) modulates place cell activity (Yanovich et al. 2009; Weible et al. 2011), this in a reproducible cell-specific manner (Dickinson et al. 2012), arguing for a specific wiring on each place cell. The MEC inputs to the hippocampus are organized indeed in a specific fashion with LII projecting specifically to DG and CA3 and LIII projecting to CA1 and Sub. It was recently shown that MEC LII projects massively to CA2 (Rowland et al. 2011; Cui et al. 2012), revalorizing the role of CA2 in the place cell system (Jones and McHugh 2011). The recent finding of grid cell modules (Burgalossi et al. 2011; Stensola et al. 2012) suggests that those inputs could be modular.

The **lesion or inactivation** of regions containing grid cells leads to an impairment of place cell spatial specificity, place cell spatial stability or place cell field size. The original EC lesion study showed impaired spatial specificity of place cells (Miller and Best 1980), yet because of the extent of the lesion and the number of cells recorded, its result was only indicative. More precise lesion/inactivation studies reported **reduced activity and stability, and changed field size** (Van Cauter et al. 2008); (Brun et al. 2008; Yanovich et al. 2009; Schlesiger et al. 2012). Furthermore, a transient inactivation of MEC inputs induces place cell **remapping** (Yanovich et al. 2009; Dimauro et al. 2012). Lesions limited to specific sub-layers of the MEC showed targeted impairment in specific HF subfields: cell loss in MEC LIII led to increased field size and instability in CA1 place cells, but not in CA3 (Brun et al. 2008), however MEC LII inactivation influenced CA1 activity (yet possibly through CA2 or CA3 inputs). Paper #2 by showing the existence of grid cells in PrS and PaS shed a new light on the interpretation of PrS and PaS lesions resulting in impairment of spatial specificity (Liu et al. 2004) or spatial stability (Calton et al. 2003).

This body of work suggests that **grid cells are not necessary** to generate place cells in the hippocampus but that they may **contribute to their stabilization** in a framework. This hypothesis was further confirmed by the facts that during septum inactivation, leading to the disruption of the MEC and PaS grid pattern, place cell signal in novel environment subsist but is less stable.

Border/boundary inputs

Another prominent model of place cell formation is based on inputs from **boundary-responsive cells** whose discharge is a function of the distance and the orientation of the rats respective to the boundaries of the environment (O'Keefe and Burgess 1996; Hartley et al. 2000; Barry et al. 2006; Lever et al. 2009; Burgess and O'Keefe 2011). Some early models hypothesized that place cells result from the summation of these inputs while more recent ones claimed that these inputs stabilized the place cells firing and anchored them in a reference frame. Experimentally, border responsive cells were found in the MEC, PrS, PaS and Sub and those areas project both to the place cells and grid cell system (papers #1 and #2) (Savelli et al. 2008; Lever et al. 2009). Developmental data shows that border cell maturation precedes that of the place and the grid cells (Bjerknes et al. 2012). This evidence points to a probable role of border/BV cells in place cell generation, yet it is not clear whether this role is direct

or through their influence on grid cells. Moreover, it is not yet established what is at the origin of the border cell signal though some studies are starting to give some indications (Brandon et al. 2011; Bonnevie et al. 2012; Brandon et al. 2012)

Self-motion, motor, velocity information and theta oscillations

Place cell firing rate is modulated by running speed and oscillates at a theta rhythm which itself is modulated by speed (McNaughton et al. 1983); (Rivas et al. 1996); (Geisler et al. 2007). Precise temporal investigations show that place cell activity oscillates slightly faster than the local field potential. The consequence of this is that spikes belonging to one cell occur earlier and earlier in the theta phase when the animal passes through a field (see 2.3). This phenomenon is called **phase precession** (O'Keefe and Recce 1993). It was shown that, in addition to their spatial rate code, place cells present an even more reliable spatial temporal code in the form of the theta phase they are firing at (Huxter et al. 2003; Huxter et al. 2008). Several model are based on these observation to explain place cell generation(Burgess and O'Keefe 1996) while others are based on velocity inputs (see above)

The **theta** hypothesis has been somehow moderated by experimental data. Septum inactivation does not have as strong an impact on place cell activity as on grid cells though it disrupts their theta modulation (Mizumori et al. 1989; Leutgeb and Mizumori 1999; Ikonen et al. 2002); Koening 2011). It produces a remapping and instability of place cells in novel environments, which may be due to the indirect effect on grid cells (Brandon et al. 2012). Furthermore, place cells were recorded in bats in the field in the absence of continuous theta (Ulanovsky and Moss 2007).

PER lesions induce instability and remapping of place cells (Muir and Bilkey 2001) and impair place cells' temporal coding and velocity modulation (Muir and Bilkey 2003). The PER may thus provide information about self-movements to the place cell system. The **retrosplenial cortex** is also thought to transmit self-motion information to the HR. Its transient inactivation induces a remapping of place cells (Cooper and Mizumori 2001). It would be very interesting to test the effect of PER and retrosplenial cortex disruption on the grid cell system and the effect of post parietal cortex on both grid and place system (Whitlock et al. 2012). It was recently shown that the genetic inactivation of **cerebellum** plasticity led to impairment of place cells regarding their use self-motion information (Rochefort et al. 2011). One should note that **POR** lesions have minimal effect on place cells (Nerad et al. 2009).

Non-spatial inputs

As stated in 2.3.5, non-spatial features also modulate place cell activity. This is particularly visible for **rate remapping**. Some authors (Jeffery 2011) proposed a **contextual gating model** that supposes the integration of contextual information on the distal dendritic tree in a similar way as in the study by (Branco and Hausser 2011), where high gain and a larger temporal window of action would explain the influence of non-spatial information on the place cell firing rate. This contrasts with proximal inputs, which will have more effect on the temporal coding.

Contextual or non-spatial information are very vague terms that encompass many different types of information. Several areas previously characterized for coding for specific non-spatial features or inducing specific behavioural states, have been identified as modulating place cell activity. Those areas includes the **prefrontal cortex** (PFC), important for planning (Kyd and Bilkey 2003; Kyd and Bilkey 2005) through the action of the **reuniens** (Ito et al. 2012), the **ventral tegmental area** (VTA) involved in motivation and reward through the **dopaminergic system** (Martig and Mizumori 2011), the **locus coeruleus** (LC) involved in stress through the noradrenergic system (Berridge et al. 1993), the **septum** involved in attention through the cholinergic system (see above for inactivation of the septum), the **LEC** important for object recognition (Lu et al. 2012; Morales et al. 2012), and the **amygdala** involved in fear and emotions (Kim et al. 2012). It will be interesting to see the effect on dorsal place cells of inactivation/lesion of the **ventral hippocampus** as it might convey non-spatial information (Royer et al. 2010). It is tempting to imagine a plastic system of Hebbian strengthening of synapses and attractor network stabilization linked to experience, behaviour relevance and context.

III.IV On how to use the anatomy to follow up the spatial signal (paper #3)

Knowledge on anatomy and connectivity is essential to understand how the signal is generated. The **example of the findings on grid cells** illustrate such a principle well. Several studies have shown that place cells' spatial firing specificity persists in spite of removal of intrahippocampus inputs (DG: (McNaughton et al. 1989); CA3: (Brun et al. 2002)). These results led to hypotheses that the spatial inputs could come from outside the hippocampus. Based on connectivity results, the EC acts as a hub in the HR, between sensory inputs and the HF. That positioned it as a perfect candidate. Further lesion studies allowed identification of the involvement of the dorsal portion in spatial memory (Steffenach et al. 2005). This, together with the knowledge of the

topographical organization of EC inputs on the HF, dorsal to dorsal and ventral to ventral (Witter et al. 1989), led to the investigation of the dorso-lateral band of the MEC and the discovery of grid cells. The rationale behind the investigation of the PrS and PaS in paper #2 followed some of the same reasoning by **recording upstream** of the MEC. A cohort of inactivation studies follow similar principles by targeting areas whose efferences are numerous to the area that contains the brain signal of interest (Brandon et al. 2011; Koenig et al. 2011; Bonnevie et al. 2012)

IV. Perspectives on the behavioural function of the spatial code

I have already briefly discussed in II.I how the data presented in this thesis influence the concept of **information coding** based on the example of spatial coding. I will here expand on how this information is **used** for addressing wider behavioural functions such as **navigation** and **memory**.

IV. I Role in navigation

Throughout this thesis, I have mainly focused on the output of spatial cognition: the **dynamic representation** of the external space and one's self-position. Mostly, however, I have neglected the use of this representation for a **behavioural purpose**, which, in the case of spatial cognition, is **navigation**.

I established previously how place, HD, grid and border cells together build a neural network that is the substrate of this dynamic representation of the space, integrating positional, directional, motion and metric information.

I would like here to discuss briefly how the activity of these cells is linked to accurate navigation. As stated in 1.2.2, one can define navigation as the **capacity to plan and execute a goal-directed path** (Gallistel 1990). Accurate navigation can be reached through different strategies that can be revealed by specific behavioural paradigms. Among these different navigation strategies, one often distinguishes between **landmark navigation** and **path integration navigation**.

A consequent body of work shows that the **integrity** of the **diverse HR areas** and the **place, HD, grid and border systems** correlate with performances in navigational tasks requiring path integration elements (see 1.3.4.2). Furthermore, the actual **behaviour** of the rat **correlates** with the **representation** shown by the **place cell system** (Bures et al. 1997; Lenck-Santini et al. 2002; Dupret et al. 2010) and the **HD cell system** (Dudchenko and Taube 1997; Valerio and Taube 2012). This is also probably true for grid and border cells but it remains to be demonstrated.

The dominant consensus is that these different systems work together: **HD cells** giving a **sense of direction**, **grid cells** providing information about **metric, velocity and distance**, **border cells** providing information about the **boundary** of the environment. Together they **anchor the map** in a **reference framework** and send information to the HF whose **place cells integrate** it with **non-spatial input** from other areas to **compute self-location**. In that model the HD, grid and border cell systems together form a **universal metric, context-independent, rigid system** (Moser and Moser 2008) that helps the place cells to generate **multiple context-dependent plastic cognitive maps,** as originally proposed (O'Keefe and Nadel 1978). In this, it supports the idea that **part of the experience is pre-structured in the brain,** as envisioned by **Kant** (Kant 1781). This map system **interacts with other cognitive systems** to give an **adapted behavioural answer** to a given situation.

IV.II Extrapolation to role in memory and learning

As stated in 1.3.4.1, many studies have shown that the HR function is not limited to spatial cognition. In particular, it is greatly involved in **episodic memory and learning**. This observation leads us to ask whether the spatial code observed in the HR is, in fact, a partial reflection of a **more general memory code**.

Any **mnemonic episode** can be decomposed into three components: **What** happened, **where** and **when** (see 1.2.4). In this context, the **spatial component** is the **easiest to visualize** when recording from a **rat**. Thus, can place cells in fact be **memory cells**? Several studies have shown that **place cells convey non-spatial information** (see 2.3.5), notably information seemingly linked to the "**when**" component (e.g. (Manns et al. 2007; Pastalkova et al. 2008; Itskov et al. 2011; MacDonald et al. 2011) and the "**what**" component (e.g. (Hampson et al. 1993; Wiebe and Staubli 1999; Wood et al. 1999; Lenck-Santini et al. 2008; Liu et al. 2012). Though the codes of HD, grid and border cells are more strictly attuned to spatial features, non-spatial features have been shown to influence their firing (see 2.3.5). Furthermore, many cells in the **PHR** code for such **non-spatial features** (e.g. (Young et al. 1997; Petrulis et al. 2005). **MEC** cells were recently found to code for **time** in a fashion similar to that in which they code for space in grid cells (Kim et al. 2012; Kraus et al. 2012). This led to the hypothesis that the ensemble of the spatial coding mechanisms described in the HR could be translated to temporal (when) or contextual (what) modalities. This idea is further supported by **recordings of single**

units in the human HR (medial temporal lobe) that respond specifically to the presentation of precise items (Kreiman et al. 2000; Kreiman et al. 2000; Quiroga et al. 2005; Quiroga et al. 2008; Cerf et al. 2010).

Precise study of spatial and non-spatial features showed that, in the rat, they seem to be distributed along **anatomical gradients within structures**. A prominent gradient has been found in the **HF along the dorso-ventral axis** where the dorsal part is more involved in spatial cognition and the ventral part in fear, reward and goal coding ((Kjelstrup et al. 2002; Steffenach et al. 2005; Royer et al. 2010; van der Meer and Redish 2011; Manganaro et al. 2012; Ruediger et al. 2012), supported by different connections, intrinsic cellular properties and proteomics (Dong et al. 2009; van Strien et al. 2009; Adhikari et al. 2010; Fanselow and Dong 2010; Adhikari et al. 2011; Valenti et al. 2011; Marcelin et al. 2012). As I previously stated, the same dorso-ventral axis also supports a **scale gradient** with small field place cells in dorsal and larger fields in ventral (Kjelstrup et al. 2008). These two findings are not mutually exclusive and the dorso-ventral axis could support several gradients. This dorso-ventral dissociation is evocative of the famous **two-streams hypothesis** of visual neural processing (Goodale and Milner 1992).

Another important gradient I mentioned often in this thesis is the **medio-lateral distribution in the entorhinal cortex** where the medial part is more devoted to spatial information and the lateral entorhinal cortex to context and object information (Fyhn et al. 2004; Hargreaves et al. 2005; Kerr et al. 2007; Yoganarasimha et al. 2011; Deshmukh et al. 2012; Igarashi et al. 2012; Keene et al. 2012; Morales et al. 2012; Morrissey et al. 2012) supposedly based on the **PER/POR pathway dissociation** (Burwell et al. 2004; Furtak et al. 2007; van Strien et al. 2009). The MEC and LEC have distinct patterns of projection towards the HF (van Strien et al. 2009). This probably led to another pattern of spatial coding distribution in the **CA1** (Henriksen et al. 2010) and **Sub** (Kim et al. 2012) along the **proximal-distal axis**. Therefore some mechanisms observed in the dorsal or medial portion of an area could very well be observed in another area but under a non-spatial output.

CONCLUSION

This thesis explores the localization of cognitive functions. It takes the example of spatial cognition and delves into the notion of the nature and origin of the spatial

neuronal code and its distribution over the hippocampal region network. It proceeds to the question of the behavioural function of the spatial neural code and links it to navigation and memory.

The work presented here is mainly based on *in vivo* unit recording in freely behaving rats and on the anatomical identification of the subareas of the hippocampal region through the establishment of cyto- and chemo-architectonic markers. Its main finding is that the spatial code is distributed over a large network that includes several subsystems. Specifically, the articles supporting this thesis characterize and quantify in several subareas of the parahippocampal region (i.e. the medial entorhinal cortex, the presubiculum and the parasubiculum) the existence of diverse neuronal types coding for boundaries, metrics, velocity and directional signal, and probably contributing to a global position signal: the border, grid and head direction cells. The second important result of the work presented here is to provide a much-needed tool for experimentalists in the form of a three-dimensional atlas of the hippocampal region that focuses on the description of anatomical borders and is integrated with a web-based virtual microscope application.

The final output (representation) of the HD, grid, place and border cell systems seems to be the most accessible in the HR, yet other brain areas are involved in the generation and stabilization of the signal. One can access the spatial code at the level of either single neuron or the network through the summation of individual coding in cell assemblies and through the emergence of global activity oscillations. The network also contributes to the generation and stabilization of the signal at the single cell level, which is generated based on their cellular and network properties, through the integration of multiple signals. Therefore, it is interesting to consider these systems as dynamic, interdependent and collaborative widespread circuits.

Since their discovery, there has been a shift the definitions of place, HD and grid cells due the multiplication of studies on their diverse properties and the improvement of recording and other experimental tools. The articles presented here contribute to this evolution and together these changes have influenced the original theoretical concept of the cognitive map (O'Keefe and Nadel 1978) and built on the idea of a universal metric map (Moser et al. 2008; Moser and Moser 2008).

Studying spatial neural coding modalities allows, by extension, insights into general information coding, computation and the dynamic interaction between mental representation and behavioural outcome. As knowledge acquisition is central to

spatial cognition, study of the latter is intimately linked to learning and memory. This link is reinforced by the fact that a large number of studies point to the HR as crucial for both spatial cognition and declarative memory. A recent review of experimental data develops this notion that similar neural algorithms are involved in both spatial cognition and memory (Buzsaki and Moser 2013).

These observations come from the analysis of rat neural activity. As the hippocampal region is a highly phylogenetically conserved brain area, however, many of these observations may be translated to humans and help the understanding and control of terrible neurologic pathologies such as epilepsy and Alzheimer's disease.

LEGAL AND ETHICAL ASPECTS

All animal experiments performed in the course of work for this thesis were conducted in strict compliance with the ethical regulations of the Norwegian Animal Welfare Act (Love om dyrevern, no73 av 20.desember 1974), and European legislation (i.e. the European convention for the protection of vertebrate animals used for experimentation and other scientific purposes). Breeding and maintenance of the rats was also done according to the highest possible standards. All scientists conducting the experiments had successfully completed a course in laboratory animal science for FELASA (Federation of Laboratory Animal Science Associations) category C researcher. Other scientists performing the *in vivo* experiments were carefully trained.

All of the experiments required intact neuronal circuits and preserved connectivity among multiple brain areas and many experiments required a behavioural analysis. Thus, *in vivo* recordings in the brain using animals was essential. Rats were used because: (a) they are the most widely used animals that have sophisticated spatial and other types of behaviours; (b) the anatomy and physiology of the rat and mouse brains are well described; and (c) the proposed procedures had been specifically designed and successfully used in these species.

During the experiments all efforts were made to keep the number of animals to the absolute minimum necessary (reduction). Sufficient animal welfare was a priority (refinement). All reasonable steps were taken to ensure the humane treatment of animals, so as to minimize their discomfort, distress and pain. To avoid or keep to the minimum the suffering of animals, sedation, aseptic techniques, anaesthesia and the best possible post-operative care were delivered.

ANNEXES

Annex 1: Basic physiology

Very schematically, a typical **neuron** can be divided into three parts: the dendrites, the cellular body (or soma) and the axon. The **first** part **receives the information** and consists of the **dendrite**, which is a thin structure arising from the cellular body and often branching multiple times, giving rise to the so-called "dendritic tree". Many dendrites can come to the soma. The **second** part is the cellular body or **soma** of the neuron and it **integrates the information** it receives from the many dendrites. Finally, the **third** part is the single **axon**, emerging at the so called "axon hillock" from the soma, which **further propagates the information**. There is only one axon per soma, however it can branch multiple times before reaching its targets. The place where two neurons connect is called the **synapse**. This is an extremely **simplistic view** as, for instance, information can be received directly on the soma, or integration can happen at the dendritic level.

Depending on the neuronal compartment considered, the **information** is either **electric** (by the travelling or the condensation of charged ions) or **chemical** (by the concentration of chemical substances such as neurotransmitters). Charges are unequally distributed in the brain so that when a neuron is quiescent (not activated) the inside of the neuron (intracellular potential) is kept more negative than the outside (extracellular potential) by the action of ion pumps. This charge difference generates the (negative) **resting membrane potential** and varies among different neuronal types.

The information travels via electrical impulses called **action potentials** (AP) along the neuron axons via the exchange of electrical charges due to the successive opening and closing of **ion channels**. APs are emitted at the axon hillocks located at the base of the neuron soma and result from the summation of all the activity arriving there. APs all have the same amplitude so that the intensity of the **signal is coded in rate** (numbers of APs per seconds). When an AP comes to the axon terminal, which synapses with the targeted neurons, its charge generates modifications such as the fusion of **neurotransmitter** vesicles with the membrane of the neuron. That way, neurotransmitters are released in the **synaptic cleft**. These neurotransmitters can then bind with the membrane receptor of the postsynaptic density located, for instance, on the dendritic tree. Each category of neurotransmitter has its specific **receptors**. The

activation of a receptor often leads directly or indirectly to **depolarization** (intracellular compartment less negatively charged) or **hyperpolarization** (intracellular compartment more negatively charged). The result of this change in polarization is further transmitted along the dendrite to the soma, which then integrates all information coming from all the dendrites. If the **sum of all information** rises above a certain **threshold**, an **AP** (or spike) is emitted by the neuron. The neuron is activated. After generating an AP, a neuron needs a certain amount of time (some msec) before being able to generate a second one. This time is the period necessary to restore the resting potential and is called the **refractory period**.

Neurons are classified according to their **location** but also their **physiological and morphological properties**, which reflect how they process the information. These properties include the number and organization of the dendrites, the shape of their soma, the length and branching of their axons, resting membrane potential, threshold for action potential, refractory periods, channel and receptor distributions, synapse type, and neurotransmitter type. In the central nervous system, one can generally discriminate between three types of neurons: the excitatory principal cells, the inhibitory cells and the cells from the neuromodulation systems. The **excitatory principal cells** transmit an excitatory signal mediated via the release of glutamate at their synapses, which tends to depolarize the targeted neuron. The **inhibitory cells** are also called interneurons and often have a local inhibitory action due to the shortness of their axons. They principally release gamma-aminobutyric acid (GABA) at their synapses in the CNS which leads to the hyperpolarization of the targeted neuron. Finally, the **neuromodulation systems** consist of different types of neurons, whose neurotransmitters (e.g. acetylcholine, dopamine, noradrenaline, serotonine) behave more as modulators of the activity of the excitatory and inhibitory inputs to their targeted areas.

The study of the neurons' physiological properties can be done at **different resolutions**. One can be interested at the **local global activity** resulting from the sum of all neurons in a given area (local field potential (LFP)). When studying LFP, one can see the emergence of **oscillatory rhythms** resulting from the synchronous discharge of a neuronal population. On the other hand, one can look at the **discharge** of **individual neurons**, or even more precisely at the **membrane, channel, receptor or molecular properties** of the neuron or of its different **sub-compartments**

(dendrites, soma, axon, synapse). These different studies can be performed *in vivo* and thus correlated with the behaviour of the animal as it is shown in the experimental work supporting this thesis or *in vitro* in precise controlled conditions, on cortical slices or neural cultures.

Annex 2: Characterization (methodological considerations)

Discharge and temporal properties

A basic way to characterize neurons is by their firing parameters. One of the first things to consider is whether the neuron is active or not, and if it is active, to what extent. This is measured by the mean firing rate (i.e. average activity of the neuron over the recording period) and the peak-firing rate (i.e. maximum firing rate reached during the recording session). To describe the discharge further, one can look in more detail at the firing of the neurons over time. A neuron can have sporadic/discrete activity (i.e. one spike from time to time); it can burst (alternation of very high firing and silence) or it can have persistent firing (i.e. constant spiking). These features can be measured with the bursting index and the interval interspike (ISI).

The vast majority of the work presented in this thesis is based on *in vivo* extracellular multi-unit recordings in behaving rats. Therefore, in most cases it is not possible to establish with certainty from which cell one is recording: whether it is a principal cell or an interneuron, if the signal is picked from a cellular body or by passing-by fibres. However, some measures have been established to narrow the doubts about the cellular type. The analyses of the waveform (e.g. peak to trough, half width), temporal autocorrelation (and notably length of the refractory period) and the ISI help in that sense. These different measures depend on the quality of the signal (signal to noise ratio) and the quality of cell isolation (cluster Median Mahalanobis distances; Schmitzer-Torbert 2005). The experimenter has to establish the amplitude threshold under which neurons will not be considered (this measure is highly dependent on the distance from the recording electrode).

Map/graph construction

To analyse the correlates of a neuron, one can plot its firing rate as a function of the position or the head direction of the rat. Sometimes these functions present themselves as triangular or Gaussian. The next step is then to translate this function in graphic terms such as rate maps or polar plots. Most of the spatial and directional measures are based on these graphs. One should consider that these graphs are highly influenced by the chosen binning and smoothing, and by the behaviour of the animal (sampling).

General spatial properties

Many quantitative parameters allow the fine analysis of spatial modulation of these

neurons. Among them, spatial information is a measure of the extent to which a cell's firing can be used to predict the position of the animal. Two equivalent measures are used. The spatial information content computes the "spatial information per spike" which is a measure of how much information about spatial location is conveyed by a single impulse of a given cell (Skaggs et al. 1996). The spatial information rate reports this information per time and is then in bytes per second. The spatial coherence is linked to the correlation between neighbouring bins of the place field.

Field properties

A prerequisite to studying the properties of a field is to define such a field. The firing field is estimated as a contiguous region of at least X cm^2 where the firing rate was above X% of the peak rate (example: 200 cm^2 and 20% (Fyhn 2004)). It is convenient to define a firing field as a group of pixels that occupies a continuous part of the apparatus, where the firing rate in each pixel must be greater than some selected threshold. Pixels that do not satisfy the firing rate criterion are excluded from the field, even if surrounded by field pixels. The continuity condition is that a candidate pixel must share at least one edge with a pixel already known to be in the field; a corner is not enough (Lewis 1977). This permits the member pixels to be found with a recursive algorithm. The minimum field size is set at nine pixels; this avoids the absurdity of referring to fields for cells that are nearly silent (cf. Fig. 5E). In addition, only the largest field in a session is considered, in order to bypass the question whether averages should be taken across units or across fields (Muller 1987).

Place fields can be described in terms of their shape, their size (i.e. scale), their numbers and their spatial distribution within the apparatus. One can also look at their directionality i.e. whether the cell is active independently of direction in which the rat is entering the considered place field (Muller 1987). This was developed in section 2.2.2.2.

Additional ways to describe a field are based on the firing of the studied neurons relative to this field. One can measure the intra-field firing and the extra-field firing (or background firing), and their ratio (i.e. signal-to-noise ratio), which gives an indication of the specificity of the field modulation. The intensity of the field is given by the peak-firing rate. The sparsity of the firing field is a measure of how diffuse the unit firing is in the spatial domain. For illustration, if a unit fires equally all over the apparatus, the information per spike is 0 and sparsity is 1; if a unit fires evenly over

one half of the apparatus but never fires in the other half, the information per spike is 1 bit and sparsity is 0.5 (Skaggs 1993, Hargreaves 2007). It is calculated as the ratio between the square mean rate and the mean square rate (Fyhn 2004). Finally, one can look at the rate contour of the firing to see how homogenous the firing is in the field and whether there are several peaks.

Grid properties

Grid cells are place-modulated neurons with periodically spaced firing fields. The vertices of the firing fields define, for each cell, a triangular or hexagonal array spanning the entire environment in a crystal-like manner. Grid cells can be described in terms of their phase, their orientation and their spacing. The grid phase is the x,y displacement relative to an external reference point. The grid orientation is the tilt relative to an external reference axis. The grid spacing is the distance between the centres of each node/field. One should note that grid cells could also be characterized according to their field properties. For example, parameters, which could be considered, are the scale of the fields, their shape, their individual in-field firing rate, the global extra-field firing rate etc. (see above sub-paragraph on field properties).

A grid score has been developed to determine objectively whether a particular neuron is a grid cell or not. Hereafter I will describe the latest version of this score. This grid score is based on a spatial autocorrelation map. The degree of spatial periodicity ("gridness" or "grid scores") is determined for each recorded cell by taking a circular sample of the autocorrelogram, centred on the central peak but with the central peak itself excluded, and then comparing rotated versions of this sample. The Pearson correlation of this circle with its rotation in α degrees is obtained for angles of 60° and 120°, on the one hand, and 30°, 90° and 150° on the other. The cell's grid score is defined as the minimum difference between any of the elements in the first group and any of the elements in the second. This score is 60^{o} rotational symmetry-based (Sargolini 2006, Langston 2010, Boccara 2010).

In these studies, a cell is defined as a grid cell when the grid score exceeded the significance level estimated from shuffled rate maps for all cells recorded in the brain region. Shuffling is performed on a cell-by-cell basis. For each trial of the shuffling procedure, the entire sequence of spikes fired by the cell is time-shifted along the animal's path by a random interval between 20 s and 20 s less than the length of the trial, with the end of the trial wrapped to the beginning. This procedure

was repeated 100 times for each cell, yielding, for example, a total of 10,000 permutations for 100 cells. For each permutation, a firing rate map and an autocorrelation map are constructed and a grid score is calculated. The 99th percentile is read out from the overall distribution of grid scores in the shuffled data for each region. Grid cells are then defined as cells in the recorded data that had grid scores higher than the 99th percentile of the shuffled data for the respective region. The use of a statistical criterion for grid cells differs from previous work defining grid cells as cells with grid scores above a fixed threshold.

In Boccara (2010), grid spacing was defined as the radius of the circle around the centre of the autocorrelation map that gave the highest grid score. In the same study, grid orientation was defined by first establishing vectors from the centre of the autocorrelation map to each of the three first vertices of the inner hexagon in a counterclockwise direction, starting from a camera-defined reference line of 0 degrees. The mean orientation of these vectors (with angles α, β and γ) was defined as $(\alpha + (\beta - 60) + (\gamma - 180))/3$. The angle between this orientation and the camera-defined reference line was taken as the orientation of the grid.

Directional properties

Most directional parameters are based on the neuron's directional tuning curve that correlates the neuron's firing rate versus the rat's head direction. The shape of this directional tuning curve gives an indication about the cell's directional properties. For example, if it is multi-peaked it means the cell is multidirectional. The peak of the tuning curve is referred to as the peak-firing rate of the cell and the animal's head direction at the peak is the preferred firing direction of the cell. The strength of directional tuning can be estimated by computing the length of the mean vector for the circular distribution of firing rate. The range of directional headings over which activity is elevated above baseline levels (background firing rate usually defined as below one spike/sec) is referred to as the directional firing range (Taube 2003). The breadth of directional tuning can also be expressed by the angular standard deviation of the mean vector, which is the resultant vector across all radial bins divided by the sum of the individual vector lengths (Sargolini 2006). A third method is to determine the half-width of the directional tuning curve (the width of the region in which the rate is higher than 50% of the peak rate) (Boccara 2010). It might also be interesting to calculate the asymmetry ratio (i.e. whether the slope is more pronounced on one

side of the firing peak than on the other).

A directional information rate (or content) can be calculated in a manner similar to the spatial information rate (or spatial information content).

There are currently no clear criteria for how directional a neuron must be to be classified as a head direction cell. Recent studies (Boccara 2010; Langston 2010; Lever 2010) have tried to address this issue by determining a threshold for calling a cell directionally modulated. In these studies, head direction-modulated cells are defined as cells with mean vector lengths significantly exceeding the degree of directional tuning that would be expected by chance. Threshold values are determined for each brain region considered by a shuffling procedure performed in the same way as for grid cells (see 2.2.2.3, grid properties). For each permutation trial, the entire sequence of spikes fired by the cell is time-shifted along the rat's path by a random interval between 20 s, on one side, and, on the other side, 20 s less than the length of the trial, with the end of the trial wrapped to the beginning. A head-direction tuning curve is then constructed, and the mean vector length is calculated. The distribution of mean vector lengths is computed for the entire set of permutations from all cells in the sample (number of cells in the region considered x 100 permutations per cell). Cells are defined as directionally modulated if the mean vector from the recorded data was longer than the 99th percentile of mean vector lengths in the distribution generated from the shuffled data.

Temporal properties

So far I have described the activity of single units in the brain. By using different filters one can record the global activity in one region, which is the sum of the synchronized activity of all the units (excitatory and inhibitory) that can be recorded in a certain diameter. This regional global activity is called local field potential (LFP). The LFP is sometimes referred to as electroencephalogram (EEG), which measures the global brain activity along the human scalp. The LFP can show oscillations at a variety of frequencies. These oscillations or brain rhythms are often associated with different states of brain functioning (e.g. exploration, sleep). The study of the LFP in the hippocampal and parahippocampal region is beyond the scope of this thesis. However, I will consider briefly the relationship of the unit's activity with one of the most prominent rhythms in the hippocampal/parahippocampal region, the theta

rhythm (4–11 Hz). This rhythm is mostly associated with exploration, alertness/attention and speed.

By looking at the temporal autocorrelation of a cell, one can examine whether there is an increase of the activity at regular intervals. For instance, if the activity increases every 10 milliseconds, it means that the neuron is theta modulated (1/4–1/11 msec). Theta rhythm is observed in the LFP (peak frequencies). In Paper #2, we defined individual cells as theta-modulated if the mean spectral power within 1 Hz of the peak in the 4–11 Hz frequency range of the spike-train autocorrelogram is at least five times greater than the mean spectral power between 0 and 125 Hz.

In theta-modulated neurons, one can see a temporal code. This temporal code is made by the incidence of spikes across the 360^{o} of the theta cycle. Theta phase locking is estimated for each cell as the length of the mean vector for the distribution of firing rate across the 360^{o} of the theta cycle.

Speed/velocity properties

Units firing can be modulated by linear or angular speed/velocity modulation (see Sharp, McNaughton, Barnes, Maurer). One should keep in mind that the power of theta oscillations is correlated to the linear speed of the rodent.

Conjunctive properties

Cells can be modulated by different factors. Therefore in the study of place cells, the question of their directionality will sometimes be considered. On the same lines, some studies focus on the speed and velocity of HD, place or grid cells. One of the clearest cases of conjunctive properties is the so-called conjunctive cells in the MEC, which present grid and head direction modulation. For such cells to be active the rat needs to be in one of the grid nodes and have its head in the preferred direction for firing (Sargolini 2006).

Dynamic properties

As stated in section 2.1, place, head direction and grid cells can be tested in terms of their two main basic properties: stability and plasticity. So far, I have mostly described static parameters. However, the study of their dynamic parameters represents a huge body of work. The stability of a firing pattern is measured by correlation of spatial, directional and firing properties within and between sessions.

REFERENCES

Acar, F., S. Naderi, et al. (2005). "Herophilus of Chalcedon: A pioneer in neuroscience." Neurosurgery **56**(4): 861-7.

Adhikari, A., M. A. Topiwala, et al. (2010). "Synchronized activity between the ventral hippocampus and the medial prefrontal cortex during anxiety." Neuron **65**(2): 257-69.

Adhikari, A., M. A. Topiwala, et al. (2011). "Single units in the medial prefrontal cortex with anxiety-related firing patterns are preferentially influenced by ventral hippocampal activity." Neuron **71**(5): 898-910.

Aggleton, J. P. and M. W. Brown (1999). "Episodic memory, amnesia, and the hippocampal-anterior thalamic axis." Behav Brain Sci **22**(3): 425-44; discussion 44-89.

Aguirre, G. K. and M. D'Esposito (1999). "Topographical disorientation: a synthesis and taxonomy." Brain **122 (Pt 9)**: 1613-28.

Ahmed, O. J. and M. R. Mehta (2009). "The hippocampal rate code: anatomy, physiology and theory." Trends Neurosci **32**(6): 329-38.

Ahmed, O. J. and M. R. Mehta (2012). "Running speed alters the frequency of hippocampal gamma oscillations." J Neurosci **32**(21): 7373-83.

Alenda, A., L. Ginzberg, et al. (2010). "Modulation of grid cell firing by changes in context." SfN abstract.

Allen, K., J. N. Rawlins, et al. (2012). "Hippocampal place cells can encode multiple trial-dependent features through rate remapping." J Neurosci **32**(42): 14752-66.

Alme, C. B., R. A. Buzzetti, et al. (2010). "Hippocampal granule cells opt for early retirement." Hippocampus **20**(10): 1109-23.

Alonso, A. and E. Garcia-Austt (1987). "Neuronal sources of theta rhythm in the entorhinal cortex of the rat. II. Phase relations between unit discharges and theta field potentials." Exp Brain Res **67**(3): 502-9.

Alonso, A. and R. R. Llinas (1989). "Subthreshold Na+-dependent theta-like rhythmicity in stellate cells of entorhinal cortex layer II." Nature **342**(6246): 175-7.

Altman, J. and G. D. Das (1965). "Post-natal origin of microneurones in the rat brain." Nature **207**(5000): 953-6.

Alvarez, P., P. A. Lipton, et al. (2001). "Differential effects of damage within the hippocampal region on memory for a natural, nonspatial Odor-Odor Association." Learn Mem **8**(2): 79-86.

Amaral, D. G. (1978). "A Golgi study of cell types in the hilar region of the hippocampus in the rat." J Comp Neurol **182**(4 Pt 2): 851-914.

Amaral, D. G., C. Dolorfo, et al. (1991). "Organization of CA1 projections to the subiculum: a PHA-L analysis in the rat." Hippocampus **1**(4): 415-35.

Amaral, D. G., R. Insausti, et al. (1987). "The entorhinal cortex of the monkey: I. Cytoarchitectonic organization." J Comp Neurol **264**(3): 326-55.

Amaral, D. G., N. Ishizuka, et al. (1990). "Neurons, numbers and the hippocampal network." Prog Brain Res **83**: 1-11.

Amaral, D. G. and M. P. Witter (1989). "The three-dimensional organization of the hippocampal formation: a review of anatomical data." Neuroscience **31**(3): 571-91.

Ambrogini, P., D. Lattanzi, et al. (2004). "Morpho-functional characterization of neuronal cells at different stages of maturation in granule cell layer of adult rat dentate gyrus." Brain Res **1017**(1-2): 21-31.

Andersen, P., (ed.) (2007). The Hippocampus book. Oxford, Oxford University Press.

Andersen, P., B. Holmqvist, et al. (1966). "Entorhinal activation of dentate granule cells." Acta Physiol Scand **66**(4): 448-60.

Anderson, M. I. and K. J. Jeffery (2003). "Heterogeneous modulation of place cell firing by changes in context." J Neurosci **23**(26): 8827-35.

Atkinson, R. C. and R. M. Shiffrin (1968). Human memory: A proposed system and its control processes. The psychology of learning and motivation (Volume 2). K. W. Spence and J. T. Spence (eds.). New York, Academic Press**:** 89-195.

Barnea, A. and F. Nottebohm (1994). "Seasonal recruitment of hippocampal neurons in adult free-ranging black-capped chickadees." Proc Natl Acad Sci U S A **91**(23): 11217-21.

Barnes, C. A. (1979). "Memory deficits associated with senescence: a neurophysiological and behavioral study in the rat." J Comp Physiol Psychol **93**(1): 74-104.

Barnes, C. A., B. L. McNaughton, et al. (1990). "Comparison of spatial and temporal characteristics of neuronal activity in sequential stages of hippocampal processing." Prog Brain Res **83**: 287-300.

Barry, C., D. Bush, et al. (2012). "Models of grid cells and theta oscillations." Nature **488**(7409): E1-2; discussion E-3.

Barry, C., L. L. Ginzberg, et al. (2012). "Grid cell firing patterns signal environmental novelty by expansion." Proc Natl Acad Sci U S A: 17687-92.

Barry, C., R. Hayman, et al. (2007). "Experience-dependent rescaling of entorhinal grids." Nat Neurosci **10**(6): 682-4.

Barry, C., J. G. Heys, et al. (2012). "Possible role of acetylcholine in regulating spatial novelty effects on theta rhythm and grid cells." Front Neural Circuits **6**: 5.

Barry, C., C. Lever, et al. (2006). "The boundary vector cell model of place cell firing and spatial memory." Rev Neurosci **17**(1-2): 71-97.

Bassett, J. P. and J. S. Taube (2001). "Neural correlates for angular head velocity in the rat dorsal tegmental nucleus." J Neurosci **21**(15): 5740-51.

Bassett, J. P., M. L. Tullman, et al. (2007). "Lesions of the tegmentomammillary circuit in the head direction system disrupt the head direction signal in the anterior thalamus." J Neurosci **27**(28): 7564-77.

Battaglia, F. P., G. R. Sutherland, et al. (2004). "Local sensory cues and place cell directionality: additional evidence of prospective coding in the hippocampus." J Neurosci **24**(19): 4541-50.

Bayer, S. A. (1980). "Development of the hippocampal region in the rat. I. Neurogenesis examined with 3H-thymidine autoradiography." J Comp Neurol **190**(1): 87-114.

Bayer, S. A. (1980). "Development of the hippocampal region in the rat. II. Morphogenesis during embryonic and early postnatal life." J Comp Neurol **190**(1): 115-34.

Beck, A. (1890). "Die Ströme der Nervencentren." Centralbl Physiol **4**: 572–3.

Bergson, H. (1910). Matter and memory. London, Allen & Unwin (Authorised translation by Nancy Margaret Paul and W. Scott Palmer).

Bernhard, C. (1872). "Des fonctions du cerveau." Rev deux mondes **98**: 373-85.

Berridge, C. W., M. E. Page, et al. (1993). "Effects of locus coeruleus inactivation on electroencephalographic activity in neocortex and hippocampus." Neuroscience **55**(2): 381-93.

Best, P. J. and K. R. Thompson (1984). SfN abstract.

Bjaalie, J. G. (2002). "Opinion: Localization in the brain: new solutions emerging." Nat Rev Neurosci **3**(4): 322-5.

Bjerknes, T. L., N. Dagslott, et al. (2012). "Representation of geometrical borders in the developing rat." SfN abstract: 702.09.

Blackstad, T. W. (1956). "Commissural connections of the hippocampal region in the rat, with special reference to their mode of termination." J Comp Neurol **105**(3): 417-537.

Blair, H. T., J. Cho, et al. (1999). "The anterior thalamic head-direction signal is abolished by bilateral but not unilateral lesions of the lateral mammillary nucleus." J Neurosci **19**(15): 6673-83.

Blair, H. T., K. Gupta, et al. (2008). "Conversion of a phase- to a rate-coded position signal by a three-stage model of theta cells, grid cells, and place cells." Hippocampus **18**(12): 1239-55.

Blair, H. T., B. W. Lipscomb, et al. (1997). "Anticipatory time intervals of head-direction cells in the anterior thalamus of the rat: implications for path integration in the head-direction circuit." J Neurophysiol **78**(1): 145-59.

Blair, H. T. and P. E. Sharp (1995). "Anticipatory head direction signals in anterior thalamus: evidence for a thalamocortical circuit that integrates angular head motion to compute head direction." J Neurosci **15**(9): 6260-70.

Bland, B. H. (1986). "The physiology and pharmacology of hippocampal formation theta rhythms." Prog Neurobiol **26**(1): 1-54.

Bliss, T., G. Collingridge, et al. (2007). Synaptic plasticity in the hippocampus The hippocampus book. P. Andersen (ed.) Oxford, Oxford University Press**:** 343-474.

Bliss, T. V. and G. L. Collingridge (1993). "A synaptic model of memory: long-term potentiation in the hippocampus." Nature **361**(6407): 31-9.

Bliss, T. V. and T. Lømo (1973). "Long-lasting potentiation of synaptic transmission in the dentate area of the anaesthetized rabbit following stimulation of the perforant path." J Physiol **232**(2): 331-56.

Bloom, F. E., A. Lazerson, et al. (2006). Brain, mind and behavior, 3rd ed, W H Freeman.

Boccara, C. N., F. Sargolini, et al. (2010). "Grid cells in pre- and parasubiculum." Nat Neurosci **13**(8): 987-94.

Bonnevie, T., B. Dunn, et al. (2012). "Entorhinal grid cells require excitatory drive from the hippocampus " SfN Abstract: 702.12.

Bostock, E., R. U. Muller, et al. (1991). "Experience-dependent modifications of hippocampal place cell firing." Hippocampus **1**(2): 193-205.

Braak, H. and E. Braak (1991). "Neuropathological stageing of Alzheimer-related changes." Acta Neuropathol **82**(4): 239-59.

Bragin, A., G. Jando, et al. (1995). "Gamma (40-100 Hz) oscillation in the hippocampus of the behaving rat." J Neurosci **15**(1 Pt 1): 47-60.

Branco, T. and M. Hausser (2011). "Synaptic integration gradients in single cortical pyramidal cell dendrites." Neuron **69**(5): 885-92.

Brandon, M. P., A. R. Bogaard, et al. (2012). "Head direction cells in the postsubiculum do not show replay of prior waking sequences during sleep." Hippocampus **22**(3): 604-18.

Brandon, M. P., A. R. Bogaard, et al. (2011). "Reduction of theta rhythm dissociates grid cell spatial periodicity from directional tuning." Science **332**(6029): 595-9.

Brandon, M. P., J. Koenig, et al. (2012). "Septal inactivation eliminates grid cell spatial periodicity and causes instability of hippocampal place cells in novel environments." SfN Abstract: 203.05.

Brankack, J., M. Stewart, et al. (1993). "Current source density analysis of the hippocampal theta rhythm: associated sustained potentials and candidate synaptic generators." Brain Res **615**(2): 310-27.

Brazhnik, E. S., R. U. Muller, et al. (2003). "Muscarinic blockade slows and degrades the location-specific firing of hippocampal pyramidal cells." J Neurosci **23**(2): 611-21.

Breese, C. R., R. E. Hampson, et al. (1989). "Hippocampal place cells: stereotypy and plasticity." J Neurosci **9**(4): 1097-111.

Brett, M., I. S. Johnsrude, et al. (2002). "The problem of functional localization in the human brain." Nat Rev Neurosci **3**(3): 243-9.

Broca, P. R. (1861). "Sur le siège de la faculté du langage articulé suivies d'une observation d'aphémie (perte de la parole)." Bull Soc Anat **6**: 330–57

Brodal, A. (1947). "The hippocampus and the sense of smell; a review." Brain **70**(Pt 2): 179-222.

Brodmann, K. (1909). Vergleichende Lokalisationslehre der Grosshirnrinde in ihren Prinzipien dargestellt auf Grund des Zellenbauers. Leipzig.
Brun, V. H., S. Leutgeb, et al. (2008). "Impaired spatial representation in CA1 after lesion of direct input from entorhinal cortex." Neuron **57**(2): 290-302.
Brun, V. H., M. K. Otnass, et al. (2002). "Place cells and place recognition maintained by direct entorhinal-hippocampal circuitry." Science **296**(5576): 2243-6.
Brun, V. H., T. Solstad, et al. (2008). "Progressive increase in grid scale from dorsal to ventral medial entorhinal cortex." Hippocampus **18**(12): 1200-12.
Buckley, M. J. and D. Gaffan (1997). "Impairment of visual object-discrimination learning after perirhinal cortex ablation." Behav Neurosci **111**(3): 467-75.
Buetfering, C., A. Kevin, et al. (2012). "Identification and characterization of parvalbumin-expressing interneurons in the medial entorhinal cortex of behaving mice." SfN Abstract: 921.10.
Burak, Y. and I. R. Fiete (2009). "Accurate path integration in continuous attractor network models of grid cells." PLoS Comput Biol **5**(2): e1000291.
Bures, J., A. A. Fenton, et al. (1997). "Place cells and place navigation." Proc Natl Acad Sci U S A **94**(1): 343-50.
Burgalossi, A., L. Herfst, et al. (2011). "Microcircuits of functionally identified neurons in the rat medial entorhinal cortex." Neuron **70**(4): 773-86.
Burgess, N. (2008). "Grid cells and theta as oscillatory interference: theory and predictions." Hippocampus **18**(12): 1157-74.
Burgess, N., C. Barry, et al. (2007). "An oscillatory interference model of grid cell firing." Hippocampus **17**(9): 801-12.
Burgess, N. and J. O'Keefe (1996). "Neuronal computations underlying the firing of place cells and their role in navigation." Hippocampus **6**(6): 749-62.
Burgess, N. and J. O'Keefe (2011). "Models of place and grid cell firing and theta rhythmicity." Curr Opin Neurobiol **21**(5): 734-44.
Burke, S. N., A. P. Maurer, et al. (2012). "Representation of three-dimensional objects by the rat perirhinal cortex." Hippocampus **22**(10): 2032-44.
Burke, S. N., A. P. Maurer, et al. (2011). "The influence of objects on place field expression and size in distal hippocampal CA1." Hippocampus **21**(7): 783-801.
Burwell, R. D. (2000). "The parahippocampal region: Corticocortical connectivity." Ann N Y Acad Sci **911**: 25-42.
Burwell, R. D. and D. G. Amaral (1998). "Perirhinal and postrhinal cortices of the rat: interconnectivity and connections with the entorhinal cortex." J Comp Neurol **391**(3): 293-321.
Burwell, R. D. and D. M. Hafeman (2003). "Positional firing properties of postrhinal cortex neurons." Neuroscience **119**(2): 577-88.
Burwell, R. D., M. P. Saddoris, et al. (2004). "Corticohippocampal contributions to spatial and contextual learning." J Neurosci **24**(15): 3826-36.
Burwell, R. D., M. L. Shapiro, et al. (1998). "Positional firing properties of perirhinal cortex neurons." Neuroreport **9**(13): 3013-8.
Burwell, R. D., M. P. Witter, et al. (1995). "Perirhinal and postrhinal cortices of the rat: a review of the neuroanatomical literature and comparison with findings from the monkey brain." Hippocampus **5**(5): 390-408.
Buschman, T. J. and E. K. Miller (2010). "Shifting the spotlight of attention: evidence for discrete computations in cognition." Front Hum Neurosci **4**: 194.
Bussey, T. J., J. Duck, et al. (2000). "Distinct patterns of behavioural impairments resulting from fornix transection or neurotoxic lesions of the perirhinal and postrhinal cortices in the rat." Behav Brain Res **111**(1-2): 187-202.
Bussey, T. J., J. L. Muir, et al. (1999). "Functionally dissociating aspects of event memory: the effects of combined perirhinal and postrhinal cortex lesions on object and place memory in the rat." J Neurosci **19**(1): 495-502.
Buzsaki, G. (2002). "Theta oscillations in the hippocampus." Neuron **33**(3): 325-40.

Buzsaki, G. (2004). "Large-scale recording of neuronal ensembles." Nat Neurosci **7**(5): 446-51.
Buzsaki, G. (2005). "Theta rhythm of navigation: link between path integration and landmark navigation, episodic and semantic memory." Hippocampus **15**(7): 827-40.
Buzsaki, G. (2010). "Neural syntax: cell assemblies, synapsembles, and readers." Neuron **68**(3): 362-85.
Buzsaki, G. (2011). "Hippocampus." Scholarpedia **6**(1): 1468.
Buzsaki, G., C. A. Anastassiou, et al. (2012). "The origin of extracellular fields and currents--EEG, ECoG, LFP and spikes." Nat Rev Neurosci **13**(6): 407-20.
Buzsaki, G. and A. Draguhn (2004). "Neuronal oscillations in cortical networks." Science **304**(5679): 1926-9.
Buzsaki, G., Z. Horvath, et al. (1992). "High-frequency network oscillation in the hippocampus." Science **256**(5059): 1025-7.
Buzsaki, G., L. W. Leung, et al. (1983). "Cellular bases of hippocampal EEG in the behaving rat." Brain Res **287**(2): 139-71.
Buzsaki, G. and E. I. Moser (2013). "Memory, navigation and theta rhythm in the hippocampal-entorhinal system." Nat Neurosci **16**(2): 130-8.
Cacucci, F., C. Lever, et al. (2004). "Theta-modulated place-by-direction cells in the hippocampal formation in the rat." J Neurosci **24**(38): 8265-77.
Calton, J. L., R. W. Stackman, et al. (2003). "Hippocampal place cell instability after lesions of the head direction cell network." J Neurosci **23**(30): 9719-31.
Calton, J. L. and J. S. Taube (2005). "Degradation of head direction cell activity during inverted locomotion." J Neurosci **25**(9): 2420-8.
Cameron, H. A. and R. D. McKay (2001). "Adult neurogenesis produces a large pool of new granule cells in the dentate gyrus." J Comp Neurol **435**(4): 406-17.
Canto, C. B., N. Koganezawa, et al. (2012). "All layers of medial entorhinal cortex receive presubicular and parasubicular inputs." J Neurosci **32**(49): 17620-31.
Canto, C. B. and M. P. Witter (2012). "Cellular properties of principal neurons in the rat entorhinal cortex. I. The lateral entorhinal cortex." Hippocampus **22**(6): 1256-76.
Canto, C. B. and M. P. Witter (2012). "Cellular properties of principal neurons in the rat entorhinal cortex. II. The medial entorhinal cortex." Hippocampus **22**(6): 1277-99.
Carr, H. Y. (1952). Free Precession Techniques in Nuclear Magnetic Resonance. Cambridge, MA.
Carr, M. F., M. P. Karlsson, et al. (2012). "Transient slow gamma synchrony underlies hippocampal memory replay." Neuron **75**(4): 700-13.
Carr, V. A., J. Rissman, et al. (2010). "Imaging the human medial temporal lobe with high-resolution fMRI." Neuron **65**(3): 298-308.
Cassel, J. C., S. Cassel, et al. (1998). "Fimbria-fornix vs selective hippocampal lesions in rats: effects on locomotor activity and spatial learning and memory." Neurobiol Learn Mem **69**(1): 22-45.
Caton, R. (1875). British Medical Journal.
Cerf, M., N. Thiruvengadam, et al. (2010). "On-line, voluntary control of human temporal lobe neurons." Nature **467**(7319): 1104-8.
Chakraborty, S., M. I. Anderson, et al. (2004). "Context-independent directional cue learning by hippocampal place cells." Eur J Neurosci **20**(1): 281-92.
Chang, E. H. and P. T. Huerta (2012). "Neurophysiological correlates of object recognition in the dorsal subiculum." Front Behav Neurosci **6**: 46.
Charcot, J. M. (1878). Leçons sur les maladies du système nerveux.
Chawla, M. K., J. F. Guzowski, et al. (2005). "Sparse, environmentally selective expression of Arc RNA in the upper blade of the rodent fascia dentata by brief spatial experience." Hippocampus **15**(5): 579-86.

Chen, L. L., L. H. Lin, et al. (1994). "Head-direction cells in the rat posterior cortex. I. Anatomical distribution and behavioral modulation." Exp Brain Res **101**(1): 8-23.

Chen, Q. S., B. L. Kagan, et al. (2000). "Impairment of hippocampal long-term potentiation by Alzheimer amyloid beta-peptides." J Neurosci Res **60**(1): 65-72.

Cheng, S. and L. M. Frank (2008). "New experiences enhance coordinated neural activity in the hippocampus." Neuron **57**(2): 303-13.

Cheng, S. and L. M. Frank (2011). "The structure of networks that produce the transformation from grid cells to place cells." Neuroscience **197**: 293-306.

Chrobak, J. J. and G. Buzsaki (1998). "Operational dynamics in the hippocampal-entorhinal axis." Neurosci Biobehav Rev **22**(2): 303-10.

Clark, B. J., J. P. Bassett, et al. (2010). "Impaired head direction cell representation in the anterodorsal thalamus after lesions of the retrosplenial cortex." J Neurosci **30**(15): 5289-302.

Clark, B. J., J. E. Brown, et al. (2012). "Head direction cell activity in the anterodorsal thalamus requires intact supragenual nuclei." J Neurophysiol **108**(10): 2767-84.

Clark, B. J., M. J. Harris, et al. (2012). "Control of anterodorsal thalamic head direction cells by environmental boundaries: comparison with conflicting distal landmarks." Hippocampus **22**(2): 172-87.

Clark, B. J., A. Sarma, et al. (2009). "Head direction cell instability in the anterior dorsal thalamus after lesions of the interpeduncular nucleus." J Neurosci **29**(2): 493-507.

Clark, B. J. and J. S. Taube (2011). "Intact landmark control and angular path integration by head direction cells in the anterodorsal thalamus after lesions of the medial entorhinal cortex." Hippocampus **21**(7): 767-82.

Clark, B. J. and J. S. Taube (2012). "Vestibular and attractor network basis of the head direction cell signal in subcortical circuits." Front Neural Circuits **6**: 7.

Clark, B. J., S. Valerio, et al. (2011). "Disrupted grid and head direction cell signal in the entorhinal cortex and parasubiculum after lesions of the head direction system." SfN Abstract: 729.11.

Clarke, E. and K. E. Dewhurst (1996). An Illustrated History of Brain Function. Imaging the Brain from Antiquity to the Present San Francisco, Norman.

Climer, J. R., E. L. Newman, et al. (2012). "Properties of temporal coding by entorhinal grid cells " SfN Abstract: 293.16.

Cohen, D. (1968). "Magnetoencephalography: evidence of magnetic fields produced by alpha-rhythm currents." Science **161**(3843): 784-6.

Cohen, L. G., P. Celnik, et al. (1997). "Functional relevance of cross-modal plasticity in blind humans." Nature **389**(6647): 180-3.

Colgin, L. L. (2011). "Neuroscience: Periodicity without rhythmicity." Nature **479**(7371): 46-7.

Colgin, L. L. (2011). "Oscillations and hippocampal-prefrontal synchrony." Curr Opin Neurobiol **21**(3): 467-74.

Colgin, L. L., T. Denninger, et al. (2009). "Frequency of gamma oscillations routes flow of information in the hippocampus." Nature **462**(7271): 353-7.

Colgin, L. L., S. Leutgeb, et al. (2010). "Attractor-map versus autoassociation based attractor dynamics in the hippocampal network." J Neurophysiol **104**(1): 35-50.

Colgin, L. L. and E. I. Moser (2010). "Gamma oscillations in the hippocampus." Physiology (Bethesda) **25**(5): 319-29.

Colgin, L. L., E. I. Moser, et al. (2008). "Understanding memory through hippocampal remapping." Trends Neurosci **31**(9): 469-77.

Cooper, B. G. and S. J. Mizumori (2001). "Temporary inactivation of the retrosplenial cortex causes a transient reorganization of spatial coding in the hippocampus." J Neurosci **21**(11): 3986-4001.

Corkin, S. (2002). "What's new with the amnesic patient H.M.?" Nat Rev Neurosci **3**(2): 153-60.
Cormack, A. M. (1973). "Reconstruction of densities from their projections, with applications in radiological physics." Phys Med Biol **18**(2): 195-207.
Couey, J. J., A. W. Witoelar, et al. (2012). "Medial entorhinal cortex layer ii stellate cells are embedded within a recurrent inhibitory network " SfN Abstract: 702.06.
Crivellato, E. and D. Ribatti (2007). "Soul, mind, brain: Greek philosophy and the birth of neuroscience." Brain Res Bull **71**(4): 327-36.
Csicsvari, J., H. Hirase, et al. (1999). "Oscillatory coupling of hippocampal pyramidal cells and interneurons in the behaving Rat." J Neurosci **19**(1): 274-87.
Csicsvari, J., B. Jamieson, et al. (2003). "Mechanisms of gamma oscillations in the hippocampus of the behaving rat." Neuron **37**(2): 311-22.
Cui, Z., C. R. Gerfen, et al. (2012). "Hypothalamic and other connections with the dorsal CA2 area of the mouse hippocampus." J Comp Neurol.
Damasio, H., T. Grabowski, et al. (1994). "The return of Phineas Gage: clues about the brain from the skull of a famous patient." Science **264**(5162): 1102-5.
Dandy, W. E. (1919). "Roentgenography of the brain after the injection of air into the spinal canal." Ann Surg **70**(4): 397-403.
Danglot, L., A. Triller, et al. (2006). "The development of hippocampal interneurons in rodents." Hippocampus **16**(12): 1032-60.
Darwin, C. (1859). On the origin of species by means of natural selection. London, J. Murray.
Darwin, C. (1873). "Origin of Certain Instincts." Nature **7**(179): 417–8.
de Almeida, L., M. Idiart, et al. (2009). "The input-output transformation of the hippocampal granule cells: from grid cells to place fields." J Neurosci **29**(23): 7504-12.
de Almeida, L., M. Idiart, et al. (2012). "The single place fields of CA3 cells: a two-stage transformation from grid cells." Hippocampus **22**(2): 200-8.
de Castro, J. M. (1974). "A selective spatial discrimination deficit after fornicotomy in the rat." Behav Biol **12**(3): 373-82.
Deacon, T. W., H. Eichenbaum, et al. (1983). "Afferent connections of the perirhinal cortex in the rat." J Comp Neurol **220**(2): 168-90.
Deisseroth, K., G. Feng, et al. (2006). "Next-generation optical technologies for illuminating genetically targeted brain circuits." J Neurosci **26**(41): 10380-6.
Derdikman, D. (2009). "Are the boundary-related cells in the subiculum boundary-vector cells?" J Neurosci **29**(43): 13429-31.
Derdikman, D., J. R. Whitlock, et al. (2009). "Fragmentation of grid cell maps in a multicompartment environment." Nat Neurosci **12**(10): 1325-32.
Deshmukh, S. S., J. L. Johnson, et al. (2012). "Perirhinal cortex represents nonspatial, but not spatial, information in rats foraging in the presence of objects: comparison with lateral entorhinal cortex." Hippocampus **22**(10): 2045-58.
Deshmukh, S. S. and J. J. Knierim (2011). "Representation of non-spatial and spatial information in the lateral entorhinal cortex." Front Behav Neurosci **5**: 69.
Dhillon, A. and R. S. Jones (2000). "Laminar differences in recurrent excitatory transmission in the rat entorhinal cortex in vitro." Neuroscience **99**(3): 413-22.
Dickinson, J. R., A. P. Weible, et al. (2012). "Transgenic activation of the same entorhinal inputs leads to the same hippocampal network response." SfN Abstract: 397.22.
Diekelmann, S. and J. Born (2010). "The memory function of sleep." Nat Rev Neurosci **11**(2): 114-26.
Diekelmann, S., C. Buchel, et al. (2011). "Labile or stable: opposing consequences for memory when reactivated during waking and sleep." Nat Neurosci **14**(3): 381-6.
Dimauro, A. J., J. W. Rueckemann, et al. (2012). "Optogenetic inactivation of dorsocaudal medial entorhinal cortex causes remapping in dorsal CA1 place cells." SfN Abstract: 203.15.

Doeller, C. F., C. Barry, et al. (2010). "Evidence for grid cells in a human memory network." Nature **463**(7281): 657-61.
Dolorfo, C. L. and D. G. Amaral (1998). "Entorhinal cortex of the rat: topographic organization of the cells of origin of the perforant path projection to the dentate gyrus." J Comp Neurol **398**(1): 25-48.
Dombeck, D. A., C. D. Harvey, et al. (2010). "Functional imaging of hippocampal place cells at cellular resolution during virtual navigation." Nat Neurosci **13**(11): 1433-40.
Domnisoru, C., A. A. Kinkhabwala, et al. (2012). "Membrane potential dynamics of grid cells during virtual navigation." SfN Abstract: 702.15.
Dong, H. W., L. W. Swanson, et al. (2009). "Genomic-anatomic evidence for distinct functional domains in hippocampal field CA1." Proc Natl Acad Sci U S A **106**(28): 11794-9.
Dragoi, G. and G. Buzsaki (2006). "Temporal encoding of place sequences by hippocampal cell assemblies." Neuron **50**(1): 145-57.
Dragoi, G. and S. Tonegawa (2011). "Preplay of future place cell sequences by hippocampal cellular assemblies." Nature **469**(7330): 397-401.
Dranovsky, A. and R. Hen (2006). "Hippocampal neurogenesis: regulation by stress and antidepressants." Biol Psychiatry **59**(12): 1136-43.
Dudchenko, P. A., J. P. Goodridge, et al. (1997). "The effects of disorientation on visual landmark control of head direction cell orientation." Exp Brain Res **115**(2): 375-80.
Dudchenko, P. A. and J. S. Taube (1997). "Correlation between head direction cell activity and spatial behavior on a radial arm maze." Behav Neurosci **111**(1): 3-19.
Dudchenko, P. A. and L. E. Zinyuk (2005). "The formation of cognitive maps of adjacent environments: evidence from the head direction cell system." Behav Neurosci **119**(6): 1511-23.
Dudek, S. M. and M. F. Bear (1992). "Homosynaptic long-term depression in area CA1 of hippocampus and effects of N-methyl-D-aspartate receptor blockade." Proc Natl Acad Sci U S A **89**(10): 4363-7.
Dunn, B., A. Witoelar, et al. (2012). "An inhibitory network of grid cells " SfN Abstract: 702.08.
Dupret, D., J. O'Neill, et al. (2010). "The reorganization and reactivation of hippocampal maps predict spatial memory performance." Nat Neurosci **13**(8): 995-1002.
Dyer, F. C. and J. L. Gould (1981). "Honey bee orientation: a backup system for cloudy days." Science **214**(4524): 1041-2.
Eacott, M. J. and G. Norman (2004). "Integrated memory for object, place, and context in rats: a possible model of episodic-like memory?" J Neurosci **24**(8): 1948-53.
Ego-Stengel, V. and M. A. Wilson (2010). "Disruption of ripple-associated hippocampal activity during rest impairs spatial learning in the rat." Hippocampus **20**(1): 1-10.
Egorov, A. V., B. N. Hamam, et al. (2002). "Graded persistent activity in entorhinal cortex neurons." Nature **420**(6912): 173-8.
Eichenbaum, H. and N. J. Cohen (2001). From conditioning to conscious recollection. New York, Oxford Univiversuty Press.
Eichenbaum, H., P. Dudchenko, et al. (1999). "The hippocampus, memory, and place cells: is it spatial memory or a memory space?" Neuron **23**(2): 209-26.
Eichenbaum, H., A. Fagan, et al. (1988). "Hippocampal system dysfunction and odor discrimination learning in rats: impairment or facilitation depending on representational demands." Behav Neurosci **102**(3): 331-9.
Eichenbaum, H., M. Kuperstein, et al. (1987). "Cue-sampling and goal-approach correlates of hippocampal unit activity in rats performing an odor-discrimination task." J Neurosci **7**(3): 716-32.

Eichenbaum, H. and P. A. Lipton (2008). "Towards a functional organization of the medial temporal lobe memory system: role of the parahippocampal and medial entorhinal cortical areas." Hippocampus **18**(12): 1314-24.
Eichenbaum, H., P. Mathews, et al. (1989). "Further studies of hippocampal representation during odor discrimination learning." Behav Neurosci **103**(6): 1207-16.
Eichenbaum, H. and R. J. Robitsek (2009). "Olfactory memory: a bridge between humans and animals in models of cognitive aging." Ann N Y Acad Sci **1170**: 658-63.
Eijkenboom, M., A. Blokland, et al. (2000). "Modelling cognitive dysfunctions with bilateral injections of ibotenic acid into the rat entorhinal cortex." Neuroscience **101**(1): 27-39.
Ekstrom, A. D., M. J. Kahana, et al. (2003). "Cellular networks underlying human spatial navigation." Nature **425**(6954): 184-8.
Ekstrom, A. D., J. Meltzer, et al. (2001). "NMDA receptor antagonism blocks experience-dependent expansion of hippocampal "place fields"." Neuron **31**(4): 631-8.
Ennaceur, A., N. Neave, et al. (1996). "Neurotoxic lesions of the perirhinal cortex do not mimic the behavioural effects of fornix transection in the rat." Behav Brain Res **80**(1-2): 9-25.
Epstein, R. and N. Kanwisher (1998). "A cortical representation of the local visual environment." Nature **392**(6676): 598-601.
Epsztein, J., M. Brecht, et al. (2011). "Intracellular determinants of hippocampal CA1 place and silent cell activity in a novel environment." Neuron **70**(1): 109-20.
Epsztein, J., A. K. Lee, et al. (2010). "Impact of spikelets on hippocampal CA1 pyramidal cell activity during spatial exploration." Science **327**(5964): 474-7.
Esposito, M. S., V. C. Piatti, et al. (2005). "Neuronal differentiation in the adult hippocampus recapitulates embryonic development." J Neurosci **25**(44): 10074-86.
Etienne, A. S. (1980). "The orientation of the golden hamster to its nest-site after the elimination of various sensory cues." Experientia **36**(9): 1048-50.
Fanselow, M. S. and H. W. Dong (2010). "Are the dorsal and ventral hippocampus functionally distinct structures?" Neuron **65**(1): 7-19.
Fenno, L., O. Yizhar, et al. (2011). "The development and application of optogenetics." Annu Rev Neurosci **34**: 389-412.
Fenton, A. A., G. Csizmadia, et al. (2000). "Conjoint control of hippocampal place cell firing by two visual stimuli. I. The effects of moving the stimuli on firing field positions." J Gen Physiol **116**(2): 191-209.
Fenton, A. A., H. Y. Kao, et al. (2008). "Unmasking the CA1 ensemble place code by exposures to small and large environments: more place cells and multiple, irregularly arranged, and expanded place fields in the larger space." J Neurosci **28**(44): 11250-62.
Fenton, A. A., W. W. Lytton, et al. (2010). "Attention-like modulation of hippocampus place cell discharge." J Neurosci **30**(13): 4613-25.
Fenton, A. A. and R. U. Muller (1998). "Place cell discharge is extremely variable during individual passes of the rat through the firing field." Proc Natl Acad Sci U S A **95**(6): 3182-7.
Fenton, A. A., M. Wesierska, et al. (1998). "Both here and there: simultaneous expression of autonomous spatial memories in rats." Proc Natl Acad Sci U S A **95**(19): 11493-8.
Ferbinteanu, J. and M. L. Shapiro (2003). "Prospective and retrospective memory coding in the hippocampus." Neuron **40**(6): 1227-39.
Ferbinteanu, J., P. Shirvalkar, et al. (2011). "Memory modulates journey-dependent coding in the rat hippocampus." J Neurosci **31**(25): 9135-46.
Finney, E. M., I. Fine, et al. (2001). "Visual stimuli activate auditory cortex in the deaf." Nat Neurosci **4**(12): 1171-3.

Flourens, P. (1824). Recherches expérimentales sur les propriétés et les fonctions du système nerveux dans les animaux vertébrés. Paris, Chez Crevot.
Fodor, J. A. (1983). The modularity of mind. Cambridge, Mass., MIT Press.
Foster, D. J. and M. A. Wilson (2006). "Reverse replay of behavioural sequences in hippocampal place cells during the awake state." Nature **440**(7084): 680-3.
Foster, T. C., C. A. Castro, et al. (1989). "Spatial selectivity of rat hippocampal neurons: dependence on preparedness for movement." Science **244**(4912): 1580-2.
Fox, S. E. and J. B. Ranck, Jr. (1975). "Localization and anatomical identification of theta and complex spike cells in dorsal hippocampal formation of rats." Exp Neurol **49**(1 Pt 1): 299-313.
Frank, L. M., E. N. Brown, et al. (2000). "Trajectory encoding in the hippocampus and entorhinal cortex." Neuron **27**(1): 169-78.
Frank, L. M., E. N. Brown, et al. (2001). "A comparison of the firing properties of putative excitatory and inhibitory neurons from CA1 and the entorhinal cortex." J Neurophysiol **86**(4): 2029-40.
Frank, L. M., G. B. Stanley, et al. (2004). "Hippocampal plasticity across multiple days of exposure to novel environments." J Neurosci **24**(35): 7681-9.
Frank, M. G., N. P. Issa, et al. (2001). "Sleep enhances plasticity in the developing visual cortex." Neuron **30**(1): 275-87.
Fransen, E., B. Tahvildari, et al. (2006). "Mechanism of graded persistent cellular activity of entorhinal cortex layer v neurons." Neuron **49**(5): 735-46.
Freund, T. F. and G. Buzsaki (1996). "Interneurons of the hippocampus." Hippocampus **6**(4): 347-470.
Fricke, R. and W. M. Cowan (1977). "An autoradiographic study of the development of the entorhinal and commissural afferents to the dentate gyrus of the rat." J Comp Neurol **173**(2): 231-50.
Fricke, R. and W. M. Cowan (1978). "An autoradiographic study of the commissural and ipsilateral hippocampo-dentate projections in the adult rat." J Comp Neurol **181**(2): 253-69.
Fricke, R. A. and D. A. Prince (1984). "Electrophysiology of dentate gyrus granule cells." J Neurophysiol **51**(2): 195-209.
Fricker, D., C. Dinocourt, et al. (2009). "Pyramidal cells of rodent presubiculum express a tetrodotoxin-insensitive Na+ current." J Physiol **587**(Pt 17): 4249-64.
Frisch, K. v. and M. Lindauer (1954). "Himmel und Erde in Konkurrenz bei der Orientierung der Bienen." Naturwissenschaften **41**(11): 245-53.
Fritsch, G. and E. Hitzig (1870). "Ueber die elektrische Erregbarkeit des Grosshirns." Archiv fuer Anatomie, Physiologie und wissenschaftliche Medicin: 330-2.
Fuhs, M. C. and D. S. Touretzky (2006). "A spin glass model of path integration in rat medial entorhinal cortex." J Neurosci **26**(16): 4266-76.
Funahashi, M., E. Harris, et al. (1999). "Re-entrant activity in a presubiculum-subiculum circuit generates epileptiform activity in vitro." Brain Res **849**(1-2): 139-46.
Funahashi, M. and M. Stewart (1997). "Presubicular and parasubicular cortical neurons of the rat: electrophysiological and morphological properties." Hippocampus **7**(2): 117-29.
Furtak, S. C., J. R. Moyer, Jr., et al. (2007). "Morphology and ontogeny of rat perirhinal cortical neurons." J Comp Neurol **505**(5): 493-510.
Furtak, S. C., S. M. Wei, et al. (2007). "Functional neuroanatomy of the parahippocampal region in the rat: the perirhinal and postrhinal cortices." Hippocampus **17**(9): 709-22.
Fyhn, M., T. Hafting, et al. (2007). "Hippocampal remapping and grid realignment in entorhinal cortex." Nature **446**(7132): 190-4.
Fyhn, M., T. Hafting, et al. (2008). "Grid cells in mice." Hippocampus **18**(12): 1230-8.
Fyhn, M., S. Molden, et al. (2002). "Hippocampal neurons responding to first-time dislocation of a target object." Neuron **35**(3): 555-66.

Fyhn, M., S. Molden, et al. (2004). "Spatial representation in the entorhinal cortex." Science **305**(5688): 1258-64.
Gaffan, D. and A. Parker (1996). "Interaction of perirhinal cortex with the fornix-fimbria: memory for objects and "object-in-place" memory." J Neurosci **16**(18): 5864-9.
Gage, F. H., G. Kempermann, et al. (1998). "Multipotent progenitor cells in the adult dentate gyrus." J Neurobiol **36**(2): 249-66.
Galani, R., L. E. Jarrard, et al. (1997). "Effects of postoperative housing conditions on functional recovery in rats with lesions of the hippocampus, subiculum, or entorhinal cortex." Neurobiol Learn Mem **67**(1): 43-56.
Galani, R., S. Obis, et al. (2002). "A comparison of the effects of fimbria-fornix, hippocampal, or entorhinal cortex lesions on spatial reference and working memory in rats: short versus long postsurgical recovery period." Neurobiol Learn Mem **77**(1): 1-16.
Galani, R., I. Weiss, et al. (1998). "Spatial memory, habituation, and reactions to spatial and nonspatial changes in rats with selective lesions of the hippocampus, the entorhinal cortex or the subiculum." Behav Brain Res **96**(1-2): 1-12.
Gallagher, M. and M. T. Koh (2011). "Episodic memory on the path to Alzheimer's disease." Curr Opin Neurobiol **21**(6): 929-34.
Gallistel, C. R. (1990). "Representations in animal cognition: an introduction." Cognition **37**(1-2): 1-22.
Garofalo, I., (ed.) (1997). Anonimi Medici: De morbis acutis et chroniis. Leiden, EJ Brill.
Ge, S., E. L. Goh, et al. (2006). "GABA regulates synaptic integration of newly generated neurons in the adult brain." Nature **439**(7076): 589-93.
Geisler, C., D. Robbe, et al. (2007). "Hippocampal place cell assemblies are speed-controlled oscillators." Proc Natl Acad Sci U S A **104**(19): 8149-54.
Geller, A. I. and A. Freese (1990). "Infection of cultured central nervous system neurons with a defective herpes simplex virus 1 vector results in stable expression of Escherichia coli beta-galactosidase." Proc Natl Acad Sci U S A **87**(3): 1149-53.
Ginther, M. R., D. F. Walsh, et al. (2011). "Hippocampal neurons encode different episodes in an overlapping sequence of odors task." J Neurosci **31**(7): 2706-11.
Giocomo, L. M., T. Bonnevie, et al. (2011). "Topographical organization of head direction and border cells in medial entorhinal cortex." SfN Abstract: 726.07.
Giocomo, L. M., T. Bonnevie, et al. (2012). "The topographical organization of head direction signals in medial entorhinal cortex " SfN Abstract: 702.05.
Giocomo, L. M. and M. E. Hasselmo (2008). "Time constants of h current in layer ii stellate cells differ along the dorsal to ventral axis of medial entorhinal cortex." J Neurosci **28**(38): 9414-25.
Giocomo, L. M. and M. E. Hasselmo (2009). "Knock-out of HCN1 subunit flattens dorsal-ventral frequency gradient of medial entorhinal neurons in adult mice." J Neurosci **29**(23): 7625-30.
Giocomo, L. M., S. A. Hussaini, et al. (2011). "Grid cells use HCN1 channels for spatial scaling." Cell **147**(5): 1159-70.
Giocomo, L. M., M. B. Moser, et al. (2011). "Computational models of grid cells." Neuron **71**(4): 589-603.
Giocomo, L. M., E. A. Zilli, et al. (2007). "Temporal frequency of subthreshold oscillations scales with entorhinal grid cell field spacing." Science **315**(5819): 1719-22.
Girardeau, G., K. Benchenane, et al. (2009). "Selective suppression of hippocampal ripples impairs spatial memory." Nat Neurosci **12**(10): 1222-3.
Glasgow, S. D. and C. A. Chapman (2007). "Local generation of theta-frequency EEG activity in the parasubiculum." J Neurophysiol **97**(6): 3868-79.
Glasgow, S. D. and C. A. Chapman (2008). "Conductances mediating intrinsic theta-frequency membrane potential oscillations in layer II parasubicular neurons." J Neurophysiol **100**(5): 2746-56.

Glasgow, S. D., I. Glovaci, et al. (2012). "Cholinergic suppression of excitatory synaptic transmission in layers II/III of the parasubiculum." Neuroscience **201**: 1-11.
Glasier, M. M., R. L. Sutton, et al. (1995). "Effects of unilateral entorhinal cortex lesion and ganglioside GM1 treatment on performance in a novel water maze task." Neurobiol Learn Mem **64**(3): 203-14.
Golgi, C. (1886). Sulla fina anatomia degli organi centrali del sistema nervoso Milano, Hoepli.
Golob, E. J., R. W. Stackman, et al. (2001). "On the behavioral significance of head direction cells: neural and behavioral dynamics during spatial memory tasks." Behav Neurosci **115**(2): 285-304.
Golob, E. J. and J. S. Taube (1999). "Head direction cells in rats with hippocampal or overlying neocortical lesions: evidence for impaired angular path integration." J Neurosci **19**(16): 7198-211.
Golob, E. J., D. A. Wolk, et al. (1998). "Recordings of postsubiculum head direction cells following lesions of the laterodorsal thalamic nucleus." Brain Res **780**(1): 9-19.
Good, M. and R. C. Honey (1997). "Dissociable effects of selective lesions to hippocampal subsystems on exploratory behavior, contextual learning, and spatial learning." Behav Neurosci **111**(3): 487-93.
Goodale, M. A. and A. D. Milner (1992). "Separate visual pathways for perception and action." Trends Neurosci **15**(1): 20-5.
Goodridge, J. P., P. A. Dudchenko, et al. (1998). "Cue control and head direction cells." Behav Neurosci **112**(4): 749-61.
Goodridge, J. P. and J. S. Taube (1997). "Interaction between the postsubiculum and anterior thalamus in the generation of head direction cell activity." J Neurosci **17**(23): 9315-30.
Goodridge, J. P. and D. S. Touretzky (2000). "Modeling attractor deformation in the rodent head-direction system." J Neurophysiol **83**(6): 3402-10.
Gothard, K. M., K. L. Hoffman, et al. (2001). "Dentate gyrus and CA1 ensemble activity during spatial reference frame shifts in the presence and absence of visual input." J Neurosci **21**(18): 7284-92.
Gothard, K. M., W. E. Skaggs, et al. (1996). "Dynamics of mismatch correction in the hippocampal ensemble code for space: interaction between path integration and environmental cues." J Neurosci **16**(24): 8027-40.
Gould, E. (2007). Structural Plasticity. The hippocampus book. P. Andersen (ed.) Oxford, Oxford University Press**:** 321-42.
Gould, E. and P. Tanapat (1999). "Stress and hippocampal neurogenesis." Biol Psychiatry **46**(11): 1472-9.
Goutagny, R., J. Jackson, et al. (2009). "Self-generated theta oscillations in the hippocampus." Nat Neurosci **12**(12): 1491-3.
Gradinaru, V., F. Zhang, et al. (2010). "Molecular and cellular approaches for diversifying and extending optogenetics." Cell **141**(1): 154-65.
Grastyan, E., K. Lissak, et al. (1959). "Hippocampal electrical activity during the development of conditioned reflexes." Electroencephalogr Clin Neurophysiol **11**(3): 409-30.
Green, J. D. and A. A. Arduini (1954). "Hippocampal electrical activity in arousal." J Neurophysiol **17**(6): 533-57.
Griffin, A. L., H. Eichenbaum, et al. (2007). "Spatial representations of hippocampal CA1 neurons are modulated by behavioral context in a hippocampus-dependent memory task." J Neurosci **27**(9): 2416-23.
Gu, Y., M. Arruda-Carvalho, et al. (2012). "Optical controlling reveals time-dependent roles for adult-born dentate granule cells." Nat Neurosci **15**(12): 1700-6.
Gupta, A. S., M. A. van der Meer, et al. (2012). "Segmentation of spatial experience by hippocampal theta sequences." Nat Neurosci **15**(7): 1032-9.

Gupta, K., N. J. Beer, et al. (2013). "Medial Entorhinal Grid Cells and Head Direction Cells Rotate with a T-Maze More Often During Less Recently Experienced Rotations." Cereb Cortex: Epub ahead of print.
Hafting, T., M. Fyhn, et al. (2008). "Hippocampus-independent phase precession in entorhinal grid cells." Nature **453**(7199): 1248-52.
Hafting, T., M. Fyhn, et al. (2005). "Microstructure of a spatial map in the entorhinal cortex." Nature **436**(7052): 801-6.
Hallock, H. L. and A. L. Griffin (2012). "Dynamic coding of dorsal hippocampal neurons between tasks that differ in structure and memory demand." Hippocampus **23**(2): 169-86.
Hammarberg, G. (1895). Studien über Klinik und Pathologie der Idiotie nebst Untersuchungen über die normale Anatomie der Hirnrinde. Uppsala.
Hampson, R. E., C. J. Heyser, et al. (1993). "Hippocampal cell firing correlates of delayed-match-to-sample performance in the rat." Behav Neurosci **107**(5): 715-39.
Hardman, R., D. J. Evans, et al. (1997). "Evidence for recovery of spatial learning following entorhinal cortex lesions in mice." Brain Res **758**(1-2): 187-200.
Hargreaves, E. L., G. Rao, et al. (2005). "Major dissociation between medial and lateral entorhinal input to dorsal hippocampus." Science **308**(5729): 1792-4.
Hargreaves, E. L., D. Yoganarasimha, et al. (2007). "Cohesiveness of spatial and directional representations recorded from neural ensembles in the anterior thalamus, parasubiculum, medial entorhinal cortex, and hippocampus." Hippocampus **17**(9): 826-41.
Harley, C. W. (1972). "Hippocampal lesions and two cue discrimination in the rat." Physiol Behav **9**(3): 343-8.
Harlow, J. M. (1848). "Passage of an iron rod through the head." Boston Medical and Surgical Journal **39**: 389-93.
Harris, K. D., J. Csicsvari, et al. (2003). "Organization of cell assemblies in the hippocampus." Nature **424**(6948): 552-6.
Harris, K. D., D. A. Henze, et al. (2002). "Spike train dynamics predicts theta-related phase precession in hippocampal pyramidal cells." Nature **417**(6890): 738-41.
Hartley, T., N. Burgess, et al. (2000). "Modeling place fields in terms of the cortical inputs to the hippocampus." Hippocampus **10**(4): 369-79.
Hartley, T., E. A. Maguire, et al. (2003). "The well-worn route and the path less traveled: distinct neural bases of route following and wayfinding in humans." Neuron **37**(5): 877-88.
Harvey, C. D., F. Collman, et al. (2009). "Intracellular dynamics of hippocampal place cells during virtual navigation." Nature **461**(7266): 941-6.
Hassabis, D., D. Kumaran, et al. (2007). "Patients with hippocampal amnesia cannot imagine new experiences." Proc Natl Acad Sci U S A **104**(5): 1726-31.
Hasselmo, M. E. (2008). "Grid cell mechanisms and function: contributions of entorhinal persistent spiking and phase resetting." Hippocampus **18**(12): 1213-29.
Hasselmo, M. E. and L. M. Giocomo (2006). "Cholinergic modulation of cortical function." J Mol Neurosci **30**(1-2): 133-5.
Hasselmo, M. E., L. M. Giocomo, et al. (2007). "Grid cell firing may arise from interference of theta frequency membrane potential oscillations in single neurons." Hippocampus **17**(12): 1252-71.
Hasselmo, M. E. and J. McGaughy (2004). "High acetylcholine levels set circuit dynamics for attention and encoding and low acetylcholine levels set dynamics for consolidation." Prog Brain Res **145**: 207-31.
Hausser, M., N. Spruston, et al. (2000). "Diversity and dynamics of dendritic signaling." Science **290**(5492): 739-44.
Hayman, R., M. A. Verriotis, et al. (2011). "Anisotropic encoding of three-dimensional space by place cells and grid cells." Nat Neurosci **14**(9): 1182-8.

Hayman, R. M. and K. J. Jeffery (2008). "How heterogeneous place cell responding arises from homogeneous grids--a contextual gating hypothesis." Hippocampus **18**(12): 1301-13.
Head, H. and G. Holmes (1911). "Sensory Disturbances from Cerebral Lesions." Brain **34**(2-3): 102.
Hebb, D. O. (1949). The organization of behavior: A neuropsychological theory. New York, John Wiley.
Hendrickson, C. W., R. J. Kimble, et al. (1969). "Hippocampal lesions and the orienting response." J Comp Physiol Psychol **67**(2): 220-7.
Henriksen, E. J., L. L. Colgin, et al. (2010). "Spatial representation along the proximodistal axis of CA1." Neuron **68**(1): 127-37.
Hensch, T. K. (2005). "Critical period plasticity in local cortical circuits." Nat Rev Neurosci **6**(11): 877-88.
Henze, D. A. and G. Buzsaki (2001). "Action potential threshold of hippocampal pyramidal cells in vivo is increased by recent spiking activity." Neuroscience **105**(1): 121-30.
Hetherington, P. A. and M. L. Shapiro (1997). "Hippocampal place fields are altered by the removal of single visual cues in a distance-dependent manner." Behav Neurosci **111**(1): 20-34.
Heys, J. G., L. M. Giocomo, et al. (2010). "Cholinergic modulation of the resonance properties of stellate cells in layer II of medial entorhinal cortex." J Neurophysiol **104**(1): 258-70.
Heys, J. G., C. F. Moss, et al. (2012). "Bat and rats: A cross-species comparison of resonance and membrane potential sag in medial entorhinal cortex." SfN Abstract: 293.14.
Heys, J. G., N. W. Schultheiss, et al. (2012). "Effects of acetylcholine on neuronal properties in entorhinal cortex." Front Behav Neurosci **6**: 32.
Ho, A. S., E. Hori, et al. (2011). "Hippocampal neuronal responses during signaled licking of gustatory stimuli in different contexts." Hippocampus **21**(5): 502-19.
Ho, S. A., E. Hori, et al. (2008). "Hippocampal place cell activity during chasing of a moving object associated with reward in rats." Neuroscience **157**(1): 254-70.
Hopfield, J. J. (1982). "Neural networks and physical systems with emergent collective computational abilities." Proc Natl Acad Sci U S A **79**(8): 2554-8.
Hubel, D. H. and T. N. Wiesel (1959). "Receptive fields of single neurones in the cat's striate cortex." J Physiol **148**: 574-91.
Hughlings-Jackson, J. (1884). "On affectations of speech from disease of the brain (2)." Brit Med J(12): 703-7.
Hussaini, S. A., K. A. Kempadoo, et al. (2011). "Increased size and stability of CA1 and CA3 place fields in HCN1 knockout mice." Neuron **72**(4): 643-53.
Huxley, T. H. (1861). "On the zoological relations of man with the lower animals." Natural History Review **1**.
Huxter, J., N. Burgess, et al. (2003). "Independent rate and temporal coding in hippocampal pyramidal cells." Nature **425**(6960): 828-32.
Huxter, J. R., T. J. Senior, et al. (2008). "Theta phase-specific codes for two-dimensional position, trajectory and heading in the hippocampus." Nat Neurosci **11**(5): 587-94.
Iaria, G., M. Petrides, et al. (2003). "Cognitive strategies dependent on the hippocampus and caudate nucleus in human navigation: variability and change with practice." J Neurosci **23**(13): 5945-52.
Igarashi, K. M., L. Lu, et al. (2012). "Olfactory learning-induced coherence between beta/slow-gamma oscillations in hippocampal area CA1 and lateral entorhinal cortex " SfN Abstract: 702.03.
Ikonen, S., R. McMahan, et al. (2002). "Cholinergic system regulation of spatial representation by the hippocampus." Hippocampus **12**(3): 386-97.

Insausti, R. (1993). "Comparative anatomy of the entorhinal cortex and hippocampus in mammals." Hippocampus **3 Spec No**: 19-26.
Insausti, R., M. T. Herrero, et al. (1997). "Entorhinal cortex of the rat: cytoarchitectonic subdivisions and the origin and distribution of cortical efferents." Hippocampus **7**(2): 146-83.
Ito, H. T., M. P. Witter, et al. (2012). "Representation of behavioral context in the nucleus reuniens for CA1 place cells." SfN Abstract: 702.04.
Itskov, V., C. Curto, et al. (2011). "Cell assembly sequences arising from spike threshold adaptation keep track of time in the hippocampus." J Neurosci **31**(8): 2828-34.
Jackson, J. and A. D. Redish (2007). "Network dynamics of hippocampal cell-assemblies resemble multiple spatial maps within single tasks." Hippocampus **17**(12): 1209-29.
Jackson, W. J. and P. N. Strong, Jr. (1969). "Differential effects of hippocampal lesions upon sequential tasks and maze learning by the rat." J Comp Physiol Psychol **68**(3): 442-50.
Jacobs, J., M. J. Kahana, et al. (2010). "A sense of direction in human entorhinal cortex." Proc Natl Acad Sci U S A **107**(14): 6487-92.
Jadhav, S. P., C. Kemere, et al. (2012). "Awake hippocampal sharp-wave ripples support spatial memory." Science **336**(6087): 1454-8.
Jarrard, L. E. (1978). "Selective hippocampal lesions: differential effects on performance by rats of a spatial task with preoperative versus postoperative training." J Comp Physiol Psychol **92**(6): 1119-27.
Jarrard, L. E. (1983). "Selective hippocampal lesions and behavior: effects of kainic acid lesions on performance of place and cue tasks." Behav Neurosci **97**(6): 873-89.
Jeewajee, A., C. Barry, et al. (2012). "Theta phase precession of grid and place cell firing in 2d." SfN Abstract: 918.09.
Jeewajee, A., C. Barry, et al. (2008). "Grid cells and theta as oscillatory interference: electrophysiological data from freely moving rats." Hippocampus **18**(12): 1175-85.
Jeewajee, A., C. Lever, et al. (2008). "Environmental novelty is signaled by reduction of the hippocampal theta frequency." Hippocampus **18**(4): 340-8.
Jeffery, K. J. (1998). "Learning of landmark stability and instability by hippocampal place cells." Neuropharmacology **37**(4-5): 677-87.
Jeffery, K. J. (2011). "Place cells, grid cells, attractors, and remapping." Neural Plast **2011**: 182602.
Jeffery, K. J. and J. M. O'Keefe (1999). "Learned interaction of visual and idiothetic cues in the control of place field orientation." Exp Brain Res **127**(2): 151-61.
Jezek, K., E. J. Henriksen, et al. (2011). "Theta-paced flickering between place-cell maps in the hippocampus." Nature **478**(7368): 246-9.
Ji, D. and M. A. Wilson (2007). "Coordinated memory replay in the visual cortex and hippocampus during sleep." Nat Neurosci **10**(1): 100-7.
Johnson, A. and A. D. Redish (2007). "Neural ensembles in CA3 transiently encode paths forward of the animal at a decision point." J Neurosci **27**(45): 12176-89.
Johnson, A., K. Seeland, et al. (2005). "Reconstruction of the postsubiculum head direction signal from neural ensembles." Hippocampus **15**(1): 86-96.
Johnson, G. A., A. Badea, et al. (2010). "Waxholm space: an image-based reference for coordinating mouse brain research." Neuroimage **53**(2): 365-72.
Jonas, P. and G. Buzsaki (2007). "Neural inhibition." Scholarpedia **2**(9): 3286.
Jones, M. W. and T. J. McHugh (2011). "Updating hippocampal representations: CA2 joins the circuit." Trends Neurosci **34**(10): 526-35.
Jones, S. P., O. Rahimi, et al. (2003). "Maturation of granule cell dendrites after mossy fiber arrival in hippocampal field CA3." Hippocampus **13**(3): 413-27.
Jouvet, M. (1969). "Biogenic amines and the states of sleep." Science **163**(3862): 32-41.

Jung, M. W. and B. L. McNaughton (1993). "Spatial selectivity of unit activity in the hippocampal granular layer." Hippocampus **3**(2): 165-82.
Jung, M. W., S. I. Wiener, et al. (1994). "Comparison of spatial firing characteristics of units in dorsal and ventral hippocampus of the rat." J Neurosci **14**(12): 7347-56.
Jung, R. and A. Kornmüller (1938). "Eine Methodik der Ableitung Iokalisierter Potentialschwankungen aus subcorticalen Hirngebieten." European Archives of Psychiatry and Clinical Neuroscience **109**(1): 1-30.
Kamondi, A., L. Acsady, et al. (1998). "Theta oscillations in somata and dendrites of hippocampal pyramidal cells in vivo: activity-dependent phase-precession of action potentials." Hippocampus **8**(3): 244-61.
Kandel, E. R. and W. A. Spencer (1961). "Electrophysiology of hippocampal neurons. II. After-potentials and repetitive firing." J Neurophysiol **24**: 243-59.
Kant, I. (1781). Critik der reinen Vernunft. Riga, Hartknoch.
Kaplan, M. S. and J. W. Hinds (1977). "Neurogenesis in the adult rat: electron microscopic analysis of light radioautographs." Science **197**(4308): 1092-4.
Karlsson, M. P. and L. M. Frank (2009). "Awake replay of remote experiences in the hippocampus." Nat Neurosci **12**(7): 913-8.
Kealy, J. and S. Commins (2011). "The rat perirhinal cortex: A review of anatomy, physiology, plasticity, and function." Prog Neurobiol **93**(4): 522-48.
Keene, C. S., R. W. Komorowski, et al. (2012). "Object and context related neuronal activity in lateral and medial entorhinal cortices in a conditional discrimination task." SfN Abstract: 203.13.
Kentros, C. G., N. T. Agnihotri, et al. (2004). "Increased attention to spatial context increases both place field stability and spatial memory." Neuron **42**(2): 283-95.
Kerr, K. M., K. L. Agster, et al. (2007). "Functional neuroanatomy of the parahippocampal region: the lateral and medial entorhinal areas." Hippocampus **17**(9): 697-708.
Kesner, R. P. and R. Giles (1998). "Neural circuit analysis of spatial working memory: role of pre- and parasubiculum, medial and lateral entorhinal cortex." Hippocampus **8**(4): 416-23.
Kesner, R. P. and D. S. Olton (1990). Neurobiology of comparative cognition. Hillsdale, N.J., L. Erlbaum Associates.
Kessels, R. P., E. H. de Haan, et al. (2001). "Varieties of human spatial memory: a meta-analysis on the effects of hippocampal lesions." Brain Res Brain Res Rev **35**(3): 295-303.
Khabbaz, A., M. S. Fee, et al. (2000). "A compact converging electrode microdrive for recording head direction cells in mice." Soc Neurosci Abstr **26**: 984.
Kim, E. J., E. S. Kim, et al. (2012). "Amygdalar stimulation produces alterations on firing properties of hippocampal place cells." J Neurosci **32**(33): 11424-34.
Kim, S. M., S. Ganguli, et al. (2012). "Spatial information outflow from the hippocampal circuit: distributed spatial coding and phase precession in the subiculum." J Neurosci **32**(34): 11539-58.
Kimble, D. P. (1963). "The effects of bilateral hippocampal lesions in rats." J Comp Physiol Psychol **56**: 273-83.
Kimble, D. P. and R. J. Kimble (1970). "The effect of hippocampal lesions on extinction and "hypothesis" behavior in rats." Physiol Behav **5**(7): 735-8.
King, C., M. Recce, et al. (1998). "The rhythmicity of cells of the medial septum/diagonal band of Broca in the awake freely moving rat: relationships with behaviour and hippocampal theta." Eur J Neurosci **10**(2): 464-77.
Kirk, I. J. (1998). "Frequency modulation of hippocampal theta by the supramammillary nucleus, and other hypothalamo-hippocampal interactions: mechanisms and functional implications." Neurosci Biobehav Rev **22**(2): 291-302.
Kirkby, D. L. and G. A. Higgins (1998). "Characterization of perforant path lesions in rodent models of memory and attention." Eur J Neurosci **10**(3): 823-38.

Kjelstrup, K. B., T. Solstad, et al. (2008). "Finite scale of spatial representation in the hippocampus." Science **321**(5885): 140-3.
Kjelstrup, K. G., F. A. Tuvnes, et al. (2002). "Reduced fear expression after lesions of the ventral hippocampus." Proc Natl Acad Sci U S A **99**(16): 10825-30.
Kjonigsen, L. J., T. B. Leergaard, et al. (2011). "Digital atlas of anatomical subdivisions and boundaries of the rat hippocampal region." Front Neuroinform **5**: 2.
Klausberger, T., P. J. Magill, et al. (2003). "Brain-state- and cell-type-specific firing of hippocampal interneurons in vivo." Nature **421**(6925): 844-8.
Klausberger, T. and P. Somogyi (2008). "Neuronal diversity and temporal dynamics: the unity of hippocampal circuit operations." Science **321**(5885): 53-7.
Klink, R. and A. Alonso (1993). "Ionic mechanisms for the subthreshold oscillations and differential electroresponsiveness of medial entorhinal cortex layer II neurons." J Neurophysiol **70**(1): 144-57.
Klink, R. and A. Alonso (1997). "Muscarinic modulation of the oscillatory and repetitive firing properties of entorhinal cortex layer II neurons." J Neurophysiol **77**(4): 1813-28.
Knierim, J. J. (2002). "Dynamic interactions between local surface cues, distal landmarks, and intrinsic circuitry in hippocampal place cells." J Neurosci **22**(14): 6254-64.
Knierim, J. J. and D. A. Hamilton (2011). "Framing spatial cognition: neural representations of proximal and distal frames of reference and their roles in navigation." Physiol Rev **91**(4): 1245-79.
Knierim, J. J., H. S. Kudrimoti, et al. (1995). "Place cells, head direction cells, and the learning of landmark stability." J Neurosci **15**(3 Pt 1): 1648-59.
Knierim, J. J., H. S. Kudrimoti, et al. (1998). "Interactions between idiothetic cues and external landmarks in the control of place cells and head direction cells." J Neurophysiol **80**(1): 425-46.
Knierim, J. J. and B. L. McNaughton (2001). "Hippocampal place-cell firing during movement in three-dimensional space." J Neurophysiol **85**(1): 105-16.
Knierim, J. J., B. L. McNaughton, et al. (2000). "Three-dimensional spatial selectivity of hippocampal neurons during space flight." Nat Neurosci **3**(3): 209-10.
Knight, R., R. Hayman, et al. (2011). "Geometric cues influence head direction cells only weakly in nondisoriented rats." J Neurosci **31**(44): 15681-92.
Kobayashi, T., H. Nishijo, et al. (1997). "Task-dependent representations in rat hippocampal place neurons." J Neurophysiol **78**(2): 597-613.
Kobayashi, T., A. H. Tran, et al. (2003). "Contribution of hippocampal place cell activity to learning and formation of goal-directed navigation in rats." Neuroscience **117**(4): 1025-35.
Koene, R. A. and M. E. Hasselmo (2007). "First-in-first-out item replacement in a model of short-term memory based on persistent spiking." Cereb Cortex **17**(8): 1766-81.
Koenig, J., A. N. Linder, et al. (2011). "The spatial periodicity of grid cells is not sustained during reduced theta oscillations." Science **332**(6029): 592-5.
Kohler, C. (1985). "Intrinsic projections of the retrohippocampal region in the rat brain. I. The subicular complex." J Comp Neurol **236**(4): 504-22.
Kohler, C. (1986). "Intrinsic connections of the retrohippocampal region in the rat brain. II. The medial entorhinal area." J Comp Neurol **246**(2): 149-69.
Kohler, C. (1988). "Intrinsic connections of the retrohippocampal region in the rat brain: III. The lateral entorhinal area." J Comp Neurol **271**(2): 208-28.
Komorowski, R. W., J. R. Manns, et al. (2009). "Robust conjunctive item-place coding by hippocampal neurons parallels learning what happens where." J Neurosci **29**(31): 9918-29.
Kosel, K. C., G. W. Van Hoesen, et al. (1983). "A direct projection from the perirhinal cortex (area 35) to the subiculum in the rat." Brain Res **269**(2): 347-51.
Kosik, K. S. (2003). "Beyond phrenology, at last." Nat Rev Neurosci **4**(3): 234-9.

Kraus, B. J., M. P. Brandon, et al. (2012). "Medial entorhinal cortical neurons exhibit temporally-modulated firing patterns during stationary treadmill running." SfN Abstract: 203.14.
Kreiman, G., C. Koch, et al. (2000). "Category-specific visual responses of single neurons in the human medial temporal lobe." Nat Neurosci **3**(9): 946-53.
Kreiman, G., C. Koch, et al. (2000). "Imagery neurons in the human brain." Nature **408**(6810): 357-61.
Krieg, W. J. (1946). "Connections of the cerebral cortex; the albino rat; structure of the cortical areas." J Comp Neurol **84**: 277-323.
Krieg, W. J. (1946). "Connections of the cerebral cortex; the albino rat; topography of the cortical areas." J Comp Neurol **84**: 221-75.
Kropff, E. and A. Treves (2008). "The emergence of grid cells: Intelligent design or just adaptation?" Hippocampus **18**(12): 1256-69.
Krupic, J., N. Burgess, et al. (2012). "Neural representations of location composed of spatially periodic bands." Science **337**(6096): 853-7.
Kubie, J. L. and R. U. Muller (1991). "Multiple representations in the hippocampus." Hippocampus **1**(3): 240-2.
Kudrimoti, H. S., J. J. Knierim, et al. (1996). "Dynamics of visual cue control over head direction cells." Ann N Y Acad Sci **781**: 642-4.
Kuhn, H. G., H. Dickinson-Anson, et al. (1996). "Neurogenesis in the dentate gyrus of the adult rat: age-related decrease of neuronal progenitor proliferation." J Neurosci **16**(6): 2027-33.
Kulkarni, M., K. Zhang, et al. (2011). "Single-cell persistent activity in anterodorsal thalamus." Neurosci Lett **498**(3): 179-84.
Kveim, O., J. Setekleiv, et al. (1964). "Differential effects of hippocampal lesions on maze and passive avoidance learning in rats." Exp Neurol **9**: 59-72.
Kyd, R. J. and D. K. Bilkey (2003). "Prefrontal cortex lesions modify the spatial properties of hippocampal place cells." Cereb Cortex **13**(5): 444-51.
Kyd, R. J. and D. K. Bilkey (2005). "Hippocampal place cells show increased sensitivity to changes in the local environment following prefrontal cortex lesions." Cereb Cortex **15**(6): 720-31.
Langley, J. N. and C. S. Sherrington (1884). "Secondary Degeneration of Nerve Tracts following removal of the Cortex of the Cerebrum in the Dog." J Physiol **5**(2): 49-126.
Langston, R. F., J. A. Ainge, et al. (2010). "Development of the Spatial Representation System in the Rat." Science **328**(5985): 1576-80.
Lash, L. (1964). "Response Discriminability and the Hippocampus." J Comp Physiol Psychol **57**: 251-6.
Lashley, K. (1950). "In search of the engram." Society of Experimental Biology Symposium **4**: 454–82.
Laurberg, S. (1979). "Commissural and intrinsic connections of the rat hippocampus." J Comp Neurol **184**(4): 685-708.
Lavenex, P. and D. G. Amaral (2000). "Hippocampal-neocortical interaction: a hierarchy of associativity." Hippocampus **10**(4): 420-30.
Lavenex, P. B., D. G. Amaral, et al. (2006). "Hippocampal lesion prevents spatial relational learning in adult macaque monkeys." J Neurosci **26**(17): 4546-58.
Lavenex, P. B. and P. Lavenex (2009). "Spatial memory and the monkey hippocampus: not all space is created equal." Hippocampus **19**(1): 8-19.
Lee, A. K., J. Epsztein, et al. (2009). "Head-anchored whole-cell recordings in freely moving rats." Nat Protoc **4**(3): 385-92.
Lee, A. K., I. D. Manns, et al. (2006). "Whole-cell recordings in freely moving rats." Neuron **51**(4): 399-407.
Lee, A. L., W. O. Ogle, et al. (2002). "Stress and depression: possible links to neuron death in the hippocampus." Bipolar Disord **4**(2): 117-28.

Lee, D., B. J. Lin, et al. (2012). "Hippocampal place fields emerge upon single-cell manipulation of excitability during behavior." Science **337**(6096): 849-53.
Lee, H., J. W. Ghim, et al. (2012). "Hippocampal neural correlates for values of experienced events." J Neurosci **32**(43): 15053-65.
Lee, I. and J. Kim (2010). "The shift from a response strategy to object-in-place strategy during learning is accompanied by a matching shift in neural firing correlates in the hippocampus." Learn Mem **17**(8): 381-93.
Lee, I., G. Rao, et al. (2004). "A double dissociation between hippocampal subfields: differential time course of CA3 and CA1 place cells for processing changed environments." Neuron **42**(5): 803-15.
Lee, I., D. Yoganarasimha, et al. (2004). "Comparison of population coherence of place cells in hippocampal subfields CA1 and CA3." Nature **430**(6998): 456-9.
Lenck-Santini, P. P., A. A. Fenton, et al. (2008). "Discharge properties of hippocampal neurons during performance of a jump avoidance task." J Neurosci **28**(27): 6773-86.
Lenck-Santini, P. P., R. U. Muller, et al. (2002). "Relationships between place cell firing fields and navigational decisions by rats." J Neurosci **22**(20): 9035-47.
Leung, L. S. and C. Y. Yim (1986). "Intracellular records of theta rhythm in hippocampal CA1 cells of the rat." Brain Res **367**(1-2): 323-7.
Leung, L. W., F. H. Lopes da Silva, et al. (1982). "Spectral characteristics of the hippocampal EEG in the freely moving rat." Electroencephalogr Clin Neurophysiol **54**(2): 203-19.
Leung, L. W. and C. Y. Yim (1991). "Intrinsic membrane potential oscillations in hippocampal neurons in vitro." Brain Res **553**(2): 261-74.
Leutgeb, J. K., S. Leutgeb, et al. (2007). "Pattern separation in the dentate gyrus and CA3 of the hippocampus." Science **315**(5814): 961-6.
Leutgeb, S., J. K. Leutgeb, et al. (2005). "Independent codes for spatial and episodic memory in hippocampal neuronal ensembles." Science **309**(5734): 619-23.
Leutgeb, S., J. K. Leutgeb, et al. (2004). "Distinct ensemble codes in hippocampal areas CA3 and CA1." Science **305**(5688): 1295-8.
Leutgeb, S. and S. J. Mizumori (1999). "Excitotoxic septal lesions result in spatial memory deficits and altered flexibility of hippocampal single-unit representations." J Neurosci **19**(15): 6661-72.
Leutgeb, S., K. E. Ragozzino, et al. (2000). "Convergence of head direction and place information in the CA1 region of hippocampus." Neuroscience **100**(1): 11-9.
Lever, C., S. Burton, et al. (2009). "Boundary vector cells in the subiculum of the hippocampal formation." J Neurosci **29**(31): 9771-7.
Lever, C., S. Burton, et al. (2010). "Environmental novelty elicits a later theta phase of firing in CA1 but not subiculum." Hippocampus **20**(2): 229-34.
Lever, C., T. Wills, et al. (2002). "Long-term plasticity in hippocampal place-cell representation of environmental geometry." Nature **416**(6876): 90-4.
Lewis, F. T. (1923). "The significance of the term Hippocampus." J Comp Neurol **35**(3): 213-30.
Lewis, P. (1977). Maps and statistics. London, Methuen.
Li, X. G., P. Somogyi, et al. (1994). "The hippocampal CA3 network: an in vivo intracellular labeling study." J Comp Neurol **339**(2): 181-208.
Lipton, P. A., J. A. White, et al. (2007). "Disambiguation of overlapping experiences by neurons in the medial entorhinal cortex." J Neurosci **27**(21): 5787-95.
Lisman, J. and A. D. Redish (2009). "Prediction, sequences and the hippocampus." Philos Trans R Soc Lond B Biol Sci **364**(1521): 1193-201.
Lisman, J. E. and M. A. Idiart (1995). "Storage of 7 +/- 2 short-term memories in oscillatory subcycles." Science **267**(5203): 1512-5.
Liu, P. and D. K. Bilkey (1998). "Perirhinal cortex contributions to performance in the Morris water maze." Behav Neurosci **112**(2): 304-15.

Liu, P. and D. K. Bilkey (2002). "The effects of NMDA lesions centered on the postrhinal cortex on spatial memory tasks in the rat." Behav Neurosci **116**(5): 860-73.
Liu, P., L. E. Jarrard, et al. (2001). "Excitotoxic lesions of the pre- and parasubiculum disrupt object recognition and spatial memory processes." Behav Neurosci **115**(1): 112-24.
Liu, P., L. E. Jarrard, et al. (2004). "Excitotoxic lesions of the pre- and parasubiculum disrupt the place fields of hippocampal pyramidal cells." Hippocampus **14**(1): 107-16.
Liu, X., S. Ramirez, et al. (2012). "Optogenetic stimulation of a hippocampal engram activates fear memory recall." Nature **484**(7394): 381-5.
Llinas, R. R. (1988). "The intrinsic electrophysiological properties of mammalian neurons: insights into central nervous system function." Science **242**(4886): 1654-64.
Logothetis, N. K., O. Eschenko, et al. (2012). "Hippocampal-cortical interaction during periods of subcortical silence." Nature **491**(7425): 547-53.
Lokhorst, G. J. and T. T. Kaitaro (2001). "The originality of Descartes' theory about the pineal gland." J Hist Neurosci **10**(1): 6-18.
Lorente de Nó, R. (1921). "La corteza cerebral del ratón. Primera contribución. La corteza acústica." Trab Lab Invest **19**: 147-88.
Lorente de Nó, R. (1934). "Studies of the structure of the cerebral cortex. II. Continuation of the study of the ammonic system." J Psychol Neurol **46**: 113-77.
Lu, L., J. K. Leutgeb, et al. (2012). "The lateral entorhinal cortex and rate coding in the hippocampus." SfN Abstract: 702.07.
Lubenov, E. V. and A. G. Siapas (2009). "Hippocampal theta oscillations are travelling waves." Nature **459**(7246): 534-9.
Lynch, G. S., T. Dunwiddie, et al. (1977). "Heterosynaptic depression: a postsynaptic correlate of long-term potentiation." Nature **266**(5604): 737-9.
MacDonald, C. J., K. Q. Lepage, et al. (2011). "Hippocampal "time cells" bridge the gap in memory for discontiguous events." Neuron **71**(4): 737-49.
Macmillan, M. (2000). "Restoring Phineas Gage: a 150th retrospective." J Hist Neurosci **9**(1): 46-66.
Madison, D. V. and R. A. Nicoll (1984). "Control of the repetitive discharge of rat CA 1 pyramidal neurones in vitro." J Physiol **354**: 319-31.
Maguire, E. A., T. Burke, et al. (1996). "Topographical disorientation following unilateral temporal lobe lesions in humans." Neuropsychologia **34**(10): 993-1001.
Maguire, E. A., R. S. Frackowiak, et al. (1997). "Recalling routes around london: activation of the right hippocampus in taxi drivers." J Neurosci **17**(18): 7103-10.
Maguire, E. A., R. Nannery, et al. (2006). "Navigation around London by a taxi driver with bilateral hippocampal lesions." Brain **129**(Pt 11): 2894-907.
Maine de Biran, P. (1804). Influence de l'habitude sur la faculte de penser. Ouvrage qui a remporté le prix sur cette question, proposée par la classe des sciences morales et politiques de l'institut national. Déterminer quelle est l'influence de l'habitude sur la faculté de penser; ou, en d'autres termes, faire voir l'effet. Paris, Henrichs.
Malenka, R. C. and M. F. Bear (2004). "LTP and LTD: an embarrassment of riches." Neuron **44**(1): 5-21.
Malkova, L. and M. Mishkin (2003). "One-trial memory for object-place associations after separate lesions of hippocampus and posterior parahippocampal region in the monkey." J Neurosci **23**(5): 1956-65.
Manganaro, A., J. O'Neill, et al. (2012). "Encoding of reward-associated features in the ventral hippocampus during spatial learning." SfN Abstract: 497.27.
Mankin, E. A., F. T. Sparks, et al. (2012). "Neuronal code for extended time in the hippocampus." Proc Natl Acad Sci U S A **109**(47): 19462-7.
Manns, J. R. and H. Eichenbaum (2009). "A cognitive map for object memory in the hippocampus." Learn Mem **16**(10): 616-24.

Manns, J. R., M. W. Howard, et al. (2007). "Gradual changes in hippocampal activity support remembering the order of events." Neuron **56**(3): 530-40.
Manns, J. R., E. A. Zilli, et al. (2007). "Hippocampal CA1 spiking during encoding and retrieval: relation to theta phase." Neurobiol Learn Mem **87**(1): 9-20.
Marcelin, B., Z. Liu, et al. (2012). "Dorsoventral differences in intrinsic properties in developing CA1 pyramidal cells." J Neurosci **32**(11): 3736-47.
Markie, P. (2012). "Rationalism vs. Empiricism." The Stanford Encyclopedia of Philosophy (Summer 2012 Edition) Retrieved December 30th 2012, from http://plato.stanford.edu/entries/rationalism-empiricism/.
Markus, E. J., C. A. Barnes, et al. (1994). "Spatial information content and reliability of hippocampal CA1 neurons: effects of visual input." Hippocampus **4**(4): 410-21.
Markus, E. J., Y. L. Qin, et al. (1995). "Interactions between location and task affect the spatial and directional firing of hippocampal neurons." J Neurosci **15**(11): 7079-94.
Marozzi, E., L. Ginzberg, et al. (2012). "Contextual modulation of grid cells in entorhinal cortex " SfN Abstract: 293.06.
Martig, A. K. and S. J. Mizumori (2011). "Ventral tegmental area disruption selectively affects CA1/CA2 but not CA3 place fields during a differential reward working memory task." Hippocampus **21**(2): 172-84.
Mason, A. (1993). "Electrophysiology and burst-firing of rat subicular pyramidal neurons in vitro: a comparison with area CA1." Brain Res **600**(1): 174-8.
Maurer, A. P., S. N. Burke, et al. (2012). "Greater running speeds result in altered hippocampal phase sequence dynamics." Hippocampus **22**(4): 737-47.
Maurer, A. P., S. L. Cowen, et al. (2006). "Organization of hippocampal cell assemblies based on theta phase precession." Hippocampus **16**(9): 785-94.
Maurer, A. P., S. R. Vanrhoads, et al. (2005). "Self-motion and the origin of differential spatial scaling along the septo-temporal axis of the hippocampus." Hippocampus **15**(7): 841-52.
McHugh, T. J., K. I. Blum, et al. (1996). "Impaired hippocampal representation of space in CA1-specific NMDAR1 knockout mice." Cell **87**(7): 1339-49.
McHugh, T. J., M. W. Jones, et al. (2007). "Dentate gyrus NMDA receptors mediate rapid pattern separation in the hippocampal network." Science **317**(5834): 94-9.
McIntosh, A. R. (1999). "Mapping cognition to the brain through neural interactions." Memory **7**(5-6): 523-48.
McNaughton, B. L., C. A. Barnes, et al. (1996). "Deciphering the hippocampal polyglot: the hippocampus as a path integration system." J Exp Biol **199**(Pt 1): 173-85.
McNaughton, B. L., C. A. Barnes, et al. (1989). "Hippocampal granule cells are necessary for normal spatial learning but not for spatially-selective pyramidal cell discharge." Exp Brain Res **76**(3): 485-96.
McNaughton, B. L., C. A. Barnes, et al. (1983). "The contributions of position, direction, and velocity to single unit activity in the hippocampus of freely-moving rats." Exp Brain Res **52**(1): 41-9.
McNaughton, B. L., F. P. Battaglia, et al. (2006). "Path integration and the neural basis of the 'cognitive map'." Nat Rev Neurosci **7**(8): 663-78.
McNaughton, B. L., L. L. Chen, et al. (1991). "'Dead reckoning', landmark learning, and the sense of direction: A neurophysiological and computational hypothesis." J Cog Neurosci **3**: 190-202.
McNaughton, B. L., S. J. Mizumori, et al. (1994). "Cortical representation of motion during unrestrained spatial navigation in the rat." Cereb Cortex **4**(1): 27-39.
Mehta, M. R. (2011). "Contribution of Ih to LTP, place cells, and grid cells." Cell **147**(5): 968-70.
Mehta, M. R., C. A. Barnes, et al. (1997). "Experience-dependent, asymmetric expansion of hippocampal place fields." Proc Natl Acad Sci U S A **94**(16): 8918-21.

Mehta, M. R., A. K. Lee, et al. (2002). "Role of experience and oscillations in transforming a rate code into a temporal code." Nature **417**(6890): 741-6.
Mehta, M. R., M. C. Quirk, et al. (2000). "Experience-dependent asymmetric shape of hippocampal receptive fields." Neuron **25**(3): 707-15.
Merabet, L. B. and A. Pascual-Leone (2010). "Neural reorganization following sensory loss: the opportunity of change." Nat Rev Neurosci **11**(1): 44-52.
Miller, R. (1989). "Cortico-hippocampal interplay: Self-organizing phase-locked loops for indexing memory." Psychobiology **17**(2): 115-28.
Miller, V. M. and P. J. Best (1980). "Spatial correlates of hippocampal unit activity are altered by lesions of the fornix and endorhinal cortex." Brain Res **194**(2): 311-23.
Milner, B. (1958). "Psychological defects produced by temporal lobe excision." Res Publ Assoc Res Nerv Ment Dis **36**: 244-57.
Mishkin, M. (1978). "Memory in monkeys severely impaired by combined but not by separate removal of amygdala and hippocampus." Nature **273**(5660): 297-8.
Mitchell and J. Ranck (1977). SfN Abstract.
Mitchell, S. J. and J. B. Ranck, Jr. (1980). "Generation of theta rhythm in medial entorhinal cortex of freely moving rats." Brain Res **189**(1): 49-66.
Mittelstaedt, M. L. and H. Mittelstaedt (1980). "Homing by path integration in a mammal." Naturwissenschaften **67**: 566-67.
Mizumori, S. J., B. L. McNaughton, et al. (1989). "A comparison of supramammillary and medial septal influences on hippocampal field potentials and single-unit activity." J Neurophysiol **61**(1): 15-31.
Mizumori, S. J., B. L. McNaughton, et al. (1989). "Preserved spatial coding in hippocampal CA1 pyramidal cells during reversible suppression of CA3c output: evidence for pattern completion in hippocampus." J Neurosci **9**(11): 3915-28.
Mizumori, S. J., D. Y. Miya, et al. (1994). "Reversible inactivation of the lateral dorsal thalamus disrupts hippocampal place representation and impairs spatial learning." Brain Res **644**(1): 168-74.
Mizumori, S. J., K. E. Ragozzino, et al. (1999). "Hippocampal representational organization and spatial context." Hippocampus **9**(4): 444-51.
Mizumori, S. J., K. E. Ward, et al. (1992). "Medial septal modulation of entorhinal single unit activity in anesthetized and freely moving rats." Brain Res **570**(1-2): 188-97.
Mizumori, S. J. and J. D. Williams (1993). "Directionally selective mnemonic properties of neurons in the lateral dorsal nucleus of the thalamus of rats." J Neurosci **13**(9): 4015-28.
Mohamed, W. (2008). "The Edwin Smith Surgical Papyrus: Neuroscience in Ancient Egypt." Retrieved October 1st 2012, from http://www.ibro.info/Pub/Pub_Main_Display.asp?LC_Docs_ID=3199.
Moita, M. A., S. Rosis, et al. (2004). "Putting fear in its place: remapping of hippocampal place cells during fear conditioning." J Neurosci **24**(31): 7015-23.
Montgomery, S. M., M. I. Betancur, et al. (2009). "Behavior-dependent coordination of multiple theta dipoles in the hippocampus." J Neurosci **29**(5): 1381-94.
Morales, E. A., E. Marozzi, et al. (2012). "Investigating the origin of contextual inputs to hippocampal place cells." SfN Abstract: 293.02.
Morris, R. G., P. Garrud, et al. (1982). "Place navigation impaired in rats with hippocampal lesions." Nature **297**(5868): 681-3.
Morris, R. G., F. Schenk, et al. (1990). "Ibotenate Lesions of Hippocampus and/or Subiculum: Dissociating Components of Allocentric Spatial Learning." Eur J Neurosci **2**(12): 1016-28.
Morris, R. G. M. (1981). "Spatial localization does not require the presence of local cues." Learning and Motivation **12**(2): 239-60.

Morrissey, M. D., G. Maal-Bared, et al. (2012). "Functional dissociation within the entorhinal cortex for memory retrieval of an association between temporally discontiguous stimuli." J Neurosci **32**(16): 5356-61.
Moscovitch, M., L. Nadel, et al. (2006). "The cognitive neuroscience of remote episodic, semantic and spatial memory." Curr Opin Neurobiol **16**(2): 179-90.
Moser, E., M. B. Moser, et al. (1993). "Spatial learning impairment parallels the magnitude of dorsal hippocampal lesions, but is hardly present following ventral lesions." J Neurosci **13**(9): 3916-25.
Moser, E. I., K. A. Krobert, et al. (1998). "Impaired spatial learning after saturation of long-term potentiation." Science **281**(5385): 2038-42.
Moser, E. I., E. Kropff, et al. (2008). "Place cells, grid cells, and the brain's spatial representation system." Annu Rev Neurosci **31**: 69-89.
Moser, E. I. and M. B. Moser (2008). "A metric for space." Hippocampus **18**(12): 1142-56.
Moser, M. B. and E. I. Moser (2000). "Pretraining and the function of hippocampal long-term potentiation." Neuron **26**(3): 559-61.
Moser, M. B., E. I. Moser, et al. (1995). "Spatial learning with a minislab in the dorsal hippocampus." Proc Natl Acad Sci U S A **92**(21): 9697-701.
Muir, G. M. and D. K. Bilkey (2001). "Instability in the place field location of hippocampal place cells after lesions centered on the perirhinal cortex." J Neurosci **21**(11): 4016-25.
Muir, G. M. and D. K. Bilkey (2003). "Theta- and movement velocity-related firing of hippocampal neurons is disrupted by lesions centered on the perirhinal cortex." Hippocampus **13**(1): 93-108.
Muir, G. M., J. E. Brown, et al. (2009). "Disruption of the head direction cell signal after occlusion of the semicircular canals in the freely moving chinchilla." J Neurosci **29**(46): 14521-33.
Muir, G. M. and J. S. Taube (2002). "The neural correlates of navigation: do head direction and place cells guide spatial behavior?" Behav Cogn Neurosci Rev **1**(4): 297-317.
Muir, G. M. and J. S. Taube (2004). "Head direction cell activity and behavior in a navigation task requiring a cognitive mapping strategy." Behav Brain Res **153**(1): 249-53.
Muller, R. U., E. Bostock, et al. (1994). "On the directional firing properties of hippocampal place cells." J Neurosci **14**(12): 7235-51.
Muller, R. U. and J. L. Kubie (1987). "The effects of changes in the environment on the spatial firing of hippocampal complex-spike cells." J Neurosci **7**(7): 1951-68.
Muller, R. U., J. L. Kubie, et al. (1987). "Spatial firing patterns of hippocampal complex-spike cells in a fixed environment." J Neurosci **7**(7): 1935-50.
Muller, R. U., J. B. Ranck, Jr., et al. (1996). "Head direction cells: properties and functional significance." Curr Opin Neurobiol **6**(2): 196-206.
Muller, R. U., M. Stead, et al. (1996). "The hippocampus as a cognitive graph." J Gen Physiol **107**(6): 663-94.
Mumby, D. G. and J. P. Pinel (1994). "Rhinal cortex lesions and object recognition in rats." Behav Neurosci **108**(1): 11-8.
Murray, E. A., T. J. Bussey, et al. (2007). "Visual perception and memory: a new view of medial temporal lobe function in primates and rodents." Annu Rev Neurosci **30**: 99-122.
Murray, E. A. and M. Mishkin (1986). "Visual recognition in monkeys following rhinal cortical ablations combined with either amygdalectomy or hippocampectomy." J Neurosci **6**(7): 1991-2003.
Myhrer, T. (1975). "Maze performance in rats with hippocampal perforant paths lesions: some aspects of functional recovery." Physiol Behav **15**(5): 433-7.

Naber, P. A., F. H. Lopes da Silva, et al. (2001). "Reciprocal connections between the entorhinal cortex and hippocampal fields CA1 and the subiculum are in register with the projections from CA1 to the subiculum." Hippocampus **11**(2): 99-104.

Nadel, L., J. Willner, et al. (1985). Cognitive maps and environmental context. Context and Learning. P. D. Balsam and A. Tomie (eds.). Hillsdale NJ, Erlbaum**:** 385–406.

Nagahara, A. H., T. Otto, et al. (1995). "Entorhinal-perirhinal lesions impair performance of rats on two versions of place learning in the Morris water maze." Behav Neurosci **109**(1): 3-9.

Nakashiba, T., J. D. Cushman, et al. (2012). "Young dentate granule cells mediate pattern separation, whereas old granule cells facilitate pattern completion." Cell **149**(1): 188-201.

Nakashiba, T., J. Z. Young, et al. (2008). "Transgenic inhibition of synaptic transmission reveals role of CA3 output in hippocampal learning." Science **319**(5867): 1260-4.

Nakazawa, K., T. J. McHugh, et al. (2004). "NMDA receptors, place cells and hippocampal spatial memory." Nat Rev Neurosci **5**(5): 361-72.

Nakazawa, K., L. D. Sun, et al. (2003). "Hippocampal CA3 NMDA receptors are crucial for memory acquisition of one-time experience." Neuron **38**(2): 305-15.

Navratilova, Z., L. M. Giocomo, et al. (2012). "Phase precession and variable spatial scaling in a periodic attractor map model of medial entorhinal grid cells with realistic after-spike dynamics." Hippocampus **22**(4): 772-89.

Navratilova, Z., L. T. Hoang, et al. (2012). "Experience-dependent firing rate remapping generates directional selectivity in hippocampal place cells." Front Neural Circuits **6**: 6.

Nerad, L., P. Liu, et al. (2009). "Bilateral NMDA lesions centered on the postrhinal cortex have minimal effects on hippocampal place cell firing." Hippocampus **19**(3): 221-7.

Newman, E. L., S. N. Gillet, et al. (2012). "Effects of cholinergic modulation on interactions of entorhinal cortex and hippocampus as measured by theta modulation of high and low gamma in the rat." SfN Abstract: 293.12.

Nitz, D. and B. McNaughton (2004). "Differential modulation of CA1 and dentate gyrus interneurons during exploration of novel environments." J Neurophysiol **91**(2): 863-72.

Nolan, M. F., G. Malleret, et al. (2004). "A behavioral role for dendritic integration: HCN1 channels constrain spatial memory and plasticity at inputs to distal dendrites of CA1 pyramidal neurons." Cell **119**(5): 719-32.

Nunez, A., E. Garcia-Austt, et al. (1987). "Intracellular theta-rhythm generation in identified hippocampal pyramids." Brain Res **416**(2): 289-300.

Nyberg, L. (2005). "Any novelty in hippocampal formation and memory?" Curr Opin Neurol **18**(4): 424-8.

O'Keefe, J. (1976). "Place units in the hippocampus of the freely moving rat." Exp Neurol **51**(1): 78-109.

O'Keefe, J. and N. Burgess (1996). "Geometric determinants of the place fields of hippocampal neurons." Nature **381**(6581): 425-8.

O'Keefe, J. and N. Burgess (2005). "Dual phase and rate coding in hippocampal place cells: theoretical significance and relationship to entorhinal grid cells." Hippocampus **15**(7): 853-66.

O'Keefe, J. and D. H. Conway (1978). "Hippocampal place units in the freely moving rat: why they fire where they fire." Exp Brain Res **31**(4): 573-90.

O'Keefe, J. and J. Dostrovsky (1971). "The hippocampus as a spatial map. Preliminary evidence from unit activity in the freely-moving rat." Brain Res **34**(1): 171-5.

O'Keefe, J. and L. Nadel (1978). The Hippocampus as a Cognitive Map. Oxford, Clarendon Press.

O'Keefe, J., L. Nadel, et al. (1975). "Fornix lesions selectively abolish place learning in the rat." Exp Neurol **48**(1): 152-66.

O'Keefe, J. and M. L. Recce (1993). "Phase relationship between hippocampal place units and the EEG theta rhythm." Hippocampus **3**(3): 317-30.
O'Keefe, J. and A. Speakman (1987). "Single unit activity in the rat hippocampus during a spatial memory task." Exp Brain Res **68**(1): 1-27.
O'Neill, J., T. Senior, et al. (2006). "Place-selective firing of CA1 pyramidal cells during sharp wave/ripple network patterns in exploratory behavior." Neuron **49**(1): 143-55.
Ogawa, S., T. M. Lee, et al. (1990). "Brain magnetic resonance imaging with contrast dependent on blood oxygenation." Proc Natl Acad Sci U S A **87**(24): 9868-72.
Oldendorf, W. H. (1961). "Isolated flying spot detection of radiodensity discontinuities--displaying the internal structural pattern of a complex object." Ire Trans Biomed Electron **BME-8**: 68-72.
Olton, D. S. (1972). "Discrimination reversal performance after hippocampal lesions: an enduring failure of reinforcement and non-reinforcement to direct behavior." Physiol Behav **9**(3): 353-6.
Olton, D. S. (1977). "The function of septo-hippocampal connections in spatially organized behaviour." Ciba Found Symp(58): 327-49.
Olton, D. S. (1979). "Mazes, maps, and memory." Am Psychol **34**(7): 583-96.
Olton, D. S., M. Branch, et al. (1978). "Spatial correlates of hippocampal unit activity." Exp Neurol **58**(3): 387-409.
Olton, D. S., J. A. Walker, et al. (1982). "A disconnection analysis of hippocampal function." Brain Res **233**(2): 241-53.
Olypher, A. V., P. Lansky, et al. (2002). "Properties of the extra-positional signal in hippocampal place cell discharge derived from the overdispersion in location-specific firing." Neuroscience **111**(3): 553-66.
Ono, T., K. Nakamura, et al. (1991). "Place recognition responses of neurons in monkey hippocampus." Neurosci Lett **121**(1-2): 194-8.
Oswald, C. J. and M. Good (2000). "The effects of combined lesions of the subicular complex and the entorhinal cortex on two forms of spatial navigation in the water maze." Behav Neurosci **114**(1): 211-7.
Otto, T. and H. Eichenbaum (1992). "Neuronal activity in the hippocampus during delayed non-match to sample performance in rats: evidence for hippocampal processing in recognition memory." Hippocampus **2**(3): 323-34.
Otto, T., F. Schottler, et al. (1991). "Hippocampus and olfactory discrimination learning: effects of entorhinal cortex lesions on olfactory learning and memory in a successive-cue, go-no-go task." Behav Neurosci **105**(1): 111-9.
Overstreet-Wadiche, L. S., A. L. Bensen, et al. (2006). "Delayed development of adult-generated granule cells in dentate gyrus." J Neurosci **26**(8): 2326-34.
Overstreet-Wadiche, L. S., D. A. Bromberg, et al. (2006). "Seizures accelerate functional integration of adult-generated granule cells." J Neurosci **26**(15): 4095-103.
Park, E., D. Dvorak, et al. (2011). "Ensemble place codes in hippocampus: CA1, CA3, and dentate gyrus place cells have multiple place fields in large environments." PLoS One **6**(7): e22349.
Parron, C., B. Poucet, et al. (2006). "Cooperation between the hippocampus and the entorhinal cortex in spatial memory: a disconnection study." Behav Brain Res **170**(1): 99-109.
Parron, C. and E. Save (2004). "Evidence for entorhinal and parietal cortices involvement in path integration in the rat." Exp Brain Res **159**(3): 349-59.
Passingham, R. E., K. E. Stephan, et al. (2002). "The anatomical basis of functional localization in the cortex." Nat Rev Neurosci **3**(8): 606-16.
Pastalkova, E., V. Itskov, et al. (2008). "Internally generated cell assembly sequences in the rat hippocampus." Science **321**(5894): 1322-7.

Pastoll, H., H. L. Ramsden, et al. (2012). "Intrinsic electrophysiological properties of entorhinal cortex stellate cells and their contribution to grid cell firing fields." Front Neural Circuits **6**: 17.
Pavlides, C. and J. Winson (1989). "Influences of hippocampal place cell firing in the awake state on the activity of these cells during subsequent sleep episodes." J Neurosci **9**(8): 2907-18.
Paxinos, G. (2004). The Rat nervous system. Amsterdam, Elsevier.
Pearce, J. M., A. D. Roberts, et al. (1998). "Hippocampal lesions disrupt navigation based on cognitive maps but not heading vectors." Nature **396**(6706): 75-7.
Penfield, W. (1952). "Memory mechanisms." AMA Arch Neurol Psychiatry **67**(2): 178-98.
Penfield, W. and T. C. Erickson (1941). Epilepsy and Cerebral Localization: A Study of the Mechanism, Treatment and Prevention of Epileptic Seizures.
Petrulis, A., P. Alvarez, et al. (2005). "Neural correlates of social odor recognition and the representation of individual distinctive social odors within entorhinal cortex and ventral subiculum." Neuroscience **130**(1): 259-74.
Petsche, H. and C. Stumpf (1962). "[The origin of theta-rhytm in the rabbit hippocampus]." Wien Klin Wochenschr **74**: 696-700.
Peyrache, A., F. P. Battaglia, et al. (2011). "Inhibition recruitment in prefrontal cortex during sleep spindles and gating of hippocampal inputs." Proc Natl Acad Sci U S A **108**(41): 17207-12.
Phelps, E. A. (2004). "Human emotion and memory: interactions of the amygdala and hippocampal complex." Curr Opin Neurobiol **14**(2): 198-202.
Phelps, M. E., E. J. Hoffman, et al. (1975). "Application of annihilation coincidence detection to transaxial reconstruction tomography." J Nucl Med **16**(3): 210-24.
Piccolino, M. (1998). "Animal electricity and the birth of electrophysiology: the legacy of Luigi Galvani." Brain Res Bull **46**(5): 381-407.
Plunkett, R. P., B. D. Faulds, et al. (1973). "Place learning in hippocampectomized rats." Bull Psychon **2**: 79-80.
Pokorny, J. and T. Yamamoto (1981). "Postnatal ontogenesis of hippocampal CA1 area in rats. I. Development of dendritic arborisation in pyramidal neurons." Brain Res Bull **7**(2): 113-20.
Pravdich-Neminsky, V. (1913). "Ein Versuch der Registrierung der elektrischen Gehirnerscheinungen." Zbl Physiol **27**: 951–60.
Quirk, G. J., R. U. Muller, et al. (1990). "The firing of hippocampal place cells in the dark depends on the rat's recent experience." J Neurosci **10**(6): 2008-17.
Quirk, G. J., R. U. Muller, et al. (1992). "The positional firing properties of medial entorhinal neurons: description and comparison with hippocampal place cells." J Neurosci **12**(5): 1945-63.
Quiroga, R. Q., R. Mukamel, et al. (2008). "Human single-neuron responses at the threshold of conscious recognition." Proc Natl Acad Sci U S A **105**(9): 3599-604.
Quiroga, R. Q., L. Reddy, et al. (2005). "Invariant visual representation by single neurons in the human brain." Nature **435**(7045): 1102-7.
Raimondo, J. V., L. Kay, et al. (2012). "Optogenetic silencing strategies differ in their effects on inhibitory synaptic transmission." Nat Neurosci **15**(8): 1102-4.
Ramirez-Amaya, V., D. F. Marrone, et al. (2006). "Integration of new neurons into functional neural networks." J Neurosci **26**(47): 12237-41.
Ramirez-Amaya, V., A. Vazdarjanova, et al. (2005). "Spatial exploration-induced Arc mRNA and protein expression: evidence for selective, network-specific reactivation." J Neurosci **25**(7): 1761-8.
Ramón y Cajal, S. (1893). "Estructura del asta de Ammon y fascia dentata." Ann Soc Esp His Nat **22**: 53–114.
Ramón y Cajal, S. (1901). "Significación probable de las células de axon corto." Trab Lab Invest Biol Univ Madrid **1**: 151-7.

Ramón y Cajal, S. (1909). Histologie du système nerveux de l'homme et des vertebretes. Paris, A. Maloine.
Ranck, J. B., Jr. (1973). "Studies on single neurons in dorsal hippocampal formation and septum in unrestrained rats. I. Behavioral correlates and firing repertoires." Exp Neurol **41**(2): 461-531.
Ranck, J. B., Jr. (1984). "Head-direction cells in the deep cell layers of dorsal presubiculum in freely moving rats." Soc Neurosci **10**: 599.
Redish, A. D. (1999). Beyond the cognitive map. Cambridge, MA, MIT Press.
Redish, A. D., F. P. Battaglia, et al. (2001). "Independence of firing correlates of anatomically proximate hippocampal pyramidal cells." J Neurosci **21**(5): RC134.
Redish, A. D., E. S. Rosenzweig, et al. (2000). "Dynamics of hippocampal ensemble activity realignment: time versus space." J Neurosci **20**(24): 9298-309.
Reifenstein, E., M. B. Stemmler, et al. (2012). "Entorhinal phase precession in open environments." SfN Abstract: 808.11.
Remme, M. W., M. Lengyel, et al. (2010). "Democracy-independence trade-off in oscillating dendrites and its implications for grid cells." Neuron **66**(3): 429-37.
Renshaw, B., A. Forbes, et al. (1940). "Activity of isocortex and hippocampus: Electrical studies with microelectrodes." J Neurophysiol **3**: 74-105.
Resnik, E., J. M. McFarland, et al. (2012). "The effects of GluA1 deletion on the hippocampal population code for position." J Neurosci **32**(26): 8952-68.
Richardson, M. P., B. A. Strange, et al. (2004). "Encoding of emotional memories depends on amygdala and hippocampus and their interactions." Nat Neurosci **7**(3): 278-85.
Riches, V. (1972). The effect of hippocampal lesions on spatial learning. B.Sc. Thesis, University College London.
Rivard, B., Y. Li, et al. (2004). "Representation of objects in space by two classes of hippocampal pyramidal cells." J Gen Physiol **124**(1): 9-25.
Rivas, J., J. M. Gaztelu, et al. (1996). "Changes in hippocampal cell discharge patterns and theta rhythm spectral properties as a function of walking velocity in the guinea pig." Exp Brain Res **108**(1): 113-8.
Robertson, R. G., E. T. Rolls, et al. (1999). "Head direction cells in the primate pre-subiculum." Hippocampus **9**(3): 206-19.
Rochefort, C., A. Arabo, et al. (2011). "Cerebellum shapes hippocampal spatial code." Science **334**(6054): 385-9.
Rogozea, R. and J. Ungher (1968). "Changes in orienting activity of cat induced by chronic hippocampal lesions." Exp Neurol **21**(2): 176-86.
Rolls, E. T. (2007). "An attractor network in the hippocampus: theory and neurophysiology." Learn Mem **14**(11): 714-31.
Rorden, C. and H. O. Karnath (2004). "Using human brain lesions to infer function: a relic from a past era in the fMRI age?" Nat Rev Neurosci **5**(10): 813-9.
Rose, M. (1927). "Die sog. Riechrinde beim Menschen und beim Affen.

II. Teil des "Allocortex bei Tier und Mensch"." J Psychol Neurol **34**: 262-401.
Rose, M. (1929). "Cytoarchitektonischer Atlas der Grobhirnrinde der Maus." J Psychol Neurol **40**: 1-32.
Rosenbaum, R. S., F. Gao, et al. (2005). ""Where to?" remote memory for spatial relations and landmark identity in former taxi drivers with Alzheimer's disease and encephalitis." J Cogn Neurosci **17**(3): 446-62.
Rosenbaum, R. S., S. Priselac, et al. (2000). "Remote spatial memory in an amnesic person with extensive bilateral hippocampal lesions." Nat Neurosci **3**(10): 1044-8.
Rosenzweig, M. R., D. Krech, et al. (1962). "Effects of environmental complexity and training on brain chemistry and anatomy: a replication and extension." J Comp Physiol Psychol **55**: 429-37.

Rowland, D. C., A. Weible, et al. (2011). "Quantitative mapping of monosynaptic inputs to entorhinal layer II neurons via transgenically-targeted rabies virus suggests a strong direct projection from hippocampal area CA2." SfN Abstract: 513.03.
Rowland, D. C., Y. Yanovich, et al. (2011). "A stable hippocampal representation of a space requires its direct experience." Proc Natl Acad Sci U S A **108**(35): 14654-8.
Royer, S., A. Sirota, et al. (2010). "Distinct representations and theta dynamics in dorsal and ventral hippocampus." J Neurosci **30**(5): 1777-87.
Royer, S., B. V. Zemelman, et al. (2012). "Control of timing, rate and bursts of hippocampal place cells by dendritic and somatic inhibition." Nat Neurosci **15**(5): 769-75.
Rudy, J. W. and R. J. Sutherland (1989). "The hippocampal formation is necessary for rats to learn and remember configural discriminations." Behav Brain Res **34**(1-2): 97-109.
Ruediger, S., D. Spirig, et al. (2012). "Goal-oriented searching mediated by ventral hippocampus early in trial-and-error learning." Nat Neurosci **15**(11): 1563-71.
Sala, I. (1891). "Zur feineren Anatomie des grossen Seepferdefusses." Zeitschr Wiss Zool **52**.
Samsonovich, A. and B. L. McNaughton (1997). "Path integration and cognitive mapping in a continuous attractor neural network model." J Neurosci **17**(15): 5900-20.
Santarelli, L. and M. D. Saxe (2003). "Substance P antagonists: meet the new drugs, same as the old drugs? Insights from transgenic animal models." CNS Spectr **8**(8): 589-96.
Santoro, G., M. D. Wood, et al. (2009). "The anatomic location of the soul from the heart, through the brain, to the whole body, and beyond: a journey through Western history, science, and philosophy." Neurosurgery **65**(4): 633-43; discussion 43.
Sargolini, F., M. Fyhn, et al. (2006). "Conjunctive representation of position, direction, and velocity in entorhinal cortex." Science **312**(5774): 758-62.
Save, E., A. Cressant, et al. (1998). "Spatial firing of hippocampal place cells in blind rats." J Neurosci **18**(5): 1818-26.
Save, E., L. Nerad, et al. (2000). "Contribution of multiple sensory information to place field stability in hippocampal place cells." Hippocampus **10**(1): 64-76.
Savelli, F. and J. J. Knierim (2012). "Flexible framing of spatial representations in the hippocampal formation " SfN Abstract: 812.13.
Savelli, F., D. Yoganarasimha, et al. (2008). "Influence of boundary removal on the spatial representations of the medial entorhinal cortex." Hippocampus **18**(12): 1270-82.
Scalia, F. and S. S. Winans (1975). "The differential projections of the olfactory bulb and accessory olfactory bulb in mammals." J Comp Neurol **161**(1): 31-55.
Schaffer, K. (1892). "Beitrag zur histologie der Amnionshorn-formation." Arch Mikr Anat **39**: 511-632.
Scharfman, H. E. (1995). "Electrophysiological evidence that dentate hilar mossy cells are excitatory and innervate both granule cells and interneurons." J Neurophysiol **74**(1): 179-94.
Schenk, F. and R. G. Morris (1985). "Dissociation between components of spatial memory in rats after recovery from the effects of retrohippocampal lesions." Exp Brain Res **58**(1): 11-28.
Schlesiger, M. I., J. B. Hales, et al. (2012). "Hippocampal place cell stability after lesions of the grid cell area in the medial entorhinal cortex." SfN Abstract: 203.02.
Schmidt-Hieber, C. and M. Hausser (2012). "Probing cellular mechanisms of spatial navigation in the medial entorhinal cortex " SfN Abstract: 702.16.
Schmidt-Hieber, C., P. Jonas, et al. (2004). "Enhanced synaptic plasticity in newly generated granule cells of the adult hippocampus." Nature **429**(6988): 184-7.
Scoville, W. B. and B. Milner (1957). "Loss of recent memory after bilateral hippocampal lesions." J Neuropsychiatry Clin Neurosci **12**(1): 103-13.

Segal, M. and S. Landis (1974). "Afferents to the hippocampus of the rat studied with the method of retrograde transport of horseradish peroxidase." Brain Res **78**(1): 1-15.

Shapiro, M. L. and J. Ferbinteanu (2006). "Relative spike timing in pairs of hippocampal neurons distinguishes the beginning and end of journeys." Proc Natl Acad Sci U S A **103**(11): 4287-92.

Shapiro, M. L., H. Tanila, et al. (1997). "Cues that hippocampal place cells encode: dynamic and hierarchical representation of local and distal stimuli." Hippocampus **7**(6): 624-42.

Sharp, P. E. (1997). "Subicular cells generate similar spatial firing patterns in two geometrically and visually distinctive environments: comparison with hippocampal place cells." Behav Brain Res **85**(1): 71-92.

Sharp, P. E., H. T. Blair, et al. (1996). "Neural network modeling of the hippocampal formation spatial signals and their possible role in navigation: a modular approach." Hippocampus **6**(6): 720-34.

Sharp, P. E., H. T. Blair, et al. (2001). "The anatomical and computational basis of the rat head-direction cell signal." Trends Neurosci **24**(5): 289-94.

Sharp, P. E., H. T. Blair, et al. (1995). "Influences of vestibular and visual motion information on the spatial firing patterns of hippocampal place cells." J Neurosci **15**(1 Pt 1): 173-89.

Sharp, P. E. and C. Green (1994). "Spatial correlates of firing patterns of single cells in the subiculum of the freely moving rat." J Neurosci **14**(4): 2339-56.

Sharp, P. E. and K. Koester (2008). "Lesions of the mammillary body region severely disrupt the cortical head direction, but not place cell signal." Hippocampus **18**(8): 766-84.

Sharp, P. E., J. L. Kubie, et al. (1990). "Firing properties of hippocampal neurons in a visually symmetrical environment: contributions of multiple sensory cues and mnemonic processes." J Neurosci **10**(9): 3093-105.

Sheline, Y. I., P. W. Wang, et al. (1996). "Hippocampal atrophy in recurrent major depression." Proc Natl Acad Sci U S A **93**(9): 3908-13.

Shen, J., C. A. Barnes, et al. (1997). "The effect of aging on experience-dependent plasticity of hippocampal place cells." J Neurosci **17**(17): 6769-82.

Shinder, M. E. and J. S. Taube (2011). "Active and passive movement are encoded equally by head direction cells in the anterodorsal thalamus." J Neurophysiol **106**(2): 788-800.

Si, B., S. Romani, et al. (2012). "Continuous attractor network model for conjunctive space-velocity tuning." SfN Abstract: 293.03.

Siegel, M., T. H. Donner, et al. (2012). "Spectral fingerprints of large-scale neuronal interactions." Nat Rev Neurosci **13**(2): 121-34.

Sills, J. B., B. W. Connors, et al. (2012). "Electrophysiological and morphological properties of neurons in layer 5 of the rat postrhinal cortex." Hippocampus **22**(9): 1912-22.

Silva, A. J., R. Paylor, et al. (1992). "Impaired spatial learning in alpha-calcium-calmodulin kinase II mutant mice." Science **257**(5067): 206-11.

Simonnet, J., E. Eugene, et al. (2012). "Cellular neuroanatomy of rat presubiculum." Eur J Neurosci **37**(4): 583-97.

Sinnamon, H. M. (2005). "Hippocampal theta activity and behavioral sequences in a reward-directed approach locomotor task." Hippocampus **15**(4): 518-34.

Sinnamon, H. M. (2005). "Hippocampal theta activity related to elicitation and inhibition of approach locomotion." Behav Brain Res **160**(2): 236-49.

Skaggs, W. E., J. J. Knierim, et al. (1995). "A model of the neural basis of the rat's sense of direction." Adv Neural Inf Process Syst **7**: 173-80.

Skaggs, W. E. and B. L. McNaughton (1998). "Spatial firing properties of hippocampal CA1 populations in an environment containing two visually identical regions." J Neurosci **18**(20): 8455-66.
Skaggs, W. E., B. L. McNaughton, et al. (1996). "Theta phase precession in hippocampal neuronal populations and the compression of temporal sequences." Hippocampus **6**(2): 149-72.
Smith, D. M. and S. J. Mizumori (2006). "Learning-related development of context-specific neuronal responses to places and events: the hippocampal role in context processing." J Neurosci **26**(12): 3154-63.
Smith, E. E. and S. M. Kosslyn (2007). Cognitive psychology. Upper Saddle River, N.J., Pearson/Prentice Hall.
Smith, G. E. (1919). "A Preliminary Note on the Morphology of the Corpus Striatum and the Origin of the Neopallium." J Anat **53**(Pt 4): 271-91.
Snyder, J. S., N. Kee, et al. (2001). "Effects of adult neurogenesis on synaptic plasticity in the rat dentate gyrus." J Neurophysiol **85**(6): 2423-31.
Solstad, T., C. N. Boccara, et al. (2008). "Representation of geometric borders in the entorhinal cortex." Science **322**(5909): 1865-8.
Solstad, T., E. I. Moser, et al. (2006). "From grid cells to place cells: a mathematical model." Hippocampus **16**(12): 1026-31.
Song, E., S. E. Fox, et al. (2012). "Neuronal representations of two visual stimuli modifications on the network level of the spatial cognition in rat brain " SfN Abstract: 293.05.
Song, E. Y., Y. B. Kim, et al. (2005). "Role of active movement in place-specific firing of hippocampal neurons." Hippocampus **15**(1): 8-17.
Song, H., G. Kempermann, et al. (2005). "New neurons in the adult mammalian brain: synaptogenesis and functional integration." J Neurosci **25**(45): 10366-8.
Spiers, H. J., N. Burgess, et al. (2001). "Bilateral hippocampal pathology impairs topographical and episodic memory but not visual pattern matching." Hippocampus **11**(6): 715-25.
Sporns, O. and G. Tononi (2007). Structural determinants of functional brain dynamics. Handbook of Brain Connectivity. V. K. Jirsa and A. R. McIntosh (eds.). Berlin, Heidelberg, Springer Verlag**:** 117-48.
Spruston, N. and C. McBain (2007). Structural and Functional Properties of Hippocampal Neurons. The hippocampus book. P. Andersen (ed.) Oxford, Oxford University Press.
Squire, L. R. (1986). "Mechanisms of memory." Science **232**(4758): 1612-9.
Squire, L. R. (1992). "Memory and the hippocampus: a synthesis from findings with rats, monkeys, and humans." Psychol Rev **99**(2): 195-231.
Squire, L. R. (2004). "Memory systems of the brain: a brief history and current perspective." Neurobiol Learn Mem **82**(3): 171-7.
Stackman, R. W., A. S. Clark, et al. (2002). "Hippocampal spatial representations require vestibular input." Hippocampus **12**(3): 291-303.
Stackman, R. W., E. J. Golob, et al. (2003). "Passive transport disrupts directional path integration by rat head direction cells." J Neurophysiol **90**(5): 2862-74.
Stackman, R. W. and J. S. Taube (1997). "Firing properties of head direction cells in the rat anterior thalamic nucleus: dependence on vestibular input." J Neurosci **17**(11): 4349-58.
Stackman, R. W. and J. S. Taube (1998). "Firing properties of rat lateral mammillary single units: head direction, head pitch, and angular head velocity." J Neurosci **18**(21): 9020-37.
Stackman, R. W., M. L. Tullman, et al. (2000). "Maintenance of rat head direction cell firing during locomotion in the vertical plane." J Neurophysiol **83**(1): 393-405.

Staley, K. J., T. S. Otis, et al. (1992). "Membrane properties of dentate gyrus granule cells: comparison of sharp microelectrode and whole-cell recordings." J Neurophysiol **67**(5): 1346-58.
Stefanacci, L., E. A. Buffalo, et al. (2000). "Profound amnesia after damage to the medial temporal lobe: A neuroanatomical and neuropsychological profile of patient E. P." J Neurosci **20**(18): 7024-36.
Steffenach, H. A., R. S. Sloviter, et al. (2002). "Impaired retention of spatial memory after transection of longitudinally oriented axons of hippocampal CA3 pyramidal cells." Proc Natl Acad Sci U S A **99**(5): 3194-8.
Steffenach, H. A., M. Witter, et al. (2005). "Spatial memory in the rat requires the dorsolateral band of the entorhinal cortex." Neuron **45**(2): 301-13.
Stensola, H., T. Stensola, et al. (2012). "The entorhinal grid map is discretized." Nature **492**(7427): 72-8.
Stephan, H. (1975). Allocortex. Berlin, Springer.
Steward, O. (1976). "Topographic organization of the projections from the entorhinal area to the hippocampal formation of the rat." J Comp Neurol **167**(3): 285-314.
Stewart, M. (1997). "Antidromic and orthodromic responses by subicular neurons in rat brain slices." Brain Res **769**(1): 71-85.
Stumpf, C. (1965). "The Fast Component in the Electrical Activity of Rabbit's Hippocampus." Electroencephalogr Clin Neurophysiol **18**: 477-86.
Super, H. and E. Soriano (1994). "The organization of the embryonic and early postnatal murine hippocampus. II. Development of entorhinal, commissural, and septal connections studied with the lipophilic tracer DiI." J Comp Neurol **344**(1): 101-20.
Sutherland, R. J., I. Q. Whishaw, et al. (1983). "A behavioural analysis of spatial localization following electrolytic, kainate- or colchicine-induced damage to the hippocampal formation in the rat." Behav Brain Res **7**(2): 133-53.
Swanson, L. W. (1977). "The anatomical organization of septo-hippocampal projections." Ciba Found Symp(58): 25-48.
Swanson, L. W. and C. Kohler (1986). "Anatomical evidence for direct projections from the entorhinal area to the entire cortical mantle in the rat." J Neurosci **6**(10): 3010-23.
Tahvildari, B., E. Fransen, et al. (2007). "Switching between 'On' and 'Off' states of persistent activity in lateral entorhinal layer III neurons." Hippocampus **17**(4): 257-63.
Tamamaki, N. and Y. Nojyo (1995). "Preservation of topography in the connections between the subiculum, field CA1, and the entorhinal cortex in rats." J Comp Neurol **353**(3): 379-90.
Tanila, H. (1999). "Hippocampal place cells can develop distinct representations of two visually identical environments." Hippocampus **9**(3): 235-46.
Tanila, H., M. L. Shapiro, et al. (1997). "Discordance of spatial representation in ensembles of hippocampal place cells." Hippocampus **7**(6): 613-23.
Tarin, P. (1750). Adversaria Anatomica. Paris, Moreau.
Tashiro, A., H. Makino, et al. (2007). "Experience-specific functional modification of the dentate gyrus through adult neurogenesis: a critical period during an immature stage." J Neurosci **27**(12): 3252-9.
Taube, J. S. (1995). "Head direction cells recorded in the anterior thalamic nuclei of freely moving rats." J Neurosci **15**(1 Pt 1): 70-86.
Taube, J. S. (1995). "Place cells recorded in the parasubiculum of freely moving rats." Hippocampus **5**(6): 569-83.
Taube, J. S. (1998). "Head direction cells and the neurophysiological basis for a sense of direction." Prog Neurobiol **55**(3): 225-56.
Taube, J. S. (2007). "The head direction signal: origins and sensory-motor integration." Annu Rev Neurosci **30**: 181-207.

Taube, J. S. (2010). "Interspike interval analyses reveal irregular firing patterns at short, but not long, intervals in rat head direction cells." J Neurophysiol **104**(3): 1635-48.
Taube, J. S. (2011). "Head direction cell firing properties and behavioural performance in 3-D space." J Physiol **589**(Pt 4): 835-41.
Taube, J. S. and J. P. Bassett (2003). "Persistent neural activity in head direction cells." Cereb Cortex **13**(11): 1162-72.
Taube, J. S. and H. L. Burton (1995). "Head direction cell activity monitored in a novel environment and during a cue conflict situation." J Neurophysiol **74**(5): 1953-71.
Taube, J. S., J. P. Kesslak, et al. (1992). "Lesions of the rat postsubiculum impair performance on spatial tasks." Behav Neural Biol **57**(2): 131-43.
Taube, J. S. and R. U. Muller (1998). "Comparisons of head direction cell activity in the postsubiculum and anterior thalamus of freely moving rats." Hippocampus **8**(2): 87-108.
Taube, J. S., R. U. Muller, et al. (1990). "Head-direction cells recorded from the postsubiculum in freely moving rats. I. Description and quantitative analysis." J Neurosci **10**(2): 420-35.
Taube, J. S., R. U. Muller, et al. (1990). "Head-direction cells recorded from the postsubiculum in freely moving rats. II. Effects of environmental manipulations." J Neurosci **10**(2): 436-47.
Teipel, S. J., J. C. Pruessner, et al. (2006). "Comprehensive dissection of the medial temporal lobe in AD: measurement of hippocampus, amygdala, entorhinal, perirhinal and parahippocampal cortices using MRI." J Neurol **253**(6): 794-800.
Teng, E. and L. R. Squire (1999). "Memory for places learned long ago is intact after hippocampal damage." Nature **400**(6745): 675-7.
Terrazas, A., M. Krause, et al. (2005). "Self-motion and the hippocampal spatial metric." J Neurosci **25**(35): 8085-96.
Thal, D. R., C. Schultz, et al. (2000). "Amyloid beta-protein (Abeta)-containing astrocytes are located preferentially near N-terminal-truncated Abeta deposits in the human entorhinal cortex." Acta Neuropathol **100**(6): 608-17.
Thompson, L. T. and P. J. Best (1989). "Place cells and silent cells in the hippocampus of freely-behaving rats." J Neurosci **9**(7): 2382-90.
Thompson, L. T. and P. J. Best (1990). "Long-term stability of the place-field activity of single units recorded from the dorsal hippocampus of freely behaving rats." Brain Res **509**(2): 299-308.
Toga, A. W., P. M. Thompson, et al. (2006). "Towards multimodal atlases of the human brain." Nat Rev Neurosci **7**(12): 952-66.
Tolman, E. C. (1948). "Cognitive maps in rats and men." Psychol Rev **55**(4): 189-208.
Touretzky, D. S. and A. D. Redish (1996). "Theory of rodent navigation based on interacting representations of space." Hippocampus **6**(3): 247-70.
Tse, D., R. F. Langston, et al. (2007). "Schemas and memory consolidation." Science **316**(5821): 76-82.
Tsuno, Y., N. W. Schultheiss, et al. (2012). "In vivo intracellular recording of medial entorhinal cortex neurons and cholinergic effects in urethane anesthetized rats." SfN Abstract: 648.06.
Tulving, E. (1985). "How Many Memory Systems Are There?" Am Psychol **40**(4): 385-98.
Ulanovsky, N. and C. F. Moss (2007). "Hippocampal cellular and network activity in freely moving echolocating bats." Nat Neurosci **10**(2): 224-33.
Ungher, J., R. Rogozea, et al. (1971). "The influence of partial bilateral fornicotomy on the orienting-investigating reaction in cat. Behavioural and EEG correlates." Rev Roum Neurol **8**(1): 35-45.
Valenti, O., D. J. Lodge, et al. (2011). "Aversive stimuli alter ventral tegmental area dopamine neuron activity via a common action in the ventral hippocampus." J Neurosci **31**(11): 4280-9.

Valerio, S. and J. S. Taube (2012). "Path integration: how the head direction signal maintains and corrects spatial orientation." Nat Neurosci **15**(10): 1445-53.
Van Cauter, T., B. Poucet, et al. (2008). "Unstable CA1 place cell representation in rats with entorhinal cortex lesions." Eur J Neurosci **27**(8): 1933-46.
van der Meer, M. A. and A. D. Redish (2011). "Theta phase precession in rat ventral striatum links place and reward information." J Neurosci **31**(8): 2843-54.
van Praag, H., A. F. Schinder, et al. (2002). "Functional neurogenesis in the adult hippocampus." Nature **415**(6875): 1030-4.
van Strien, N. M., N. L. Cappaert, et al. (2009). "The anatomy of memory: an interactive overview of the parahippocampal-hippocampal network." Nat Rev Neurosci **10**(4): 272-82.
VanCauter, T., J. R. Whitlock, et al. (2012). "Impaired spatial periodicity of grid cells in a novel environment." SfN Abstract: 702.01.
Vanderwolf, C. H. (1969). "Hippocampal electrical activity and voluntary movement in the rat." Electroencephalogr Clin Neurophysiol **26**(4): 407-18.
Vann, S. D. and M. M. Albasser (2011). "Hippocampus and neocortex: recognition and spatial memory." Curr Opin Neurobiol **21**(3): 440-5.
Vazdarjanova, A. and J. F. Guzowski (2004). "Differences in hippocampal neuronal population responses to modifications of an environmental context: evidence for distinct, yet complementary, functions of CA3 and CA1 ensembles." J Neurosci **24**(29): 6489-96.
Vertes, R. P. (2005). "Hippocampal theta rhythm: a tag for short-term memory." Hippocampus **15**(7): 923-35.
Vinogradova, O. S. (2001). "Hippocampus as comparator: role of the two input and two output systems of the hippocampus in selection and registration of information." Hippocampus **11**(5): 578-98.
von Bonin, G. and P. Bailey (1947). The neocortex of Macaca mulatta. Urbana, IL, University of Illinois Press.
Von heimendahl, M. and M. Brecht (2012). "Dopaminergic action and hippocampal global remapping " SfN Abstract: 810.28.
Walsh, V. and A. Cowey (2000). "Transcranial magnetic stimulation and cognitive neuroscience." Nat Rev Neurosci **1**(1): 73-9.
Walther, C. (2002). "Hippocampal terminology: concepts, misconceptions, origins." Endeavour **26**(2): 41-4.
Wan, H., J. P. Aggleton, et al. (1999). "Different contributions of the hippocampus and perirhinal cortex to recognition memory." J Neurosci **19**(3): 1142-8.
Wang, S., B. W. Scott, et al. (2000). "Heterogenous properties of dentate granule neurons in the adult rat." J Neurobiol **42**(2): 248-57.
Warburton, E. C., A. Baird, et al. (2001). "The conjoint importance of the hippocampus and anterior thalamic nuclei for allocentric spatial learning: evidence from a disconnection study in the rat." J Neurosci **21**(18): 7323-30.
Watanabe, Y., E. Gould, et al. (1992). "Stress induces atrophy of apical dendrites of hippocampal CA3 pyramidal neurons." Brain Res **588**(2): 341-5.
Wehner, R. and V. Srinivasan (1981). "Searching Behaviour of Desert Ants, Genus Cataglyphis (Formicidae, Hymenoptera)." J Comp Physiol **142**: 315-38.
Weible, A. P., D. C. Rowland, et al. (2011). "Transgenically-targeted increase in the activity of medial entorhinal layer II neurons induces reversible field expansion and remapping of CA1 place cells." SfN Abstract: 729.09.
Welday, A. C., I. G. Shlifer, et al. (2011). "Cosine directional tuning of theta cell burst frequencies: evidence for spatial coding by oscillatory interference." J Neurosci **31**(45): 16157-76.
Wernicke, C. (1874). Der aphasische Symptomencomplex: Eine psychologische Studie auf anatomischer Basis. Breslau, Cohn & Weigert.

Whishaw, I. Q. (1972). "Hippocampal electroencephalographic activity in the Mongolian gerbil during natural behaviours and wheel running and in the rat during wheel running and conditioned immobility." Can J Psychol **26**(3): 219-39.
Whishaw, I. Q. (1987). "Hippocampal, granule cell and CA3-4 lesions impair formation of a place learning-set in the rat and induce reflex epilepsy." Behav Brain Res **24**(1): 59-72.
Whishaw, I. Q. and B. Kolb (2005). The Behavior of the laboratory rat. A handbook with tests. Oxford, Oxford University Press.
Whishaw, I. Q. and H. Maaswinkel (1998). "Rats with fimbria-fornix lesions are impaired in path integration: a role for the hippocampus in "sense of direction"." J Neurosci **18**(8): 3050-8.
Whishaw, I. Q. and C. H. Vanderwolf (1973). "Hippocampal EEG and behavior: changes in amplitude and frequency of RSA (theta rhythm) associated with spontaneous and learned movement patterns in rats and cats." Behav Biol **8**(4): 461-84.
White, N. M. and R. J. McDonald (2002). "Multiple parallel memory systems in the brain of the rat." Neurobiol Learn Mem **77**(2): 125-84.
Whitlock, J. R. and D. Derdikman (2012). "Head direction maps remain stable despite grid map fragmentation." Front Neural Circuits **6**: 9.
Whitlock, J. R., A. J. Heynen, et al. (2006). "Learning induces long-term potentiation in the hippocampus." Science **313**(5790): 1093-7.
Whitlock, J. R., G. Pfuhl, et al. (2012). "Functional split between parietal and entorhinal cortices in the rat." Neuron **73**(4): 789-802.
Whittington, M. A., R. D. Traub, et al. (1995). "Synchronized oscillations in interneuron networks driven by metabotropic glutamate receptor activation." Nature **373**(6515): 612-5.
Wiebe, S. (2000). "Epidemiology of temporal lobe epilepsy." Can J Neurol Sci **27 Suppl 1**: S6-10; discussion S20-1.
Wiebe, S. P. and U. V. Staubli (1999). "Dynamic filtering of recognition memory codes in the hippocampus." J Neurosci **19**(23): 10562-74.
Wiener, S. I. (1993). "Spatial and behavioral correlates of striatal neurons in rats performing a self-initiated navigation task." J Neurosci **13**(9): 3802-17.
Wiener, S. I., A. Berthoz, et al. (2002). "Multisensory processing in the elaboration of place and head direction responses by limbic system neurons." Brain Res Cogn Brain Res **14**(1): 75-90.
Wiener, S. I., C. A. Paul, et al. (1989). "Spatial and behavioral correlates of hippocampal neuronal activity." J Neurosci **9**(8): 2737-63.
Wiig, K. A. and D. K. Bilkey (1994). "The effects of perirhinal cortical lesions on spatial reference memory in the rat." Behav Brain Res **63**(1): 101-9.
Wiig, K. A. and R. D. Burwell (1998). "Memory impairment on a delayed non-matching-to-position task after lesions of the perirhinal cortex in the rat." Behav Neurosci **112**(4): 827-38.
Wikenheiser, A. M. and A. D. Redish (2011). "Changes in reward contingency modulate the trial-to-trial variability of hippocampal place cells." J Neurophysiol **106**(2): 589-98.
Willis, T. (1664). Cerebri anatome, cui accessit nervorum descripto et usus. London.
Wills, T. J., F. Cacucci, et al. (2010). "Development of the hippocampal cognitive map in preweanling rats." Science **328**(5985): 1573-6.
Wills, T. J., C. Lever, et al. (2005). "Attractor dynamics in the hippocampal representation of the local environment." Science **308**(5723): 873-6.
Wilson, M. A. and B. L. McNaughton (1993). "Dynamics of the hippocampal ensemble code for space." Science **261**(5124): 1055-8.
Wilson, M. A. and B. L. McNaughton (1994). "Reactivation of hippocampal ensemble memories during sleep." Science **265**(5172): 676-9.

Winocur, G. and C. B. Breckenridge (1973). "Cue-dependent behavior of hippocampally damaged rats in a complex maze." J Comp Physiol Psychol **82**(3): 512-22.
Winocur, G., M. Moscovitch, et al. (2005). "Preserved spatial memory after hippocampal lesions: effects of extensive experience in a complex environment." Nat Neurosci **8**(3): 273-5.
Winson, J. (1978). "Loss of hippocampal theta rhythm results in spatial memory deficit in the rat." Science **201**(4351): 160-3.
Wirak, D. O., R. Bayney, et al. (1991). "Regulatory region of human amyloid precursor protein (APP) gene promotes neuron-specific gene expression in the CNS of transgenic mice." EMBO J **10**(2): 289-96.
Witter, M. P. and D. G. Amaral (2004). Hippocampal formation. The Rat Nervous System San Diego, CA, Elsevier Academic Press. **3:** 635-704.
Witter, M. P., H. J. Groenewegen, et al. (1989). "Functional organization of the extrinsic and intrinsic circuitry of the parahippocampal region." Prog Neurobiol **33**(3): 161-253.
Wood, E. R., P. A. Dudchenko, et al. (1999). "The global record of memory in hippocampal neuronal activity." Nature **397**(6720): 613-6.
Wood, E. R., P. A. Dudchenko, et al. (2000). "Hippocampal neurons encode information about different types of memory episodes occurring in the same location." Neuron **27**(3): 623-33.
Woollett, K. and E. A. Maguire (2011). "Acquiring "the Knowledge" of London's layout drives structural brain changes." Curr Biol **21**(24): 2109-14.
Wyble, B. P., J. M. Hyman, et al. (2004). "Analysis of theta power in hippocampal EEG during bar pressing and running behavior in rats during distinct behavioral contexts." Hippocampus **14**(5): 662-74.
Xie, X., R. H. Hahnloser, et al. (2002). "Double-ring network model of the head-direction system." Phys Rev E Stat Nonlin Soft Matter Phys **66**(4 Pt 1): 041902.
Yanovich, Y., D. C. Rowland, et al. (2009). "The NMDA receptor antagonist CPP prevents the long-term stability of head-direction and conjunctive cells in the mouse entorhinal cortex " SfN Abstract: 480.3.
Yartsev, M. M., M. P. Witter, et al. (2011). "Grid cells without theta oscillations in the entorhinal cortex of bats." Nature **479**(7371): 103-7.
Ye, J., S.-J. Zhang, et al. (2012). "Optogenetic dissection of the entorhinal-hippocampal space circuit." SfN Abstract: 702.13.
Ylinen, A., I. Soltesz, et al. (1995). "Intracellular correlates of hippocampal theta rhythm in identified pyramidal cells, granule cells, and basket cells." Hippocampus **5**(1): 78-90.
Yoder, R. M., B. J. Clark, et al. (2011). "Origins of landmark encoding in the brain." Trends Neurosci **34**(11): 561-71.
Yoder, R. M. and J. S. Taube (2009). "Head direction cell activity in mice: robust directional signal depends on intact otolith organs." J Neurosci **29**(4): 1061-76.
Yoder, R. M. and J. S. Taube (2011). "Projections to the anterodorsal thalamus and lateral mammillary nuclei arise from different cell populations within the postsubiculum: implications for the control of head direction cells." Hippocampus **21**(10): 1062-73.
Yoganarasimha, D. and J. J. Knierim (2005). "Coupling between place cells and head direction cells during relative translations and rotations of distal landmarks." Exp Brain Res **160**(3): 344-59.
Yoganarasimha, D., G. Rao, et al. (2011). "Lateral entorhinal neurons are not spatially selective in cue-rich environments." Hippocampus **21**(12): 1363-74.
Yoganarasimha, D., X. Yu, et al. (2006). "Head direction cell representations maintain internal coherence during conflicting proximal and distal cue rotations: comparison with hippocampal place cells." J Neurosci **26**(2): 622-31.

Yoshida, M., E. Fransen, et al. (2008). "mGluR-dependent persistent firing in entorhinal cortex layer III neurons." Eur J Neurosci **28**(6): 1116-26.
Yoshida, M. and M. E. Hasselmo (2009). "Persistent firing supported by an intrinsic cellular mechanism in a component of the head direction system." J Neurosci **29**(15): 4945-52.
Yoshida, M., A. Jochems, et al. (2012). "Spike frequency adaptation and medium spike after hyperpolarization potential are differentially distributed along the dorso-ventral axis in layer II neurons from the medial entorinal cortex." SfN Abstract: 702.26.
Young, B. J., G. D. Fox, et al. (1994). "Correlates of hippocampal complex-spike cell activity in rats performing a nonspatial radial maze task." J Neurosci **14**(11 Pt 1): 6553-63.
Young, B. J., T. Otto, et al. (1997). "Memory representation within the parahippocampal region." J Neurosci **17**(13): 5183-95.
Yu, X., D. Yoganarasimha, et al. (2006). "Backward shift of head direction tuning curves of the anterior thalamus: comparison with CA1 place fields." Neuron **52**(4): 717-29.
Zhang, K. (1996). "Representation of spatial orientation by the intrinsic dynamics of the head-direction cell ensemble: a theory." J Neurosci **16**(6): 2112-26.
Zhang, S. J., J. Ye, et al. (2013). "Optogenetic dissection of entorhinal-hippocampal functional connectivity." Science **340**(6128): 1232627.
Zhu, X. O., M. W. Brown, et al. (1995). "Neuronal signalling of information important to visual recognition memory in rat rhinal and neighbouring cortices." Eur J Neurosci **7**(4): 753-65.
Zilles, K. and K. Amunts (2010). "Centenary of Brodmann's map--conception and fate." Nat Rev Neurosci **11**(2): 139-45.
Zilli, E. A. (2012). "Models of grid cell spatial firing published 2005-2011." Front Neural Circuits **6**: 16.
Zilli, E. A. and M. E. Hasselmo (2010). "Coupled noisy spiking neurons as velocity-controlled oscillators in a model of grid cell spatial firing." J Neurosci **30**(41): 13850-60.
Zola-Morgan, S. and L. R. Squire (1984). "Preserved learning in monkeys with medial temporal lesions: sparing of motor and cognitive skills." J Neurosci **4**(4): 1072-85.
Zola-Morgan, S., L. R. Squire, et al. (1986). "Human amnesia and the medial temporal region: enduring memory impairment following a bilateral lesion limited to field CA1 of the hippocampus." J Neurosci **6**(10): 2950-67.
Zola-Morgan, S., L. R. Squire, et al. (1989). "Lesions of the hippocampal formation but not lesions of the fornix or the mammillary nuclei produce long-lasting memory impairment in monkeys." J Neurosci **9**(3): 898-913.
Zugaro, M. B., A. Arleo, et al. (2003). "Rapid spatial reorientation and head direction cells." J Neurosci **23**(8): 3478-82.
Zugaro, M. B., A. Arleo, et al. (2004). "Rat anterodorsal thalamic head direction neurons depend upon dynamic visual signals to select anchoring landmark cues." Eur J Neurosci **20**(2): 530-6.
Zugaro, M. B., E. Tabuchi, et al. (2000). "Influence of conflicting visual, inertial and substratal cues on head direction cell activity." Exp Brain Res **133**(2): 198-208.

Paper I

8. M. J. Kiel, O. H. Yilmaz, T. Iwashita, C. Terhorst, S. J. Morrison, *Cell* **121**, 1109 (2005).
9. D. A. Sipkins *et al.*, *Nature* **435**, 969 (2005).
10. Materials and methods are available as supporting material on *Science* Online.
11. A. Peled *et al.*, *Science* **283**, 845 (1999).
12. T. Lapidot, O. Kollet, *Leukemia* **16**, 1992 (2002).
13. H. E. Broxmeyer, *Curr. Opin. Hematol.* **15**, 49 (2008).
14. D. J. Ceradini *et al.*, *Nat. Med.* **10**, 858 (2004).
15. C. Hitchon *et al.*, *Arthritis Rheum.* **46**, 2587 (2002).
16. B. Nervi, D. C. Link, J. F. DiPersio, *J. Cell. Biochem.* **99**, 690 (2006).
17. G. Calandra *et al.*, *Bone Marrow Transplant.* **41**, 331 (2008).
18. W. Bensinger *et al.*, *J. Clin. Oncol.* **13**, 2547 (1995).
19. N. Okumura *et al.*, *Blood* **87**, 4100 (1996).
20. R. L. Driessen, H. M. Johnston, S. K. Nilsson, *Exp. Hematol.* **31**, 1284 (2003).
21. L. K. Ashman, *Int. J. Biochem. Cell Biol.* **31**, 1037 (1999).
22. S. Sharma *et al.*, *Stem Cells Dev.* **15**, 755 (2006).
23. N. Théou-Anton *et al.*, *Br. J. Cancer* **94**, 1180 (2006).
24. K. A. Giehl, U. Nagele, M. Vokenandt, C. Berking, *J. Cutan. Pathol.* **34**, 7 (2007).
25. G. Bellone *et al.*, *Int. J. Oncol.* **29**, 851 (2006).
26. M. Tao *et al.*, *Cytokine* **12**, 699 (2000).
27. R. Zheng, K. Klang, N. C. Gorin, D. Small, *Leuk. Res.* **28**, 121 (2004).

28. We thank A. Chenn, K. Cohen, L. Godley, and R. Salgia for critical discussions and reading of the manuscript; A. Chenn for assistance with retroviral cell transduction; A. Wickrema for help with CD34$^+$ purification; V. Bindokas for imaging expertise; and S. Gurbuxani for assistance with histopathology interpretation. Supported by a grant from the Illinois Regenerative Medicine Institute (IRMI), an NIH (National Cancer Institute) K08 award (5K08CA112126-02), and an NIH Director's DP2 award (1DP2OD002160-01). A patent application related to this work has been filed by the University of Chicago.

Supporting Online Material

www.sciencemag.org/cgi/content/full/322/5909/1861/DC1
Materials and Methods
Figs. S1 to S13
Movies S1 and S2

7 August 2008; accepted 19 November 2008
10.1126/science.1164390

Representation of Geometric Borders in the Entorhinal Cortex

Trygve Solstad, Charlotte N. Boccara,* Emilio Kropff,* May-Britt Moser, Edvard I. Moser†

We report the existence of an entorhinal cell type that fires when an animal is close to the borders of the proximal environment. The orientation-specific edge-apposing activity of these "border cells" is maintained when the environment is stretched and during testing in enclosures of different size and shape in different rooms. Border cells are relatively sparse, making up less than 10% of the local cell population, but can be found in all layers of the medial entorhinal cortex as well as the adjacent parasubiculum, often intermingled with head-direction cells and grid cells. Border cells may be instrumental in planning trajectories and anchoring grid fields and place fields to a geometric reference frame.

An animal's current position in the environment is encoded by a network of hippocampal and parahippocampal neurons with diverse spatial firing properties. Within this network, at least three cell types contribute to the computation of self-location: place cells, which fire when the animal moves through a particular location in space (*1*–*3*); head-direction cells, which fire when the animal is facing in a certain direction (*4*–*7*); and grid cells, whose multiple sharply localized firing fields form a remarkably regular triangular pattern across the environment (*3*, *7*–*9*). In addition to these cell types, computational models posit the existence of cortical "boundary vector cells," whose activity patterns encode the animal's distance from salient geometric borders (*10*, *11*). Based on predictions from these models, we investigated whether proximity to borders is represented by specific cell types in the entorhinal spatial representation circuit (*12*).

A total of 624 principal cells were recorded from the dorsocaudal quarter of the medial entorhinal cortex (MEC) and adjacent parasubiculum in 13 rats (fig. S1). Neural activity was sampled while these animals foraged in enclosures with moveable walls and barriers. The animals were first tested in a square enclosure (1 m by 1 m or 1.5 m by 1.5 m) with 50-cm-high walls. Many recorded cells were grid cells and head-direction cells (*7*–*9*), but in addition the data included a previously unknown class of entorhinal cells that fired exclusively along one or several walls of the enclosure (Fig. 1 and fig. S2). These cells were identified by computing, for each cell, the difference between the maximal length of a wall touching upon a single firing field and the average distance of the fields from the nearest wall, divided by the sum of those values (*12*). Border scores ranged from –1 for cells with central firing fields to +1 for cells with fields that perfectly lined up along at least one entire wall. "Border cells" were defined as spatially stable cells with border scores above 0.5. A total of 69 cells from 12 animals passed this criterion (Fig. 1 and fig. S2) (*13*). In these cells, 86.0 ± 0.6% of the spikes occurred closer to the walls than to the center of the box per unit of time [mean ± SEM; $t(68) = 17.4$, one-sample t test, $P < 0.001$; expected value 75%]. Only 3.6 ± 1.0% of the

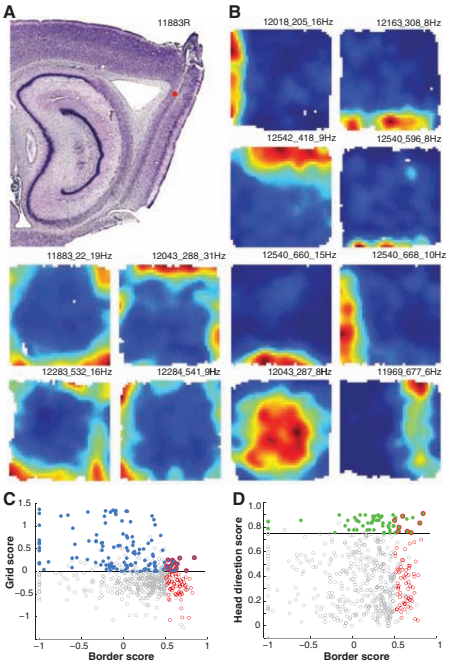

Fig. 1. Examples of border cells in the MEC and adjacent parasubiculum. (**A**) Sagittal Nissl-stained section showing a representative recording location in the MEC (red dot, recording location; rat number and hemisphere (R, right) are indicated; see fig. S1 for all other recording positions). (**B**) Color-coded rate maps for 12 border cells. Red is maximum, dark blue is zero. Pixels not covered are white. Animal numbers (five digits), cell numbers (two or three digits), and peak firing rates are indicated above each panel. Cells 287 and 677 did not pass the criterion for border cells because the fields were located at some distance from the wall; the number of such cells was fewer than 10. See fig. S2 for the complete set of rate maps, trajectories, and directional tuning curves, and representative waveforms and tetrode clusters. (**C** and **D**) Scatter plots showing correlation between border scores and grid scores (C) or head-direction scores (D) (*12*). Each dot in the scatter plot corresponds to one cell (red, border cells; blue, grid cells; green, head-direction cells; gray, cells not passing any criterion, including cells with high spatial or directional scores but low stability; double-colored dots, cells that satisfy criteria for two cell classes). Horizontal lines indicate thresholds for grid and head-direction cells.

Kavli Institute for Systems Neuroscience and Centre for the Biology of Memory, Norwegian University of Science and Technology, 7489 Trondheim, Norway.

*These authors contributed equally to this work.
†To whom correspondence should be addressed. E-mail: edvard.moser@ntnu.no

central area was part of a firing field [expected value 25%; $t(68) = 22.1$, $P < 0.001$]. Fifty-two of the cells fired along a single wall; the remaining 17, mostly from the deep layers of the MEC, had fields along two, three, or four walls (fig. S2A). On average, the border field along the dominant wall covered 75.4 ± 1.8% of the length of the wall. The mean distance between the active bins in the field and the wall was 8.4 ± 0.3% of the box length. An additional set of fewer than 10 cells, excluded by the formal criterion, had fields that were parallel to the box walls but separated by a stripe of inactivity between the walls and the field (Fig. 1B, cells 287 and 677). The activity pattern of the border cells was fundamentally different from that of grid cells and head-direction cells recorded simultaneously on the same tetrodes [Fig. 1, C and D, and supporting online material (SOM) text]. Border cells were found in all layers of the MEC and in the adjacent parasubiculum (fig. S1 and SOM text). Thirty-one of 69 border cells were modulated by the theta rhythm (fig. S3).

If the activity was determined by the walls rather than other localized variables, the cells should continue to fire along their preferred walls after changes in the length of the box, and the mean firing distance from the nearest wall might remain unchanged. This prediction was confirmed for most of the cells that were classified as border cells in the small square enclosure. Extending the 1-m–by–1-m square to a 1-m–by–2-m or 2-m–by–1-m rectangle caused a corresponding extension of the firing field if the field was parallel to the extended wall but not if its long axis was orthogonal to the direction of extension (44 cells; Fig. 2A and fig. S4). The fraction of spikes along the walls per unit of time was not changed [79.9 ± 1.7% in the square and 80.8 ± 1.5% in the rectangles; paired t test, $t(43) = 0.45$]. The proportion of the central area covered by firing fields [5.0 ± 1.0% in the square and 7.9 ± 1.5% in the rectangle; paired t test, $t(43) = 2.3$, $P < 0.05$] remained far below the chance level of 25% [for the rectangle, $t(43) = 11.8$, < 0.001], suggesting that the firing was indeed controlled by the walls of the environment.

Do border cells primarily encode the periphery of the environment or are they tuned to barriers more generally, irrespective of their continuity with the other borders? We recorded the activity of 22 border cells after inserting a discrete wall into the square enclosure (*11*, *12*) (Fig. 2B and figs. S5 and S6). Only cells with fields along a single wall were analyzed (12 cells). When the wall was inserted in parallel with the original firing field, an additional field emerged in the rate map of all cells, although only 9 of the new fields met our selection criteria for quantitative analysis. In all 12 cases, the new field lined up along the inserted wall. The new field and the parent field were always on the same side of the insert relative to the distal room cues (for example, both were on the east side in Fig. 2B). The new field covered 68.7 ± 8.2% of the inserted wall on this side. The coverage of the opposite side (the side that faced the parent field) was 0 in all cases. Reducing the height of the barrier from 50 cm to 5 cm did not abolish the new field as long as the animal's trajectory was impeded (fig. S6; three experiments).

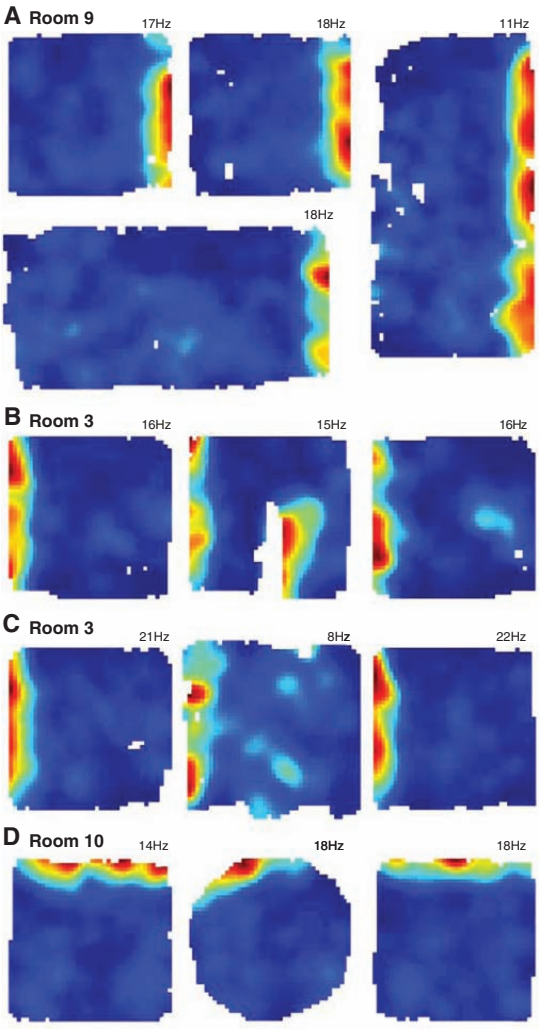

Fig. 2. Border cells express proximity to boundaries in a number of environmental configurations. (**A** to **D**) Color-coded rate maps for a representative border cell in boxes with different geometric configurations (cell 205 of rat 12018). Each panel shows one trial. Symbols are as in Fig. 1B. (A) The border field follows the walls when the square enclosure is stretched to a rectangle. (B) Introducing a discrete wall (white pixels) inside the square causes a new border field to appear (middle panel). The new field has the same orientation relative to distal cues as the original field on the peripheral wall. (C) Border fields persist after removal of the box walls (middle panel). Without walls, the drop along the edges was 60 cm. (D) Preserved firing along borders across rooms and geometrical shapes. All trials in (D) were recorded in a different room than those in (A) to (C). The conditions favor hippocampal global remapping between rooms and rate remapping within rooms (*12*, *16*, *22*) (fig. S9).

To determine whether border cells also respond to boundaries other than walls, the box walls were removed and the animals were tested on the remaining open surface, which now had a 60-cm drop on all four sides. In general, border fields could still be identified (Fig. 2C and figs. S7 and S8). The fraction of spikes along the walls per unit of time was not changed significantly [84.4 ± 1.5% with walls, 80.3 ± 3.1% without walls, $t(9) = 1.8$, $P > 0.10$], although the fraction of the central area that was part of a firing field increased [2.8 ± 2.1% with walls, 11.2 ± 4.1 without walls, $t(9) = 2.5$, $P < 0.05$; expected value 25%, $t(9) = 3.3$, $P < 0.01$]. The persistence of activity along the edges suggests that the cells respond to a variety of borders.

Unlike place cells (*14*, *15*), grid cells and head-direction cells retain their basic activity pattern across environments (*5*, *9*, *16*, *17*). To determine whether border cells are similarly context-independent, we first compared the activity of 27 cells in two different rooms, using square recording boxes in each room. The fraction of spikes along the walls, normalized by dwell times, did not change between the rooms [83.0 ± 1.5% versus 84.7 ± 1.3%; paired t test, $t(26) = 1.41$, $P > 0.15$; Fig. 2, B and C, versus D], nor did the proportion of the central area that was part of a firing field [11.5 ± 4.1% versus 7.5 ± 2.8%; $t(26) = 0.98$, $P > 0.30$]. We also compared the firing patterns of 21 border cells in two differently shaped enclosures, a square and a circle,

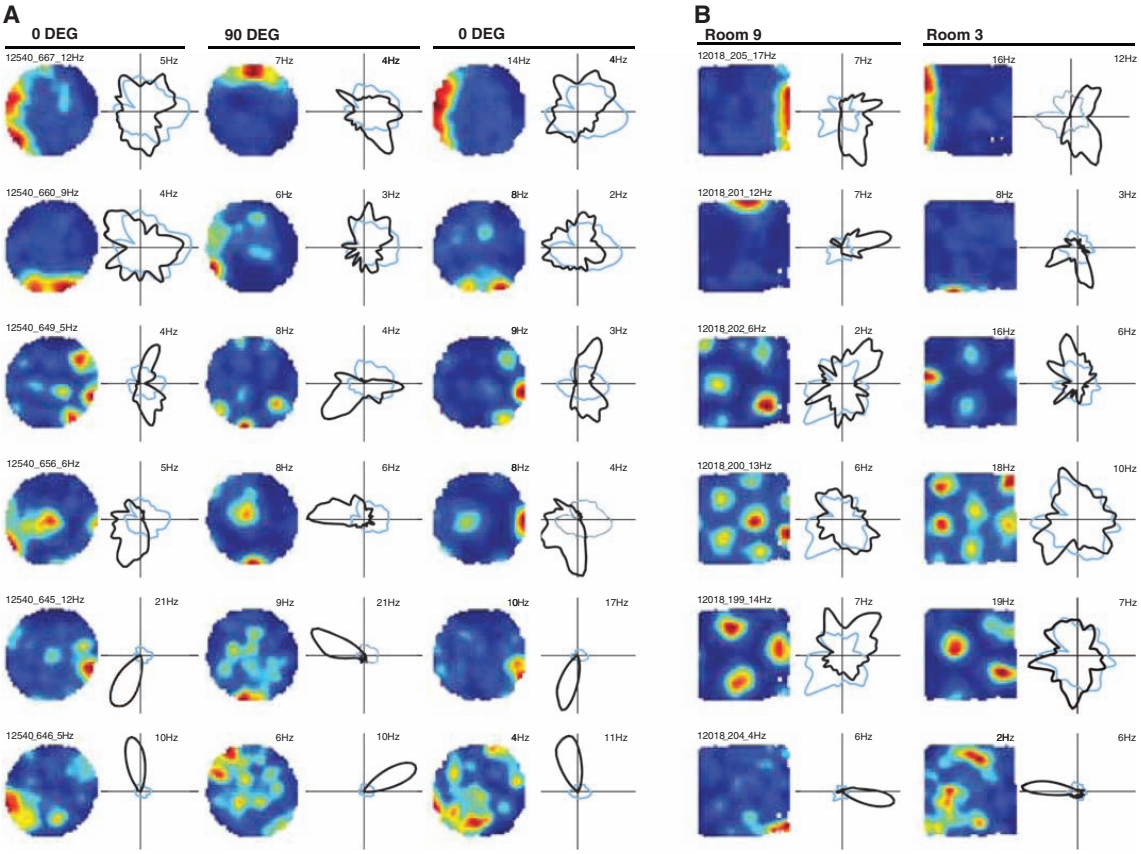

Fig. 3. Border cells, grid cells, and head-direction cells respond coherently to environmental manipulations. (**A**) Rate and head-direction maps for two border cells (top two rows), two grid cells with some head-directional modulation (middle two rows), and two head-direction cells (bottom two rows) recorded simultaneously before and after the rotation of a polarizing cue card (left and right columns, 0°; middle column, 90°). The polar plots show firing rate as a function of head direction (black traces) and the time that the rat faced each direction (blue traces). Peak firing rate is indicated. (**B**) Rate maps and polar plots for two border cells (top two rows), three grid cells (middle three rows), and one head-direction cell (bottom row) in two different rooms. The cells were recorded simultaneously.

in a single room (Fig. 2D and fig. S9). Again, the time-normalized fraction of spikes along the walls was not different [square, 87.1 ± 1.0%; circle, 85.0 ± 1.6%; paired *t* test, $t(20) = 1.67$, $P > 0.10$; Fig. 2D] and the firing fields covered a similar proportion of the central area of the environments [6.1 ± 2.2% and 12.7 ± 4.3; $t(20) = 1.95$, $P > 0.05$]. The persistence of border-related activity across environments, under conditions that often lead to realignment in grid cells and remapping in place cells (*16*) (fig. S8), suggests that the firing of these cells is primarily defined by geometric borders and less by the content of the environment or the training history of the animal.

Does the representation of borders, grid positions, and directions remain coherent across environments? We recorded 10 border cells along with grid cells and head-direction cells in five experiments. When the cue card on the wall of the circle was rotated 90°, simultaneously recorded border cells always rotated in concert (three experiments; pairwise difference in rotation 1°, 1°, and 9°; Fig. 3A). The same was observed with simultaneously recorded border cells and grid cells (mean difference between cell types 0°, 7.2°, and 9.5°; Fig. 3A) and with simultaneously recorded border cells and head-direction cells (mean difference 8.5°, 12.5°, and 13.6°; Fig. 3A; two of these experiments also included grid cells). When the animals were tested in different rooms, differences in the relative orientation of simultaneously recorded border cells were retained; that is, cells with fields on opposite walls in one room also fired along opposite walls in the other room, and their relation to grid cells and head-direction cells remained constant (Fig. 3B).

Taken together, these findings provide evidence for a previously unknown cell type in the spatial representation circuit of the MEC. Border cells have firing fields that line up along selected geometric borders of the proximal environment, irrespective of their length and continuity with other borders. The observation of border cells across all layers of the MEC confirms predictions from computational models that posit the existence of a boundary-responsive cortical cell population upstream of the hippocampus (*10*, *11*, *18*). Given that border cells are distributed widely in the circuit, information about obstacles and borders should be accessible to the majority of the entorhinal grid cells as well as to external target regions involved in path planning (*19*). By defining the perimeter of the environment, border cells may serve as reference frames for place representations within that environment, determining the firing locations of grid cells in the MEC as well as of place cells in the hippocampus and spatially selective cells in other cortical regions (*20*) (SOM text).

References and Notes

1. J. O'Keefe, J. Dostrovsky, *Brain Res.* **34**, 171 (1971).
2. J. O'Keefe, L. Nadel, *The Hippocampus as a Cognitive Map* (Clarendon, Oxford, 1978).

3. E. I. Moser, E. Kropff, M.-B. Moser, *Annu. Rev. Neurosci.* **31**, 69 (2008).
4. J.B. Ranck Jr., in *Electrical Activity of the Archicortex*, G. Buzsáki, C. H. Vanderwolf, Eds. (Akademiai Kiado, Budapest, Hungary, 1985), pp. 217–220.
5. J. S. Taube, R. U. Muller, J. B. Ranck Jr., *J. Neurosci.* **10**, 420 (1990).
6. J. S. Taube, *Annu. Rev. Neurosci.* **30**, 181 (2007).
7. F. Sargolini *et al*., *Science* **312**, 758 (2006).
8. M. Fyhn, S. Molden, M. P. Witter, E. I. Moser, M.-B. Moser, *Science* **305**, 1258 (2004).
9. T. Hafting, M. Fyhn, S. Molden, M.-B. Moser, E. I. Moser, *Nature* **436**, 801 (2005).
10. T. Hartley, N. Burgess, C. Lever, F. Cacucci, J. O'Keefe, *Hippocampus* **10**, 369 (2000).
11. C. Barry *et al*., *Rev. Neurosci.* **17**, 71 (2006).
12. Materials and methods are available as supporting material on *Science* Online.
13. The proportion of border cells in the medial entorhinal cell population is overestimated because experiments were often not started on days with no known border cells in the cell sample. The estimates should be taken as an upper limit.
14. E. Bostock, R. U. Muller, J. L. Kubie, *Hippocampus* **1**, 193 (1991).
15. L. L. Colgin, E. I. Moser, M.-B. Moser, *Trends Neurosci.* **31**, 469 (2008).
16. M. Fyhn, T. Hafting, A. Treves, M.-B. Moser, E. I. Moser, *Nature* **446**, 190 (2007).
17. D. Yoganarasimha, X. Yu, J. J. Knierim, *J. Neurosci.* **26**, 622 (2006).
18. A small number of boundary-modulated cells has also been reported downstream of the hippocampus, in the subiculum (*11*), but whether these signals are derived from local neurons or from entorhinal axons [as in (*21*)] has not been established.
19. J. R. Whitlock, R. J. Sutherland, M. P. Witter, M.-B. Moser, E. I. Moser, *Proc. Natl. Acad. Sci. U.S.A.* **105**, 14755 (2008).
20. D. A. Nitz, *Neuron* **49**, 747 (2006).
21. J. K. Leutgeb, S. Leutgeb, M.-B. Moser, E. I. Moser, *Science* **315**, 961 (2007).
22. S. Leutgeb *et al*., *Science* **309**, 619 (2005).
23. We thank N. Burgess and a number of other colleagues for helpful discussion and suggestions; M. P. Witter for advice about electrode location; M. Fyhn for donating an implanted animal; and A. M. Amundsgård, E. Sjulstad, I. M. F. Hammer, K. Haugen, K. Jenssen, R. Skjerpeng, H. Waade, and T. Åsmul for technical assistance. The work was supported by the Kavli Foundation, the Centre of Excellence scheme of the Norwegian Research Council, and a European Commission Framework 7 project (SPACEBRAIN).

Supporting Online Material

www.sciencemag.org/cgi/content/full/322/5909/1865/DC1
Materials and Methods
SOM Text
Figs. S1 to S12
References

26 September 2008; accepted 10 November 2008
10.1126/science.1166466

www.sciencemag.org/cgi/content/full/322/5909/1865/DC1

Supporting Online Material for

Representation of Geometric Borders in the Entorhinal Cortex

Trygve Solstad, Charlotte N. Boccara, Emilio Kropff, May-Britt Moser, Edvard I. Moser*

*To whom correspondence should be addressed. E-mail: edvard.moser@ntnu.no

Published 19 December 2008, *Science* **322**, 1865 (2008)
DOI: 10.1126/science.1166466

This PDF file includes:

Materials and Methods
SOM Text
Figs. S1 to S12
References

Supporting Online Material

1. Materials and Methods

Subjects

Thirteen male Long-Evans rats were used for the experiment. The animals were housed individually in transparent plexiglass cages (45 × 30 × 35 cm) in a temperature and humidity-controlled vivarium near the recording rooms. All rats were maintained on a 12-h light/ 12-h dark schedule. Testing occurred in the dark phase. The rats were kept at 85-90% of free-feeding body weight and food deprived 18-24 h before each training and recording trial. Body weight at the time of surgery was 350-400 g. Water was available ad libitum.

Surgery

The rats were anesthetized i.p. with Equithesin (pentobarbital and chloral hydrate; 1.0 ml/ 250 g body weight) after brief exposure to an isoflurane-filled chamber. They were then implanted with two microdrives, one in each hemisphere, each connected to four tetrodes cut flat at the same level. The tetrodes were made of 17 μm polyimide-coated platinum-iridium (90% - 10%) wire. The electrode tips were platinum-plated to reduce electrode impedances to ~200 kΩ at 1 kHz. Tetrodes aimed for the deep layers of MEC were implanted at AP 0.3-0.8 in front of the sinus, ML 4.0-4.8 mm from the midline, and DV 1.4 under the dura. Implants were oriented at an 0-15 degree angle in the anterior direction in the sagittal plane. A jeweller's screw fixed to the skull served as a ground electrode. The microdrive was secured to the skull using jewellers' screws and dental cement. After surgery, the rats were allowed 2-3 days of recovery before handling and/or habituation to the test environments was resumed.

Data collection

Before each recording trial, the rat rested on a towel in a large flower pot on a pedestal. The rat was connected to the recording equipment via AC-coupled unity-gain operational amplifiers close to the rat's head, using a counterbalanced cable that allowed the animal to move freely in the pot and the recording boxes. Over the course of 10-30 days, the tetrodes were lowered in steps of 50 μm or less until single neurons could be isolated at appropriate depths. When the signal amplitudes exceeded ~4 times the noise level (r.m.s. 20-30 μV), and the units were stable for more than 6 h, data were recorded in the first experiment. After each finished set of experiments, the tetrodes were moved further until new well-separated cells were encountered.

Recorded signals were amplified 8 000 to 25 000 times and band-pass filtered between 0.8 and 6.7 kHz. Triggered spikes were stored to disk at 48 kHz (50 samples per waveform, 8 bits/sample) with a 32 bit time stamp (clock rate at 96 kHz). EEG was recorded single-ended from one the electrodes. The EEG was amplified 3000-10 000 times, lowpass-filtered at 500 Hz, sampled at 4800 Hz, and stored with the unit data. By means of an overhead video camera the recording system tracked the position of two light-emitting diodes (LEDs), one large and one small, on the head stage (sampling rate 50 Hz). The LEDs were separated by 5-10 cm and aligned with the body axis of the rat.

Apparatus and training procedures

In parallel with the turning of the tetrodes, over the course of 2-4 weeks, the animals were trained to run around in black aluminium enclosures of different shapes and sizes located in different rooms that were all polarized by a white cue card. Running was motivated by randomly scattering crumbs of chocolate or vanilla biscuits in the recording enclosures. In the

first experiment (Fig. 1 and 2A), 12 animals ran in a modular aluminium recording enclosure that could be expanded or contracted to take one of three shapes: a small square (100 × 100 × 50 cm high), a rectangle with the longest side in the *x* direction (200 × 100 × 50 cm high), or a rectangle with the longest side in the *y* direction (100 × 200 × 50 cm high). The sequence of testing was A-B-A'-C-A'' (in a small subset of the experiments, A'' was not included). A polarizing white cue card (45 cm × 50 cm) was displayed at a constant location on the west wall midway between the corners. Each session lasted 10, 15, or 20 minutes. Intertrial intervals were 1-15 min.

In 9 rats, the experiments in squares and rectangles were succeeded by tests in the square enclosure in which a separate wall (50 cm long × 50 cm high) was inserted between the centre of one of the external walls and the centre of the box (Fig. 2B). Trials were 10 min. Data was also recorded for 10 min before the wall was inserted and for 10 min after it was removed.

Seven rats were tested after removal of the external walls of the enclosure (10 min with walls, 10 - 20 min without, 10 min with walls; Fig. 2C). The external walls rested centrally on a square table (110 cm long × 110 cm). There was a 60 cm drop from the table down to the floor on the trials without walls.

Six rats were tested in a sequence of differently shaped environments: first a square box (100 × 100 cm or 150 × 150 cm, 50 cm high), then a circle (100 or 150 cm diameter, 50 cm high), and then the same square as on the initial trial (Fig. 2D and S9). Only the walls of the environment were changed; the surface remained the same, as did the food reward. These conditions generally favour rate remapping in the hippocampus and the spatial phase or orientation of grid fields in the entorhinal cortex remain unchanged (*16*, *22*). Intertrial

intervals were 10 min. In 6 experiments (4 rats), the cue card on the wall of the circular box was rotated 90° and back on separate trials. All rotation experiments were performed with black curtains around the enclosure to mask distal cues. Between the trials, the rat rested on a pedestal outside the curtains. The floor was cleaned with water between each trial.

In 7 animals, more than one recording room was used during the course of experiments (baseline recordings in the small square, squares vs. rectangles, wall inserts, removal of walls, and circle vs. square; e.g., Fig. 2A vs. 2BC vs. 2D). Firing properties were compared across rooms in those experiments.

Spike sorting and cell classification

Spike sorting was performed offline using graphical cluster-cutting software. Clustering was performed manually in two-dimensional projections of the multidimensional parameter space (consisting of waveform amplitudes), using autocorrelation and crosscorrelation functions as additional separation tools (Fig. S2D). Putative excitatory cells were distinguished from putative interneurons using a combination of spike width, average rate and the occasional presence of bursts (*8*). Putative interneurons were not included in any analysis.

Nearly all border cells in layers II and V of MEC, and in parasubiculum and the transition zone between parasubiculum, postrhinal cortex and MEC, had broad waveforms and low average rates (Fig. S2D). Border cells in layer III of MEC had shorter peak-to-trough latencies (Fig. S2D) but because all cells on tetrodes in this layer (including grid cells) had narrow waveforms, it is unlikely that the waveforms originate exclusively from bypassing fibers. Layer III cells were thus not excluded. In all layers, clusters of border cells were generally similar in shape and amplitude to those of grid cells in the same area (Fig. S2D; *8*).

Firing rates, place fields and spatial scale measurement

Position estimates were based on tracking of the LED closest to the centre of the rat's head. The tracked positions were smoothed with a 15 point mean filter offline. To characterize firing fields, the position data were sorted into bins of 2.5 cm × 2.5 cm and the firing rate was determined for each bin. A spatial smoothing algorithm was used. The average rate in any bin x was estimated as:

$$\lambda(x) = \sum_{i=1}^{n} g(\tfrac{s_i - x}{h}) \Big/ \int_0^T g(\tfrac{y(t) - x}{h}) dt$$

where g is a smoothing kernel, h is a smoothing factor, n is the number of spikes, s_i the location of the i-th spike, $y(t)$ the location of the rat at time t, and [0, T] the period of the recording. A Gaussian kernel was used for g and h = 5 cm. In order to avoid error from extrapolation, we considered positions more than 5 cm away from the tracked path as unvisited. A firing field was estimated as a contiguous region of at least 200 cm^2 where the firing rate was above 30% of the peak rate. Additional fields were identified by deleting the detected field from the rate map and iterating the search for contiguous firing regions in the remaining part of the rate map until no additional fields were found. The cell's peak rate was estimated as the highest firing rate observed in any bin of the smoothed rate map. Mean firing rate was calculated as the total number of spikes divided by trial duration. The spatial correlation between neural activity on consecutive trials in the same enclosure was estimated by correlating the rates of firing in corresponding bins of the pair of smoothed rate maps for each cell.

Analysis of border cells

Putative border fields were identified first by identifying collections of neighboring pixels with firing rates higher than 0.3 times the maximum firing rate and covering a total area of at least 200 cm^2. For all experiments in square or rectangular environments, the coverage of a given wall of by a field was then estimated as the fraction of pixels along the wall that was occupied by the field, and c_M was defined as the maximum coverage of any single field over any of the four walls of the environment. The mean firing distance d_m was computed by averaging the distance to the nearest wall over all pixels in the map belonging to some of its fields, weighted by the firing rate. To achieve this, the firing rate was normalized by its sum over all pixels belonging to some field, resembling a probability distribution. Finally, d_m was normalized by half of the shortest side of the environment (i.e. the largest possible distance to its perimeter) so as to obtain a fraction between 0 and 1. A border score was defined by comparing d_m with the maximum coverage of any wall by a single field c_M,

$$b = \frac{c_M - d_m}{c_M + d_m}.$$

Border scores ranged from -1 for cells with central firing fields to +1 for cells with fields that perfectly line up along at least one entire wall. Intuitively, the border scores provide an idea of the expansion of fields across walls rather than away from them. It should be noted that the measure saturates when the width of the field approaches half the length of the environment.

'Border cells' were defined as cells with border scores above 0.5. Only cells with stable border fields (spatial correlation > 0.5) were included in the sample. In experiments with walls inserted into the recording enclosure, the analysis was restricted to border cells with fields along a single wall, i.e. cells where the border score for the preferred wall was at least twice as high as the score for any of the remaining three walls.

Analysis of grid cells

The structure of all rate maps was evaluated by calculating the spatial autocorrelation for each smoothed rate map (*7*). Autocorrelograms were based on Pearson's product moment correlation coefficient with corrections for edge effects and unvisited locations. With $\lambda\ (x, y)$ denoting the average rate of a cell at location (x, y), the autocorrelation between the fields with spatial lags of τ_x and τ_y was estimated as:

$$r(\tau_x, \tau_y) = \frac{n\sum \lambda(x,y)\lambda(x-\tau_x, y-\tau_y) - \sum \lambda(x,y)\sum \lambda(x-\tau_x, y-\tau_y)}{\sqrt{n\sum \lambda(x,y)^2 - \left(\sum \lambda(x,y)\right)^2}\sqrt{n\sum \lambda(x-\tau_x, y-\tau_y)^2 - \left(\sum \lambda(x-\tau_x, y-\tau_y)\right)^2}}$$

where the summation is over all n pixels in $\lambda\ (x, y)$ for which rate was estimated for both $\lambda\ (x, y)$ and $\lambda\ (x - \tau_x, y - \tau_y)$. Autocorrelations were not estimated for lags of τ_x, τ_y where $n < 20$.

The degree of spatial periodicity (gridness) was determined for each recorded cell by selecting a ring around the center of the autocorrelogram containing the 6 closest fields (*7*). The Pearson Correlation of this ring with its rotation in α degrees was obtained for angles of 60° and 120° on one side and 30°, 90° and 150° on the other. A grid score *g* was defined as the minimum difference between any of the elements in the first group and any of the elements in the second.

A cells was classified as a grid cell when the correlations at 60º and 120º of rotation exceeded each of the correlations at 30 º, 90 º and 150º (grid score > 0). For some analyses (counts of grid fields and estimates of grid spacing), a threshold of 0.30 was used. If fewer than 6 peaks

were identified, the circle was fitted around the outermost peak. The central peak was not included in the analysis.

For each grid cell, the spacing of the grid was defined as the distance from the central peak to the vertices of the inner hexagon in the autocorrelogram (the median of the six distances). The orientation of the grid was defined as the angle between a camera-fixed reference line (0°) and the vector to the nearest vertex of the inner hexagon in the counterclockwise direction (*9*).

Analysis of head-direction cells

The rat's head direction was calculated for each tracker sample from the projection of the relative position of the two LEDs onto the horizontal plane, corrected for the possible angle between the placement of the two LEDs and the rat's true heading. The directional tuning function for each cell was obtained by plotting the firing rate as a function of the rat's directional heading, divided into bins of 1 degree. Gaussian smoothing with a standard deviation of 5.1 degrees was applied. The preferred firing direction was defined as the circular mean of the directional tuning function. Based on the preferred firing direction, a head direction score was computed for each cell, with the aim of identifying unimodal and concentrated head direction distributions. To achieve this, the circular mean α and the arc around it containing half of the distribution $\Delta\alpha$ were obtained. The head direction score was defined as

$$h = 1 - \frac{\Delta\alpha}{180^\circ},$$

in such a way that for a delta distribution $h=1$ while for a uniform distribution $h=0$.

Head direction cells were defined as cells with $h > 0.75$, i.e. those cells where the arc containing half of the distribution was smaller than 45 degrees, i.e. 22.5 degrees to each side of the preferred firing direction). Only cells with stable directional preferences (circular correlation > 0.5) were included in the sample.

A subset of 8 border cells also satisfied the criteria for head direction cells. For each of these cells, a new rate map was constructed that only included positions and spikes sampled while the rat was looking in a direction *hd* inside the central quartiles of the distribution:

$$hd \in [\alpha - \frac{\Delta\alpha}{2}, \alpha + \frac{\Delta\alpha}{2}]$$

Fig. S12B shows firing fields for these cells after correction for directional tuning.

Rotation experiment

In a subset of the experiments in the circular environment, the cue card was moved 90 degrees along the arc of the circle on one of the trials in order to determine if simultaneously recorded border cells, grid cells and head direction cells rotated coherently (Fig. 3). To identify the angle of rotation for grid cells, border cells and head direction cells, the map or directional tuning curve in the rotation trial was rotated in steps of 1 degree and for each step the Pearson correlation coefficient with the original map in the unrotated baseline trial was obtained. The angle of rotation was defined as the angle that gave maximal correlation between the rotated maps.

Theta analysis

Theta modulation of individual cells was determined from their spike-train autocorrelation functions. A cell was defined as theta modulated if the mean power within 1 Hz of each side of the peak in the 5-12 Hz frequency range was at least 10 times greater than the mean spectral power

highpass filtered at 2 Hz (*S1*). Theta activity in the local field potential was analysed by filtering EEG from the entorhinal tetrodes off-line (*S2*). An acausal (zero phase shift) FFT bandpass filter was applied to the signals. The filter function was constructed using a Hamming window. For the low cut-off frequencies, 5 and 6 Hz were chosen for the stopband and passband, respectively; 10 and 11 Hz were chosen for high passband and stopband cut-off frequencies.

Histology and reconstruction of recording positions

Electrodes were not moved after the final recording session. The rats received an overdose of either Equithesin or Pentobarbital and were perfused transcardially with 0.9% saline followed by 4% formaldehyde. The brains were extracted and stored in 4 % formaldehyde. At least 24 hours later, the brains were quickly frozen, cut in sagital sections (30 μm) using a cryostat, mounted and stained with cresyl violet. Every section in the area of the tetrode trace was retained.
The positions of the tips of the recording electrodes were determined from digital pictures.
The measurements were made using AxioVision (LE Rel. 4.3). A shrinkage coefficient was calculated by dividing the distance measured from the surface of the brain to the tips of the recording electrode by the last depth of the electrodes. In case of multiple recordings along the dorsoventral extent of the electrode trace, the position of the electrodes at recording was extrapolated using the read-out of the tetrode turning protocol, adjusted for shrinkage.

2. Supporting Text

Distribution of border cells

Border cells were found in all layers of the MEC (layer II: 16/96 cells, 17%; layer III: 16/128 cells, 13%; layer V: 18/186 cells, 10%; layer 6: 4/44 cells, 9%; Fig. S1 and S2). A few border cells were encountered also in dorsal parasubiculum (7/100 cells, 7%) and in the transition area of MEC, parasubiculum and postrhinal cortex (8/70 cells, 11%). The cells were often co-localized with grid cells and head direction cells. Differences in theta modulation across layers are reported in Fig. S3.

Firing properties of border cells in extended boxes

There was no change in the mean rate of the border cells in the experiments where the square recording environment was extended to a rectangle (square: 1.80 ± 0.23, rectangle: 1.83 ± 0.27, $t(43) = 0.28$), although the peak rate increased slightly in the extended enclosure (square: 9.0 ± 0.8; rectangle: 10.5 ± 1.1; $t(43) = 2.1$, $P < 0.05$). When the rat was returned to the small square after the rectangle, rate maps were similar to those recorded on the baseline trial (spatial correlation: $r = 0.74 \pm 0.02$ for first versus second square; $r = 0.64 \pm 0.06$ for first versus third square; Fig. 2A and S4).

Border cells are distinct from grid cells

The activity of the cells that passed the criterion for border cells was fundamentally different from that of grid cells and head direction cells that were recorded simultaneously on the same tetrodes (Fig. 1CD). Grid cells were defined as cells with a positive grid score, which is reflective of hexagonally spaced firing (101 cells; *7*, *9*). There was minimal overlap between the populations of grid cells and border cells; 14 of the 69 border cells had positive grid scores but

the scores were all very low, ranging from 0.01 to 0.30. Typical grid cells had higher scores, ranging up to 1.37. Grid cells generally had low border scores (correlation between grid and border scores: $r = -0.30$, $P < 0.001$, $N = 611$; Fig. 1C). The percentage of spikes along the walls of the square, normalized by dwell times, was no larger for grid cells than expected from a flat spatial distribution (observed: 75.1 ± 0.5%; expected: 75%). The same was true for the proportion of the central area covered by firing fields (29.0 ± 2.0%; expected: 25%; $t(188) = 1.98$, $P = 0.05$), suggesting, not surprisingly, that grid fields are as common at the centre as at the periphery of the enclosure.

Grid cells generally showed an increase in the number of identified firing fields in the long rectangular environment compared to the small square (rectangle: 4.5 ± 0.3 fields; square: 2.6 ± 0.2; all cells with grid scores > 0.30; $t(57) = 8.4$, $P < 0.001$; Fig. S10A). The rectangle was 2.0 times larger than the square; the number of fields was 1.76 times larger. In the majority of the experiments, the size of the individual grid fields and the spacing between them were preserved (Fig. S10A). In a small number of trials, the grid fields scaled up in the extended direction (Fig. 10B; as in *S3*). On average, however, there was no significant difference in grid spacing between the stretched rectangular environment and the smaller square (46.6 ± 0.6 cm vs. 45.8 ± 1.0 cm, respectively; all cells with grid scores > 0.30; $t(42) = 0.96$). Insertion of the barrier did not disrupt the periodicity or vertex locations of the grid fields and no new fields appeared along the insert in any of these cells (Fig. S11).

Border cells are distinct from head direction cells

Although a subset of the border cells showed some modulation by head direction (Fig. 1D), the firing fields of border cells were not merely caused by overrepresentation of certain head directions at the periphery of the environment (Fig. S2BC). The degree of directional tuning was

quantified for each cell of the entire sample by computing the head direction with the circular mean firing rate (the 'preferred' head direction) and then determining the arc around this direction that contained half of the spike distribution. Cells were classified as head direction cells when this arc was smaller than 45 degrees and their head direction was stable across sessions (stability was defined as a directional correlation of more than 0.5). By this criterion, 68 cells in the total sample were modulated by head direction. These cells, as a group, did not fire more along the walls than in the centre of the box (75.9 ± 0.8% of the spikes occurred in the outer part; expected: 75.0%; $t(67) = 1.1$, $P > 0.25$). A subset of 8 head direction cells also passed the criterion for border cells; the remaining 61 border cells had wide directional tuning curves (mean arc for all border cells: 110 degrees; Fig. S2C). There was no correlation between border and head direction scores ($r = 0.05$, $P > 0.20$, $N = 590$; Fig. 1D) and, in the sample of border cells, the distribution of the head direction with the strongest firing was uniform and thus did not coincide with the orientation of the walls (Rayleigh test, $z = 2.1$, $P > 0.10$; S12A). The contribution of head direction modulation in the 8 directionally modulated border cells was further analyzed by computing rate maps selectively for time segments with head directions in the central quartiles of the directional tuning curve of the cell. In at least 4 of these 8 cells, a border field was still present (Fig. S12B).

Collectively, these observations suggest that grid cells, head direction cells and border cells are distinct populations, although both grid cells and border cells contain some cells that are modulated by head direction. This directional modulation does not account for the border-related activity, however.

Interdependence of entorhinal-hippocampal functional cell types

With the discovery of entorhinal border cells, the entorhinal spatial representation circuit contains three distinct cell types – border cells, grid cells (*8*, *9*), and head direction cells (*7*), in

addition to border cells and grid cells that are modulated by head direction. Collectively these cell types are likely to contribute to a dynamically updated map-like entorhinal representation of the animal's location and orientation in the environment (*3*, *7-9*, *S4-S6*). The existence of border cells, grid cells, and head direction cells in the same local circuit, and the coherent properties of these cell types across environments, suggests that the three cell types operate as an integrated map across large parts of the MEC.

The four functional cell types of the entorhinal-hippocampal system are strongly interdependent. Place cells may be derived from grid cells by summation of signals from cells with different grid spacing and grid orientation (*S4-S7*), grid cells may receive directional inputs from head direction cells in the presubiculum or the entorhinal cortex itself (*4-7*), and border cells may influence grid cells and place cells, directly or indirectly.

Border cells may calibrate spatial representations

The neural mechanisms for representation of self-location in grid cells have not been determined but are likely to involve interactions between self-motion cues and learned associations with the external environment (*3*, *9*, *S4-S6*). The fact that animals may confound rotationally equivalent positions in rectangular environments even when these positions differ in non-geometrical features, such as brightness or texture (*S8*), points to geometrical shape as one of the key external determinants of the brain's spatial representations (*S8*, *S9*). Border cells may be part of the circuit by which entorhinal and other representations get calibrated by the local borders of the environment.

Border cells represent both local and global borders

The fact that border fields line up along discrete walls and inserts suggests that many border cells respond to low-level features of spatial geometry, such as vertical surfaces and corners, rather

than the global shape of the environment. This subset of the border cells may extract specific features of the spatial environment, much in the same way that cells in the striate cortex signal the contours of a visual image (*S10*). Other cells, particularly in the deep layers of MEC, have fields along the entire periphery of the environment and may respond to borders more globally. The existence of a large subpopulation with preferential responses to individual walls and inserts is consistent with studies showing that spatial discrimination is determined primarily by local geometrical features (*S11*).

Border cells vs. place cells

Border cells are also distinct from place cells. Whereas border cells fire unconditionally at borders in all environments, place cells are active only in a subset of the environments, and the firing locations in these environments may vary from one to the other (*14*,*15*). Hippocampal place cells may also be controlled by barriers (*S12*) but usually they do not line up along the wall, they are not orientation-specific, and they do not respond unconditionally to borders. Unlike entorhinal border cells (Fig. 2B), cells with fields at an internal barrier do not have additional, similarly oriented fields along the perimeter of the recording box (*S12*). These differences suggest that hippocampal neurons may not treat barriers differently from other discrete objects (*S13*-*S15*).

3. Supporting Figures

Figure_S1, page_1

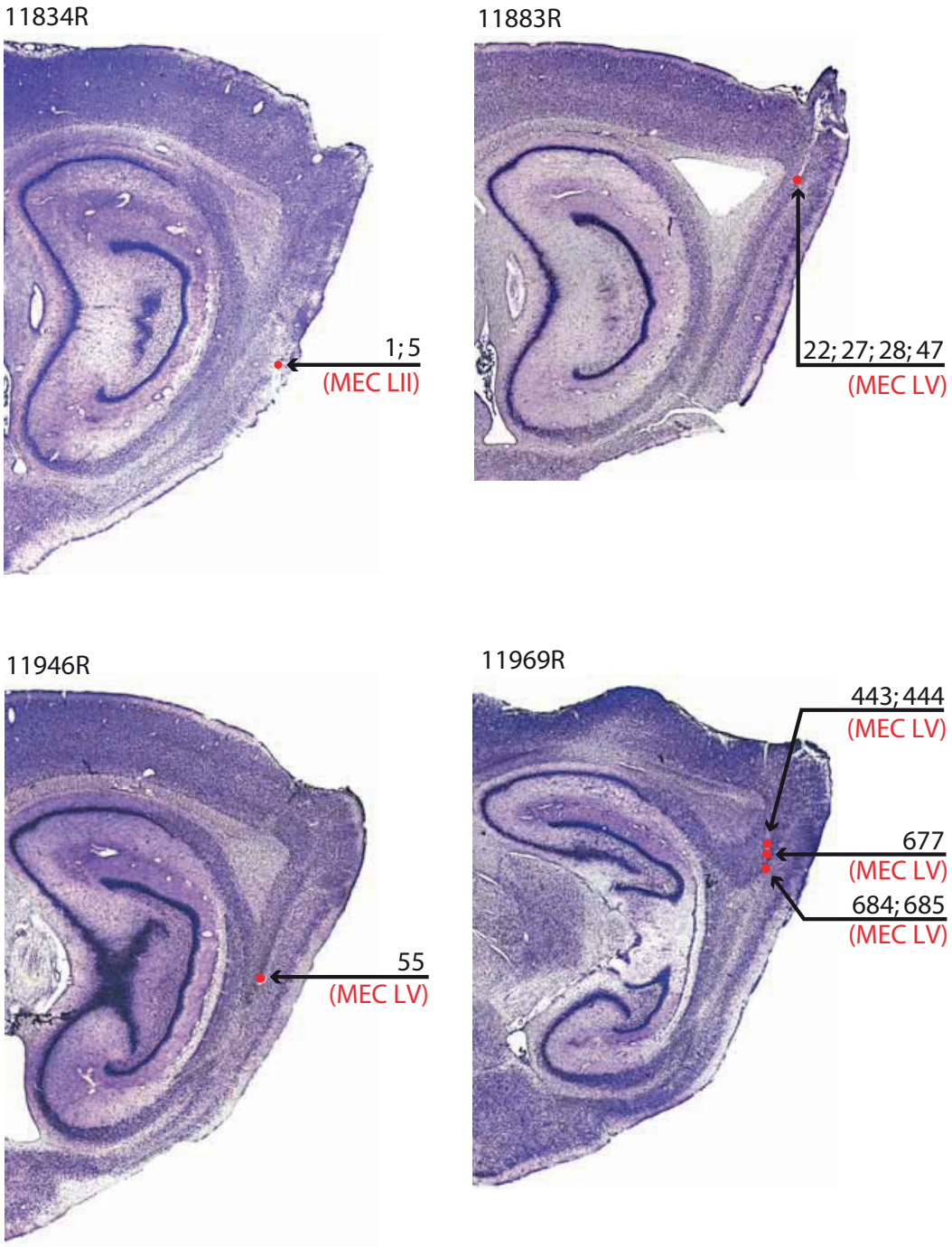

12017R

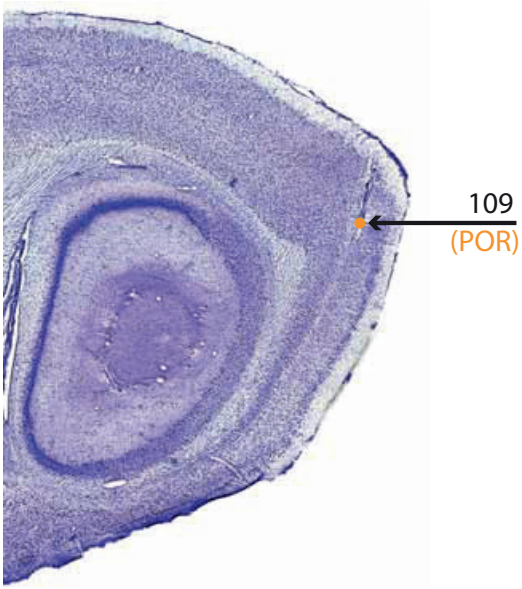

12018R

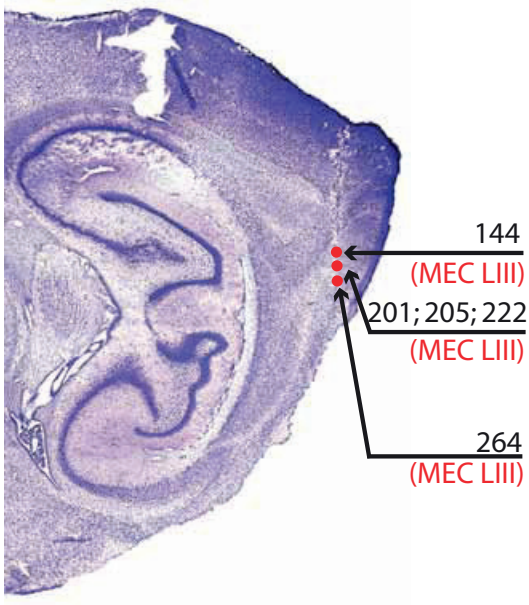

12018L

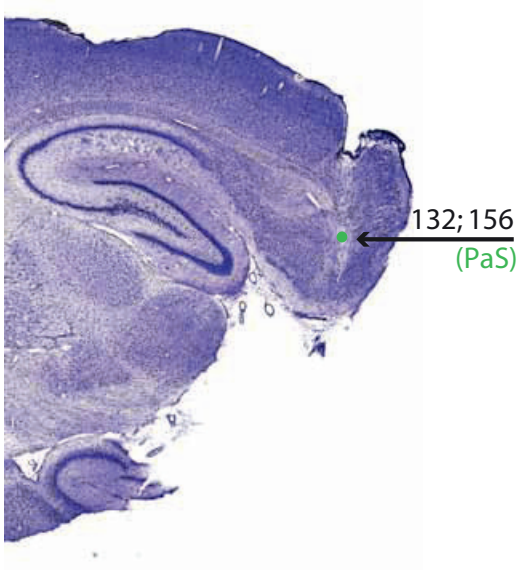

12043R

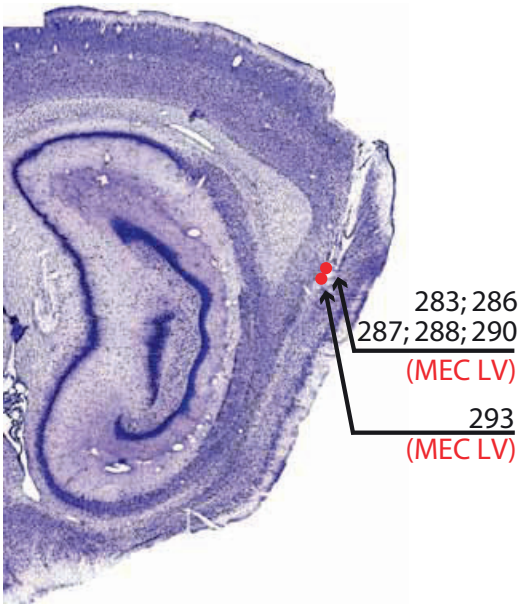

12043L

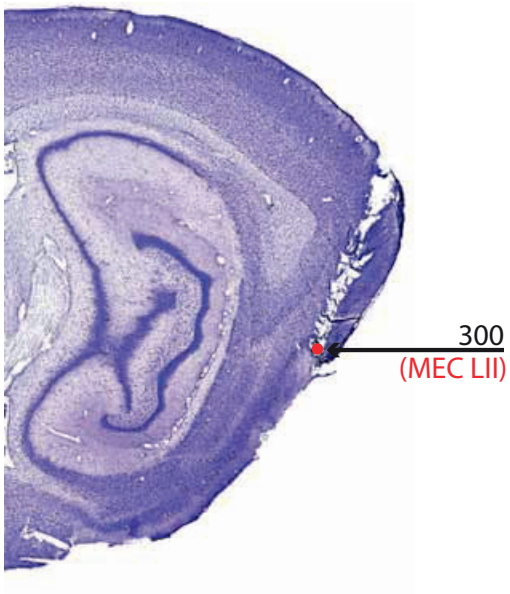

12163L

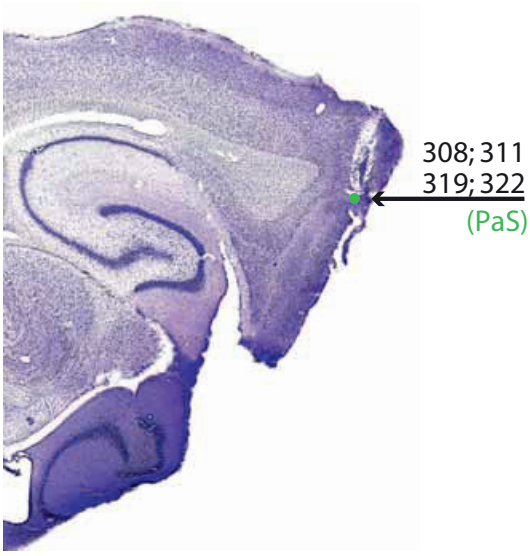

12283L

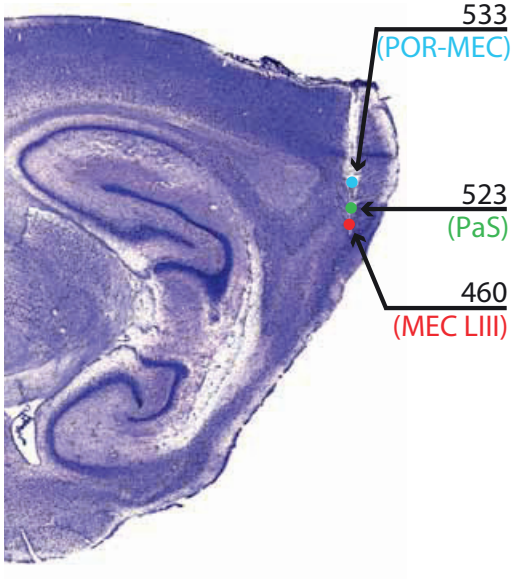

12283R

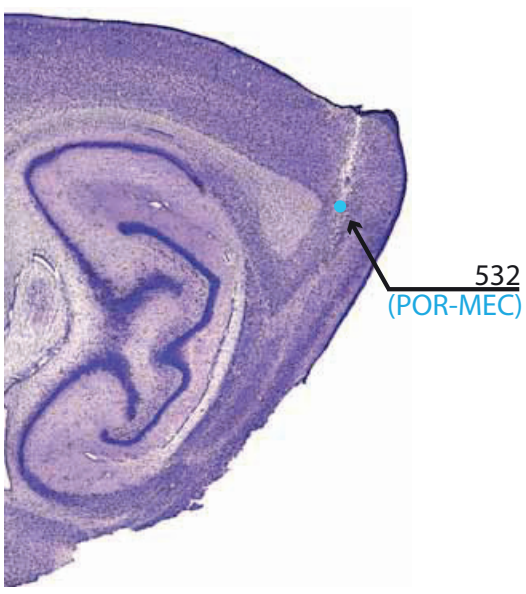

12284R

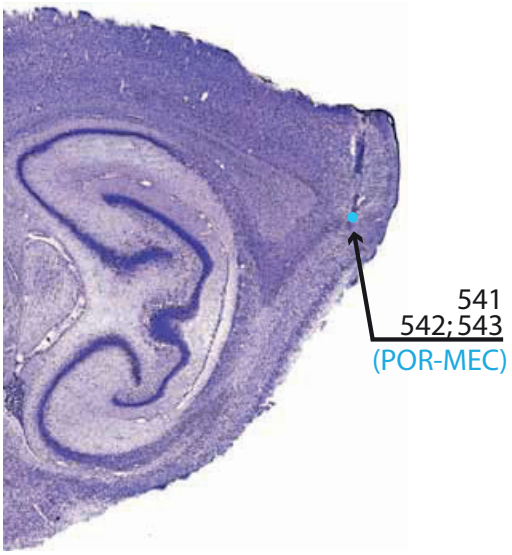

12540L

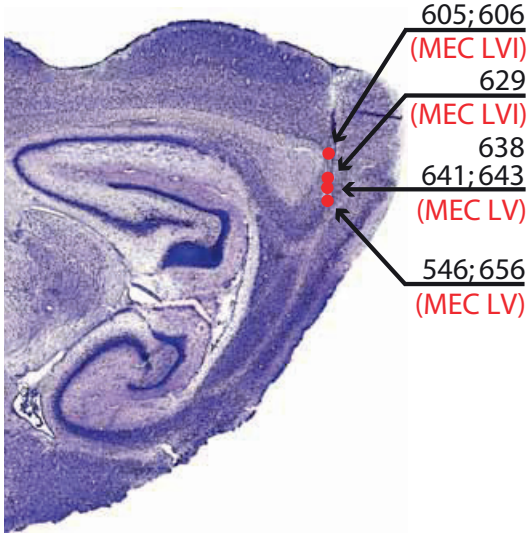

12540R

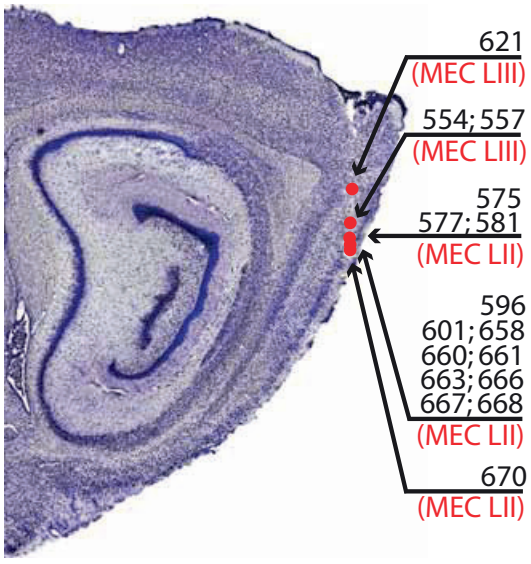

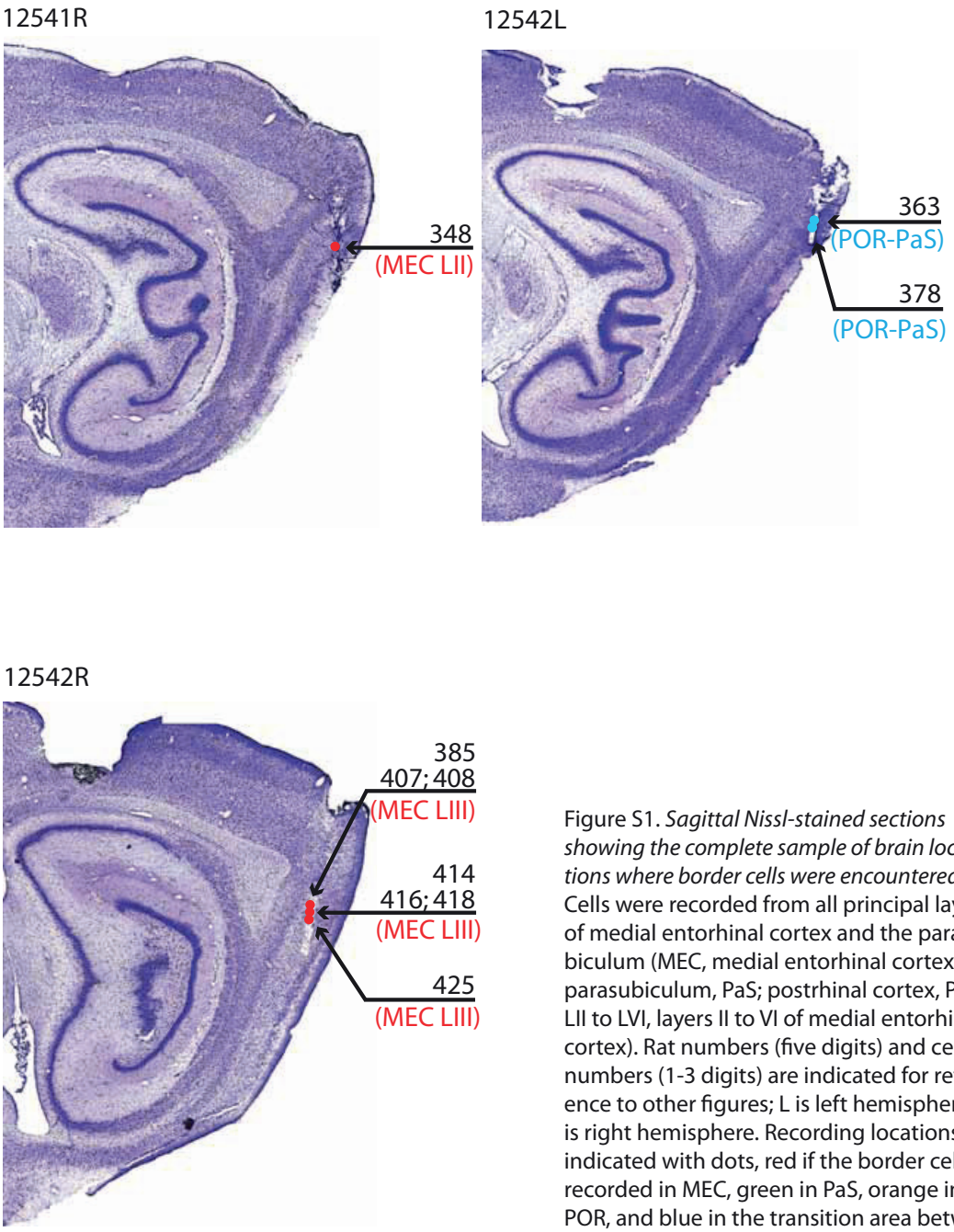

Figure S1. *Sagittal Nissl-stained sections showing the complete sample of brain locations where border cells were encountered.* Cells were recorded from all principal layers of medial entorhinal cortex and the parasubiculum (MEC, medial entorhinal cortex; parasubiculum, PaS; postrhinal cortex, POR; LII to LVI, layers II to VI of medial entorhinal cortex). Rat numbers (five digits) and cell numbers (1-3 digits) are indicated for reference to other figures; L is left hemisphere, R is right hemisphere. Recording locations are indicated with dots, red if the border cell was recorded in MEC, green in PaS, orange in POR, and blue in the transition area between POR and MEC or PaS.

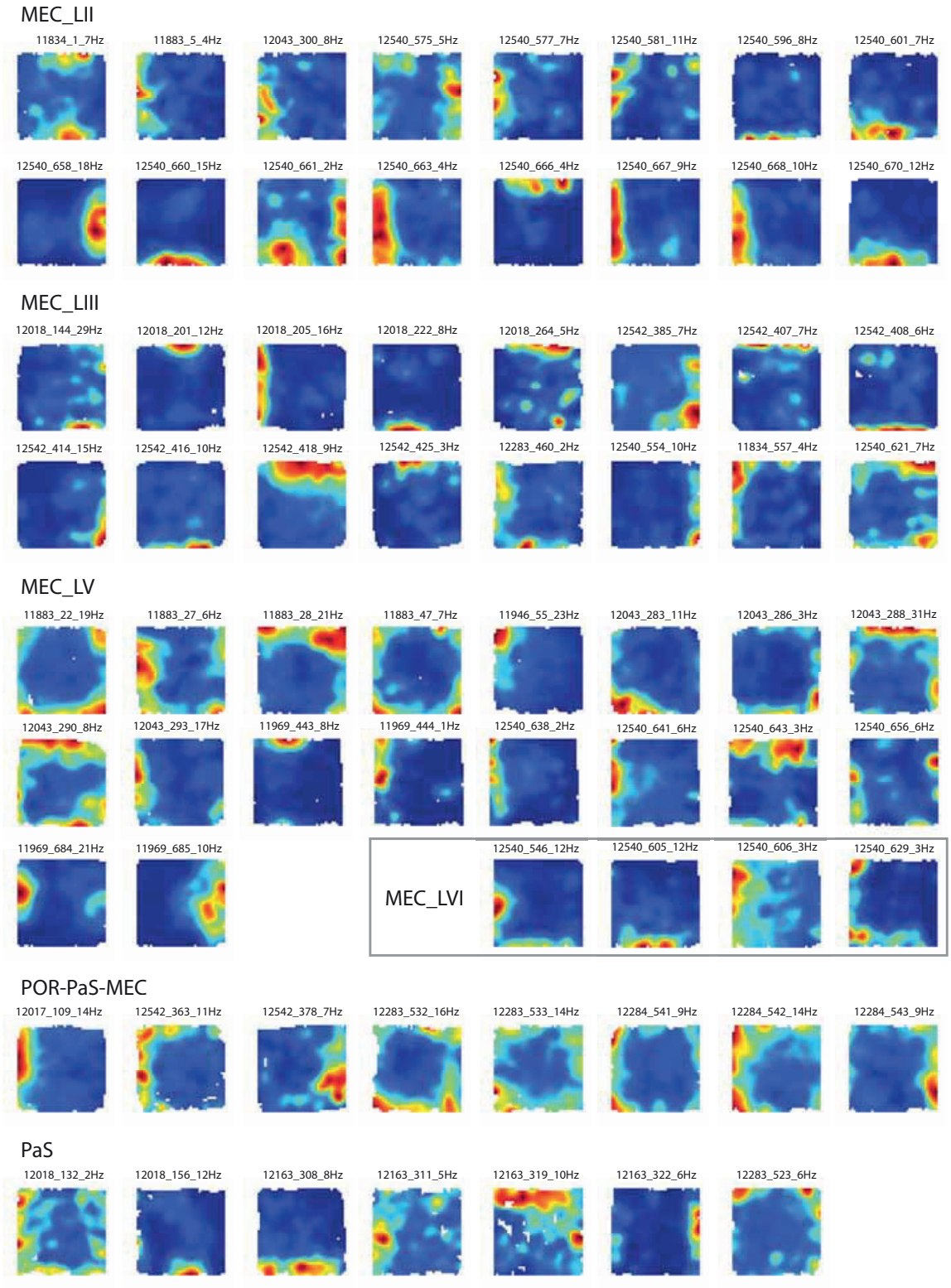

Figure S2A. *Colour-coded rate maps showing firing fields in the small square box for the entire sample of cells classified as border cells (border score > 0.50).* Cells are sorted according to brain region and cell layer (MEC, medial entorhinal cortex; LII-LVI: layers II to VI; PaS, parasubiculum; POR-PaS-MEC, transition between postrhinal cortex, parasubiculum and medial entorhinal cortex). Each panel shows the rate map of one cell. Red is maximum, dark blue is zero. Pixels not covered are white. Animal numbers (five digits), cell numbers (1-3 digits), and peak firing rates are indicated above each panel. A subset of these cells are shown in Fig. 1. See Figure S2B for path diagrams and Figure S2C for directional modulation of the same cell sample. Note slight overrepresentation of cells with border fields along mulitple walls in the deep layers of MEC (compared to the superficial layers).

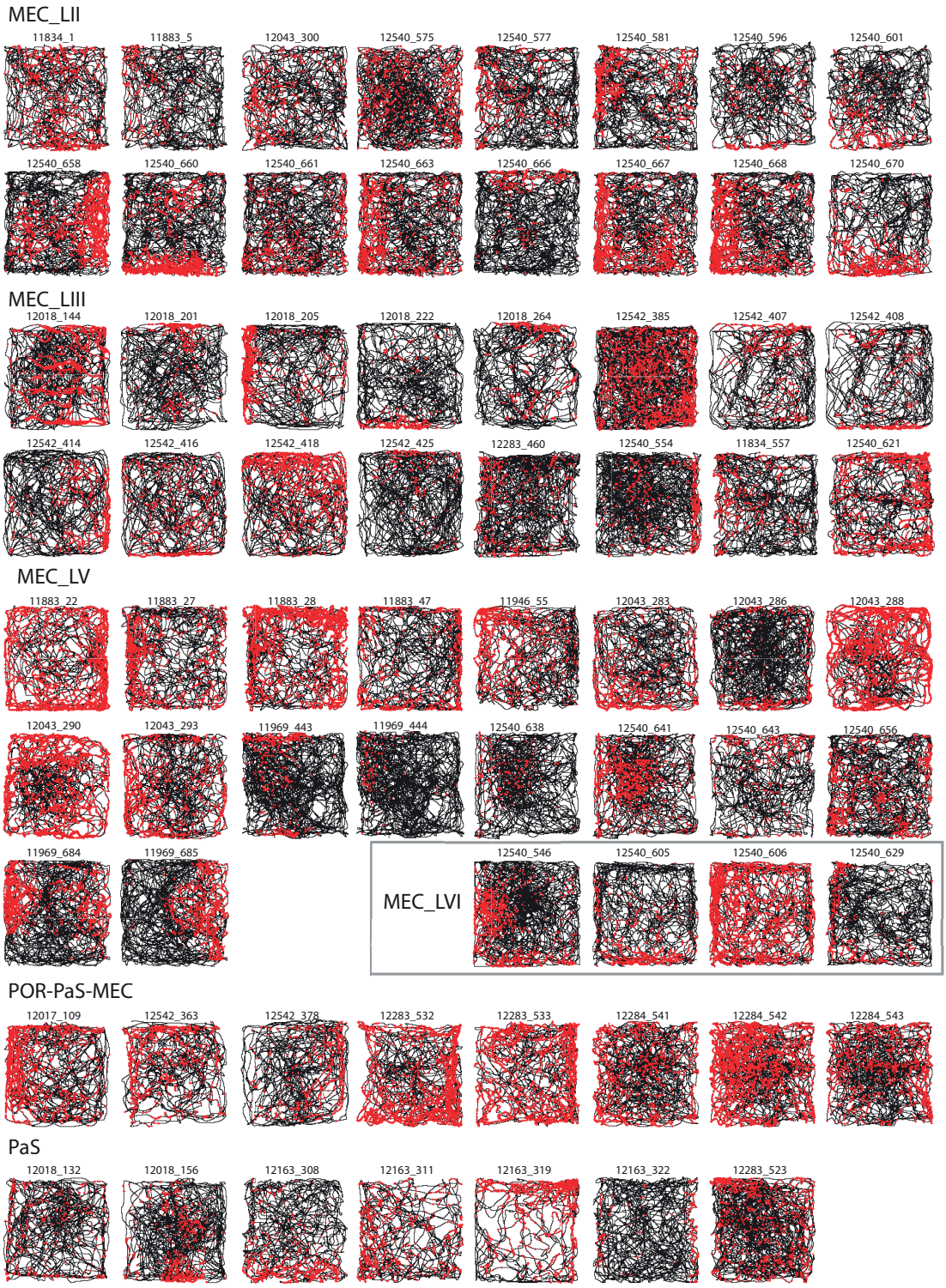

Figure S2B. *Trajectories with spike locations for the complete sample of border cells (same cells as in Fig. S2A; same figure layout).* Trajectories are in black. Each red dot corresponds to the location of one spike of the cell. Cells are sorted according to brain region and cell layer as in Fig. S2A. Note that nearly all cells classified as border cells had activity along the walls independently of the direction of running; only a small subset, shown in Fig.S2C, was modulated by head direction but their directional tuning generally did not account for their border-related firing fields (see also Fig. S12). The most striking exceptions may be cell 144, which is probably a head direction cell (Fig. S12B), and cell 656, which may be a grid cell (Fig. S9).

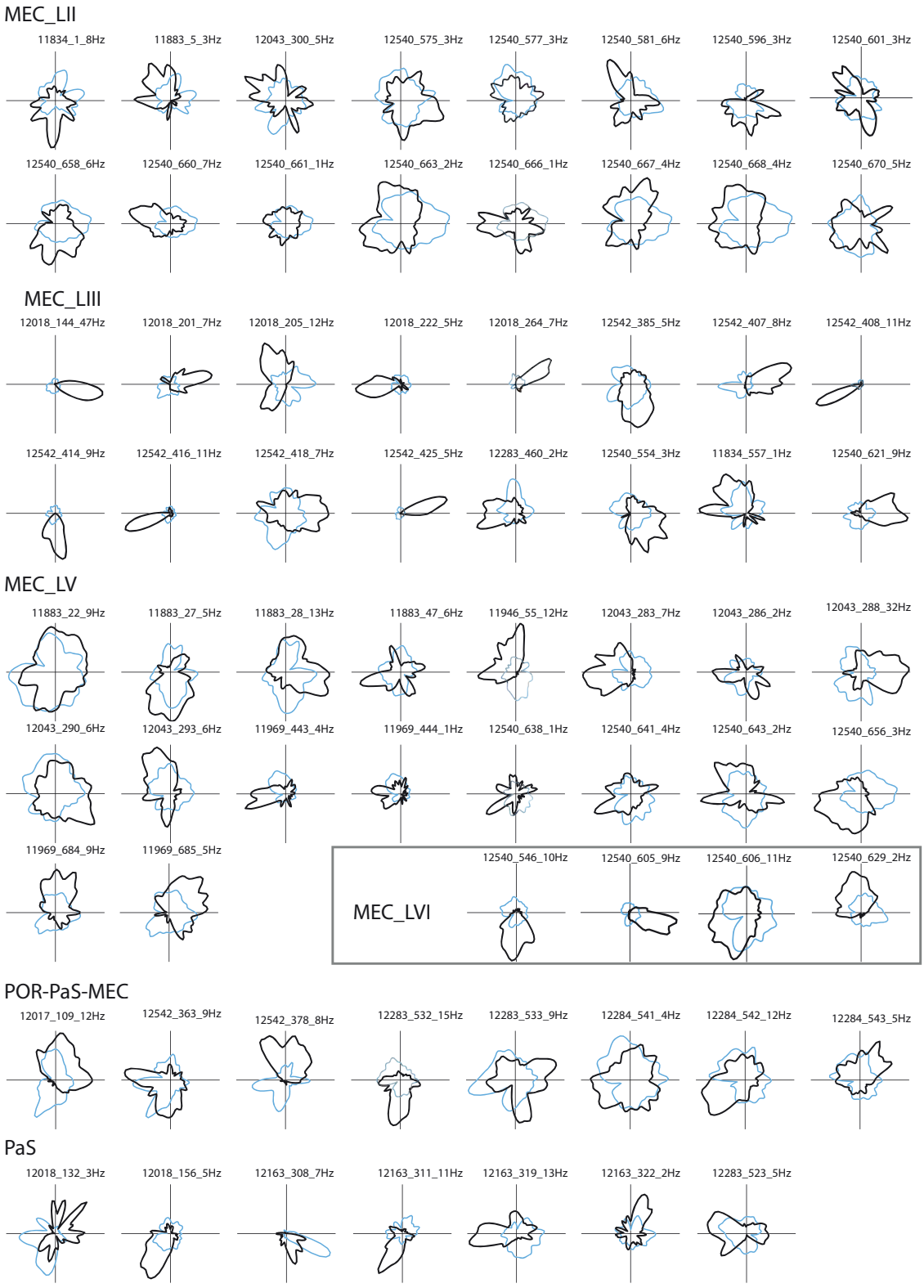

Figure S2C. *Head direction tuning in border cells.* Polar plots show, for each border cell in Fig. S2A and B, the firing rate as a function of head direction (black) and the amount of time that the rat faced each direction (blue trace). Rat number, cell number, and peak firing rates are indicated. A subset of 8 border cells in layers III-VI and parasubiculum showed significant modulation by head direction (head direction scores >0.75; see Fig. S12).

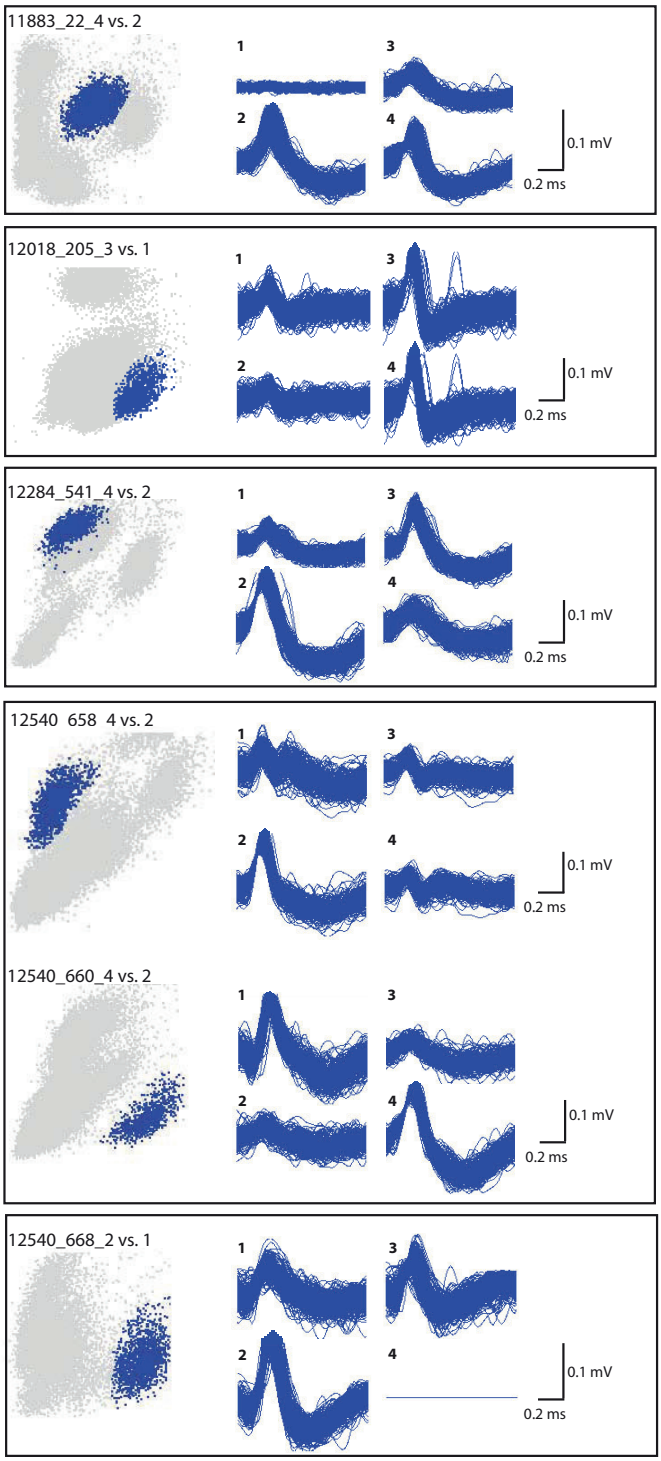

Figure S2D. *Cluster diagrams and waveforms of border cells recorded with tetrodes in MEC*. Left, Scatterplot showing relation between peak-to-trough amplitudes of all signals recorded on two electrodes of one tetrode in 5 experiments with one or several border cells (one box per experiment and tetrode). Only one of 6 electrode combinations is shown for each experiment. Each dot represents one sampled signal. Rat number (5 digits), cell number (3 digits) and electrode combinations are indicated. Clusters in the scatterplot are likely to correspond to spikes originating from the same cell. Clusters in blue refer to cells that satisfy criteria for border cells. Right, Waveforms of the cell that corresponds to the blue cluster to the left. Waveforms are shown for each of the four electrodes (1-4) of the tetrode. Note that peak-to-trough latencies are generally long, suggesting that the waveforms originate from local cells rather than bypassing axons. The mean latency (± S.E.M.) from peak to trough for the waveform on the electrode with the largest amplitude was 0.317 ± 0.016 ms. The mean amplitude, measured from peak to trough, was 0.162 ± 0.005 mV. Layer III border cells had shorter peak-to-trough latencies than border cells in other layers (layer II: 0.322 ± 0.029; layer III: 0.162 ± 0.026; layer V: 0.384 ± 0.0.021; parasubiculum and transition areas: 0.366 ± 0.023; one-way ANOVA: $F(3,68) = 14.6$, $P < 0.001$, layer III significantly different from all other layers with Bonferroni test, no other differences); however, all grid cells that were recorded on the same layer III tetrodes also had short-peak-to-trough latencies (data not shown).

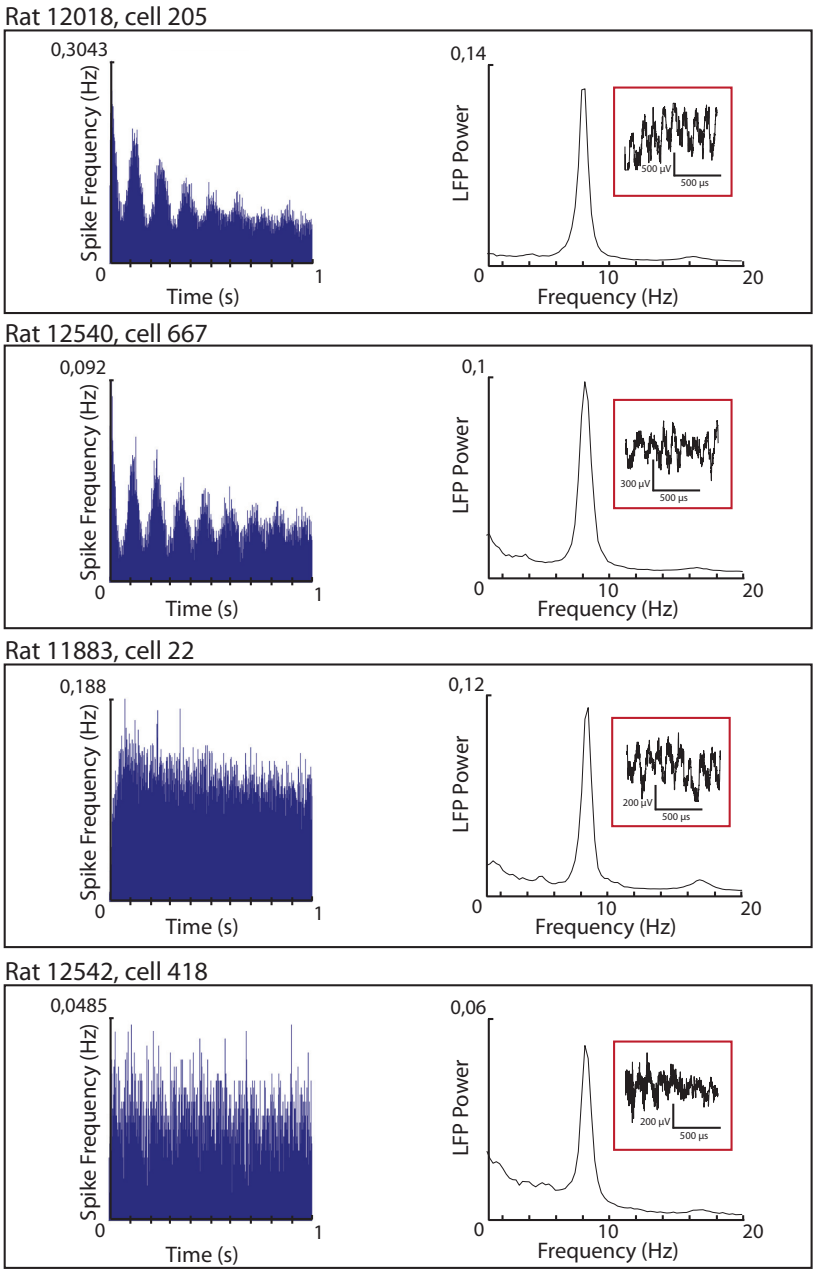

Figure S3. *Theta modulation of four border cells in medial entorhinal cortex.* Left: Autocorrelation diagrams showing distribution of interspike times for two border cells that were theta modulated (top) and two that were not (bottom). Average number of spikes per second is shown for bins of 2 ms. Right: Power spectra showing theta modulation of field EEG during recording of the cells to the left. Inset: Examples of EEG traces showing theta activity in the field in all cases. A cell was defined as theta modulated if the mean power within 1 Hz of each side of the peak in the 5-12 Hz frequency range was at least 10 times greater than the mean spectral power highpass-filtered at 2 Hz (*S1*). By this criterion, 31 out of 69 border cells were theta-modulated. The proportion of theta-modulated border cells was similar to that of simultaneously recorded grid cells (46 of 81; *S2*). Layer II contained a larger proportion of theta modulated cells than the deep layers (layer II: 10/16 cells, 63%; layer III: 7/16 cells, 44%; layer V: 5/18 cells, 28%; layer VI: 1/4 cells, 25%; PaS: 5/7 cells, 71%; other: 3/8 cells, 38%; the difference between layer II and layers V-VI was significant (P = 0.03, binomial test).

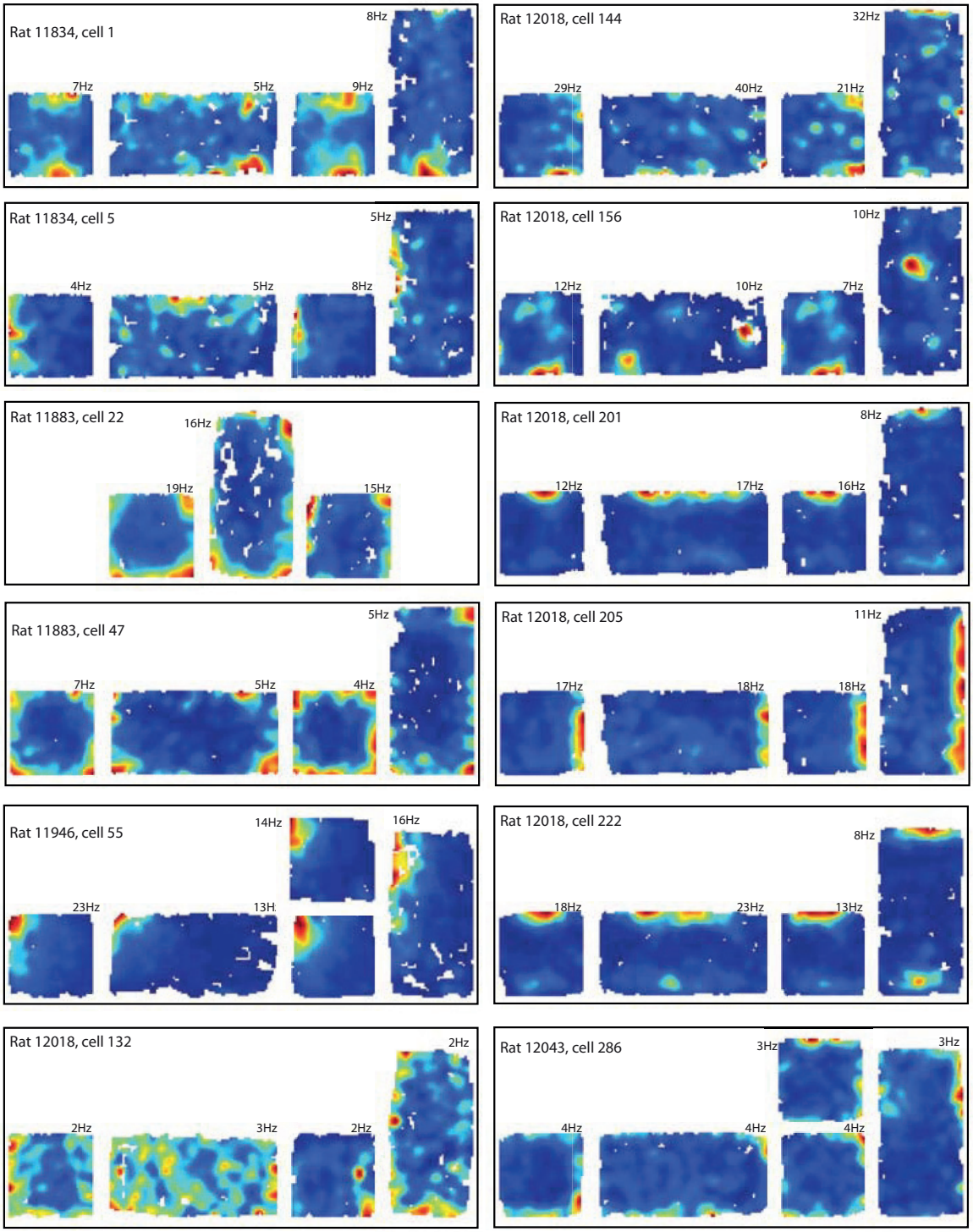
Rat 11834, cell 1
7Hz
5Hz
9Hz
8Hz
Rat 12018, cell 144
29Hz
40Hz
21Hz
32Hz
Rat 11834, cell 5
4Hz
5Hz
8Hz
5Hz
Rat 12018, cell 156
12Hz
10Hz
7Hz
10Hz
Rat 11883, cell 22
19Hz
16Hz
15Hz
Rat 12018, cell 201
12Hz
17Hz
16Hz
8Hz
Rat 11883, cell 47
7Hz
5Hz
4Hz
5Hz
Rat 12018, cell 205
17Hz
18Hz
18Hz
11Hz
Rat 11946, cell 55
23Hz
13Hz
14Hz
16Hz
Rat 12018, cell 222
18Hz
23Hz
13Hz
8Hz
Rat 12018, cell 132
2Hz
3Hz
2Hz
2Hz
Rat 12043, cell 286
4Hz
4Hz
4Hz
3Hz
3Hz

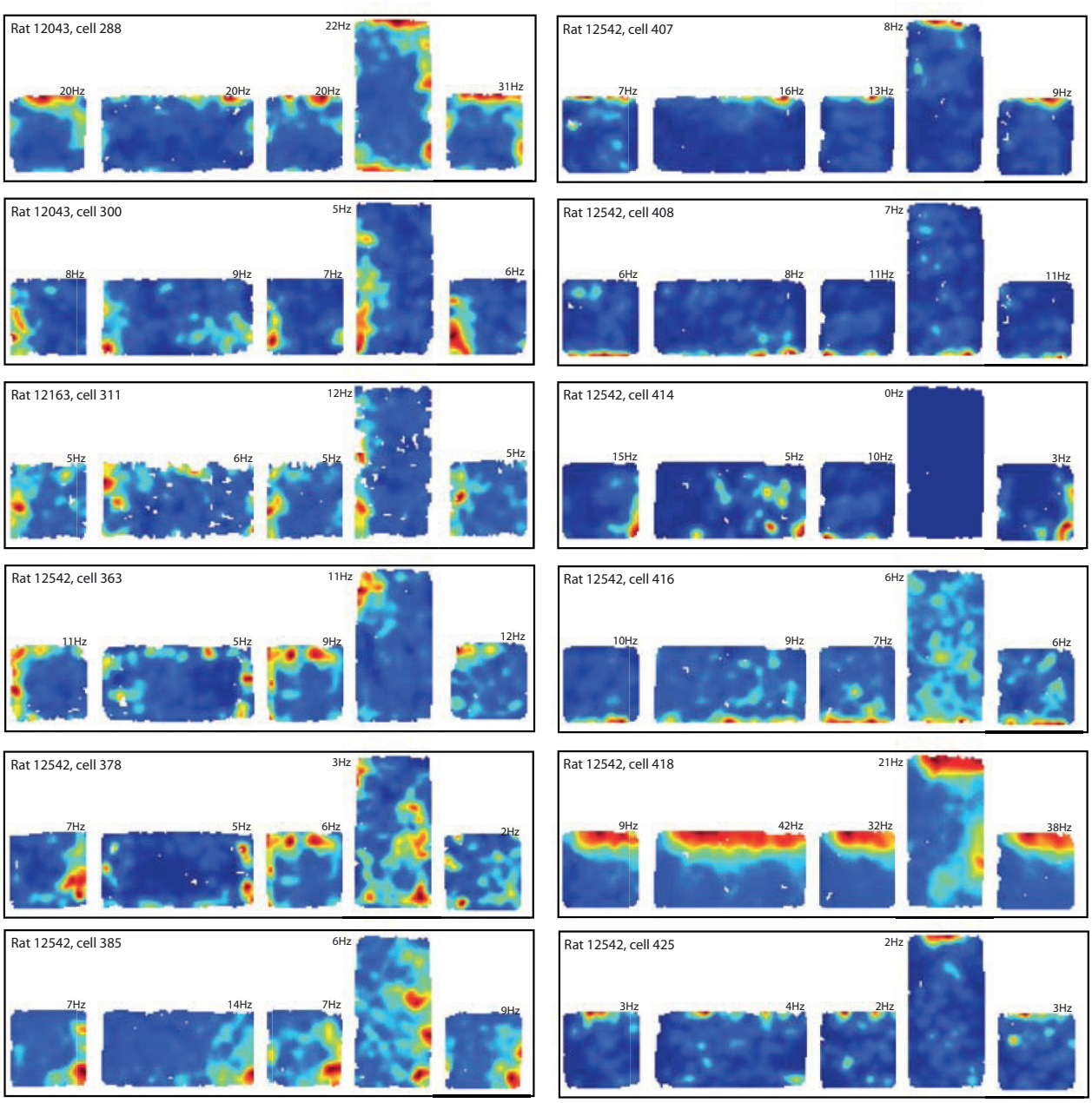
Rat 12043, cell 288
20Hz
20Hz
20Hz
22Hz
31Hz
Rat 12542, cell 407
7Hz
16Hz
13Hz
8Hz
9Hz
Rat 12043, cell 300
8Hz
9Hz
7Hz
5Hz
6Hz
Rat 12542, cell 408
6Hz
8Hz
11Hz
7Hz
11Hz
Rat 12163, cell 311
5Hz
6Hz
5Hz
12Hz
5Hz
Rat 12542, cell 414
15Hz
5Hz
10Hz
0Hz
3Hz
Rat 12542, cell 363
11Hz
5Hz
9Hz
11Hz
12Hz
Rat 12542, cell 416
10Hz
9Hz
7Hz
6Hz
6Hz
Rat 12542, cell 378
7Hz
5Hz
6Hz
3Hz
2Hz
Rat 12542, cell 418
9Hz
42Hz
32Hz
21Hz
38Hz
Rat 12542, cell 385
7Hz
14Hz
7Hz
6Hz
9Hz
Rat 12542, cell 425
3Hz
4Hz
2Hz
2Hz
3Hz

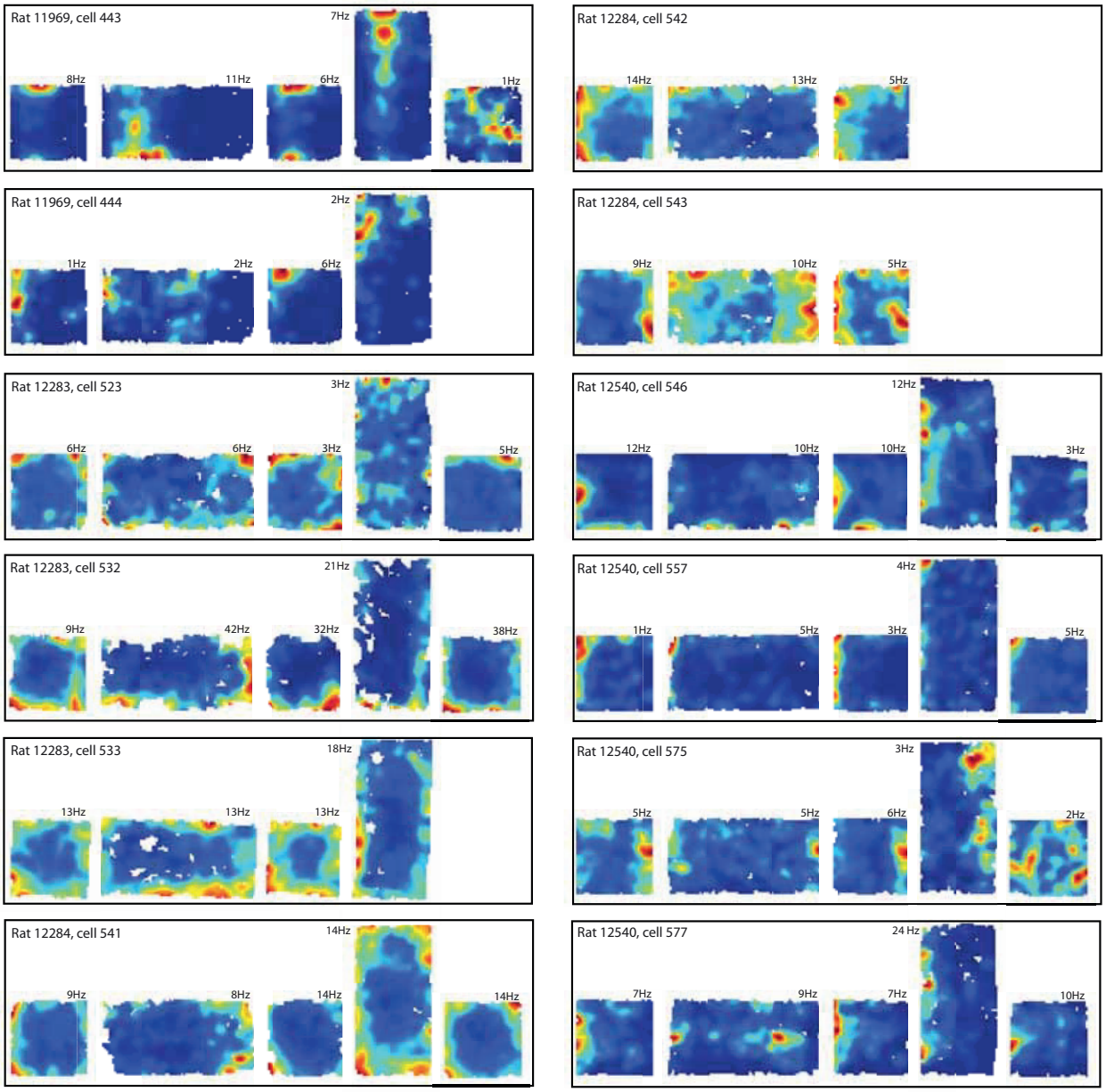
Rat 11969, cell 443
8Hz
11Hz
6Hz
7Hz
1Hz
Rat 12284, cell 542
14Hz
13Hz
5Hz
Rat 11969, cell 444
1Hz
2Hz
6Hz
2Hz
Rat 12284, cell 543
9Hz
10Hz
5Hz
Rat 12283, cell 523
6Hz
6Hz
3Hz
3Hz
5Hz
Rat 12540, cell 546
12Hz
10Hz
10Hz
12Hz
3Hz
Rat 12283, cell 532
9Hz
42Hz
32Hz
21Hz
38Hz
Rat 12540, cell 557
1Hz
5Hz
3Hz
4Hz
5Hz
Rat 12283, cell 533
13Hz
13Hz
13Hz
18Hz
Rat 12540, cell 575
5Hz
5Hz
6Hz
3Hz
2Hz
Rat 12284, cell 541
9Hz
8Hz
14Hz
14Hz
14Hz
Rat 12540, cell 577
7Hz
9Hz
7Hz
24 Hz
10Hz

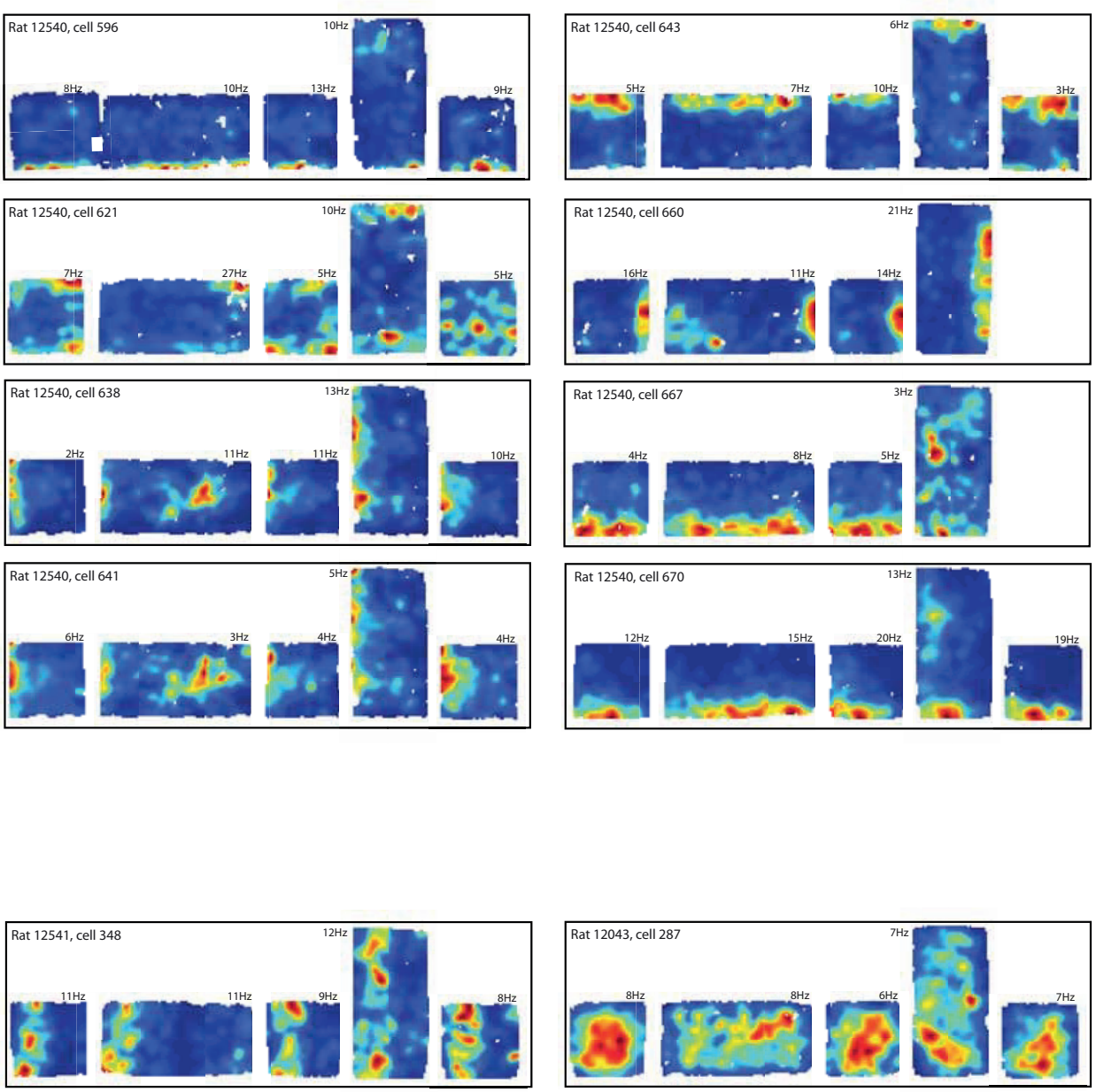

Fig. S4. *Colour-coded rate maps showing firing fields for the entire sample of border cells recorded in square and rectangular versions of the same enclosure (4 pages).* Each box in the figure shows one experiment, with trials shown in chronological order from left to right. Page 1-3 and the 8 panels at the top of page 4 show cells that passed the criterion for border cells in the square enclosure (border scores > 0.50; 44 cells). The two bottom cells on page 4 are cells that did not pass the criterion but nonetheless appeared to show border-associated activity (see also Fig. 1). Cell 348 fired in parallel with one of the walls but at a certain distance from it; cell 287 fired throughout the central part of the enclosure but was silent near the borders (antiborder cell). Red indicates maximum firing rate, dark blue is zero firing. Pixels not covered are white. Animal numbers, cell numbers and peak rates are indicated. Note that, in the rectangle, border fields remain anchored to the wall(s) at which firing occurs in the square environment and that, with less than 5 exceptions, no new fields appeared in the new open space when the box is stretched. Three of the exceptional cases had positive gridness scores (cells 156, 577 and 638). For electrode positions, see Fig. S1.

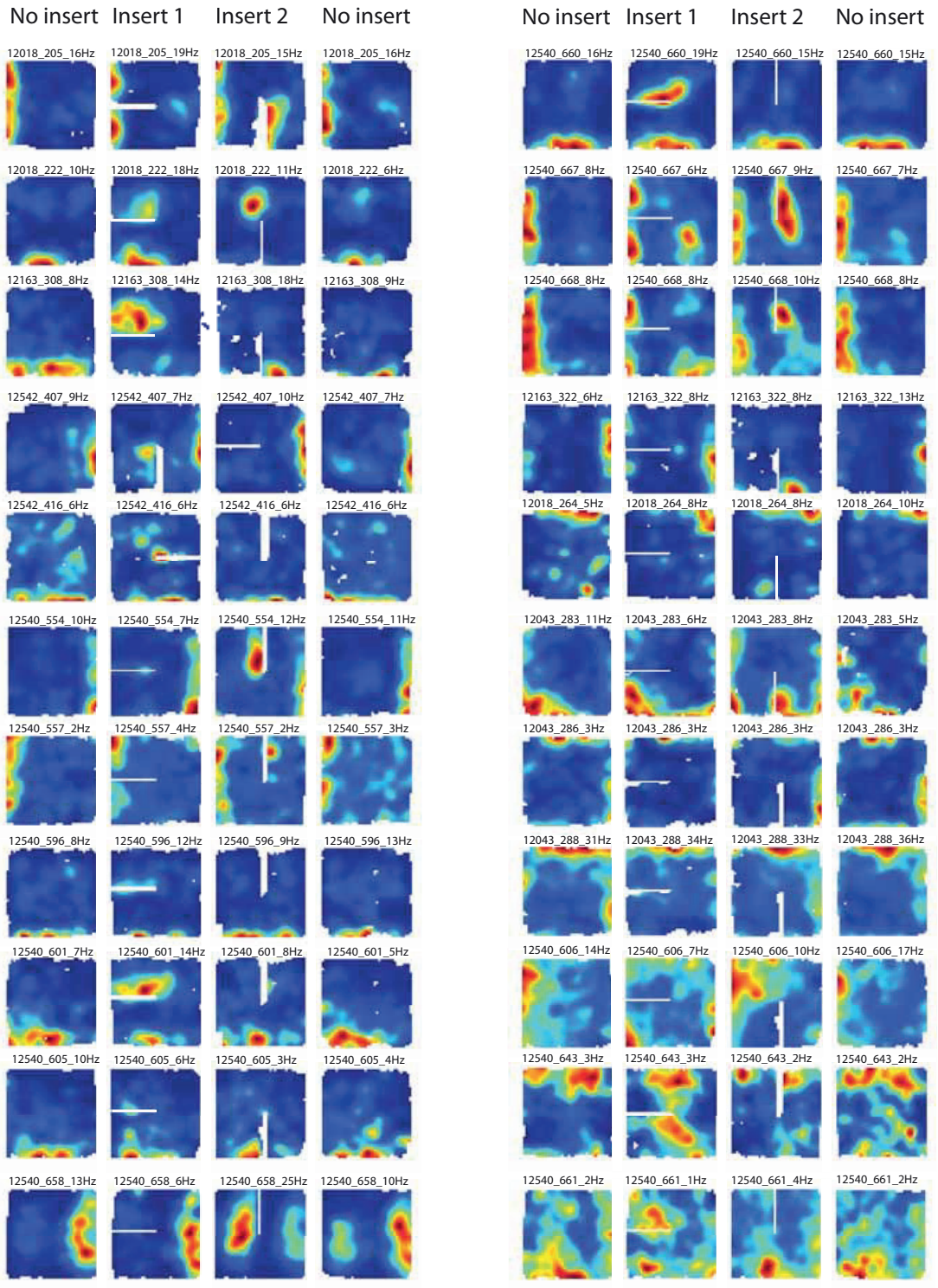

Figure S5. *Colour-coded rate maps showing firing fields for the entire sample of border cells recorded before and after introducing a discrete wall inside the square enclosure.* Four trials are shown for each experiment; the wall was inserted on the two middle trials (horizontal and vertical orientation, respectively). Animal numbers (5 digits), cell numbers (3 digits) and peak rates are indicated. Red is maximum, dark blue is zero. Pixels not covered are white. The position of the insert can be seen as a stripe of white pixels extending from the west wall and the north or south wall, respectively. Fourteen cells had fields along a single wall of the enclosure in the baseline condition (all cells in the left half of the figure and the three first cells in the right half). In these cells, a new field appeared when the insert was parallel to the wall along which the original field was anchored. The new field was always on the same side of the associated wall as the original field, relative to the distal cues. Note the remnant of the new field after removal of the insert on the fourth trial in some cells. In cells with fields on multiple walls, new fields were often not observed. For electrode positions, see Fig. S1.

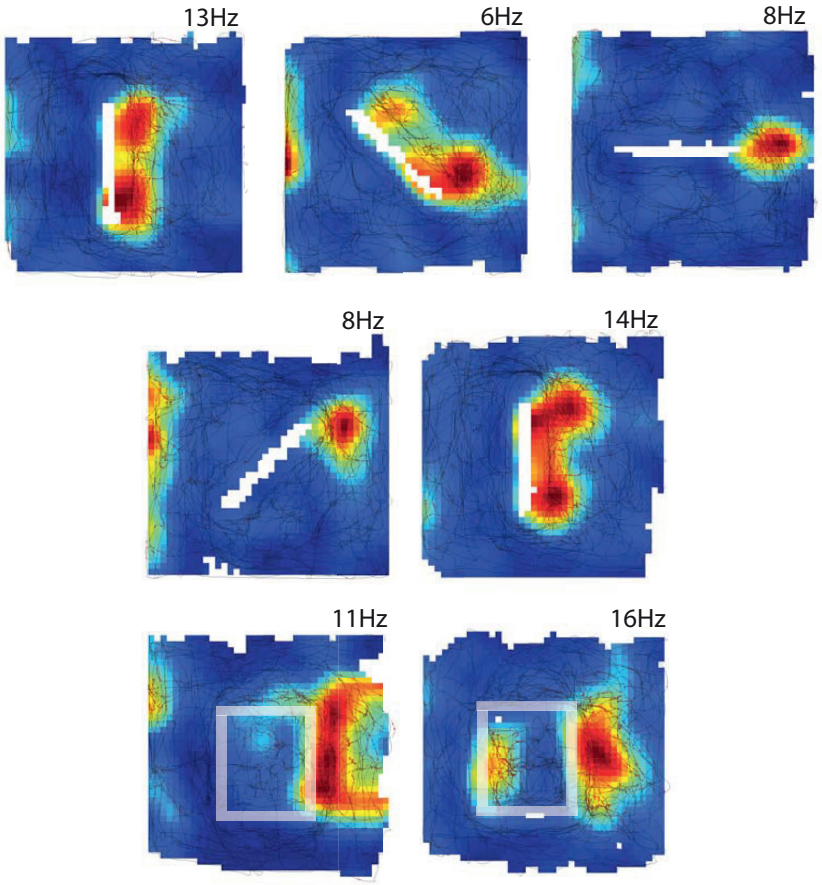

Figure S6. *Effect of changing wall orientation and wall height (rat 12018, cell 205)*. A discrete 50-cm wall was placed in the center of an elevated table with a 60 cm drop on all four sides. Between successive trials, the wall was rotated 45 degrees (upper and middle rows). On the two last trials (bottom row), the wall was replaced with a 5 cm rectangular barrier (left, a 5 cm high table; right, a 5 cm high fence). The rat could climb over the barrier. Rate maps are colour-coded as in Fig. 1. The trajectory is superimposed on the rate map (black trace). The position of the insert is visible as a stripe of white or grey pixels. Peak rates are indicated. Note persistence of an orientation-specific border field in spite of reduced height.

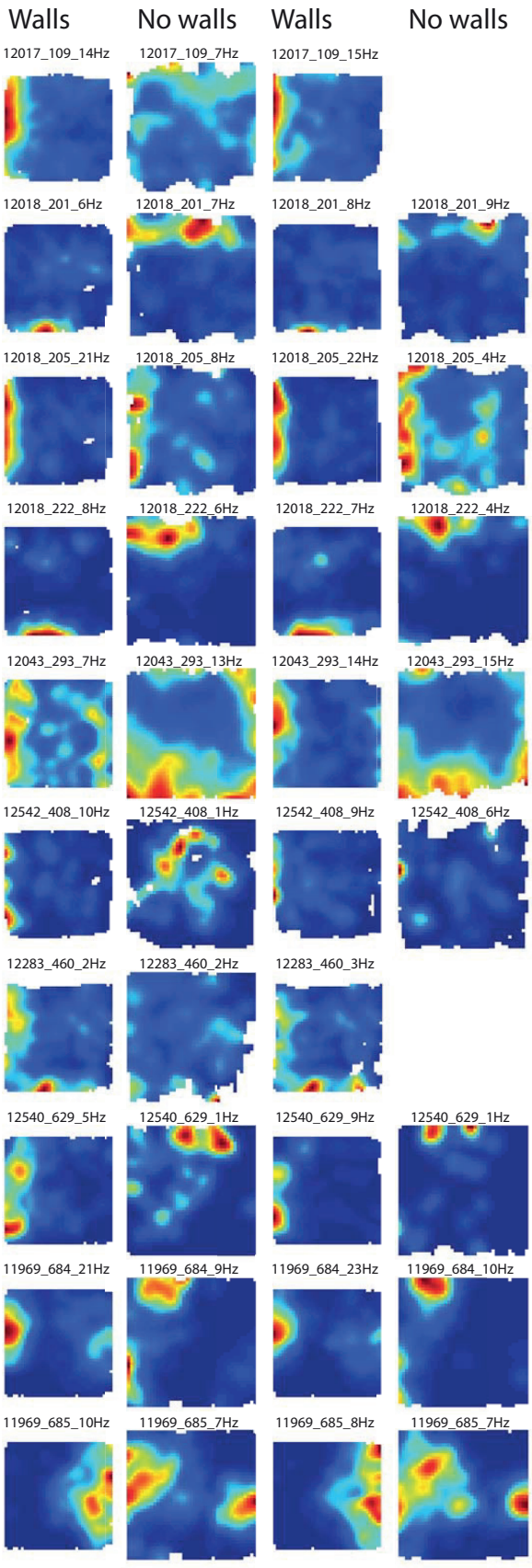

Figure S7. *Colour-coded rate maps showing firing fields for the entire sample of border cells recorded before and after removal of the walls.* Red is maximum, dark blue is zero. Pixels not covered are white. Animal numbers (5 digits), cell numbers (3 digits) and peak rates are indicated. The sequence of testing is from left to right. Border fields were often but not always maintained after removal of the external walls. In at least one experiment, the fields moved to a different border (cell 222; see also Fig. S8). For electrode positions, see Fig. S1. Colours are scaled individually for each trial (note occasional trials with 1 Hz peak rate, where the cell is essentially silent).

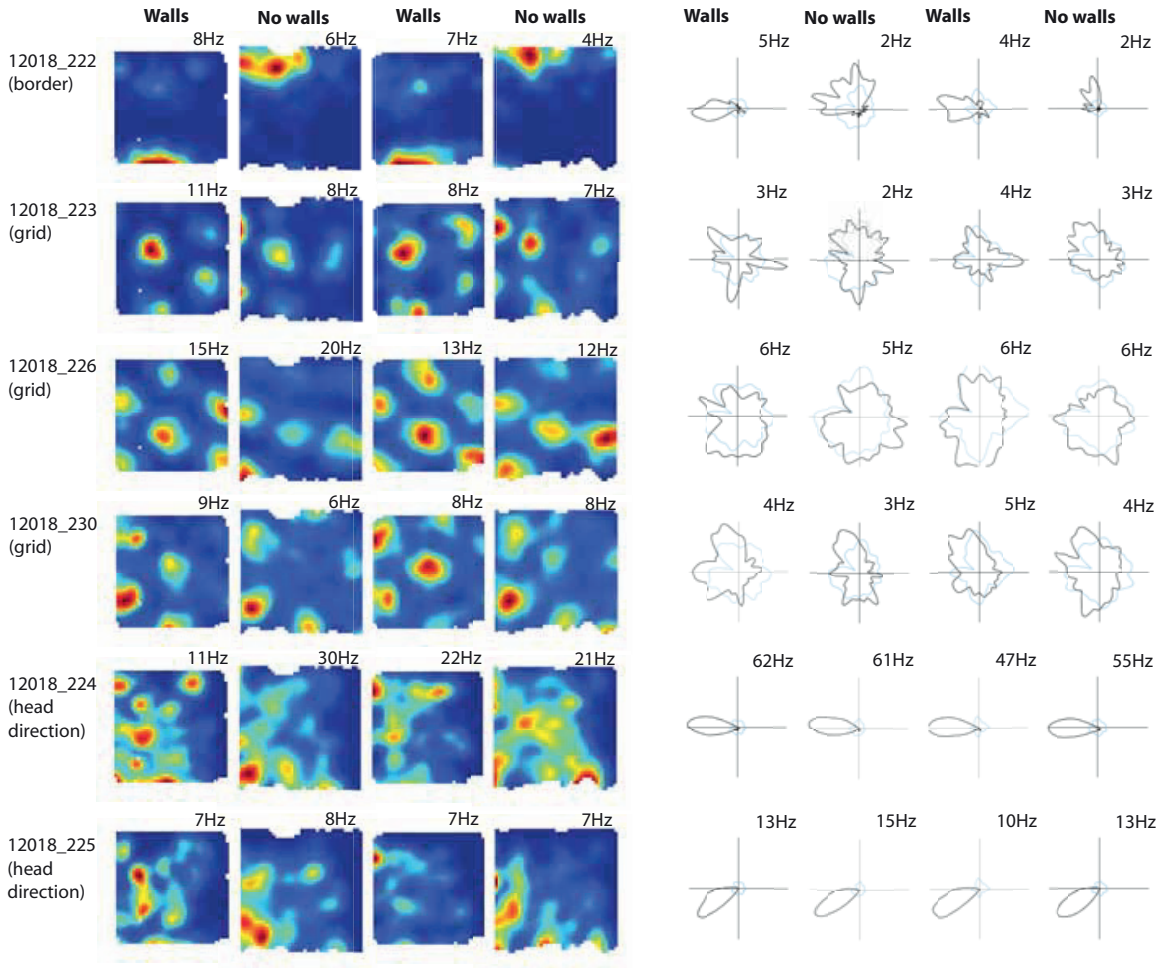

Figure S8. *Relocation of border field coincides with realignment of the grid representation*. The figure shows rate maps (left) and directional maps (right) for a border cell (top), three grid cells (middle), and two head direction cells (bottom) recorded simultaneously in the medial entorhinal cortex before and after removal of the external walls of the recording enclosure (as in Fig. S7). Animal and cell numbers are indicated to the left. Trials are presented chronologically from left to right in each panel. Symbols as in Fig. 1 and 4. Removing the walls changed the spatial phase but not the orientation of the grid fields (*16*). Head direction preferences remained stable. Note that the shift in grid phase was accompanied by a change in the wall preference of the border cell. Previous work has shown that grid realignments are accompanied by remapping in the hippocampal place cell population (*16*).

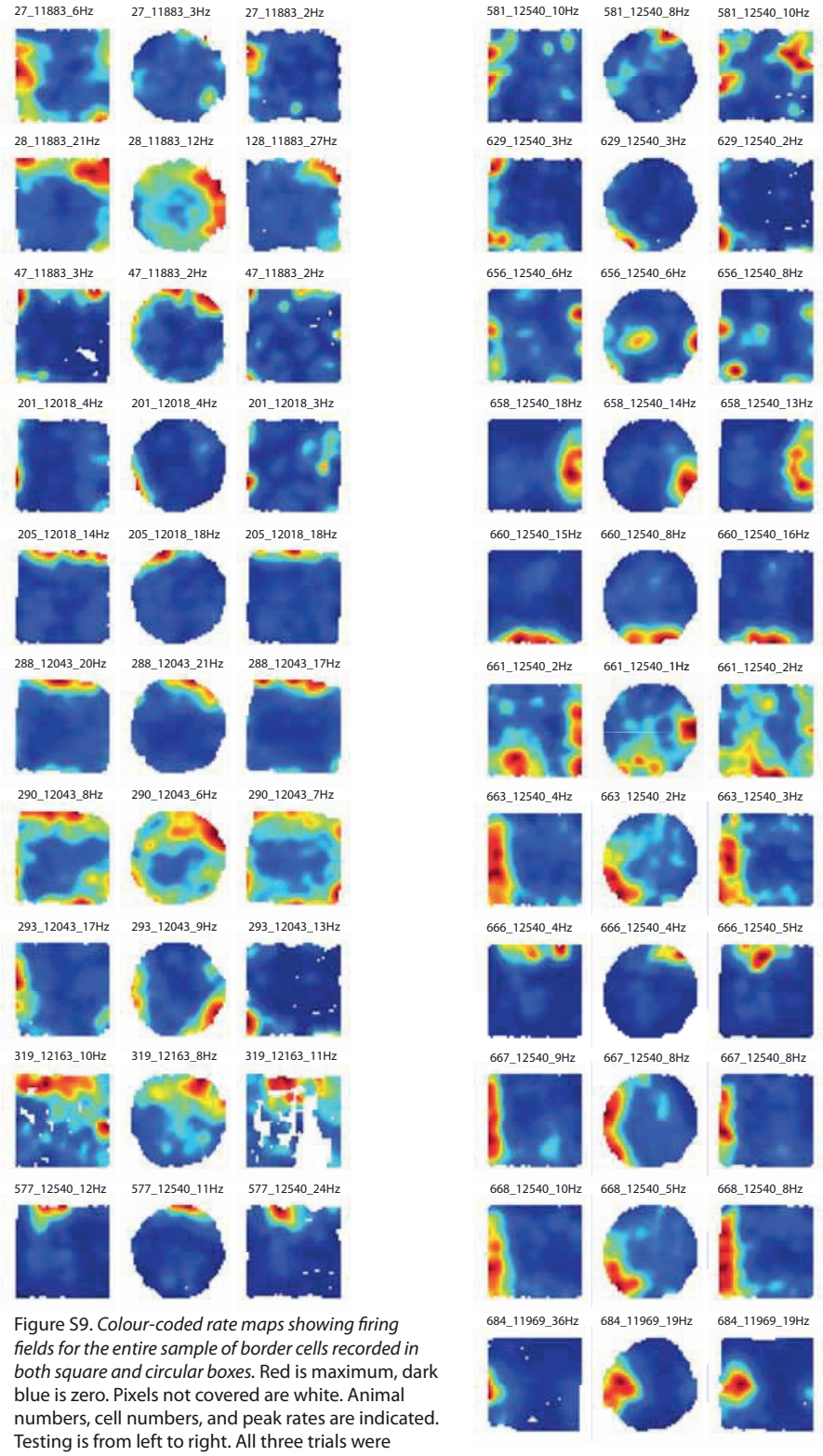

Figure S9. *Colour-coded rate maps showing firing fields for the entire sample of border cells recorded in both square and circular boxes.* Red is maximum, dark blue is zero. Pixels not covered are white. Animal numbers, cell numbers, and peak rates are indicated. Testing is from left to right. All three trials were performed in the same room. For cell numbers 47, 201, 205, 577, and 684, the room was different from the one shown in Fig. S2A. Note that border fields are maintained across box shapes. Cell 656 is a possible exception but the rate map suggests that this cell may be a grid cell (with most of the grid vertices at the walls in the square environment). The vertices of simultaneously recorded grid cells did not appear to move, suggesting that the spatial phase of the grid was constant and that global remapping may not have occurred in the hippocampus (*16*). More substantial interventions, e.g. with changes in floor texture and food rewards accompanying the shape change, might be associated with displacement of border fields and grid fields as well as global remapping in the hippocampus (*16*).

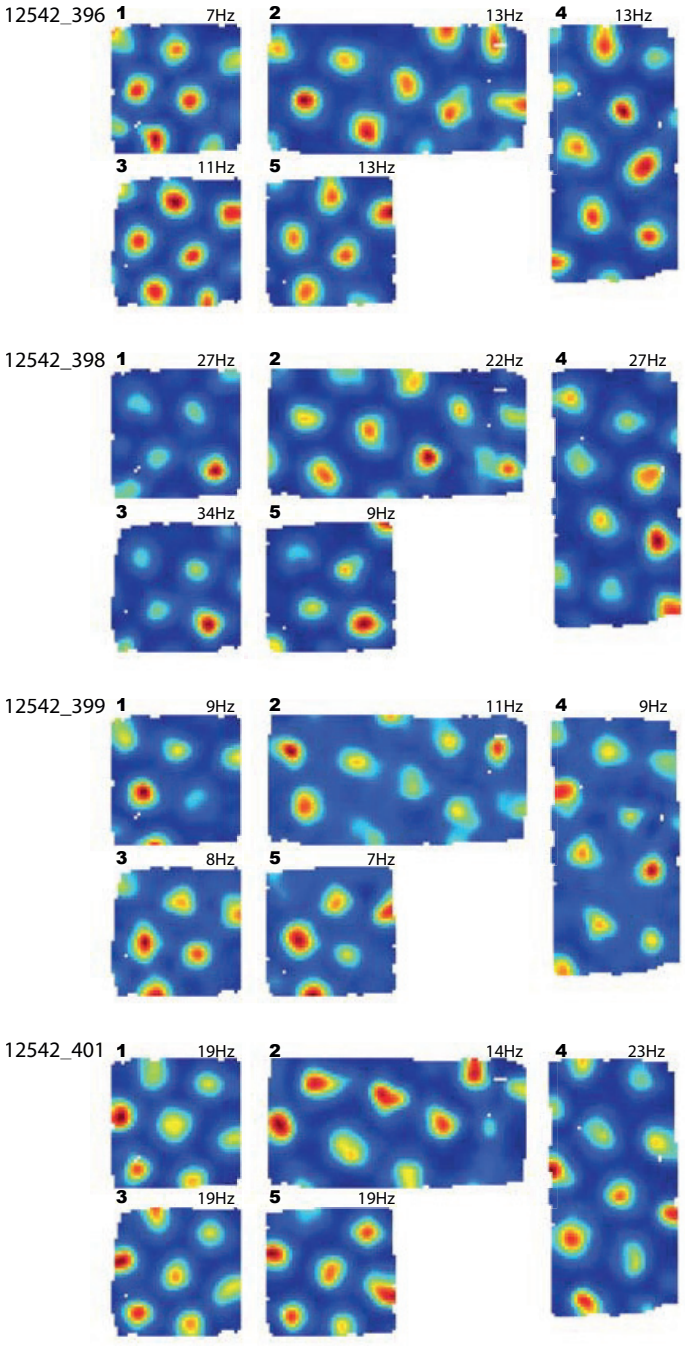

Figure S10A. *Colour-coded rate maps showing firing fields of non-scaling grid cells in the square and rectangular versions of the recording enclosure.* Red is maximum, dark blue is zero. Pixels not covered are white. All data are from one trial in one rat. Rat and cell numbers are indicated to the left; trial number and peak rate are shown above each rate map. Note increase in number of grid fields after extension of the environment. There was minimal scaling of the grid fields in this experiment.

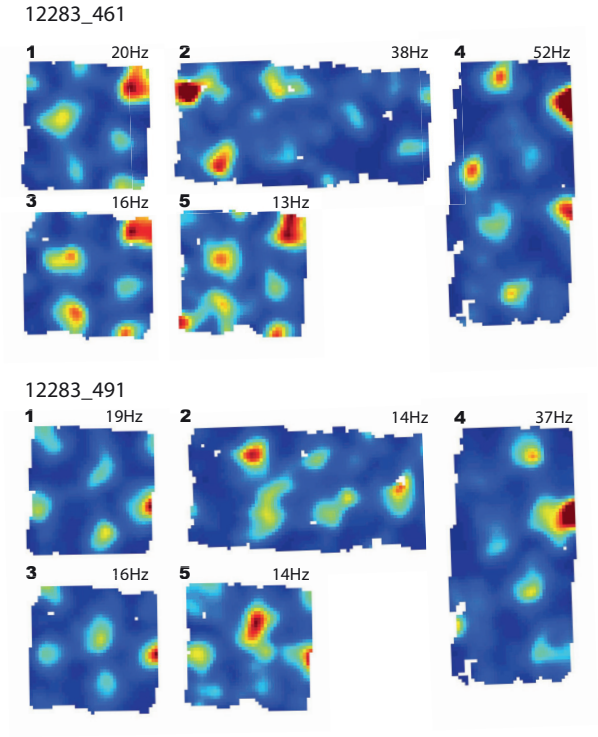

Figure S10B. *Colour-coded rate maps showing firing fields of two re-scaling grid cells in the square and rectangular versions of the recording enclosure.* Animal, cell and trial numbers are indicated (5, 3 and 1 digits, respectively); peak firing rate is shown above each panel. The colour scale extends from 0 to the peak rate of the first trial; higher frequencies are shown in dark red. Note increased distance between grid fields in the extended direction after changing the square into a rectangle in this particular experiment.

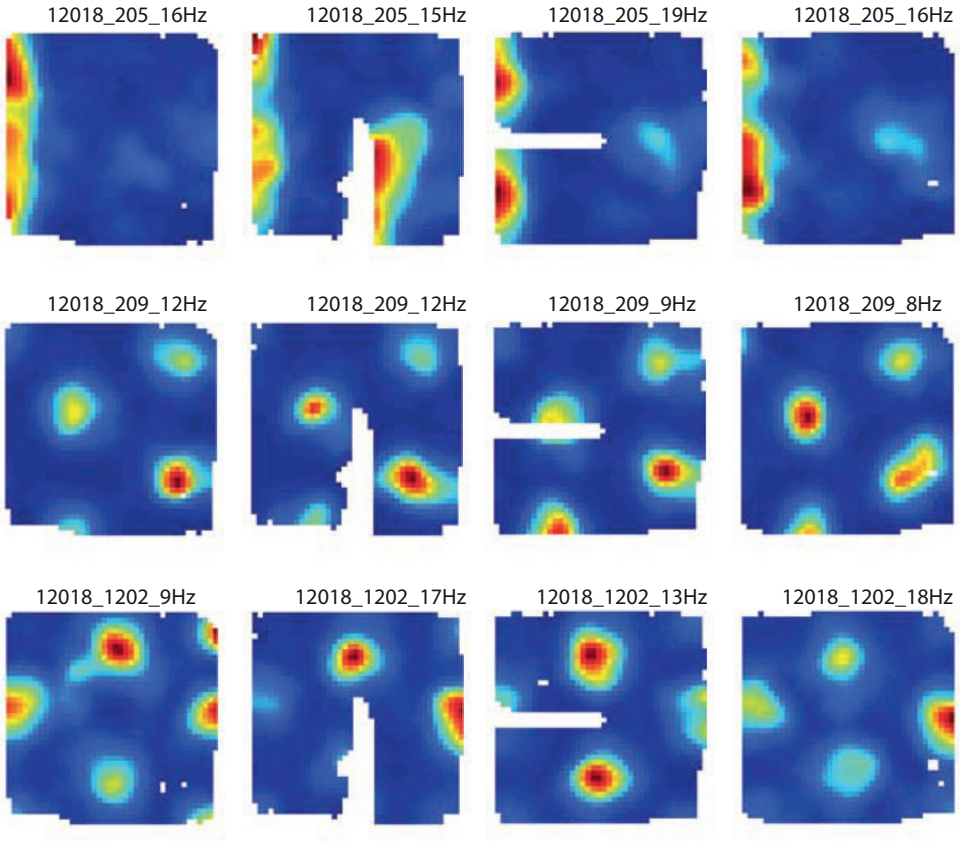

Figure S11. *Colour-coded rate maps showing firing fields of simultaneously recorded border and grid cells after introduction of a discrete wall inside the square enclosure.* Red is maximum, dark blue is zero. Pixels not covered are white. Animal numbers, cell numbers and peak rates are indicated. Testing is from left to right. A new field emerged only in the border cell. The vertex positions of the grid cells were maintained and no additional fields could be observed.

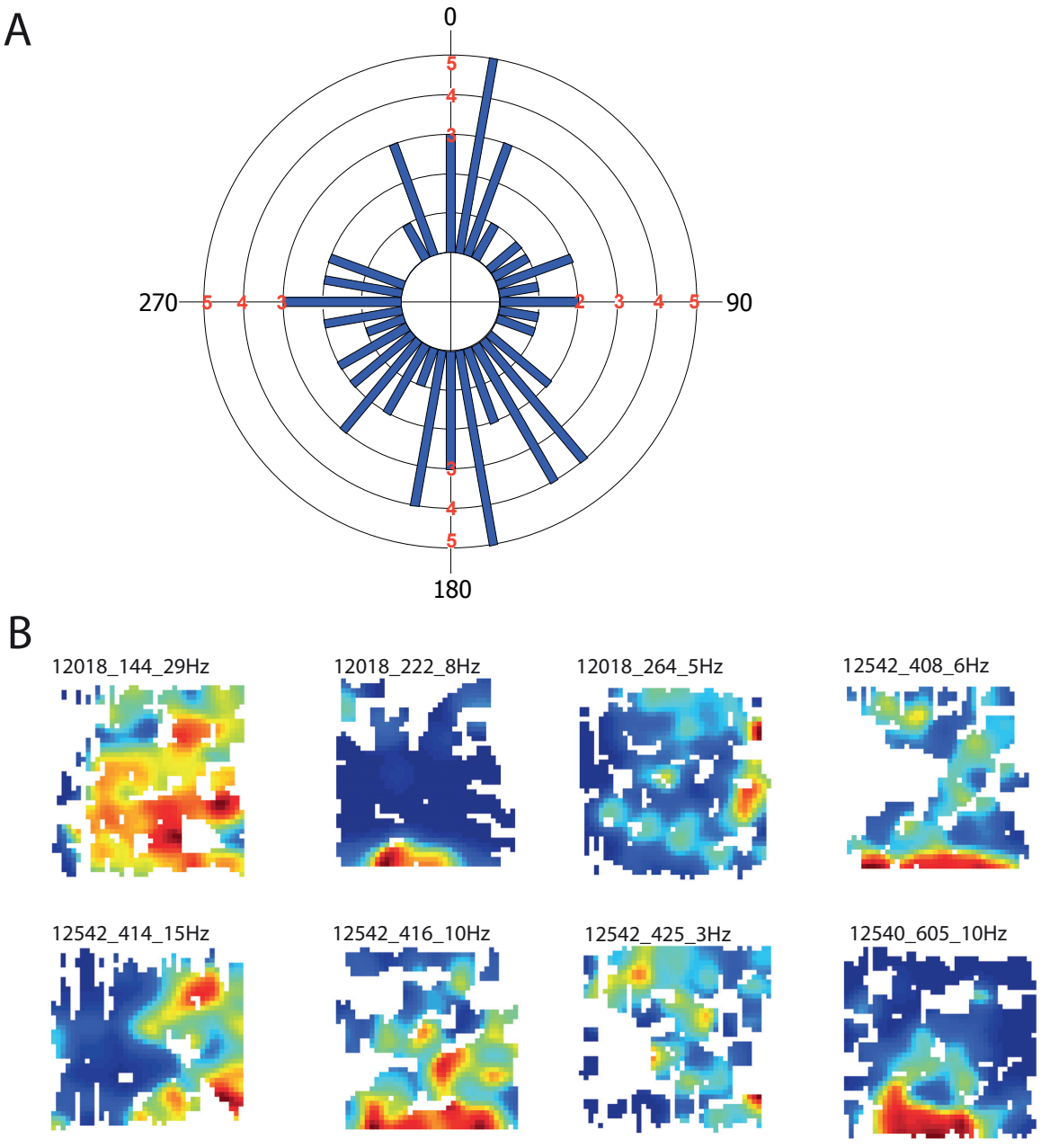

Figure S12. *Border fields are not dependent on head direction tuning*. **A**, Circular distribution of head-directional firing preferences across the entire sample of border cells. Note that preferred head direction is distributed evenly, in contrast to the orientation of the border fields, which is parallel to the walls of the enclosure (i.e., their orientations are in multiples of 90 degrees). Red numbers along the axes indicate frequency. **B**, Colour-coded rate maps showing direction-controlled firing fields for the subset of 8 border cells with suprathreshold head direction modulation in the square enclosure (stable directional tuning and a head direction index greater than 0.75, i.e. more than half of the spike distribution within an arc of 45 degrees; see Fig. S2C). These rate maps include only time segments when the rat is looking in a direction that falls within the central quartiles of the distribution of firing directions around the circular mean firing direction for the cell. Red is maximum, dark blue is zero. Pixels not covered at the preferred firing direction are white. Animal numbers, cell numbers and peak rates are indicated. Note that border-associated activity persists in 4 or 5 of these cells after controlling for head direction, suggesting that, with very few exceptions (primarily cells 144 and 425), border fields were not caused by head direction modulation.

4. Supporing References and Notes

S1. A. Jeewajee, C. Lever, S. Burton, J. O'Keefe, N. Burgess. *Hippocampus* **18**, 340 (2008).

S2. T. Hafting, M. Fyhn, T. Bonnevie, M.-B. Moser, E.I. Moser. *Nature* **453**, 1248 (2008).

S3. C. Barry, R. Hayman, N. Burgess, K.J. Jeffery. *Nat. Neurosci*. **10**, 682 (2007).

S4. B.L. McNaughton, F.P. Battaglia, O. Jensen, E.I. Moser, M.-B. Moser. *Nat. Rev. Neurosci*. **7**, 663 (2006).

S5. M.C. Fuhs, D.S. Touretzky. *J. Neurosci*. **26**, 4266 (2006).

S6. J. O'Keefe, N. Burgess. *Hippocampus* **15**, 853 (2005).

S7. T. Solstad, E.I. Moser, G.T. Einevoll. *Hippocampus* **16**, 1026 (2006).

S8. K. Cheng. *Cognition* **23**, 149 (1986).

S9. C.R. Gallistel. *The organization of learning*. MIT Press (Cambridge, MA, 1990).

S10. D.H. Hubel, T.N. Wiesel. *Proc. R. Soc. Lond. B Biol. Sci.* **198**, 1 (1977).

S11. J.M. Pearce, M.A. Good, P.M. Jones, A. McGregor. *J. Exp. Psychol. Anim. Behav. Process*. **30**, 135 (2004).

S12. B. Rivard, Y. Li, P.P. Lenck-Santini, B. Poucet, R.U. Muller. *J. Gen. Physiol*. **124**, 9 (2004).

S13. K.M. Gothard, W.E. Skaggs, K.M. Moore, B.L. McNaughton. *J. Neurosci*. **16**, 823(1996).

S14. A. Cressant, R.U. Muller, B. Poucet. *Hippocampus* **9**, 423 (1999).

S15. M. Fyhn, S. Molden, S. Hollup, M.-B. Moser, E.I. *Neuron* **35**, 555 (2002).

Paper II

nature neuroscience

Grid cells in pre- and parasubiculum

Charlotte N Boccara[1], Francesca Sargolini[1,2], Veslemøy Hult Thoresen[1], Trygve Solstad[1], Menno P Witter[1], Edvard I Moser[1] & May-Britt Moser[1]

Allocentric space is mapped by a widespread brain circuit of functionally specialized cell types located in interconnected subregions of the hippocampal-parahippocampal cortices. Little is known about the neural architectures required to express this variety of firing patterns. In rats, we found that one of the cell types, the grid cell, was abundant not only in medial entorhinal cortex (MEC), where it was first reported, but also in pre- and parasubiculum. The proportion of grid cells in pre- and parasubiculum was comparable to deep layers of MEC. The symmetry of the grid pattern and its relationship to the theta rhythm were weaker, especially in presubiculum. Pre- and parasubicular grid cells intermingled with head-direction cells and border cells, as in deep MEC layers. The characterization of a common pool of space-responsive cells in architecturally diverse subdivisions of parahippocampal cortex constrains the range of mechanisms that might give rise to their unique functional discharge phenotypes.

From the early studies of maze learning in the rat, it became gradually accepted that animals form internal maps of their proximal spatial environment[1]. Today, a widespread brain circuit is known to be involved in the representation of external space[2,3]. A unique property of this circuit is the existence of several functionally specialized cell types. The first cell type to be characterized was the place cell[4]. Place cells are hippocampal cells that fire if and only if the animal is in a specific location. Different, but overlapping, subsets of place cells are active in different environments and, in each environment, different place cells have different firing fields[5–7]. Collectively, place cells form a multitude of spatial maps individualized to the variety of environments that the animal has experienced[6,8,9]. The discovery of place cells was followed by the description of a directional signal in a different part of the network[10,11]. Cells in the dorsal presubiculum (postsubiculum), a parahippocampal region with strong indirect connections to the hippocampus[12], have been found to fire whenever animals face a particular direction in the environment, irrespective of where they are or what they are doing[11,13]. Such head-direction cells have subsequently been described in a number of cortical and subcortical regions[13]. More recently, a third type of spatial representation has been described in the MEC, at the interface between presubiculum, hippocampus and neocortex[14]. The key cell type of this representation is the grid cell[15]. Grid cells are place-modulated neurons with periodically spaced firing fields. The vertices of the firing fields define, for each cell, a triangular or hexagonal array spanning the entire environment in a crystal-like manner[15]. The phase and orientation of the grid pattern is determined by the unique cues of each environment. Grid cells colocalize with head-direction cells[16], as well as a recently described fourth cell type, referred to as border cells[17]. Border cells are entorhinal cells that signal specific geometric boundaries of the local environment[17,18]. All entorhinal cell types are active in all environments and preserve their internal spatial and directional firing relationships when animals move from one environment to another[17,19], suggesting that these cells, unlike the place cells of the hippocampus, are part of a path integration–dependent metric applied universally across environments[2,19,20].

Although several components of the spatial representation network have been characterized, little is known about the mechanisms by which functionally specific firing profiles are generated and integrated. The breadth of mechanisms that could potentially account for spatially and directionally localized firing is particularly apparent for grid cells. Grid patterns may be generated from intracellular processes such as interference between intrinsic membrane oscillations[21,22], as well as network processes in which firing patterns are translated across associative networks in accordance with the animal's movement[20,23,24]. One way to constrain the number of candidate mechanisms would be to determine whether cells with common functional properties, such as grid cells, depend on specific neuronal morphologies or network architectures. Until now, systematic mapping of grid cells has been limited to MEC, where the scale of the grid is topographically mapped along the dorsoventral axis[14,15,25] and layer II is functionally different from deeper layers[16,26]. Attempts to explain the periodic firing structure of grid cells have consequently focused on resonance properties and intrinsic connectivity patterns characteristic of the MEC network. To determine whether grid patterns are expressed in brain regions with other properties, we recorded activity from the dorsal parts of presubiculum and parasubiculum, two cytoarchitecturally distinct areas that give rise to some of the strongest external inputs to MEC[12]. Grid cells were abundant in both regions. Similar to the deeper layers of MEC, pre- and parasubiculum contained a mixture of grid cells, head-direction cells and border cells, suggesting that the firing patterns of these cell classes can be generated in architecturally diverse neural systems.

[1]Kavli Institute for Systems Neuroscience and Centre for the Biology of Memory, MTFS, Norwegian University of Science and Technology, Trondheim, Norway. [2]Laboratoire de Neurobiologie de la Cognition – CNRS, UMR 6155 – Pôle 3C, Université de Provence, Marseille, France. Correspondence should be addressed to E.I.M. (edvard.moser@ntnu.no).

Received 25 March; accepted 25 June; published online 25 July 2010; doi:10.1038/nn.2602

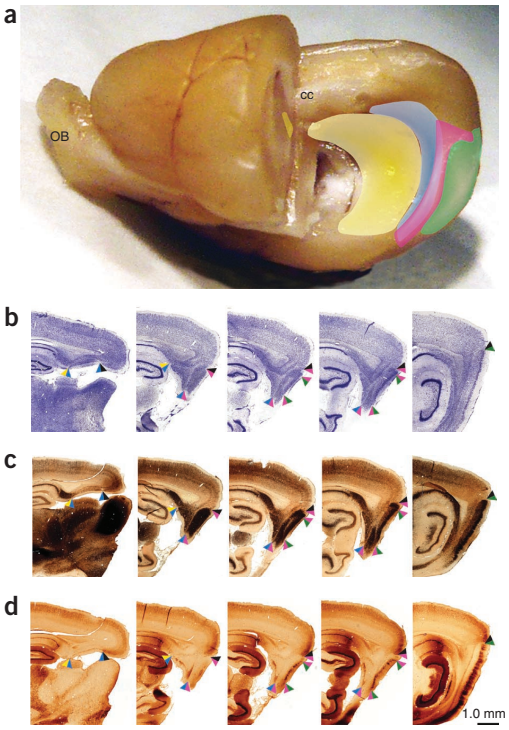

Figure 1 Relative positions of pre- and parasubiculum in the rat brain. (**a**) Ventral-lateral view of a whole rat brain, with partial removal of the posterior half of the left hemisphere to enable a midsagittal view of the right hemisphere. Shown are three-dimensional outlines of hippocampal formation (yellow), presubiculum (blue), parasubiculum (pink) and MEC (green) in the right hemisphere. cc, corpus callosum; OB, olfactory bulb. (**b**) Nissl-stained sagittal sections arranged from medial (left) to lateral (right) to show the positions of presubiculum, parasubiculum and MEC. (**c**) Sagittal sections stained for parvalbumin (same brain as in **b**; adjacent sections). Note the dark staining of superficial layers of MEC and parasubiculum (see **Supplementary Fig. 1** for an outline of parahippocampal subregions and layers). (**d**) Sagittal sections stained for calbindin (same brain as in **b** and **c**, adjacent sections). Calbindin staining was absent in parasubiculum, whereas layer II of MEC and presubiculum showed relatively strong staining. The calbindin stains clearly show that the parasubiculum curves around the dorsal end of MEC, with a small portion of parasubiculum appearing dorsal to the superficial layers of MEC on a limited range of sagittal sections. Arrowheads in **b**–**d** indicate borders of hippocampus (subiculum, yellow), presubiculum (blue), parasubiculum (pink), MEC (green) and other regions (black).

RESULTS

Histological borders, tetrode localization and cell sample

To determine the exact location of the tetrodes in the various subdivisions of the parahippocampal cortex (**Fig. 1a**), we first established histological landmarks that are visible with Nissl staining (**Fig. 1b**). The clearest distinction is between the hippocampus (subiculum) and the parahippocampal areas. The hippocampus is a three-layered cortex, whereas parahippocampal areas have six layers, with superficial cell layers (II and III) separated from deep layers (V and VI) by the thin, cell-sparse lamina dissecans (layer IV). Nissl stains show clear differences between the superficial layers of presubiculum, parasubiculum and MEC[12]. Cell bodies in superficial layers of presubiculum were smaller and more compact than in MEC and parasubiculum. Layers II and III were clearly separable in MEC and dorsal presubiculum, with layer II showing denser staining than layer III. In the parasubiculum, this laminar differentiation was virtually absent and layers II and III showed markedly similar cell sizes, packing densities and staining for Nissl substance (**Fig. 1b**).

Cytoarchitectonic features are less informative about borders in the deep parahippocampal layers. To distinguish regional borders in all layers, we immunostained sections for parvalbumin (**Fig. 1c**) and calbindin (**Fig. 1d**), which are differentially expressed in the interneuron populations of hippocampal and parahippocampal subregions. Parvalbumin immunoreactivity changed from intense in MEC layer II to weak in deep layers of parasubiculum (**Fig. 1c** and **Supplementary Fig. 1**). Calbindin staining was strong in layer II of PrS and MEC, weak in the other layers of these two areas and completely absent in parasubiculum (**Fig. 1d**).

On the basis of the histological criteria developed above, a total of 1,182 well-isolated cells was estimated to be recorded from dorsal pre- and parasubiculum in 13 rats (17 hemispheres). All recordings were made during food-motivated running in square or circular open fields. We assigned 654 cells from seven rats to the presubiculum and 528 cells, also from seven rats, to the parasubiculum. The recording positions were distributed across all principal cell layers of pre- and parasubiculum (**Supplementary Fig. 2**). The data from pre- and parasubiculum were compared with a sample of 630 cells from MEC (15 rats). The entorhinal cells were taken from a previous study[16] and reanalyzed with criteria and procedures identical to those used for pre- and parasubiculum. Separation of spike clusters was not different in pre- and parasubiculum (**Supplementary Fig. 3**). Clusters in these areas were slightly better separated than in MEC (**Supplementary Fig. 3**).

Grid cells

Grid cells were observed in presubiculum (**Fig. 2**) and parasubiculum (**Fig. 3**). Both regions contained cells with multiple discrete firing fields organized in a hexagonal pattern across the space covered by the rat during the recording trial. The regular spacing of the firing fields was verified by spatial autocorrelation analyses[15,16], which, for all grid cells, showed a periodic hexagonal pattern similar to that of the rate maps (**Figs. 2**–**4**; the ten cells with the highest grid scores in each area are shown in **Supplementary Figs. 4** and **5**).

To quantify the hexagonal periodicity of pre- and parasubiculum cells, we computed a grid score for each cell by first taking a circular sample of the autocorrelogram, centered on the central peak, but with the central peak itself excluded, and then comparing rotated versions of this sample[16] (**Supplementary Fig. 6**). The Pearson correlation of this circle, with its rotation in α degrees, was obtained for angles of 60° and 120°, and for 30°, 90° and 150°. The cell's grid score was defined as the minimum difference between any of the elements in the first group and any of the elements in the second. A cell was defined as a grid cell when the grid score exceeded the significance level estimated from shuffled rate maps for all cells recorded in the brain region[27,28]. Shuffling was performed on a cell-by-cell basis. For each trial of the shuffling procedure, the entire sequence of spikes fired by the cell was time-shifted along the rat's path by a random interval between 20 s and 20 s less than the length of the trial, with the end of the trial wrapped to the beginning. This procedure was repeated 100 times for each cell, yielding a total of 65,400 permutations for the 654 presubiculum cells, 52,800 permutations for the 528 parasubiculum cells and 63,000 permutations for the 630 MEC cells. For each permutation, a firing rate map and an autocorrelation map

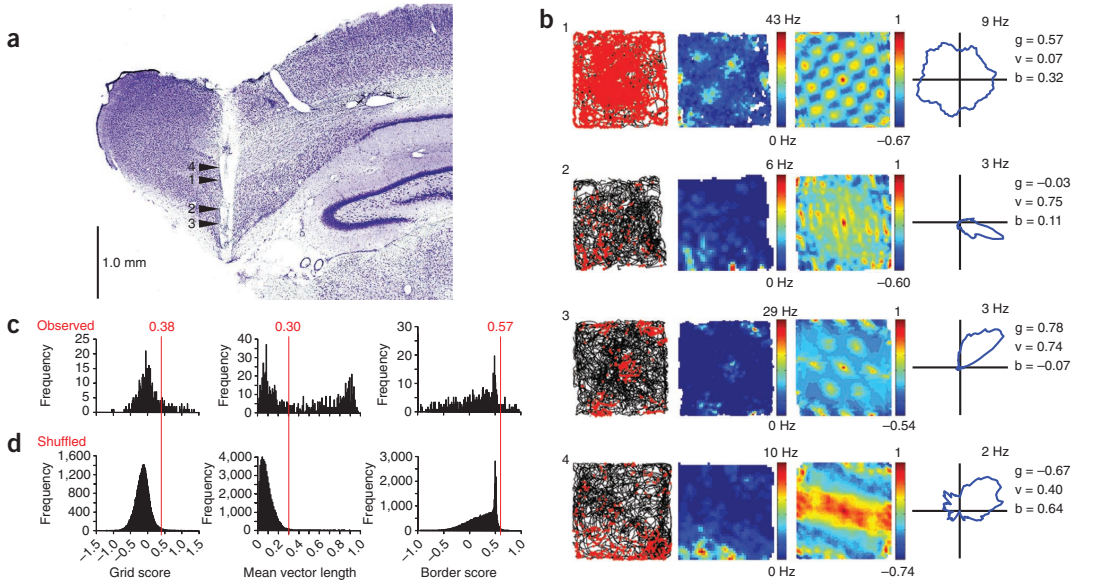

Figure 2 Functional cell types of the presubiculum. (**a**) Nissl-stained sagittal brain section showing location of recording positions (arrowheads) in dorsal presubiculum of a representative rat (**Supplementary Fig. 2** shows the complete set of recording sites). (**b**) Trajectory with spike positions (left), rate maps (middle left), autocorrelation maps (middle right) and directional plots (right) of four representative presubiculum cells recorded during running in an open field. Each row shows data from one cell. The width of the open field was 100 cm (bottom row) or 200 cm (three upper rows). The trajectory in the left diagram is black; firing locations are superimposed in red. Each red dot corresponds to one spike. Rate maps and autocorrelation maps are color-coded, with color scale bars and minimum and maximum values to the right of each map. Pixels not covered are white. The scale of the autocorrelation diagrams is twice the scale of the rate maps (for example, 400 cm versus 200 cm side lengths in the three upper plots). The directional plots show firing rate as a function of head direction. Grid scores (g), mean vector length (v) and border scores (b) are provided for each cell to the right of the polar plot. Note presence of grid cells (1), head-direction cells (2), conjuctive head-direction × grid cells (3) and border cells (4) in the presubiculum. Numbers refer to recording sites in **a**. (**c**) Distribution of grid scores, mean vector length and border scores for the entire sample of presubiculum cells (top, observed), as well as randomly shuffled rate maps from the same sample of presubiculum cells (bottom, shuffled; 65,400 permutations). Red line and number indicate 99th percentile for the shuffled data. Note the abundance of presubiculum cells with grid, head-direction and border scores above the 99th percentile level.

were constructed and a grid score was calculated. The 99th percentile was read out from the overall distribution of grid scores in the shuffled data for each region. Grid cells were then defined as cells in the recorded data that had grid scores higher than the 99th percentile of the shuffled data for the respective region (for 95th percentile thresholds, see **Supplementary Fig. 7**).

Using these criteria, we found 84 grid cells in the presubiculum, corresponding to 12.8% of the cell sample in this area, and 107 in the parasubiculum, corresponding to 20.3% (**Figs. 2** and **3**; **Supplementary Fig. 7**). These numbers are significantly larger than expected by random selection from the shuffled distribution (presubiculum, $Z = 30.4$, $P < 0.001$; parasubiculum, $Z = 44.5$, $P < 0.001$; large-sample binomial tests with expected P_0 of 0.01). The proportion of grid cells was lower in presubiculum than in parasubiculum ($Z = 3.45$, $P < 0.001$) and lower in both pre- and parasubiculum than in MEC (222 of 630 cells, 35.2%; presubiculum versus MEC, $Z = 9.42$, $P < 0.001$; parasubiculum versus MEC, $Z = 5.63$, $P < 0.001$; **Fig. 4**). Cells with high grid scores were found in all three areas (**Figs. 2c**, **3c** and **4c**, and **Supplementary Figs. 4** and **5**); however, the mean scores of those cells that passed the 99th-percentile criterion were significantly lower in presubiculum than in parasubiculum (0.715 ± 0.029 versus 0.852 ± 0.027, $t_{189} = 3.47$, $P < 0.001$) and MEC (0.938 ± 0.019, $t_{304} = 6.22$, $P < 0.001$) and lower in parasubiculum than in MEC ($t_{327} = 2.56$, $P = 0.01$). Grid cells were present in all layers of pre- and parasubiculum (**Supplementary Figs. 8** and **9**). The uniformity across layers in these areas contrasted with the distribution in MEC, where the proportion of grid cells was significantly higher in superficial than in deep layers (layer II, 50.0%; layer III, 46.7%; layer V, 21.5%; layer VI, 25.0%; superficial versus deep, $Z = 6.00$, $P < 0.001$; **Fig. 5**).

The local organization of grid cells in pre- and parasubiculum shared many features with the grid-cell network in MEC[15,16]. As in MEC, the grid phase was distributed; that is, the vertices of co-localized grid cells were generally offset relative to each other (**Fig. 6a–c**). Grid orientation and grid spacing were relatively constant between colocalized neurons in all three areas (average s.d. for simultaneously recorded cells in presubiculum, parasubiculum and MEC were 6.9 ± 1.7, 6.0 ± 1.1 and 4.4 ± 0.6 degrees, respectively, for grid orientation and 13.7 ± 4.4, 10.2 ± 1.8 and 10.0 ± 1.2 cm, respectively, for grid spacing; $t < 2.33$, $P > 0.05$ after correction for multiple comparisons; **Fig. 6d**). The mean values for grid spacing were 68.9 ± 3.1, 67.3 ± 1.9 and 69.9 ± 3.0 cm, respectively.

Head-direction cells

The majority of the presubiculum cells were modulated by head direction (**Fig. 2**), as expected[11]. Direction-modulated cells were also abundant in the parasubiculum (**Fig. 3**). Many head-direction cells in these two regions also satisfied the criterion for grid cells, mirroring

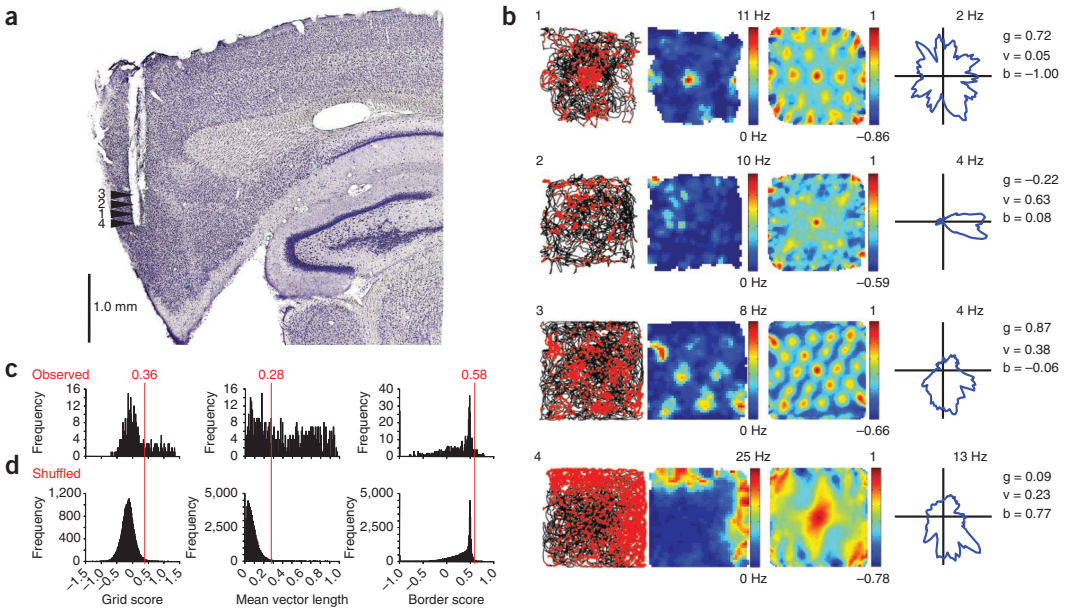

Figure 3 Functional cell types of the parasubiculum. (**a**) Nissl-stained sagittal brain section showing location of recording positions (arrowheads) in the dorsal parasubiculum of a representative rat (for recording sites in other rats, see **Supplementary Fig. 2**). (**b**) Trajectory maps (left), rate maps (middle left), autocorrelation maps (middle right) and directional plots (right) of representative parasubiculum cells. Data are presented as in **Figure 2**. The width of the open field was 100 cm. The parasubiculum contained grid cells (1), head-direction cells (2), conjunctive head-direction × grid cells (3) and border cells (4). Numbers refer to recording sites in **a**. (**c**) Distribution of grid scores, mean vector length and border scores for the entire sample of parasubiculum cells (top, observed), as well as randomly shuffled rate maps from the same sample of parasubiculum cells (bottom, shuffled; 52,800 permutations). Red lines indicate 99th percentile for the shuffled data; values are indicated. Note the abundance of grid cells, head-direction cells and border cells (cells with scores above the 99th percentile significance level).

the 'conjunctive' firing properties of layer III-VI cells in MEC (**Fig. 4**; the ten cells with the strongest directional modulation in each area are shown in **Supplementary Figs. 10** and **11**).

The directional modulation of each individual cell was quantified by computing the length of the mean vector (the Rayleigh vector) for the distribution of firing rate across all head directions. A cell was classified as being direction modulated if the mean vector length exceeded the 99th percentile of a distribution of mean vector lengths for shuffled data generated from the entire set of cells recorded in the relevant brain area[27,28]. Of the 654 cells, 351 passed this criterion in the presubiculum (53.7%), as did 309 out of 528 cells in the parasubiculum (58.5%) and 240 out of 435 cells in MEC (55.1%). These proportions are substantially larger than expected by random selection from the shuffled distribution (presubiculum, $Z = 135.4$, $P < 0.001$; parasubiculum, $Z = 132.8$, $P < 0.001$; MEC, $Z = 113.6$, $P < 0.001$). The proportion of head-direction cells did not vary between areas ($Z < 1.67$, $P > 0.05$), but the laminar organization differed. Superficial and deep layers of pre- and parasubiculum had similar numbers of directional cells (**Supplementary Figs. 8** and **9**), whereas the number was substantially lower in the superficial layers of MEC, with almost no directional cells in layer II (**Fig. 5**).

Although sharply tuned head-direction cells existed in all regions (**Figs. 2c**, **3c** and **4c**, and **Supplementary Figs. 10** and **11**), the sensitivity to direction in such cells was, on average sharper, in presubiculum than in parasubiculum and MEC (mean vector length, 0.727 ± 0.010 versus 0.632 ± 0.011 and 0.612 ± 0.012, respectively, $t_{658} = 6.51$, $P < 0.001$ and $t_{589} = 6.87$, $P < 0.001$; half-width of the directional tuning curve, 53.0 ± 1.4 versus 67.4 ± 1.9 and 66.5 ± 2.3 degrees, respectively, $t_{655} = 6.49$, $P < 0.001$ and $t_{586} = 5.47$, $P < 0.001$). Head-direction cells in parasubiculum and MEC were not different ($t < 0.70$). In all three regions, the distribution of head direction scores had a bimodal shape (**Figs. 2c**, **3c** and **4c**). The lower limit of the cluster of highly directional cells in these distributions corresponded approximately to the 99th percentile of the shuffled distribution. Taken together, the observations suggest that head-direction cells are abundant across all areas of the parahippocampal cortex, but the directional tuning is stronger in presubiculum than parasubiculum and MEC.

A considerable fraction of head-direction cells in pre- and parasubiculum also satisfied the criterion for grid cells (**Figs. 2b**, **3b** and **4b**). The proportion of such conjunctive cells[16] in the head direction–modulated cell population was lower in presubiculum than in parasubiculum (8.5% versus 20.7%, $Z = 4.46$, $P < 0.001$). Conjunctive cells were present in similar numbers in deep layers of MEC (layer V, 22.5%; layer VI, 9.0%). The largest proportion of conjunctive cells was recorded in layer III of MEC (50.6% of the head-direction cells). In presubiculum and MEC, the directional tuning of head-direction cells with a grid correlate was lower than that of head-direction cells with no such correlate (**Supplementary Fig. 4**).

Border cells

Border cells fire when the animal is close to one or several local boundaries of the environment, such as the walls of the recording box[17,18]. We identified border cells by computing, for each cell, the difference between the maximal length of a wall touching on a single

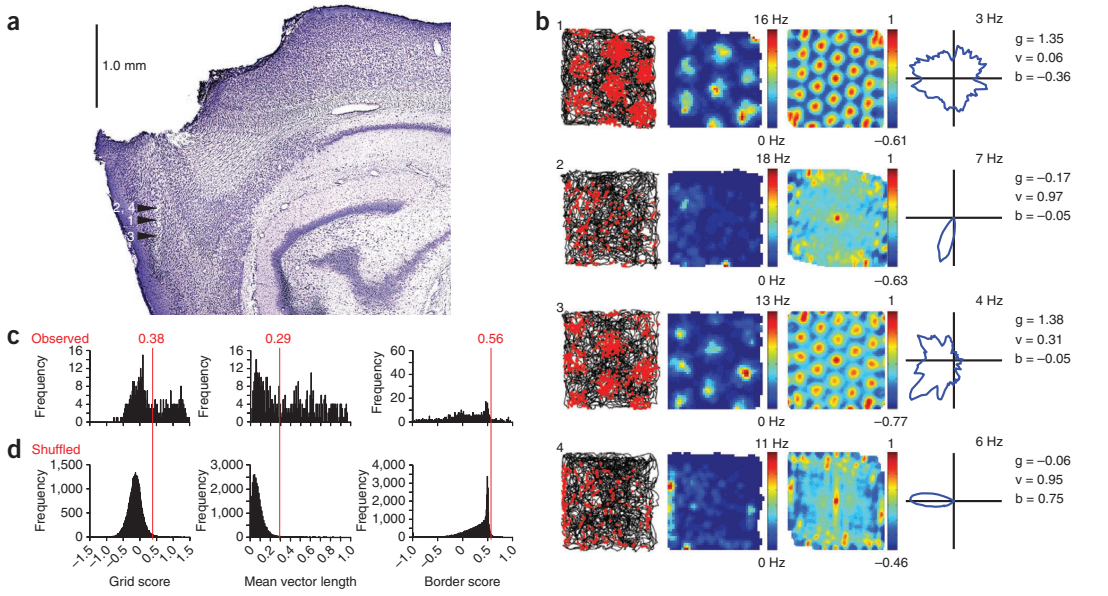

Figure 4 Functional cell types of MEC[16]. (**a**) Nissl-stained sagittal brain section showing location of recording positions (arrowheads) in the dorsal MEC of a representative rat. (**b**) Trajectory maps (left), rate maps (middle left), autocorrelation maps (middle right) and directional plots (right) of representative MEC cells. Data are presented as in **Figure 2**. The width of the open field was 100 cm. Note existence of grid cells (1), head-direction cells (2), conjunctive head-direction × grid cells (3) and border cells (4). Numbers refer to recording sites in **a**. (**c**) Distribution of grid scores, mean vector length and border scores for the entire sample of MEC cells (top, observed), as well as randomly shuffled rate maps from the same sample of MEC cells (bottom, shuffled; 63,000 permutations). Red lines indicate 99th percentile for the shuffled data; values are indicated.

firing field and the average distance of the firing locations from the nearest wall, divided by the sum of those values[17]. A cell was classified as a border cell if this border score was larger than the 99th percentile of a distribution of border scores for shuffled data generated from the entire set of cells recorded in the relevant brain region.

Of 654 cells, 59 passed the 99th percentile criterion in the presubiculum (9.0%; **Fig. 2**), as did 28 of 528 cells in the parasubiculum (5.3%; **Fig. 3**). This is a significantly larger fraction than expected by random selection from the shuffled distribution (presubiculum, $Z = 20.6$, $P < 0.001$; parasubiculum, $Z = 9.94$, $P < 0.001$; large-sample binomial tests with expected P_0 of 0.01; the five cells with the highest border scores in each area are shown in **Supplementary Figs. 12** and **13**). The proportion of border cells in these regions was comparable to the proportion estimated in the MEC sample (40 of 630 cells, 6.3%, $Z = 13.5$, $P < 0.001$, binomial tests with P_0 of 0.01; **Fig. 4**).

Theta rhythmicity

Theta rhythmicity was observed in the local field potential in pre- and parasubiculum, as well as MEC (peak frequencies of 6.97 ± 0.13, 7.84 ± 0.05 and 7.91 ± 0.07 Hz, respectively). Individual cells were defined as being theta modulated if the mean spectral power within 1 Hz of the peak in the 4–11-Hz frequency range of the spike-train autocorrelogram was at least fivefold greater than the mean spectral power between 0 and 125 Hz[27,28]. Following this criterion, 26.3% of the cells in presubiculum, 44.7% in parasubiculum and 55.6% in MEC were theta modulated (**Fig. 7** and **Supplementary Fig. 14**).

The fraction of theta-modulated cells was significantly lower in presubiculum than in parasubiculum ($Z = 6.61$, $P < 0.001$) and significantly lower in parasubiculum than in MEC ($Z = 3.68$, $P < 0.001$). In MEC, the percentage increased from deep to superficial (layer VI, 32.5%; layer V, 34.2%; layer III, 77.0%; layer II, 85.4%; deep versus superficial, $Z = 11.6$, $P < 0.001$; **Fig. 8**). Strong theta modulation was primarily observed in grid cells, although some head-direction cells and border cells were theta rhythmic in all three regions (**Fig. 7** and **Supplementary Figs. 14** and **15**). Theta phase locking, estimated for each cell as the length of the mean vector for the distribution of firing rate across the 360 degrees of the theta cycle, was strong in parasubiculum and some layers of MEC, but weak in presubiculum (**Supplementary Fig. 14**).

DISCUSSION

We found that grid cells are not exclusive to MEC. Grid cells were abundant in dorsal pre- and parasubiculum, although, on average, grid cells in these regions exhibited weaker rotational symmetry than their entorhinal counterparts. Grid cells in pre- and parasubiculum were colocalized with head-direction cells and border cells and many of the grid cells were conjunctively modulated by head direction, as in layers III–VI of MEC[16,17]. Colocalized grid cells had fields with relatively similar spacing and orientation. Our results clearly suggest that the distribution of functional cell types does not follow the intrinsic cytoarchitectural borders of the parahippocampal cortex; each functional cell type was expressed across an extended region including MEC, presubiculum and parasubiculum.

We found that place and direction are represented in overlapping regions of the parahippocampal cortex. Our data reinforce that of early studies suggesting that the presubiculum contains a functionally diverse cell population, with head-direction cells corresponding to only one subset of the neural population[11]. The presence of grid cells in pre- and parasubiculum is also consistent with later studies

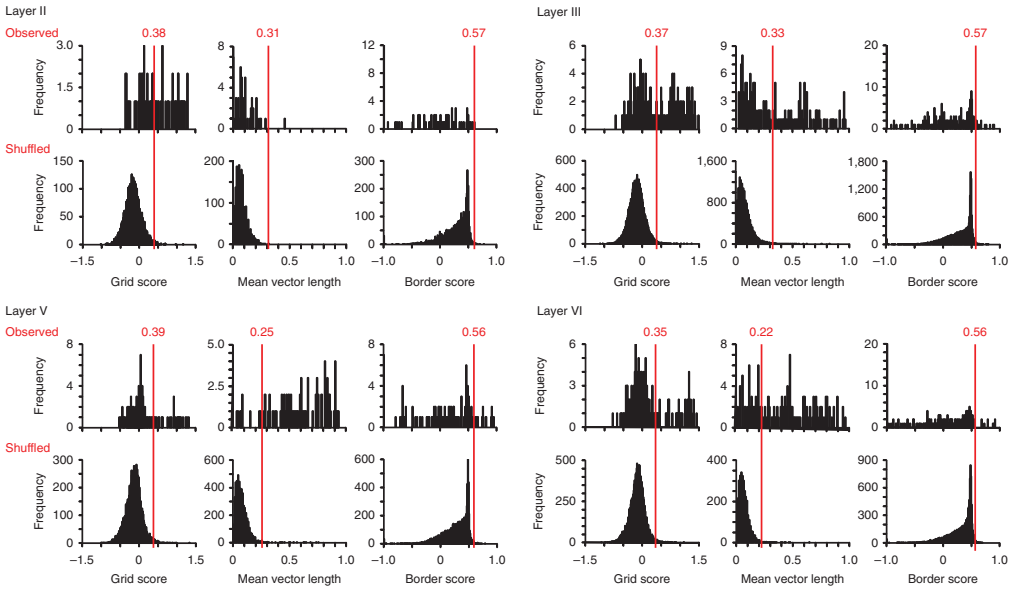

Figure 5 Distribution of grid scores, mean vector length and border scores for the 630 MEC cells[16], sorted by layers. In each panel, the top row shows the distributions of values in the recorded data, whereas the bottom row shows the corresponding distributions for randomly shuffled rate maps from all cells in the respective layers. The red lines indicate the 99th percentile values. The largest proportion of grid cells was recorded in layer II, followed by layer III. Layer II did not have more directional cells than would be expected by chance.

that found place-specific firing patterns in these regions. Place-modulated cells with large and distributed firing fields have been observed in both presubiculum[29,30] and parasubiculum[29,31–33]. The recording environments used in those studies were generally too small to determine whether the firing fields represented individual nodes of a periodic grid; however, the conjunction of directional and place-specific firing in many of these cells[29,32] and the presence of strong theta modulation in those neurons[29] suggests that the data originate from the same functional cell population as the one that we examined. Taken together, these findings indicate that the majority of pre- and parasubiculum neurons have properties similar to layer III–VI cells of MEC.

Despite the functional similarity of cell types in MEC and pre- and parasubiculum, quantitative differences were present (**Fig. 8**). First, for grid cells, there was a clear difference between superficial layers of MEC and the rest of the parahippocampal circuit. Although cells with markedly regular grid patterns were present in all of the subregions, the number of grid cells decreased

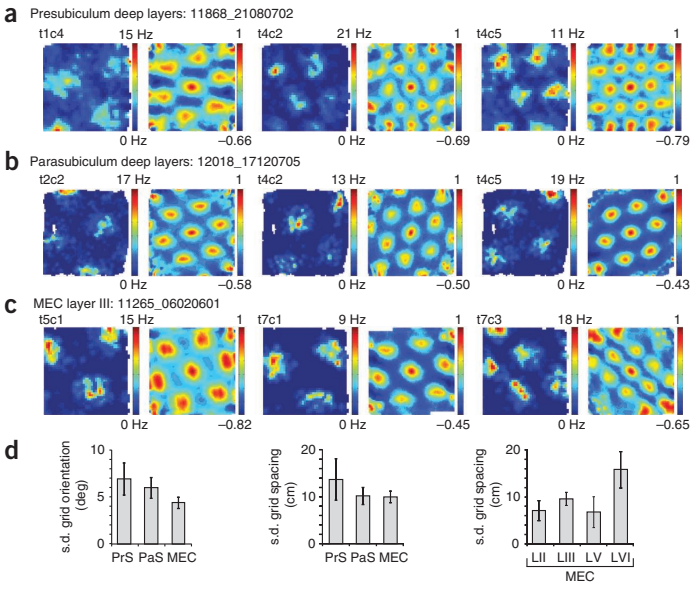

Figure 6 Grid spacing and grid orientation in local ensembles of grid cells in presubiculum and parasubiculum. (**a**–**c**) Representative rate and autocorrelation maps for three simultaneously recorded grid cells (**a**, presubiculum; **b**, parasubiculum; **c**, MEC; rat, trial and cell number are indicated). The width of the open field was 100 cm in **a** and **c** and 150 cm in **b**. Colocalized grid cells had relatively similar grid orientation and grid scale[15]. (**d**) s.d. of grid orientation and grid spacing for sets of simultaneously recorded colocalized cells in presubiculum (PrS), parasubiculum (PaS) and MEC (mean ± s.e.m.; right panel shows layers of MEC). Average values for grid spacing were similar.

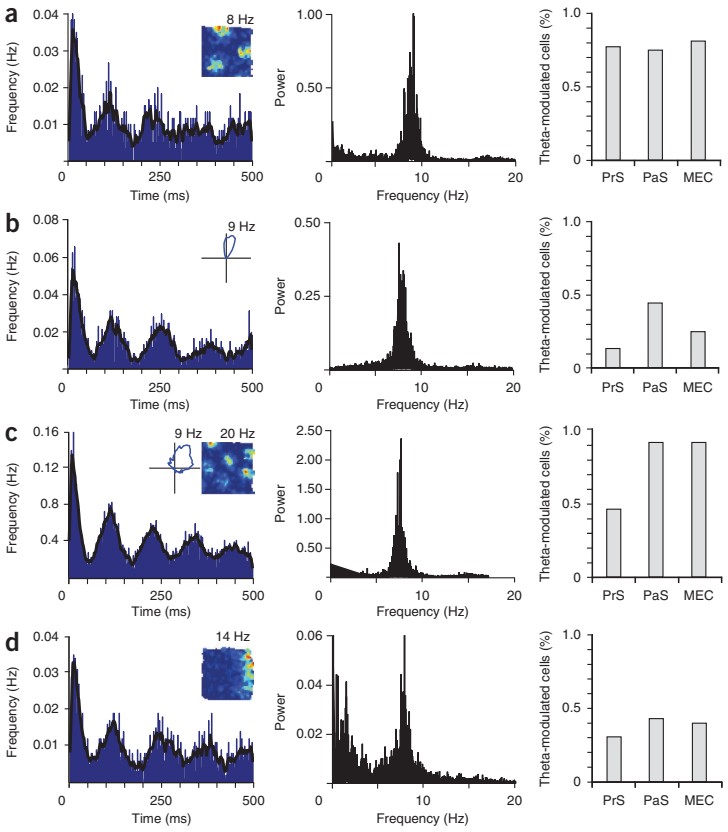

Figure 7 Theta modulation of functional cell types in presubiculum, parasubiculum and MEC. (**a**–**d**) Four theta-modulated cells are shown (**a**, grid cell; **b**, head-direction cell; **c**, conjuctive head-direction × grid cell; **d**, border cell). Left to right, panels show spike-time autocorrelation diagrams (inserts, spatial or directional rate maps), EEG power spectra and percentages of theta-modulated cells in each parahippocampal region. The width of the test box was 100 cm in each case.

from layers II, III to layers V, VI of MEC. In addition, the average rotational symmetry of the grid fields decreased from MEC to para- and presubiculum. This reduction was accompanied by a decrease in theta rhythmicity. In each region, theta modulation correlated strongly with grid scores. The decline in theta-grid activity was paralleled by an increase in directional modulation; directional tuning was weakest in layer II of MEC and sharpest in the presubiculum. These patterns are consistent with observations of covariance between grid scale and intracellular theta frequency[34] and suggest a mechanistic link between theta rhythms and grid patterns[21,22]. They also suggest that the representation of head direction is uncoupled from the theta rhythm.

Although the mechanisms for grid and head direction signals have not been determined, our findings may provide some clues about the range of network architectures able to generate such discharge patterns. In principle, grid, direction and border patterns in pre- and parasubiculum could be inherited passively from parent cells with similar properties in the MEC[15–17] or, for border cells, from boundary-associated cells in the subiculum[35]. The relatively weak nature of the projection from MEC to pre- and parasubiculum[36,37] speaks against inheritance in this direction. Instead, projection cells in pre- or parasubiculum may impose firing patterns on cells in MEC, in the direction where connections are stronger[37]. This would require a symmetry-enhancing mechanism in MEC as well as a mechanism for maintaining precise grid and direction patterns in the presence of competing inputs from the local network or from other brain regions. A third, and possibly more likely, scenario is that grid and direction correlates are generated locally in each parahippocampal region. This would suggest that such discharge phenotypes can be expressed by a relatively broad variety of network morphologies. By identifying the common properties of these networks, it may be possible to determine the necessary conditions for the observed firing profiles. It is currently not known whether the three parahippocampal regions share a common set of wiring principles; however, recurrent connectivity has been reported both in some layers of MEC[38–40] and in the presubiculum and parasubiculum[41,42]. Moreover, in all three regions, individual cells exhibit strong theta modulation and the theta modulation is correlated with periodic firing fields. Intracellular subthreshold theta oscillations have been reported in principal cells of MEC[43] as well as the parasubiculum[44,45], suggesting that grid patterns may be linked mechanistically to the ability of individual cells to uncouple from the field theta rhythm[21,22]. Another point of convergence includes the reduced frequency adaptation[46] and persistent firing[47] of cells in the presubiculum, which is reminiscent of the lack of adaptation described in layers III–VI of the MEC[48]. Persistent firing may contribute to directional tuning as well as grid fields[49]. Finally, all three areas interface inputs from the subiculum

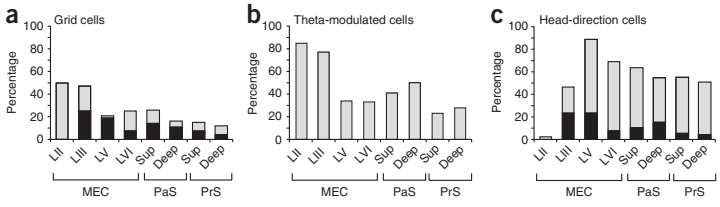

Figure 8 Distribution of grid cells, theta-modulated cells and head direction–modulated cells in the parahippocampal cortex. (**a**–**c**) The distributions of each cell type across layers of MEC, presubiculum and parasubiculum are shown (**a**, grid cells; **b**, theta-modulated cells; **c**, head-direction cells). The subset of cells with conjunctive grid × head-direction properties are indicated in dark gray in **a** and **c**. Note the parallel decrease in numbers of grid cells and theta-modulated cells from the superficial (sup) layers of MEC to the deep MEC layers and the pre- and parasubiculum.

with signals from anterior and midline nuclei of the thalamus and the retrosplenial cortex[12], although only MEC receives direct input from CA1 of the hippocampus. The critical common properties of the three networks remain to be identified, but the characterization of a joint pool of grid cells and head-direction cells in architecturally diverse subdivisions of the parahippocampal cortex constrains the range of mechanisms that could give rise to their unique functional discharge phenotypes.

METHODS

Methods and any associated references are available in the online version of the paper at http://www.nature.com/natureneuroscience/.

Note: Supplementary information is available on the Nature Neuroscience website.

ACKNOWLEDGMENTS

We thank R. Skjerpeng for programming, D. Derdikman for help with code, J. Ainge for donating an implanted rat, and A.M. Amundgård, I. Hammer, K. Haugen, K. Jenssen and H. Waade for technical assistance. This work was supported by the Kavli Foundation and a Centre of Excellence grant from the Norwegian Research Council.

AUTHOR CONTRIBUTIONS

C.N.B., F.S., M.P.W., E.I.M. and M.-B.M. planned and interpreted the study. M.-B.M. provided training and supervision. C.N.B., F.S. and T.S. performed surgeries. C.N.B. and M.P.W. performed histological reconstructions. C.N.B., F.S., V.H.T. and T.S. recorded the data. C.N.B., F.S., E.I.M. and M.-B.M. carried out the analyses. C.N.B. and E.I.M. wrote the paper. Data from a previous study[16] were reanalyzed by C.N.B. and E.I.M.

COMPETING FINANCIAL INTERESTS

The authors declare no competing financial interests.

Published online at http://www.nature.com/natureneuroscience/.
Reprints and permissions information is available online at http://www.nature.com/reprintsandpermissions/.

1. Tolman, E.C. Cognitive maps in rats and men. *Psychol. Rev.* **55**, 189–208 (1948).
2. Moser, E.I., Kropff, E. & Moser, M.-B. Place cells, grid cells, and the brain's spatial representation system. *Annu. Rev. Neurosci.* **31**, 69–89 (2008).
3. Whitlock, J.R., Sutherland, R.J., Witter, M.P., Moser, M.B. & Moser, E.I. Navigating from hippocampus to parietal cortex. *Proc. Natl. Acad. Sci. USA* **105**, 14755–14762 (2008).
4. O'Keefe, J. & Dostrovsky, J. The hippocampus as a spatial map. Preliminary evidence from unit activity in the freely-moving rat. *Brain Res.* **34**, 171–175 (1971).
5. O'Keefe, J. & Conway, D.H. Hippocampal place units in the freely moving rat: why they fire where they fire. *Exp. Brain Res.* **31**, 573–590 (1978).
6. Muller, R.U. & Kubie, J.L. The effects of changes in the environment on the spatial firing of hippocampal complex-spike cells. *J. Neurosci.* **7**, 1951–1968 (1987).
7. Leutgeb, S., Leutgeb, J.K., Treves, A., Moser, M.-B. & Moser, E.I. Distinct ensemble codes in hippocampal areas CA3 and CA1. *Science* **305**, 1295–1298 (2004).
8. O'Keefe, J. & Nadel, L. *The Hippocampus as a Cognitive Map* (Clarendon Press, Oxford University Press, Oxford, 1978).
9. Colgin, L.L., Moser, E.I. & Moser, M.-B. Understanding memory through hippocampal remapping. *Trends Neurosci.* **31**, 469–477 (2008).
10. Ranck, J.B. Head direction cells in the deep cell layer of dorsal presubiculum in freely moving rats. in *Electrical Activity of the Archicortex* (eds. G. Buzsáki & C.H. Vanderwolf) 217–220 (Akademiai Kiado, Budapest, 1985).
11. Taube, J.S., Muller, R.U. & Ranck, J.B. Jr. Head-direction cells recorded from the postsubiculum in freely moving rats. I. Description and quantitative analysis. *J. Neurosci.* **10**, 420–435 (1990).
12. Witter, M.P. & Amaral, D.G. Hippocampal formation. in *The Rat Nervous System* (ed. G. Paxinos) 637–703 (Academic, San Diego, 2004).
13. Taube, J.S. The head direction signal: origins and sensory-motor integration. *Annu. Rev. Neurosci.* **30**, 181–207 (2007).
14. Fyhn, M., Molden, S., Witter, M.P., Moser, E.I. & Moser, M.B. Spatial representation in the entorhinal cortex. *Science* **305**, 1258–1264 (2004).
15. Hafting, T., Fyhn, M., Molden, S., Moser, M.B. & Moser, E.I. Microstructure of a spatial map in the entorhinal cortex. *Nature* **436**, 801–806 (2005).
16. Sargolini, F. *et al.* Conjunctive representation of position, direction and velocity in entorhinal cortex. *Science* **312**, 758–762 (2006).
17. Solstad, T., Boccara, C., Kropff, E., Moser, M.B. & Moser, E.I. Representation of geometric borders in the entorhinal cortex. *Science* **322**, 1865–1868 (2008).
18. Savelli, F., Yoganarasimha, D. & Knierim, J.J. Influence of boundary removal on the spatial representations of the medial entorhinal cortex. *Hippocampus* **18**, 1270–1282 (2008).
19. Fyhn, M., Hafting, T., Treves, A., Moser, M.B. & Moser, E.I. Hippocampal remapping and grid realignment in entorhinal cortex. *Nature* **446**, 190–194 (2007).
20. McNaughton, B.L., Battaglia, F.P., Jensen, O., Moser, E.I. & Moser, M.-B. Path integration and the neural basis of the "cognitive map". *Nat. Rev. Neurosci.* **7**, 663–678 (2006).
21. Burgess, N., Barry, C. & O'Keefe, J. An oscillatory interference model of grid cell firing. *Hippocampus* **17**, 801–812 (2007).
22. Hasselmo, M.E., Giocomo, L.M. & Zilli, E.A. Grid cell firing may arise from interference of theta frequency membrane potential oscillations in single neurons. *Hippocampus* **17**, 1252–1271 (2007).
23. Fuhs, M.C. & Touretzky, D.S. A spin glass model of path integration in rat medial entorhinal cortex. *J. Neurosci.* **26**, 4266–4276 (2006).
24. Burak, Y. & Fiete, I.R. Accurate path integration in continuous attractor network models of grid cells. *PLOS Comput. Biol.* **5**, e1000291 (2009).
25. Brun, V.H. *et al.* Progressive increase in grid scale from dorsal to ventral medial entorhinal cortex. *Hippocampus* **18**, 1200–1212 (2008).
26. Hafting, T., Fyhn, M., Bonnevie, T., Moser, M.-B. & Moser, E.I. Hippocampus-independent phase precession in entorhinal grid cells. *Nature* **453**, 1248–1252 (2008).
27. Langston, R.F. *et al.* Development of the spatial representation system in the rat. *Science* **328**, 1576–1580 (2010).
28. Wills, T., Cacucci, F., Burgess, N. & O'Keefe, J. Development of the hippocampal cognitive map in preweanling rats. *Science* **328**, 1573–1576 (2010).
29. Cacucci, F., Lever, C., Wills, T.J., Burgess, N. & O'Keefe, J. Theta-modulated place-by-direction cells in the hippocampal formation in the rat. *J. Neurosci.* **24**, 8265–8277 (2004).
30. Taube, J.S. Place cells recorded in the parasubiculum of freely moving rats. *Hippocampus* **5**, 569–583 (1995).
31. Sharp, P.E. Multiple spatial/behavioral correlates for cells in the rat postsubiculum: multiple regression analysis and comparison to other hippocampal areas. *Cereb. Cortex* **6**, 238–259 (1996).
32. Hargreaves, E.L., Yoganarasimha, D. & Knierim, J.J. Cohesiveness of spatial and directional representations recorded from neural ensembles in the anterior thalamus, parasubiculum, medial entorhinal cortex and hippocampus. *Hippocampus* **17**, 826–841 (2007).
33. Hargreaves, E.L., Rao, G., Lee, I. & Knierim, J.J. Major dissociation between medial and lateral entorhinal input to the dorsal hippocampus. *Science* **308**, 1792–1794 (2005).
34. Giocomo, L.M., Zilli, E.A., Fransen, E. & Hasselmo, M.E. Temporal frequency of subthreshold oscillations scales with entorhinal grid cell field spacing. *Science* **315**, 1719–1722 (2007).
35. Lever, C., Burton, S., Jeewajee, A., O'Keefe, J. & Burgess, N. Boundary vector cells in the subiculum of the hippocampal formation. *J. Neurosci.* **29**, 9771–9777 (2009).
36. Köhler, C. Intrinsic connections of the retrohippocampal region in the rat brain. II. The medial entorhinal area. *J. Comp. Neurol.* **246**, 149–169 (1986).
37. van Groen, T. & Wyss, J.M. The connections of presubiculum and parasubiculum in the rat. *Brain Res.* **518**, 227–243 (1990).
38. Klink, R. & Alonso, A. Morphological characteristics of layer II projection neurons in the rat medial entorhinal cortex. *Hippocampus* **7**, 571–583 (1997).
39. Dhillon, A. & Jones, R.S. Laminar differences in recurrent excitatory transmission in the rat entorhinal cortex *in vitro*. *Neuroscience* **99**, 413–422 (2000).
40. Kumar, S.S., Jin, X., Buckmaster, P.S. & Huguenard, J.R. Recurrent circuits in layer II of medial entorhinal cortex in a model of temporal lobe epilepsy. *J. Neurosci.* **27**, 1239–1246 (2007).
41. Köhler, C. Intrinsic projections of the retrohippocampal region in the rat brain. I. The subicular complex. *J. Comp. Neurol.* **236**, 504–522 (1985).
42. Funahashi, M. & Stewart, M. Presubicular and parasubicular cortical neurons of the rat: functional separation of deep and superficial neurons *in vitro*. *J. Physiol. (Lond.)* **501**, 387–403 (1997).
43. Alonso, A. & Llinas, R.R. Subthreshold Na_s-dependent theta-like rhythmicity in stellate cells of entorhinal cortex layer II. *Nature* **342**, 175–177 (1989).
44. Glasgow, S.D. & Chapman, C.A. Local generation of theta-frequency EEG activity in the parasubiculum. *J. Neurophysiol.* **97**, 3868–3879 (2007).
45. Glasgow, S.D. & Chapman, C.A. Conductances mediating intrinsic theta-frequency membrane potential oscillations in layer II parasubicular neurons. *J. Neurophysiol.* **100**, 2746–2756 (2008).
46. Fricker, D., Dinocourt, C., Eugène, E., Wood, J. & Miles, R. Pyramidal cells of rodent presubiculum express a tetrodotoxin-insensitive Na^+ current. *J. Physiol. (Lond.)* **587**, 4249–4264 (2009).
47. Yoshida, M. & Hasselmo, M.E. Persistent firing supported by an intrinsic cellular mechanism in a component of the head direction system. *J. Neurosci.* **29**, 4945–4952 (2009).
48. Egorov, A.V., Hamam, B.N., Fransén, E., Hasselmo, M.E. & Alonso, A.A. Graded persistent activity in entorhinal cortex neurons. *Nature* **420**, 173–178 (2002).
49. Hasselmo, M.E. Grid cell mechanisms and function: contributions of entorhinal persistent spiking and phase resetting. *Hippocampus* **18**, 1213–1229 (2008).

ONLINE METHODS

Subjects and surgeries. Neuronal activity was recorded from 28 male Long-Evans rats (3–5 months old, 350–450 g at implantation, housed and food deprived as in described previously[16]). We recorded activity from either presubiculum or parasubiculum in 13 of the rats. The remaining 15 had recording electrodes in MEC. The data from the MEC rats have been published previously[16], but were reanalyzed with criteria and procedures similar to those used for pre- and parasubiculum to enable direct quantitative comparison. All experiments were approved by the National Animal Research Authority of Norway.

Tetrodes, consisting of four twisted electrodes per microdrive, were implanted at anterior-posterior 0.3–2.4 mm in front of the transverse sinus, mediolateral 3.7–4.5 mm from the midline and dorsovental 1.4–1.8 mm below the dura, depending on the intended target site in pre- or parasubiculum (one or two microdrives per rat[17]). Six pre- or parasubicular implants were angled 8–15 degrees in the anterior direction in the sagittal plane. All entorhinal implants were angled and positioned as described previously[14].

Data collection. General data collection procedures have been described previously[17]. All data from pre- and parasubiculum were tracked with two LEDs, one large and one small, 5–10 cm apart on the head stage (sampling rate of 50 Hz). Approximately 30% of the data from MEC (195 of 630 cells) were collected with one LED only; these data were not included in analyses of modulation by head direction.

The rats collected crumbs of vanilla or chocolate biscuit thrown randomly into a 50-cm-high square or circular box with black floor and black walls surrounded by black curtains. More than 80% of the experiments in each brain region were performed in the square; the remaining data were collected in the circle. The width of the square box was 100 cm. For 26 of the 630 MEC cells and 90 of the 1,182 cells in pre- and parasubiculum, we used a larger box (150, 180 or 220 cm). Ten cells in pre- or parasubiculum were recorded in a small box (50 cm or 70 cm). The diameter of the circular box was 200 cm. The location of the boxes was constant between trials. All boxes were polarized by a white cue card (50 × 50 cm)[17]. Tests in the 100-cm box consisted of two 10-min trials with a 5-min intertrial interval; tests in the larger boxes consisted of two or three consecutive 10-min trials.

Spike sorting, cell classification and rate maps. Spike sorting was performed offline using graphical cluster-cutting software (**Supplementary Fig. 3**). Position estimates were based on tracking of one of the LEDs on the head stage. Only epochs with instantaneous running speeds of 2.5 cm s^{-1} or more were included. To characterize firing fields, we sorted the position data into 2.5 cm × 2.5 cm bins and smoothed the path with a 21-sample boxcar window filter (400 ms, ten samples on each side). Firing-rate distributions were determined for trials with more than 80% coverage by counting the number of spikes in each bin as well as the time spent per bin. Maps for number of spikes and time were smoothed individually using a quasi-Gaussian kernel over the surrounding 5 × 5 bins[27]. Firing rates were determined by dividing spike number and time for each bin of the two smoothed maps. The peak rate was defined as the rate in the bin with the highest rate in the firing rate map.

Analysis of grid cells. The structure of the rate maps was evaluated for all cells with more than 100 spikes by calculating the spatial autocorrelation for each smoothed rate map[16]. The degree of spatial periodicity (gridness or grid scores) was determined for each recorded cell by taking a circular sample of the autocorrelogram, centered on the central peak, but with the central peak excluded, and comparing rotated versions of this sample[16,17] (**Supplementary Fig. 6**). Grid cells were defined as cells in which rotational symmetry–based grid scores exceeded the 99th percentile of a distribution of grid scores for shuffled recordings from the entire population of cells in the same brain region (presubiculum, parasubiculum, or MEC)[27,28]. Details of the shuffling procedure are provided in the main text. For analyses with a 95th percentile threshold, see **Supplementary Figure 7**. The use of a statistical criterion for grid cells differs from previous work defining grid cells as cells with grid scores above a fixed threshold[16,17].

Grid spacing was defined as the radius of the circle around the center of the autocorrelation map that gave the highest grid score. Grid orientation was defined by first establishing vectors from the center of the autocorrelation map to each of the three first vertices of the inner hexagon in the counterclockwise direction, starting from a camera-defined reference line of 0 degrees. The mean orientation of these vectors (with angles α, β and γ) was defined as $(\alpha + (\beta - 60) + (\gamma - 180))/3$. The angle between this orientation and the camera-defined reference line was taken as the orientation of the grid. Grid spacing and grid orientation of simultaneously recorded colocalized grid cells were compared for all trials with two or more simultaneously recorded grid cells.

Analysis of head-direction cells. Directional analyses were only performed for experiments with two LEDs (all cells in pre- and parasubiculum, 435 of the MEC cells). The rat's head direction was calculated for each tracker sample from the projection of the relative position of the two LEDs onto the horizontal plane. The directional tuning function for each cell was obtained by plotting the firing rate as a function of the rat's directional heading, divided into bins of 3 degrees and smoothed with a 14.5-degree mean window filter (14 bins on each side)[27]. To minimize the contribution of inhomogeneous sampling on directional tuning estimates, we accepted data only if all directional bins were covered by the rat.

The strength of directional tuning was estimated by computing the length of the mean vector for the circular distribution of firing rate. Head direction–modulated cells were defined as cells with mean vector lengths significantly exceeding the degree of directional tuning that would be expected by chance[27,28]. Threshold values were determined for each brain region (presubiculum, parasubiculum, MEC) by a shuffling procedure performed in the same way as for grid cells. For each permutation trial, the entire sequence of spikes fired by the cell was time-shifted along the rat's path by a random interval between 20 s on one side and, on the other side, 20 s less than the length of the trial, with the end of the trial wrapped to the beginning, a head-direction tuning curve was then constructed, and the mean vector length was calculated. The distribution of mean vector lengths was computed for the entire set of permutations from all cells in the sample (~60,000 permutations per brain region; 100 permutations per cell). Cells were defined as directionally modulated if the mean vector from the recorded data was longer than the 99th percentile of mean vector lengths in the distribution generated from the shuffled data. Directional tuning was estimated also for each cell by determining the half-width of the directional tuning curve (the width of the region in which the rate was higher than 50% of the peak rate).

Analysis of border cells. Border cells were identified by computing, for each cell, the difference between the maximal length of a wall touching on any single firing field of the cell and the average distance of the field from the nearest wall, divided by the sum of those values[17]. Firing fields were defined as collections of neighboring pixels with firing rates 0.3-fold higher than the cell's peak firing rate that cover a total area of at least 200 cm^2. Border scores ranged from −1 for cells with central firing fields to +1 for cells with fields that perfectly line up along at least one entire wall. Border cells were defined as cells with border scores significantly exceeding the degree of wall-related firing that would be expected by chance. The significance level was determined for each brain region (presubiculum, parasubiculum, MEC) by a shuffling procedure performed for experiments in the square boxes in the same way as for grid cells and head-direction cells. For each permutation trial, the entire sequence of spikes fired by the cell was time-shifted along the rat's path by a random interval between 20 s and 20 s less than the length of the trial, with the end of the trial wrapped to the beginning, a rate map was then constructed and a border score was calculated. The distribution of border scores was computed for the entire set of permutations from all cells in the sample (~60,000 permutations per brain region; 100 per cell) and the 99th percentile was determined. Cells were defined as being directionally modulated if the border score from the recorded data was higher than the 99th percentile for border scores in the distribution generated from the shuffled data.

Theta rhythm and theta modulation. To estimate variations in neural activity across the theta cycle, we filtered local EEG off-line, as described previously[27]. Theta modulation of individual neurons was determined from the Fast Fourier Transform–based power spectrum of the spike-train autocorrelation functions of the cells. A cell was defined as being theta modulated if the mean power within 1 Hz of each side of the peak in the 4–5- to 10–11-Hz frequency range was at least fivefold greater than the mean spectral power between 0 Hz and 125 Hz[27]. Theta phase locking was estimated for each cell as the length of the mean vector for the distribution of firing rate across the 360 degrees of the theta cycle.

Histology and reconstruction of recording positions. Electrodes were not moved after the final recording session. The rats were killed with an overdose of Equithesin and were transcardially perfused with 0.9% saline (wt/vol) followed by 4% formaldehyde (wt/vol). The brains were extracted and stored in 4% formaldehyde. At least 24 h later, the brains were quickly frozen, cut in sagittal sections (30 μm) using a cryostat, mounted and stained with cresyl violet. Every section in the area of the tetrode trace was retained. For some brains, only every third section was used for cresyl violet staining; the other sections were used for parvalbumin and calbindin staining.

Immunostaining was performed on equally spaced series of sagittal sections, cut on a cryostat or freezing sliding microtome. Sections were rinsed three times for 10 min in 125 nM phosphate buffer (pH 7.4) and pre-incubated for 1.5 h in 5% normal goat serum (wt/vol) in a solution of 50 mM Tris, 0.87% NaCl (wt/vol) and 0.5% Triton X-100 (TBS-TX, wt/vol). All rinses in between incubation steps were with TBS-TX. Subsequent to rinsing, sections were incubated with monoclonal mouse primary antibodies to parvalbumin (Sigma-Aldrich P3088, 1:2,000 in TBS-TX) or calbindin (D-28K, Swant, 1:4,000 in TBS-TX) for 48 h at 4 °C. Sections were subsequently incubated in a secondary goat anti mouse antibody coupled to biotin (Sigma Aldrich B7151, 1:100 in TBS-TX for 90 min at 20–22 °C), followed by incubation with the Vector ABC kit according to specifications of the manufacturer (Vector Laboratories, Peroxidase standard PK-Vectastain ABC kit 400). For visualization, sections were rinsed in Tris/HCl solution and subsequently reacted with diaminobenzidine[50]. Sections were mounted on glass slides from a 0.2% gelatin solution and dried. Sections on slides were dehydrated through increasing concentrations of ethanol to xylene and coverslipped with Entellan (Merck).

The positions of the tips of the recording electrodes were determined from digital pictures of the brain sections. The measurements were made using AxioVision (LE Rel. 4.3). A shrinkage coefficient was calculated[17]. The laminar location of the recording electrodes in MEC was determined on the basis of cytoarchitectonic criteria (**Supplementary Fig. 2**).

50. Wouterlood, F.G., Härtig, W., Brückner, G. & Witter, M.P. Parvalbumin-immunoreactive neurons in the entorhinal cortex of the rat: localization, morphology, connectivity and ultrastructure. *J. Neurocytol.* **24**, 135–153 (1995).

doi:10.1038/nn.2602

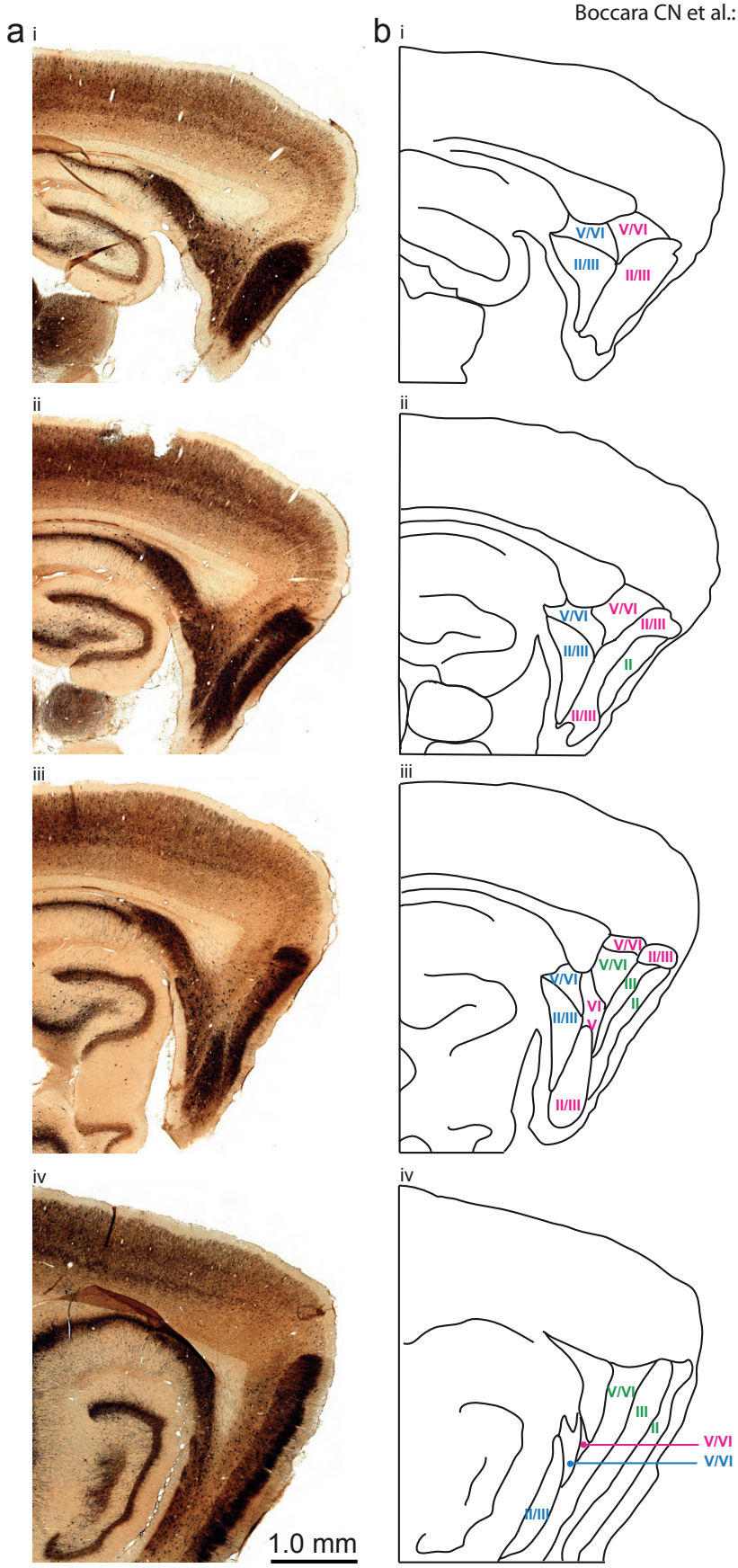

Supplementary Figure 1. Differences in intensity of parvalbumin immunoreactivity. **a**, Series of sagittal sections from medial (i, top) to lateral (iv, bottom) stained for parvalbumin (same sections as in the four panels to the right in Fig. 1c). A gradient of neuropil staining intensity is present, ranging from very dense in MEC layer II, dense in superficial (layer II/III) parasubiculum, moderate in MEC layer III and in both superficial (layer II/III) and deep (layers V/VI) presubiculum, weak in deep (layer V/VI) MEC and deep (layer V/VI) parasubiculum to negative in layer I of all areas. The deep layers of parasubiculum show different staining intensity patterns along the dorsoventral axis. At ventral levels, the staining intensity is uniformly very weak. At most dorsal levels, layer V is slightly darker than layer VI. This is different from the deep layers of MEC, which at all levels show a uniformly weak intensity of staining. All differential staining patterns have been corroborated in series of coronal and horizontal sections (Kjonigsen et al 2009, SFN Abstr 101.11). **b**, Delimitation of the different layers and subdivisons based on parvalbumin staining. MEC layers are labeled in green, parasubiculum layers in pink, presubiculum layers in blue.

Presubiculum layers

Parasubiculum layers

MEC layers

MEC layers were distinguished in the following way: Layer II of MEC is characterized by fairly large, densely packed neurons that stain densely for both parvalbumin and Nissl substance. Layer III is a wider layer consisting of regularly arranged, lightly stained large-to-medium sized cells that are predominantly of the pyramidal type. The deep border of layer III is lamina dissecans (layer IV). Layer V is multi-laminated and comprises different sizes of pyramidal cells that show a radial arrangement. Layer VI comprises a wider variety of neuron-types of different sizes that are oriented parallel to the pial surface.

Supplementary Figure 2, Part 1

Rat 11492 (L), PrS_deep-sup

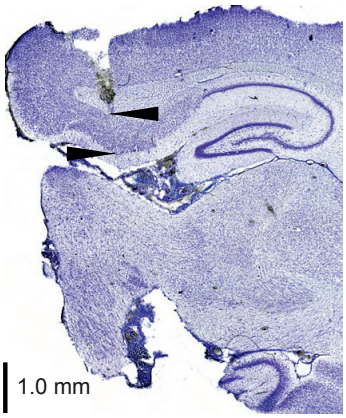

Rat 11492 (R), PrS_deep-sup

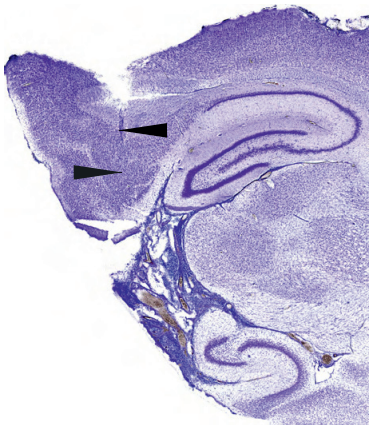

Rat 11539(R), PrS_deep

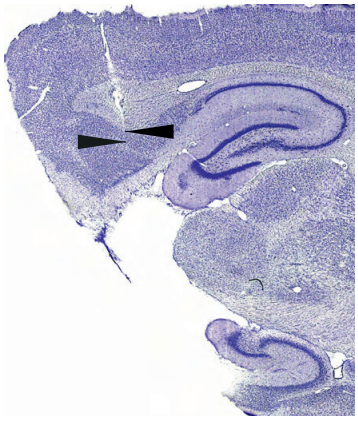

Rat 11573(R), PrS_deep-sup

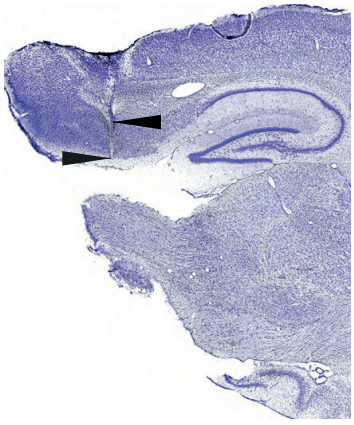

Rat# 11579(L), PrS_deep-sup

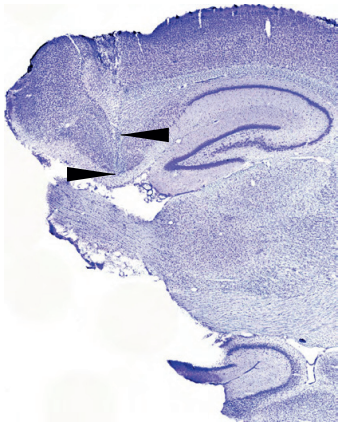

Rat 11579(R), PrS_deep-sup

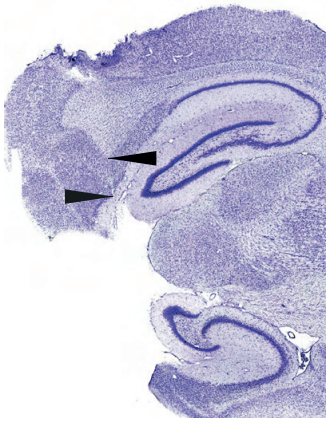

Nature Neuroscience: doi:10.1038/nn.2602

Supplementary Figure 2, Part 2

Rat 11584 (L), PrS_deep-sup

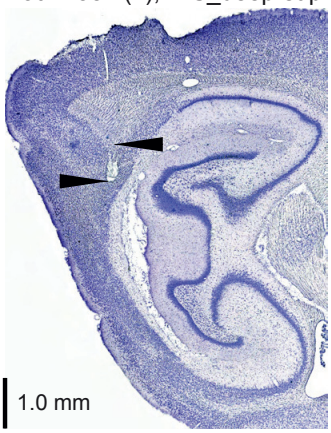

Rat 11584 (R), PrS_deep-sup

Rat 11666(R), PrS_deep-sup

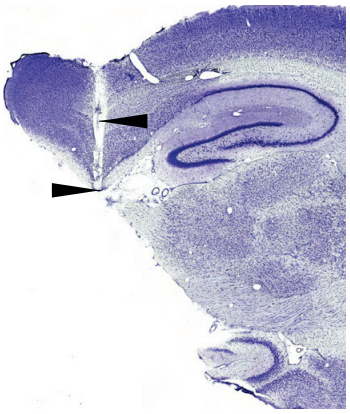

Rat 11868(L), PrS_deep-sup

Rat 11868 (R), PrS_deep-sup, PaS_sup

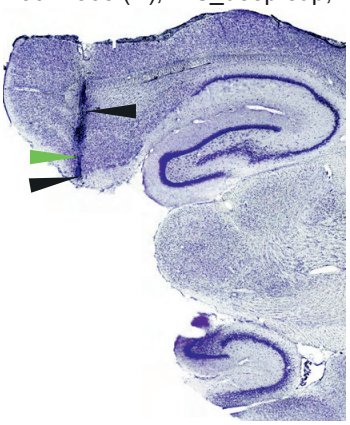

Nature Neuroscience: doi:10.1038/nn.2602

Supplementary Figure 2, Part 3

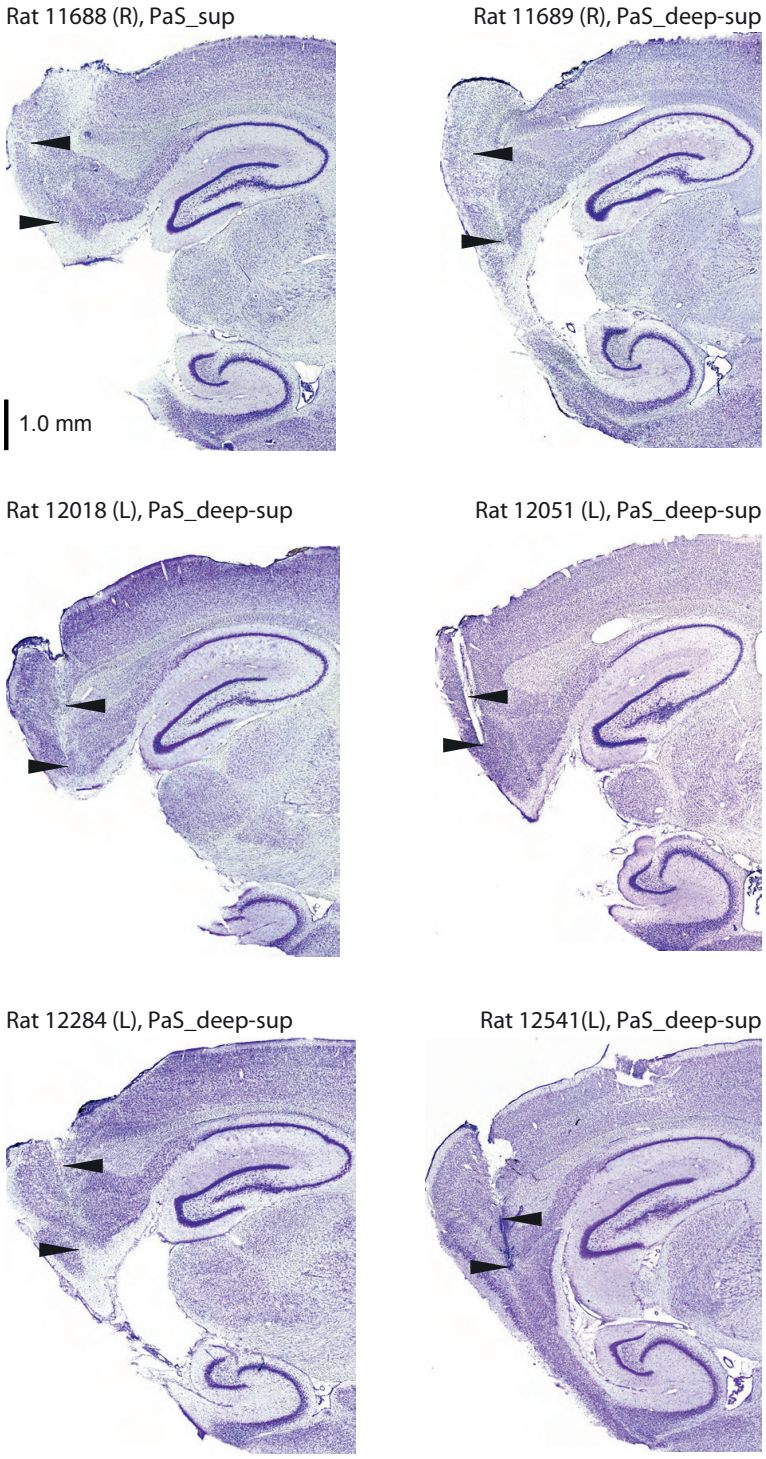

Supplementary Figure 2. Recording locations in presubiculum (part 1-2) and parasubiculum (part 2-3). Sagittal Nissl-stained brain sections show electrode tracks for all rats with recordings in these regions. Start and end recording locations are indicated by black arrowheads. Labels indicate rat number, hemisphere (L, left; R, right), brain area (PrS, presubiculum; PaS, parasubiculum), and whether recordings were obtained from deep and/or superficial (sup) layers. Green arrowhead in Part 2 indicates border between pre- and parasubiculum.

The laminar location of the recording electrodes in PrS, PaS and MEC was determined on the basis of cytoarchitectonic criteria. In pre- and parasubiculum, the superficial layers (II, III) are clearly demarcated from the deeper layers (V, VI) by the presence of the cell-sparse lamina dissecans.

Nature Neuroscience: doi:10.1038/nn.2602

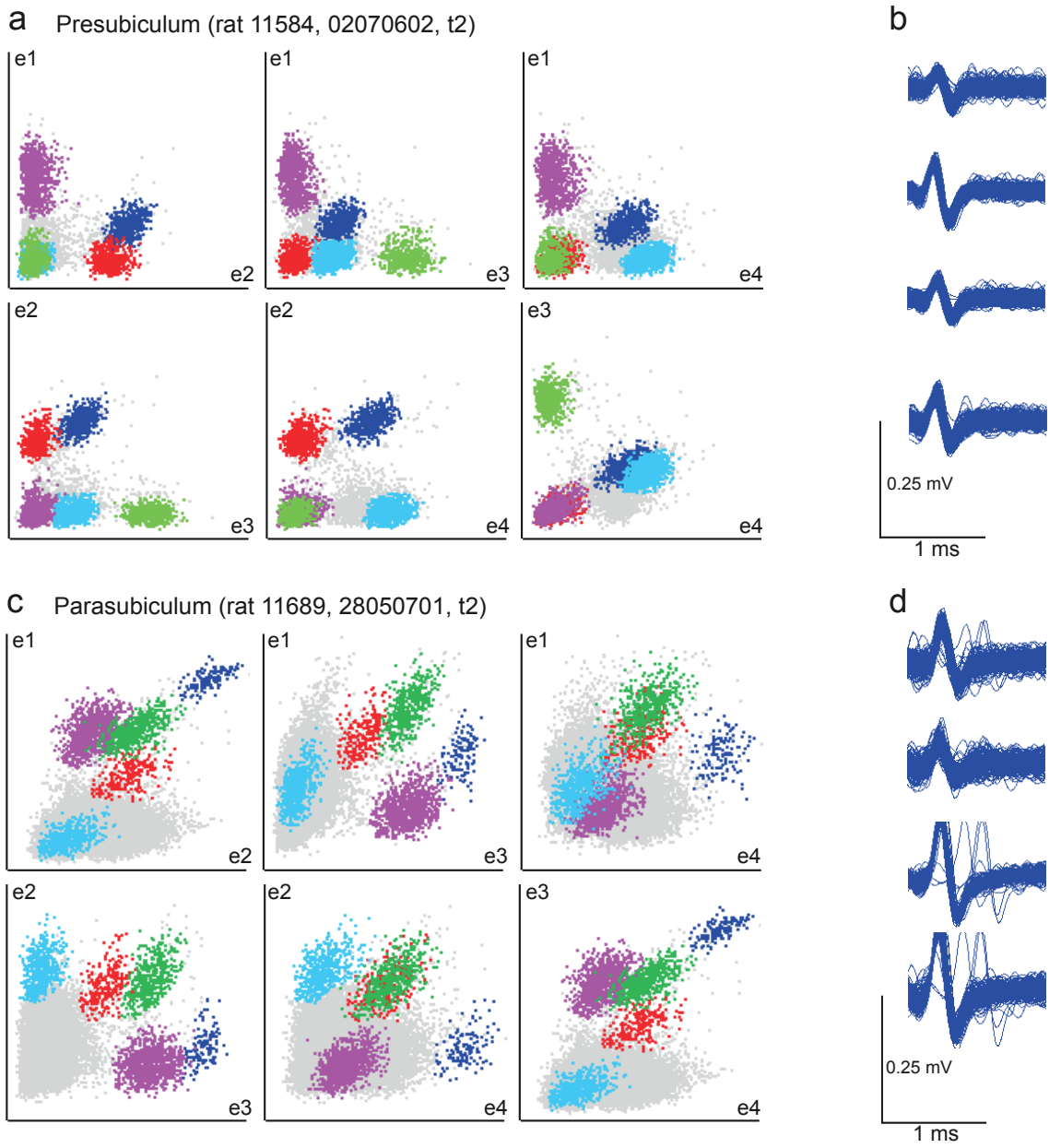

Supplementary Figure 3. Cluster diagrams and waveforms from presubiculum (**a,b**) and parasubiculum (**c,d**). **ac**, Scatterplots showing relation between peak-to-trough amplitudes of all signals recorded on each pair of electrodes on a given tetrode. All six electrode combinations are shown for each experiment. Rat number, trial, tetrode number (t) and electrode numbers (e1-e4) are indicated. Each dot represents one sampled signal. Clusters in the scatterplot are likely to correspond to spikes that originate from the same cell. The dark blue, red and purple clusters in **a** refer to head direction cells. In **c**, all clusters except the dark blue one refer to head direction cells. The dark blue cluster refers to a grid cell. **bd**, All waveforms of the cell corresponding to the blue cluster in the scatterplot to the left. Waveforms are shown for each of the four electrodes (e1-e4) of the tetrode. The examples show that the separation of clusters and waveforms in pre- and parasubiculum was qualitatively similar. This was confirmed in quantitative analyses of cluster separation in the total cell sample. Cluster separation was estimated by calculating distances between clustered spikes of different cells ('isolation distances') in Mahalonobis space (Schmitzer-Torbert, N. et al. Quantitative measures of cluster quality for use in extracellular recordings. Neurosci. 131, 1-11 (2005)). Median Mahalonobis distances were 35.0 for presubiculum, 32.1 for parasubiculum, and 23.8 for MEC. There was no significant difference between pre- and parasubiculum but clusters in MEC were less well-separated (pre- vs. parasubiculum: $Z = 1.02$, $P > 0.30$, ; MEC vs. presubiculum: $Z = 7.68$, $P < 0.001$; MEC vs. parasubiculum: $Z = 6.24$, $P < 0.001$). Recordings from principal neurons with cell bodies in pre- and parasubiculum were distinguished from putative interneurons and axonal recordings according to waveforms and firing rate. Waveforms of accepted cells were generally shorter in presubiculum than parasubiculum (peak-to-trough amplitudes: 264 ± 6 μs for presubiculum, 303 ± 6 μs for parasubiculum, 287 ± 5 μs for MEC; pre- vs. parasubiculum: $t(1180) = 4.23$, $P < 0.001$; presubiculum vs. MEC: $t(1280) = 2.83$, $P < 0.005$). Note that although the combination of short spikes and high average rates is common in layers predominated by interneurons, e.g. layer I of MEC, certainty about classification of cell types must await studies with intracellular recording or specific staining of extracellularly identified neurons. The mean firing rates of accepted pre- and parasubiculum cells (± S.E.M.) were 1.88 ± 0.14 Hz and 1.53 ± 0.12 Hz, respectively. The average rate of the accepted MEC cells was 2.08 ± 0.08 Hz.

Nature Neuroscience: doi:10.1038/nn.2602

Supplementary Figure 4, Part 1

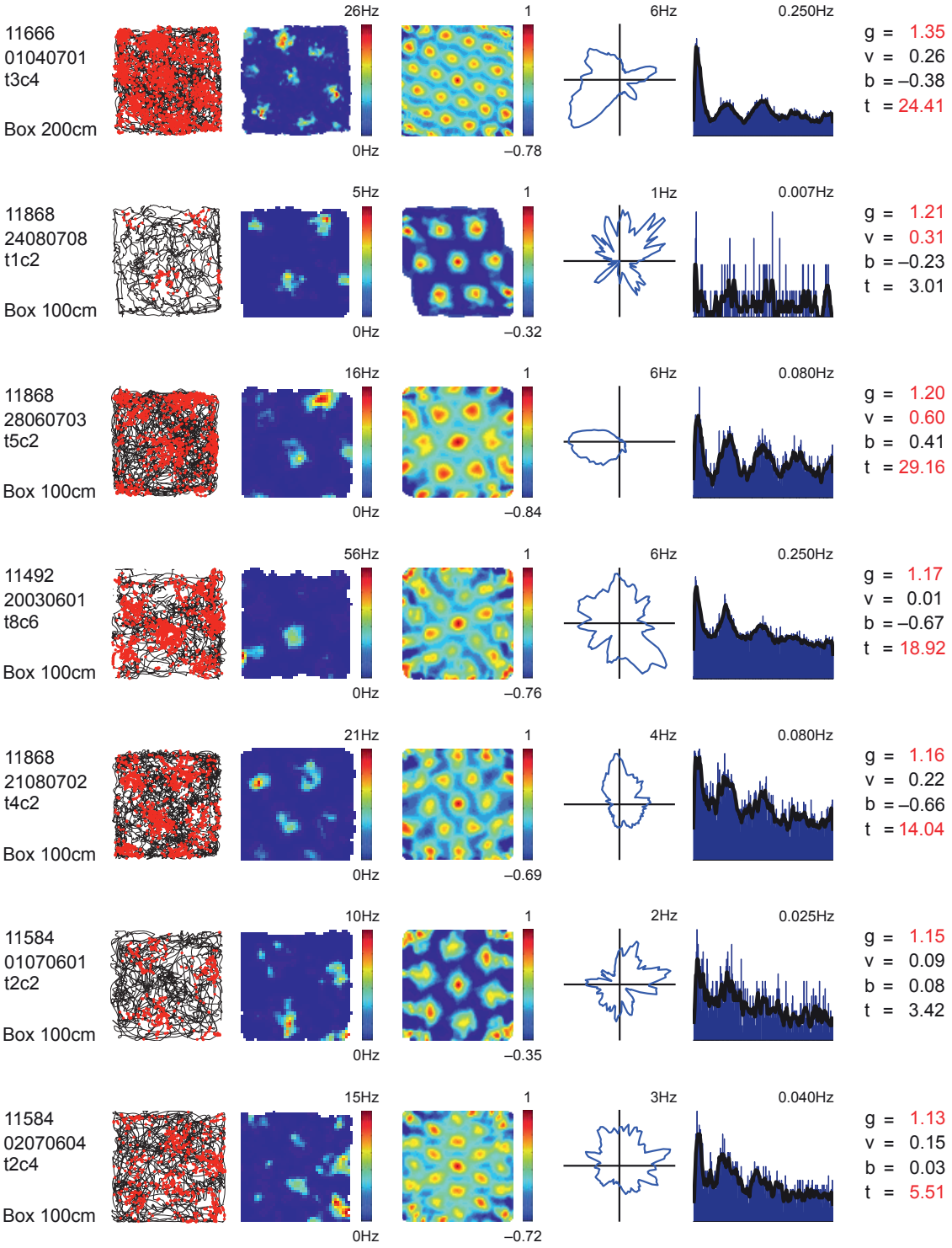

Nature Neuroscience: doi:10.1038/nn.2602

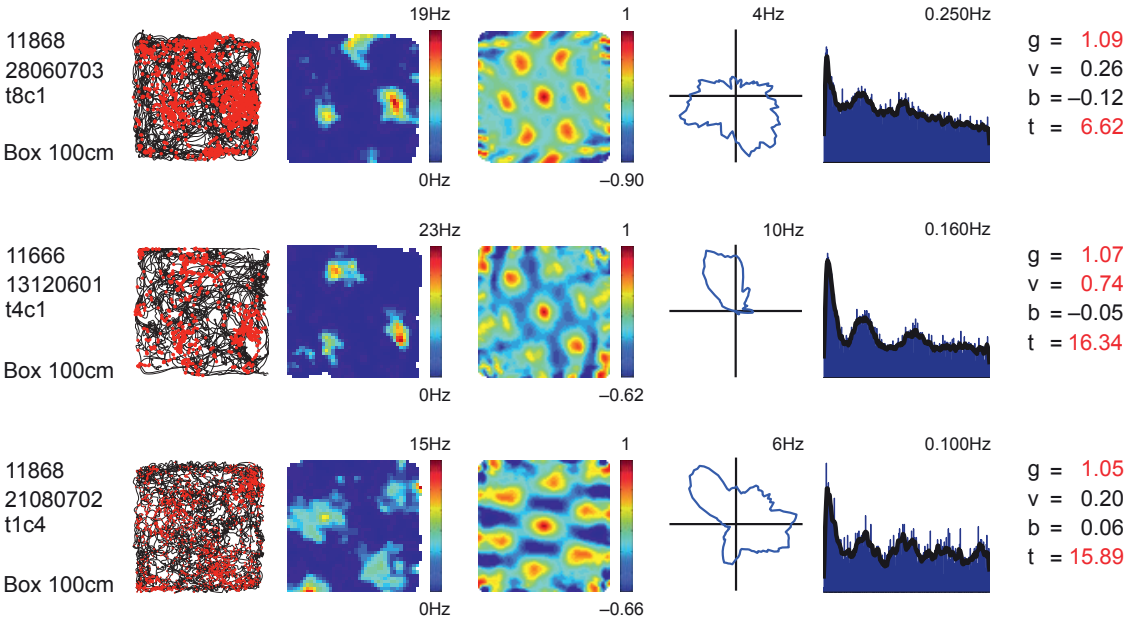

Supplementary Figure 4. The ten cells with the highest grid scores in presubiculum in the square box (Parts 1 and 2). Each row shows data for one cell. Left to right: rat, trial, tetrode (t) and cell (c) numbers and box size; trajectory with spike positions; colour-coded rate map and autocorrelation map; directional plot; spike-time autocorrelation diagram (0-500 ms); the cell's grid score g, mean vector length v, border score b, and theta modulation t (power at theta peak ± 1 Hz divided by power across the entire spectrum). 99th-percentile significance levels for presubiculum were as follows: g = 0.377, v = 0.298, and b = 0.575; all cells with higher values were classified as grid cells, head direction cells, and border cells, respectively. Values passing the threshold are marked in red. Colour scale bars show range of firing rates and autocorrelation values, respectively. Peak rates are indicated in rate and direction plots. Maximal frequency on the y-axis is indicated in the spike-time autocorrelograms.

Additional analyses were performed to examine the stability of the grid fields in pre- and parasubiculum and MEC. Stability was determined by measuring spatial correlations between the first and second half of the trial. These correlations were lower in presubiculum than parasubiculum and lower in both pre- and parasubiculum than in MEC (0.362 ± 0.024 for presubiculum, 0.458 ± 0.019 for parasubiculum, and 0.558 ± 0.012 for MEC; means ± S.E.M.; presubiculum vs. parasubiculum: $t(189) = 3.23$; presubiculum vs. MEC: $t(304) = 7.98$; parasubiculum vs. MEC: $t(327) = 4.54$; all $P < 0.001$); however, the differences were largely explained by differences in grid scores. When the stability was investigated separately for grid cells with high scores (above 1.0), the regional difference in stability was no longer significant (presubiculum: 0.516 ± 0.038, parasubiculum: 0.514 ± 0.023, MEC: 0.570 ± 0.015; presubiculum vs. parasubiculum: $t(51) = 0.04$; presubiculum vs. MEC: $t(120) = 1.31$; parasubiculum vs. MEC: $t(139) = 1.88$; all $P > 0.05$).

Supplementary Figure 5, Part 1

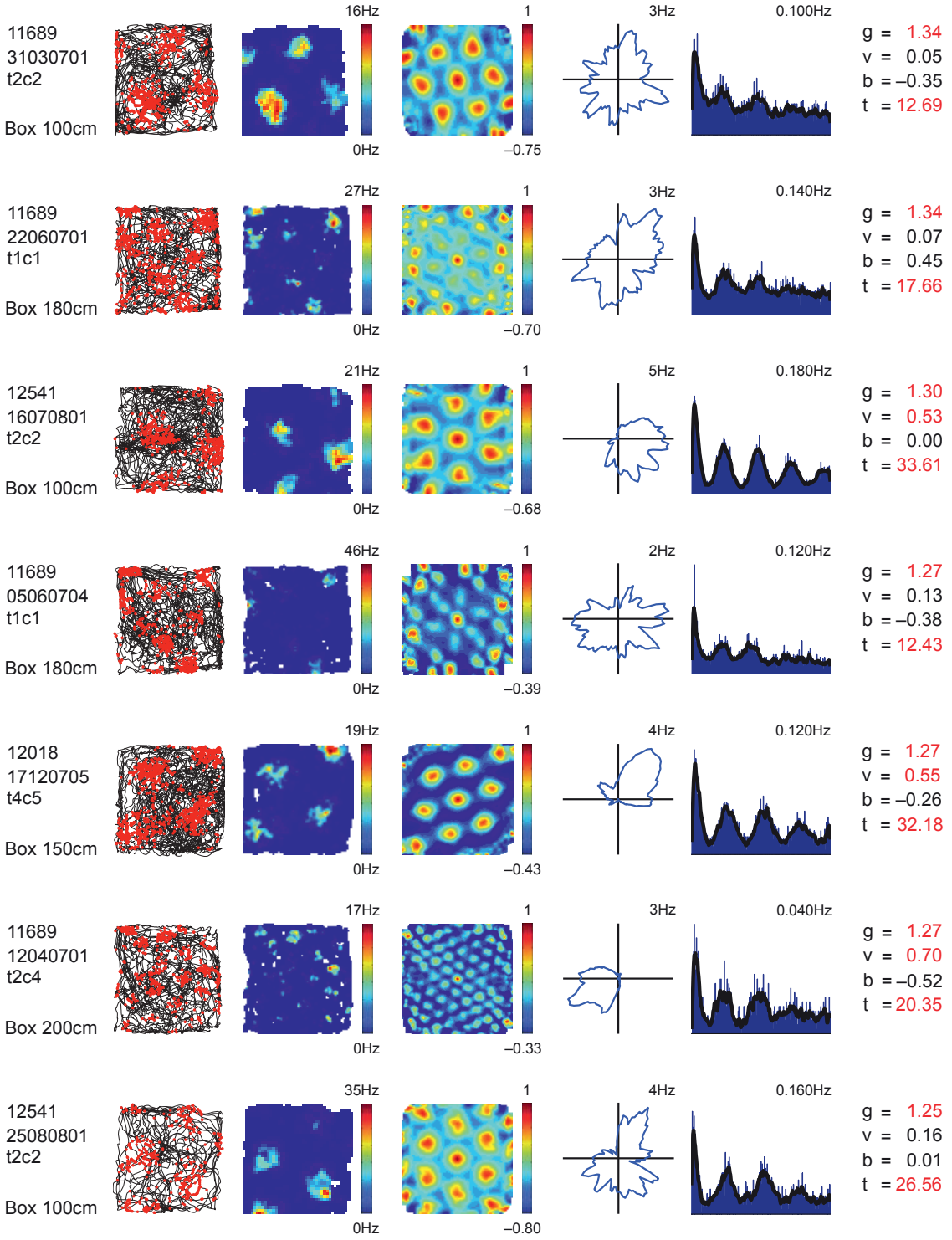

Supplementary Figure 5, Part 2

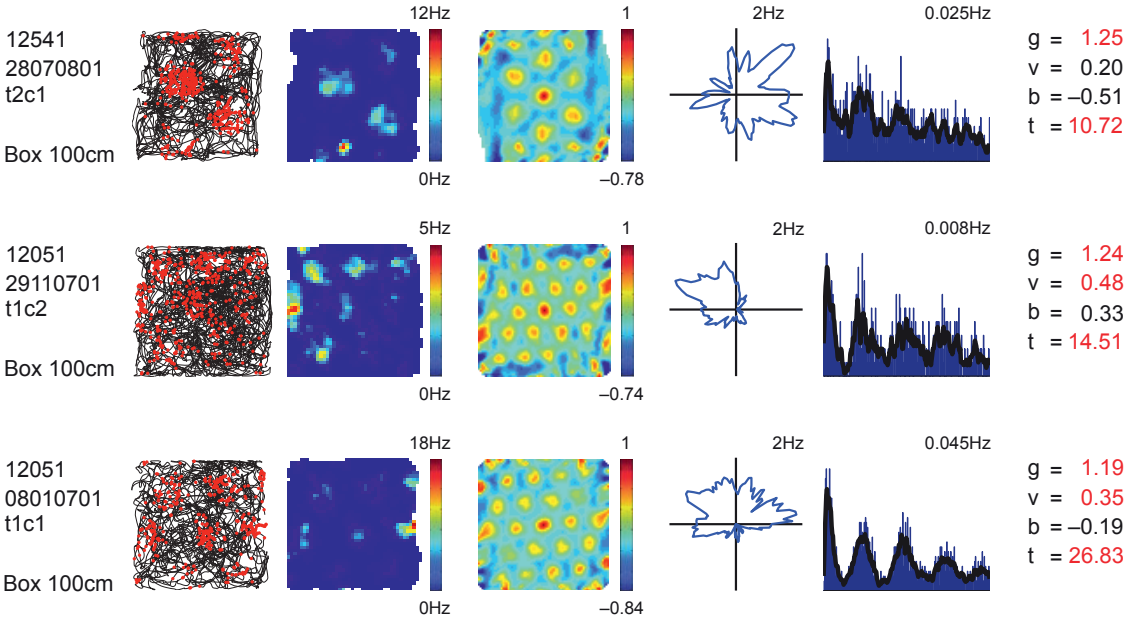

Supplementary Figure 5. The ten cells with the highest grid scores in parasubiculum in the square box (Parts 1 and 2). Each row shows data for one cell. Left to right: rat, trial, tetrode (t) and cell (c) numbers and box size; trajectory with spike positions; colour-coded rate map and autocorrelation map; directional plot; spike-time autocorrelation diagram (0-500 ms); the cell's grid score g, mean vector length v, border score b, and theta modulation t (power at theta peak ± 1 Hz divided by power across the entire spectrum). 99th-percentile significance levels for parasubiculum were as follows: g = 0.364, v = 0.284, and b = 0.575; all cells with higher values were classified as grid cells, head direction cells, and border cells, respectively. Values passing the threshold are marked in red. Colour scale bars show range of firing rates and autocorrelation values, respectively. Peak rates are indicated in rate and direction plots. Maximal frequency on the y-axis is indicated in the spike-time autocorrelograms.

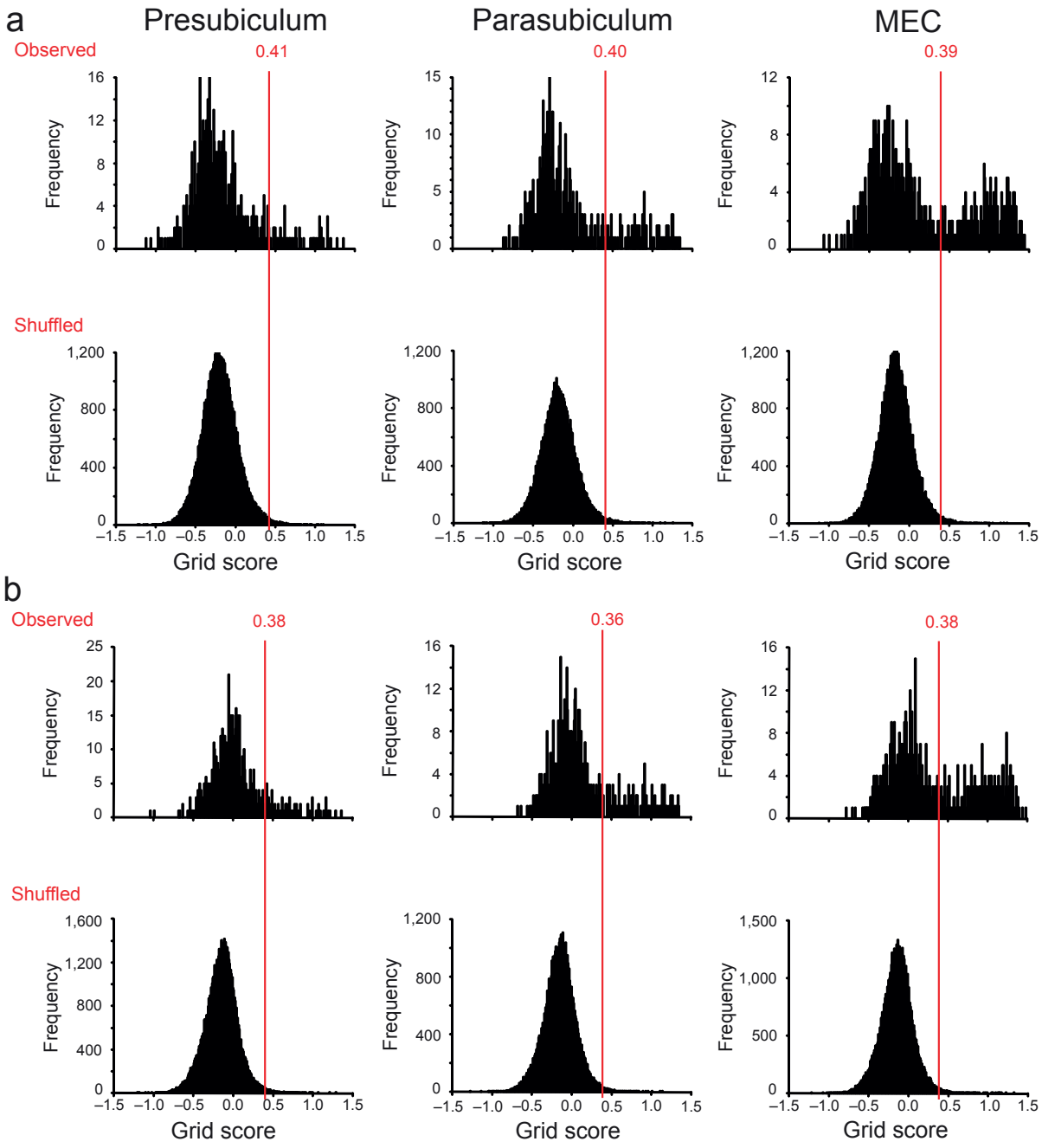

Supplementary Figure 6. Comparison of two methods for estimating rotational symmetry of grid cells. In both cases, the degree of spatial periodicity ('gridness') was determined for each cell by rotating a circular sample around the centre of the autocorrelation map in steps of 30° and computing the correlation between each rotated map and the original. The two methods differed in the way the radius of the circular sample was determined. Method 1 (Fixed radius) confined the analysis to the area defined by a circle around the outermost peak of the six peaks closest to the centre of the autocorrelation map, with peaks defined as 16 or more contiguous bins of 2.5 cm × 2.5 cm above a threshold of r = 0. If fewer than 6 peaks were identified, the circle was fitted around the outermost peak. Grid scores were defined as the minimum difference between any of the correlations at 60 and 120° of rotation and any of the correlations at 30, 90 and 150°. Method 2 (Moving radius) computed correlations in a similar way, but for a range of circular samples, by expanding the outer radius in steps of 1 bin (2.5 cm) from a minimum of 10 cm more than the boundary of the central field to a maximum of 10 cm less than the width of the recording box (i.e. 90 cm, 140 cm, 170 cm or 210 cm), as in ref. 27. Grid scores were then defined as the largest difference between the two groups of rotation angles (60 and 120° vs. 30, 90 and 150°) obtained for any radius.

The figure shows the distributions of grid scores obtained with each of the two methods in each brain region ('observed') as well as randomly shuffled rate maps for the same regions ('shuffled'; see main text for shuffling procedure). **a**, Method 1 (Fixed radius); **b**, Method 2 (Moving radius). Red lines and numbers indicate 99th percentiles for the shuffled data. Note that the difference between the two estimates was minimal. Method 2 was chosen in the rest of the study because this method does not rely on successful identification of peaks in the autocorrelogram, which can be unreliable for grids with poorly defined peaks.

Nature Neuroscience: doi:10.1038/nn.2602

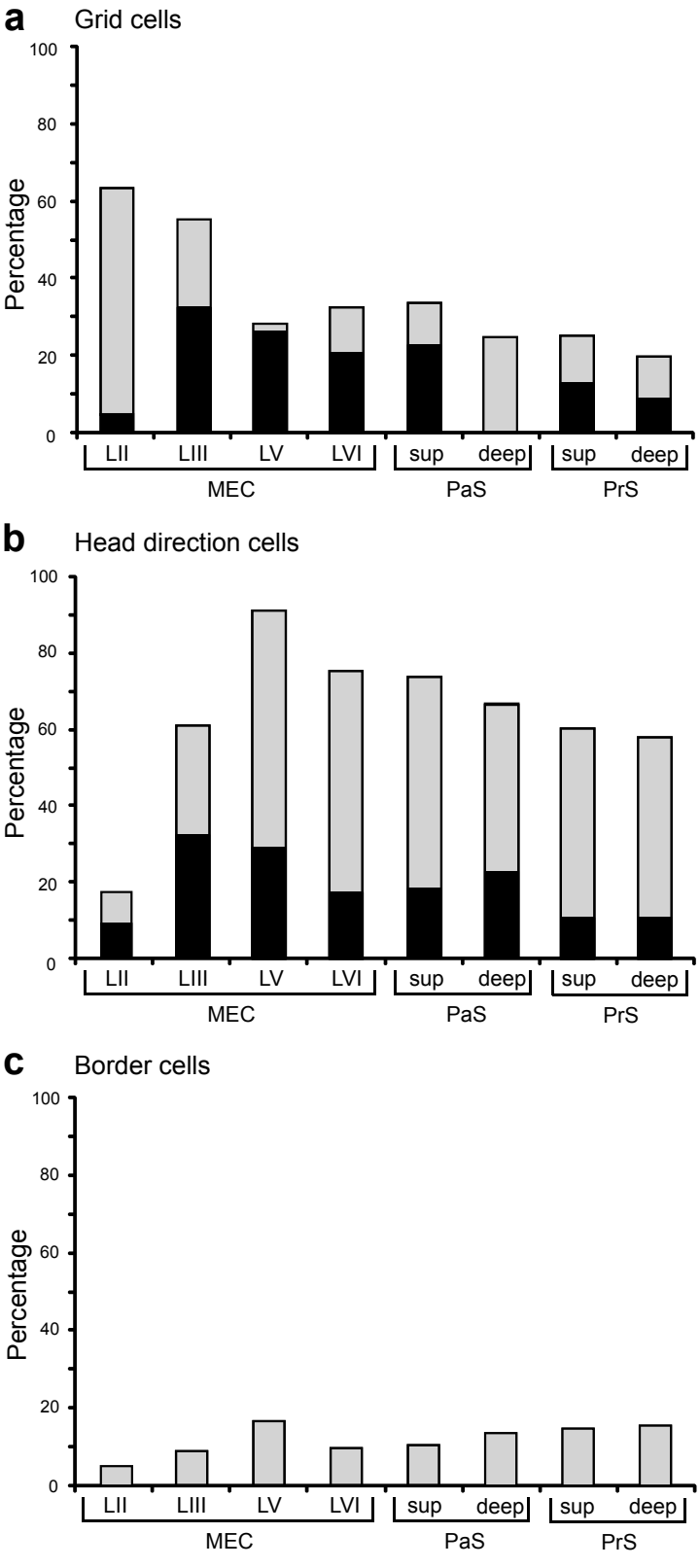

Supplementary Figure 7. Distribution of grid cells (**a**), head direction cells (**b**), and border cells (**c**) in the parahippocampal cortex when a 95th-percentile significance level is used to define the cell types, as in ref.s 27 and 28 (for all other analyses in this study, a 99th percentile threshold was used). The 95th percentile was read out from the distribution of scores in the shuffled data for each region. Grid cells, head direction cells and border cells were defined, respectively, as cells in the recorded data that had grid scores, mean vector lengths, or border scores higher than the 95th percentile of the shuffled data. The figure shows the percentage of each cell type across layers of medial entorhinal cortex, parasubiculum and presubiculum (MEC = medial entorhinal cortex, PaS = parasubiculum, PrS = presubiculum, L = layer, sup = superficial layers). The proportions of cells with conjunctive grid × head direction properties are indicated in dark grey. The distribution pattern was similar to the pattern obtained with a 99th- percentile criterion (Fig. 8).

Nature Neuroscience: doi:10.1038/nn.2602

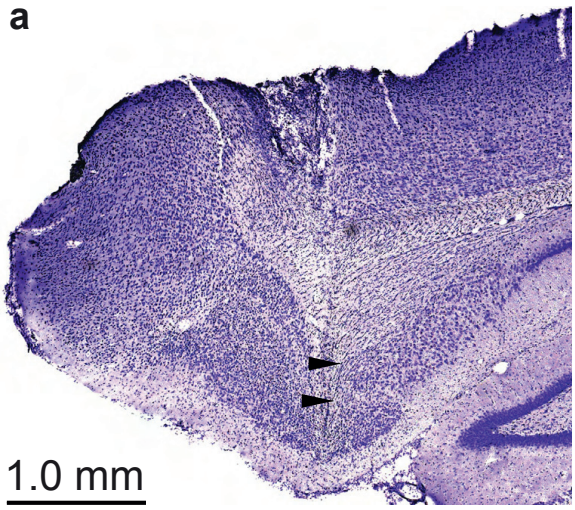

Supplementary Figure 8. Laminar distribution of grid cells, head direction cells and border cells in the presubiculum. **a**, Nissl-stained sagittal brain section showing location of recording positions (arrowheads) in deep layers (layers V-VI; top) and superficial layers (layers II-III; bottom) of the presubiculum in a representative animal. **bc**, Distribution of grid scores, mean vector length and border scores for deep (**b**) and superficial (**c**) layers. Top rows show distribution of recorded values ('observed'); bottom rows show distributions for randomly shuffled rate maps from all cells of each layer ('shuffled'). The red lines indicate the 99th-percentile significance level of the shuffled distributions; the value is indicated above each line. Note similar proportions of grid cells, head direction cells and border cells in superficial and deep layers (grid cells: 11.1% vs. 14.7%; directional cells: 51.0 vs. 55.1%) .

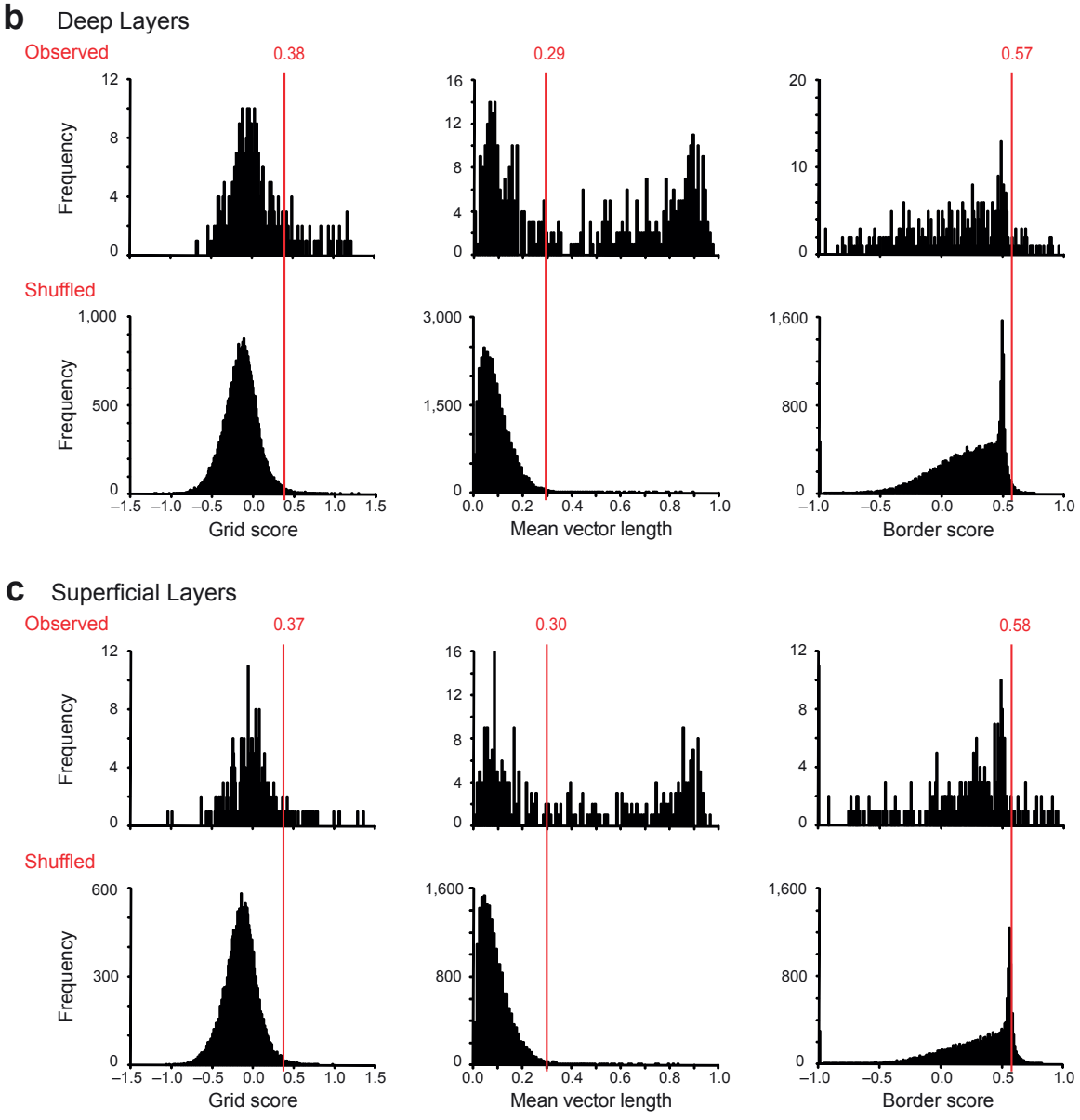

Nature Neuroscience: doi:10.1038/nn.2602

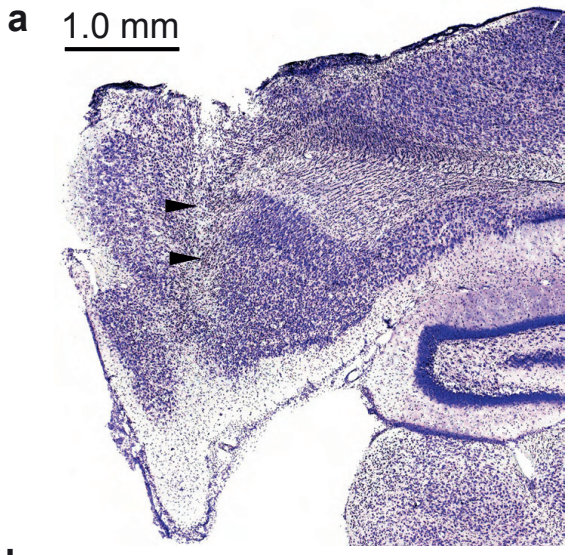

Supplementary Figure 9. Laminar distribution of grid cells, head direction cells and border cells in the parasubiculum. **a**, Nissl-stained sagittal brain section showing location of recording positions (arrowheads) in deep layers (layers V-VI; top) and superficial layers (layers II-III; bottom) of the parasubiculum in a representative animal. **bc**, Distribution of grid scores, mean vector length and border scores for each layer of the parasubiculum. Top rows show distribution of recorded values ('observed'); bottom panels show distributions for randomly shuffled rate maps from all cells in each layer ('shuffled'). The red lines indicate the 99th-percentile significance level; the values are indicated above each line. Grid cells were slightly more abundant in deep layers than superficial layers (26.3% vs. 15.8%, Z = 2.98, P < 0.005). Deep and superficial layers had similar numbers of directional cells (63.8 and 54.9%, respectively).

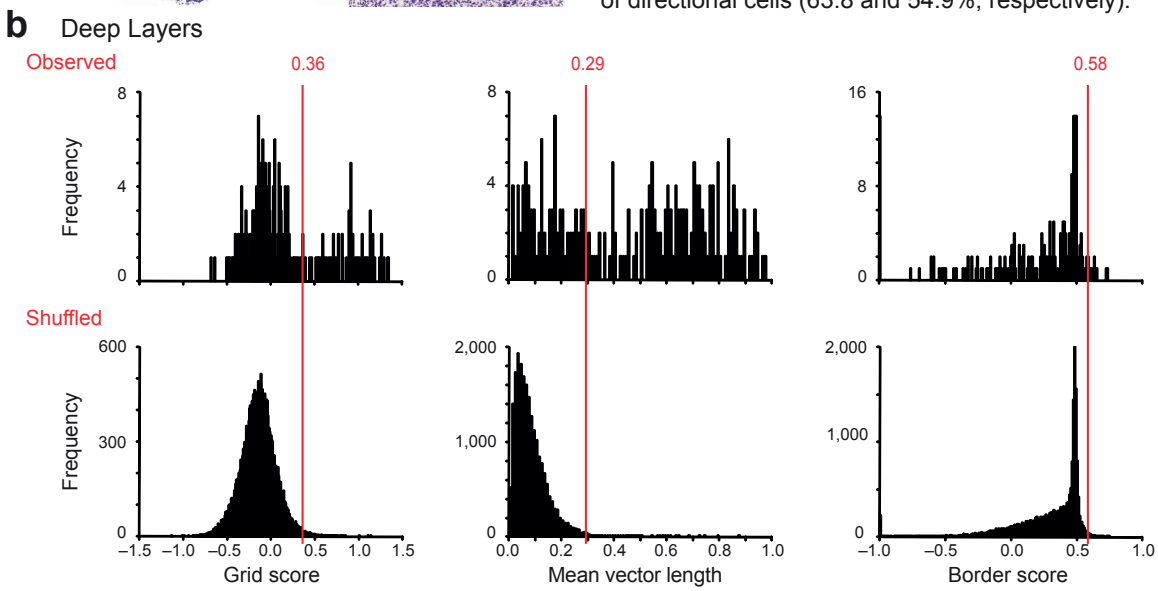

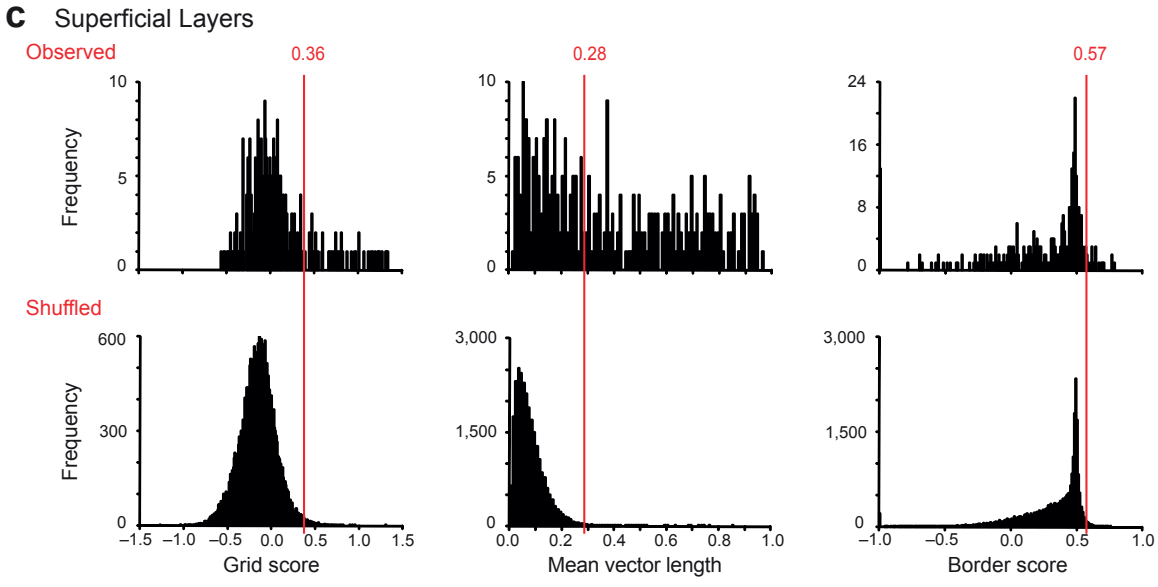

Nature Neuroscience: doi:10.1038/nn.2602

Supplementary Figure 10, Part 1

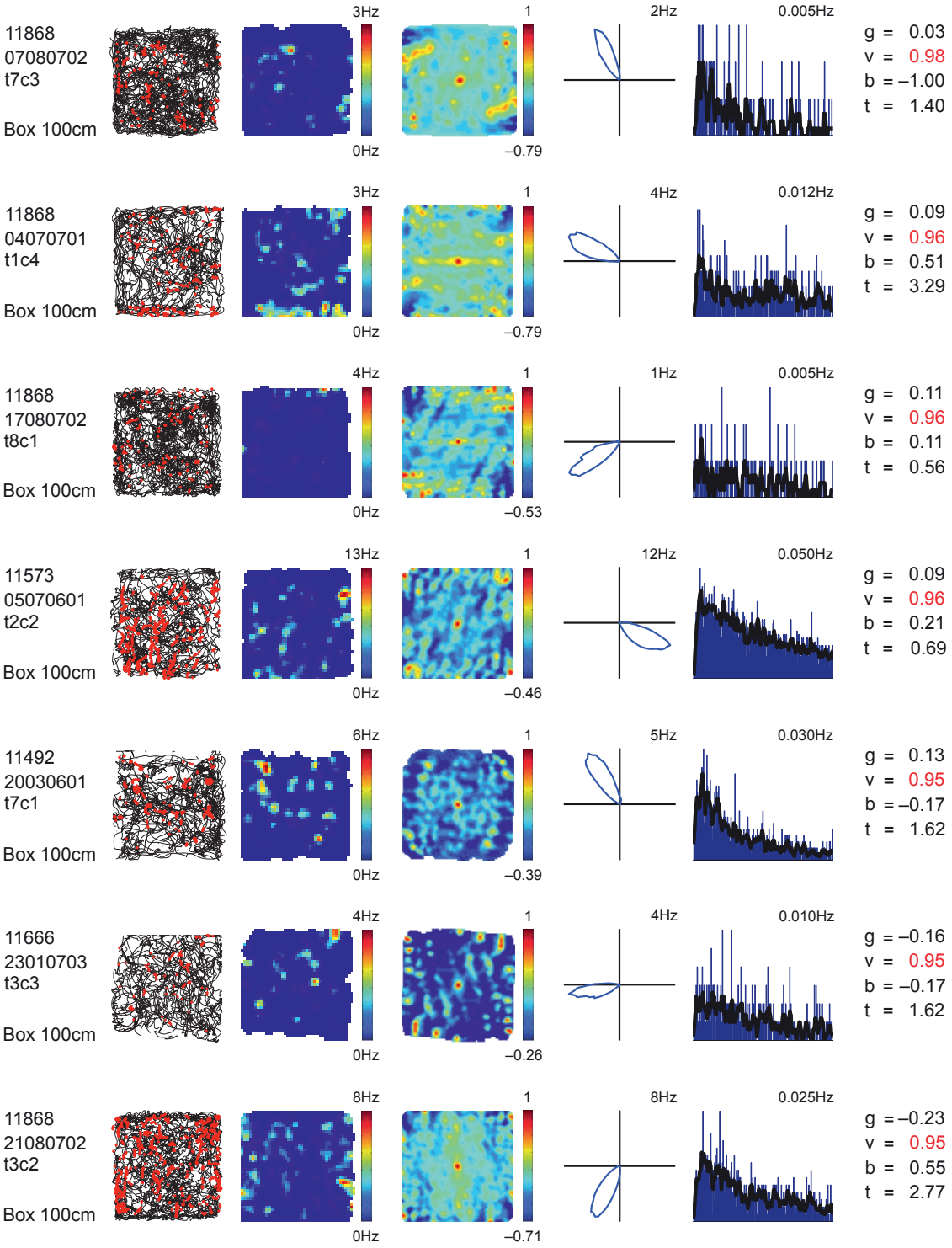

Supplementary Figure 10, Part 2

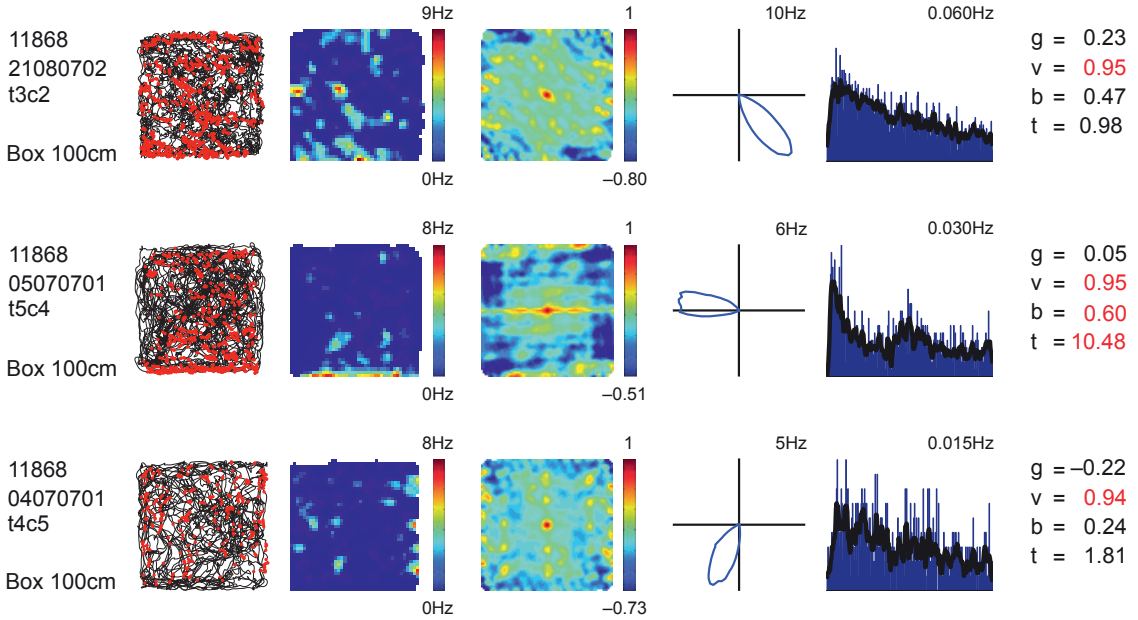

Supplementary Figure 10. The ten cells with the highest direction scores (mean vector lengths) in presubiculum (Parts 1 and 2). Each row shows data for one cell. Left to right: rat , trial, tetrode (t) and cell (c) numbers and box size; colour-coded rate map and autocorrelation map; directional plot; spike-time autocorrelation diagram (0-500 ms); the cell's grid score g, mean vector length v, border score b, and theta modulation t (power at theta peak ± 1 Hz divided by power across the entire spectrum). 99th-percentile significance levels for presubiculum were as follows: g = 0.377, v = 0.298, and b = 0.575; all cells with higher values were classified as grid cells, head direction cells, and border cells, respectively. Values passing the threshold are marked in red. Colour scale bars show range of firing rates and autocorrelation values, respectively.Peak rates are indicated in rate and direction plots. Maximal frequency on the y-axis is indicated in the spike-time autocorrelograms.

An analysis of the stability of the directional preferences, expressed as angular correlations between directional rate maps for the first and second half of the trial, showed no regional difference (presubiculum: 0.882 ± 0.009; parasubiculum: 0.834 ± 0.009; MEC: 0.888 ± 0.014).

The directional tuning of presubicular head direction cells with a grid correlate was lower than that of head direction cells with no such correlate (mean vector lengths of 0.663 ± 0.023 and 0.733 ± 0.010, respectively, $t(349) = 1.97$, $P = 0.05$). A similar tendency was observed in MEC (with grid: 0.575 ± 0.017; without grid: 0.636 ± 0.014, $t(195) = 2.0$, $p < 0.05$). In parasubiculum, the effect was not significant (0.596 ± 0.018 vs. 0.642 ± 0.013; $t(307) = 1.8$, $P > 0.05$).

Supplementary Figure 11, Part 1

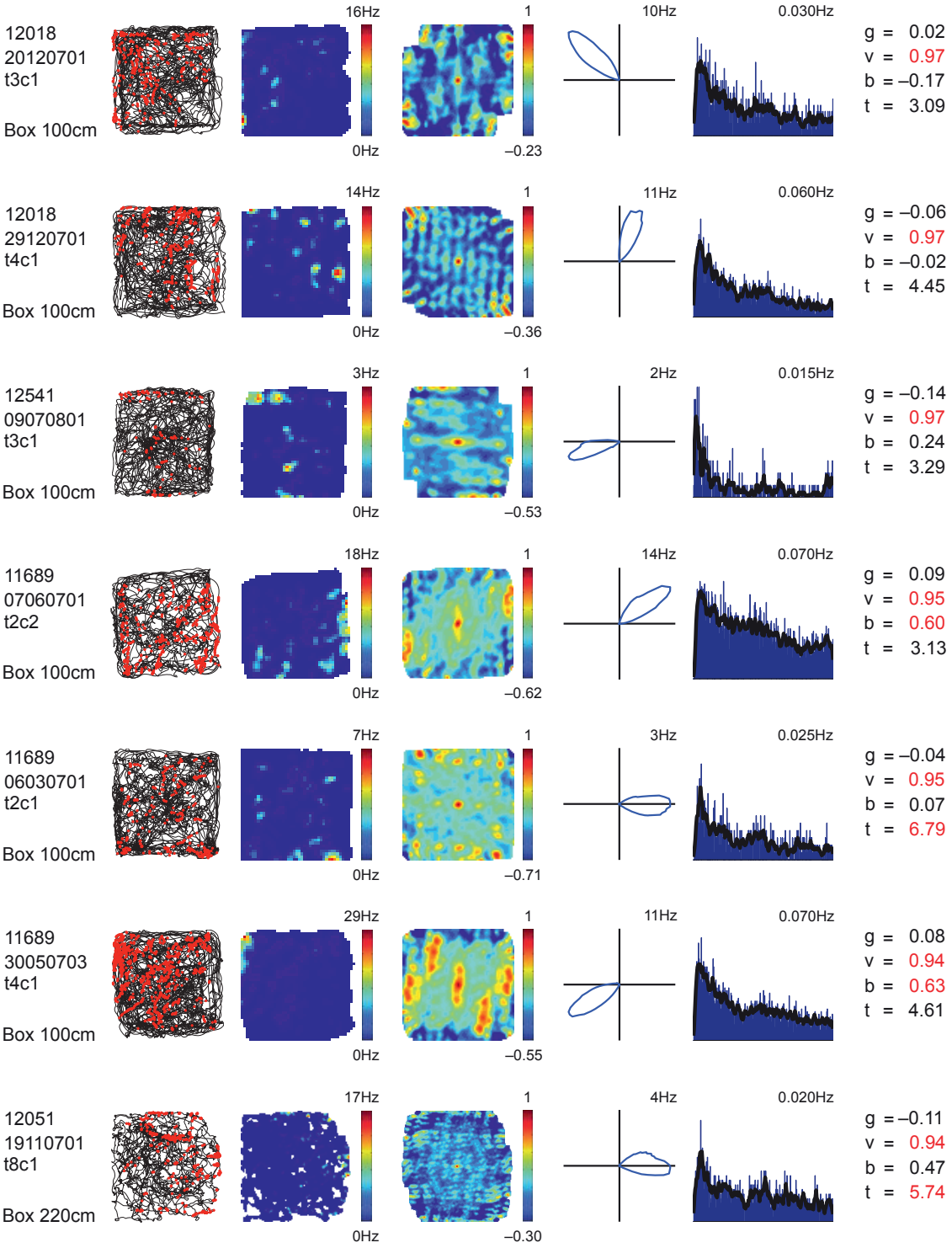

Supplementary Figure 11, Part 2

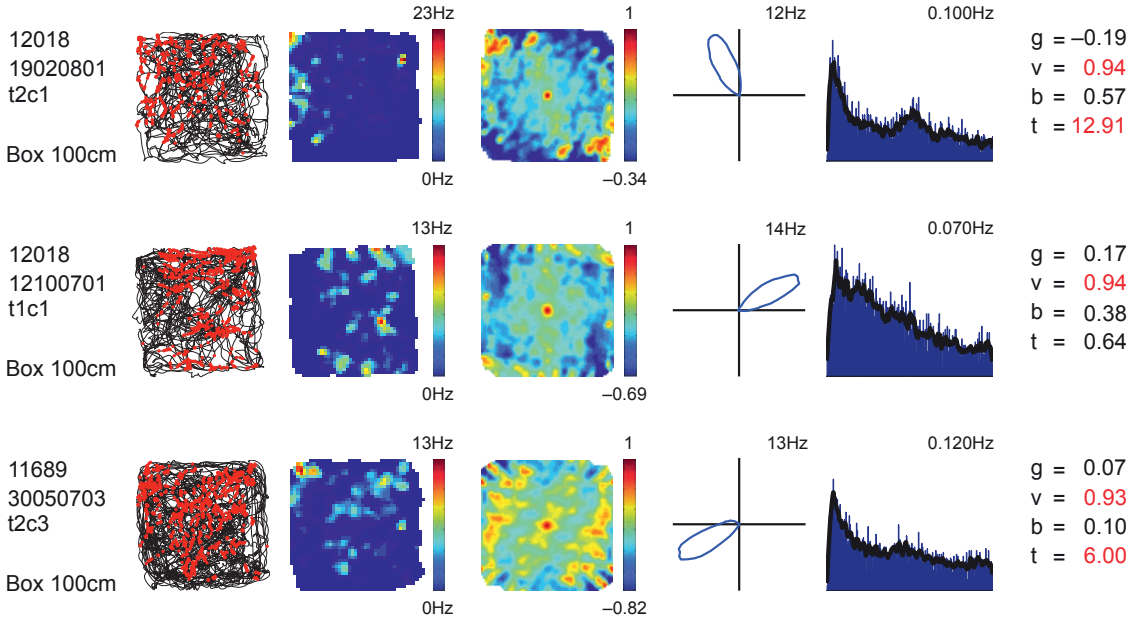

Supplementary Figure 11. The ten cells with the highest direction scores (mean vector lengths) in parasubiculum (Parts 1 and 2). Each row shows data for one cell. Left to right: rat , trial, tetrode (t) and cell (c) numbers and box size; colour-coded rate map and autocorrelation map; directional plot; spike-time autocorrelation diagram (0-500 ms); the cell's grid score g, mean vector length v, border score b, and theta modulation t (power at theta peak ± 1 Hz divided by power across the entire spectrum). 99th-percentile significance levels for parasubiculum were as follows: g = 0.364, v = 0.284, and b = 0.575; all cells with higher values were classified as grid cells, head direction cells, and border cells, respectively. Values passing the threshold are marked in red. Colour scale bars show range of firing rates and autocorrelation values, respectively. Peak rates are indicated in rate and direction plots. Maximal frequency on the y-axis is indicated in the spike-time autocorrelograms.

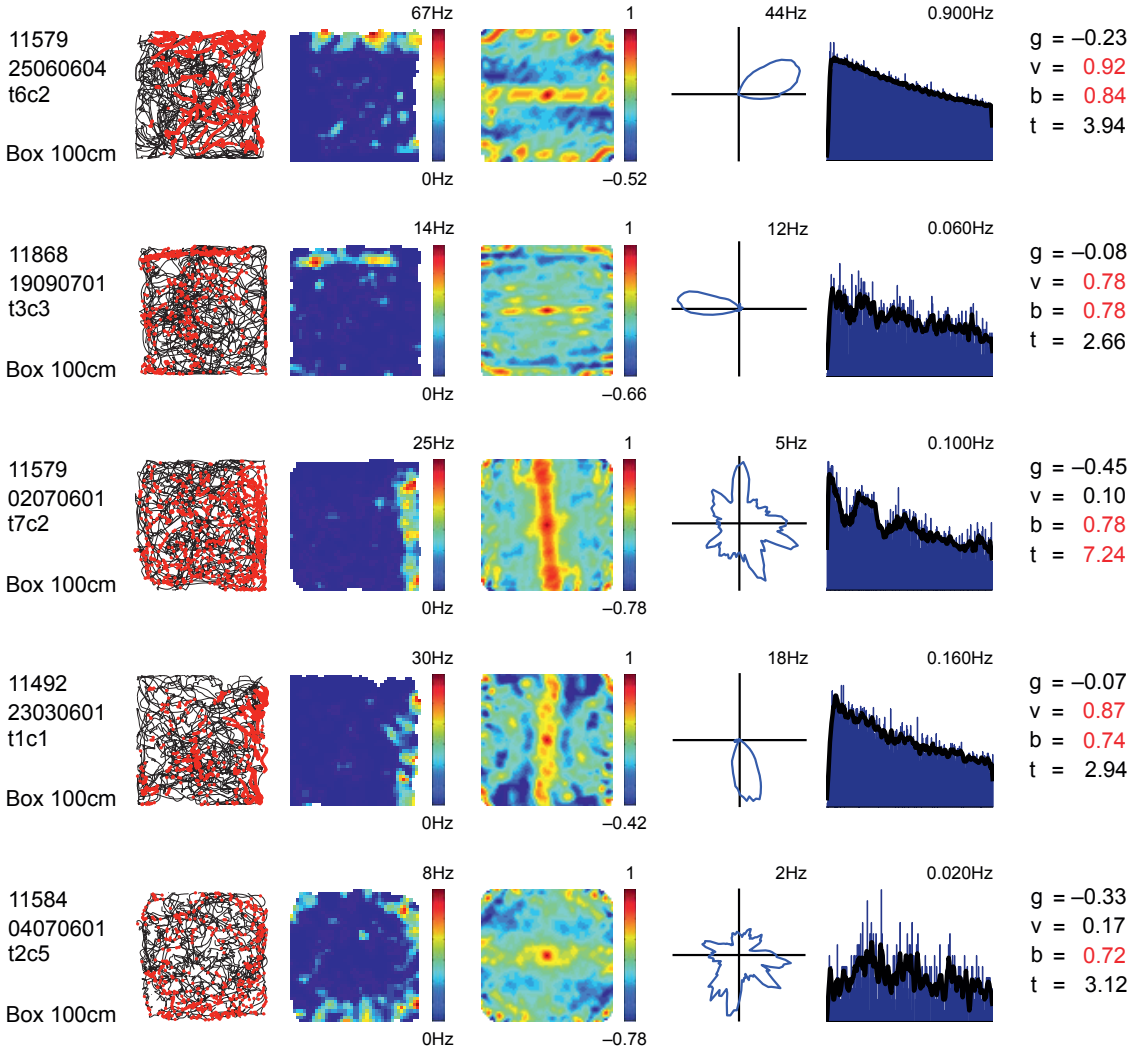

Supplementary Figure 12. The five cells with the highest border scores in the square box in presubiculum. Each row shows data for one cell. Left to right: rat, trial, tetrode (t) and cell (c) numbers and box size; trajectory with spike positions; colour-coded rate map and autocorrelation map; directional plot; spike-time autocorrelation diagram (0-500 ms); the cell's grid score g, mean vector length v, border score b, and theta modulation t (power at theta peak ± 1 Hz divided by power across the entire spectrum). 99th-percentile significance levels for presubiculum were as follows: g = 0.377, v = 0.298, and b = 0.575; all cells with higher values were classified as grid cells, head direction cells, and border cells, respectively. Values passing the threshold are marked in red. Colour scale bars show range of firing rates and autocorrelation values, respectively. Peak rates are indicated in rate and direction plots. Maximal frequency on the y-axis is indicated in the spike-time autocorrelograms.

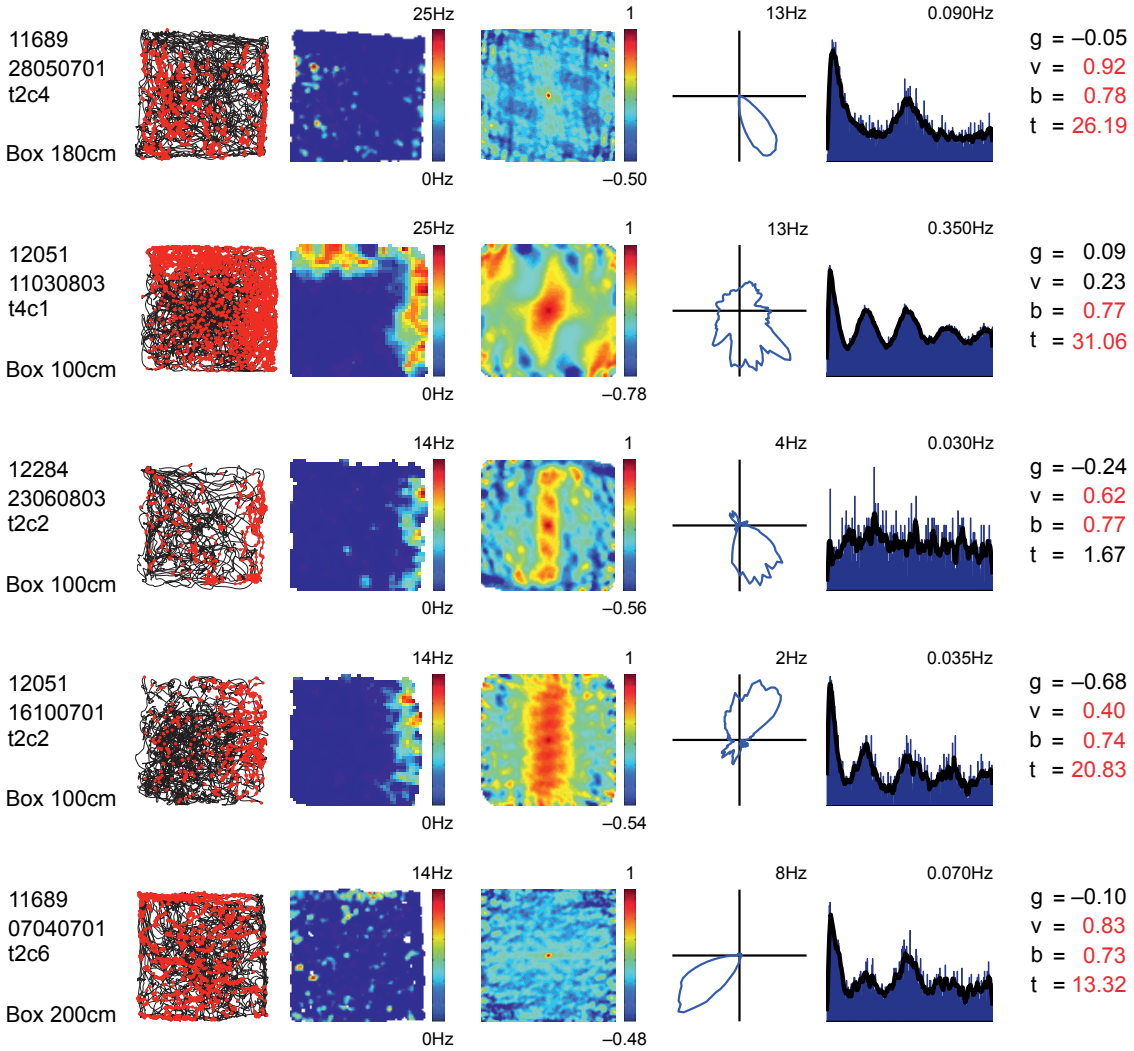

Supplementary Figure 13. The five cells with the highest border scores in parasubiculum. Each row shows data for one cell. Left to right: rat, trial, tetrode (t) and cell (c) numbers and box size; trajectory with spike positions; colour-coded rate map and autocorrelation map; directional plot; spike-time autocorrelation diagram (0-500 ms); the cell's grid score g, mean vector length v, border score b, and theta modulation t (power at theta peak ± 1 Hz divided by power across the entire spectrum). 99th-percentile significance levels for parasubiculum were as follows: g = 0.364, v = 0.284, and b = 0.575; all cells with higher values were classified as grid cells, head direction cells, and border cells, respectively. Values passing the threshold are marked in red. Colour scale bars show range of firing rates and autocorrelation values, respectively. Peak rates are indicated in rate and direction plots. Maximal frequency on the y-axis is indicated in the spike-time autocorrelograms.

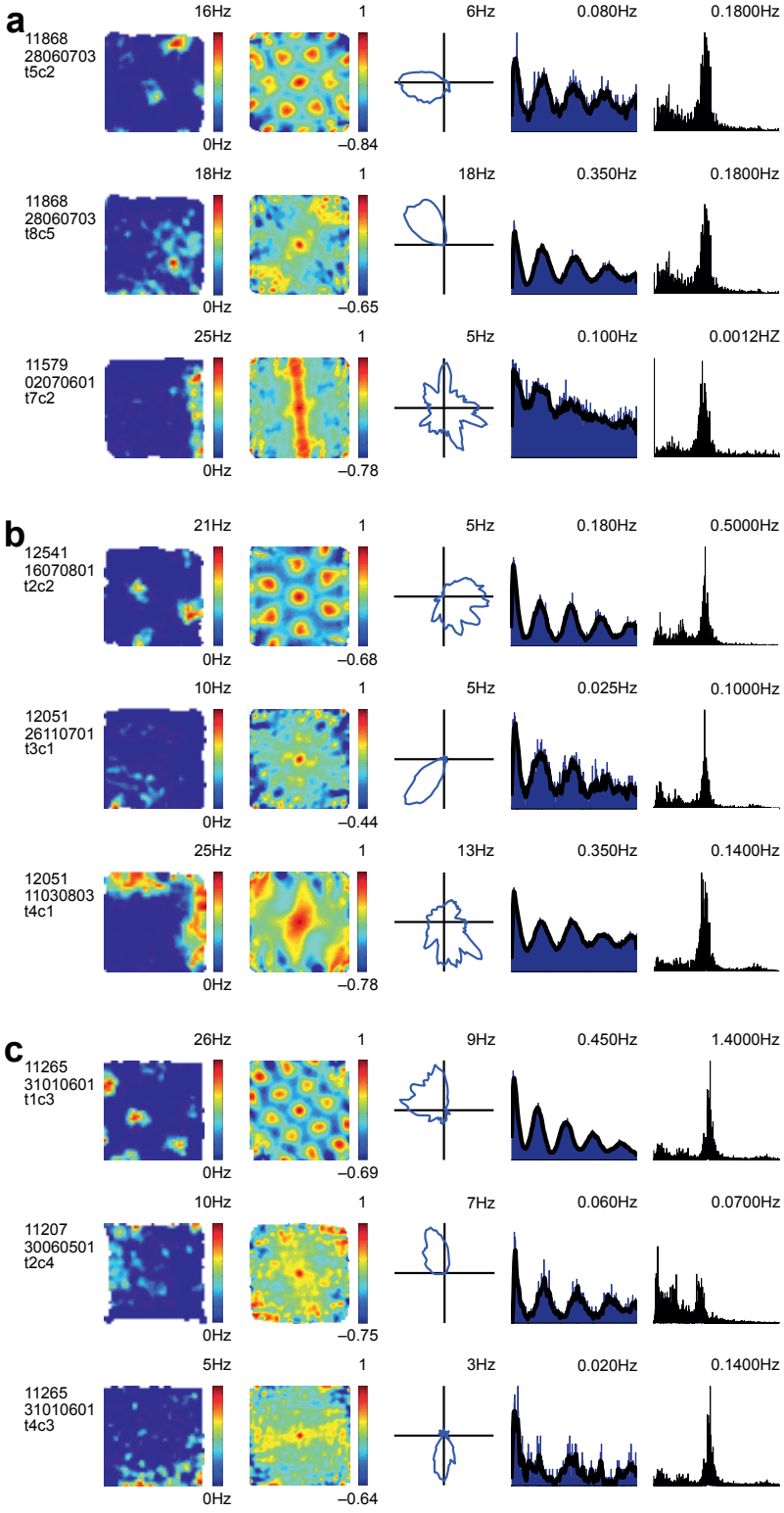

Supplementary Figure 14. Spatial and directional firing properties of cells with strong theta modulation (**a**, presubiculum; **b**, parasubiculum; **c**, MEC). Each panel shows a head direction cell, a grid cell, and a border cell. Each row corresponds to one cell. From left to right: Rat, trial, tetrode (t) and cell (c) numbers; colour-coded rate map and autocorrelation map; directional plot; spike-time autocorrelation diagram (0-500 ms), and EEG power spectrum (0-20Hz). Peak rates are indicated in rate and direction plots. Maximal frequencies on the y-axis are indicated in the spike-time autocorrelograms and power spectra.

Quantitative analyses showed that theta modulation was observed more strongly in grid cells than head-direction and border cells. The proportion of theta-modulated grid cells was larger than the proportion of theta-modulated cells with head direction or border modulation (presubiculum: 65.4% vs. 16.0% and 31.0%, $Z > 4.04$, $P < 0.001$; parasubiculum 64.6% vs. 51.2% and 21.5%, $Z > 3.02$, $P < 0.001$; MEC: 84.2% vs. 39.7% and 40.0%, $Z > 5.25$, $P < 0.001$). The proportion of theta-modulated grid cells was higher in superficial layers of MEC (layer II: 88%; layer III: 90%) than in deep layers (layer V: 62%; layer VI: 70%) or in pre- or parasubiculum. The percentage of theta-modulated cells was, in turn, higher among head-direction cells with conjunctive grid activity than among pure head direction-modulated cells (presubiculum: 46.7% vs. 13.1%, $Z = 4.80$, $P < 0.001$; parasubiculum: 92.2% vs. 44.7%, $Z = 6.82$, $P < 0.001$; MEC: 95.1 % vs. 20.7%; $Z = 10.3$, $P < 0.001$). The peak theta frequency determined from the distribution of inter-spike intervals was higher than the peak theta frequency of the field potential in the presubiculum (7.84 ± 0.07 Hz vs. 6.97 ± 0.13 Hz, $t(171) = 5.53$, $P < 0.001$, paired t-test) and the MEC (8.24 ± 0.05 Hz vs. 7.91 ± 0.07 Hz, $t(351) = 3.58$, $P < 0.001$) but not in the parasubiculum (7.78 ± 0.08 Hz vs. 8.08 ± 0.05 Hz).

Theta phase locking, estimated for each cell as the length of the mean vector for the distribution of firing rate across the 360 degrees of the theta cycle, was strong in parasubiculum and some layers of MEC but weak in presubiculum (parasubiculum: mean vector length across degrees of theta cycle: 0.448 ± 0.012 for all theta-modulated cells and 0.465 ± 0.018 for theta-modulated grid cells; MEC layer VI: 0.226 ± 0.018 and 0.155 ± 0.018, respectively; MEC layer V: 0.333 ± 0.026 and 0.356 ± 0.042; MEC layer III: 0.337 ± 0.018 and 0.367 ± 0.025; MEC layer II: 0.216 ± 0.019 and 0.185 ± 0.024; presubiculum: 0.205 ± 0.010 and 0.175 ± 0.015). In MEC, phase locking was weaker in layer II than layer III, as expected when many or most layer II cells exhibit phase precession ($t(242) = 3.89$, $P < 0.001$).

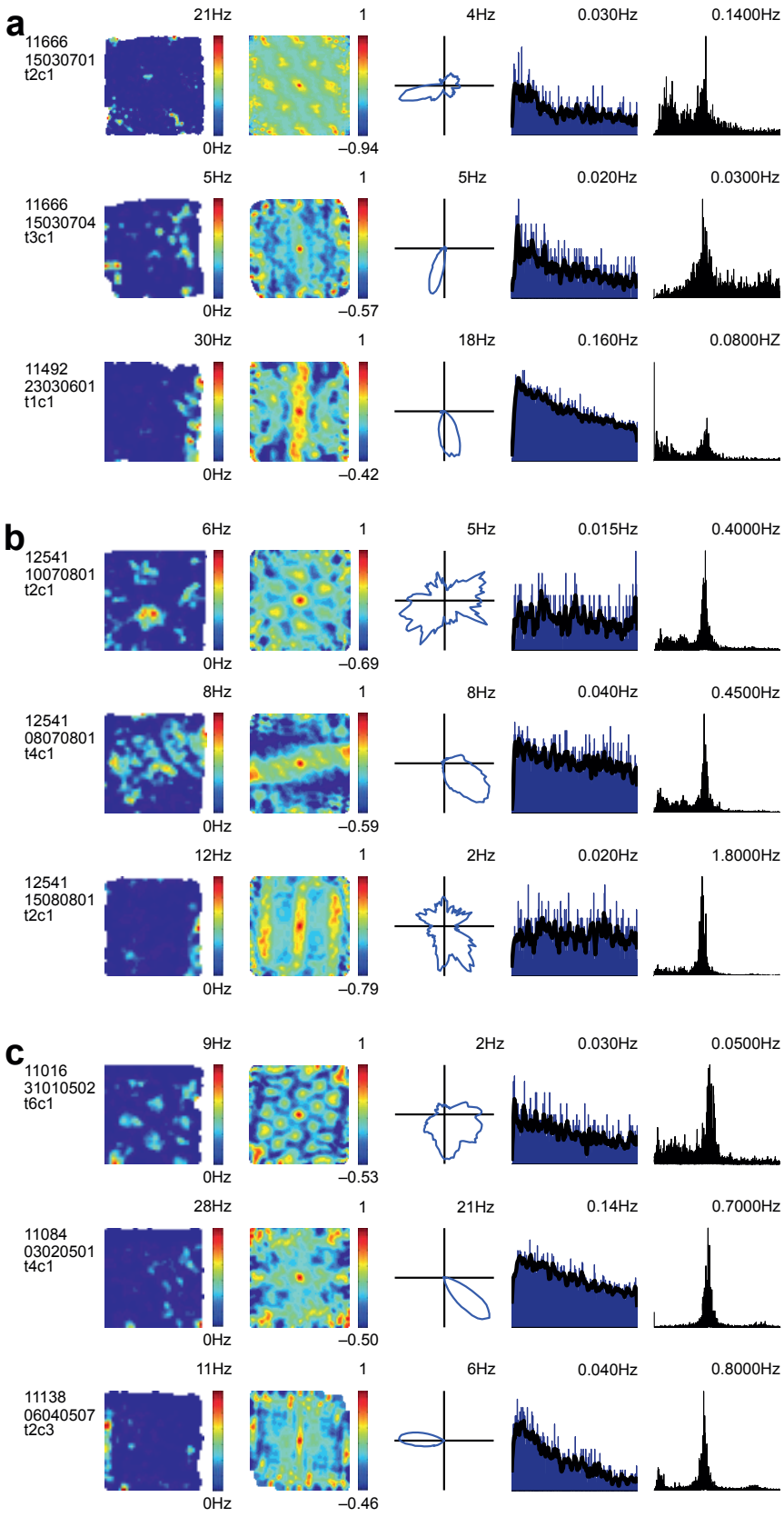

Supplementary Figure 15. Spatial and directional firing properties of cells with weak theta modulation (**a**, presubiculum; **b**, parasubiculum; **c**, MEC). Each panel shows a grid cell or conjunctive cells, a head direction cell, and a border cell. Each row corresponds to one cell. From left to right: Rat, trial, tetrode and cell numbers; colour-coded rate map and autocorrelation map; directional plot; spike-time autocorrelation diagram (0-500 ms), and EEG power spectrum (0-20Hz). Characteristic firing patterns are expressed in spite of weak expression of theta modulation. Peak rates are indicated in rate and direction plots. Maximal frequencies on the y-axis are indicated in the spike-time autocorrelograms and power spectra.

Paper III

A THREE-PLANE ARCHITECTONIC ATLAS OF THE RAT HIPPOCAMPAL REGION.

Boccara CN[1*], Kjønigsen LJ[2*], Hammer I[1], Bjålie J[2], Leergaard TB[2], Witter MP[1]

[1]Kavli Institute for System Neuroscience, Centre for the Biology of Memory, Norwegian University of Science and Technology (NTNU), Trondheim, Norway

[2]Centre for Molecular Biology and Neuroscience, Institute of Basic Medical Sciences, University of Oslo, Oslo, Norway

*Both authors contributed equally to the study

Number of pages: 42 (text) + 4 (figures)

Number of figures: 4

Address correspondence to:

Menno P. Witter Ph.D.

Kavli Institute for System Neuroscience

Centre for the Biology of Memory

MTFS

7498 Trondheim, Norway

+47 73598249

Email: menno.witter@ntnu.no

Key words: Cytoarchitectonic, chemoarchitectonic, hippocampus, parahippocampal region, horizontal plane, sagittal plane, coronal plane

Abstract
The hippocampal region, comprising the hippocampal formation and the parahippocampal region, has been for decades one of the most intensely studied parts of the brain. The increased understanding of its functional diversity and complexity has led to an increased demand for specificity in experimental procedures and manipulations. In view of the complex three-dimensional structure of the region, precisely positioned experimental approaches require a fine-grained architectural description of the region that is available and readable to non-anatomically experienced experimentalists. In this paper we provide the first cyto- and chemoarchitectural description of the hippocampal region at high resolution and in the three standard sectional planes: coronal, horizontal and sagittal. The atlas is based on series of adjacent sections stained for neurons and for a number of chemical marker substances, relying mainly on immunopositivity for parvalbumin and calbindin. All borders defined in one plane have been crosschecked against their counterparts in the other two planes. The entire dataset will be made available as a web-based interactive application.

Introduction

Brain functional studies are based on increasingly precise experimental manipulations targeted at specific region or sub-regions. Their success strongly depends on the availability of a standardized methodology to represent the exact three-dimensional position of either the manipulation or the brain region whose functionality is assessed. For example, the behavioral correlates of brain lesions can only be interpreted if the position and extent of the lesion is well documented. Similarly, without an accurate determination of electrode positions, unit recordings in freely behaving animal are essentially meaningless.

For decades, numerous studies contributed to establish the rodent hippocampal region partition in functionally different domains showing striking disparities in morphological and biophysical cellular properties, as well as in intrinsic and extrinsic connectivity, and in behavioral correlates of their activity. The latter was specifically supported by a large body of work characterizing neurons coding for precise variable of the external space out of which four main categories have been identified in specific areas of the hippocampus region: the place cells in the cornu ammonis (CA) fields (O'Keefe and Dostrovsky 1971) and the dentate gyrus (Olton et al. 1978); the head direction cells (HDC) in the dorsal portion of the presubiculum (Ranck 1984; Taube et al. 1990) the medial part of the entorhinal cortex (Sargolini et al. 2006)) and the dorsal portion of the parasubiculum (Boccara et al. 2010)); the grid cells in the medial entorhinal cortex (Hafting et al. 2005) and in the dorsal pre- and parasubiculum (Boccara et al. 2010); and cells coding for the border of the environment in the medial entorhinal cortex, dorsal pre- and parasubiculum (Savelli et al. 2008; Solstad et al. 2008; Boccara et al. 2010) and in the subiculum (Lever et al. 2009). Beside spatial correlates, other types of coding have been observed in the hippocampal region. Notably, cells coding for objects were recorded in the lateral entorhinal (Zhu et al. 1995; Young et al. 1997; Wan et al. 1999; Deshmukh and Knierim 2011). Similar neural correlates of object recognition memory or novelty were observed in perirhinal cortex (Zhu et al. 1995; Burke et al. 2012), but also in the postrhinal cortex (Burwell and Hafeman 2003) and the subiculum (Chang and Huerta 2012).

The improvement of experimental and recording tools permitted to reveal specializations at an increasingly finer anatomical scale. Such example of

intrastructural functional differentiation exists between the medial and the lateral entorhinal cortices (Fyhn et al. 2004; Hargreaves et al. 2005; Steffenach et al. 2005; Witter and Moser 2006). Another example is the finding of a topographical gradient of place and grid cell scale along the longitudinal axes of the hippocampal formation (Moser et al. 1993; Kjelstrup et al. 2008) and the medial entorhinal cortex (Hafting et al. 2005; Sargolini et al. 2006; Brun et al. 2008)(Hafting et al., 2005; Sargolini et al., 2006; Brun et al., 2008). Other examples concern the distribution of spatial information along a proximodistal gradient in the CA1 (Henriksen et al. 2010) and in the subiculum (Kim et al. 2012). Such within structure functional segmentations are often mirrored by corresponding connectional differences as is the case for medial and lateral entorhinal cortex (Witter et al. 1989) and gradients of connectivity along the longitudinal axis of the hippocampal formation (van Strien et al. 2009).

The development of techniques targeting either individual cells such as *in vivo* whole cell or juxtacellular recording or imaging (Harvey et al. 2009; Lee et al. 2009; Burgalossi et al. 2011), and genetically engineered selection/inactivation of neurons in a specific region/sub-region/cell population notably through optogenetic (Gradinaru et al. 2010; Akam et al. 2012; Raimondo et al. 2012), pushes the boundaries of neural investigation. In this context, a lack of proper identification of the investigated area can drastically change the interpretation of the results. Our aim here is to describe a pragmatic yet detailed set of criteria to recognize the many different areas of the hippocampal region and even identified markers that allow identifying the anatomical borders between subdivisions and layers within an area.

The complexity of the hippocampal region, both in terms of its detailed functional partition between and within subdivisions, as well as its intricate three-dimensional curvatures, makes it a difficult structure to experimentally probe in a reliable way. The currently available stereotaxic brain atlases (Swanson 2004; Paxinos and Watson 2009) or previously published accounts of the cytoarchitectonic features of subdivisions of the rat hippocampal region (Blackstad 1956; Haug 1976; Insausti 1993; Burwell et al. 1995; Insausti et al. 1997; Burwell 2001; Witter and Amaral 2004) lack sufficient spatial resolution in the three standard planes of sectioning. To remedy this problem, we set out to provide a fine-grained anatomical description of the parahippocampal-hippocampal region as encountered in coronal, horizontal and sagittal sections of the rat brain. Our description is based on cyto- and chemoarchitectonic features observed in histological sections stained for NeuN,

calbindin, and parvalbumin. It presents recently re-evaluated borders, as determined by complementary staining methods focusing on criteria that apply to all three planes. In contrast to most of the current architectonic descriptions of the region, we not only provide overall descriptions of features of each of the different subdivisions, but also particularly focus on the detailed description of the anatomical borders. All areas and the borders between have been integrated in a web-based application (http://www.rbwb.org), providing an unrivalled interactive three-dimensional atlas (Kjonigsen et al. 2011). This interactive and flexible framework offers a unique tool for experimentalist to help them to find their way in the complex anatomy of the hippocampal region.

Methods

The anatomical descriptions are based on histological material from eight young adult rats. The brains of two male Long-Evans rats (bodyweights around 220 g; Charles River, Denmark) were used to prepare the final illustrations. All experimental procedures were carried out in compliance with National Institute of Health and European Community guidelines for the use and care of laboratory animals, and care was taken to use as low numbers of animals as possible, still aiming for reliable and sufficient data to generate a three-plane atlas.

To prepare the atlas sections and their digital images, we used modifications of standard protocols that have been described previously (Insausti et al. 1997) Kjønigsen et al 2011). In short, animals were given an overdose of Equithesin and perfused transcardially with 250 ml ringer solution at 37°C followed by 300 ml 4% freshly prepared paraformaldehyde in 0.1M phosphate buffer (pH 7.4), using a peristaltic pump (WPI). The brains were extracted and put in 4% paraformaldehyde at 4°C overnight. After being cryoprotected in 2% dimethyl sulfoxide (DMSO, Merck) in 0.125 M PB and 20% glycerine (Merck) at least overnight, 50 µm sections were prepared on a freezing microtome (Microm HM 30 ThermoScientific, Oslo, Norway) and collected in 6 equally spaced series.

Two brains were selected to prepare the atlas figures. Of one brain, the left hemisphere was cut horizontally, while the right hemisphere was cut sagitally. The second brain was cut in the coronal plane. While cutting, one series was mounted directly onto Superfrost plus-slides and stained with cresyl violet for cytoarchitectural orientation and to be used as a matrix when mounting the sections used for immunohistochemistry. Three of the series were immunostained for the neuronal stain NeuN, and the calcium-binding proteins parvalbumin (PV) and calbindin D-28 (CB), respectively, using modified previously published protocols, PV: (Cuello et al. 1983; Wouterlood et al. 1995); CB: (Wouterlood et al. 2001); NeuN: (Mullen et al. 1992). All sections were rinsed 3 times for 10 minutes in 125 nM phosphate buffer (pH 7.4) and pre-incubated for 1.5 hour in 5% normal goat serum in a solution of 50 mM Tris, 0.87% sodium chloride and 0.5% Triton X-100 (TBS-TX). All rinses in between incubation steps were with TBS-TX. Subsequent to rinsing, individual series of sections were incubated with monoclonal mouse primary antibodies against parvalbumin (Sigma-Aldrich P3088, 1:2000 in TBS-TX) or against calbindin D-28K

(Swant, 1:4000 in TBS-TX), or against NeuN (Chemicon, 1:1000) for 24-48 hours at 4°C. After rinsing, sections were incubated in a secondary goat anti mouse antibody coupled to biotin (Sigma Aldrich B7151, 1:100 in TBS-TX for 90 min at room temperature), followed by incubation with the Vector ABC kit according to specifications of the manufacturer (Vector laboratories Inc., Peroxidase standard PK-Vectastain ABC kit 400). For visualization, sections were rinsed in Tris/HCl solution and subsequently reacted with diaminobenzidine (Wouterlood et al. 1995). Sections were mounted on glass slides from a 0.2% gelatin solution and dried. Sections on slides were dehydrated through increasing concentrations of ethanol to xylene and coverslipped with Entellan (Merck, Darmstadt, Germany).

In addition we used sections taken from a brain of a female Wistar rat (body weight 200-220 g; Harlan, Zeist, The Netherlands) that was perfused with a sulphide containing fixative according to the sulphide-silver staining protocol as originally described by Timm to stain for the presence of zinc (Haug 1976). We have additionally used sections taken from female Wistar and Long Evans brains stained for acetylcholinesterase (AChE; (Loyez 1910; Kluver and Barrera 1953; Tago et al. 1986) or BlackGold s2 myelin stains (Schmued et al. 2008), as well as SMI-32 (Voelker et al. 2004) and calretinin (Wouterlood et al. 2007).

High-resolution brightfield digital images of the stained sections were obtained with an automated scanning microscopical device (Mirax midi, Zeiss, Germany) at a resolution of 0,46 µm/pixel. All images were subsequently exported at a resolution appropriate for publication (300 DPI) and contrast and brightness was adjusted with the use of Adobe Photoshop CS (Adobe Systems Inc., San Jose, CA, USA) to assure equal-luminance images of all sections. The original high-resolution files were used to prepare the images to be presented in a zoomifiable format in the online database.

In order to delineate subdivisions, we applied two different approaches. First, all sections from the series stained for NeuN, PV and CB have been digitally drawn using Neurolucida imaging software (Micro-Brightfield, Inc., Colchester, USA). This program enables to directly draw the visual image under the microscope, producing a digital computer representation, while maintaining relationships between adjoining sections. Borders as visualized with the different staining methods were indicated in each section. Subsequently, the drawings of the adjacent differently stained sections were merged and linearly scaled to fit. This allows an easy assessment of the degree

of overlap between borders drawn on the basis of the differential expression patterns of the markers used. In a second approach, digital images of three adjacent sections that were differently stained sections were merged as individual layers into a single file, using Adobe Photoshop CS, and linearly scaled and rotated to get the best match between adjacent sections. Using adjustments in transparency, the coincidence of borders in each of the different stains can be easily visualized.

This procedure was applied to all sections prepared in the three different planes of sectioning. Criteria to delineate subdivisions in the hippocampal region were derived from previously published accounts (Insausti et al. 1997; Witter and Amaral 2004; Kjonigsen et al. 2011). The criteria were first independently applied to all sections of the three series. Subsequently, each of the delineations specific for a particular plane of sectioning were transferred to a standard 3D brain (Kjonigsen et al in prep) and checked for consistency with the independently generated delineations in the other two planes. Discrepancies present in the three independently derived datasets were checked by comparing individually generated 3D-reconstructions and corrected.

Results

Nomenclature

The hippocampal region consists of two main structures: the hippocampal formation (HF) and the parahippocampal region (PHR). The HF, also sometimes referred to as hippocampus, includes the dentate gyrus (DG), the Cornu Ammonis (CA) regions 1, 2, and 3, or hippocampus proper, and the subiculum (Sub). We additionally differentiate a separate, yet poorly understood part, referred to as the gyrus fasciolaris, or fasciola cinereum (Stephan 1975). The PHR comprises the presubiculum (PrS), the parasubiculum (PaS), the entorhinal cortex (EC), the perirhinal cortex (PER) and the postrhinal cortex (POR). The defining difference between HF and PHR is the number of layers. The HF is a three-layer cortex, consisting of a molecular layer, directly deep to the pia, a cellular layer, and deep to the latter the so-called polymorph layer. In contrast, PHR is considered to have six different layers. These are from outside in, the molecular layer and the cellular layers II-VI. In case of EC, PrS and PaS, layer IV is a cell-poor layer, generally referred to as the lamina dissecans. The positions of these cortical regions in the rat brain are illustrated in Figure 1.

We defined three principal axes used throughout the paper to describe anatomical positions: the rostrocaudal axis (also referred to as anteroposterior), the dorsoventral axis and the mediolateral axis. In addition, notwithstanding the curvature of HF, the longitudinal axis of HF is referred to as dorsoventral axis, whereas the axis perpendicular to this is referred to as the transverse axis. When describing positions along the transverse axis of HF, portions located closer to DG are referred to as proximal and those further away from DG are called distal. It should be pointed out that all these terms do not imply that within the individual subdivisions of HF separate entities exist such as a proximal CA1 versus a distal CA1, or a ventral and a dorsal CA1. In case of PHR, a similar set of axes is now commonly accepted, although the differences in curvatures of substructures necessarily lead to some adaptations. In case of PrS and PaS, different locations are described using the dorsoventral and transverse proximodistal terminology. For the remaining EC, PER and POR, we opted to maintain the proximodistal transverse terminology, yet the longitudinal axis partially overlapping with a dorsoventral axis, will be referred to as the anteroposterior axis. A fourth axis is used to describe the radial, laminar, or superficial to deep position within the different subdivisions. This radial axis is such

that layer I is the most superficial layer, closest to the pia, and layer VI the deepest. It is essential to point out that both HF and PHR are curved in a complex way such that the radial outside-in relation can have many different orientations in the brain (Figure 1). This, for example, leads to the fusion of the pial surface of one half of DG with this of the remaining hippocampal subfields. The fusion between the two cortical sheets, characterized by the presence of a series of blood vessels, is called the hippocampal fissure.

ARCHITECTONIC DESCRIPTION

All of the subdivisions of the hippocampal region have been originally identified based solely on cytoarchitectonic features apparent with neuronal marker such as Nissl or NeuN. However, the position of some borders was unclear until chemoarchitectonic features were recently taken into account to settle the debates. Such features can be revealed by immuno-staining for parvalbumin and calbindin, two proteins that are differentially expressed in the neuron populations of hippocampal and parahippocampal sub-regions.

In the following paragraphs, each subfield will be presented: first by a general overview of its position in the brain in relation to its neighbors, second by its overall cytoarchitectonic characteristics, and third by a precise description of the cytoarchitectonic and chemoarchitectonic features marking its borders with its neighbors. To avoid duplication, we will describe each border only once, such that for each new subdivision, when applicable, only the border with the proximally adjacent neighbour will be described in detail.

Hippocampal formation

The hippocampal formation (HF) in the rat is a c-shaped structure positioned in the posterior half or the hemisphere. The dorsoanterior portion of HF borders the dorsal tip of the septal complex in the midline of the brain, while the most ventral tip is positioned more laterally in the hemisphere, adjacent and directly posterior to the amygdaloid complex (Figure. 1). The HF is characterized by its marked three-layered organization, typical of the allocortex, see Nomenclature (Stephan 1975). The superficial layer is a plexiform layer and contains only very few neurons. The middle layer is a thin and densely packed principal cell layer. The inner layer is a dense and fibrous polymorph layer with embedded dispersed neurons. The HF subfields are, from proximal to distal along the transverse axis: the dentate gyrus (DG), the Cornu

Amnonis (CA) fields 1, 2 and 3 and the subiculum. In this account we further differentiate a poorly understood region generally referred to as the fasciola (or fasciola cinereum; FC). In coronal and horizontal sections, this part almost looks like an additional mini-hippocampus, situated directly medial to the most dorsal tip of HF. Careful analysis of the adult hippocampus supports previous accounts that FC actually is a continuation of the longitudinal extent of HF, bending medially (Stephan 1975). In this sense FC is comparable to the uncal portion of the primate anterior hippocampus, while the dorsal tip of HF would be comparable to the primate genu, except that the curve in the rat is located at the dorsal tip, while in the primate it is located at the ventral tip. The FC can be further subdivided into small subfields characterized by a dominance of granule cells (FC-DG), and large and small pyramidal cells (FG-CA3 and FG-CA1/Sub, respectively). However for the present account we opted to refrain from subdividing FC.

The **Dentate gyrus (DG)** is the most medial and proximal portion of HF. The outer plexiform layer is called the molecular layer and its inner polymorph layer is referred to as the hilus. When stained for a neuronal marker such as NeuN, DG is characterized by a single curved cell layer, densely packed with granule cells. The curve presents itself as a V-shaped, or C-shaped structure, depending on the dorsoventral level of the HF (Amaral et al. 2007). Each limb of the V (or C) is referred to as a blade. The blade directly adjacent to the hippocampal fissure and the other hippocampal fields is known as the enclosed blade. It is also sometimes called the suprapyramidal, dorsal, or inner blade. For the opposite portion of the granule cell layer the term “exposed blade” will be used here, yet some authors refer to it as the infrapyramidal, ventral, outer, or free blade. The rat granule cells lack basal dendrites but have an extensive apical dendritic tuft, extending into the molecular layer, reaching the pial surface. The granular cell axons are called the mossy fibers.

Chemoarchitectonics features are instrumental to clearly distinguish DG from its neighbouring hippocampal fields, especially through differences in calbindin (Calb) staining patterns. The DG is more darkly stained than all its neighbors, except for the distal CA1. The border between DG and the distal CA1 is marked by the hippocampus fissure and by the contrast between the uniformly dark DG molecular layer and the very dark “fibrous” pattern of CA1. Within the DG, there is a staining gradient from a very dark granular cell layer and dark molecular layer to an

intermediately stained hilus. Most, if not all, granule cells are labelled while there is only a low number of calbindin positive neurons in the hilus. In addition, one can see a deep adjacent layer of unstained neurons apposing the granular cells. Those neurons likely correspond to the layer of interneuron that partially stain positive for parvalbumin.

The **Cornu Ammonis or Ammons Horn (CA)**, also known as hippocampus proper, is characterized by a thin layer of densely packed pyramidal cells, embedded in an outer plexiform layer and an inner rather thin polymorph layer, the stratum oriens, that borders the fibre-containing alveus. The outer plexiform layer contains the apical dendrites of the pyramidal cells. It is divided into a number of sub-layers, which will be described within the context of each of the respective subfields CA1, CA2 and CA3. Some authors have differentiated a field CA4. However, it is ill-defined in respect to the DG hilus, therefore this practice will not be followed here (Witter and Amaral 2004). The CA field is bordered by DG proximally, and meets Sub at its most distal part.

Area CA3 is characterized by the presence of a densely packed layer of large pyramidal cells. The outer plexiform layer of CA3 is subdivided from deep to superficial into stratum lucidum, stratum radiatum, and stratum lacunosum-moleculare. The stratum radiatum is named after the regular parallel alignment of pyramidal neuron apical dendrites. In addition, it contains many of the hippocampus local axons. The stratum lacunosum-moleculare is located between the stratum radiatum and the hippocampal fissure. Axons of major extrinsic inputs travel and terminate in this sublayer. The stratum lucidum is sandwiched between the pyramidal cell layer and the stratum radiatum. It contains the mossy fibres that originate in DG.

The border between the CA3 proximal part and the DG hilus is hard to identify in conventionally stained sections, but calbindin stained preparations show an abrupt change in two neuropil staining features. As mentioned above, the positive hilus contrasts from the overall unstained CA3 neuropil, with the exception of the calbindin-positive mossy fibres originating from DG in the hilus and running confined to stratum lucidum.

Area CA2 contains a mixture of large and small pyramidal cells. The cell layer tends to be a bit thicker than in CA1. The large pyramidal cells are similar in size to those

seen in CA3, whereas the smaller ones are similar in size to those of CA1. Except for its lack of stratum lucidum the laminar profile of CA2 is comparable to CA3. The border between CA2 and CA3 is principally characterised by a slight widening of the pyramidal layer.

Chemoarcitectonic features highlight the identification of this border with the lack of stratum lucidum marked by only limited or absent calbindin positive mossy fibers and the presence of a much higher density of quite large parvalbumin-positive neurons compared to CA3.

A striking feature of **area CA1** is its very regular homogeneous cell layer, comprizing a few rows of medium-sized pyramidal neurons, smaller than the pyramidal cells of CA3. The transition between CA2 and CA1 coincides with a sudden drop in the pyramidal cell size, observable in sections stained for NeuN.

This border is also clearly marked by chemoarchitectonic features as CA1 superficial pyramidal cells and the neuropil between the stratum radiatum (sr) and stratum lacunosum-moleculare (sl-m) stain positive for calbindin, features not seen in CA2. In addition, CA1 sl-m stains positive for parvalbumin and create a continuous appearance, which is absent in CA2.

The **subiculum (Sub)** is the third main component of the HF. It is dorsally located between CA1 and the retrosplenial cortex and ventrally, between CA1 and the presubiculum (PrS). Over most of its extent, Sub encompasses a well-differentiated multilayered pyramidal cell layer. Between the pyramidal layer and the hippocampal fissure/pial surface, one can find the outer plexiform layer, referred to as the molecular layer. The latter can be subdivided into a deep portion continuous with CA1 sr and a superficial portion continuous with CA1 slm. These sublayers are not easy to detect by any of the markers used, yet they largely reflects the differential termination of intrinsic and extrinsic connections similar to what has been described for all CA fields. The border between CA1 and Sub is clear cytoarchitectonically through a widening of the pyramidal cell layer from a thin layer with darkly stained and more densely packed neurons in CA1 to a larger and less organized layer presenting lightly stained and slightly larger pyramidal cells. Along most of the long axis of the subiculum, the subicular cell sheet is distally continuous with the deep layers of PrS. The precise border between Sub and the deep layer of PrS is generally crescent-shaped and characterized by a subtle change from a homogeneous layer of

cells in Sub to a more radially organized cell layer in PrS (See below for a detailed description of the border). At the most dorsal extreme, Sub borders directly with the retrosplenial cortex (RSC). This border is abrupt and characterized by a sudden increase in the number of cell layers as well as the emergence of a densely packed outer granular layer (layer II) in RSC.

Chemoarchitectonically, the CA1-Sub border is visible in calbindin stained sections, since superficially positioned neurons in CA1 are positive for that protein and not stained in Sub. Although the CA1/Sub border seems easy to establish, it is in practice not possible to determine whether a particular dendrite in the transition area belongs to a CA1 or Sub neuron. This is due to the fact that this border is oriented obliquely to the transverse axis. This orientation is apparent when focusing on the small area where calbindin positive small CA1 pyramids are positioned superficially to the most proximal Sub neurons.

Parahippocampal region

The parahippocampal region (PHR) includes several six-layered cortical areas reciprocally connected to the HF and each other. It can be divided into five main structures: the presubiculum (PrS), the parasubiculum (PaS), the entorhinal cortex (EC), the perirhinal cortex (PER) and the postrhinal cortex (POR). Some of these areas have been further divided in a variety of different ways. For the present account, we will divide the PER into areas 35 and 36 (Burwell 2001) and the EC in medial entorhinal cortex (MEC) and lateral entorhinal cotex (LEC);. MEC is further subdivided into the caudal entorhinal (CE) and medial entorhinal (ME) areas while the LEC is subdivided into the dorsolateral (DLE), dorsal-intermediate (DIE), and ventral-intermediate entorhinal (VIE) areas (Insausti et al. 1997). The amygdalo-entorhinal cortex is not included here in the EC (Witter and Amaral 2004).

The **presubiculum (PrS)** is a multilayered cortical area, which takes its name from the fact that on its lateral side it juxtaposes the subiculum (Sub) over most of the longitudinal dorsoventral extent. On the other side it meets the parasubiculum, again along a large part of the longitudinal extent. PrS has been divided into a dorsal and a ventral portion, coinciding with subtle differences in connectivity (van Groen and Wyss 1990). The dorsal portion of PrS has also been named the postsubiculum, or Brodmann's area 48, while the ventral PrS is also referred to as Brodmann's area 27

(Brodmann 1909). However these subdivisions are not used in the present account. At the dorsal extreme, PrS borders the retrosplenial cortex and the visual cortex.

Alike all PHR structures, the PrS contains six layers. The first layer (LI) is the acellular molecular layer. The second (LII) and third (LIII) layers together form the superficial layers while layers five (LV) and six (LVI) are the deep layers. A cell sparse layer, generally termed lamina dissecans or layer IV separates the superficial from the deep layers. LII is easily identifiable in Nissl or NeuN stained sections, it consists of a thin superficial sheet of small darkly stained and densely packed pyramidal cells, while the broader neighbouring LIII is lighter and present a looser cell arrangement. In dorsal PrS, layer II is often fragmented, forming little clusters of cells. The deep layers can be recognized by their columnar arrangement. The main cytoarchitectonic characteristic differentiating the deep layers from each other is that LV consists of one or two rows of large pyramidal cells while layer VI harbors a variety of generally smaller neuron types.

Cell density and cell size allow to reliably position the border of PrS with most of its neighbouring structures. Complementary information comes from chemoarchitectonic staining (see below). As stated previously, the transition between Sub and PrS is characterized by an increase in number of layers, which also indicates the border of the HF with the PHR (Stephan 1975). One can observe the sudden emergence of a superficial cortical sheet, strictly separated by the lamina dissecans from the deeper continuation of the subicular sheet. The border between the subiculum and layers V and VI of PrS is crescent shaped and can be easily recognized using cytoarchitectonic features. While most subicular cells are approximately of the same size, with no apparent layered features being apparent, PrS cell bodies are smaller and more densely packed. In addition, the PrS deep layer columnar arrangement clearly separates it from the adjacent Sub. The border between PrS with retrosplenial or the visual cortex is marked by the presence of the lamina dissecans in PrS opposed to its absence in the two other structures. In addition, the outer granular layer II of the retrosplenial cortex presents a sudden increase in density compared to PrS. Morevover, the overall radial organization of PrS deep layers is replaced with a more diffuse arrangement in the retrosplenial cortex and a laminar arrangement in the visual cortex.

The distribution of immunoreactivity for calbindin allows differentiating PrS from its neigbours. PrS LII presents a moderate to strong reactivity along most of its

extent while the other layers are quite weakly stained. This strong calbindin positivity in PrS LII contrasts with the absence of reactivity for calbindin in Sub and PaS. However, one should be aware of a much weaker reaction in the most dorso-medial portion of PrS LII (figure 2: D10-12), and thus use for that portion other criteria. Parvalbumin reactivity is not strikingly different between PrS and its neighbors, however it may confirm border positions based on other criteria. PrS superficial layers show a slightly stronger reactivity than the deep layers, while the lamina dissecans appears as a clear unstained thin stripe. This distribution of reactivity changes abruptly at the border with the retrosplenial cortex, which is characterized by a more laminated pattern with an overall dense staining in LII, LIV and LV contrasting with a weaker staining in LIII and LVI (figure 3: C12, figure 2: C1-3). The border of PrS with PaS will be described below, in the PaS section.

The **parasubiculum (PaS)** is a narrow part of PHR, wedged in between PrS and EC. The most dorsal portion of PaS curves around EC such that a small portion of PaS appears dorsal to the most caudodorsal part of MEC, bordering the postrhinal cortex (POR) laterally. This portion has often been mistaken for EC. The PaS, or Brodmann's area 49 has been subdivided into two portions (area 49a and 49b) (Brodmann 1909), yet based on the lack of clearly established functional differences, we opted not to further divide PaS

The cytoarchitecture of PaS looks very similar to that of the PrS. It is a six layers-cortex, with superficial cell layers (LII-III) separated from deep layers (LV-VI) by the thin cell-sparse lamina dissecans (layer IV). Yet, contrary to what is observed in the PrS, the laminar differentiation of the superficial layers (LII/III) is virtually absent. In addition, PaS cell bodies are uniformly bigger, less compact and stain only moderately for Nissl substance.

PaS deep layers cannot easily be distinguished from those in PrS, EC, and POR in classical neuronal stains, yet immunochemistry markers do facilitate their delineation. A striking feature of PaS is its absence of reactivity for calbindin, which contrasts with the moderate to strong reactivity to that protein of the superficial layers of PrS, EC and POR. Furthermore, parvalbumin immunoreactivity contributes to establish the PaS/PrS border. The distribution of this protein contrasts between PrS, which shows a quite homogeneous pattern with a uniform number of positive neurons and only a small difference of overall staining intensity between deep and superficial

layers, and PaS, which presents a clearer lamination with a higher number of positive neurons in the superficial layers accompanied by a corresponding difference in staining intensity of the neuropil. In addition, the generally stronger reactivity for parvalbumin in the deep layers of PrS contrasts with the lower staining intensity in those of PaS, providing the only useful criterion to determine the deep layer border between the two areas.

The **entorhinal cortex (EC)** is a large cortical area that forms a cap-like structure occupying the latero-ventro-caudal domain of the hemisphere. It is essentially the center part of the PHR and therefore it borders to the other four divisions of PHR. On its rostral side, the EC juxtaposes the piriform cortex laterally, and the periamygdaloid cortex and the posterior cortical nucleus of the amygdala, medially. The transition between the EC and its anterior neighbors takes place approximately at the midst of the amygdaloid fissure. There the EC progressively decreases in width, such that it eventually extends anteriorly for approximately 2 mm as a narrow strip. This anterior extension is delimited ventromedially by the piriform cortex, and dorsolaterally by the perirhinal cortex (PER). The latter area continuous to border EC more caudally while the dorsocaudal border of EC is with the postrhinal cortex (POR) that wraps around the EC. Medially, the EC is bordered over most of its rostrocaudal extent by the parasubiculum (PaS; Figure 1).

The EC is commonly divided into a lateral entorhinal cortex (LEC) and a medial entorhinal cortex (MEC) (Witter and Amaral 2004), also referred to as Brodmann's areas 28a and 28b respectively (Brodmann 1909). In recent years, the EC in primates has been subdivided further and in an attempt to maintain some level of comparability, the rat EC was subsequently similarly subdivided (Insausti et al. 1997). Following the latter account, EC includes five different areas. The MEC is subdivided into caudal entorhinal (CE) and medial entorhinal (ME) areas and LEC into dorsal lateral entorhinal (DLE), dorsal intermediate entorhinal (DIE) and ventral intermediate entorhinal (VIE) areas. Originally, a sixth area was described as part of LEC, the so-called amygdaloid entorhinal transition (AE) since preliminary observations suggested that AE projected to the dentate gyrus (Insausti et al. 1997). However more elaborate studies refuted that claim (Pitkanen et al. 2000), thus AE is here not considered as part of EC (Witter and Amaral 2004).

As all parahippocampal areas, the EC is a six-layered cortex. Cytoarchitectonically, EC layer I is a quite narrow molecular layer containing very few small neuronal somata. Layer II is thin and densely packed with medium to large dark cells, mainly of the stellate type. Layer III and V contain mostly medium-sized pyramids that are moderately stained. Finally, the cell population in layer VI is more varied in cell types, yet this layer stained moderately and homogenously in Nissl throughout the whole EC. In MEC, deep layers (V-VI) are clearly distinguishable from superficial layers (II-III), as the thin acellular layer IV, i.e. lamina dissecans, separates them. In LEC, this layer IV is rather poorly developed. The five subdivisions (CE, ME, DLE, DIE and VIE) are differentiated based on subtle cytoarchitectonic differences and mainly serve detailed anatomical comparisons. Therefore the LEC/MEC distinction is sufficient for most practical purposes (Witter et al. 1989; Insausti et al. 1997).

The border between EC and the olfactory (posterior piriform cortex) and the periamygdaloid cortex is indicated by a reduction in the number of cell layers from six to three, whereby losing the lamina dissecans and layers deep to it, while maintaining layers I-III. Layer II is characterized in Nissl stain by darkly stained large neurons, while in layer III a slight drop in staining density for calbindin can be observed. The most medial border between EC and the amygdala is with the posterior cortical nucleus and is easily identifiable by a lack of laminar organization of the amygdala.

The medial border of EC with PaS is defined best by combining cyto- and chemoarchitectonic criteria. The border at the superficial layer level can be identified based on the clear lamination seen EC due to the intensely stained LII, contrasting with the PaS cytoarchitectural uniformity of staining with Nissl or NeuN. This border may be confirmed by sections stained for calbindin, which exhibit a moderate to strong staining of the deepest cells of EC LII that contrast with a non-reactive PaS. This difference is particularly helpful in identifying the small extension of PaS that curves around the dorsal end of the EC (Fig. 1). Staining with parvalbumin show similar contrasting results between a clear lamination of the EC superficial layer with LII being very densely and LIII moderately stained, opposed to the uniform dense staining of PaS. Parvalbumin reactivity is also instrumental in defining the border between Pas and EC deep layers. Deep layers in EC show throughout a uniformly weak intensity of staining which contrast with either even weaker reactivity in the

more ventral parts of PaS (figure 2: A3; figure 3: C10), or the more laminated pattern at more dorsal levels of PaS (figure 2: A2; figure 3: C10-11) with LV being slightly denser than layer VI. The reader is referred to each subfield paragraph (see below) for a more specific description of the border of each EC subfield with PaS.

The **Medial entorhinal cortex (MEC)** is subdivided into caudal entorhinal (CE) and medial entorhinal (ME) areas. Although the name may be taken to indicate that MEC is the most medial portion of EC, that statement is only partially correct, since the most caudodorsal portion of EC is also part of MEC (Fig 1). However, the medial border of EC coincides with the medial border of MEC, which thus borders PaS, POR and Sub. MEC naturally has part of its lateral border with LEC as well as with POR.

The characteristic feature of MEC is the overall regular organization and clear lamination. The superficial layers II and III are clearly separated from the deep layers by a well-developed acellular layer IV or lamina dissecans. In NeuN or Nissl staining, LII presents itself as a well developed, regularly packed ensemble of medium to large darkly stained stellate cells. Layer III contains medium sized pyramids that are homogeneously distributed along the entire extent of MEC showing a slightly higher density in the superficial half of the layer The deep layers show a clear columnar or radially oriented organization. Most of these features change rather abruptly at the border with LEC, such that LEC overall looks way less homogeneously and regularly organized. An extensive description of the MEC/LEC border will be provided in the LEC section.

The **caudal entorhinal area (CE)** constitutes the ventral part of the caudal pole of the rat hemisphere. At the very caudal extreme, CE spans the mediolateral extent of the entorhinal cortex, from the rhinal fissure laterally to the border with PaS medially. It is relevant to note that in sagittal sections it may appear as if CE borders PrS (Figure 3: A9). This is essentially an artefact due to the fact that their respective Layer VI are difficult to separate. The lateral and dorsal-lateral border of CE is mainly with POR, although a limited ventral-anterior portion of CE borders parts of LEC. More ventral-medially, CE is positioned adjacent to ME.

Cytoarchitectonically, CE layer I presents some sparse neurons and is sharply delimited from layer II, which consists of a continuous band of medium to large darkly stained and regularly packed stellate cells. At its medial extreme, layer II

typically increases its width. Layer III is wide and presents the typical MEC cytoarchitecture (see above) and so is layer V, whose neurons are loosely arranged at the border with the clear lamina dissecans but tightly packed deeper in the layer. Layer VI is broad and not clearly demarcated from the white matter. Neurons in the deep layers V and VI of CE are radially organized.

The border between CE and PaS is easy to discern in the superficial layers based on the difference of lamination between MEC and PaS (see above) and the absence of reactivity for calbindin in PaS (see above). The border between the deep layers of these two structures is marked by the absence of reactivity for parvalbumin in PaS at that level, which contrasts with the moderate positivity of staining in CE LV and VI.

The **medial entorhinal area (ME)** occupies the most ventromedial portion of the entorhinal cortex. It is located on the medial and caudomedial bank of the amygdaloid fissure. The caudal border of ME is with the caudal entorhinal area (CE), and medially the border is with the parasubiculum (PaS). Rostromedially, the parasubiculum is replaced by the most anterior remnant of the presubiculum (PrS). Laterally and anteriorly, ME borders the ventral intermediate entorhinal area (VIE). The extreme anterolateral part of the ME borders the periamygdaloid area (PA), whereas the most anteromedial aspect meets the amygdaloid-hippocampal transition (AHT).

The overall cytoarchitectonic features of ME are comparable to those of CE. The most striking changes that delineate the border between the two subdivisions of MEC are an overall less conspicuous lamination in ME compared to this of CE. ME superficial layers are less homogeneous than their CE counterparts. ME LII brakes up into two or three clusters of cells, which makes it less sharply delineated from both LI and LIII, while ME LIII tends to split into sublayers. Differences exist also in the deep layers. Layer V of both areas can be subdivided into sub-layers, a superficial layer Va and a deep layer Vb and the main contrast between CE and ME is in the superficial portion. CE LVa is sparsely populated by large pyramidal cells, while ME is characterized by a more regularly build LVa with a higher number of large pyramidals positioned at regular intervals. Immunocytochemical markers provide complementary information on the ME/CE border. CE shows a strong reactivity for calbindin of both neuropil and neurons limited to LII, whereas in ME this reactivity

extends into the superficial portion of LIII. In staining for parvalbumin, CE superficial layers exhibit moderate homogeneous reactivity contrary to ME where parvalbumin positive neuropil is sparse to absent.

The border between ME and PaS is similar to that described above for CE and PaS. The borders with the PA and the AHT are marked by the absence of lamination in the superficial layers of these areas and the absence of clearly developed deep layers. In addition, the positivity for calbindin is higher superficially in AHT than in ME.

The **Lateral entorhinal cortex (LEC)** is positioned ventral and lateral to the MEC. Its medial and caudal border is thus with MEC, while laterally LEC is flanked by PER, area 35, over its entire rostrocaudal extent. The rostral border is with the posterior piriform cortex laterally and with the amygdalo-entorhinal transition and periramygdaloid cortex more medially.

Cytoarchitectonically, either with Nissl or NeuN, the neurons in LEC LII are slightly smaller, not as darkly stained and less densely packed compared to MEC LII. Quite often they do not form a continuous layer but tend to break up into cellular groups or islands. LEC LIII pyramids are less regularly distributed than in MEC. Layer IV of LEC is either poorly developed, which contrasts with the clear lamina dissecans of MEC. The deep layers lack the columnar organization typically seen in MEC.

The **ventral intermediate entorhinal (VIE)** area starts approximately at the same rostrocaudal level as its medial neighbor ME. The anterior border of VIE is with the amygdalo-entorhinal transition area laterally, and with the periamygdaloid cortex and the posterior cortical nucleus of the amygdala, medially.

In general, the layers of VIE are less well developed anteriorly, where they tend to merge. LII stellate cells are smaller and less stained than their counterparts in ME. They are organized in clumps that are very close to each other, rendering a continuous appearance of a thinner LII when studied with low magnification. According to several authors (Caballero-Bleda and Witter 1993) the outer portion of layer III of VIE should be considered part of layer II and designated as layer IIb to differentiate it from the more superficial layer IIa. The densely packed medium-size pyramids in LIII form irregular clusters surrounded by empty spaces in opposition to the more homogenous organization observed in ME. Although very little or no

separation exists between LIII and LV, they can still be easily differentiated based on the characteristic presence of big darkly stained pyramidal cells through the whole LV. The presence of these big darkly stained cells is also a marker for the border with ME where they are restricted to the outer part of LV. The cell density in LV decreases at the border with the rather thin layer VI.

The absence of the lamina dissecans and the deep layer columnar arrangement are the main markers of the border between VIE and ME. This border also stands out based on chemoarchitectural features. In VIE, there are almost no positive neurons that stain for calbindin and for the neuropil, the superficial half of LI is moderately to weakly stained, and so is LII, while the whole extent of LIII is positive (Figure 1: D2-4; Figure 4: D17-18). In contrast, in ME, calbindin positive neuropil is found mainly in LI, LII and superficial LIII and positive neurons in LII.

The border between VIE and the amygdaloid region is characterized primarly by the change from VIE having multiple cell layers into areas that essentially have only one clearly defined cell layer sandwiched between molecular and polymorph layers (Figure 2: B8-9). Subtle chemoarchitectural differences do exist but do not really contribute to the description of this border.
The border between VIE and DIE will be described in the DIE paragraph.

The **dorsal intermediate entorhinal area (DIE)** forms the ventrolateral portion of the LEC. It forms a strip of LEC that runs parallel to the rhinal fissure and thus to PER. Caudally it borders with CE and laterally with DLE, whereas medially, most of its extent borders VIE. The rostral border is with the posterior piriform cortex.

Layer I of DIE is quite narrow and contains very few scattered neurons. LII and LIII respect the classic cytoarchitectures of EC. LII consists of a fairly densely packed and homogenous thin layer of big rounded darkly stained neurons. LIII is wide with a narrow, densely packed outer zone where the neurons are arranged in clusters, and a less dense, irregular inner zone. Similarly to VIE, the outer portion of LIII of DIE can be considered part of LII and named layer IIb. A characteristic feature of the DIE is that while LIV is very poorly developed or absent, LIII is clearly separated from LII along much of its extent by a very thin, relatively acellular band. LV is rather narrow and comprises loosely arranged medium to large pyramids that are not as darkly stained as those in VIE or ME. This difference is particularly striking in LVa of these areas. Whereas in ME and to a slightly lesser extent in VIE,

LVa comprises a more or less continuous row of large, darkly stained pyramids, such cells are only present incidentally in DIE. LVI is a narrow and compact, and together with LV lack a columnar arrangement.

The border between CE and DIE is marked by CE conspicuous lamina dissecans. Both areas have an overall comparable layer II. Layer III changes from having an irregular neuronal organization with neurons clusters surrounded by empty areas in DIE to a much more regularly organized layer with equally spaced neurons in CE. . The columnar like arrangements seen in layers V and VI of CE also breaks down in DIE such that the appearance of layers V and VI is more laminar. In addition the border features a sudden increase in the number of large darkly stained neurons in layer V in DIE compared to CE. Chemoarchitectonically the two regions are somewhat similar, in particular when comparing DIE with the adjacent lateral portion of CE. However, at the border calbindin positivity in DIE is present in both layers II and III while in CE, this is almost exclusive present layer II. When comparing sections stained for parvalbumin, it is obvious that CE has very strong positivity contrasting with the moderate staining in DIE and the weak staining in VIE.

The VIE and DIE share a number of features since they both are part of the LEC. However, there are still sufficient cytoarchitectonic and chemoarchitectonic differences to distinguish between the two. Layer II of VIE is narrow and organized in clumps that are very close to each other, rendering a continuous appearance when studied with low magnification which contrasts with DIE layer II. There is no acellular band separating layer II from layer III in VIE. Although LIII of VIE is generally thinner than in DIE this does not hold true in their border region. No major differences between the two areas are apparent in deep layers V and VI, with the exception that the border between layer V and the lamina dissecans is very much obscured in DIE compared to VIE and the latter area also contains much more large, darkly stained pyramidal cells than DIE does. Looking at chemoarchitectonic features, calbindin is strongly expressed in deep layer I, layer II and III in VIE, both in neurons and neuropil. In DIE, the staining in layers I and III is less dense, but the staining of individual neurons in layer II is more intense in DIE than in VIE.

The **dorsal lateral entorhinal area (DLE)** forms a strip of cortex closely related to the rhinal fissure, and therefore it is the only entorhinal area entirely located on the lateral aspect of the rat's cerebral hemisphere. At caudal levels it occupies both banks

of the rhinal fissure, while anteriorly it lies ventrally to it. It is positioned between the perirhinal cortex (PER) dorsally and the dorsal intermediate entorhinal area (DIE) ventrally. Similar to DIE, DLE extends along most of the rostrocaudal extent of the entorhinal cortex (EC), as is seen in coronal sections. Rostrally, DLE is replaced by the posterior piriform cortex. Although variable between animals, the very anterolateral part of the caudal enthorinal area (CE) generally abuts a posterior extension of the DLE.

Layer I of DLE is not very thick, and differs characteristically from what is seen in all other subdivisions of the EC in that it is populated by neurons that look like displaced layer II cells. Layer II is classic for EC (see above). Layer III is rather thin, and the cells are organized in horizontal rows, parallel to the surface curvature of the rhinal fissure. The outer portion of that layer is more densely packed than the inner one. A not sharply delineated and cell sparse layer IV separates layers III and V. Layer V has only a few very big and darkly stained pyramids, while the remaining neurons are medium-sized. Layer VI is more compact than layer V, and its cells are larger than their counterparts in the immediately adjacent DIE. Layer VI is obliquely oriented, so that the long axes of the neurons are parallel to the surface of the ventral bank of the rhinal fissure. Overall, both layers V and VI make an oblique and in some instances slightly curved border with the adjacent PER.

The border between DLE and CE in the superficial layers can be established by focusing on rather subtle differences. As stated above, DLE layer II cells tend to spread into the molecular layer, while this feature is not seen in CE. Also the packing in the superficial layers of DLE is much more irregular than in CE and the lamina dissecans is less marked in DLE compared to CE. Using immunoreactivity for calbindin provides additional information since CE shows strong staining almost exclusively in layer II, whereas in DLE staining is also present in layer III. In addition, CE deep layers have a columnar organization, whereas the DLE deep layers lack that feature.

There are striking and defining differences in the way cells are organized into layers between DLE and DIE. DIE layer II stellates are organized in a denser and more homogeneously packed layer than in DLE without invading the thinner molecular layer. In addition, a very narrow, relatively acellular band separates layer II from layer III in much of the DIE extent, which is not seen in DLE. DLE layer III is thinner than in DIE and presents a very different cell organization. In DIE, one can

clearly see a narrow, more densely packed outer zone with its neurons arranged in cell clusters, and a less densely and irregularly packed inner zone. This contrasts with the horizontal organization in DLE described above. Moreover in DIE the lamina dissecans is less conspicuous than in DLE. Layers V and VI do not show striking architectonic differences. When considering additional markers, it is apparent that whereas layer II of DLE stains rather strongly for calbindin both in terms of neurons as well as neuropil, in DIE the neuropil staining is less dense such that the individual positive neurons are easy to see. Using parvalbumin, the border between the two regions coincides with a gradual loss of the positive staining in layer III: moderate in DLE, light to absent in DIE.

The **perirhinal cortex (PER)** comprises two narrow strips of cortex, area 35 (PER 35) and area 36 (PER 36), which are adjacent to one another and situated around the rhinal sulcus, having a rostrocaudal extent almost similar to that of LEC (Figure 1) The PER 36 is quite often referred to as ectorhinal cortex, in which case PER 35 is referred to as the perirhinal cortex (Paxinos and Watson 1998). The rostral border of PER is with the insular cortex and it is generally accepted that this border coincides with the emergence of the claustrum, when looking into coronal sections. Its posterior border is with POR and generally positioned slightly rostral to the ventrally adjacent border between DLE and CE (see below). Anteriorly, the PER includes the fundus of the rhinal sulcus, both banks, and the dorsally adjacent cortex. More posteriorly, PER 35 and PER 36 are situated respectively inside and dorsal to the fundus of the posterior rhinal sulcus. It is generally accepted that when the claustrum is no longer visible, insular cortex is no longer present and is replaced by PER (Burwell 2001).

The **perirhinal area 35 (PER 35)** is bordered dorsally by PER 36 and ventrally and caudally by the entorhinal cortex (EC) and in some instances a small part of POR. The anterior border is with the agranular portion of the insular cortex. PER 35 may extend a bit more rostrally compared to PER 36. Some authors have further subdivided PER 35 into dorsal and ventral portions (Burwell 2001), but this subdivision is not applied here.

PER 35 tends to have a fairly thick layer I, a feature that is likely associated with the rhinal sulcus rather than with a cytoarchitectural region. Neurons in PER 35 exhibit a modified radial organization such that they form a shallow U-shaped arc

beginning at the pial surface ventral to the rhinal sulcus and ending at the white matter deep to the rhinal sulcus. PER 35 is further characterized by large, darkly stained, heart-shaped pyramidal cells in layer V. These cells are progressively smaller at more caudal levels of that area. Layers II and III of PER 35 tend to be merged, giving the impression of a fairly homogeneous, thick superficial neuronal sheet of lightly stained medium sized neurons bordered by the distinctive layer V cells. Layer VI is a narrow layer populated by medium sized neurons that, particularly at more dorsal levels when close to the border with PER 36, are rather similar to those of layer V. Layer VI exhibits the most clearly the typical crescent-like organization of PER 35.

The border between EC and PER 35 can be easily established based on cytoarchitectonic criteria. Indeed while DLE bordering the PER 35 shows a clear lamination in its superficial layers with layer II cells being larger and darkly stained than layer III cells, PER 35 superficial layers are homogeneously packed and do not seem different one from the other. In addition the lack of a lamina dissecans in PER 35 differentiates it clearly from the adjacent DLE. Regarding the deeper layers, the border between DLE and PER 35 is not conspicuous with the exception of the overall orientation of the neurons, which follow the above-mentioned crescent shape in PER 35 but not in DLE. The border between EC and PER 35 stands out with a stain for the distribution of the calcium-binding protein parvalbumin. The portion of DLE superficial layers, close to the border, stains heavily positive for parvalbumin and contrasts with an abrupt loss of staining in area 35. Vice-versa, in material stained for the calcium-binding protein calbindin, a marked increase of staining in area 35 is noticeable. Although not used in this atlas as a marker, a comparable sudden increase in staining intensity is noticeable when staining for the presence of heavy metals such as TIMM stain (Burwell et al. 1995; Naber et al. 1999; Burwell 2001).

The anterior border of PER 35 with the insular cortex has been described in detail in previous accounts (Burwell 2001) and is largely based on differences in cytoarchitectonic features. Here we essentially adopted this description. In short, PER 35 is characterized by the absence of the granular LIV seen in the insular cortex. Additionally, PER 35 deep layers are highly contrasted with layer V containing heart-shaped neurons and being thicker than LVI. On the other hand, the insular cortex deep layers are of approximately equal thickness and LV lacks the large darkly stained heart-shaped neurons. In addition, there are no claustral cells present in PER 35 deep to LVI.

The **perirhinal area 36 (PER 36)** is bordered dorsally by the ventral temporal cortex (Tev), ventrally by PER 35 and caudally by POR, which is situated mostly dorsal to the rhinal sulcus. The anterior border is with the granular and dysgranular portions of the insular cortex. Area 36 has been subdivided into three subfields: areas 36d, 36v, and 36p according to Burwell (Burwell 2001), but this subdivision will not be used here.

In general, PER 36 is characterized by a well-differentiated laminar organization of all principal layers. The LII of PER 36 is composed of aggregates of lightly-stained, medium-sized cells, while LIII presents itself as a homogeneous layer populated with medium-sized pyramidal cells. This patchy layer II is a good indicator to differentiate area 36 from Tev. The more dorsal part of PER 36 shows the presence of a granular LIV, which becomes dysgranular closer to the ventral border with PER 35. Throughout LIV appears to merge with LV. The outer sublayer is similar to layer V in packing density and staining characteristics of cells. In the inner sublayer, cells are flattened parallel to the surface of the external capsule. The thick, bilaminate layer VI is characteristic of area 36 and allows distinguishing it from the dorsally adjacent Tev and the ventrally adjacent area 35.

Chemoarchitectonics help to further delineate PER 36. While parvalbumin positivity is essentially absent in PER 35, the staining intensity increases gradually in PER 36 and provides the impression of a laminar distribution with the neuropil in LII and superficial LIII being moderately positive, in deep LIII and LIV less positive, in LV strongly positive, and finally in LVI weakly positive. In Tev, staining intensity for parvalbumin is more or less homogeneous in layers II-IV and dramatically increases in LV where it contrast with the somehow less intense reactivity seen in the adjacent PER 36 LV. The distribution of calbindin gives additional information on PER 36 borders. The reactivity for that protein tends to be stronger in the superficial layers of PER 36 than in their counterpart in PER 35, but slightly weaker than in their counterparts in Tev. The anterior border between PER 36 and insular cortex is comparable to that described for PER 35 (Burwell 2001).

The **postrhinal cortex (POR)** is associated with the rhinal sulcus by being positioned largely dorsal to it. POR is located caudally to PER 36 and rises steeply and wraps obliquely around the caudal pole of EC. Thus, it is difficult to discern and limited in its rostrocaudal extent when viewed in coronal sections. In most cases, POR arises at

the caudal limit of the angular bundle when subicular cells are no longer present in coronal sections. Another landmark is the shortening of the PrS in the dorsoventral dimension and the insertion of a cell-sparse region deep to PrS that borders the underlying white matter. The POR has been subdivided into dorsal and ventral portions (Burwell 2001) but this subdivision is not applied here. The ventral border over most of its anterior-posterior extent is with the entorhinal cortex (EC), although at the most medial portion of that border, EC is occasionally replaced by PaS. The extent to which POR borders with PaS is very variable between animals. Anteriorly, the superficial layers lie in the fundus of the rhinal sulcus, but the deep cortical layers in the fundus still belong to the ventrally adjacent EC. Caudally the region assumes a position above the fundus and is dorsally bordered at more rostral levels by temporal cortex and more caudally with occipital cortex, including visual and retrosplenial domains.

POR is singled from its neighbors by its overall absence of marked lamination. A distinctive feature is the presence of ectopic layer II cells at anterior levels of POR near the border with EC and PER. These ectopic cells have been noticed in all animals included in this study, although there is variability in how prominent they are. At these anterior levels, layers II and III can be differentiated from one another because layer III cells are less densely packed. Caudally, however, layer II is not easily separable from layer III. A granular layer IV is distinguishable in POR but less so at caudal levels. Layer V is composed of small pyramid-shaped cells. Layer VI, which is fused together with layer V, is composed of fusiform cells and elongated pyramids that are oriented almost parallel with the angular bundle.

The border between PER and POR is not very easy to detect. It can be based on POR bilaminate appearance where layers II and III are more or less fused and layer V and VI have merged and are quite similar in appearance. Most specifically, POR can be differentiated from PER by the presence of ectotopic layer II cells. These patches of LII cells into LI, give LII a distinctively irregular appearance (Burwell et al. 1995).

The border between POR and EC/PaS is also visible based on these ectopic layer II POR cells and the absence of clear laminar structure in POR superficial layers. Staining with an antibody against the calcium-binding protein parvalbumin makes these borders stand out. Whereas MEC and PaS close to the border are darkly stained, POR is only lightly stained. A similar pattern is observed in the AChE-

stained material. In contrast, in material stained for the calcium-binding protein calbindin, a marked strong staining in POR is noticeable, which is absent from the directly adjacent part of EC and PaS. Although not used in this atlas as a marker, a comparable sudden increase in staining intensity is noticeable when staining for the presence of heavy metals in Timm staining (Burwell et al. 1995; Naber et al. 1999; Burwell 2001).

The dorsal borders of the POR with the temporal cortex anteriorly and with the occipital cortex posteriorly are difficult to discern. A major marker is the increased differentiation between layers II and III, as well as a more prominent layer IV. As described previously (Burwell 2001), we confirmed in our material that cortical areas dorsal to POR express a higher level of myelin (not illustrated).

Discussion

The hippocampal region of the rat comprises a large number of areas, described by various authors over a period of more than a century. This series of descriptive papers essentially started with the description by Ramon y Cajal and his student Lorente de Nó of the hippocampus and its main subdivisions, and the subdivisions of the parahippocampal region, as we know them today (Ramón y Cajal 1909; Lorente de Nó 1933; Lorente de Nó 1934) Many studies have followed, either aiming to describe all the subfields (Witter and Amaral 2004), or they focussed on one area, providing a more detailed description, often resulting in further subdivisions of the area of interest, e.g. (Insausti et al. 1997; Burwell 2001). This resulted in somewhat fragmented and often inconsistent delineations, which hampers the use of such architectonic descriptions as a way to describe experimental results. The present account establishes a set of precise criteria that allows the identification of anatomical borders between all currently recognized subareas of the rat hippocampal region.

In the past decades, many studies have highlighted functional and connectional heterogeneity of many of the now recognized hippocampal and parahippocampal subareas. However, the lack or inconsistencies of clear standardized criteria to delineate the subareas may have caused imprecision in the anatomical identification of experimental observation and manipulations (Hafting et al. 2005; Barry et al. 2007; Burgalossi et al. 2011). Those interpretation errors may multiply as the accuracy of experimental tools is increasing. Some examples of these recent technical advances strongly dependent on a fine histological interpretation are the new viral, transgenic and optogenetic approaches which allow the specific manipulation of the activity of selected neural populations (Gradinaru, Zhang et al. 2010; Raimondo, Kay et al. 2012; Zhang, Ye et al. 2013), whole-cell in vivo recordings (Lee, Manns et al. 2006; Burgalossi, Herfst et al. 2011; Domnisoru, Kinkhabwala et al. 2012; Gu, Arruda-Carvalho et al. 2012) and high-resolution functional imaging (Dombeck, Harvey et al. 2010).

Previously published anatomical descriptions quite often lack precision or reliability by either considering criteria only valid for one sectioning plane or by not focusing on the whole hippocampal region. In addition, these descriptions often may not pay attention to subtle variations, and the number of illustrations provided is limited, leaving room for interpretation errors and inconsistencies. Most importantly,

almost all accounts described the overall or average architectonical features of the hippocampal and parahippocampal subareas, but failed to highlight the criteria that define the borders between those areas. The atlas presented here focuses on these markers and defines a set of cytoarchitectonic criteria apparent in simple neuronal staining that allow distinguishing between neighbouring hippocampal areas. In the absence of clear differences in neuronal staining, the present work establishes an additional set of chemoarchitectonic criteria made apparent with immuno-staining against two calcium-binding proteins, calbindin and parvalbumin. The significant advantage of our approach compare to previous accounts is that the boundaries we described are verified in all three major sectional plans (i.e. coronal, sagittal and horizontal). In addition, the boundaries as applied in any of these three planes have been verified in the other two, to assure that they are consistent throughout. Inconsistencies were easily detected and borders readjusted by mapping the single plane delineations onto a standard three-dimensional rat brain (Kjonigsen et al. in prep).

The choice for the markers used in the present atlas to define the various hippocampal and parahippocampal subareas is based on pragmatic considerations and on proven robustness. Both Nissl stain and staining for NeuN provide a reliable cytoarchitectonic visualization. Yet, the Nissl stain is unfortunately not always stable with respect to the density of the staining pattern. Therefore we privileged the use of NeuN, which is a more stable procedure and provides comparable images. Such stability is needed to obtain high-resolution digital images of all sections for the interactive web-based atlas (Kjonigsen et al. 2011). The selection of calbindin and parvalbumin to further delineates the borders between areas was based on previously published data (Insausti et al. 1997; Naber et al. 1999; Burwell 2001; Naber et al. 2001; Boccara et al. 2010). This literature demonstrates that these two markers, combined with NeuN, provide a powerful, stable and thus reliable, easy approach to delineate all subdivisions for the purpose of both descriptive and experimental studies. Other staining have been reported very useful to highlight some specific borders: for instance staining for heavy metals using the TIMM method or staining for dynorphin, acetylcholinesterase, myelin or nonphosphorylated neurofilament protein with an antibody against SMI-32. Yet we did not include their pattern of expression in the present atlas, as they did not add additional information to the three procedures presented here.

Most of the anatomical borders of the current atlas are similar to what had been presented in previous accounts. However some borders were reappraised based on the availability of three different planes of sectioning and of differential preparations with calbindin or parvalbumin (see some examples below). Though special attention was given to the three dimensional coherence of the described borders and their definitions, it is apparent that differences in staining intensity do exist in the various planes of sectioning. Such discrepancies have been highlighted in the text. Some disparities might also exist between animals, not only between strains but also within strains. Some of this variation may be related to age or sex, but other remains unexplained for and unpredictable. For example, we observed a striking diversity in the dorsolateral extent of the parasubiculum. In some animals the parasubiculum may extent slightly laterally, just dorsal to MEC, where it borders POR. While in other animals, PaS may extend further laterally such that it actually separates to dorsal MEC from POR over a substantial part of the dorsal MEC border. This can be clearly seen in sagittal sections and has led some authors to mistakenly conclude that this part of PaS was the medial-dorsal tip of MEC (Burgalossi et al. 2011). The use of differential staining, notably calbindin, highlights that misconception and establishes the curvature of the PaS around the MEC (Figure 2: A9-11).

Though many borders are striking, others are more difficult to identify when looking at a single section. Yet, those uncertainties can often be resolved by looking at the emergence of a specific marker in several adjacent sections or by choosing the adequate sectioning plane or even combining results from several sectioning planes. Again a striking example is the delicate delineation between POR, MEC and PaS in coronal and horizontal sections. The process of positioning these borders is facilitated by either working with sagittal sections or by an analysis of multiple adjacent horizontal sections. Another example is the contrast between the difficult positioning of the border between LEC and PER in sagittal sections and how strikingly clear it is in coronal sections. While constructing the present atlas, we used the three dimensional visualization to facilitate the correct positioning of the LEC/PER border in sagittal sections.

The nomenclature proposed in the present atlas is quite standard. We opted to divide the hippocampal region into the hippocampal formation (HF) and the parahippocampal region (PHR) based on their laminar features. The structures we

included here in the HF are the dentate gyrus (DG), fields CA3, CA2, and CA1, and the subiculum (Sub). These HF structures form a continuum of three-layered cortex, also called alleocortex, that contrast with the PHR structures, which consist of the pre- and parasubiculum , and the entorhinal, perirhinal and postrhinal cortex (respectively PrS, PaS, EC, PER and POR). These areas were grouped as constituting the PHR based on varied arguments such as their specific connectivity to the HF. In 1923, Lewis published a historical and etymological work on the anatomy of the hippocampus where he attributes to Arantius (1587) the fatherhood of the appellation and to Duvernoy the first illustration of the structure (1729). He further reported that Winsløw introduced for the first time the idea of horn, by comparing the curvature of the structure to this of a ram's horn and that Garengeot (1742) proposed the latin term Cornu Ammonis (acronym CA), which stands for Ammon's horn, in reference to the Egyptian god often depicted as having the head of a ram (Lewis 1923). The initial histological work from Golgi (Golgi 1886), Sala (Sala 1891), Schaffer (Schaffer 1892) and Ramón y Cajal (Ramón y Cajal 1893) helped to establish some of the different subfield of the hippocampal region. The original nomenclature is mostly derived from the analysis of Golgi-stained material by Ramón y Cajal and his student, Lorenté de Nó. This initial work was later revised based on new techniques. Already in the earliest cytoarchitectonic descriptions of the mammalian cortex, cortices were classified based on their number of layers with the two major types being the allocortex and the neocortex (or isocortex) that presented six-layers. In addition, transitional zones have been suggested to exist between the three-layered and six-layered cortical areas: the periallocortex and proisocortex (Stephan 1975). Even though the six layers are not always clearly visible in all structures of the PHR, one can see a salient increase in number of layers at the transition with the HF. For example, the Sub/PrS border is characterized by the sudden emergence of an additional cortical sheet positioned superficially to and strictly separated from the deeper continuation of the subicular sheet by a cell-free zone, termed lamina dissecans. At the border between EC, PER and POR the lamina dissecans disappears, giving way to a more homogeneously layered cortex, that resembles the six-layered neocortex. However, in contrast to the adjacent neocortex, PER and POR do not have a marked granular cell layer IV.

We divided here the HF in DG, CA1, CA2, CA3 and Sub. This definition is quite commonly accepted nowodays. The first description of the DG was actually the

one of the hippocampus by Arantius. About 200 years later, Tarin (Tarin 1750) described anew that structure and called it the fascia dentate derived from the Latin *dentatus* (tooth-like), in reference to its shape. The denomination "dentate gyrus" dates from 1861 (Huxley 1861), yet Cajal used the term "fascia dentata". Lorenté de Nó (Lorente de Nó 1921; Lorente de Nó 1934) divided the hippocampus proper in four subfields and he named them CA1, CA2, CA3 and CA4, following on Garengeot Cornu Ammonis. CA4 designate the terminal portion of the hippocampal pyramidal cell layer that inserts within the limbs formed by the granule cell layer of the DG or the hilus as if it were a portion of the hippocampus yet it was later designated as belonging to the dentate gyrus (Blackstad 1956; Amaral 1978). The use of the term CA4 has remained inconsistent and will therefore not be used in the present account, especially as calbindin staining permit to distinguish the clearly positive neuropil of the hilus from the proximal part of CA3. The hippocampus proper can clearly be divided into two major regions, a large-celled proximal region and a smaller-celled distal region. Ramón y Cajal (1909) called these two regions 'regio inferior' and 'regio superior', respectively. However, the terminology of Lorente de Nó in CA1-4 has achieved more common usage. His CA3 and CA2 fields are equivalent to the large-celled regio inferior of Ramon y Cajal and his CA1 is equivalent to regio superior. In addition to differences in the size of the pyramidal cells in CA3 and CA1, there is a clear-cut connectional difference. The CA3 pyramidal cells receive a mossy fiber input from DG and CA1 pyramidal cells do not. The CA2 field has been a matter of some controversy. As originally defined by Lorente de Nó, it was a narrow zone of cells interposed between CA3 and CA1 that had large cell bodies like CA3 but did not receive mossy fiber innervation like CA3 cells. Although the validity of this subdivision has often been questioned, the bulk of evidence indicates that indeed there is a narrow CA2 (approximately 250 μm), located distal to the end bulb of the mossy fiber projection. This region has connectional and functional differences (Jones and McHugh 2011; Piskorowski and Chevaleyre 2012) when compared with the other hippocampal fields. In many respects, CA2 resembles a terminal portion of the CA3 field, yet in other ways CA2 is quite distinct from both CA3 and CA1. The subiculum is the Latin for "support". Ramon y Cajal used that term to describe a supporting area of the hippocampus (Ramón y Cajal 1909). However the area was not clearly delineated until Lorenté de Nó limited the subiculum to the three-layer cortex adjacent to CA1 where the thin-packed cell layer typical of the DG and the CA fields

gets much wider and less organized (Lorente de Nó 1934). Note that a number of authors use the term "subicular complex" to indicate a conglomerate of cytoarchitectonically different, relatively small cortical fields including the Sub, the PrS and the PaS, yet we do not consider these areas as belonging together based on their different layering.

In the present account we mostly used cyto- and chemoarchitectonic criteria to subdivide the cortex, yet connectivity often provide relevant information confirming architectonically defined borders and nomenclature. Such information was at the source of our definition of the PHR structures as being PrS, PaS, EC, POR and PER. We further subdivided some of these areas as indicated below. We have chosen to use the term presubiculum without further subdividing this structure due to its overall homogeneity in connectivity and histochemical appearance (Blackstad 1956; Haug 1976; Witter et al. 1989; Witter 2002; Honda and Ishizuka 2004; Honda et al. 2008). However, one should not that in the past, several authors have recognized the septal portion of PrS as a separated area named postsubiculum and equivalent to the area 48 (region post- or retrosubicularis) according to Brodmann (Rose and Woolsey 1948; Swanson and Cowan 1977; Vogt and Miller 1983; van Groen and Wyss 1990). Futhermore, One should be careful to avoid the confusion with the term "prosubiculum", initially used to described the transitional region between field CA1 and the subiculum proper (Vogt and Vogt 1919; Rose 1926; Lorente de Nó 1934). The prosubiculum was defined as an area where the stratum radiatum was no longer visible and where the pyramidal cell layer of CA1 merged and overlapped with subicular pyramidal cells. We follow the choice of many contemporary researchers and do not differentiate a prosubiculum by considering this area as an oblique transitional region where field CA1 gradually replaces the Sub. We decided to differentiate the parasubiculum (PaS) from the presubiculum based on several differences in connectivity and architectonics. What we define as PaS encloses Brodmann areas 49a, 49b and 29e. Area 29 has often be considered to constitute the retrosplenial cortex, yet several authors showed that this area is most probably separated and attached to the PaS (Blackstad 1956; Stephan 1975; Haug 1976). In the present account, we will consider the PaS as a whole and will not further subdivide it. The entorhinal cortex is one of the largest structures of the parahippocampal region and received recently a renewed interest due to its functional heterogeneity. Therefore, we detailed carefully its subdivision by first distinguishing between medial

and lateral entorhinal cortex (i.e. respectively MEC and LEC). Lorente de Nó was the first to subdivide the entorhinal cortex, on the basis of the projections to the hippocampal formation, in lateral, intermediate, and medial subdivisions (1933). Brodmann (Brodmann 1909), using cytoarchitectonic criteria, parceled the entorhinal cortex into two fields, a lateral area 28a and a medial area 28b. Note the confusing use by Krieg (Krieg 1946; Krieg 1946) of the term 28a for the medial division of the entorhinal cortex and the term 28b for its lateral division. Although the subdivision into a lateral and a medial entorhinal cortex appears to be generally accepted, several authors felt the need to recognize more than two subdivisions (Blackstad 1956; Haug 1976; Krettek and Price 1977; Wyss 1981). We followed this view in the atlas presented here and further subdivided the MEC in medial (ME) and caudal (CE) entorhinal cortex, and the LEC in dorsal-lateral (DLE), dorsal-intermediate (DLE) and ventral-intermediate (VIE) entorhinal cortex. The VIE and to a lesser extent ME have several features in common with the ill-defined, so-called intermediate entorhinal cortex (Blackstad 1956; Steward 1976; Wyss 1981; Ruth et al. 1982; Ruth et al. 1988). The last two PHR subareas are the perirhinal and postrhinal cortices (PER and POR). We decided no to subdivide further POR, even though some authors had proposed a distinction between dorsal and ventral areas has been proposed (Burwell 2001). In view of the absence of clear criteria to delineate these subdivions in all three planes we did not implement that nomenclature. Regarding PER, we did subdivide it into area 35 and 36 (paxinos an dwatson stereotaxic atlas; Swanson Stereotaxic atlas). In that we followed Brodmann's terminology as first described by Rose who refereed to area 35 as perirhinal cortex and area 36 as ectorhinal cortex in the mouse brain (1926). This nomenclature was used by Krieg (1946) to describe the perirhinal cortex in the rat, although his rostral border was positioned way more caudally than is done in the present account. Deacon et al (Deacon et al. 1983), noted that the rostral and caudal part of area 35 and 36 were both hodologically and cytoarchitectonically different from each other. This led him to separate the perirhinal cortex into a rostral perirhinal and a caudal postrhinal area. This separation was later confirmed by other connectivity studies and we essentially followed the delineations of that study (Burwell 2001).

The current database is integrated with an on-line application (http://www.rbwb.org), which currently consists of the updated architectonic description of each subarea and an interactive coronal atlas made available through a

virtual microscope (Kjonigsen et al. 2011). Soon, the sagittal and horizontal sections will be entered in this application. In addition, the three dimensional representations of all subdivisions will be made available through the use of a standardized representation of the rat brain, the so-called Waxholm rat brain (Johnson et al. 2010).
This atlas aims to become a standard tool for experimentalists both in the planning of experiments and in the interpretation and presentation phase of their experimental data. It provides them the opportunity to carefully decide beforehand which is the best plane of sectioning and whether multiple stains are needed in order to determine a given anatomical border. In addition to its user-friendly interactivity and flexibility, one of the advantages of this on-line atlas is that it can be easily updated with newly obtained experimental findings. Finally, we foresee that this atlas may allow to the reconciliation of diverging results through a meta-analysis of data obtained/represented in sections obtained in different planes.

Figures

Figure 1 Three-dimensional views of the hippocampal region obtained with (?): **(**A) Medial side view of one hemisphere. (B) Caudal view. (C) Lateral side view. Color code as presented in the lower panel. Dashed lines: numbers corresponding to sections presented in figure 2-4.
HF: hippocampus formation; PHR: parahippocampal region; DG: dentate gyrus; CA1-3: Cornu Ammonis 1-3, Sub: subiculum; PrS: presubiculum; PaS: parasubiculum; EC: entorhinal cortex; PER: perirhinal; POR: postrhinal; MEC: medial entorhinal cortex; LEC; lateral entorhinal cortex; 35: perirhinal area 35; 36: perirhinal area 36; CE: caudal entorhinal area; ME: medial entorhinal area; VIE; ventral intermediate entorhinal area; DIE: dorsal intermediate entorhinal area; DLE: dorsal lateral entorhinal area

Figure 2 Selected coronal sections: (A) Delimitation of the hippocampal region subareas. Color code as presented in the lower panel. (B) Nissl sections. (C) Parvalbumin sections. (D) Calbindin sections. Numbers correspond to levels presented in figure 1.
Rsc: retrosplenial cortex; see figure 1 for other acronyms

Figure 3 Selected sagittal sections: (A) Delimitation of the hippocampal region subareas. Color code as presented in the lower panel. (B) Nissl sections. (C) Parvalbumin sections. (D) Calbindin sections. Numbers correspond to levels presented in figure 1.
Te.Cx: temporal cortex; Vi.Cx: visual cortex; Rsc: retrosplenial cortex; see figure 1 for other acronyms

Figure 4 Selected horizontal sections: (A) Delimitation of the hippocampal region subareas. Color code as presented in the lower panel. (B) Nissl sections. (C) Parvalbumin sections. (D) Calbindin sections. Numbers correspond to levels presented in figure 1.
Rsc: retrosplenial cortex; see figure 1 for other acronyms

References

Akam, T., I. Oren, L. Mantoan, E. Ferenczi and D. M. Kullmann (2012). "Oscillatory dynamics in the hippocampus support dentate gyrus-CA3 coupling." Nat Neurosci **15**(5): 763-8.

Amaral, D. G. (1978). "A Golgi study of cell types in the hilar region of the hippocampus in the rat." J Comp Neurol **182**(4 Pt 2): 851-914.

Amaral, D. G., H. E. Scharfman and P. Lavenex (2007). "The dentate gyrus: fundamental neuroanatomical organization (dentate gyrus for dummies)." Prog Brain Res **163**: 3-22.

Barry, C., R. Hayman, N. Burgess and K. J. Jeffery (2007). "Experience-dependent rescaling of entorhinal grids." Nat Neurosci **10**(6): 682-4.

Blackstad, T. W. (1956). "Commissural connections of the hippocampal region in the rat, with special reference to their mode of termination." J Comp Neurol **105**(3): 417-537.

Boccara, C. N., F. Sargolini, V. H. Thoresen, T. Solstad, M. P. Witter, E. I. Moser and M. B. Moser (2010). "Grid cells in pre- and parasubiculum." Nat Neurosci **13**(8): 987-94.

Brodmann, K. (1909). Vergleichende Lokalisationslehre der Grosshirnrinde in ihren Prinzipien dargestellt auf Grund des Zellenbauers. Leipzig.

Brun, V. H., T. Solstad, K. B. Kjelstrup, M. Fyhn, M. P. Witter, E. I. Moser and M. B. Moser (2008). "Progressive increase in grid scale from dorsal to ventral medial entorhinal cortex." Hippocampus **18**(12): 1200-12.

Burgalossi, A., L. Herfst, M. von Heimendahl, H. Forste, K. Haskic, M. Schmidt and M. Brecht (2011). "Microcircuits of functionally identified neurons in the rat medial entorhinal cortex." Neuron **70**(4): 773-86.

Burke, S. N., A. P. Maurer, A. L. Hartzell, S. Nematollahi, A. Uprety, J. L. Wallace and C. A. Barnes (2012). "Representation of three-dimensional objects by the rat perirhinal cortex." Hippocampus **22**(10): 2032-44.

Burwell, R. D. (2001). "Borders and cytoarchitecture of the perirhinal and postrhinal cortices in the rat." J Comp Neurol **437**(1): 17-41.

Burwell, R. D. and D. M. Hafeman (2003). "Positional firing properties of postrhinal cortex neurons." Neuroscience **119**(2): 577-88.

Burwell, R. D., M. P. Witter and D. G. Amaral (1995). "Perirhinal and postrhinal cortices of the rat: a review of the neuroanatomical literature and comparison with findings from the monkey brain." Hippocampus **5**(5): 390-408.

Caballero-Bleda, M. and M. P. Witter (1993). "Regional and laminar organization of projections from the presubiculum and parasubiculum to the entorhinal cortex: an anterograde tracing study in the rat." J Comp Neurol **328**(1): 115-29.

Chang, E. H. and P. T. Huerta (2012). "Neurophysiological correlates of object recognition in the dorsal subiculum." Front Behav Neurosci **6**: 46.

Cuello, A. C., J. V. Priestley and M. V. Sofroniew (1983). "Immunocytochemistry and neurobiology." Q J Exp Physiol **68**(4): 545-78.

Deacon, T. W., H. Eichenbaum, P. Rosenberg and K. W. Eckmann (1983). "Afferent connections of the perirhinal cortex in the rat." J Comp Neurol **220**(2): 168-90.

Deshmukh, S. S. and J. J. Knierim (2011). "Representation of non-spatial and spatial information in the lateral entorhinal cortex." Front Behav Neurosci **5**: 69.

Fyhn, M., S. Molden, M. P. Witter, E. I. Moser and M. B. Moser (2004). "Spatial representation in the entorhinal cortex." Science **305**(5688): 1258-64.

Golgi, C. (1886). Sulla Fina Anatomia Degli Organi Centrali del Sistema Nervoso Milano, Hoepli.
Gradinaru, V., F. Zhang, C. Ramakrishnan, J. Mattis, R. Prakash, I. Diester, I. Goshen, K. R. Thompson and K. Deisseroth (2010). "Molecular and cellular approaches for diversifying and extending optogenetics." Cell **141**(1): 154-65.
Hafting, T., M. Fyhn, S. Molden, M. B. Moser and E. I. Moser (2005). "Microstructure of a spatial map in the entorhinal cortex." Nature **436**(7052): 801-6.
Hargreaves, E. L., G. Rao, I. Lee and J. J. Knierim (2005). "Major dissociation between medial and lateral entorhinal input to dorsal hippocampus." Science **308**(5729): 1792-4.
Harvey, C. D., F. Collman, D. A. Dombeck and D. W. Tank (2009). "Intracellular dynamics of hippocampal place cells during virtual navigation." Nature **461**(7266): 941-6.
Haug, F. M. (1976). "Sulphide silver pattern and cytoarchitectonics of parahippocampal areas in the rat. Special reference to the subdivision of area entorhinalis (area 28) and its demarcation from the pyriform cortex." Adv Anat Embryol Cell Biol **52**(4): 3-73.
Henriksen, E. J., L. L. Colgin, C. A. Barnes, M. P. Witter, M. B. Moser and E. I. Moser (2010). "Spatial representation along the proximodistal axis of CA1." Neuron **68**(1): 127-37.
Honda, Y. and N. Ishizuka (2004). "Organization of connectivity of the rat presubiculum: I. Efferent projections to the medial entorhinal cortex." J Comp Neurol **473**(4): 463-84.
Honda, Y., Y. Umitsu and N. Ishizuka (2008). "Organization of connectivity of the rat presubiculum: II. Associational and commissural connections." J Comp Neurol **506**(4): 640-58.
Huxley, T. H. (1861). "On the zoological relations of man with the lower animals." Natural History Review **1**.
Insausti, R. (1993). "Comparative anatomy of the entorhinal cortex and hippocampus in mammals." Hippocampus **3 Spec No**: 19-26.
Insausti, R., M. T. Herrero and M. P. Witter (1997). "Entorhinal cortex of the rat: cytoarchitectonic subdivisions and the origin and distribution of cortical efferents." Hippocampus **7**(2): 146-83.
Johnson, G. A., A. Badea, J. Brandenburg, G. Cofer, B. Fubara, S. Liu and J. Nissanov (2010). "Waxholm space: an image-based reference for coordinating mouse brain research." Neuroimage **53**(2): 365-72.
Jones, M. W. and T. J. McHugh (2011). "Updating hippocampal representations: CA2 joins the circuit." Trends Neurosci **34**(10): 526-35.
Kim, S. M., S. Ganguli and L. M. Frank (2012). "Spatial information outflow from the hippocampal circuit: distributed spatial coding and phase precession in the subiculum." J Neurosci **32**(34): 11539-58.
Kjelstrup, K. B., T. Solstad, V. H. Brun, T. Hafting, S. Leutgeb, M. P. Witter, E. I. Moser and M. B. Moser (2008). "Finite scale of spatial representation in the hippocampus." Science **321**(5885): 140-3.
Kjonigsen, L. J., T. B. Leergaard, M. P. Witter and J. G. Bjaalie (2011). "Digital atlas of anatomical subdivisions and boundaries of the rat hippocampal region." Front Neuroinform **5**: 2.
Kluver, H. and E. Barrera (1953). "A method for the combined staining of cells and fibers in the nervous system." J Neuropathol Exp Neurol **12**(4): 400-3.

Krettek, J. E. and J. L. Price (1977). "Projections from the amygdaloid complex and adjacent olfactory structures to the entorhinal cortex and to the subiculum in the rat and cat." J Comp Neurol **172**(4): 723-52.
Krieg, W. J. (1946). "Connections of the cerebral cortex; the albino rat; structure of the cortical areas." J Comp Neurol **84**: 277-323.
Krieg, W. J. (1946). "Connections of the cerebral cortex; the albino rat; topography of the cortical areas." J Comp Neurol **84**: 221-75.
Lee, A. K., J. Epsztein and M. Brecht (2009). "Head-anchored whole-cell recordings in freely moving rats." Nat Protoc **4**(3): 385-92.
Lever, C., S. Burton, A. Jeewajee, J. O'Keefe and N. Burgess (2009). "Boundary vector cells in the subiculum of the hippocampal formation." J Neurosci **29**(31): 9771-7.
Lewis, F. T. (1923). "The significance of the term Hippocampus." J Comp Neurol **35**(3): 213-30.
Lorente de Nó, R. (1921). "La corteza cerebral del ratón. Primera contribución. La corteza acústica." Trab Lab Invest **19**: 147-88.
Lorente de Nó, R. (1933). "Studies on the structure of the cerebral cortex." J Psychol Neurol **45**(381-438).
Lorente de Nó, R. (1934). "Studies of the structure of the cerebral cortex. II. Continuation of the study of the ammonic system." J Psychol Neurol **46**: 113-77.
Loyez, M. (1910). "Coloration des fibres nerveuses par la method ál'hématoxyline au fer après inclusion a la celloidine." C.R. Soc Biol (Paris) **69**: 511-3.
Moser, E., M. B. Moser and P. Andersen (1993). "Spatial learning impairment parallels the magnitude of dorsal hippocampal lesions, but is hardly present following ventral lesions." J Neurosci **13**(9): 3916-25.
Mullen, R. J., C. R. Buck and A. M. Smith (1992). "NeuN, a neuronal specific nuclear protein in vertebrates." Development **116**(1): 201-11.
Naber, P. A., M. P. Witter and F. H. Lopes da Silva (2001). "Evidence for a direct projection from the postrhinal cortex to the subiculum in the rat." Hippocampus **11**(2): 105-17.
Naber, P. A., M. P. Witter and F. H. Lopez da Silva (1999). "Perirhinal cortex input to the hippocampus in the rat: evidence for parallel pathways, both direct and indirect. A combined physiological and anatomical study." Eur J Neurosci **11**(11): 4119-33.
O'Keefe, J. and J. Dostrovsky (1971). "The hippocampus as a spatial map. Preliminary evidence from unit activity in the freely-moving rat." Brain Res **34**(1): 171-5.
Olton, D. S., M. Branch and P. J. Best (1978). "Spatial correlates of hippocampal unit activity." Exp Neurol **58**(3): 387-409.
Paxinos, G. and C. Watson (1998). The Rat Brain. In Stereotaxic Coordinates, Academic Press.
Paxinos, G. and C. Watson (2009). The Rat Brain. In stereotaxic coordinates. Amsterdam, Elsevier/AP.
Piskorowski, R. A. and V. Chevaleyre (2012). "Synaptic integration by different dendritic compartments of hippocampal CA1 and CA2 pyramidal neurons." Cellular and Molecular Life Sciences **69**(1): 75-88.
Pitkanen, A., M. Pikkarainen, N. Nurminen and A. Ylinen (2000). "Reciprocal connections between the amygdala and the hippocampal formation, perirhinal

cortex, and postrhinal cortex in rat. A review." Ann N Y Acad Sci **911**: 369-91.
Raimondo, J. V., L. Kay, T. J. Ellender and C. J. Akerman (2012). "Optogenetic silencing strategies differ in their effects on inhibitory synaptic transmission." Nat Neurosci **15**(8): 1102-4.
Ramón y Cajal, S. (1893). "Estructura del asta de Ammon y fascia dentata." Ann Soc Esp His Nat **22**.
Ramón y Cajal, S. (1909). Histologie du Systeme Nerveux de l'Homme et des Vertebretes. Paris, A. Maloine.
Ranck, J. B., Jr. (1984). "Head-direction cells in the deep cell layers of dorsal presubiculum in freely moving rats." Soc Neurosci **10**: 599.
Rose, J. E. and C. N. Woolsey (1948). "Structure and relations of limbic cortex and anterior thalamic nuclei in rabbit and cat." J Comp Neurol **89**(3): 279-347.
Rose, M. (1926). "Der allocortex bei tier und mensch." J Psychol Neurol **34**: 1-99.
Ruth, R. E., T. J. Collier and A. Routtenberg (1982). "Topography between the entorhinal cortex and the dentate septotemporal axis in rats: I. Medial and intermediate entorhinal projecting cells." J Comp Neurol **209**(1): 69-78.
Ruth, R. E., T. J. Collier and A. Routtenberg (1988). "Topographical relationship between the entorhinal cortex and the septotemporal axis of the dentate gyrus in rats: II. Cells projecting from lateral entorhinal subdivisions." J Comp Neurol **270**(4): 506-16.
Sala, I. (1891). "Zur feineren Anatomie des grossen Seepferdefusses." Zeitschr Wiss Zool **52**.
Sargolini, F., M. Fyhn, T. Hafting, B. L. McNaughton, M. P. Witter, M. B. Moser and E. I. Moser (2006). "Conjunctive representation of position, direction, and velocity in entorhinal cortex." Science **312**(5774): 758-62.
Savelli, F., D. Yoganarasimha and J. J. Knierim (2008). "Influence of boundary removal on the spatial representations of the medial entorhinal cortex." Hippocampus **18**(12): 1270-82.
Schaffer, K. (1892). "Beitrag zur histologie der Amnionshorn-formation." Arch Mikr Anat **39**: 511-632.
Schmued, L., J. Bowyer, M. Cozart, D. Heard, Z. Binienda and M. Paule (2008). "Introducing Black-Gold II, a highly soluble gold phosphate complex with several unique advantages for the histochemical localization of myelin." Brain Res **1229**: 210-7.
Solstad, T., C. N. Boccara, E. Kropff, M. B. Moser and E. I. Moser (2008). "Representation of geometric borders in the entorhinal cortex." Science **322**(5909): 1865-8.
Steffenach, H. A., M. Witter, M. B. Moser and E. I. Moser (2005). "Spatial memory in the rat requires the dorsolateral band of the entorhinal cortex." Neuron **45**(2): 301-13.
Stephan, H. (1975). Allocortex. Berlin, Springer.
Steward, O. (1976). "Topographic organization of the projections from the entorhinal area to the hippocampal formation of the rat." J Comp Neurol **167**(3): 285-314.
Swanson, L. W. (2004). Brain maps III : structure of the rat brain. An atlas with printed and electronic templates for data, models, and schematics. Amsterdam, Elsevier.

Swanson, L. W. and W. M. Cowan (1977). "An autoradiographic study of the organization of the efferent connections of the hippocampal formation in the rat." J Comp Neurol **172**(1): 49-84.
Tago, H., H. Kimura and T. Maeda (1986). "Visualization of detailed acetylcholinesterase fiber and neuron staining in rat brain by a sensitive histochemical procedure." J Histochem Cytochem **34**(11): 1431-8.
Tarin, P. (1750). Adversaria Anatomica. Paris, Moreau.
Taube, J. S., R. U. Muller and J. B. Ranck, Jr. (1990). "Head-direction cells recorded from the postsubiculum in freely moving rats. I. Description and quantitative analysis." J Neurosci **10**(2): 420-35.
van Groen, T. and J. M. Wyss (1990). "The postsubicular cortex in the rat: characterization of the fourth region of the subicular cortex and its connections." Brain Research **529**(1-2): 165-77.
van Strien, N. M., N. L. Cappaert and M. P. Witter (2009). "The anatomy of memory: an interactive overview of the parahippocampal-hippocampal network." Nat Rev Neurosci **10**(4): 272-82.
Voelker, C. C., N. Garin, J. S. Taylor, B. H. Gahwiler, J. P. Hornung and Z. Molnar (2004). "Selective neurofilament (SMI-32, FNP-7 and N200) expression in subpopulations of layer V pyramidal neurons in vivo and in vitro." Cereb Cortex **14**(11): 1276-86.
Vogt, B. A. and M. W. Miller (1983). "Cortical connections between rat cingulate cortex and visual, motor, and postsubicular cortices." J Comp Neurol **216**(2): 192-210.
Vogt, C. and O. Vogt (1919). "Allgemeinere Ergebnisse unserer Hirnforschung." J Psychol Neurol **216**(25): 192-210.
Wan, H., J. P. Aggleton and M. W. Brown (1999). "Different contributions of the hippocampus and perirhinal cortex to recognition memory." J Neurosci **19**(3): 1142-8.
Witter, M. P. (2002). The parahippocampal region: Past, present, and future. The Parahippocampal Region: Organization and Role in Cognitive Functions M. P. Witter and F. G. Wouterlood. London, Oxford Univ Press 3-20.
Witter, M. P. and D. G. Amaral (2004). Chapter 21: Hippocampal formation. The Rat Nervous System. San Diego, CA, Elsevier Academic Press. **3:** 635-704.
Witter, M. P., H. J. Groenewegen, F. H. Lopes da Silva and A. H. Lohman (1989). "Functional organization of the extrinsic and intrinsic circuitry of the parahippocampal region." Prog Neurobiol **33**(3): 161-253.
Witter, M. P. and E. I. Moser (2006). "Spatial representation and the architecture of the entorhinal cortex." Trends Neurosci **29**(12): 671-8.
Wouterlood, F. G., C. B. Canto, V. Aliane, A. J. Boekel, J. Grosche, W. Hartig, J. A. Belien and M. P. Witter (2007). "Coexpression of vesicular glutamate transporters 1 and 2, glutamic acid decarboxylase and calretinin in rat entorhinal cortex." Brain Struct Funct **212**(3-4): 303-19.
Wouterlood, F. G., J. Grosche and W. Hartig (2001). "Co-localization of calretinin and calbindin in distinct cells in the hippocampal formation of the rat." Brain Res **922**(2): 310-4.
Wouterlood, F. G., W. Hartig, G. Bruckner and M. P. Witter (1995). "Parvalbumin-immunoreactive neurons in the entorhinal cortex of the rat: localization, morphology, connectivity and ultrastructure." J Neurocytol **24**(2): 135-53.
Wyss, J. M. (1981). "An autoradiographic study of the efferent connections of the entorhinal cortex in the rat." J Comp Neurol **199**(4): 495-512.

Young, B. J., T. Otto, G. D. Fox and H. Eichenbaum (1997). "Memory representation within the parahippocampal region." J Neurosci **17**(13): 5183-95.
Zhu, X. O., M. W. Brown and J. P. Aggleton (1995). "Neuronal signalling of information important to visual recognition memory in rat rhinal and neighbouring cortices." Eur J Neurosci **7**(4): 753-65.

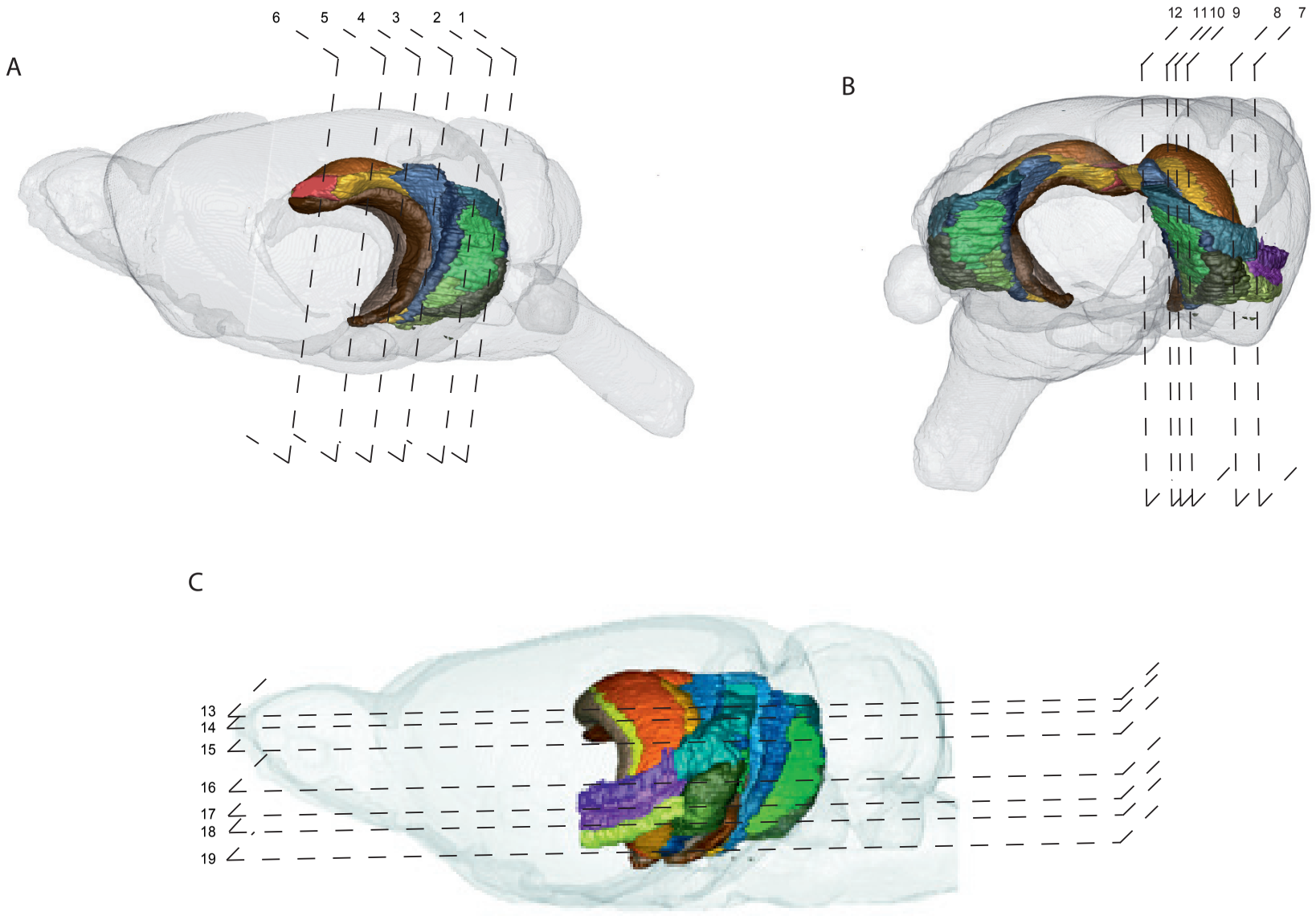
A
6
5
4
3
2
1
B
12
11
10
9
8
7
C
13
14
15
16
17
18
19

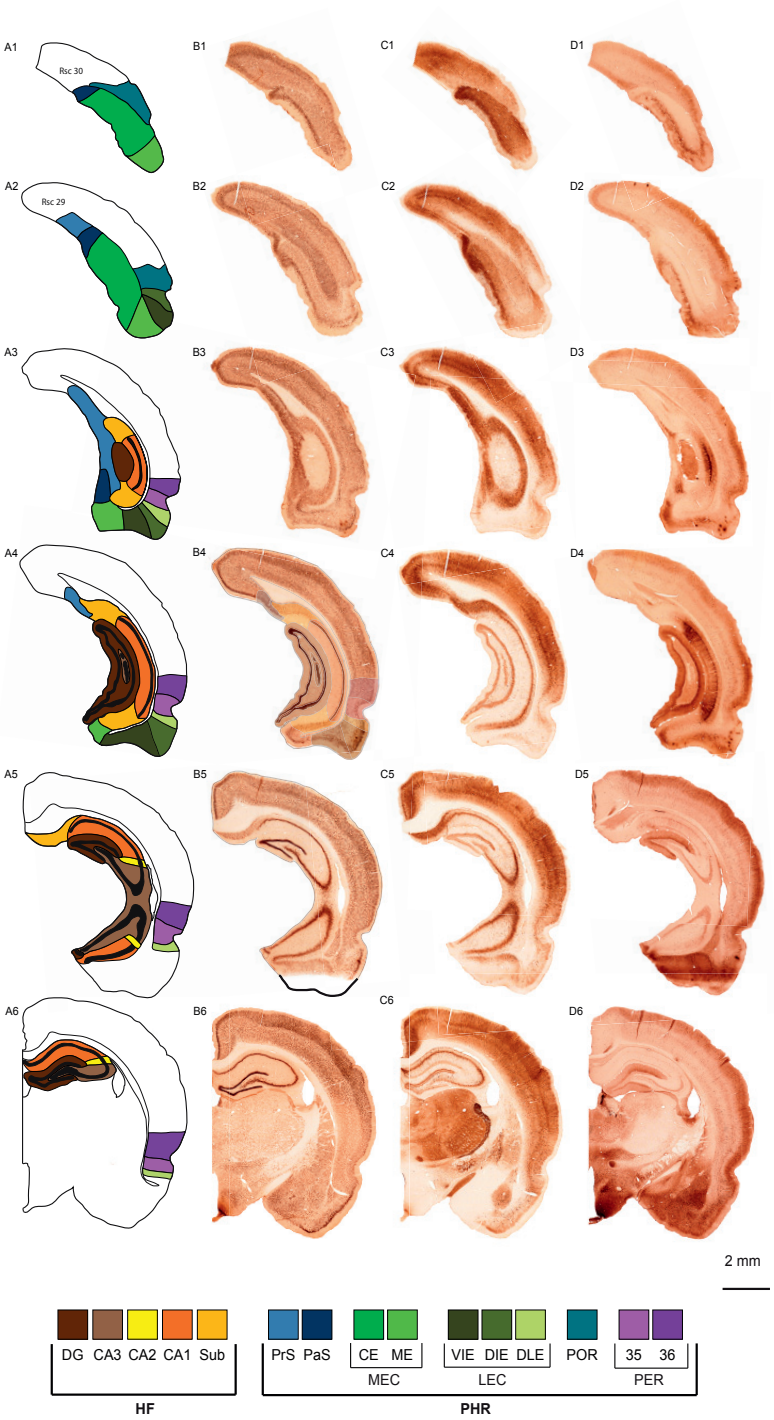
A1
Rsc 30
A2
Rsc 29
A3
A4
A5
A6
B1
B2
B3
B4
B5
B6
C1
C2
C3
C4
C5
C6
D1
D2
D3
D4
D5
D6
2 mm
DG CA3 CA2 CA1 Sub
HF
PrS PaS
CE ME
MEC
VIE DIE DLE
LEC
POR
35 36
PER
PHR

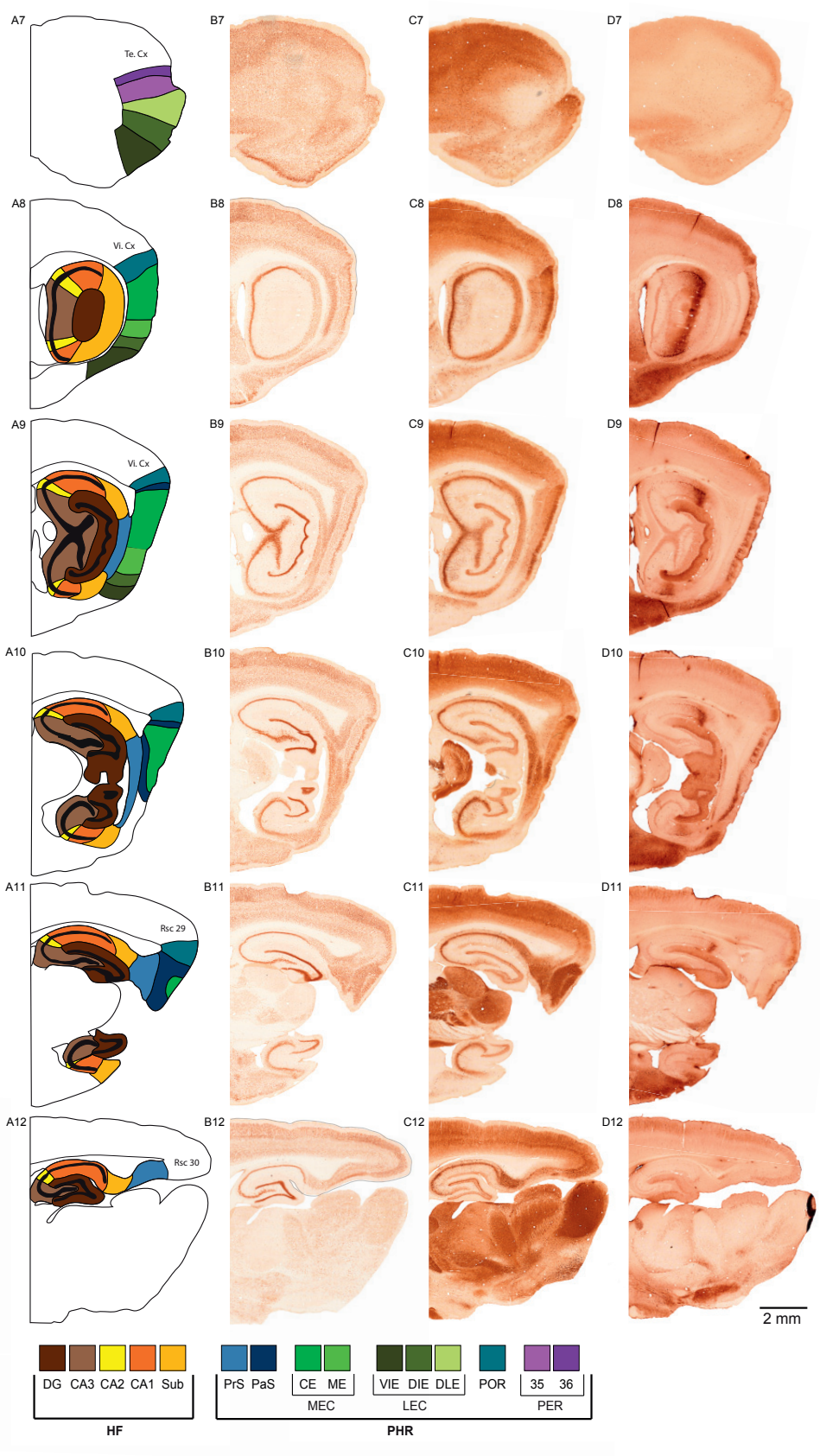
A7
B7
C7
D7
Te. Cx
A8
B8
C8
D8
Vi. Cx
A9
B9
C9
D9
Vi. Cx
A10
B10
C10
D10
A11
B11
C11
D11
Rsc 29
A12
B12
C12
D12
Rsc 30
2 mm
DG CA3 CA2 CA1 Sub
HF
PrS PaS
CE ME
MEC
VIE DIE DLE
LEC
POR
35 36
PER
PHR

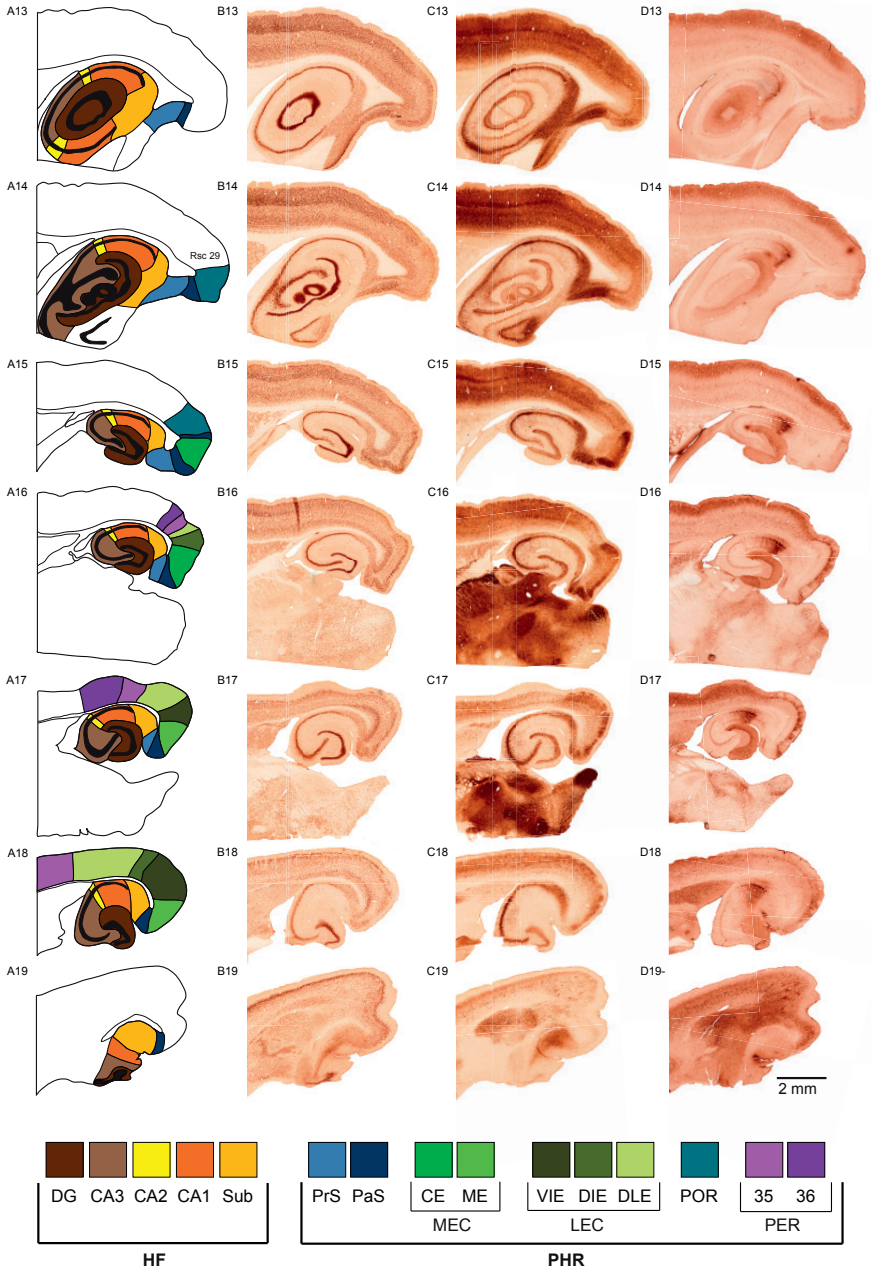
A13
B13
C13
D13
A14
B14
C14
D14
Rsc 29
A15
B15
C15
D15
A16
B16
C16
D16
A17
B17
C17
D17
A18
B18
C18
D18
A19
B19
C19
D19-
2 mm
DG CA3 CA2 CA1 Sub
HF
PrS PaS
CE ME
MEC
VIE DIE DLE
LEC
POR
35 36
PER
PHR